In this **Issue**

Highlights from this issue of *A&R* | **By Lara C. Pullen, PhD**

How Do Patients With Newly Diagnosed Systemic Lupus Erythematosus Present?

p. 91

In this issue, Mosca et al (p. 91) used data from a multicenter multiethnic cohort to describe the clinical manifestations that can be used to distinguish early systemic lupus erythematosus (SLE) from SLE-mimicking conditions. The authors reviewed clinical symptoms and serologic findings of 389 SLE patients, who received their initial diagnoses at lupus referral centers, and compared these data with the findings from 227 patients referred to the same centers for possible SLE, but who were given a different diagnosis after clinical and serologic evaluation.

Unexplained fever was more common in early SLE than in SLE-mimicking conditions (34.5% versus 13.7%), and less common features in early SLE included Raynaud's phenomenon (22.1% versus 48.5%), sicca symptoms (4.4% versus 34.4%), dysphagia (0.3% versus 6.2%), and fatigue (28.3% versus 37.0%). With regard to serologic findings, anti–double-stranded DNA, anti–β_2-glycoprotein I antibodies, positive Coombs' test results, autoimmune hemolytic anemia, hypocomplementemia, and leukopenia were more common in early SLE than in SLE-mimicking conditions.

The investigators found that symptoms detailed in the 1997 American College of Rheumatology (ACR) and the 2012 Systemic Lupus International Collaborating Clinics (SLICC) classification criteria occurred much more frequently among those with early SLE. There were differences in the classification criteria: fewer patients with early SLE were not identified as having early SLE with use of the SLICC criteria compared with the ACR criteria (16.5% versus 33.9%), and the ACR criteria demonstrated higher specificity than the SLICC criteria (91.6% versus 82.4%). The authors suggest their findings may aid in earlier diagnosis of SLE and provide information for ongoing initiatives to revise SLE classification criteria.

Impact of TNFi Versus NSAID Treatment on Radiographic Progression in Early AS

p. 82

Rheumatologists have questioned whether radiographic progression of ankylosing spondylitis (AS) can be prevented via effective treatment. In this issue, Park et al (p. 82) report that treatment with tumor necrosis factor inhibitors (TNFi) can effectively suppress inflammation and decrease radiographic progression in patients with early AS. In this study, patients in the TNFi group had longer disease duration, a higher baseline C-reactive protein (CRP) level, and a higher Bath Ankylosing Spondylitis Disease Activity Index score than patients in the control group.

When the investigators time-averaged CRP levels over radiographic intervals, they found lower CRP levels in patients treated with TNFi than in those treated with nonsteroidal antiinflammatory drugs (NSAIDs). The mean ± SD modified Stoke Ankylosing Spondylitis Spine Score (mSASSS) change over 2 years in the study population was 1.30 ± 2.97 units. Overall, an increase of 1 mg/dl time-averaged CRP level led to an increase of 1.02 mSASSS units per 2-year interval.

The researchers used a multivariable model to adjust for age, smoking status, baseline CRP level, and the presence of syndesmophytes at baseline, which resulted in the TNFi group having less mSASSS change over 2 years compared with the control group.
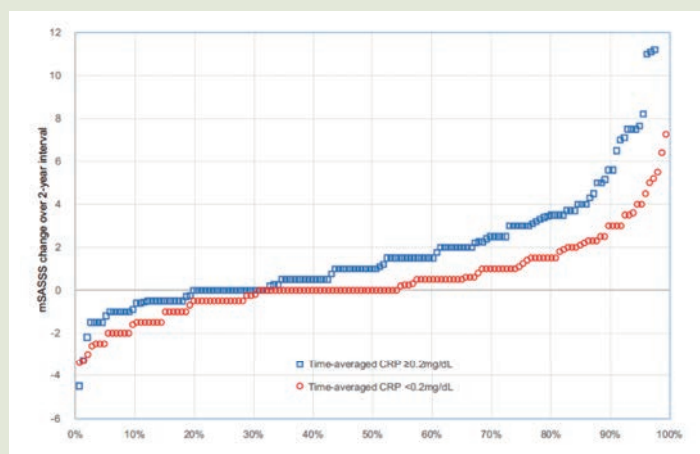

Figure 1. Cumulative probability plot showing radiographic progression during 2-year time intervals according to time-averaged CRP levels (<0.2 mg/dl versus ≥0.2 mg/dl) over individual intervals.

When time-averaged CRP was introduced into the model, it significantly influenced the mSASSS change and decreased the estimated group difference. The NSAID indices of both groups were not associated with either time-averaged CRP levels or mSASSS changes.

Association of Extensive Effusion-Synovitis With Progression of Cartilage Damage in Patients With OA and Meniscal Tear

Patients with knee osteoarthritis (OA) and meniscal tear frequently have synovitis and articular cartilage damage. In this issue, MacFarlane et al (page 73) examined a cohort of patients with OA and meniscal tear to assess the associations of baseline effusion-synovitis and the changes in effusion-synovitis with changes in cartilage damage. The authors report that the presence of extensive effusion-synovitis is associated with subsequent progression of cartilage damage over 18 months. The greatest risk of concurrent cartilage damage progression occurred in patients with extensive effusion-synovitis that persisted over time. In addition, extensive effusion-synovitis at baseline conferred a 50–70% increased risk of worsening cartilage damage depth.

The 18-month study included 221 participants from the Meniscal Tear in Osteoarthritis Research (MeTeOR) trial of surgery versus physical therapy for the treatment of meniscal tear. The investigators performed semiquantitative grading of effusion-synovitis and cartilage damage on baseline and follow-up magnetic resonance images and then dichotomized effusion-synovitis as none/small (minimal) and medium/large (extensive). Then an assessment of the association between baseline effusion-synovitis and changes in effusion-synovitis with changes in cartilage damage size and depth was conducted. The analyses were adjusted for patient demographic characteristics, treatment, and baseline cartilage damage.

The investigators found that effusion-synovitis was persistently minimal in 45.3% and persistently extensive in 21.3% of the patients. The balance of patients (33.5%) had minimal synovitis on one occasion and extensive synovitis on the other. In general, effusion-synovitis was associated with a nonsignificant 20–30% increased risk of worsening cartilage damage size. In adjusted analyses, patients with extensive effusion-synovitis at baseline had a relative risk (RR) of cartilage damage depth of 1.7. Those patients with persistently extensive effusion-synovitis had a significantly increased risk of progression of cartilage damage depth (RR 2.0) when compared to those with persistently minimal effusion-synovitis. These results are consistent with those of previous studies that have investigated the relationship between synovitis and cartilage damage.

Radiographic Progression of DIP Joint Osteoarthritis in Patients with Rheumatoid Arthritis

Distal interphalangeal (DIP) joints are generally considered to be unaffected by rheumatoid arthritis (RA). However, researchers have documented synovitis and bone marrow edema both in DIP joint osteoarthritis (OA) and RA. Although synovitis and bone marrow edema are associated with radiographic progression in hand OA and hand RA, the radiographic courses are substantially different. In this issue, Lechtenboehmer et al (p. 43) report the results of a systematic investigation of the incidence and radiographic progression of DIP joint OA in patients with concomitant RA, in relation to RA activity and patient characteristics.

The mean ± SD age of the patients was 56.1 ± 11.1 years, and the median follow-up period was 4.5 years. The researchers found that DIP joint OA was present in 60% of the patients at baseline. Higher mean age and higher mean body mass index were associated with the presence of DIP joint OA. In contrast, neither the presence of anti–citrullinated protein antibodies (ACPAs) nor the presence of rheumatoid factor were associated with DIP joint OA.

When the investigators looked at the Disease Activity Score using the erythrocyte sedimentation rate and metacarpophalangeal (MCP) joint erosions, they found that disease activity was not associated with DIP joint OA progression. Likewise, RA disease duration had no relevant effect size associated with DIP joint OA progression. Although known risk factors for DIP joint OA
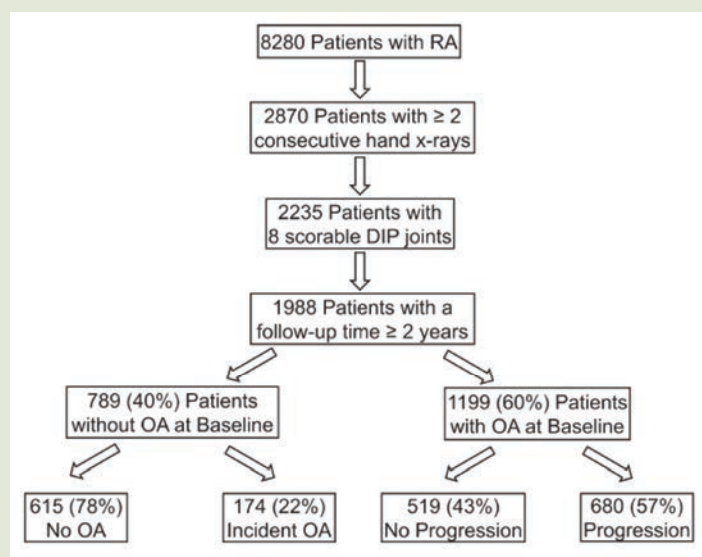

Figure 1. Patient selection process and DIP joint OA development and progression rates.

were seen in patients with RA and, given the finding that RA activity, the presence of ACPAs, and MCP joint erosions were not associated with the prevalence or progression of DIP joint OA, the researchers concluded that there are distinct roles of inflammation in the pathogenesis of RA and DIP joint OA.
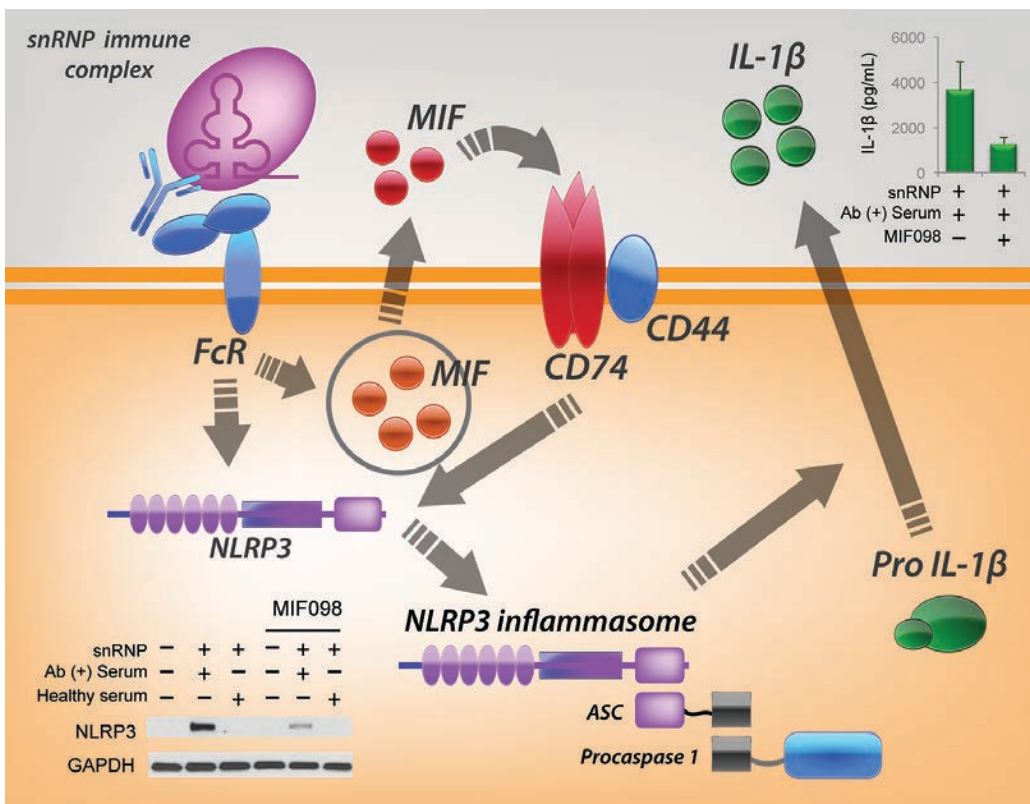
Clinical Connections

Macrophage Migration Inhibitory Factor Regulates U1 Small Nuclear RNP Immune Complex–Mediated Activation of the NLRP3 Inflammasome

CORRESPONDENCE
Insoo Kang, MD: insoo.kang@yale.edu

KEY POINTS

- The U1 snRNP immune complex induces MIF secretion and activates the NLRP3 inflammasome in human monocytes, leading to IL-1β production.

- Blocking MIF binding to its receptor CD74 suppresses NLRP3 expression and subsequent IL-1β production.

- Our findings demonstrate the upstream role of MIF in regulating U1 snRNP immune complex–mediated NLRP3 inflammasome activation in lupus.

SUMMARY

Macrophage migration inhibitory factor (MIF), produced primarily from activated monocytes and macrophages, is an upstream activator of innate immune responses. High-expression genotypes of MIF are linked to systemic lupus erythematosus (SLE; lupus) disease severity. U1 small nuclear RNP (snRNP) immune complex containing U1 snRNP and anti–U1 snRNP antibodies, which are found in SLE, induces MIF secretion and activates the NLRP3 inflammasome comprising NLRP3, ASC, and procaspase 1 in human monocytes, leading to the production of the proinflammatory cytokine interleukin-1β (IL-1β). Blocking MIF binding to its receptor CD74 with the small molecule MIF098 suppresses NLRP3 expression and subsequent IL-1β production, indicating the critical role of MIF in regulating NLRP3 inflammasome activation. These findings by Shin et al provide mechanistic insight and a therapeutic rationale for targeting MIF in subgroups of lupus patients, such as high-genotypic MIF expressers or those with anti-snRNP antibodies.

Interferon-γ–Mediated Immunopathology Potentiated by Toll-Like Receptor 9 Activation in a Murine Model of Macrophage Activation Syndrome

Weaver et al, *Arthritis Rheumatol* 2019;71:161–168.

CORRESPONDENCE
Lehn K. Weaver, MD, PhD: weaver11@email.chop.edu
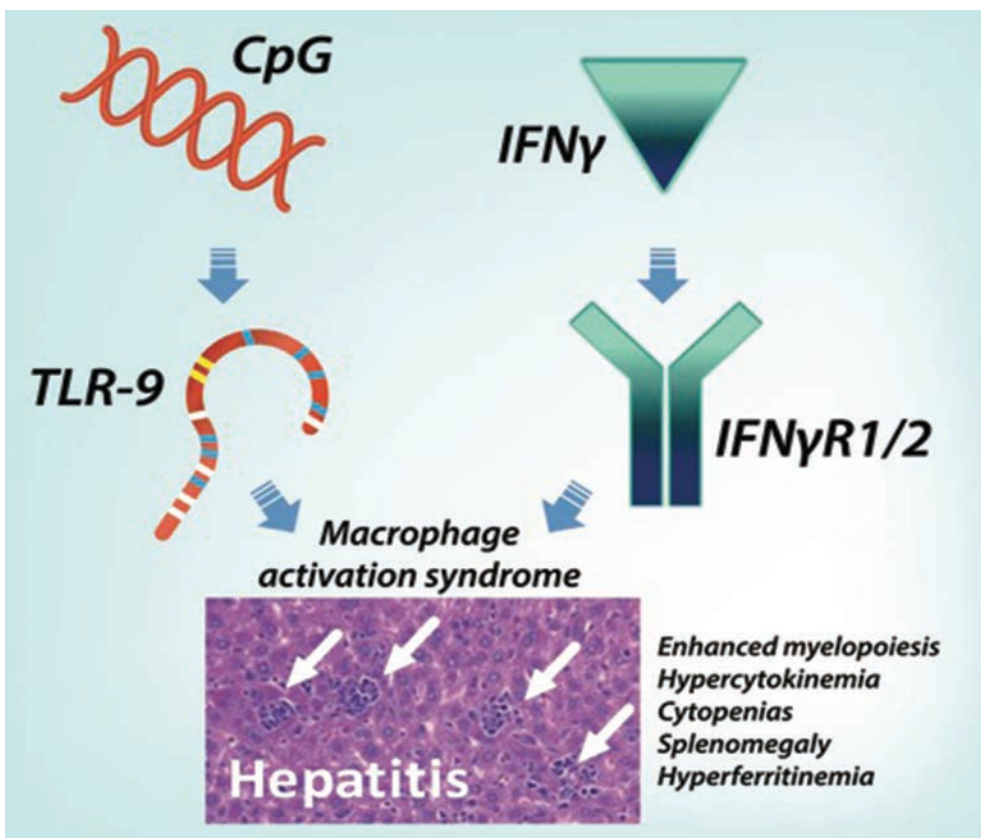
KEY POINTS

- IFNγ- and TLR-9–dependent signals are insufficient to trigger murine MAS individually.

- The pathogenesis of murine MAS requires activation of both IFNγ- and TLR-9–dependent signals to induce disease.

- Enhanced myelopoiesis by IFNγ- and TLR-9–dependent signals may be a common inflammatory pathway that synergistically amplifies immune responses in MAS.

SUMMARY

Macrophage activation syndrome (MAS) is a life-threatening complication of inflammatory rheumatologic conditions. Interferon-γ (IFNγ) is considered to be a therapeutic target for the treatment of MAS, yet the mechanisms leading to IFNγ-mediated immunopathology remain unknown. High-dose IFNγ is also insufficient to recapitulate all manifestations of MAS in murine models, suggesting additional signals potentiate IFNγ-mediated immunopathology to drive disease. As Toll-like receptor (TLR) activation has been implicated in the pathogenesis of both human and murine MAS, Weaver et al investigated whether TLR signals contribute to murine MAS. Both IFNγ and TLR-9 signaling were observed to be required for induction of MAS, as IFNγ-deficient animals develop MAS when treated with both a TLR-9 agonist and IFNγ, but not when they are treated with these inflammatory signals individually. IFNγ and TLR augmented inflammatory myelopoiesis, which may contribute to disease by accelerating the production of new TLR-9–responsive monocytes. These data demonstrate the requirement for both IFNγ- and TLR-9–dependent signals in the pathogenesis of experimental MAS.

Arthritis & Rheumatology

An Official Journal of the American College of Rheumatology
www.athritisrheum.org and wileyonlinelibrary.com

Arthritis & Rheumatology

An Official Journal of the American College of Rheumatology
www.athritisrheum.org and wileyonlinelibrary.com

VOLUME 71 • January 2019 • NO. 1

Clinical Images

Sjögren's Syndrome

Gout

Macrophage Activation Syndrome

Letters

ACR Announcements

Cover image: The figure on the cover (from Pringle et al, page 133) illustrates expression of the receptor for tumor necrosis factor in a salivary gland organoid cultured from human parotid salivary gland stem cells. Cell nuclei appear in blue and tumor necrosis factor receptor staining in red, resulting in a purple appearance in this overlap image. Expression of receptors for proinflammatory cytokines allows salivary gland stem cells to proliferate in response to proinflammatory cytokines and facilitates eventual replication-induced senescence.

AMERICAN COLLEGE
OF RHEUMATOLOGY
EDUCATION · TREATMENT · RESEARCH

Arthritis & Rheumatology

An Official Journal of the American College of Rheumatology
www.arthritisrheum.org and wileyonlinelibrary.com

EDITORIAL

A Fresh New Look, and a Fresh New Journal

Richard J. Bucala[1] iD and Marian T. Hannan[2] iD

The founding of *Arthritis & Rheumatism* (*A&R*) in 1958 by the American Rheumatism Association (now the American College of Rheumatology [ACR]) occurred at the advent of knowledge of immunologic abnormalities in patients with rheumatoid arthritis, systemic lupus erythematosus, and related disorders. Over its ensuing 60-year history, *A&R* (renamed *Arthritis & Rheumatology* in 2014) developed into a preeminent publication for disseminating research findings and advancing the field scientifically. Landmark papers addressed the role of autoantibodies and lymphocytes in rheumatic diseases and, in recent years, the clinical translation of cell- and cytokine-based paradigms of disease. Publication was expanded in 1988 with *Arthritis Care & Research* (*AC&R*), which increased the coverage of clinical research and included reports of studies analyzing economic, educational, and policy issues. Both journals have become international in scope yet remain first and foremost anchored to the academic and educational mission of the ACR.

This month introduces two initiatives by the ACR to better attend to the information and educational needs of our community, which includes not only investigators but practicing physicians and health professionals. First, *Arthritis & Rheumatology* and *Arthritis Care & Research* introduce a new article presentation format to enhance readers' experience with online and print publication. Second, the inaugural issue of *ACR Open Rheumatology*, a fully open access and online publication, debuts as the ACR's third venue for original research reports and scholarly articles.

The global expansion of research activities and scope of clinical medicine, together with the accessibility and speed of the internet, have led to an unprecedented expansion of new information and spawned alternative and innovative means of disseminating research findings. "Living" digital documents offer instantaneous links to graphical, video, and complex data files that promote discussion and continued analysis of published findings. The new formatting of the ACR's journals will facilitate these operations and improve readers' ability to access and make use of published content. It will include a clearer presentation of figures and tables, and a new font to enhance online and print reading.

Both *Arthritis & Rheumatology* and *Arthritis Care & Research* have thrived, with annual submissions numbering in the thousands, and they have become distinguished for publishing research to advance scientific rheumatology and improve clinical practice. Both journals have enjoyed great success but also are now weighted with so many submissions that they are not able to publish as much content as desired and must turn away many interesting reports and leave topical areas underserved. *ACR Open Rheumatology* will expand the ACR's portfolio of publications, which also includes *The Rheumatologist*, to better fulfill its mission to disseminate the highest-quality original research and information for rheumatologists. *ACR Open Rheumatology* will provide online access to full content to anyone, with no login or membership required. In addition, articles in *ACR Open Rheumatology* will be published under a Creative Commons Attribution-Noncommercial license, which means they can be used, reproduced, and distributed openly, with only a requisite for proper citation and noncommercial use. *ACR Open Rheumatology* will offer an added opportunity for authors to publish under the aegis of the ACR. Authors will be able to take advantage of internal resubmission from *A&R* and *AC&R* directly to *ACR Open Rheumatology*, and with expedited review (i.e., the review from *A&R* or *AC&R* could be utilized by *ACR Open Rheumatology*). Authors also may submit articles directly to *ACR Open Rheumatology*, without having submitted previously to *A&R* or *AC&R*.

In current circumstances, where the impact of biomedical research on clinical practice has never been greater, the need for thoughtful and expert peer review, professional editing, and high standards for data reporting is essential. The operating philosophy of our journals, now augmented with *ACR Open Rheumatology*, is unchanged: to offer the best publications in rheumatology for a diverse audience of researchers and health care professionals. We are excited by these new initiatives, which will better advance scientific discourse and improve clinical practice.

ACKNOWLEDGMENT

AUTHOR CONTRIBUTIONS

Drs. Bucala and Hannan drafted the article, revised it critically for important intellectual content, and approved the final version to be published.

AMERICAN COLLEGE
OF RHEUMATOLOGY
EDUCATION · TREATMENT · RESEARCH

EDITORIAL

The Evolving Art and Science of American College of Rheumatology Guidelines

Jinoos Yazdany,[1] Liron Caplan,[2] (iD) John Fitzgerald,[3] and Gabriela Schmajuk[4] (iD)

Frequently, disease management guidelines generate controversy. Earlier this year, in a research letter to *JAMA Internal Medicine,* authors critiqued American College of Rheumatology (ACR) guidelines for not being adequately evidence-based (1). When such criticisms arise, there is an important opportunity for reflection. Are ACR guidelines appropriately rigorous? Are there ways to improve upon current processes for guideline development? How can we improve the value and integrity of ACR guidelines moving forward?

The ACR guideline development process has evolved significantly over the last 2 decades. The early ACR guideline statements in the 1990s on topics such as lupus or osteoarthritis were primarily consensus statements generated by a group of experts to address key clinical management issues. Formal systematic literature reviews were generally not performed, there was no validated rating system for evaluating evidence, patients were not involved, and there was an overall lack of transparency about group processes, including conflict of interest policies. Still, these statements had advantages, including that they were written by respected leaders in the field and were simple to interpret.

In the 2000s, with calls for a more rigorous process and a growing body of evidence in rheumatology, this "eminence-based" process evolved into one that used Rand-UCLA appropriateness methodology, combined with components of the American College of Cardiology/American Heart Association evidence rating process (2). The Rand-UCLA method relied on the development of clinical scenarios and was applied to convert systematic literature review data into clinically relevant recommendations using expert opinion. Although the ACR completed a number of guidelines using this method, there were shortcom-

ings. Perhaps most importantly, the manner by which expert panels used the evidence ratings to derive their recommendations continued to be ambiguous. The method also strongly weighed evidence derived from randomized controlled trials (RCTs) over observational data without substantial consideration of a study's rigor. Systematic reviews were sometimes conducted but were not routinely published, limiting critical reappraisal of the methods. In addition, patients were minimally involved in the process, raising concerns that their interests were not adequately prioritized.

In 2012, after an evaluation of the 2011 National Academies standards for guideline development (3), the ACR overhauled its guideline development processes and began to incorporate the use of GRADE methodology (www.gradeworkinggroup.org) and also significantly increased patient involvement. All recent ACR guidelines, including the psoriatic arthritis guideline published in this issue of *Arthritis & Rheumatology* (4), now are developed using this methodology.

GRADE methodology offered advantages over previous approaches. The method consists of 2 components: 1) a systematic literature review to assess the certainty of effect estimates for each intervention considered, and 2) a recommendation strength that takes into account not only the quality of the available evidence, but also variability in patient values and preferences. GRADE standardizes the process of moving from evidence to recommendations and enables greater transparency about the judgments made during that process. A recommendation may be strong in the face of low-quality evidence in situations where convincing observational evidence exists and/or potential benefits greatly outweigh risks (or vice versa). Similarly, GRADE allows for a conditional recommendation even in the face of high-quality evidence; for example, an expensive new therapy supported by clinical trials but producing only a minimal added benefit might warrant a conditional recommendation. Importantly, the scientific evidence and the judgments of the voting panels are published to allow readers to review the specific factors underlying each recommendation.

GRADE ratings are reproducible when people with extensive experience use the method, although interrater reliability diminishes when evidence is more complex (5,6). The

[1]Jinoos Yazdany, MD, MPH: Zuckerberg San Francisco General Hospital and University of California, San Francisco; [2]Liron Caplan, MD, PhD: Rocky Mountain Region Veterans Affairs Medical Center, Aurora, Colorado; [3]John Fitzgerald, MD, PhD: University of California, Los Angeles; [4]Gabriela Schmajuk, MD, MSc: Department of Veterans Affairs and University of California, San Francisco.

Address correspondence to Jinoos Yazdany, MD, MPH, Division of Rheumatology, University of California, San Francisco, 1001 Potrero Avenue, Building 30, San Francisco, CA 94110. E-mail: jinoos.yazdany@ucsf.edu.

Submitted for publication April 12, 2018; accepted in revised form September 11, 2018.

overall benefits of GRADE, perhaps augmented by the extensive resources facilitating its implementation by the GRADE Working Group, led to rapid adoption of the method among guideline developers such as the ACR; it is now used by >80 groups (7).

But GRADE also has limitations. One limitation is that GRADE methods are not always easily adaptable to the clinical questions posed by guideline developers. GRADE is simplest to apply when high-quality evidence allows for generation of quantitative estimates of effect for each outcome. If data are qualitative or if there is significant heterogeneity between studies precluding pooling of estimates, user judgment is needed to assign levels of certainty and to develop recommendations. Guideline development using GRADE is also significantly more expensive and results in a product that is more complex to read given the detailed analyses required. Finally, GRADE assigns observational studies a default rating of "low quality," and users can then modify these evidence ratings per GRADE guidance. However, some have argued that the general approach to rating of observational data is inadequate, and that GRADE should further specify the manner by which confidence assessments should be modified (8).

This latter point is relevant in understanding why ACR guidelines include many recommendations that rely on low-quality evidence. Essentially, recommendations that do not harvest evidence from RCTs are less likely to be designated as having a high or moderate evidence rating. This poses challenges in rheumatology, where disease heterogeneity and low prevalence make RCTs challenging for many aspects of care. In addition, rheumatologists understandably seek the most guidance in areas with the lowest-quality evidence. Increasing calls for evidence-based medicine through reports such as the National Academies *Clinical Practice Guidelines We Can Trust* (3) have led some groups to restrict their recommendations to only those with high-level evidence. However, recent criticism (9,10) of American College of Physicians guidelines on topics such as gout and osteoporosis, which limited recommendations to areas with high-quality evidence despite significant observational evidence and expert consensus in other areas, suggest that a more nuanced approach is needed. Ultimately, the clinical utility of a guideline may be more in the ability to synthesize the *best available* literature with expert consensus relevant to challenging, real-world clinical situations for which little evidence exists. Limiting the scope of guidelines to only the few areas and populations where RCTs are available ignores the needs of clinicians who seek more comprehensive advice from experts in the field.

In their critique of ACR guidelines, Duarte-Garcia et al (1) noted that >50% of the ACR's 403 recommendations were classified as level C, while only one-fourth were level A. In addition, they noted cases of discordance between the evidence level and strength of recommendation, with the rheumatoid arthritis guidelines having the greatest number of strong recommendations based on weak (level C) evidence (16%). This brings up a key question: do clinicians want recommendations, regardless of the quality of the evidence? This question was recently studied in a multicenter RCT involving almost 500 clinicians (11). Investigators randomized participants to receive summaries in areas with either low- or high-quality evidence, with or without recommendations that followed GRADE. Not surprisingly, in all scenarios, the vast majority of clinicians (>80%) preferred having recommendations in addition to just evidence summaries. The fact that ACR guidelines provide recommendations, and sometimes strong recommendations, even in the face of weak evidence is consistent with that study's findings of what clinicians hope for in guidelines and with what the ACR's membership has requested.

An additional question is whether ACR is an outlier with regard to the evidence base of its guidelines, with more recommendations based on low-quality evidence compared to other specialties. In a recent systematic query of UpToDate, the most widely used reference by clinicians worldwide, 49.7% of 9,451 GRADE recommendations had low evidence/certainty, 39.8% had moderate certainty, and 10.5% had high certainty (12). Uncertainty or low-quality evidence is therefore prevalent, and in fact, the means for rheumatology are similar to those across all fields of medicine.

The ACR has remained on the forefront of evolving guideline methodology in order to maintain credibility with guideline users and disseminators. However, no methodology is perfect, and GRADE has its limitations. The ACR should continue to work with GRADE developers to address shortcomings and to contribute to the science around guideline development in general. Moreover, the ACR should continue to begin each guideline project by asking which questions are most clinically relevant and posting that list for public comment, encouraging input from patients and providers alike. Including all relevant questions, regardless of the level of evidence for the eventual recommendations, makes the final guideline more useful to all stakeholders, including patients.

While it may be argued that the ACR's current approach results in many recommendations that are not supported by high-quality evidence using current GRADE definitions, the counterargument is that these same recommendations are precisely the ones that rheumatologists and patients find the most useful. This approach is justified as long as there is 1) transparency about the quality of the evidence in these areas, 2) clarity regarding other factors that played into the guideline development group's decision making (including clinical experience and expertise, observational studies, as well as patient values and preferences), and 3) an acknowledgment that clinicians should have leeway to deviate from recommendations in areas of uncertainty. Finally, it is important to recognize that there are gaps in evidence for much of what we do as rheumatologists, and for many areas with low-quality evidence, RCTs may not be feasible. Accelerating the collection

of high-quality observational data that will facilitate closure of knowledge gaps and improve the evidence base for guidelines through efforts such as the ACR's RISE (Rheumatology Informatics System for Effectiveness) registry is therefore an important priority.

ACKNOWLEDGMENT

AUTHOR CONTRIBUTIONS

All authors drafted the article, revised it critically for important intellectual content, and approved the final version to be published.

REFERENCES

1. Duarte-Garcia A, Zamore R, Wong JB. The evidence basis for the American College of Rheumatology practice guidelines [letter]. JAMA Intern Med 2018;178:146–8.
2. Fitch K, Bernstein SJ, Aguilar MD, Burnand B, LaCalle JR, Lazaro P, et al, editors. The Rand/UCLA appropriateness method user's manual. Santa Barbara (CA): Rand Corporation; 2001.
3. Graham R, Mancher M, Wolman DM, Greenfield S, Steinberg E, editors. Clinical practice guidelines we can trust. Washington, DC: National Academies Press; 2011.
4. Singh JA, Guyatt G, Ogdie A, Gladman DD, Deal C, Deodhar A, et al. 2018 American College of Rheumatology/National Psoriasis Foundation guideline for the treatment of psoriatic arthritis. Arthritis Rheumatol 2019;51:5–34.
5. Mustafa RA, Santesso N, Brozek J, Akl EA, Walter SD, Norman G, et al. The GRADE approach is reproducible in assessing the quality of evidence of quantitative evidence syntheses. J Clin Epidemiol 2013;66:736–42.
6. Kumar A, Miladinovic B, Guyatt GH, Schunemann HJ, Djulbegovic B. GRADE guidelines system is reproducible when instructions are clearly operationalized even among the guidelines panel members with limited experience with GRADE. J Clin Epidemiol 2016;75:115–8.
7. Norris SL, Bero L. GRADE methods for guideline development: time to evolve? Ann Intern Med 2016;165:810–1.
8. Malmivaara A. Methodological considerations of the GRADE method. Ann Med 2015;47:1–5.
9. Neogi T, Mikuls TR. To treat or not to treat (to target) in gout. Ann Intern Med 2017;166:71–2.
10. Caplan L, Hansen KE, Saag KG. Response to the American College of Physicians Osteoporosis Guideline, 2017 update [editorial]. Arthritis Rheumatol 2017;69:2097–101.
11. Neumann I, Alonso-Coello P, Vandvik PO, Agoritsas T, Mas G, Akl EA, et al. Do clinicians want recommendations? A multi-center study comparing evidence summaries with and without GRADE recommendations. J Clin Epidemiol 2018;99:33–40.
12. Agoritsas T, Merglen A, Heen AF, Kristiansen A, Neumann I, Brito JP, et al. UpToDate adherence to GRADE criteria for strong recommendations: an analytical survey. BMJ Open 2017;7:e018593.

AMERICAN COLLEGE
OF RHEUMATOLOGY
EDUCATION · TREATMENT · RESEARCH

SPECIAL ARTICLE

2018 American College of Rheumatology/National Psoriasis Foundation Guideline for the Treatment of Psoriatic Arthritis

Jasvinder A. Singh,[1] iD Gordon Guyatt,[2] Alexis Ogdie,[3] Dafna D. Gladman,[4] Chad Deal,[5] Atul Deodhar,[6] Maureen Dubreuil,[7] Jonathan Dunham,[3] M. Elaine Husni,[5] Sarah Kenny,[8] Jennifer Kwan-Morley,[9] Janice Lin,[10] Paula Marchetta,[11] Philip J. Mease,[12] Joseph F. Merola,[13] Julie Miner,[14] Christopher T. Ritchlin,[15] Bernadette Siaton,[16] Benjamin J. Smith,[17] Abby S. Van Voorhees,[18] Anna Helena Jonsson,[13] Amit Aakash Shah,[19] Nancy Sullivan,[20] Marat Turgunbaev,[19] Laura C. Coates,[21] Alice Gottlieb,[22] Marina Magrey,[23] W. Benjamin Nowell,[24] Ana-Maria Orbai,[25] Soumya M. Reddy,[26] Jose U. Scher,[26] Evan Siegel,[27] Michael Siegel,[28] Jessica A. Walsh,[29] Amy S. Turner,[19] and James Reston[20]

Objective. To develop an evidence-based guideline for the pharmacologic and nonpharmacologic treatment of psoriatic arthritis (PsA), as a collaboration between the American College of Rheumatology (ACR) and the National Psoriasis Foundation (NPF).

Methods. We identified critical outcomes in PsA and clinically relevant PICO (population/intervention/comparator/outcomes) questions. A Literature Review Team performed a systematic literature review to summarize evidence supporting the benefits and harms of available pharmacologic and nonpharmacologic therapies for PsA. GRADE (Grading of Recommendations Assessment, Development and Evaluation) methodology was used to rate the quality of the evidence. A voting panel, including rheumatologists, dermatologists, other health professionals, and patients, achieved consensus on the direction and the strength of the recommendations.

Results. The guideline covers the management of active PsA in patients who are treatment-naive and those who continue to have active PsA despite treatment, and addresses the use of oral small molecules, tumor necrosis factor inhibitors, interleukin-12/23 inhibitors (IL-12/23i), IL-17 inhibitors, CTLA4-Ig (abatacept), and a JAK inhibitor (tofacitinib). We also developed recommendations for psoriatic spondylitis, predominant enthesitis, and treatment in the presence of concomitant inflammatory bowel disease, diabetes, or serious infections. We formulated recommendations for a treat-to-target strategy, vaccinations, and nonpharmacologic therapies. Six percent of the recommendations were strong and 94% conditional, indicating the importance of active discussion between the health care provider and the patient to choose the optimal treatment.

Conclusion. The 2018 ACR/NPF PsA guideline serves as a tool for health care providers and patients in the selection of appropriate therapy in common clinical scenarios. Best treatment decisions consider each individual patient situation. The guideline is not meant to be proscriptive and should not be used to limit treatment options for patients with PsA.

INTRODUCTION

Psoriatic arthritis (PsA) is a chronic inflammatory musculoskeletal disease associated with psoriasis, manifesting most commonly with peripheral arthritis, dactylitis, enthesitis, and spondylitis. Nail lesions, including pitting and onycholysis, occur in ~80–90% of patients with PsA. The incidence of PsA is ~6 per 100,000 per year, and the prevalence is ~1–2 per 1,000 in the general population (1). The annual incidence of PsA in patients with psoriasis is 2.7% (2), and the reported prevalence of PsA among patients with psoriasis has varied between 6% and 41% (1). In the majority of patients the skin symptoms develop first, followed by the arthritis; however, in some patients the skin and joint symptoms present at the same time, and in 10–15% the arthritis presents first (2).

PsA affects men and women equally. The distribution of the peripheral arthritis varies from asymmetric oligoarthritis (involving ≤4 joints) to symmetric polyarthritis (involving ≥5 joints). Distal interphalangeal joints are commonly affected and, in some patients, are the only affected joints. Axial disease, when present, usually occurs together with peripheral arthritis. Some patients present with rapidly progressive and destructive PsA–arthritis mutilans. PsA is associated with an adverse impact on health-related quality of life (3–5) and high health care costs and utilization (6,7). Greater disease activity is associated with progressive joint damage and higher mortality (8–11). Early identification of PsA and early initiation of therapy are important for improving long-term outcomes (12).

Both nonpharmacologic and pharmacologic treatment can ameliorate PsA symptoms and can occasionally result

[1]Jasvinder A. Singh, MD, MPH: University of Alabama at Birmingham and Birmingham Veterans Affairs Medical Center, Birmingham, Alabama; [2]Gordon Guyatt, MD: McMaster University, Hamilton, Ontario, Canada; [3]Alexis Ogdie, MD, MSCE, Jonathan Dunham, MD: University of Pennsylvania, Philadelphia; [4]Dafna D. Gladman, MD: University of Toronto and Toronto Western Hospital, Toronto, Ontario, Canada; [5]Chad Deal, MD, M. Elaine Husni, MD, MPH: Cleveland Clinic, Cleveland, Ohio; [6]Atul Deodhar, MD: Oregon Health & Science University, Portland; [7]Maureen Dubreuil, MD: Boston Medical Center, Boston, Massachusetts; [8]Sarah Kenny: New York, New York; [9]Jennifer Kwan-Morley, MD: Premier Orthopaedics, Malvern, Pennsylvania; [10]Janice Lin, MD, MPH: Stanford University, Stanford, California; [11]Paula Marchetta, MD, MBA: Concorde Medical Group, New York, New York; [12]Philip J. Mease, MD: Swedish-Providence Health Systems and University of Washington, Seattle, Washington; [13]Joseph F. Merola, MD, MMSc, Anna Helena Jonsson, MD, PhD: Brigham and Women's Hospital and Harvard Medical School, Boston, Massachusetts; [14]Julie Miner, PT: Comprehensive Therapy Consultants and Therapy Steps, Roswell, Georgia; [15]Christopher T. Ritchlin, MD, MPH: University of Rochester Medical Center, Rochester, New York; [16]Bernadette Siaton, MD, MEHP: University of Maryland School of Medicine, Baltimore; [17]Benjamin J. Smith, PA-C, DFAAPA: Florida State University College of Medicine School of Physician Assistant Practice, Tallahassee; [18]Abby S. Van Voorhees, MD: Eastern Virginia Medical School, Norfolk; [19]Amit Aakash Shah, MD, MPH, Marat Turgunbaev, MD, MPH, Amy S. Turner: American College of Rheumatology, Atlanta, Georgia; [20]Nancy Sullivan, James Reston, PhD, MPH: ECRI Institute, Plymouth Meeting, Pennsylvania; [21]Laura C. Coates, MD, PhD: University of Oxford, Oxford, UK; [22]Alice Gottlieb, MD, PhD: New York Medical College at Metropolitan Hospital, New York, New York; [23]Marina Magrey, MD: Case Western/MetroHealth, Cleveland, Ohio; [24]Benjamin Nowell, PhD: Global Healthy Living Foundation, Nyack, New York; [25]Ana-Maria Orbai, MD, MHS: Johns Hopkins University, Baltimore, Maryland; [26]Soumya M. Reddy, MD, Jose U. Scher, MD: New York University School of Medicine, New York, New York; [27]Evan Siegel, MD: Arthritis & Rheumatism Associates, Rockville, Maryland; [28]Michael Siegel, PhD: National Psoriasis Foundation, Portland, Oregon; [29]Jessica A. Walsh, MD: University of Utah and George E. Wahlen Veterans Affairs Medical Center, Salt Lake City, Utah.

in disease remission (Figure 1). Clinicians and patients can now choose from a wide variety of pharmacologic therapies, including symptomatic treatments such as nonsteroidal anti-inflammatory drugs (NSAIDs) and intraarticular injections, as well as immunomodulatory therapies.

The presentation of PsA is heterogeneous, and health care providers frequently face challenges when considering the various treatment options. Our objective was to develop evidence-based treatment recommendations for the management of active PsA in adults, using pharmacologic and nonpharmacologic therapies. These PsA treatment recommendations can help guide both clinicians and patients to arrive at optimal management decisions.

METHODS

Methodology overview. This guideline followed the American College of Rheumatology (ACR) guideline development process (http://www.rheumatology.org/Practice-Quality/Clinical-Support/Clinical-Practice-Guidelines). This process includes using the GRADE (Grading of Recommendations Assessment, Development and Evaluation) methodology (13–15) (www.gradeworkinggroup.org) to rate the quality of the available evidence and to develop the recommendations. ACR policy guided disclosures and the management of conflicts of interest. The full methods are presented in detail in Supplementary Appendix 1, on the *Arthritis & Rheumatology* web site at http://onlinelibrary.wiley.com/doi/10.1002/art.40726/abstract.

This work involved 4 teams selected by the ACR Quality of Care Committee after reviewing individual and group volunteer applications in response to an open request for proposals announcement: 1) a Core Leadership Team, which supervised and coordinated the project and drafted the clinical questions and manuscript; 2) a Literature Review Team, which completed the literature search and abstraction; 3) an Expert Panel, composed of patients, patient advocates, rheumatologists, dermatologists, 1 dermatologist-rheumatologist, and 1 rheumatology nurse practitioner, which developed the clinical questions (PICO [population/intervention/comparator/outcomes] questions) and decided on the scope of the guideline project; and 4) a Voting Panel, which included rheumatologists, 1 dermatologist, 1 dermatologist-rheumatologist, 1 rheumatology physician assistant, and 2 patients (1 of whom was also a physical therapist), who provided input from the patient perspective and voted on the recommendations. Additionally, a Patient Panel consisting of 9 adults with PsA reviewed the evidence and provided input on their values and preferences, which was reviewed before discussion of each section of PsA management (e.g., treatment-naive, treated, comorbidities), and was incorporated into discussions and formulation of recommendations. Supplementary Appendix 2 (http://onlinelibrary.wiley.com/doi/10.1002/art.40726/abstract) presents rosters of the team and panel members. In accordance with ACR policy, the principal investigator and the leader of the literature review team were free of conflicts, and within each team, >50% of the members were free of conflicts.

Non-pharmacologic therapies	• physical therapy, occupational therapy, smoking cessation, weight loss, massage therapy, exercise
Symptomatic treatments	• nonsteroidal anti-inflammatory drugs, glucocorticoids, local glucocorticoid injections
OSM	• methotrexate, sulfasalazine, cyclosporine, leflunomide, apremilast
TNFi	• etanercept, infliximab, adalimumab, golimumab, certolizumab pegol
IL12/23i	• ustekinumab
IL17i	• secukinumab, ixekizumab, brodalumab
CTLA4-Ig	• abatacept
JAK inhibitor	• tofacitinib

Figure 1. Pharmacologic, nonpharmacologic, and symptomatic therapies for psoriatic arthritis. Pharmacologic therapies are displayed in the blue boxes and include oral small molecules (OSMs), tumor necrosis factor inhibitor (TNFi) biologics, interleukin-17 inhibitor (IL-17i) biologics, an IL-12/23i biologic, CTLA4-immunoglobulin, and a JAK inhibitor. While there are numerous nonpharmacologic therapies available, 6 of these are addressed in this guideline. Symptomatic therapies include nonsteroidal antiinflammatory drugs, systemic glucocorticoids, and local glucocorticoid injections. Systemic glucocorticoids or local injections are not addressed in this guideline.

Framework for the PsA guideline development and scope of the guideline. Because there are numerous topics within PsA that could be addressed, at the beginning of the process the guideline panels made several decisions regarding the focus of this guideline and how to define aspects of the disease (e.g., active disease). At an initial scoping meeting, the Voting Panel and Expert Panel agreed that the project would include the management of patients with *active* PsA, defined as symptoms at an unacceptably bothersome level as reported by the patient and judged by the examining health care provider to be due to PsA based on the presence of at least 1 of the following: actively inflamed joints, dactylitis, enthesitis, axial disease, active skin and/or nail involvement, and/or extraarticular manifestations such as uveitis or inflammatory bowel disease (IBD). The health care provider may, in deciding if symptoms are due to active PsA, consider information beyond the core information from the history and physical examination, such as inflammation markers (C-reactive protein [CRP] or erythrocyte sedimentation rate [ESR]) and imaging results. At the scoping meeting, the panels decided that the guideline would address both pharmacologic and nonpharmacologic therapies for the treatment of PsA. We examined evidence regarding vaccinations, treatment in the presence of common comorbidities, and implementing a treat-to-target strategy.

In addressing pharmacologic therapies, we focused on immunomodulatory agents for long-term management rather than addressing acute symptom management (i.e., through intraarticular injections and the use of systemic glucocorticoids). Tofacitinib and ixekizumab were submitted for review and potential approval by the US Food and Drug Administration (FDA) at the time of formulation of this guideline (16,17) and for this reason, these drugs were addressed in the guideline. Both drugs have been approved for PsA since then (18,19). Tofacitinib is not included within the oral small molecules (OSM) category since its benefit/risk profile differs from that of the rest of the OSMs, especially with regard to risks (20–22), and consistent with its being considered separately in other treatment guidelines (23,24). Additionally, the panel addressed alternatives in patient subpopulations (e.g., patients with predominant enthesitis, axial disease, dactylitis, comorbidities), and greater versus lesser disease severity.

There are currently no widely agreed-upon definitions of disease severity in PsA or psoriasis. Thus, health care providers and patients should judge PsA and psoriasis severity on a case-by-case basis. For the purpose of these recommendations, severity includes not only the level of disease activity at a given time point, but also the presence or absence of poor prognostic factors and long-term damage. Examples of severe PsA disease include the presence of 1 or more of the following: a poor prognostic factor (erosive disease, dactylitis, elevated levels of inflammation mark-

ers such as ESR and CRP attributable to PsA), long-term damage that interferes with function (e.g., joint deformities), highly active disease that causes a major impairment in quality of life (i.e., active psoriatic inflammatory disease at many sites [including dactylitis, enthesitis] or function-limiting inflammatory disease at few sites), and rapidly progressive disease (Figure 2). In clinical trials, severe psoriasis has been defined as a Psoriasis Area and Severity Index (PASI) (25) score of ≥12 and a body surface area score of ≥10. However, because it is cumbersome, physicians seldom use the PASI in clinical practice. Examples of definitions of severe PsA and severe psoriasis are shown in Figure 2. Finally, because the National Psoriasis Foundation (NPF) and American Academy of Dermatology are concurrently developing psoriasis treatment guidelines, the treatment of skin psoriasis separately from the inflammatory arthritis was not included in the current ACR/NPF PsA guideline.

Systematic synthesis of the literature. Systematic searches of the published English-language literature included Ovid Medline, PubMed, Embase, and the Cochrane Library (including Cochrane Database of Systematic Reviews, Database of Abstracts of Reviews of Effects, Cochrane Central Register of Controlled Trials, and Health Technology Assessments) from the beginning of each database through November 15, 2016 (Supplementary Appendix 3, on the *Arthritis & Rheumatology* web site at http://onlinelibrary.wiley.com/doi/10.1002/art.40726/abstract); we conducted updated searches on May 2, 2017 and again on March 8, 2018. DistillerSR software (https://distillercer.com/products/distillersr-systematic-reviewsoftware/) (Supplementary Appendix 4; http://onlinelibrary.wiley.com/doi/10.1002/art.40726/abstract) was used to facilitate duplicate screening of literature search results. Reviewers entered extracted data into RevMan software (http://tech.cochrane.org/revman), and evaluated the risk of bias in primary studies using the Cochrane risk of bias tool (http://handbook.cochrane.org/). We exported RevMan files into GRADEpro software to formulate a GRADE summary of findings table (Supplementary Appendix 5; http://onlinelibrary.wiley.com/doi/10.1002/art.40726/abstract) for each PICO question (26). Additionally, a network meta-analysis was performed when sufficient studies were available. GRADE criteria provided the framework for judging the overall quality of evidence (13).

The panels chose the critical outcomes for all comparisons at the initial scoping; these included the American College of Rheumatology 20% response criteria (ACR20) (the primary outcome for most PsA clinical trials), the Health Assessment Questionnaire disability index (a measure of physical function), the PASI 75% response criteria (PASI75) (a measure of skin psoriasis improvement), and serious infections. Both the ACR20 and the PASI75 are accepted outcome measures specified by regulatory agencies, including the US FDA, for the approval of treatments for PsA (27). Serious infections are among the issues of greatest

Severe Psoriatic Arthritis	Severe Psoriasis
• Erosive disease • Elevated markers of inflammation (ESR, CRP) attributable to PsA • Long-term damage that interferes with function (i.e., joint deformities) • Highly active disease that causes a major impairment in quality of life • Active PsA at many sites including dactylitis, enthesitis • Function-limiting PsA at a few sites • Rapidly progressive disease	• PASI of 12 or more • BSA of 5-10% or more • Significant involvement in specific areas • (e.g., face, hands or feet, nails, intertriginous areas, scalp) where the burden of the disease causes significant disability • Impairment of physical or mental functioning can warrant a designation of moderate-to-severe disease despite the lower amount of surface area of skin involved

Figure 2. Examples of "severe" psoriatic arthritis (PsA) and psoriasis. The guideline development group defined severe PsA and psoriasis as the presence of 1 or more of the items listed. This is not a formal definition. There have been many definitions of severe psoriasis used over time—the items here are adapted from the 2007 National Psoriasis Foundation expert consensus statement for moderate-to-severe psoriasis (68). In clinical trials, severe psoriasis has been defined as a Psoriasis Area and Severity Index (PASI) score of ≥12 and a body surface area (BSA) score of ≥10 (25). ESR = erythrocyte sedimentation rate; CRP = C-reactive protein.

concern for patients and physicians when selecting among therapies. Other specific harms (e.g., liver toxicity with methotrexate [MTX]) were included as critical outcomes for individual comparisons. We included other outcomes, such as total infections (regardless of severity), when appropriate.

Moving from evidence to recommendations. GRADE methodology specifies that panels make recommendations based on the balance of benefits and harms, the quality of the evidence (i.e., confidence in effect estimates), and patients' values and preferences. Deciding on the balance between desirable and undesirable outcomes requires estimating the relative value patients place on those outcomes. When the literature provided very limited guidance, the experience of the Voting Panel members (including physicians, a rheumatology physician assistant, and the 2 patients present) in managing the relevant cases and issues became an important source of evidence. Values and preferences, crucial to all recommendations, derived from input from the members of the Patient Panel were particularly salient in such situations. GRADE methodology allows the panels the possibility of not coming to a decision, and a summary of the discussion is noted in such cases. However, during the development of this guideline, the Voting Panel came to a conclusion in each case scenario, and such a situation did not arise.

Consensus building. The Voting Panel voted on the direction and strength of the recommendation related to each PICO question. Recommendations required a 70% level of agreement, as used previously in other similar processes (28) and in the previous ACR guidelines (23,29,30); if 70% agreement was not achieved during an initial vote, the panel members held additional discussions before revoting. For all conditional recommendations, a written explanation is provided, describing the reasons for the decision and conditions under which the alternative choice may be preferable.

Moving from recommendations to practice. These recommendations are designed to help health care providers work with patients in selecting therapies. The presence or absence of concomitantly occurring conditions, such as IBD, uveitis, diabetes, and serious infections, and the knowledge of previous therapies, influence decisions regarding optimal management. In the context of PsA, the physical examination, which is also required for selecting therapy, includes assessment of the peripheral joints (including for dactylitis), the entheses, the spine, the skin, and the nails. Health care providers and patients must take into consideration all active disease domains, comorbidities, and the patient's functional status in choosing the optimal therapy for an individual at a given point in time.

RESULTS/RECOMMENDATIONS

How to interpret the recommendations

1. A *strong recommendation* means that the panel was *confident* that the desirable effects of following the recommendation outweigh the undesirable effects (or vice versa), so the course of action would apply to all or almost all patients, and only a small proportion of clinicians/patients not wanting to follow the recommendation. We use the phrase "*should use*" or "*should be used*" for strong recommendations.

2. A *conditional recommendation* means that the panel believed the desirable effects of following the recommendation *probably* outweigh the undesirable effects, so the course of action would apply to the majority of the patients, but a small proportion of clinicians/patients may not want to follow the recommendation. Because of this, conditional recommendations are preference sensitive and always warrant a shared decision-making approach. We use the phrase "*is recommended over*" or "*is/would be recommended*" for conditional recommendations. We specify conditions under which the less preferred drug may be used by using the phrase "*may be used*" or "*may consider*" or "*Y (less preferred drug) may be used instead of X (preferred drug)*" or "*may consider Y instead of X (preferred drug)*" for conditional recommendations.

3. Conditional recommendations were usually based on low- to very-low-quality evidence (in rare instances, moderate-quality evidence). Strong recommendations were typically based on moderate- or high-quality evidence.

4. For each recommendation, Supplementary Appendix 5 (on the *Arthritis & Rheumatology* web site at http://onlinelibrary.wiley.com/doi/10.1002/art.40726/abstract) provides details regarding the PICO questions and the GRADE evidence tables.

5. In each case, the Voting Panel's recommendation was based on a judgment of the most likely net benefit, i.e.,1) more benefit with the medication conditionally recommended with no difference in harms between the medications being compared (e.g., choosing a TNFi over OSMs in treatment-naive patients) or 2) less harm with the medication conditionally recommended and no difference in benefit (e.g., choosing abatacept over a TNFi in patients at risk of or with a history of previous infections, or preferring a different OSM over MTX in patients with PsA and diabetes due to an increased risk of liver toxicity in this subpopulation).

6. This is an evidence-based guideline, in that we explicitly use the best evidence available and present that in a transparent manner for the clinician reader/user (31,32). In some instances, this includes a randomized trial directly comparing the interventions under consideration. In other cases, in the absence of any published evidence, the best evidence comes from the collective experience of the Voting Panel and patient panel members, which in the GRADE system is rated as "very-low-quality" evidence.

Recommendations for pharmacologic interventions

Active PsA in treatment-naive patients (Table 1 and Figure 3). *All recommendations for treatment-naive patients with active PsA are conditional based on low- to very-low-quality evidence.*

In treatment-naive patients with active PsA, a TNFi biologic agent is recommended over an OSM as a first-line option (Table 1). OSMs may be used instead of a TNFi biologic in patients without severe PsA and without severe psoriasis (as defined in Methods and Figure 2; final determination of severity to be made by the patient and the health care provider), those who prefer an oral drug instead of parenteral therapy, or those with contraindications to TNFi treatment, including congestive heart failure, previous serious infections, recurrent infections, or demyelinating disease.

For treatment-naive patients with active PsA, the use of a TNFi biologic or OSM is recommended over an interleukin-17 inhibitor (IL-17i) or IL-12/23i biologic. An IL-17i or IL-12/23i biologic may be used instead of TNFi biologics in patients with severe psoriasis or contraindications to TNFi biologics, and may be used instead of OSMs in patients with severe psoriasis or severe PsA. MTX is recommended over NSAIDs in treatment-naive patients with active PsA. NSAIDs may be used instead of MTX after consideration of possible contraindications and side effect profile in patients without evidence of severe PsA or severe psoriasis and in those at risk for liver toxicity (Table 1 and Figure 3). An IL-17i biologic is recommended over an IL-12/23i biologic. IL-12/23i biologics may be used in patients who have concomitant IBD or who desire less frequent drug administration*.*

Active PsA despite treatment with an OSM (Table 2 and Figure 4). *All recommendations for patients with active PsA despite treatment with an OSM are conditional based on mostly low- to very-low-quality evidence and, in a few instances, moderate-quality evidence.*

In patients with active PsA despite OSM therapy, switching to a TNFi, an IL-17i, or an IL-12/23i biologic is recommended over switching to a different OSM (Table 2 and Figure 4). A different OSM may be used rather than a TNFi, IL-17i, or IL-12/23i in patients who prefer an oral medication or those without evidence of severe PsA or severe psoriasis; a differ-

Table 1. Recommendations for the initial treatment of patients with active psoriatic arthritis who are OSM- and other treatment–naive (PICOs 9–15)*

	Level of evidence (evidence [refs.] reviewed)†
In OSM- and other treatment–naive patients with active PsA,	
1. **Treat with a TNFi biologic over an OSM** (MTX, SSZ, LEF, CSA, or APR) (PICO 10a–e)	Low (53–66)
Conditional recommendation based on low-quality evidence; may consider an OSM if the patient does not have severe PsA,‡ does not have severe psoriasis,§ prefers oral therapy, has concern over starting a biologic as the first therapy, or has contraindications to TNFi biologics, including congestive heart failure, previous serious infections, recurrent infections, or demyelinating disease.	
2. **Treat with a TNFi biologic over an IL-17i biologic** (PICO 14)	Very low
Conditional recommendation based on very-low-quality evidence; may consider an IL-17i biologic if the patient has severe psoriasis or has contraindications to TNFi biologics, including congestive heart failure, previous serious infections, recurrent infections, or demyelinating disease.	
3. **Treat with a TNFi biologic over an IL-12/23i biologic** (PICO 13)	Very low
Conditional recommendation based on very-low-quality evidence; may consider an IL-12/23i biologic if the patient has severe psoriasis, prefers less frequent drug administration, or has contraindications to TNFi biologics, including congestive heart failure, previous serious infections, recurrent infections, or demyelinating disease.	
4. **Treat with an OSM over an IL-17i biologic** (PICO 12)	Very low
Conditional recommendation based on very-low-quality evidence; may consider an IL-17i biologic if the patient has severe psoriasis and/or severe PsA.	
5. **Treat with an OSM over an IL-12/23i biologic** (PICO 11)	Very low
Conditional recommendation based on very-low-quality evidence; may consider an IL-12/23i biologic if the patient has concomitant IBD and/or severe psoriasis and/or severe PsA or prefers less frequent drug administration.	
6. **Treat with MTX over NSAIDs** (PICO 9)	Very low (67)
Conditional recommendation based on very-low-quality evidence; may consider NSAIDs before starting MTX in patients with less active disease, after careful consideration of cardiovascular risks and renal risks of NSAIDs.	
7. **Treat with an IL-17i biologic over an IL-12/23i biologic** (PICO 15)	Very low
Conditional recommendation based on very-low-quality evidence; may consider an IL-12/23i biologic if the patient has concomitant IBD or prefers less frequent drug administration.	

* Active psoriatic arthritis (PsA) is defined as disease causing symptoms at an unacceptably bothersome level as reported by the patient, and judged by the examining clinician to be *due to PsA* based on ≥1 of the following: swollen joints, tender joints, dactylitis, enthesitis, axial disease, active skin and/or nail involvement, and extraarticular inflammatory manifestations such as uveitis or inflammatory bowel disease (IBD). Oral small molecules (OSMs) are defined as methotrexate (MTX), sulfasalazine (SSZ), leflunomide (LEF), cyclosporine (CSA), or apremilast (APR) and *do not* include tofacitinib, which was handled separately since its efficacy/safety profile is much different from that of other OSMs listed above. OSM- and other treatment–naive is defined as naive to treatment with OSMs, tumor necrosis factor inhibitors (TNFi,) interleukin-17 inhibitors (IL-17i), and IL-12/23i; patients may have received nonsteroidal antiinflammatory drugs (NSAIDs), glucocorticoids, and/or other pharmacologic and nonpharmacologic interventions.
† When there were no published studies, we relied on the clinical experience of the panelists, which was designated very-low-quality evidence.
‡ Because there are currently no widely agreed-upon definitions of disease severity, PsA severity should be established by the health care provider and patient on a case-by-case basis. For the purposes of these recommendations, severity is considered a broader concept than disease activity in that it encompasses the level of disease activity at a given time point, as well as the presence of poor prognostic factors and long-term damage. Examples of severe PsA disease include the presence of ≥1 of the following: a poor prognostic factor (erosive disease, elevated levels of inflammation markers such as C-reactive protein or erythrocyte sedimentation rate attributable to PsA), long-term damage that interferes with function (e.g., joint deformities, vision loss), highly active disease that causes major impairment in quality of life (i.e., active psoriatic inflammatory disease at many sites [including dactylitis, enthesitis] or function-limiting inflammatory disease at few sites), and rapidly progressive disease.
§ Because there are currently no widely agreed-upon definitions of disease severity, psoriasis severity should be established by the health care provider and patient on a case-by-case basis. In clinical trials, severe psoriasis has been defined as a Psoriasis Area and Severity Index (PASI) score (25) of ≥12 and a body surface area score of ≥10. In clinical practice, however, the PASI tool is not standardly utilized given its cumbersome nature. In 2007, the National Psoriasis Foundation published an expert consensus statement, which defined moderate-to-severe disease as a body surface area of ≥5% (68). In cases in which the involvement is in critical areas, such as the face, hands or feet, nails, intertriginous areas, scalp, or where the burden of the disease causes significant disability or impairment of physical or mental functioning, the disease can be severe despite the lower amount of surface area of skin involved. The need to factor in the unique circumstances of the individual patient is of critical importance, but this threshold provides some guidance in the care of patients.

Figure 3. Recommendations for the treatment of patients with active psoriatic arthritis (PsA) who are treatment-naive (no exposure to oral small molecules [OSMs] or other treatments). All recommendations are conditional based on low- to very-low-quality evidence. A conditional recommendation means that the panel believed the desirable effects of following the recommendation probably outweigh the undesirable effects, so the course of action would apply to the majority of the patients, but some may not want to follow the recommendation. Because of this, conditional recommendations are preference sensitive and always warrant a shared decision-making approach. Due to the complexity of management of active PsA, not all clinical situations and choices could be depicted in this flow chart, and therefore we show only the key recommendations. For a complete list of recommendations, please refer to the Results section of the text. For the level of evidence supporting each recommendation, see Table 1 and the related section in the Results. This figure is derived from recommendations based on PICO (population/intervention/comparator/outcomes) questions that are based on the common clinical situations. Active PsA was defined as symptoms at an unacceptably bothersome level as reported by the patient, and judged by the examining health care provider to be due to PsA based on the presence of at least 1 of the following: actively inflamed joints, dactylitis, enthesitis, axial disease, active skin and/or nail involvement, and/or extraarticular manifestations such as uveitis or inflammatory bowel disease (IBD). TNFi = tumor necrosis factor inhibitor; IL-17i = interleukin-17 inhibitor; MTX = methotrexate; NSAIDs = nonsteroidal antiinflammatory drugs.

ent OSM may be used rather than a TNFi in the presence of contraindications to TNFi biologics. A TNFi biologic is recommended over an IL-17i biologic, an IL-12/23i biologic, abatacept, or tofacitinib. An IL-17i biologic is recommended over an IL-12/23i biologic, abatacept, or tofacitinib. An IL-12/23i is recommended over abatacept or tofacitinib. In patients with contraindications to TNFi agents, an IL-12/23i, an IL-17i, abatacept, or tofacitinib may be used instead of a TNFi. In patients with severe psoriasis, an IL-12/23i or an IL-17i may be used instead of a TNFi. Tofacitinib may be used instead of a TNFi in patients preferring oral medication who do not have severe psoriasis.

Switching to another OSM is recommended over adding another OSM to the current treatment (except in the case of apremilast). Adding another OSM (except apremilast) to current treatment may be considered if the patient has exhibited partial response to the current OSM. Adding apremilast to the current OSM therapy is recommended over switching to apremilast monotherapy since most evidence for benefits of apremilast pertains to apremilast combination therapy. Switching to apremilast monotherapy may be considered instead of apremilast combination therapy if the patient has intolerable side effects with the current OSM.

Biologic monotherapy is recommended over biologic combination therapy with MTX (the most commonly used OSM in combination therapy). When switching to biologic monotherapy, stopping the OSM or tapering of the OSM are both reasonable options and depend on patient and health care provider

Table 2. Recommendations for treatment of patients with active psoriatic arthritis despite treatment with an OSM (PICOs 16–25; 67–69; 76–78)*

	Level of evidence (evidence [refs.] reviewed)†
In adult patients with active PsA despite treatment with an OSM,	
1. **Switch to a TNFi biologic over a different OSM** (PICO 23)	Moderate (62–66, 69–86)
Conditional recommendation based on moderate-quality evidence; may consider switching to a different OSM if the patient has contraindications to TNFi biologics, including congestive heart failure, previous serious infections, recurrent infections, or demyelinating disease, if the patient prefers an oral versus parenteral therapy, or in patients without evidence of severe PsA‡ or severe psoriasis.§	
2. **Switch to a TNFi biologic over an IL-17i biologic** (PICO 17)	Moderate (62–66, 72–78, 87–97)
Conditional recommendation based on moderate-quality evidence; may consider an IL-17i if the patient has severe psoriasis and/or has contraindications to TNFi biologics, including congestive heart failure, previous serious infections, recurrent infections, or demyelinating disease, and/or a family history of demyelinating disease such as multiple sclerosis.	
3. **Switch to a TNFi biologic over an IL-12/23i biologic** (PICO 16)	Moderate (62–66, 72–78, 97–102)
Conditional recommendation based on moderate-quality evidence; may consider an IL-12/23i if the patient has severe psoriasis and/or contraindications to TNFi biologics, including congestive heart failure, previous serious infections, recurrent infections, or demyelinating disease, or prefers less frequent drug administration.	
4. **Switch to a TNFi biologic over abatacept** (PICO 67)	Low (62–66, 72–78, 103, 104)
Conditional recommendation based on low-quality evidence; may consider abatacept if the patient has contraindications to TNFi biologics, including congestive heart failure, previous serious infections, recurrent infections, or demyelinating disease.	
5. **Switch to a TNFi biologic over tofacitinib** (PICO 76)	Low (62–66, 72–78, 105)
Conditional recommendation based on low-quality evidence; may consider tofacitinib if the patient has contraindications to TNFi biologics, including congestive heart failure, previous serious infections, recurrent infections, or demyelinating disease, or prefers oral medication.	
6. **Switch to an IL-17i over a different OSM** (PICO 25)	Low (79–87, 89–95)
Conditional recommendation based on low-quality evidence; may consider switching to a different OSM if the patient prefers an oral versus parenteral therapy or in patients without evidence of severe PsA or severe psoriasis.	
7. **Switch to an IL-17i biologic over an IL-12/23i biologic** (PICO 18)	Moderate (87, 89–95, 98–100, 106, 107)
Conditional recommendation based on moderate-quality evidence; may consider an IL-12/23i biologic if the patient has concomitant IBD or prefers less frequent drug administration.	
8. **Switch to an IL-17i biologic over abatacept** (PICO 69)	Low (89–95, 103, 104)
Conditional recommendation based on low-quality evidence; may consider abatacept in patients with recurrent or serious infections.	
9. **Switch to an IL-17i biologic over tofacitinib** (PICO 78)	Low (89–95, 105)
Conditional recommendation based on low-quality evidence; may consider tofacitinib if the patient prefers an oral therapy or has a history of recurrent *Candida* infections.	
10. **Switch to an IL-12/23i biologic over a different OSM** (PICO 24)	Low (79–86, 98–100)
Conditional recommendation based on low-quality evidence; may consider switching to a different OSM if the patient prefers an oral versus parenteral therapy or in patients without evidence of severe PsA or severe psoriasis.	
11. **Switch to an IL-12/23i biologic over abatacept** (PICO 68)	Low (98–100, 103, 104)
Conditional recommendation based on low-quality evidence; may consider abatacept in patients with recurrent or serious infections.	

Table 2. *(Cont'd)*

	Level of evidence (evidence [refs.] reviewed)†
12. **Switch to an IL-12/23i biologic over tofacitinib** (PICO 77)	Low (98–100, 105)
Conditional recommendation based on low-quality evidence; may consider tofacitinib if the patient prefers an oral therapy.	
13. **Add apremilast to current OSM therapy over switching to apremilast** (PICO 22b)	Low (83, 84, 108)
Conditional recommendation based on low-quality evidence; may consider switching to apremilast if the patient has intolerable side effects with the current OSM.	
14. **Switch to another OSM (except apremilast) over adding another OSM (except apremilast) to current treatment** (PICO 22a)	Low (83, 84, 108)
Conditional recommendation based on low-quality evidence; may consider adding another OSM (except apremilast) to current treatment if the patient has demonstrated partial response to the current OSM.	
15. **Switch to a TNFi biologic monotherapy over MTX and a TNFi biologic combination therapy** (PICO 19)	Low (109–111)
Conditional recommendation based on low-quality evidence; may consider MTX and TNFi biologic combination therapy if the patient has severe skin manifestations, has had a partial response to current MTX therapy, has concomitant uveitis (since uveitis may respond to MTX therapy), and if the current TNFi biologic is infliximab or adalimumab.	
16. **Switch to an IL-17i biologic monotherapy over MTX and an IL-17i biologic combination therapy** (PICO 21)	Very low
Conditional recommendation based on very-low-quality evidence; may consider MTX and an IL-17i biologic combination therapy if the patient has severe skin manifestations, has had a partial response to current MTX therapy, or has concomitant uveitis (since uveitis may respond to MTX therapy).	
17. **Switch to an IL-12/23i biologic monotherapy over MTX and an IL-12/23i biologic combination therapy** (PICO 20)	Very low
Conditional recommendation based on very-low-quality evidence; may consider MTX and an IL-12/23i biologic combination therapy if the patient has severe skin manifestations, has had a partial response to current MTX therapy, or has concomitant uveitis (since uveitis may respond to MTX therapy).	

* Active psoriatic arthritis (PsA) is defined as disease causing symptoms at an unacceptably bothersome level as reported by the patient, and judged by the examining clinician to be *due to PsA* based on ≥1 of the following: swollen joints, tender joints, dactylitis, enthesitis, axial disease, active skin and/or nail involvement, and extraarticular inflammatory manifestations such as uveitis or inflammatory bowel disease (IBD). Oral small molecules (OSMs) are defined as methotrexate (MTX), sulfasalazine, leflunomide, cyclosporine, or apremilast and *do not* include tofacitinib, which was handled separately since its efficacy/safety profile is much different from that of other OSMs listed above. TNFi = tumor necrosis factor inhibitor; IL-17i = interleukin-17 inhibitor.

† When there were no published studies, we relied on the clinical experience of the panelists, which was designated very-low-quality evidence.

‡ Because there are currently no widely agreed-upon definitions of disease severity, PsA severity should be established by the health care provider and patient on a case-by-case basis. For the purposes of these recommendations, severity is considered a broader concept than disease activity in that it encompasses the level of disease activity at a given time point, as well as the presence of poor prognostic factors and long-term damage. Examples of severe PsA disease include the presence of ≥1 of the following: a poor prognostic factor (erosive disease, elevated levels of inflammation markers such as C-reactive protein or erythrocyte sedimentation rate attributable to PsA), long-term damage that interferes with function (e.g., joint deformities, vision loss), highly active disease that causes major impairment in quality of life (i.e., active psoriatic inflammatory disease at many sites [including dactylitis, enthesitis] or function-limiting inflammatory disease at few sites), and rapidly progressive disease.

§ Because there are currently no widely agreed-upon definitions of disease severity, psoriasis severity should be established by the health care provider and patient on a case-by-case basis. In clinical trials, severe psoriasis has been defined as a Psoriasis Area and Severity Index (PASI) score (25) of ≥12 and a body surface area score of ≥10. In clinical practice, however, the PASI tool is not standardly utilized given its cumbersome nature. In 2007, the National Psoriasis Foundation published an expert consensus statement, which defined moderate-to-severe disease as a body surface area of ≥5% (68). In cases in which the involvement is in critical areas, such as the face, hands or feet, nails, intertriginous areas, scalp, or where the burden of the disease causes significant disability or impairment of physical or mental functioning, the disease can be severe despite the lower amount of surface area of skin involved. The need to factor in the unique circumstances of the individual patient is of critical importance, but this threshold provides some guidance in the care of patients.

Figure 4. Recommendations for the treatment of patients with active psoriatic arthritis (PsA) despite treatment with oral small molecules (OSMs). All recommendations are conditional based on low- to very-low-quality evidence. A conditional recommendation means that the panel believed the desirable effects of following the recommendation probably outweigh the undesirable effects, so the course of action would apply to the majority of the patients, but some may not want to follow the recommendation. Because of this, conditional recommendations are preference sensitive and always warrant a shared decision-making approach. Due to the complexity of management of active PsA, not all clinical situations and choices could be depicted in this flow chart, and therefore we show only the key recommendations. For a complete list of recommendations, please refer to the Results section of the text. For the level of evidence supporting each recommendation, see Table 2 and the related section in the Results. TNFi = tumor necrosis factor inhibitor; IL-17i = interleukin-17 inhibitor; MTX = methotrexate.

preferences. A biologic agent in combination with MTX may be used instead of biologic monotherapy if the patient has severe psoriasis, has had a partial response to current MTX therapy, or has concomitant uveitis (since uveitis may respond to MTX therapy), or in patients receiving treatment with a monoclonal antibody TNFi biologic, especially infliximab and adalimumab, to potentially delay or prevent the formation of antidrug antibodies.

Active PsA despite treatment with a TNFi biologic agent as monotherapy or in combination therapy (Table 3 and Figure 5). *All recommendations for patients with active PsA despite TNFi biologic treatment are conditional based on low- to very-low-quality evidence.*

In patients with active PsA despite treatment with TNFi biologic monotherapy, switching to a different TNFi biologic monotherapy is recommended over switching to IL-12/23i biologic, an IL-17i biologic, abatacept, or tofacitinib monotherapy or adding MTX to the current TNFi biologic (Table 3 and

Figure 5). An IL-12/23i biologic, IL-17i biologic, abatacept, or tofacitinib may be used instead of a different TNFi biologic monotherapy in the case of a primary TNFi biologic failure or a serious adverse event due to the TNFi biologic. An IL-17i or IL-12/23i biologic may be used instead of a different TNFi biologic, particularly in the presence of severe psoriasis. Abatacept may be used instead of a TNFi biologic in patients with recurrent or serious infections in the absence of severe psoriasis, based on indirect evidence of fewer hospitalized infections with abatacept compared to TNFi biologics in a population with rheumatoid arthritis (33). Tofacitinib may be used instead of a TNFi biologic if oral therapy is preferred by the patient.

In patients with active PsA despite treatment with TNFi biologic monotherapy, an IL-17i biologic is recommended over an IL-12/23i biologic, abatacept, or tofacitinib, and an IL-12/23i biologic is recommended over abatacept or tofacitinib. An IL-12/23i biologic may be considered instead of an IL-17i biologic if the patient has IBD or desires less frequent drug administration. Abatacept may be considered instead of an IL-17i or IL-

Table 3. Recommendations for treatment of patients with active psoriatic arthritis despite treatment with a TNFi biologic, as monotherapy or in combination with MTX (PICOs 26–35; 70–75)*

	Level of evidence (evidence [refs.] reviewed)†
In adult patients with active PsA despite treatment with a TNFi biologic monotherapy,	
1. **Switch to a different TNFi biologic over switching to an IL-17i biologic** (PICO 28)	Low (72, 73, 90–93, 95)
Conditional recommendation based on low-quality evidence; may consider an IL-17i if the patient had a primary TNFi biologic efficacy failure or a TNFi biologic–associated serious adverse event or severe psoriasis.‡	
2. **Switch to a different TNFi biologic over switching to an IL-12/23i biologic** (PICO 27)	Low (72, 73, 99, 100)
Conditional recommendation based on low-quality evidence; may consider an IL-12/23i if the patient had a primary TNFi biologic efficacy failure or a TNFi biologic–associated serious adverse effect or prefers less frequent drug administration.	
3. **Switch to a different TNFi biologic over switching to abatacept** (PICO 70)	Low (72, 73, 103, 104)
Conditional recommendation based on low-quality evidence; may consider abatacept if the patient had a primary TNFi biologic efficacy failure or TNFi biologic–associated serious adverse effect.	
4. **Switch to a different TNFi biologic over switching to tofacitinib** (PICO 73)	Low (62–66, 72–78, 105)
Conditional recommendation based on low-quality evidence; may consider tofacitinib if the patient prefers an oral therapy or had a primary TNFi biologic efficacy failure or a TNFi biologic–associated serious adverse effect.	
5. **Switch to a different TNFi biologic (with or without MTX) over adding MTX to the same TNFi biologic monotherapy** (PICO 26 and 26A)	Very low
Conditional recommendation based on very-low-quality evidence; may consider adding MTX when patients have demonstrated partial response to the current TNFi biologic therapy, especially if the TNFi biologic is a monoclonal antibody.	
6. **Switch to an IL-17i biologic over switching to an IL-12/23i biologic** (PICO 29)	Low (90–93, 95, 99, 100)
Conditional recommendation based on low-quality evidence; may consider an IL-12/23i if the patient has IBD or if the patient prefers less frequent drug administration.	
7. **Switch to an IL-17i biologic over abatacept** (PICO 72)	Low (90–93, 95, 103, 104, 112)
Conditional recommendation based on low-quality evidence; may consider abatacept if the patient prefers IV dosing or in patients with recurrent or serious infections.	
8. **Switch to an IL-17i biologic over tofacitinib** (PICO 75)	Low (90–93, 105)
Conditional recommendation based on low-quality evidence; may consider tofacitinib if the patient prefers an oral therapy or in patients with concomitant IBD or a history of recurrent *Candida* infections.	
9. **Switch to an IL-12/23i biologic over abatacept** (PICO 71)	Low (99, 100, 103, 104)
Conditional recommendation based on of low-quality evidence; may consider abatacept if the patient prefers IV dosing or in patients with recurrent or serious infections.	
10. **Switch to an IL-12/23i biologic over tofacitinib** (PICO 74)	Low (98–100, 105)
Conditional recommendation based on low-quality evidence; may consider tofacitinib if the patient prefers an oral therapy.	
11. **Switch to a different TNFi biologic monotherapy over switching to a different TNFi biologic and MTX combination therapy** (PICO 30)	Very low
Conditional recommendation based on very-low-quality evidence; may consider switching to a TNFi biologic and MTX combination therapy if the current TNFi biologic is infliximab.	
12. **Switch to an IL-17i biologic monotherapy over switching to an IL-17i biologic and MTX combination therapy** (PICO 32)	Very low
Conditional recommendation based on very-low-quality evidence; may consider switching to an IL-17i biologic and MTX combination therapy in patients with concomitant uveitis, as uveitis may respond to MTX therapy.	

Table 3. *(Cont'd)*

	Level of evidence (evidence [refs.] reviewed)†
13. **Switch to an IL-12/23i biologic monotherapy over switching to an IL-12/23i biologic and MTX combination therapy** (PICO 31)	Very low
Conditional recommendation based on very-low-quality evidence; may consider switching to an IL-12/23i biologic and MTX combination therapy if the patient has severe psoriasis.	
In adult patients with active PsA despite treatment with a TNFi biologic and MTX combination therapy,	
14. **Switch to a different TNFi biologic + MTX over switching to a different TNFi biologic monotherapy** (PICO 33)	Very low
Conditional recommendation based on very-low-quality evidence; may consider switching to a different TNFi biologic monotherapy if the patient has demonstrated MTX-associated adverse events, prefers to receive fewer medications, or perceives MTX as a burden.	
15. **Switch to an IL-17i biologic monotherapy over an IL-17i biologic and MTX combination therapy** (PICO 35)	Very low
Conditional recommendation based on very-low-quality evidence; may consider switching to an IL-17i biologic and MTX combination therapy if the patient had had a partial response to the existing regimen or in patients with concomitant uveitis, as uveitis may respond to MTX therapy. Continuing MTX during the transition to an IL-17i biologic was discussed as potentially beneficial to allow the new therapy time to work.	
16. **Switch to IL-12/23i biologic monotherapy over IL-12/23i biologic and MTX combination therapy** (PICO 34)	Very low
Conditional recommendation based on very-low-quality evidence; may consider switching to an IL-12/23i biologic and MTX combination therapy if the patient had had a partial response to the existing regimen or in patients with concomitant uveitis, as uveitis may respond to MTX therapy. Continuing MTX during the transition to an IL-12/23i biologic was discussed as potentially beneficial to allow the new therapy time to work.	

* Active psoriatic arthritis (PsA) is defined as disease causing symptoms at an unacceptably bothersome level as reported by the patient, and judged by the examining clinician to be *due to PsA* based on ≥1 of the following: swollen joints, tender joints, dactylitis, enthesitis, axial disease, active skin and/or nail involvement, and extraarticular inflammatory manifestations such as uveitis or inflammatory bowel disease (IBD). TNFi = tumor necrosis factor inhibitor; MTX = methotrexate; IL-17i = interleukin-17 inhibitor; IV = intravenous.
† When there were no published studies, we relied on the clinical experience of the panelists, which was designated very-low-quality evidence.
‡ Because there are currently no widely agreed-upon definitions of disease severity, psoriasis severity should be established by the health care provider and patient on a case-by-case basis. In clinical trials, severe psoriasis has been defined as a Psoriasis Area and Severity Index (PASI) score (25) of ≥12 and a body surface area score of ≥10. In clinical practice, however, the PASI tool is not standardly utilized given its cumbersome nature. In 2007, the National Psoriasis Foundation published an expert consensus statement, which defined moderate-to-severe disease as a body surface area of ≥5% (68). In cases in which the involvement is in critical areas, such as the face, hands or feet, nails, intertriginous areas, scalp, or where the burden of the disease causes significant disability or impairment of physical or mental functioning, the disease can be severe despite the lower amount of surface area of skin involved. The need to factor in the unique circumstances of the individual patient is of critical importance, but this threshold provides some guidance in the care of patients.

12/23i biologic in patients with recurrent or serious infections. Tofacitinib may be considered instead of an IL-17i biologic in patients who prefer oral therapy or have a history of recurrent or severe *Candida* infections. Tofacitinib may be considered instead of an IL-12/23i biologic in patients who prefer oral therapy. For each biologic (TNFi, IL-12/23i, or IL-17i), monotherapy is recommended over combination with MTX. Combination therapy with biologic and MTX may be used instead of biologic monotherapy in the presence of severe psoriasis, partial response to current MTX therapy, concomitant uveitis (since uveitis may respond to MTX therapy), and if the current TNFi biologic is infliximab or adalimumab (for immunogenicity prevention).

Under circumstances in which combination therapy with a TNFi biologic and MTX is used and active PsA persists, switching to a different TNFi with MTX is recommended over monotherapy with a different TNFi. Continuing MTX treatment during TNFi transition was seen as beneficial because TNFi biologics may have more sustained efficacy when used in combination with MTX, but evidence is limited (34). Monotherapy with a different TNFi biologic may be used if the patient has had MTX-associated adverse events, prefers to receive fewer medications, or perceives MTX treatment as a burden. IL-12/23i or IL-17i biologic monotherapy is recommended over either of these agents in combination with MTX. Combination therapy with an IL-17i or IL-12/23 biologic and MTX may be used instead of switching to biologic monotherapy
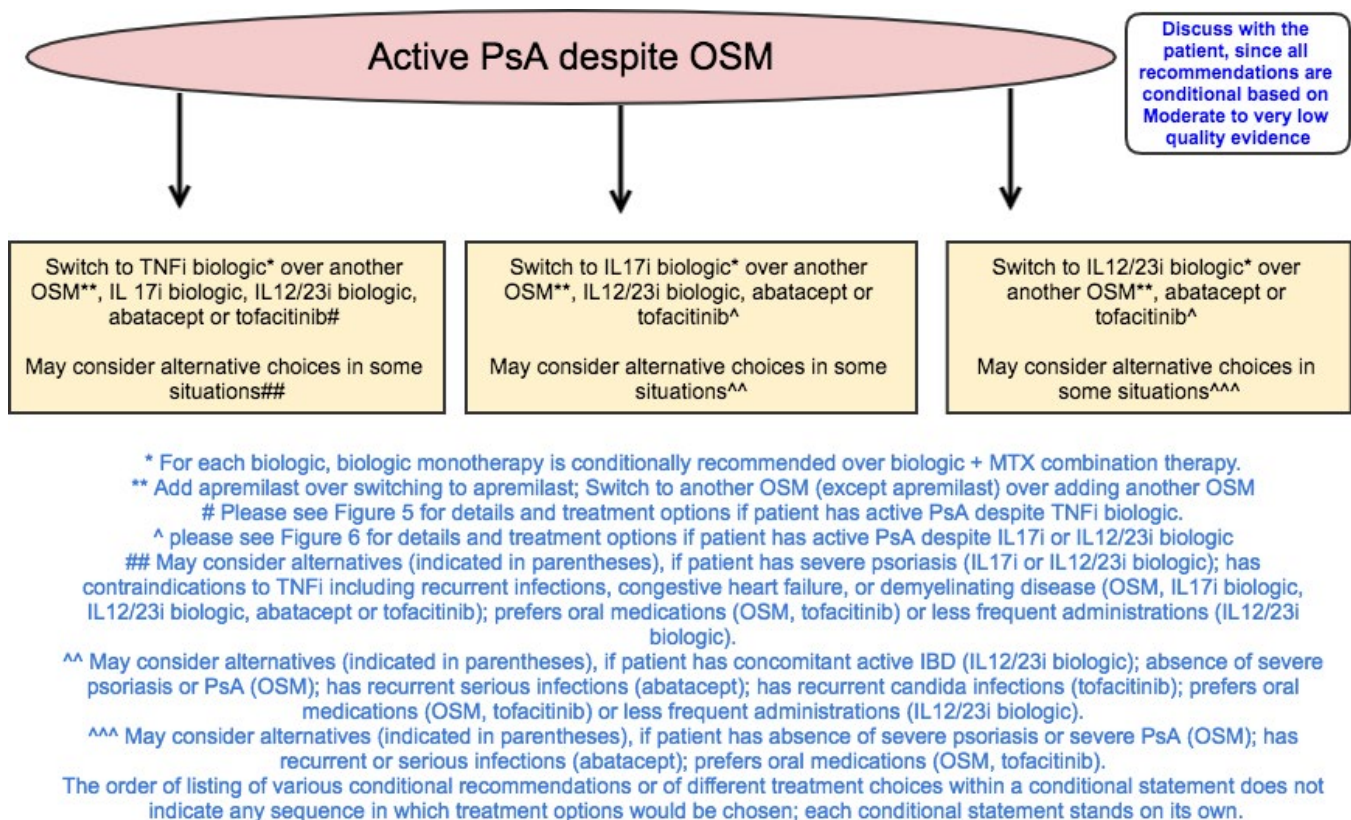
Figure 5. Recommendations for the treatment of patients with active psoriatic arthritis (PsA) despite treatment with a tumor necrosis factor inhibitor (TNFi) as monotherapy or as combination therapy with methotrexate (MTX). All recommendations are conditional based on low- to very-low-quality evidence. A conditional recommendation means that the panel believed the desirable effects of following the recommendation probably outweigh the undesirable effects, so the course of action would apply to the majority of the patients, but some may not want to follow the recommendation. Because of this, conditional recommendations are preference sensitive and always warrant a shared decision-making approach. Due to the complexity of management of active PsA, not all clinical situations and choices could be depicted in this flow chart, and therefore we show only the key recommendations. For a complete list of recommendations, please refer to the Results section of the text. For the level of evidence supporting each recommendation, see Table 3 and the related section in the Results. IL-17i = interleukin-17 inhibitor; IV = intravenous.

if the patient had a partial response to the existing regimen and/or has concomitant uveitis that might respond to MTX therapy.

Active PsA despite treatment with an IL-17i biologic agent as monotherapy (Table 4 and Figure 6). *All recommendations for patients with active PsA despite IL-17i biologic treatment are conditional based on very-low-quality evidence.*

In patients with active PsA despite treatment with an IL-17i biologic, switching to a TNFi biologic is recommended over switching to an IL-12/23i biologic, adding MTX to the current IL-17i biologic, or switching to a different IL-17i biologic (Table 4 and Figure 6). Switching to an IL-12/23i biologic is recommended over adding MTX to the current IL-17i biologic or switching to a different IL-17i biologic. Treatment may be switched to an IL-12/23i biologic instead of a TNFi biologic if the patient has severe psoriasis or a contraindication to TNFi biologic treatment. Another

IL-17i biologic may be used instead of switching to a TNFi or IL-12/23i biologic if the patient had a secondary efficacy failure with the current IL-17i biologic, severe psoriasis, or a contraindication to TNFi treatment. MTX may be added to the current IL-17i regimen instead of switching to a TNFi or IL-12/23i biologic in patients who have had a partial response to the current IL-17i biologic.

Active PsA despite treatment with an IL-12/23i biologic agent as monotherapy (Table 4 and Figure 6). *All recommendations for patients with active PsA despite IL-12/23i biologic treatment are conditional based on very-low-quality evidence.*

In patients with active PsA despite treatment with an IL-12/23i biologic, switching to a TNFi biologic is recommended over adding MTX to the current regimen or switching to an IL-17i biologic

Table 4. Recommendations for treatment of patients with active psoriatic arthritis despite treatment with an IL-17i or an IL-12/23i biologic monotherapy (PICOs 36–43)*

	Level of evidence†
In adult patients with active PsA despite treatment with an IL-17i biologic monotherapy,	
1. **Switch to a TNFi biologic over switching to an IL-12/23i biologic** (PICO 39)	Very low
Conditional recommendation based on very-low-quality-evidence; may consider switching to IL- 12/23i if the patient has contraindications to TNFi biologics, including congestive heart failure, previous serious infections, recurrent infections, or demyelinating disease, or prefers less frequent drug administration.	
2. **Switch to a TNFi biologic over switching to a different IL-17i biologic** (PICO 42)	Very low
Conditional recommendation based on very-low-quality evidence; may consider switching to a different IL-17i if the patient had had a secondary efficacy failure to current IL-17i, or severe psoriasis, or contraindications to TNFi biologics, including congestive heart failure, previous serious infections, recurrent infections, or demyelinating disease.	
3. **Switch to a TNFi biologic over adding MTX to an IL-17i biologic** (PICO 41)	Very low
Conditional recommendation based on very-low-quality evidence; may consider adding MTX to an IL-17i if the patient had had a partial response to the existing regimen or if the patient has contraindications to TNFi biologics, including congestive heart failure, previous serious infections, recurrent infections, or demyelinating disease.	
4. **Switch to an IL-12/23i biologic over switching to a different IL-17i biologic** (PICO 43)	Very low
Conditional recommendation based on very-low-quality evidence; may consider switching to a different IL-17i if the patient had had a secondary efficacy failure to current IL-17i or severe psoriasis,‡ or if the patient has contraindications to TNFi biologics, including congestive heart failure, previous serious infections, recurrent infections, or demyelinating disease.	
5. **Switch to an IL-12/23i biologic over adding MTX to an IL-17i biologic** (PICO 40)	Very low
Conditional recommendation based on very-low-quality evidence; may consider adding MTX to an IL-17i if the patient had had a partial response to the existing regimen.	
In adult patients with active PsA despite treatment with an IL-12/23i biologic monotherapy,	
6. **Switch to a TNFi biologic over switching to an IL-17i biologic** (PICO 38)	Very low
Conditional recommendation based on very-low-quality evidence; may consider an IL-17i if the patient has severe psoriasis or contraindications to TNFi biologics, including congestive heart failure, previous serious infections, recurrent infections, or demyelinating disease.	
7. **Switch to a TNFi biologic over adding MTX to an IL-12/23i biologic** (PICO 36)	Very low
Conditional recommendation based on very-low-quality evidence; may consider adding MTX in patients in whom the severe psoriasis is not responding to the current therapy, or if the patient has contraindications to TNFi biologics, including congestive heart failure, previous serious infections, recurrent infections, or demyelinating disease.	
8. **Switch to an IL-17i biologic over adding MTX to an IL-12/23i biologic** (PICO 37).	Very low
Conditional recommendation based on very-low-quality evidence; may consider adding MTX in patients with only partial response to the current therapy or in those who potentially have not had enough time to adequately respond.	

* Active psoriatic arthritis (PsA) is defined as disease causing symptoms at an unacceptably bothersome level as reported by the patient, and judged by the examining clinician to be *due to PsA* based on ≥1 of the following: swollen joints, tender joints, dactylitis, enthesitis, axial disease, active skin and/or nail involvement, and extraarticular inflammatory manifestations such as uveitis or inflammatory bowel disease. IL-17i = interleukin-17 inhibitor; TNFi = tumor necrosis factor inhibitor; MTX = methotrexate.
† When there were no published studies—as was the case with all of the recommendations presented in this table—we relied on the clinical experience of the panelists, which was designated very-low-quality evidence.
‡ Because there are currently no widely agreed-upon definitions of disease severity, psoriasis severity should be established by the health care provider and patient on a case-by-case basis. In clinical trials, severe psoriasis has been defined as a Psoriasis Area and Severity Index (PASI) score (25) of ≥12 and a body surface area score of ≥10. In clinical practice, however, the PASI tool is not standardly utilized given its cumbersome nature. In 2007, the National Psoriasis Foundation published an expert consensus statement, which defined moderate-to-severe disease as a body surface area of ≥5% (68). In cases in which the involvement is in critical areas, such as the face, hands or feet, nails, intertriginous areas, scalp, or where the burden of the disease causes significant disability or impairment of physical or mental functioning, the disease can be severe despite the lower amount of surface area of skin involved. The need to factor in the unique circumstances of the individual patient is of critical importance, but this threshold provides some guidance in the care of patients.

Figure 6. Recommendations for the treatment of patients with active psoriatic arthritis (PsA) despite treatment with interleukin-17 inhibitor (IL-17i) or IL-12/23i biologic monotherapy. All recommendations are conditional based on low- to very-low-quality of evidence. A conditional recommendation means that the panel believed the desirable effects of following the recommendation probably outweigh the undesirable effects, so the course of action would apply to the majority of the patients, but some may not want to follow the recommendation. Because of this, conditional recommendations are preference sensitive and always warrant a shared decision-making approach. Due to the complexity of management of active PsA, not all clinical situations and choices could be depicted in this flow chart, and therefore we show only the key recommendations. For a complete list of recommendations, please refer to the Results section of the text. For the level of evidence supporting each recommendation, see Table 4 and the related section in the Results. TNFi = tumor necrosis factor inhibitor; MTX = methotrexate.

(Table 4 and Figure 6). Switching to an IL-17i biologic is recommended over adding MTX to the current therapy. Treatment may be switched to an IL-17i biologic instead of a TNFi biologic if the patient has severe psoriasis or a contraindication to TNFi biologic treatment. MTX may be added to the current IL-12/23i biologic therapy instead of switching to a TNFi or an IL-17i biologic in patients with a partial response to the current therapy; MTX may also be added to the current IL-12/23i biologic therapy instead of switching to a TNFi biologic in the presence of contraindications to TNFi biologics.

Treat-to-target (Table 5). *This recommendation for patients with active PsA is conditional based on low-quality evidence.*

In patients with active PsA, using a treat-to-target strategy is recommended over not following a-treat-to-target strategy. One may consider not using a treat-to-target strategy in patients in whom there are concerns related to increased adverse events, costs of therapy, and patient burden of medications associated with tighter control.

Active PsA with psoriatic spondylitis/axial disease despite treatment with NSAIDs (Table 5). *All recommendations for patients with active PsA with psoriatic spondylitis/ axial disease despite NSAID treatment are conditional based on very-low-quality evidence.*

The ACR/Spondylitis Association of America/Spondyloarthritis Research and Treatment Network recommendations for patients with axial spondyloarthritis (35) should be followed for patients with axial PsA. OSMs are not effective for axial disease (35). In patients with active axial PsA despite NSAID treatment, a TNFi biologic is recommended over an IL-17i or IL-12/23i biologic, and an IL-17i biologic is recommended over an IL-12/23i biologic. An IL-17i biologic may be used instead of a TNFi biologic if the patient has severe psoriasis or a contraindication to TNFi biologic treatment (Table 5). We recommend *not using* an IL-12/23i biologic since 3 randomized trials of an IL-12/23i biologic (ustekinumab) in patients with axial spondyloarthritis (a related condition) were stopped because the key primary and secondary end points were not achieved (36–38); the safety profile was reportedly consistent with that observed in past ustekinumab studies.

Table 5. Recommendations for treatment of patients with active psoriatic arthritis including treat-to-target, active axial disease, enthesitis, or active inflammatory bowel disease (PICOs 44–55; 58–62)*

	Level of evidence (evidence [refs.] reviewed)†
In adult patients with active PsA,	
1. **Use a treat-to-target strategy over not following a treat-to-target strategy** (PICO 44)	Low (113)
Conditional recommendation based on low-quality evidence; may consider not following a treat-to-target strategy in patients in whom higher frequency and/or severity of adverse events, higher cost of therapy, or higher patient burden of medications with tighter control are a concern.	
In patients with active PsA with psoriatic spondylitis/axial disease despite treatment with NSAIDs,‡	
2. **Switch to a TNFi biologic over switching to an IL-17i biologic** (PICO 46)	Very low
Conditional recommendation based on very-low-quality evidence; may consider switching to an IL-17i biologic if the patient has contraindications to TNFi biologics, congestive heart failure, previous serious infections, recurrent infections, or demyelinating disease, or if the patient has severe psoriasis.§	
3. **Switch to a TNFi biologic over switching to an IL-12/23i biologic** (PICO 45)	Very low
Conditional recommendation based on very-low-quality evidence; switching to an IL-12/23i biologic is *not* considered since recent trials in axial SpA were stopped.	
4. **Switch to an IL-17i biologic over switching to an IL-12/23i** (PICO 47)	Very low
Conditional recommendation based on very-low-quality evidence; switching to an IL-12/23i biologic is *not* considered since recent trials in axial SpA were stopped.	
In adult patients with active PsA and predominant enthesitis who are both OSM- and biologic treatment–naive,¶	
5. **Start oral NSAIDs over an OSM (specifically apremilast)** (PICO 48)	Very low
Conditional recommendation based on very-low-quality evidence; may consider starting an OSM (specifically apremilast) if the patient has active joint disease and/or skin disease or contraindications to the use of NSAIDs, including cardiovascular disease, peptic ulcer disease, or renal disease or impairment.	
6. **Start a TNFi biologic over an OSM (specifically apremilast)** (PICO 48A)	Very low
Conditional recommendation based on very-low-quality evidence; may consider starting an OSM (specifically apremilast) if the patient prefers an oral treatment as the first therapy or the patient has contraindications to TNFi biologics, including recurrent infections, congestive heart failure, or demyelinating disease.	
7. **Start tofacitinib over an OSM (specifically apremilast)** (PICO 55)	Very low
Conditional recommendation based on very-low-quality evidence; may consider starting an OSM (specifically apremilast) if the patient has recurrent infections.	
In adult patients with active PsA and predominant enthesitis despite treatment with OSM,	
8. **Switch to a TNFi biologic over an IL-17i biologic** (PICO 53)	Low (72, 73, 76, 89, 90, 92)
Conditional recommendation based on low-quality evidence; may consider switching to an IL-117i if the patient has severe psoriasis or contraindications to TNFi biologics, including congestive heart failure, previous serious infections, recurrent infections, or demyelinating disease.	
9. **Switch to a TNFi biologic over an IL-12/23i biologic** (PICO 52)	Low (72, 73, 76, 98, 100)
Conditional recommendation based on low-quality evidence; may consider switching to an IL-12/23i if the patient has severe psoriasis or contraindications to TNFi biologics, including congestive heart failure, previous serious infections, recurrent infections, or demyelinating disease, or if the patient prefers less frequent drug administration.	
10. **Switch to a TNFi biologic over switching to another OSM** (PICO 49)	Low (72, 73, 76, 83–85)
Conditional recommendation based on low-quality evidence; may consider switching to another OSM# if the patient prefers an oral medication over an injection, or if the patient has contraindications to TNFi biologics, including congestive heart failure, previous serious infections, recurrent infections, or demyelinating disease.	

Table 5. *(Cont'd)*

	Level of evidence (evidence [refs.] reviewed)†
11. **Switch to an IL-17i biologic over an IL-12/23i biologic** (PICO 54)	Low (89, 90, 92, 93, 98–100)
Conditional recommendation based on low-quality evidence; may consider switching to an IL-12/23i if the patient has concomitant IBD or if the patient prefers less frequent drug administration.	
12. **Switch to an IL-17i biologic over switching to another OSM** (PICO 51)	Low (83–86, 89, 90, 92, 93)
Conditional recommendation based on low-quality evidence; may consider switching to another OSM if the patient prefers an oral medication.	
13. **Switch to an IL-12/23i biologic over switching to another OSM** (PICO 50)	Low (83–86, 98, 100)
Conditional recommendation based on low-quality evidence; may consider switching to another OSM# if the patient prefers an oral medication over an injection, or if there are contraindications to an IL- 12/23i, such as severe recurrent infections.	
In adult patients with active PsA and concomitant active IBD who are both OSM- and biologic treatment–naive,	
14. **Start a monoclonal antibody TNFi biologic over an OSM** (PICO 62)	Very low (114)
Conditional recommendation based on very-low-quality evidence; may consider starting an OSM if the patient prefers an oral medication, or if the patient has contraindications to TNFi biologics, including congestive heart failure, previous serious infections, recurrent infections, or demyelinating disease.	
In adult patients with active PsA and concomitant active IBD despite treatment with an OSM,	
15. **Switch to a monoclonal antibody TNFi biologic over a TNFi biologic soluble receptor biologic (i.e., etanercept)** (PICO 58)	Moderate (115–117)
Strong recommendation supported by moderate-quality evidence, showing TNFi monoclonal antibody biologics are effective in IBD but indirect evidence shows a TNFi biologic soluble receptor biologic is not effective for the treatment of IBD.	
16. **Switch to a TNFi monoclonal antibody biologic over an IL-17i biologic** (PICO 59)	Moderate (50)
Strong recommendation supported by moderate-quality evidence showing monoclonal antibody TNFi biologics are effective for IBD while an IL-17i biologic is not effective for IBD.	
17. **Switch to a TNFi biologic monoclonal antibody biologic over an IL-12/23i biologic** (PICO 61)	Very low
Conditional recommendation based on very-low-quality evidence; may consider switching to an IL- 12/23i biologic if the patient has contraindications to TNFi biologics, including congestive heart failure, previous serious infections, recurrent infections, or demyelinating disease, or prefers less frequent drug administration.	
18. **Switch to an IL-12/23i biologic over switching to an IL-17i biologic** (PICO 60)	Moderate (50)
Strong recommendation supported by moderate-quality evidence showing IL-12/23i biologic is effective for IBD while an IL-17i biologic is not effective for IBD.	

* Active psoriatic arthritis (PsA) is defined as disease causing symptoms at an unacceptably bothersome level as reported by the patient, and judged by the examining clinician to be *due to PsA* based on ≥1 of the following: swollen joints, tender joints, dactylitis, enthesitis, axial disease, active skin and/or nail involvement, and extraarticular inflammatory manifestations such as uveitis or inflammatory bowel disease (IBD).
† When there were no published studies, we relied on the clinical experience of the panelists, which was designated very-low-quality evidence.
‡ Axial disease is generally treated according to the American College of Rheumatology/Spondylitis Association of America/Spondyloarthritis Research and Treatment Network recommendations for spondyloarthritis (SpA).
§ Because there are currently no widely agreed-upon definitions of disease severity, psoriasis severity should be established by the health care provider and patient on a case-by-case basis. In clinical trials, severe psoriasis has been defined as a Psoriasis Area and Severity Index (PASI) score (25) of ≥12 and a body surface area score of ≥10. In clinical practice, however, the PASI tool is not standardly utilized given its cumbersome nature. In 2007, the National Psoriasis Foundation published an expert consensus statement, which defined moderate-to-severe disease as a body surface area of ≥5% (68). In cases in which the involvement is in critical areas, such as the face, hands or feet, nails, intertriginous areas, scalp, or where the burden of the disease causes significant disability or impairment of physical or mental functioning, the disease can be severe despite the lower amount of surface area of skin involved. The need to factor in the unique circumstances of the individual patient is of critical importance, but this threshold provides some guidance in the care of patients.
¶ Oral small molecules (OSMs) are defined as methotrexate (MTX), sulfasalazine, leflunomide, cyclosporine, or apremilast and *do not* include tofacitinib, which was handled separately since its efficacy/safety profile is much different from that of other OSMs listed above. OSM- and biologic treatment–naive is defined as naive to treatment with OSMs, tumor necrosis factor inhibitors (TNFi,), interleukin-17 inhibitors (IL-17i), and IL-12/23i; patients may have received nonsteroidal antiinflammatory drugs (NSAIDs), glucocorticoids, and/or other pharmacologic and nonpharmacologic interventions.
# It should be noted that for the enthesitis questions (PICO 49, 50, and 51), the existing evidence was mainly drawn from the apremilast studies, as no randomized controlled trial report described enthesitis outcomes for the other OSMs.

Active PsA with predominant enthesitis in treatment-naive patients and despite treatment with an OSM (Table 5). *All recommendations for patients with active PsA with predominant enthesitis are conditional based on low- to very-low-quality evidence. (This section names apremilast among all OSMs specifically for recommendations, since of the OSMs, only apremilast has shown efficacy for enthesitis.)*

In treatment-naive PsA patients with predominant enthesitis, a TNFi biologic is recommended over an OSM as a first-line option. Apremilast may be used instead of a TNFi biologic if the patient prefers an oral therapy or has contraindications to TNFi. Oral NSAIDs are recommended over starting an OSM unless the patient has cardiovascular disease, peptic ulcer disease, renal disease (or impairment), or severe psoriasis or PsA, in which case apremilast may be given instead of NSAIDs. Tofacitinib is recommended over apremilast for treatment-naive patients with predominant enthesitis. Apremilast may be used instead of tofacitinib in patients with recurrent infections.

In patients with active PsA with predominant enthesitis despite treatment with an OSM (used for other manifestations of PsA), a TNFi biologic, an IL-17i biologic, or an IL-12/23i biologic is recommended over switching to another OSM. Apremilast may be used in patients who prefer oral therapy or who have recurrent infections or contraindications to TNFi biologics. A TNFi biologic is recommended over an IL-17i or IL-12/23i biologic. An IL-17i or IL-12/23i biologic may be used instead of a TNFi biologic in patients with severe psoriasis or contraindications to TNFi. An IL-17i biologic is recommended over an IL-12/23i biologic. An IL-12/23i biologic may be used instead of a TNFi biologic in patients who prefer less frequent drug administration, and instead of an IL-17i biologic in patients with concomitant IBD or who prefer less frequent drug administration.

Active PsA with concomitant active IBD (Table 5). *All recommendations for patients with active PsA with concomitant active IBD are strong based on moderate-quality evidence, except for 2 conditional recommendations based on very-low-quality evidence.*

Active PsA in OSM- and biologic treatment–naive patients with concomitant active IBD. In patients with active PsA with concomitant active IBD who have not received OSM or biologic treatment, a monoclonal antibody TNFi biologic (excludes etanercept, which is a fusion molecule/soluble receptor biologic) is recommended over an OSM (Table 5). An OSM may be used in patients without severe PsA who prefer oral therapy or have contraindications to TNFi biologics.

Active PsA despite treatment with an OSM in patients with concomitant active IBD. In patients with active PsA with concomitant active IBD despite treatment with an OSM, a monoclonal antibody TNFi biologic or an IL-12/23i biologic *should be used* over an IL-17i biologic, and a monoclonal antibody TNFi biologic *should be used* over a TNFi soluble receptor biologic (etanercept) (*all strong recommendations* [Table 5]). A monoclonal antibody TNFi biologic is recommended over an IL-12/23i biologic (conditional recommendation). An IL-12/23i biologic may be used instead of a monoclonal antibody TNFi biologic in patients with contraindications to TNFi biologics or who prefer less frequent drug administration.

Active PsA with comorbidities (Table 6). *All recommendations for patients with active PsA with comorbidities are conditional based on low- to very-low-quality evidence, except those for patients with serious infections, which are strong based on moderate-quality evidence.*

Active PsA in OSM- and biologic treatment–naive patients with concomitant diabetes. In patients with active PsA with concomitant active diabetes who have not received OSM or biologic treatment, an OSM other than MTX is recommended over a TNFi biologic, due to the concern about the higher prevalence of fatty liver disease and liver toxicity with MTX use in this patient population (39,40) (Table 6). A TNFi biologic may be used instead of an OSM in the presence of severe PsA or severe psoriasis or when diabetes is well controlled (i.e., with a potentially lower risk of infections)*.*

Active PsA in OSM- and biologic treatment–naive patients with frequent serious infections. In patients with active PsA who have frequent serious infections and have not received OSM or biologic treatment, an OSM *should be used* over a TNFi biologic as a first-line treatment since there is a black box warning against the use of a TNFi biologic in patients with frequent serious infections (*strong recommendation*). An IL-12/23i or IL-17i biologic is recommended over a TNFi biologic (conditional recommendation [Table 6]). A TNFi biologic may be used instead of an IL-12/23i biologic in patients with severe PsA and instead of an IL-17i biologic in patients with concomitant IBD.

Active PsA in patients requiring killed or live attenuated vaccinations when starting biologic treatment (Table 7). *All recommendations for vaccinations in patients with active PsA are conditional based on very-low-quality evidence.*

It is recommended that the biologic treatment be started and the killed vaccines administered (as indicated based on patient age, sex, and immunization history per recommendations of the Centers for Disease Control and Prevention [41]) in patients with active PsA over delaying the biologic to give the killed vaccines. Delaying the start of the biologic is recommended over not delaying to administer a live attenuated vaccination in patients with active PsA (Table 7). If PsA manifestations are severe and delaying the start of the biologic is not desirable, starting the biologic and administering the live attenuated vaccines at the same time might be considered.

Table 6. Recommendations for treatment of patients with active psoriatic arthritis and comorbidities, including concomitant diabetes and recurrent serious infections (PICOs 63–66)*

	Level of evidence (evidence [refs.] reviewed)†
In adult patients with active PsA and diabetes who are both OSM- and biologic treatment–naive,‡	
1. **Start an OSM other than MTX over a TNFi biologic** (PICO 63a)	Very low (118, 119)
Conditional recommendation based on very-low-quality evidence; may consider starting a TNFi, if the patient has severe PsA§ or severe/active skin disease,¶ when diabetes is well controlled.	
In adult patients with active PsA and frequent serious infections who are both OSM- and biologic treatment–naive,	
2. **Start an OSM over a TNFi biologic** (PICO 64)	Moderate (33, 120)
Strong recommendation supported by moderate-quality evidence, including a black box warning against the use of a TNFi biologic with regard to increased risk of serious infection.	
3. **Start an IL-12/23i biologic over a TNFi biologic** (PICO 65)	Very low (33)
Conditional recommendation based on very-low-quality evidence; may consider starting a TNFi if the patient has severe PsA.	
4. **Start an IL-17i biologic over a TNFi biologic** (PICO 66)	Very low
Conditional recommendation based on very-low-quality evidence; may consider starting a TNFi biologic in patients with concomitant IBD.	

* Active psoriatic arthritis (PsA) is defined as disease causing symptoms at an unacceptably bothersome level as reported by the patient, and judged by the examining clinician to be *due to PsA* based on ≥1 of the following: swollen joints, tender joints, dactylitis, enthesitis, axial disease, active skin and/or nail involvement, and extraarticular inflammatory manifestations such as uveitis or inflammatory bowel disease (IBD).

† When there were no published studies, we relied on the clinical experience of the panelists, which was designated very-low-quality evidence.

‡ Oral small molecules (OSMs) are defined as methotrexate (MTX), sulfasalazine, leflunomide, cyclosporine, or apremilast and *do not* include tofacitinib, which was handled separately since its efficacy/safety profile is much different from that of other OSMs listed above. OSM- and other treatment–naive is defined as naive to treatment with OSMs, tumor necrosis factor inhibitors (TNFi), interleukin-17 inhibitors (IL-17i), and IL-12/23i; patients may have received nonsteroidal antiinflammatory drugs, glucocorticoids, and/or other pharmacologic and nonpharmacologic interventions.

§ Because there are currently no widely agreed-upon definitions of disease severity, PsA severity should be established by the health care provider and patient on a case-by-case basis. For the purposes of these recommendations, severity is considered a broader concept than disease activity in that it encompasses the level of disease activity at a given time point, as well as the presence of poor prognostic factors and long-term damage. Examples of severe PsA disease include the presence of ≥1 of the following: a poor prognostic factor (erosive disease, elevated levels of inflammation markers such as C-reactive protein or erythrocyte sedimentation rate attributable to PsA), long-term damage that interferes with function (e.g., joint deformities, vision loss), highly active disease that causes major impairment in quality of life (i.e., active psoriatic inflammatory disease at many sites [including dactylitis, enthesitis] or function-limiting inflammatory disease at few sites), and rapidly progressive disease.

¶ Because there are currently no widely agreed-upon definitions of disease severity, psoriasis severity should be established by the health care provider and patient on a case-by-case basis. In clinical trials, severe psoriasis has been defined as a Psoriasis Area and Severity Index (PASI) score (25) of ≥12 and a body surface area score of ≥10. In clinical practice, however, the PASI tool is not standardly utilized given its cumbersome nature. In 2007, the National Psoriasis Foundation published an expert consensus statement, which defined moderate-to-severe disease as a body surface area of ≥5% (68). In cases in which the involvement is in critical areas, such as the face, hands or feet, nails, intertriginous areas, scalp, or where the burden of the disease causes significant disability or impairment of physical or mental functioning, the disease can be severe despite the lower amount of surface area of skin involved. The need to factor in the unique circumstances of the individual patient is of critical importance, but this threshold provides some guidance in the care of patients.

Recommendations for nonpharmacologic interventions in patients with active PsA regardless of pharmacologic treatment status (Table 8)

All recommendations for nonpharmacologic interventions for patients with active PsA are conditional based on low- to very-low-quality evidence, except that for smoking cessation, which is a strong recommendation.

It is recommended that patients with active PsA use some form or combination of exercise, physical therapy, occupational therapy, massage therapy, and acupuncture over not using these modalities as tolerated. Low-impact exercise (e.g., tai chi, yoga, swimming) is recommended over high-impact exercise (e.g., running). High-impact exercises may be performed instead of low-impact exercises by patients who prefer the former and

Table 7. Recommendations for vaccination in patients with active psoriatic arthritis (PICOs 56–57)*

	Level of evidence (evidence [refs.] reviewed)†
In adult patients with active PsA needing vaccinations,‡	
1. **Start the biologic and administer killed vaccines over delaying the start of biologic to administer killed vaccines** (PICO 56)	Very low (121–126)
Conditional recommendation based on very-low-quality evidence; may consider delaying the start of biologic to administer killed vaccines due to patient preference based on patient belief about vaccine efficacy.	
2. **Delay the start of biologic to administer live attenuated vaccines over starting the biologic and administering live attenuated vaccines** (PICO 57)	Very low (127)
Conditional recommendation based on very-low-quality evidence; may consider starting the biologic and administering live attenuated vaccines in patients with very active severe joint§ or skin¶ disease who prefer no delay in biologic initiation.	

* Active psoriatic arthritis (PsA) is defined as disease causing symptoms at an unacceptably bothersome level as reported by the patient, and judged by the examining clinician to be *due to PsA* based on ≥1 of the following: swollen joints, tender joints, dactylitis, enthesitis, axial disease, active skin and/or nail involvement, and extraarticular inflammatory manifestations such as uveitis or inflammatory bowel disease.
† When there were no published studies, we relied on the clinical experience of the panelists, which was designated very-low-quality evidence.
‡ Vaccines as indicated by patient age, sex, and immunization history per recommendations from the Centers for Disease Control and Prevention and available at: https://www.cdc.gov/vaccines/schedules/downloads/adult/adult-combined-schedule.pdf.
§ Because there are currently no widely agreed-upon definitions of disease severity, PsA severity should be established by the health care provider and patient on a case-by-case basis. For the purposes of these recommendations, severity is considered a broader concept than disease activity in that it encompasses the level of disease activity at a given time point, as well as the presence of poor prognostic factors and long-term damage. Examples of severe PsA disease include the presence of ≥1 of the following: a poor prognostic factor (erosive disease, elevated levels of inflammation markers such as C-reactive protein or erythrocyte sedimentation rate attributable to PsA), long-term damage that interferes with function (e.g., joint deformities, vision loss), highly active disease that causes major impairment in quality of life (i.e., active psoriatic inflammatory disease at many sites [including dactylitis, enthesitis] or function-limiting inflammatory disease at few sites), and rapidly progressive disease.
¶ Because there are currently no widely agreed-upon definitions of disease severity, psoriasis severity should be established by the health care provider and patient on a case-by-case basis. In clinical trials, severe psoriasis has been defined as a Psoriasis Area and Severity Index (PASI) score (25) of ≥12 and a body surface area score of ≥10. In clinical practice, however, the PASI tool is not standardly utilized given its cumbersome nature. In 2007, the National Psoriasis Foundation published an expert consensus statement, which defined moderate-to-severe disease as a body surface area of ≥5% (68). In cases in which the involvement is in critical areas, such as the face, hands or feet, nails, intertriginous areas, scalp, or where the burden of the disease causes significant disability or impairment of physical or mental functioning, the disease can be severe despite the lower amount of surface area of skin involved. The need to factor in the unique circumstances of the individual patient is of critical importance, but this threshold provides some guidance in the care of patients.

have no contraindications to high-impact exercises (Table 8). Clinicians *should* encourage patients to stop smoking, offering cessation aids, due to a demonstrated effectiveness of smoking cessation in randomized trials in other conditions and in the general population (42–44) (*strong recommendation*). In PsA patients who are overweight or obese, weight loss is recommended in order to potentially increase pharmacologic response.

All strong recommendations in this guideline are also listed separately in Supplementary Appendix 6, at http://onlinelibrary.wiley.com/doi/10.1002/art.40726/abstract.

DISCUSSION

We present herein the first ACR/NPF guideline for the treatment of psoriatic arthritis. The goal of this guideline is to assist health care providers in managing active PsA in their patients, including optimizing therapy. PsA is a heterogene-

ous and multifaceted inflammatory disease, and its different clinical features (e.g., peripheral arthritis, psoriasis, nail disease, enthesitis, dactylitis, axial disease) sometimes respond differently to therapy. Despite an expansion in the number of new therapies for PsA, there remains limited comparative efficacy/effectiveness evidence to inform treatment decisions. Thus, most of our recommendations are based on low-quality evidence and are conditional. The conditional recommendations convey that, although the suggested course of action will be best for many patients, there will be some patients in whom, considering their comorbidities and/or their values and preferences, the alternative represents the best choice. The guideline will be updated as new evidence from comparative studies becomes available.

A Patient Panel meeting was held prior to the Voting Panel meeting to gain insight into patients' values and preferences for the pharmacologic/nonpharmacologic intervention comparisons being addressed. We recognize that patient preferences are an important part of our treatment recommendations. Findings from the Patient Panel meeting were discussed throughout the Voting Panel

Table 8. Recommendations for treatment of patients with active psoriatic arthritis with nonpharmacologic interventions (PICOs 1–8)*

	Level of evidence (evidence [refs.] reviewed)†
In adult patients with active PsA,	
1. **Recommend exercise over no exercise** (PICO 1)	Low (128)
Conditional recommendation based on low-quality evidence; may consider no exercise in patients with existing muscle/tendon injury or multiple inflamed symptomatic joints with worsening pain with exercise.	
2. **Recommend low-impact exercise (e.g., tai chi, yoga, swimming) over high-impact exercise (e.g., running)** (PICO 2)	Very low
Conditional recommendation based on very-low-quality evidence; may consider high-impact exercise due to patient preference.	
3. **Recommend physical therapy over no physical therapy** (PICO 3)	Very low
Conditional recommendation based on very-low-quality evidence; may consider no physical therapy due to patient preference, out-of-pocket cost, distance to physical therapy site, or lack of transportation.	
4. **Recommend occupational therapy over no occupational therapy** (PICO 4)	Low (129, 130)
Conditional recommendation based on low-quality evidence; may consider no occupational therapy due to patient preference, out-of-pocket cost, distance to occupational therapy site, or lack of transportation.	
5. **Recommend weight loss over no weight loss for patients who are overweight/obese** (PICO 5)	Low (131–133)
Conditional recommendation based on low-quality evidence; may consider no weight loss due to additional patient burden involved with weight-loss program.	
6. **Recommend massage therapy over no massage therapy** (PICO 7)	Very low (134)
Conditional recommendation based on very-low-quality evidence; may consider no massage therapy due to associated costs.	
7. **Recommend acupuncture over no acupuncture** (PICO 8)	Very low (135)
Conditional recommendation based on very-low-quality evidence; may consider no acupuncture due to associated costs.	
8. **Recommend smoking cessation over no smoking cessation** (PICO 6)	Moderate (136, 137)
Strong recommendation supported by moderate-quality evidence, rated down for indirectness.	

* Active psoriatic arthritis (PsA) is defined as disease causing symptoms at an unacceptably bothersome level as reported by the patient, and judged by the examining clinician to be *due to PsA* based on ≥1 of the following: swollen joints, tender joints, dactylitis, enthesitis, axial disease, active skin and/or nail involvement, and extraarticular inflammatory manifestations such as uveitis or inflammatory bowel disease.
† When there were no published studies, we relied on the clinical experience of the panelists, which was designated very-low-quality evidence.

meeting to ensure that patient input was incorporated into the final PsA guideline. Examples of patient feedback included strong value on therapies that are effective (e.g., prevent further damage, and improve quality of life, social participation, and function) and safe (especially having low adverse event profiles). In particular, patients discussed the negative impact of adverse events (e.g., fatigue, nausea, and malaise) on quality of life and social participation, and thus the risk for these adverse events weighed heavily in patients' decision-making. The concept of treat-to-target was challenging for patients. Although they saw value in improved outcomes, they also thought this strategy could increase costs to the patient (e.g., copayments, time traveling to more frequent appointments, etc.) and potentially increase adverse events. Therefore, a detailed con-

versation with the patient is needed to make decisions regarding treat-to-target. To help ensure that the recommendations were patient-centered, 2 patients were members of the Voting Panel.

While using a treat-to-target approach over not using a treat-to-target approach was discussed by the Voting Panel, we did not address specific targets to be recommended or used. There have been 2 international meetings to discuss potential targets: the use of either minimal disease activity (MDA) or disease activity in psoriatic arthritis (DAPSA) (45,46). The treatment target for PsA would likely be MDA or DAPSA, although a different target may be chosen through patient–provider discussion.

The ACR/NPF PsA guideline conditionally recommends a TNFi biologic over an OSM agent in patients with active PsA. The

available low-quality evidence is inconclusive regarding the efficacy of OSMs in management of PsA, whereas there is moderate-quality evidence of the benefits of TNFi biologics, in particular regarding their impact on the prevention of disease progression and joint damage. In making their recommendation, the panel recognized the cost implications, but put considerations of quality of evidence for benefit over other considerations. This guideline provides recommendations for early and aggressive therapy in patients with newly diagnosed PsA.

The recommendation is, however, conditional, and the panel recognized several potential exceptions to it. Circumstances in which a patient may choose an OSM over a TNFi biologic may include mild-to-moderate disease, a preference of oral over parenteral therapy, or concerns regarding adverse effects of a biologic. A TNFi biologic would not be a good choice in patients with contraindications, including congestive heart failure, previous serious infections, recurrent infections, or demyelinating disease.

During the development of the Group for Research and Assessment of Psoriasis and Psoriatic Arthritis recommendations (47) and the European League Against Rheumatism (EULAR) recommendations (48) for the treatment of PsA, panel members also challenged the decision to put OSMs first in those recommendations. For the EULAR recommendations, the final decision was made based on the lower cost of these medications, a consideration our panel placed lower than the quality of evidence for benefit.

In patients with concomitant IBD, the Voting Panel made strong recommendations favoring a monoclonal antibody TNFi or an IL-12/23i biologic over an IL-17i biologic or a TNFi receptor biologic (etanercept). This was based on moderate-quality evidence showing that TNFi biologics and ustekinumab (an IL-12/23i biologic) are effective for the management of IBD, whereas etanercept (a TNFi receptor biologic) and secukinumab (an IL-17i biologic) are not (49,50).

When the evidence was low or very-low quality, the panel could not be confident in the judgment of net benefit—thus the conditional recommendation. Often, low- or very-low-quality evidence came from indirect evidence, for instance from rheumatoid arthritis (33) or, in the absence of studies, from clinical experience (Supplementary Appendix 5, on the Arthritis & Rheumatology web site at http://onlinelibrary.wiley.com/doi/10.1002/art.40726/abstract). When data on comparative benefits and comparative harms were similar between two medications, the panel explicitly preferred and recommended the medication for which longer-term harms were more well-known, and in which the physician experience in patients with PsA was longer, supplementing with harms data/experience from related rheumatic conditions, where these medications are commonly used. In each case, judgments of net benefit involved explicit consideration of values and preferences, including input from Patient Panel members of the Voting Panel as well as the full Patient Panel that met prior to the Voting Panel meeting.

We recognize that these recommendations do not account for the full complexity of PsA or the full range of possible therapies (e.g., glucocorticoids were not addressed). The high degree of heterogeneity in the presentation and course of PsA coupled with the involvement of multiple domains in a single patient cannot be captured in a single algorithm. In addition, reporting of disease measures and differences in inclusion/exclusion criteria in PsA clinical trials makes it difficult to compare therapies across trials. The impact of alternative therapies on important outcomes such as joint damage still remains to be elucidated. Vaccination recommendations with tofacitinib were not included, as it was not yet approved for PsA when the PICO questions were drafted and only a limited number of PICO questions could be feasibly included for voting. Additional topics, including vaccination in the setting of tofacitinib, will be addressed in a subsequent guideline update.

The ACR has decided to use GRADE methodology in the development of guidelines for the management of rheumatic diseases. The GRADE methodology specifies that panels make recommendations based on a consideration of the balance of relative benefits and harms of the treatment options under consideration, the quality of the evidence (i.e., confidence in the evidence based on the lowest quality of the critical outcomes—high, moderate, low, or very low), and patients' values and preferences. The rating of the quality of evidence for each clinical situation (PICO question) helped to inform the strength of the recommendation (strong or conditional) (51).

The use of GRADE (not used in other PsA treatment recommendations) allowed an explicit consideration of the overall evidence, including the balance of benefits and harms of treatments, the incorporation of patient values and preferences, and cost considerations to judge the tradeoff. This approach led to transparency in decision making by the Voting Panel for each clinical scenario and the formulation of these recommendations. Consistent with GRADE guidance, the Voting Panel usually offered a strong recommendation in the presence of moderate- or high-quality rating of the evidence, and a conditional recommendation in the presence of very-low or low-quality evidence (although recommendations can also be conditional in the setting of moderate-quality evidence, and in certain circumstances strong in the face of low-quality evidence) (15). The other merits of the ACR/NPF process undertaken included a comprehensive literature search, the consideration of each comparison in light of the available evidence, the diverse composition of the Voting Panel, the inclusion of all of the available therapies (e.g., IL-17i biologics, an IL-12/23i biologic, abatacept, and tofacitinib) in the decision-making process (including those approved for psoriasis or rheumatoid arthritis but not yet for PsA, ensuring that the guideline would not be out of date by the time it was published), and the inclusion of population subsets, such as those with predominant enthesitis and/or IBD.

Limitations of the guideline include the limited comparative evidence to inform selection of therapies (i.e., primary comparative benefit/efficacy and harms evidence) and the inability to include all possible clinical scenarios due to the necessity of keeping the task feasible. Because the American Academy of Dermatology and the NPF are currently developing a guideline addressing therapy for psoriasis, our guideline did not address treatment of isolated psoriasis. Another limitation is that we searched only English-language literature. The major limitation of the work arises from the limitations in the evidence.

In this guideline, we often used indirect comparisons among trials/therapies, frequently relying on network meta-analysis. Stratified analyses among subgroups (e.g., treatment-naive, inadequate response to a TNFi biologic agent) were rarely reported separately in primary trials, limiting our ability to perform network meta-analyses in these important subgroups. For most clinical scenarios (PICO questions) there were few or no head-to-head comparison studies identified in the literature review. Thus, the quality of evidence was most often low or very low, and only occasionally moderate (Supplementary Appendix 5; http://onlinelibrary.wiley.com/doi/10.1002/art.40726/abstract). This led to nearly all recommendations being conditional, with a few strong recommendations in cases in which there was sufficient evidence (including that from outside of PsA) to make the Voting Panel confident in selecting one option over the comparator. A flow chart or ranking of treatments requires strong recommendation; when recommendations are conditional/weak it means that the right course of action differs between patients. When the right course of action differs between patients, it is inappropriate to make the flow chart and establish treatment ranking or a hierarchy of treatment options (14).

The 2018 ACR/NPF guideline for the treatment of PsA will assist patients and their health care providers in making challenging disease management decisions. More comparative data are needed to inform treatment selection. Several ongoing trials, including a trial to compare a TNFi biologic combination therapy with a TNFi biologic monotherapy and MTX monotherapy (52), will inform treatment decisions. We anticipate future updates to the guideline when new evidence is available.

ACKNOWLEDGMENTS

AUTHOR CONTRIBUTIONS

REFERENCES

1. Ogdie A, Weiss P. The epidemiology of psoriatic arthritis. Rheum Dis Clin North Am 2015;41:545–68.

2. Ritchlin CT, Colbert RA, Gladman DD. Psoriatic arthritis. N Engl J Med 2017;376:2095–6.

3. Husted JA, Gladman DD, Farewell VT, Cook RJ. Health-related quality of life of patients with psoriatic arthritis: a comparison with patients with rheumatoid arthritis. Arthritis Rheum 2001;45:151–8.

4. Adams R, Walsh C, Veale D, Bresnihan B, FitzGerald O, Barry M. Understanding the relationship between the EQ-5D, SF-6D, HAQ and disease activity in inflammatory arthritis. Pharmacoeconomics 2010;28:477–87.

5. Singh JA, Strand V. Spondyloarthritis is associated with poor function and physical health-related quality of life. J Rheumatol 2009;36:1012–20.

6. Javitz HS, Ward MM, Farber E, Nail L, Vallow SG. The direct cost of care for psoriasis and psoriatic arthritis in the United States. J Am Acad Dermatol 2002;46:850–60.

7. Singh JA, Strand V. Health care utilization in patients with spondyloarthropathies. Rheumatology (Oxford) 2009;48:272–6.

8. Bond SJ, Farewell VT, Schentag CT, Gladman DD. Predictors for radiological damage in psoriatic arthritis: results from a single centre. Ann Rheum Dis 2007;66:370–6.

9. Cresswell L, Chandran V, Farewell VT, Gladman DD. Inflammation in an individual joint predicts damage to that joint in psoriatic arthritis. Ann Rheum Dis 2011;70:305–8.

10. Gladman DD, Farewell VT, Wong K, Husted J. Mortality studies in psoriatic arthritis: results from a single outpatient center. II. Prognostic indicators for death. Arthritis Rheum 1998;41:1103–10.

11. Gladman DD. Mortality in psoriatic arthritis. Clin Exp Rheumatol 2008;26 Suppl 51:S62–5.

12. Gladman DD. Early psoriatic arthritis. Rheum Dis Clin North Am 2012;38:373–86.

13. Guyatt GH, Oxman AD, Vist GE, Kunz R, Falck-Ytter Y, Alonso-Coello P, et al. GRADE: an emerging consensus on rating quality of evidence and strength of recommendations. BMJ 2008;336:924–6.

14. Andrews J, Guyatt G, Oxman AD, Alderson P, Dahm P, Falck-Ytter Y, et al. GRADE guidelines: 14. Going from evidence to recommendations: the significance and presentation of recommendations. J Clin Epidemiol 2013;66:719–25.

15. Andrews JC, Schunemann HJ, Oxman AD, Pottie K, Meerpohl JJ, Coello PA, et al. GRADE guidelines: 15. Going from evidence to recommendation—determinants of a recommendation's direction and strength. J Clin Epidemiol 2013;66:726–35.

16. Pfizer. Press release: Pfizer Announces U.S. FDA Filing acceptance of supplemental new drug application for Xeljanz (tofacitinib citrate) for the treatment of adult patients with active psoriatic arthritis. 2017. URL: https://press.pfizer.com/press-release/pfizer-announces-us-fda-filing-acceptance-supplemental-new-drug-application-xeljanz-to.

17. Reuters. Brief: Eli Lilly files supplemental biologics license application with FDA for Taltz. 2017. URL: http://www.reuters.com/article/brief-eli-lilly-files-supplemental-biolo-idUSFWN1JC0KM.

18. National Psoriasis Foundation. FDA approves Xeljanz for psoriatic arthritis. 2017. URL: https://www.psoriasis.org/advance/fda-approves-xeljanz-psoriatic-arthritis.

19. National Psoriasis Foundation. FDA approves Taltz for psoriatic arthritis. 2017. URL: https://www.psoriasis.org/advance/fda-approves-taltz-psoriatic-arthritis.

20. Cohen SB, Tanaka Y, Mariette X, Curtis JR, Lee EB, Nash P, et al. Long-term safety of tofacitinib for the treatment of rheumatoid arthritis up to 8.5 years: integrated analysis of data from the global clinical trials. Ann Rheum Dis 2017;76:1253–62.

21. Strand V, Ahadieh S, French J, Geier J, Krishnaswami S, Menon S, et al. Systematic review and meta-analysis of serious infections with tofacitinib and biologic disease-modifying antirheumatic drug treatment in rheumatoid arthritis clinical trials. Arthritis Res Ther 2015;17:362.

22. Kuo CM, Tung TH, Wang SH, Chi CC. Efficacy and safety of tofacitinib for moderate-to-severe plaque psoriasis: a systematic review and meta-analysis of randomized controlled trials. J Eur Acad Dermatol Venereol 2018;32:355–62.

23. Singh JA, Saag KG, Bridges SL Jr, Akl EA, Bannuru RR, Sullivan MC, et al. 2015 American College of Rheumatology guideline for the treatment of rheumatoid arthritis. Arthritis Care Res (Hoboken) 2016;68:1–25.

24. Singh JA, Saag KG, Bridges SL Jr, Akl EA, Bannuru RR, Sullivan MC, et al. 2015 American College of Rheumatology guideline for the treatment of rheumatoid arthritis. Arthritis Rheumatol 2016;68:1–26.

25. Feldman SR. A quantitative definition of severe psoriasis for use in clinical trials. J Dermatolog Treat 2004;15:27–9.

26. Guyatt GH, Oxman AD, Kunz R, Atkins D, Brozek J, Vist G, et al. GRADE guidelines: 2. Framing the question and deciding on important outcomes. J Clin Epidemiol 2011;64:395–400.

27. European Medicines Agency. Guideline on clinical investigation of medicinal products for the treatment of psoriatic arthritis. 2006. URL: http://www.ema.europa.eu/docs/en_GB/document_library/Scientific_guideline/2009/09/WC500003413.pdf.

28. Jaeschke R, Guyatt GH, Dellinger P, Schunemann H, Levy MM, Kunz R, et al. Use of GRADE grid to reach decisions on clinical practice guidelines when consensus is elusive. BMJ 2008;337:a744.

29. Saag KG, Teng GG, Patkar NM, Anuntiyo J, Finney C, Curtis JR, et al. American College of Rheumatology 2008 recommendations for the use of nonbiologic and biologic disease-modifying antirheumatic drugs in rheumatoid arthritis. Arthritis Rheum 2008;59:762–84.

30. Singh JA, Furst DE, Bharat A, Curtis JR, Kavanaugh AF, Kremer JM, et al. 2012 update of the 2008 American College of Rheumatology recommendations for the use of disease-modifying antirheumatic drugs and biologic agents in the treatment of rheumatoid arthritis. Arthritis Care Res (Hoboken) 2012;64:625–39.

31. Neumann A, Akl E, Vandvik P, Agoritsas T, Alonso-Coello P, Rind D, et al. How to use a patient management recommendation: clinical practice guidelines and decision analyses. Users' guides to the medical literature: a manual for evidence-based clinical practice. New York (NY): McGraw-Hill; 2014.

32. Neumann I, Santesso N, Akl EA, Rind DM, Vandvik PO, Alonso-Coello P, et al. A guide for health professionals to interpret and use recommendations in guidelines developed with the GRADE approach. J Clin Epidemiol 2016;72:45–55.

33. Yun H, Xie F, Delzell E, Levitan EB, Chen L, Lewis JD, et al. Comparative risk of hospitalized infection associated with biologic agents in rheumatoid arthritis patients enrolled in Medicare. Arthritis Rheumatol 2016;68:56–66.

34. Favalli EG, Selmi C, Becciolini A, Biggioggero M, Ariani A, Santilli D, et al. Eight-year retention rate of first-line tumor necrosis factor inhibitors in spondyloarthritis: a multicenter retrospective analysis. Arthritis Care Res (Hoboken) 2017;69:867–74.

35. Ward MM, Deodhar A, Akl EA, Lui A, Ermann J, Gensler LS, et al. American College of Rheumatology/Spondylitis Association of America/Spondyloarthritis Research and Treatment Network 2015 recommendations for the treatment of ankylosing spondylitis and nonradiographic axial spondyloarthritis. Arthritis Rheumatol 2016;68:282–98.

36. Janssen Research & Development, LLC, sponsor. An efficacy and safety study of ustekinumab in participants with active non-radiographic axial spondyloarthritis. ClinicalTrials.gov identifier: NCT02407223; 2017.

37. Janssen Research & Development, LLC, sponsor. A study to evaluate the efficacy and safety of ustekinumab in the treatment of anti-TNFα naive participants with active radiographic axial spondyloarthritis. ClinicalTrials.gov identifier: NCT02437162; 2018.

38. Janssen Research & Development, LLC, sponsor. A study to evaluate the efficacy and safety of ustekinumab in the treatment of anti-TNFα refractory participants with active radiographic axial spondyloarthritis. ClinicalTrials.gov identifier: NCT02438787; 2018.

39. Maybury CM, Jabbar-Lopez ZK, Wong T, Dhillon AP, Barker JN, Smith CH. Methotrexate and liver fibrosis in people with psoriasis: a systematic review of observational studies. Br J Dermatol 2014;171:17–29.

40. Miele L, Vallone S, Cefalo C, La Torre G, Di Stasi C, Vecchio FM, et al. Prevalence, characteristics and severity of non-alcoholic fatty liver disease in patients with chronic plaque psoriasis. J Hepatol 2009;51:778–86.

41. Centers for Disease Control and Prevention. Recommended immunization schedules for adults aged 19 years or older. URL: https://www.cdc.gov/vaccines/schedules/hcp/adult.html.

42. Critchley J, Capewell S. Smoking cessation for the secondary prevention of coronary heart disease. Cochrane Database Syst Rev 2004:CD003041.

43. Critchley JA, Capewell S. Mortality risk reduction associated with smoking cessation in patients with coronary heart disease: a systematic review. JAMA 2003;290:86–97.

44. Taylor G, McNeill A, Girling A, Farley A, Lindson-Hawley N, Aveyard P. Change in mental health after smoking cessation: systematic review and meta-analysis. BMJ 2014;348:g1151.

45. Coates LC, Fransen J, Helliwell PS. Defining minimal disease activity in psoriatic arthritis: a proposed objective target for treatment. Ann Rheum Dis 2010;69:48–53.

46. Schoels MM, Aletaha D, Alasti F, Smolen JS. Disease activity in psoriatic arthritis (PsA): defining remission and treatment success using the DAPSA score. Ann Rheum Dis 2016;75:811–8.

47. Coates LC, Kavanaugh A, Mease PJ, Soriano ER, Acosta-Felquer ML, Armstrong AW, et al. Group for Research and Assessment of Psoriasis and Psoriatic Arthritis 2015 treatment recommendations for psoriatic arthritis. Arthritis Rheumatol 2016;68:1060–71.

48. Gossec L, Smolen JS, Ramiro S, de Wit M, Cutolo M, Dougados M, et al. European League Against Rheumatism (EULAR) recommendations for the management of psoriatic arthritis with pharmacological therapies: 2015 update. Ann Rheum Dis 2016;75:499–510.

49. Cohen BL, Sachar DB. Update on anti-tumor necrosis factor agents and other new drugs for inflammatory bowel disease. BMJ 2017;357:j2505.

50. Hueber W, Sands BE, Lewitzky S, Vandemeulebroecke M, Reinisch W, Higgins PD, et al. Secukinumab, a human anti-IL-17A monoclonal antibody, for moderate to severe Crohn's disease: unexpected results of a randomised, double-blind placebo-controlled trial. Gut 2012;61:1693–700.

51. Balshem H, Helfand M, Schunemann HJ, Oxman AD, Kunz R, Brozek J, et al. GRADE guidelines: 3. Rating the quality of evidence. J Clin Epidemiol 2011;64:401–6.

52. Mease PJ, Gladman DD, Samad AS, Coates LC, Liu LX, Aras GA, et al. Design and rationale of the Study of Etanercept and Methotrexate in Combination or as Monotherapy in Subjects with Psoriatic Arthritis (SEAM-PsA). RMD Open 2018;4:e000606.

53. Baranauskaite A, Raffayova H, Kungurov NV, Kubanova A, Venalis A, Helmle L, et al. Infliximab plus methotrexate is superior to methotrexate alone in the treatment of psoriatic arthritis in methotrexate-naive patients: the RESPOND study. Ann Rheum Dis 2012;71:541–8.

54. Heiberg MS, Kaufmann C, Rodevand E, Mikkelsen K, Koldingsnes W, Mowinckel P, et al. The comparative effectiveness of anti-TNF therapy and methotrexate in patients with psoriatic arthritis: 6 month results from a longitudinal, observational, multicentre study. Ann Rheum Dis 2007;66:1038–42.

55. Eder L, Thavaneswaran A, Chandran V, Gladman DD. Tumour necrosis factor α blockers are more effective than methotrexate in the inhibition of radiographic joint damage progression among patients with psoriatic arthritis. Ann Rheum Dis 2014;73:1007–11.

56. Barker J, Hoffmann M, Wozel G, Ortonne JP, Zheng H, van Hoogstraten H, et al. Efficacy and safety of infliximab vs. methotrexate in patients with moderate-to-severe plaque psoriasis: results of an open-label, active-controlled, randomized trial (RESTORE1). Br J Dermatol 2011;165:1109–17.

57. Saurat JH, Stingl G, Dubertret L, Papp K, Langley RG, Ortonne JP, et al. Efficacy and safety results from the randomized controlled comparative study of adalimumab vs. methotrexate vs. placebo in patients with psoriasis (CHAMPION). Br J Dermatol 2008;158:558–66.

58. Kingsley GH, Kowalczyk A, Taylor H, Ibrahim F, Packham JC, McHugh NJ, et al. A randomized placebo-controlled trial of methotrexate in psoriatic arthritis. Rheumatology (Oxford) 2012;51:1368–77.

59. Gupta AK, Grober JS, Hamilton TA, Ellis CN, Siegel MT, Voorhees JJ, et al. Sulfasalazine therapy for psoriatic arthritis: a double blind, placebo controlled trial. J Rheumatol 1995;22:894–8.

60. Combe B, Goupille P, Kuntz JL, Tebib J, Liote F, Bregeon C. Sulphasalazine in psoriatic arthritis: a randomized, multicentre, placebo-controlled study. Br J Rheumatol 1996;35:664–8.

61. Farr M, Kitas GD, Waterhouse L, Jubb R, Felix-Davies D, Bacon PA. Sulphasalazine in psoriatic arthritis: a double-blind placebo-controlled study. Br J Rheumatol 1990;29:46–9.

62. Mease PJ, Gladman DD, Ritchlin CT, Ruderman EM, Steinfeld SD, Choy EH, et al. Adalimumab for the treatment of patients with moderately to severely active psoriatic arthritis: results of a double-blind, randomized, placebo-controlled trial. Arthritis Rheum 2005;52:3279–89.

63. Gladman DD, Mease PJ, Cifaldi MA, Perdok RJ, Sasso E, Medich J. Adalimumab improves joint-related and skin-related functional impairment in patients with psoriatic arthritis: patient-reported outcomes of the Adalimumab Effectiveness in Psoriatic Arthritis Trial. Ann Rheum Dis 2007;66:163–8.

64. Mease PJ, Kivitz AJ, Burch FX, Siegel EL, Cohen SB, Ory P, et al. Etanercept treatment of psoriatic arthritis: safety, efficacy, and effect on disease progression. Arthritis Rheum 2004;50:2264–72.

65. Mease PJ, Woolley JM, Singh A, Tsuji W, Dunn M, Chiou CF. Patient-reported outcomes in a randomized trial of etanercept in psoriatic arthritis. J Rheumatol 2010;37:1221–7.

66. Mease PJ, Goffe BS, Metz J, VanderStoep A, Finck B, Burge DJ. Etanercept in the treatment of psoriatic arthritis and psoriasis: a randomised trial. Lancet 2000;356:385–90.

67. Abu-Shakra M, Gladman DD, Thorne JC, Long J, Gough J, Farewell VT. Longterm methotrexate therapy in psoriatic arthritis: clinical and radiological outcome. J Rheumatol 1995;22:241–5.

68. Pariser DM, Bagel J, Gelfand JM, Korman NJ, Ritchlin CT, Strober BE, et al. National Psoriasis Foundation clinical consensus on disease severity. Arch Dermatol 2007;143:239–42.

69. Karanikolas GN, Koukli EM, Katsalira A, Arida A, Petrou D, Komninou E, et al. Adalimumab or cyclosporine as monotherapy and in combination in severe psoriatic arthritis: results from a prospective 12-month nonrandomized unblinded clinical trial. J Rheumatol 2011;38:2466–74.

70. Bachelez H, van de Kerkhof PC, Strohal R, Kubanov A, Valenzuela F, Lee JH, et al. Tofacitinib versus etanercept or placebo in moderate-to-severe chronic plaque psoriasis: a phase 3 randomised non-inferiority trial. Lancet 2015;386:552–61.

71. Reich K, Gooderham M, Green L, Bewley A, Zhang Z, Khanskaya I, et al. The efficacy and safety of apremilast, etanercept and placebo in patients with moderate-to-severe plaque psoriasis: 52-week results from a phase IIIb, randomized, placebo-controlled trial (LIBERATE). J Eur Acad Dermatol Venereol 2017;31:507–17.

72. Mease PJ, Fleischmann R, Deodhar AA, Wollenhaupt J, Khraishi M, Kielar D, et al. Effect of certolizumab pegol on signs and symptoms in patients with psoriatic arthritis: 24-week results of a phase 3 double-blind randomised placebo-controlled study (RAPID-PsA). Ann Rheum Dis 2014;73:48–55.

73. Gladman D, Fleischmann R, Coteur G, Woltering F, Mease PJ. Effect of certolizumab pegol on multiple facets of psoriatic arthritis as reported by patients: 24-week patient-reported outcome results of a phase III, multicenter study. Arthritis Care Res (Hoboken) 2014;66:1085–92.

74. Genovese MC, Mease PJ, Thomson GT, Kivitz AJ, Perdok RJ, Weinberg MA, et al. Safety and efficacy of adalimumab in treatment of patients with psoriatic arthritis who had failed disease modifying antirheumatic drug therapy. J Rheumatol 2007;34:1040–50.

75. Antoni C, Krueger GG, de Vlam K, Birbara C, Beutler A, Guzzo C, et al. Infliximab improves signs and symptoms of psoriatic arthritis: results of the IMPACT 2 trial. Ann Rheum Dis 2005;64:1150–7.

76. Kavanaugh A, McInnes I, Mease P, Krueger GG, Gladman D, Gomez-Reino J, et al. Golimumab, a new human tumor necrosis factor α antibody, administered every four weeks as a subcutaneous injection in psoriatic arthritis: twenty-four–week efficacy and safety results of a randomized, placebo-controlled study. Arthritis Rheum 2009;60:976–86.

77. Antoni CE, Kavanaugh A, Kirkham B, Tutuncu Z, Burmester GR, Schneider U, et al. Sustained benefits of infliximab therapy for dermatologic and articular manifestations of psoriatic arthritis: results from the infliximab multinational psoriatic arthritis controlled trial (IMPACT). Arthritis Rheum 2005;52:1227–36.

78. Torii H, Nakagawa H, Japanese Infliximab Study Investigators. Infliximab monotherapy in Japanese patients with moderate-to-severe plaque psoriasis and psoriatic arthritis: a randomized, double-blind, placebo-controlled multicenter trial. J Dermatol Sci 2010;59:40–9.

79. Nash P, Thaci D, Behrens F, Falk F, Kaltwasser JP. Leflunomide improves psoriasis in patients with psoriatic arthritis: an in-depth analysis of data from the TOPAS study. Dermatology 2006;212:238–49.

80. Kaltwasser JP, Nash P, Gladman D, Rosen CF, Behrens F, Jones P, et al. Efficacy and safety of leflunomide in the treatment of psoriatic arthritis and psoriasis: a multinational, double-blind, randomized, placebo-controlled clinical trial. Arthritis Rheum 2004;50:1939–50.

81. Strand V, Schett G, Hu C, Stevens RM. Patient-reported health-related quality of life with apremilast for psoriatic arthritis: a phase II, randomized, controlled study. J Rheumatol 2013;40:1158–65.

82. Schett G, Wollenhaupt J, Papp K, Joos R, Rodrigues JF, Vessey AR, et al. Oral apremilast in the treatment of active psoriatic arthritis: results of a multicenter, randomized, double-blind, placebo-controlled study. Arthritis Rheum 2012;64:3156–67.

83. Edwards CJ, Blanco FJ, Crowley J, Birbara CA, Jaworski J, Aelion J, et al. Apremilast, an oral phosphodiesterase 4 inhibitor, in patients with psoriatic arthritis and current skin involvement: a phase III, randomised, controlled trial (PALACE 3). Ann Rheum Dis 2016;75:1065–73.

84. Cutolo M, Myerson GE, Fleischmann RM, Liote F, Diaz-Gonzalez F, Van den Bosch F, et al. A phase III, randomized, controlled trial of apremilast in patients with psoriatic arthritis: results of the PALACE 2 Trial. J Rheumatol 2016;43:1724–34.

85. Kavanaugh A, Mease PJ, Gomez-Reino JJ, Adebajo AO, Wollenhaupt J, Gladman DD, et al. Longterm (52-week) results of a phase III randomized, controlled trial of apremilast in patients with psoriatic arthritis. J Rheumatol 2015;42:479–88.

86. Kavanaugh A, Mease PJ, Gomez-Reino JJ, Adebajo AO, Wollenhaupt J, Gladman DD, et al. Treatment of psoriatic arthritis in a phase 3 randomised, placebo-controlled trial with apremilast, an oral phosphodiesterase 4 inhibitor. Ann Rheum Dis 2014;73:1020–6.

87. Gottlieb AB, Langley RG, Philipp S, Sigurgeirsson B, Blauvelt A, Martin R, et al. Secukinumab improves physical function in subjects with plaque psoriasis and psoriatic arthritis: results from two randomized, phase 3 trials. J Drugs Dermatol 2015;14:821–33.

88. Langley RG, Elewski BE, Lebwohl M, Reich K, Griffiths CE, Papp K, et al. Secukinumab in plaque psoriasis—results of two phase 3 trials. N Engl J Med 2014;371:326–38.

89. Mease PJ, van der Heijde D, Ritchlin CT, Okada M, Cuchacovich RS, Shuler CL, et al. Ixekizumab, an interleukin-17A specific monoclonal antibody, for the treatment of biologic-naive patients with active psoriatic arthritis: results from the 24-week randomised, double-blind, placebo-controlled and active (adalimumab)-controlled period of the phase III trial SPIRIT-P1. Ann Rheum Dis 2017;76:79–87.

90. McInnes IB, Mease PJ, Kirkham B, Kavanaugh A, Ritchlin CT, Rahman P, et al. Secukinumab, a human anti-interleukin-17A monoclonal antibody, in patients with psoriatic arthritis (FUTURE 2): a randomised, double-blind, placebo-controlled, phase 3 trial. Lancet 2015;386:1137–46.

91. McInnes IB, Sieper J, Braun J, Emery P, van der Heijde D, Isaacs JD, et al. Efficacy and safety of secukinumab, a fully human anti-interleukin-17A monoclonal antibody, in patients with moderate-to-severe psoriatic arthritis: a 24-week, randomized, double-blind, placebo-controlled, phase II proof-of-concept trial. Ann Rheum Dis 2014;73:349–56.

92. Mease PJ, McInnes IB, Kirkham B, Kavanaugh A, Rahman P, van der Heijde D, et al. Secukinumab inhibition of interleukin-17A in patients with psoriatic arthritis. N Engl J Med 2015;373:1329–39.

93. Mease PJ, Genovese MC, Greenwald MW, Ritchlin CT, Beaulieu AD, Deodhar A, et al. Brodalumab, an anti-IL17RA monoclonal antibody, in psoriatic arthritis. N Engl J Med 2014;370:2295–306.

94. Nakagawa H, Niiro H, Ootaki K, Japanese Brodalumab Study Group. Brodalumab, a human anti-interleukin-17-receptor antibody in the treatment of Japanese patients with moderate-to-severe plaque psoriasis: efficacy and safety results from a phase II randomized controlled study. J Dermatol Sci 2016;81:44–52.

95. Papp K, Menter A, Strober B, Kricorian G, Thompson EH, Milmont CE, et al. Efficacy and safety of brodalumab in subpopulations of patients with difficult-to-treat moderate-to-severe plaque psoriasis. J Am Acad Dermatol 2015;72:436–9.

96. Griffiths CE, Reich K, Lebwohl M, van de Kerkhof P, Paul C, Menter A, et al. Comparison of ixekizumab with etanercept or placebo in moderate-to-severe psoriasis (UNCOVER-2 and UNCOVER-3): results from two phase 3 randomised trials. Lancet 2015;386:541–51.

97. Rungapiromnan W, Yiu ZZN, Warren RB, Griffiths CE, Ashcroft DM. Impact of biologic therapies on risk of major adverse cardiovascular events in patients with psoriasis: systematic review and meta-analysis of randomized controlled trials. Br J Dermatol 2017;176:890–901.

98. McInnes IB, Kavanaugh A, Gottlieb AB, Puig L, Rahman P, Ritchlin C, et al. Efficacy and safety of ustekinumab in patients with active psoriatic arthritis: 1 year results of the phase 3, multicentre, double-blind, placebo-controlled PSUMMIT 1 trial. Lancet 2013;382:780–9.

99. Gottlieb A, Menter A, Mendelsohn A, Shen YK, Li S, Guzzo C, et al. Ustekinumab, a human interleukin 12/23 monoclonal antibody, for psoriatic arthritis: randomised, double-blind, placebo-controlled, crossover trial. Lancet 2009;373:633–40.

100. Ritchlin C, Rahman P, Kavanaugh A, McInnes IB, Puig L, Li S, et al. Efficacy and safety of the anti-IL-12/23 p40 monoclonal antibody, ustekinumab, in patients with active psoriatic arthritis despite conventional non-biological and biological anti-tumour necrosis factor therapy: 6-month and 1-year results of the phase 3, multicentre, double-blind, placebo-controlled, randomised PSUMMIT 2 trial. Ann Rheum Dis 2014;73:990–9.

101. Griffiths CE, Strober BE, van de Kerkhof P, Ho V, Fidelus-Gort R, Yeilding N, et al. Comparison of ustekinumab and etanercept for moderate-to-severe psoriasis. N Engl J Med 2010;362:118–28.

102. Gupta AK, Daigle D, Lyons DC. Network meta-analysis of treatments for chronic plaque psoriasis in Canada. J Cutan Med Surg 2014;18:371–8.

103. Mease P, Genovese MC, Gladstein G, Kivitz AJ, Ritchlin C, Tak PP, et al. Abatacept in the treatment of patients with psoriatic arthritis: results of a six-month, multicenter, randomized, double-blind, placebo-controlled, phase II trial. Arthritis Rheum 2011;63:939–48.

104. Mease PJ, Gottlieb AB, van der Heijde D, FitzGerald O, Johnsen A, Nys M, et al. Efficacy and safety of abatacept, a T-cell modulator, in a randomised, double-blind, placebo-controlled, phase III study in psoriatic arthritis. Ann Rheum Dis 2017;76:1550–8.

105. Menter MA, Papp KA, Cather J, Leonardi C, Pariser DM, Krueger JG, et al. Efficacy of tofacitinib for the treatment of moderate-to-severe chronic plaque psoriasis in patient subgroups from two randomised Phase 3 trials. J Drugs Dermatol 2016;15:568–80.

106. Lebwohl M, Strober B, Menter A, Gordon K, Weglowska J, Puig L, et al. Phase 3 studies comparing brodalumab with ustekinumab in psoriasis. N Engl J Med 2015;373:1318–28.

107. Thaci D, Blauvelt A, Reich K, Tsai TF, Vanaclocha F, Kingo K, et al. Secukinumab is superior to ustekinumab in clearing skin of subjects with moderate to severe plaque psoriasis: CLEAR, a randomized controlled trial. J Am Acad Dermatol 2015;73:400–9.

108. Fraser AD, van Kuijk AW, Westhovens R, Karim Z, Wakefield R, Gerards AH, et al. A randomised, double blind, placebo controlled, multicentre trial of combination therapy with methotrexate plus ciclosporin in patients with active psoriatic arthritis. Ann Rheum Dis 2005;64:859–64.

109. Combe B, Behrens F, McHugh N, Brock F, Kerkmann U, Kola B, et al. Comparison of etanercept monotherapy and combination therapy with methotrexate in psoriatic arthritis: results from 2 clinical trials. J Rheumatol 2016;43:1063–7.

110. Zachariae C, Mork NJ, Reunala T, Lorentzen H, Falk E, Karvonen SL, et al. The combination of etanercept and methotrexate increases the effectiveness of treatment in active psoriasis despite inadequate effect of methotrexate therapy. Acta Derm Venereol 2008;88:495–501.

111. Fagerli KM, Lie E, van der Heijde D, Heiberg MS, Lexberg AS, Rodevand E, et al. The role of methotrexate co-medication in TNF-inhibitor treatment in patients with psoriatic arthritis: results from 440 patients included in the NOR-DMARD study. Ann Rheum Dis 2014;73:132–7.

112. Nash P, Kirkham B, Okada M, Rahman P, Combe B, Burmester GR, et al. Ixekizumab for the treatment of patients with active psoriatic arthritis and an inadequate response to tumour necrosis factor inhibitors: results from the 24-week randomised, double-blind, placebo-controlled period of the SPIRIT-P2 phase 3 trial. Lancet 2017;389:2317–27.

113. Coates LC, Moverley AR, McParland L, Brown S, Navarro-Coy N, O'Dwyer JL, et al. Effect of tight control of inflammation in early psoriatic arthritis (TICOPA): a UK multicentre, open-label, randomised controlled trial. Lancet 2015;386:2489–98.

114. Narula N, Marshall JK, Colombel JF, Leontiadis GI, Williams JG, Muqtadir Z, et al. Systematic review and meta-analysis: infliximab or cyclosporine as rescue therapy in patients with severe ulcerative colitis refractory to steroids. Am J Gastroenterol 2016;111:477–91.

115. Stidham RW, Lee TC, Higgins PD, Deshpande AR, Sussman DA, Singal AG, et al. Systematic review with network meta-analysis: the efficacy of anti-TNF agents for the treatment of Crohn's disease. Aliment Pharmacol Ther 2014;39:1349–62.

116. Stidham RW, Lee TC, Higgins PD, Deshpande AR, Sussman DA, Singal AG, et al. Systematic review with network meta-analysis: the efficacy of anti-tumour necrosis factor-α agents for the treatment of ulcerative colitis. Aliment Pharmacol Ther 2014;39:660–71.

117. Sandborn WJ, Hanauer SB, Katz S, Safdi M, Wolf DG, Baerg RD, et al. Etanercept for active Crohn's disease: a randomized, double-blind, placebo-controlled trial. Gastroenterology 2001;121:1088–94.

118. Rosenberg P, Urwitz H, Johannesson A, Ros AM, Lindholm J, Kinnman N, et al. Psoriasis patients with diabetes type 2 are at high risk of developing liver fibrosis during methotrexate treatment. J Hepatol 2007;46:1111–8.

119. Malatjalian DA, Ross JB, Williams CN, Colwell SJ, Eastwood BJ. Methotrexate hepatotoxicity in psoriatics: report of 104 patients from Nova Scotia, with analysis of risks from obesity, diabetes and alcohol consumption during long term follow-up. Can J Gastroenterol 1996;10:369–75.

120. US Food and Drug Administration. FDA drug safety communication: drug labels for the tumor necrosis factor-α (TNFα) blockers now include warnings about infection with Legionella and Listeria bacteria. 2011. URL: https://www.fda.gov/Drugs/DrugSafety/ucm270849.htm.

121. Kivitz AJ, Schechtman J, Texter M, Fichtner A, de Longueville M, Chartash EK. Vaccine responses in patients with rheumatoid arthritis treated with certolizumab pegol: results from a single-blind randomized phase IV trial. J Rheumatol 2014;41:648–57.

122. Franca IL, Ribeiro AC, Aikawa NE, Saad CG, Moraes JC, Goldstein-Schainberg C, et al. TNF blockers show distinct patterns of immune response to the pandemic influenza A H1N1 vaccine in inflammatory arthritis patients. Rheumatology (Oxford) 2012;51:2091–8.

123. Elkayam O, Bashkin A, Mandelboim M, Litinsky I, Comaheshter D, Levartovsky D, et al. The effect of infliximab and timing of vaccination on the humoral response to influenza vaccination in patients with rheumatoid arthritis and ankylosing spondylitis. Semin Arthritis Rheum 2010;39:442–7.

124. Kaine JL, Kivitz AJ, Birbara C, Luo AY. Immune responses following administration of influenza and pneumococcal vaccines to patients with rheumatoid arthritis receiving adalimumab. J Rheumatol 2007;34:272–9.

125. Ribeiro AC, Laurindo IM, Guedes LK, Saad CG, Moraes JC, Silva CA, et al. Abatacept and reduced immune response to pandemic 2009 influenza A/H1N1 vaccination in patients with rheumatoid arthritis. Arthritis Care Res (Hoboken) 2013;65:476–80.

126. Migita K, Akeda Y, Akazawa M, Tohma S, Hirano F, Ideguchi H, et al. Effect of abatacept on the immunogenicity of 23-valent pneumococcal polysaccharide vaccination (PPSV23) in rheumatoid arthritis patients. Arthritis Res Ther 2015;17:357.

127. Zhang J, Xie F, Delzell E, Chen L, Winthrop KL, Lewis JD, et al. Association between vaccination for herpes zoster and risk of herpes zoster infection among older patients with selected immune-mediated diseases. JAMA 2012;308:43–9.

128. Baillet A, Zeboulon N, Gossec L, Combescure C, Bodin LA, Juvin R, et al. Efficacy of cardiorespiratory aerobic exercise in rheumatoid arthritis: meta-analysis of randomized controlled trials. Arthritis Care Res (Hoboken) 2010;62:984–92.

129. Knittle K, Maes S, de Gucht V. Psychological interventions for rheumatoid arthritis: examining the role of self-regulation with a systematic review and meta-analysis of randomized controlled trials. Arthritis Care Res (Hoboken) 2010;62:1460–72.

130. Siegel S, Tencza M, Apodaca B, Poole J. Effectiveness of occupational therapy interventions for adults with rheumatoid arthritis: a systematic review. Am J Occup Ther 2017;71:1–11.

131. Di Minno MN, Peluso R, Iervolino S, Russolillo A, Lupoli R, Scarpa R, et al. Weight loss and achievement of minimal disease activity in patients with psoriatic arthritis starting treatment with tumour necrosis factor α blockers. Ann Rheum Dis 2014;73:1157–62.

132. Gisondi P, Del Giglio M, Di Francesco V, Zamboni M, Girolomoni G. Weight loss improves the response of obese patients with moderate-to-severe chronic plaque psoriasis to low-dose cyclosporine therapy: a randomized, controlled, investigator-blinded clinical trial. Am J Clin Nutr 2008;88:1242–7.

133. Al-Mutairi N, Nour T. The effect of weight reduction on treatment outcomes in obese patients with psoriasis on biologic therapy: a randomized controlled prospective trial. Expert Opin Biol Ther 2014;14:749–56.

134. Nelson L, Churilla J. Massage therapy for pain and function in patients with arthritis: a systematic review of randomized controlled trials. Am J Phys Med Rehabil 2017;96:665–72.

135. Manyanga T, Froese M, Zarychanski R, Abou-Setta A, Friesen C, Tennenhouse M, et al. Pain management with acupuncture in osteoarthritis: a systematic review and meta-analysis. BMC Complement Altern Med 2014;14:312.

136. Anthonisen NR, Skeans MA, Wise RA, Manfreda J, Kanner RE, Connett JE, et al. The effects of a smoking cessation intervention on 14.5-year mortality: a randomized clinical trial. Ann Intern Med 2005;142:233–9.

137. Mons U, Muezzinler A, Gellert C, Schottker B, Abnet CC, Bobak M, et al. Impact of smoking and smoking cessation on cardiovascular events and mortality among older adults: meta-analysis of individual participant data from prospective cohort studies of the CHANCES consortium. BMJ 2015;350:h1551.

AMERICAN COLLEGE
OF RHEUMATOLOGY
EDUCATION · TREATMENT · RESEARCH

REVIEW

Nervous System Disease in Systemic Lupus Erythematosus: Current Status and Future Directions

John G. Hanly,[1] Elizabeth Kozora,[2] Steven D. Beyea,[3] and Julius Birnbaum[4]

The American College of Rheumatology's case definitions for 19 neuropsychiatric syndromes in systemic lupus erythematosus (SLE) constitute a comprehensive classification of nervous system events in this disease. However, additional strategies are needed to determine whether a neuropsychiatric syndrome is attributable to SLE versus a competing comorbidity. Cognitive function is a clinical surrogate of overall brain health, with applications in both diagnosis and determination of clinical outcomes. Ischemic and inflammatory mechanisms are both key components of the immunopathogenesis of neuropsychiatric SLE (NPSLE), including abnormalities of the blood–brain barrier and autoantibody-mediated production of proinflammatory cytokines. Advances in neuroimaging provide a platform to assess novel disease mechanisms in a noninvasive way. The convergence of more rigorous clinical characterization, validation of biomarkers, and brain neuroimaging provides opportunities to determine the efficacy of novel targeted therapies in the treatment of NPSLE.

Introduction

Neurologic and psychiatric (NP) features of systemic lupus erythematosus (SLE), collectively referred to as neuropsychiatric SLE (NPSLE), are serious but incompletely understood manifestations of SLE. In this review we first discuss what is currently known about the classification and attribution of clinical NP events in SLE patients, the key immunopathogenetic mechanisms involved, the role of currently available neuroimaging techniques, and the standard of care in NPSLE. We then propose ways to advance knowledge through future research in NPSLE, including work on biomarkers, advanced neuroimaging, and clinical outcomes with new therapies (Table 1).

Current status of NPSLE

Classification and attribution of nervous system disease in SLE. The 1999 American College of Rheumatology (ACR) case definitions (1) for 19 NP syndromes (12 central nervous system events and 7 peripheral nervous system events) constitute a widely adopted classification of NPSLE (Figure 1). One of the challenges of such a comprehensive classification of NP events is to determine their attribution to SLE or other causes. To address this, the Systemic Lupus International Collaborating Clinics (SLICC) developed rules for use in prospective studies of NP disease in the SLICC inception cohort. Factors taken into account included 1) the interval between diagnosis of SLE and onset of NP events (i.e., the longer the NP event preceded the diagnosis of SLE, the lower the likelihood of causality), 2) concurrent non-SLE factors (i.e., identification of potential causes or contributing factors for each NP syndrome in the glossary accompanying the ACR case definitions) (1), and 3) the high frequency of some NP events in the general population (2) (i.e., making it impossible to correctly attribute these events); thus, isolated headaches, anxiety, mild depression (including mood disorders not meeting criteria for "major depressive-like episodes"), mild cognitive impairment (deficits in <3 of 8 specified cognitive domains), and polyneuropathy without electrophysiologic confirmation were not attributed to SLE (1). Using this approach (3), the proportion of NP events attributed to SLE varies

Table 1. Research goals and strategies in NPSLE*

Topic	Research goals	Strategies
NP events	Identify NP events associated with SLE Determine correct attribution of NP events to SLE and other causes	Update and revision of ACR case definitions for NP events in SLE Improvement of current attribution models through multidisciplinary, international collaborative research
Clinical outcomes for NP events	Develop response criteria for use in clinical trials of NPSLE	Use of longitudinal observational SLE cohorts to derive and validate response criteria
Pathogenesis of NPSLE	Advance knowledge on pathogenesis of NPSLE	Collaborative research involving animal models and human SLE to determine novel pathogenic mechanisms and potential therapeutic targets; includes studies on brain tissue, CSF, and peripheral blood
Diagnosis of NPSLE	Enhance diagnostic testing	Studies of novel neuroimaging techniques and candidate biomarkers in serum and CSF from well-characterized clinical cohorts
Treatment	Expand and test current and novel therapies	Clinical trials of NPSLE to determine efficacy/tolerability of symptomatic, immunosuppressive, and biologic therapies

*NPSLE = neuropsychiatric systemic lupus erythematosus; ACR = American College of Rheumatology; CSF = cerebrospinal fluid.

between 19% and 38% and affects 6–12% of newly diagnosed SLE patients in the first year of disease (4). Although the cumulative frequency of NP events increases over time in SLE patients, the proportionate attribution remains constant.

In a recent study (5), a fourth component was added to the SLICC attribution model called "favoring factors", which refers to variables that support the attribution of an NP event to SLE, derived from the European League Against Rheumatism recommendations on NPSLE (6) and an expert panel. Weights were assigned to variables of the 4 components, generating a score between 0 and 10, with a higher score indicating a greater likelihood that the NP event is attributed to SLE. Using physician determination of attribution as the comparator, the optimal cutoff score was ≥7, with a sensitivity of 87.9% and specificity of 82.6%. The addition of this fourth component increases the ability to distinguish when an NP syndrome is attributable to SLE versus a competing comorbidity.

NP events are associated with a significant negative impact on patient-reported health-related quality of life (HRQoL), regardless of attribution and adjusting for global SLE disease activity, cumulative organ damage, and medications (3,7). Thus, all NP events are of clinical significance, but the treatment pathway is dependent on the correct attribution.

Cognitive dysfunction in SLE. Notwithstanding the range of NP events in SLE, neurocognitive disorders may be considered
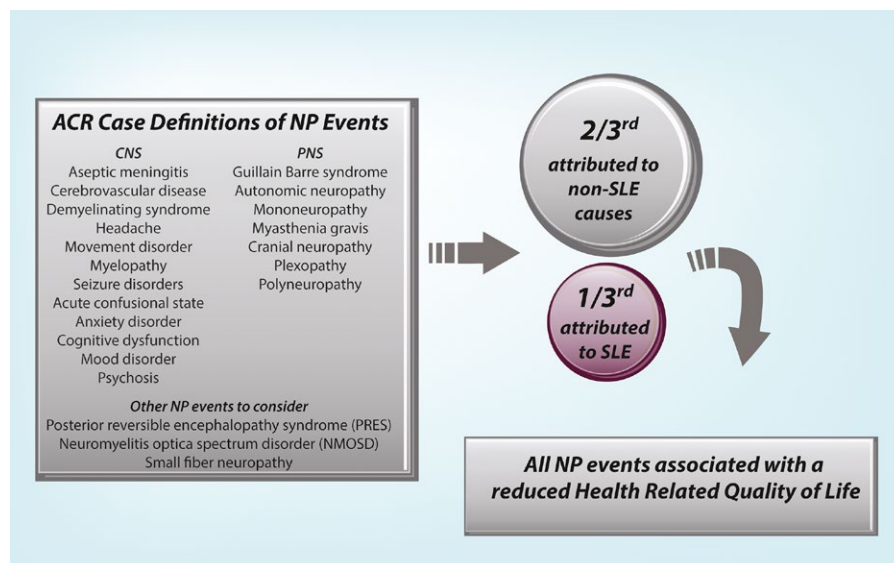
Figure 1. Nervous system events included in the American College of Rheumatology (ACR) case definitions for 12 central nervous system (CNS) manifestations and 7 peripheral nervous system (PNS) manifestations in systemic lupus erythematosus (SLE). Other neuropsychiatric (NP) manifestations that should be considered in a future revision of the ACR case definitions include posterior reversible encephalopathy syndrome, neuromyelitis optica spectrum disorder, and small-fiber neuropathy. In SLE patients, the majority of these NP events are attributed to non-SLE causes, but regardless of attribution all NP events are associated with a negative impact on health-related quality of life. Color figure can be viewed in the online issue, which is available at http://onlinelibrary.wiley.com/doi/10.1002/art.40591/abstract.

a distinct subset of NPSLE as well as a surrogate of overall brain function. Self-report measures of perceived cognitive impairment are poorly correlated with objective assessment in SLE patients (8) and are associated with concurrent anxiety, depression, and fibromyalgia. Screening measures include the Montreal Cognitive Assessment Scale (9) and computerized testing that permits efficient assessment by nonexperts, but they may fail to identify higher-level cognitive impairment (10). Thus, clinical suspicion of cognitive impairment merits formal neuropsychological testing, which is currently the most reliable and objective diagnostic approach. The ACR battery of neuropsychological tests (1) provides the recommended minimal guideline for evaluation.

The broad range of reported prevalence rates of cognitive dysfunction (14–88%) in SLE patients is due to differences in the disease spectrum of patients under study, the selection of neurocognitive tests, and the definition of impairment. More than 50% of SLE patients with overt NP disease, such as strokes and seizures, have cognitive impairment. Approximately 30% of SLE patients have isolated cognitive deficits that affect attention, memory, executive function, and processing speed. Longitudinal studies have identified fluctuating test performance, indicating evanescent cognitive dysfunction rather than persistent or progressive disease (11). Non-SLE causes of cognitive dysfunction include prior neurodevelopmental issues (e.g., learning disability, head injury), pain, mood disorders, fatigue, and medications.

Pathogenesis of NPSLE: collusion of ischemic and inflammatory mechanisms. There are complementary pathogenic pathways that align with different NPSLE manifestations (12) (Figure 2). Ischemic injury to large- and small-caliber vessels by antiphospholipid antibodies (aPL), immune complexes, and complement activation leads to focal NP events (e.g., stroke) and diffuse NP events (e.g., cognitive dysfunction). In addition, inflammation-mediated injury with increased permeability of the blood–brain barrier, intrathecal autoantibodies and immune complexes, and production of interferon-α (IFNα) and other inflammatory mediators lead to diffuse NP manifestations, such as psychosis, acute confusion, and cognitive dysfunction (12). Autoantibodies play key roles in mediating both ischemic and inflammatory disease mechanisms.

Multifocal small and large brain infarcts, consistent neuropathologic features in NPSLE (13), are frequently caused by aPL-mediated thrombosis. This acquired procoagulant state has traditionally been considered noninflammatory. However, recent evidence implicates complement activation (14) in association with focal NPSLE, psychosis, and cognitive dysfunction, suggesting an added inflammatory pathogenic component. Mice deficient in C3 and C5 components of complement are resistant to aPL-induced thrombosis and endothelial activation (15). In 31% of cases, patients with NPSLE have histopathologic deposition of classical and terminal complement components on the luminal surface of intracerebral vessels and cerebral vasculitis (13). Collectively, these data broaden the historical pathogenetic concepts of aPL-induced brain injury and identify potential therapeutic targets in NPSLE.

The blood–brain barrier provides a structural and functional interface between the brain and the circulation at the capillary level; by regulating the influx of required nutrients and efflux of toxic products, the barrier secures brain homeostasis. It is pivotal to the integrity of the neurovascular unit of pericytes, end-feet of astrocytes, and neuronal axon termini that transmit regulatory signals to the capillary endothelium. Disruption of the blood–brain barrier is associated with neurologic disorders including Alzheim-
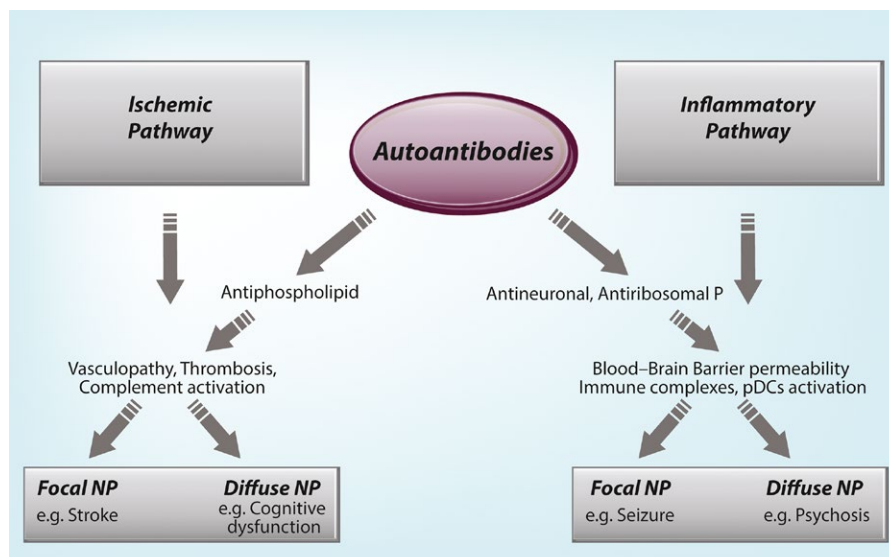
Figure 2. Summary of disease mechanisms contributing to neuropsychiatric (NP) systemic lupus erythematosus clinical events. Autoantibodies are primary drivers of the ischemic and inflammatory pathogenic pathways. pDCs = plasmacytoid dendritic cells. Color figure can be viewed in the online issue, which is available at http://onlinelibrary.wiley.com/doi/10.1002/art.40591/abstract.

er's disease, multiple sclerosis, and stroke. In SLE, enhanced blood–brain barrier permeability may result from autoantibody and immune complexes binding to the endothelial surface (16), complement activation (17), and cytokines such as TWEAK (18). Resident in the blood–brain barrier, matrix metalloproteinases (MMPs) are proteolytic enzymes which can degrade basement membranes, disrupt inter-endothelial tight junctions, and activate membrane-bound proinflammatory molecules. Blood–brain barrier disruption can also be mediated by non-SLE factors such as smoking, serious infection, and hypertension. In animal models of SLE, enhanced blood–brain barrier permeability is critical for autoantibodies to access neuronal tissue (19,20), with subsequent neuronal binding and apoptosis (21). In human studies of NPSLE, the detection of some autoantibodies in the cerebrospinal fluid (CSF) correlates with concurrent NP events (22).

Initial studies of cytokines in NPSLE indicated associations of elevated CSF interleukin-6 (IL-6) levels with seizures, and IFNα with lupus psychosis. Subsequently, further evidence of increased intrathecal IL-6 and other cytokines such as IL-10, IL-2, and IL-8 emerged (23). The sources of cytokines include neuronal, glial, and infiltrating immunocompetent cells (23). Autoantibodies (24) and RNA-protein antigens in CSF form immune complexes and initiate a proinflammatory cascade. First they bind Fcγ receptor II on plasmacytoid dendritic cells, followed by endocytosis, activation of endosomal Toll-like receptor 7, and downstream production of IFNα. Proinflammatory cytokines are also produced by blood–brain barrier endothelium following surface binding of anti–NR2 glutamate receptor (16) and anti-P antibodies (25). Another potentially important mediator may be calcium-binding protein S100ß, which is produced mainly by astrocytes. In low levels S100ß is neurotrophic, but overproduction by activated glial cells leads to loss of neuronal cells and increased permeability of the blood–brain barrier (26).

Many SLE patients have increased production of type I IFN proteins. A study in lupus-prone mice (27) identified a novel mechanism for NPSLE that is IFNα-dependent. Synaptic pruning, whereby activated brain microglial cells ingest synaptic terminals, is responsible for sculpting neuronal circuits during brain development. This also occurs in neurodegenerative diseases and possibly in SLE (27). Lupus-prone mice had lower synaptic density in association with increased synaptic pruning by activated microglial cells. This was prevented by blocking IFN signaling. In the same study, brain tissue from 4 of 6 patients with NPSLE showed increased IFN signaling in microglia and other cell types, compared to controls. These insights identify potential therapeutic targets for NPSLE, including pathogenic autoantibodies, select proinflammatory cytokines, and regulators of the blood–brain barrier.

The role of neuroimaging in the diagnosis of NPSLE. Conventional neuroimaging noninvasively localizes intracranial abnormalities, distinguishes white matter disease from gray matter disease, measures cerebral atrophy, and identifies changes in cerebral blood flow and volume. X-ray computed tomography has largely been replaced by magnetic resonance imaging (MRI) because of superior soft tissue contrast, the facility to image multiple anatomic planes, and greater sensitivity to endogenous contrast mechanisms. MRI identifies abnormalities in up to 75% of SLE patients (28,29). However, with the exception of larger cerebral infarcts and hippocampal atrophy (30), the correlation between structural anatomic changes and clinical NP manifestations is poor.

More than 50% of patients with NPSLE events (including acute confusion, psychosis, mood disorders, and headaches) have normal findings in conventional MRI scans (31). Subcortical white matter hyperintensities on T2-weighted imaging occur in 20–50% of SLE patients regardless of clinical NP disease, in up to 75% of SLE patients with aPL syndrome (APS) (32), and in 47% of healthy individuals (33). In an unselected SLE population, the volume of such lesions was associated with age, overall disease severity, and disease duration, rather than NPSLE (34). These abnormalities are regarded as nonspecific. In contrast, gray matter changes have a better correlation with clinical disease and may resolve in 2–3 weeks following an acute NP event (35). Magnetic resonance angiography is not optimal for imaging small-caliber vessels, which are primarily involved in NPSLE.

Given this lack of correlation between clinical and structural abnormalities, imaging modalities that characterize functional properties of the underlying pathology are of interest. Examples include MRI diffusion-weighted imaging (DWI), magnetization transfer imaging (MTI), and radionuclide imaging such as positron emission computed tomography (PET) and single-photon emission tomography (SPECT) (36–38).

MTI measures energy transfer between bound and unbound hydrogen molecules (e.g., between white matter and CSF), and results are expressed as a magnetic transfer ratio (MTR) (36). A decrease in bound molecules (e.g., due to demyelination) or an increase in unbound molecules (e.g., due to edema) can diminish the energy transfer or MTR. Decreased whole-brain MTR, even in the absence of other structural MRI changes, has been reported in SLE (39,40). It is reversible and most likely reflects parenchymal edema (40).

DWI measures changes in stochastic movement of water in the brain. The increase in diffusivity in patients with NPSLE (36), in combination with changes in MTI, may be due to demyelination, cerebral atrophy resulting in an increase in CSF volume, or a combination thereof (36,40). In contrast, cytotoxic edema resulting in intracellular swelling leads to decreased diffusivity and is seen more frequently in the setting of acute stroke. This differs from vasogenic edema consequent to disruption of the blood–brain barrier, which is predominantly extracellular and not associated with restricted diffusion.

PET scanning (37) and SPECT scanning (35) use tailored radiopharmaceuticals and are exquisitely sensitive. PET scanning is the most objective neuroimaging measure of brain function, but access and cost limit its applicability (37). In SLE

patients, SPECT imaging has identified both diffuse and focal deficits, which may be fixed or reversible. The findings are not specific for NPSLE and do not always correlate with clinical NP manifestations. Up to 50% of SLE patients without clinical manifestations of NP disease may have abnormal SPECT results (34), and the significance of these abnormalities is not clear.

In order to overcome the limitations of subjective interpretation, more advanced MRI-based technologies quantify results linked to a physiologic parameter of interest. One example is magnetic resonance spectroscopy, which measures the relative concentration of biochemical compounds within predetermined brain regions. N-acetylaspartate reflects the quantity of neuronal/axonal tissue (28); in NPSLE, it is decreased in structural lesions seen on MRI, as well as in normal-appearing gray and white matter (35). Other neurometabolite abnormalities reported in active NPSLE include increased choline and lactate, indicating inflammation and compromised tissue metabolism, respectively (28).

Diffusion tensor imaging uses DWI data to visualize neural tracts (tractography) and map white matter connections. Abnormalities in NPSLE likely represent demyelination and/or altered network connectivity not seen with conventional MRI sequences (40). Using brain connectivity analysis of diffusion MRI data, reduced nodal efficiency in the brain network was observed in patients with NPSLE, compared to controls (41).

Blood oxygen level–dependent functional MRI (BOLD fMRI) measures local brain deoxyhemoglobin levels, an indirect measure of brain function within gray matter (42). BOLD fMRI data are acquired either in task/stimulus-based paradigms (providing statistical parametric maps linked to a specific function), or in resting-state acquisitions (providing functional connectivity maps of brain networks such as the default mode). Preliminary studies in SLE (43) suggest compensatory adaptation of neuronal function through recruitment of additional cortical pathways. These compensatory responses maintain cognitive function in the short term but may eventually be overcome and manifest as overt cognitive impairment (41). Even SLE patients without clinical NP disease have abnormal fMRI resting-state brain intrinsic connectivity (42), raising the possibility of preclinical detection (44).

Treatment of NP events in SLE patients. Crucial to instituting the correct treatment plan (Figure 3) is determining the attribution of nervous system disease to SLE, non-SLE causes, or both. Comorbid factors such as infection, metabolic abnormalities, and cardiovascular risk factors should be considered. Implementing pharmacologic and nonpharmacologic strategies for pain, stress, anxiety and depression, poor sleep, and high blood pressure is worthwhile. Identification of ischemic and inflammatory disease pathways will guide selection of more specific therapies. Given the paucity of clinical trials in NPSLE, information on treatment and outcomes is derived from observational studies and extrapolated from experience with other organ system disease in SLE and related disorders. Short-term and long-term outcomes of NP events are generally favorable, particularly for NP events attributed to SLE (7,45).

Ischemic pathway therapies. Low-dose aspirin has been suggested for primary prevention of transient ischemic attack and ischemic stroke in SLE patients with aPL (46), but its efficacy is unproven. Secondary prevention of focal NP disease attributed to aPL requires lifelong anticoagulation therapy (47), despite the lack of controlled clinical trials in NPSLE. The
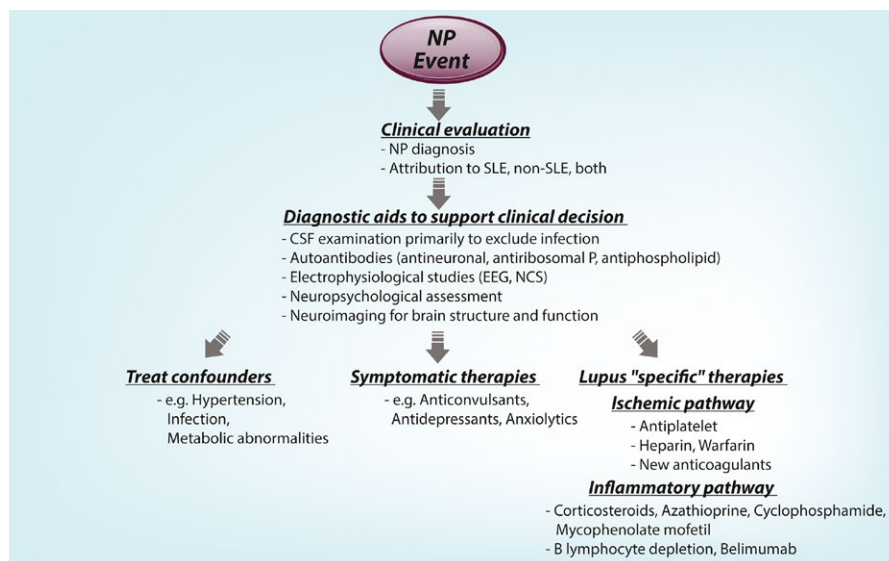
Figure 3. Diagnostic and treatment algorithm for patients with systemic lupus erythematosus (SLE) who present with neuropsychiatric (NP) events. CSF = cerebrospinal fluid; EEG = electroencephalography; NCS = nerve conduction study. Color figure can be viewed in the online issue, which is available at http://onlinelibrary.wiley.com/doi/10.1002/art.40591/abstract.

optimal target international normalized ratio in such cases is controversial, especially in the treatment of arterial events (46). Potential adjunctive therapies, especially in patients with arterial thrombosis and recurrent venous thrombosis while receiving warfarin, are antiplatelet agents, antimalarials, and statins (46).

Inflammatory pathway therapies. Evidence from other neurologic disorders such as vasculitic neuropathies and central nervous system angiitis, and from other organ manifestations of SLE (e.g., lupus nephritis), suggests that immunosuppressive agents would be beneficial in treating NPSLE. High-dose glucocorticoids, alone or in combination with azathioprine, cyclophosphamide, and mycophenolate mofetil, are reported to be effective. Only 2 of these agents have been subjected to controlled clinical trials in NPSLE (48,49), both with positive outcomes. Two observational cohort studies (50,51) showed a lower risk of seizures in SLE patients receiving antimalarial drugs, in addition to reduced brain atrophy and damage, based on MRI data (29). Experience with biologic agents in NPSLE is limited to uncontrolled studies. Off-label use of B cell depletion with rituximab has resulted in favorable outcomes in children (52) and adults (53) with NPSLE. Patients with severe NPSLE were excluded from phase III clinical trials of belimumab.

Historically, glucocorticoids have been a cornerstone in the treatment of serious manifestations of NPSLE, especially in those associated with an inflammatory pathogenic pathway (48,49). Given the evidence linking glucocorticoid use to cumulative organ damage in SLE (54) and the associated negative impact on HRQoL (55), alternative therapeutic strategies are necessary. In addition, glucocorticoids have been implicated as a cause of psychiatric symptoms in 2–60% of individuals (56–58), although it is more likely that this occurs in ~20% of cases (58). Complications of glucocorticoid therapy include affective, behavioral, and cognitive symptoms (59), which can complicate the diagnosis and attribution of NP events in SLE patients. Thus, although the use of glucocorticoids is part of the current standard of care of NPSLE, these observations suggest a therapeutic imperative to limit overall exposure.

Cognitive impairment. Although no clinical trials support antiplatelet or anticoagulant therapy for cognitive dysfunction in SLE, patients with aPL without thromboembolic phenomena had better cognitive performance with aspirin (60). Agents used for cognitive dysfunction in Alzheimer's disease (e.g., cholinesterase inhibitors, memantine) and attention deficit disorder (e.g., methylphenidate) provide alternative treatment strategies, but data on their use in SLE are limited. Memantine, a non-competitive inhibitor of glutamate at the N-methyl-D-aspartate receptor, did not produce significant cognitive improvement in SLE patients (61). Treatment approaches that target behavioral factors may be useful. For example, a psychoeducational group intervention for SLE patients with self-perceived cognitive

dysfunction was associated with improvement in memory, self-efficacy, and other aspects of cognitive function (62). Cognitive dysfunction has also been associated with poor exercise capacity in SLE patients, and an exercise training program may be an inexpensive behavioral approach to improving cognitive abilities (63).

Future studies to address challenges in NPSLE

Classification and attribution of NPSLE. Although a major advance in the field, the ACR classification for NPSLE (1) requires revision and updating. For example, entities such as posterior reversible encephalopathy syndrome and small-fiber neuropathy should be added, and further guidance on determining attribution of individual NP events is required. In addition, establishment of clinical outcome measures and response criteria is necessary to support clinical trials of current and novel therapeutic interventions. This could start with recommending instruments currently used in observational studies, such as physician assessment of NP status, patient-reported HRQoL, and cognitive performance on a standardized battery of neuropsychological tests.

Biomarkers in NPSLE. The identification and validation of biomarkers in peripheral blood and CSF would be valuable in the management of NPSLE. For example, neuron-specific enolase, a neuronal glycolytic enzyme produced mainly by astrocytes, is increased in peripheral blood following acute brain injury but is decreased in chronic disorders such as dementia, multiple sclerosis, and NPSLE. Serum levels of S100ß are increased in adults and children with NPSLE (26). The lack of disease specificity of these biomarkers requires that their use be integrated with a priori decisions about attribution of NP events. The identification of more specific biomarkers of NPSLE is required.

Neuroimaging in NPSLE. Neuroimaging technologies probing new aspects of NPSLE, combinations of multiple imaging modalities, and multidisciplinary research efforts are required. The dynamic susceptibility contrast and dynamic contrast-enhanced (DCE) scanning techniques acquire image time series following the injection of contrast agent. The spatiotemporal pattern of enhancement is a measure of cerebral blood flow and tissue perfusion properties and can determine the rate of perfusion into brain tissue. Such changes are directly linked to alterations in the blood–brain barrier. DCE MRI in a rodent model of NPSLE demonstrated compromised blood–brain barrier (64). These imaging techniques have identified abnormalities in clinical populations in association with mild traumatic brain injury (Figure 4) and thus may be of potential value in patients with NPSLE. Recent advances in MRI-based cellular and molecular imaging (65) could facilitate longitudinal human research studies without the use of ionizing radiation and with the advantage of superior spatial reso-
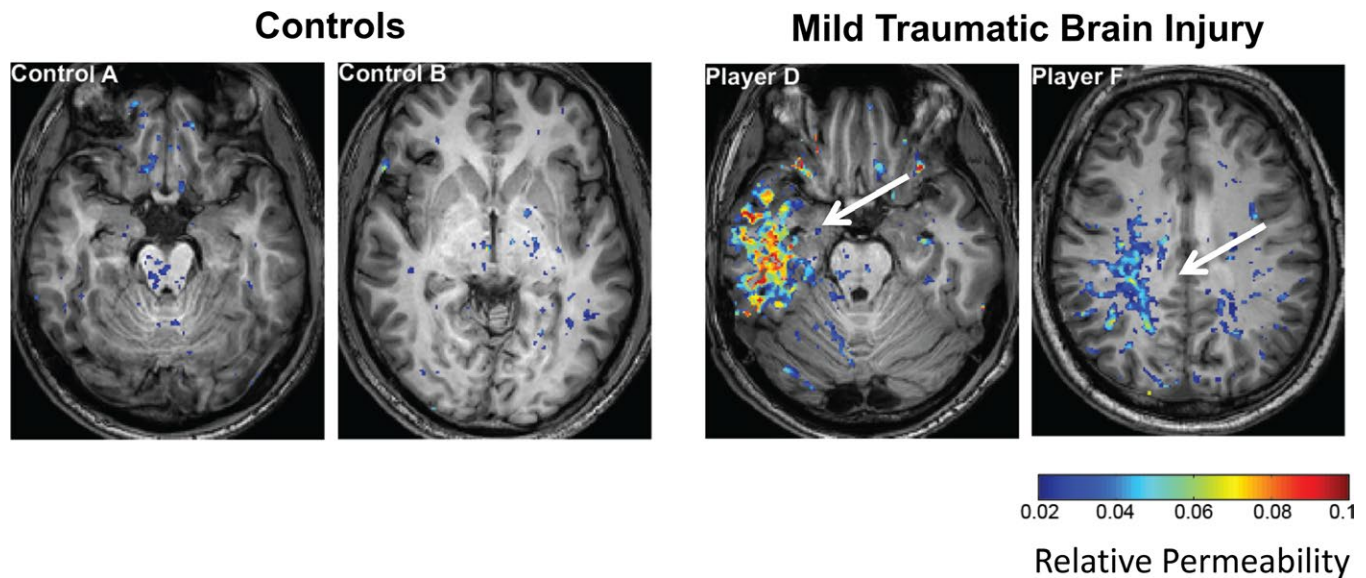
Figure 4. Representative dynamic contrast-enhanced magnetic resonance imaging scans in 2 individuals with mild traumatic brain injury (male amateur football players) and 2 controls (male track and field athletes). Increased focal permeability of the blood–brain barrier is apparent in the scans from those with mild traumatic brain injury (**arrows**) compared to the scans from the controls. Adapted, with permission, from Weissberg I, Veksler R, Kamintsky L, Saar-Ashkenazy R, Milikovsky DZ, Shelef I, et al. Imaging blood-brain barrier dysfunction in football players. JAMA Neurol 2014;71:1453–5.

lution (66). For example, preclinical studies used superparamagnetic iron oxide labeling for in vivo MRI of specific immune cells (67), which is a strategy that could be of interest in NPSLE.

Both electroencephalography (EEG) and resting-state fMRI determine brain network connectivity, but have poor spatial resolution and temporal sampling, respectively. Magnetoencephalography (MEG), the magnetic analog of EEG, produces superior spatial resolution and specificity compared to EEG, as well as superior temporal resolution compared to fMRI (68). Network connectivity studies using MEG spectral analysis exhibit signals that correspond to known functional networks (e.g., beta band measures of the sensorimotor network) (69). MEG is less accessible than MRI and EEG but could be used to study brain network changes in NPSLE.

Critically, future studies should correlate neuroimaging and clinical characterization of NP manifestations, including validated attribution models and detailed cognitive testing. Concurrent measurement of biomarkers in CSF and peripheral blood could link neuroimaging abnormalities with laboratory variables that are relatively inexpensive and rapidly measured. The linking of neuroimaging abnormalities of blood–brain barrier permeability with elevated peripheral blood levels of MMP-9 (70) or S100ß (26) could provide a convenient diagnostic tool and means of stratifying patients for clinical trials. Biomarkers of neuronal loss and reparative astrogliosis have been documented in CSF, and circulating levels of neurofilament light chain subunit (a component of myelinated axons) correlate with vascular (71), degenerative (72), and autoimmune inflammatory (73) brain disease. Enabled by the recent advances in quantitative neuroimaging, future studies will likely benefit from machine learning characterization of multimodal data sets (74), which may improve the accuracy of NPSLE detection.

Treatment of NPSLE. Controlled clinical trials of new therapies in SLE have excluded patients with severe NP manifestations. Although ethical and pragmatic reservations about recruiting patients with acute, life-threatening NP events to clinical trials are appropriate, such events are rare, and patients with other types of NP events could be studied. For example, SLE patients who have less acute NP disease (e.g., mood disorder, selected cerebrovascular disease, or cognitive impairment) would be suitable to participate in a study to determine efficacy and tolerability of symptomatic, anticoagulant, and immunosuppressive therapies. Although mood disorders have been shown to occur in 12.7% of SLE patients (45), no controlled clinical trials have been conducted to determine the optimum pharmacotherapy.

A complementary strategy for operationalizing clinical trials in NPSLE is the use of immunologic variables to stratify patient selection. A possible approach is selecting cases based on CSF autoantibody and cytokine profiles, elevated serum biomarker levels, and/or predefined neuroimaging abnormalities. Specific examples include determining the biologic effect of CSF IgG (a potent inducer of IFNα) (24), measuring anti-NR2 autoantibodies in CSF (associated with active NPSLE) (22), and measuring CSF B lymphocyte stimulator (BLyS) and IFNα levels (elevated in some patients with NPSLE) (23).

Based on NPSLE pathogenesis, there are novel therapeutic strategies worthy of study in combination with the current

standard of care. Interventions to decrease the permeability of the blood–brain barrier in a manner similar to minimizing brain injury following ischemic stroke could be advantageous in NPSLE. This could prevent autoantibodies and non–disease-specific toxins from entering the brain. Inhibiting MMPs that are resident in the blood–brain barrier, especially MMP-9 (75), by enhancing its natural inhibitor or introducing a novel biologic agent could also be beneficial in NPSLE. Two additional compounds that reduce blood–brain barrier permeability (GW0742, a peroxisome proliferator–activated receptor β/δ agonist [76], and KD025, a Rho kinase inhibitor [77]), both of which have been studied in experimental systems, could also be considered as therapies.

Reducing levels of pathogenic autoantibodies is a known strategy in the treatment of SLE. One of the challenges in NPSLE is a lack of clearly defined pathogenic autoantibodies. Although anti-NR2, anti-P, and anti–aquaporin 4 autoantibodies are elegant examples of how such a system may operate, they account for only a minority of NPSLE cases, and other autoantibodies of even greater clinical significance likely await discovery. Experience in the treatment of APS suggests that lowering aPL levels is not associated with a beneficial clinical response. However, the recent evidence implicating complement activation in APS suggests that targeting activation products such as C4d (15) may be beneficial, at least in the acute phase of aPL-mediated NPSLE.

Cytokines present another attractive therapeutic target for NPSLE. Belimumab targets BLyS, but it has not been studied specifically in NPSLE. Inhibition of type I IFNs with anifrolumab, a monoclonal antibody that binds the IFNα/β receptor, is currently in phase III clinical trials for SLE treatment, but patients with severe NPSLE are excluded. It is an attractive target for NPSLE and should be considered pending the outcome of current trials. One of the challenges with both agents is their large immunoglobulin structure that may prevent passage across the blood–brain barrier in sufficient quantity to exert a meaningful biologic effect. A strategy to circumvent this problem includes the use of glutamate, which has been shown experimentally to temporarily enhance permeability of the blood–brain barrier. This has been proposed as a means of improving drug delivery in the treatment of primary malignant brain tumors (78). Alternatively, JAK inhibitors that interfere with the JAK–STAT signaling pathway are small molecules that penetrate the blood–brain barrier (79) and reduce the production of several cytokines, including type I IFNs. Tofacitinib, a JAK1/JAK3 inhibitor, has been approved for use in rheumatoid arthritis and is currently in phase II studies for SLE treatment.

Conclusions

NP events in SLE patients are common, tend to be heterogeneous, and frequently present a diagnostic and therapeutic challenge. The therapies currently available are largely empirical and informed by both known disease mechanisms in NPSLE and effective treatments of other serious organ disease in SLE. Future studies utilizing advances in neuroimaging (28) and biomarkers (80) are necessary to enhance understanding of the immunopathogenetic mechanisms of NPSLE and to guide the design of clinical trials. Innovative strategies targeting the blood–brain barrier, specific autoantibodies, and cytokines are worthy of exploration and study.

AUTHOR CONTRIBUTIONS

All authors were involved in drafting the article or revising it critically for important intellectual content, and all authors approved the final version to be published.

REFERENCES

1. ACR Ad Hoc Committee on Neuropsychiatric Lupus Nomenclature. The American College of Rheumatology nomenclature and case definitions for neuropsychiatric lupus syndromes. Arthritis Rheum 1999;42:599–608.

2. Ainiala H, Hietaharju A, Loukkola J, Peltola J, Korpela M, Metsanoja R, et al. Validity of the new American College of Rheumatology criteria for neuropsychiatric lupus syndromes: a population-based evaluation. Arthritis Rheum 2001;45:419–23.

3. Hanly JG, Urowitz MB, Su L, Sanchez-Guerrero J, Bae SC, Gordon C, et al. Short-term outcome of neuropsychiatric events in systemic lupus erythematosus upon enrollment into an international inception cohort study. Arthritis Rheum 2008;59:721–9.

4. Hanly JG, Urowitz MB, Sanchez-Guerrero J, Bae SC, Gordon C, Wallace DJ, et al. Neuropsychiatric events at the time of diagnosis of systemic lupus erythematosus: an international inception cohort study. Arthritis Rheum 2007;56:265–73.

5. Bortoluzzi A, Scire CA, Bombardieri S, Caniatti L, Conti F, De Vita S, et al. Development and validation of a new algorithm for attribution of neuropsychiatric events in systemic lupus erythematosus. Rheumatology (Oxford) 2015;54:891–8.

6. Bertsias GK, Ioannidis JP, Aringer M, Bollen E, Bombardieri S, Bruce IN, et al. EULAR recommendations for the management of systemic lupus erythematosus with neuropsychiatric manifestations: report of a task force of the EULAR standing committee for clinical affairs. Ann Rheum Dis 2010;69:2074–82.

7. Magro-Checa C, Beaart-van de Voorde LJ, Middelkoop HA, Dane ML, van der Wee NJ, van Buchem MA, et al. Outcomes of neuropsychiatric events in systemic lupus erythematosus based on clinical phenotypes; prospective data from the Leiden NP SLE cohort. Lupus 2017;26:543–51.

8. Hanly JG, Su L, Omisade A, Farewell VT, Fisk JD. Screening for cognitive impairment in systemic lupus erythematosus. J Rheumatol 2012;39:1371–7.

9. Adhikari T, Piatti A, Luggen M. Cognitive dysfunction in SLE: development of a screening tool. Lupus 2011;20:1142–6.

10. Hanly JG, Omisade A, Su L, Farewell V, Fisk JD. Assessment of cognitive function in systemic lupus erythematosus, rheumatoid arthritis, and multiple sclerosis by computerized neuropsychological tests. Arthritis Rheum 2010;62:1478–86.

11. Hanly JG, Cassell K, Fisk JD. Cognitive function in systemic lupus erythematosus: results of a 5-year prospective study. Arthritis Rheum 1997;40:1542–3.

12. Hanly JG. Diagnosis and management of neuropsychiatric SLE. Nat Rev Rheumatol 2014;10:338–47.

13. Cohen D, Rijnink EC, Nabuurs RJ, Steup-Beekman GM, Versluis MJ, Emmer BJ, et al. Brain histopathology in patients with systemic lupus erythematosus: identification of lesions associated with clinical neuropsychiatric lupus syndromes and the role of complement. Rheumatology (Oxford) 2017;56:77–86.

14. Magro-Checa C, Schaarenburg RA, Beaart HJ, Huizinga TW, Steup-Beekman GM, Trouw LA. Complement levels and anti-C1q autoantibodies in patients with neuropsychiatric systemic lupus erythematosus. Lupus 2016;25:878–88.

15. Cohen D, Buurma A, Goemaere NN, Girardi G, le Cessie S, Scherjon S, et al. Classical complement activation as a footprint for murine and human antiphospholipid antibody-induced fetal loss. J Pathol 2011;225:502–11.

16. Yoshio T, Okamoto H, Hirohata S, Minota S. IgG anti-NR2 glutamate receptor autoantibodies from patients with systemic lupus erythematosus activate endothelial cells. Arthritis Rheum 2013;65:457–63.

17. Mahajan SD, Parikh NU, Woodruff TM, Jarvis JN, Lopez M, Hennon T, et al. C5a alters blood-brain barrier integrity in a human in vitro model of systemic lupus erythematosus. Immunology 2015;146:130–43.

18. Wen J, Doerner J, Weidenheim K, Xia Y, Stock A, Michaelson JS, et al. TNF-like weak inducer of apoptosis promotes blood brain barrier disruption and increases neuronal cell death in MRL/lpr mice. J Autoimmun 2015;60:40–50.

19. Kowal C, DeGiorgio LA, Nakaoka T, Hetherington H, Huerta PT, Diamond B, et al. Cognition and immunity: antibody impairs memory. Immunity 2004;21:179–88.

20. Bravo-Zehnder M, Toledo EM, Segovia-Miranda F, Serrano FG, Benito MJ, Metz C, et al. Anti-ribosomal P protein autoantibodies from patients with neuropsychiatric lupus impair memory in mice. Arthritis Rheumatol 2015;67:204–14.

21. Lauvsnes MB, Omdal R. Systemic lupus erythematosus, the brain, and anti-NR2 antibodies. J Neurol 2012;259:622–9.

22. Arinuma Y, Yanagida T, Hirohata S. Association of cerebrospinal fluid anti-NR2 glutamate receptor antibodies with diffuse neuropsychiatric systemic lupus erythematosus. Arthritis Rheum 2008;58:1130–5.

23. Kothur K, Wienholt L, Brilot F, Dale RC. CSF cytokines/chemokines as biomarkers in neuroinflammatory CNS disorders: a systematic review. Cytokine 2016;77:227–37.

24. Santer DM, Yoshio T, Minota S, Moller T, Elkon KB. Potent induction of IFN-α and chemokines by autoantibodies in the cerebrospinal fluid of patients with neuropsychiatric lupus. J Immunol 2009;182:1192–201.

25. Yoshio T, Hirata D, Onda K, Nara H, Minota S. Antiribosomal P protein antibodies in cerebrospinal fluid are associated with neuropsychiatric systemic lupus erythematosus. J Rheumatol 2005;32:34–9.

26. Lapa AT, Postal M, Sinicato NA, Bellini BS, Fernandes PT, Marini R, et al. S100β is associated with cognitive impairment in childhood-onset systemic lupus erythematosus patients. Lupus 2017;26:478–83.

27. Bialas AR, Presumey J, Das A, van der Poel CE, Lapchak PH, Mesin L, et al. Microglia-dependent synapse loss in type I interferon-mediated lupus. Nature 2017;546:539–43.

28. Postal M, Lapa AT, Reis F, Rittner L, Appenzeller S. Magnetic resonance imaging in neuropsychiatric systemic lupus erythematosus: current state of the art and novel approaches. Lupus 2017;26:517–21.

29. Sarbu N, Toledano P, Calvo A, Roura E, Sarbu MI, Espinosa G, et al. Advanced MRI techniques: biomarkers in neuropsychiatric lupus. Lupus 2017;26:510–6.

30. Zimmermann N, Correa DG, Kubo TA, Netto TM, Pereira DB, Fonseca RP, et al. Global cognitive impairment in systemic lupus erythematosus patients: a structural MRI study. Clin Neuroradiol 2017;27:23–9.

31. Al-Obaidi M, Saunders D, Brown S, Ramsden L, Martin N, Moraitis E, et al. Evaluation of magnetic resonance imaging abnormalities in juvenile onset neuropsychiatric systemic lupus erythematosus. Clin Rheumatol 2016;35:2449–56.

32. Van Swieten JC, van den Hout JH, van Ketel BA, Hijdra A, Wokke JH, van Gijn J. Periventricular lesions in the white matter on magnetic resonance imaging in the elderly: a morphometric correlation with arteriolosclerosis and dilated perivascular spaces. Brain 1991;114:761–74.

33. Schmidt R, Fazekas F, Kleinert G, Offenbacher H, Gindl K, Payer F, et al. Magnetic resonance imaging signal hyperintensities in the deep and subcortical white matter: a comparative study between stroke patients and normal volunteers. Arch Neurol 1992;49:825–7.

34. Sibbitt WL Jr, Jung RE, Brooks WM. Neuropsychiatric systemic lupus erythematosus. Compr Ther 1999;25:198–208.

35. Sibbitt WL Jr, Sibbitt RR, Brooks WM. Neuroimaging in neuropsychiatric systemic lupus erythematosus. Arthritis Rheum 1999;42:2026–38.

36. Bosma GP, Steens SC, Petropoulos H, Admiraal-Behloul F, van den Haak A, Doornbos J, et al. Multisequence magnetic resonance imaging study of neuropsychiatric systemic lupus erythematosus. Arthritis Rheum 2004;50:3195–202.

37. Curiel R, Akin EA, Beaulieu G, DePalma L, Hashefi M. PET/CT imaging in systemic lupus erythematosus. Ann N Y Acad Sci 2011;1228:71–80.

38. Netto TM, Zimmermann N, Rueda-Lopes F, Bizzo BC, Fonseca RP, Gasparetto EL. Neuropsychiatric lupus: classification criteria in neuroimaging studies. Can J Neurol Sci 2013;40:284–91.

39. Magro-Checa C, Ercan E, Wolterbeek R, Emmer B, van der Wee NJ, Middelkoop HA, et al. Changes in white matter microstructure suggest inflammatory origin of neuropsychiatric systemic lupus erythematosus. Arthritis Rheumatol 2016;68:1945–54.

40. Ercan E, Ingo C, Tritanon O, Magro-Checa C, Smith A, Smith S, et al. A multimodal MRI approach to identify and characterize microstructural brain changes in neuropsychiatric systemic lupus erythematosus. Neuroimage Clin 2015;8:337–44.

41. Xu M, Tan X, Zhang X, Guo Y, Mei Y, Feng Q, et al. Alterations of white matter structural networks in patients with non-neuropsychiatric systemic lupus erythematosus identified by probabilistic tractography and connectivity-based analyses. Neuroimage Clin 2017;13:349–60.

42. Niu C, Tan X, Liu X, Han K, Niu M, Xu J, et al. Cortical thickness reductions associate with abnormal resting-state functional connectivity in non-neuropsychiatric systemic lupus erythematosus. Brain Imaging Behav 2018;12:674–84.

43. Barraclough M, Elliott R, McKie S, Parker B, Bruce IN. Cognitive dysfunction and functional magnetic resonance imaging in systemic lupus erythematosus. Lupus 2015;24:1239–47.

44. Papadaki EZ, Boumpas DT. Non-conventional MRI techniques in neuropsychiatric systemic lupus erythematosis (NPSLE): emerging tools to elucidate the pathophysiology and aid the diagnosis and management. In: Bright P, editor. Neuroimaging: clinical applications. London: IntechOpen Limited; 2012. p. 441–66.

45. Hanly JG, Su L, Urowitz MB, Romero-Diaz J, Gordon C, Bae SC, et al. Mood disorders in systemic lupus erythematosus: results from an international inception cohort study. Arthritis Rheumatol 2015;67:1837–47.

46. De Amorim LC, Maia FM, Rodrigues CE. Stroke in systemic lupus erythematosus and antiphospholipid syndrome: risk factors, clinical manifestations, neuroimaging, and treatment. Lupus 2017;26:529–36.

47. Hanly JG. The nervous system and lupus. In: Lahita RG, editor. Systemic lupus erythematosus. 5th ed. Cambridge (MA): Academic Press; 2011. p. 727–46.

48. Barile-Fabris L, Ariza-Andraca R, Olguin-Ortega L, Jara LJ, Fraga-Mouret A, Miranda-Limon JM, et al. Controlled clinical trial of IV cyclophosphamide versus IV methylprednisolone in severe neurological manifestations in systemic lupus erythematosus. Ann Rheum Dis 2005;64:620–5.

49. Denburg SD, Carbotte RM, Denburg JA. Corticosteroids and neuropsychological functioning in patients with systemic lupus erythematosus. Arthritis Rheum 1994;37:1311–20.

50. Andrade RM, Alarcon GS, Gonzalez LA, Fernandez M, Apte M, Vila LM, et al. Seizures in patients with systemic lupus erythematosus: data from LUMINA, a multiethnic cohort (LUMINA LIV). Ann Rheum Dis 2008;67:829–34.

51. Hanly JG, Urowitz MB, Su L, Gordon C, Bae SC, Sanchez-Guerrero J, et al. Seizure disorders in systemic lupus erythematosus results from an international, prospective, inception cohort study. Ann Rheum Dis 2012;71:1502–9.

52. Dale RC, Brilot F, Duffy LV, Twilt M, Waldman AT, Narula S, et al. Utility and safety of rituximab in pediatric autoimmune and inflammatory CNS disease. Neurology 2014;83:142–50.

53. Narvaez J, Rios-Rodriguez V, de la Fuente D, Estrada P, Lopez-Vives L, Gomez-Vaquero C, et al. Rituximab therapy in refractory neuropsychiatric lupus: current clinical evidence. Semin Arthritis Rheum 2011;41:364–72.

54. Ruiz-Arruza I, Lozano J, Cabezas-Rodriguez I, Medina JA, Ugarte A, Erdozain JG, et al. Restrictive use of oral glucocorticoids in systemic lupus erythematosus and prevention of damage without worsening long-term disease control: an observational study. Arthritis Care Res (Hoboken) 2018;70:582–91.

55. Legge A, Doucette S, Hanly JG. Predictors of organ damage progression and effect on health-related quality of life in systemic lupus erythematosus. J Rheumatol 2016;43:1050–6.

56. Bolanos SH, Khan DA, Hanczyc M, Bauer MS, Dhanani N, Brown ES. Assessment of mood states in patients receiving long-term corticosteroid therapy and in controls with patient-rated and clinician-rated scales. Ann Allergy Asthma Immunol 2004;92:500–5.

57. Lewis DA, Smith RE. Steroid-induced psychiatric syndromes: a report of 14 cases and a review of the literature. J Affect Disord 1983;5:319–32.

58. The Boston Collaborative Drug Surveillance Program. Acute adverse reactions to prednisone in relation to dosage. Clin Pharmacol Ther 1972;13:694–8.

59. Dubovsky AN, Arvikar S, Stern TA, Axelrod L. The neuropsychiatric complications of glucocorticoid use: steroid psychosis revisited. Psychosomatics 2012;53:103–15.

60. McLaurin EY, Holliday SL, Williams P, Brey RL. Predictors of cognitive dysfunction in patients with systemic lupus erythematosus. Neurology 2005;64:297–303.

61. Petri M, Naqibuddin M, Sampedro M, Omdal R, Carson KA. Memantine in systemic lupus erythematosus: a randomized, double-blind placebo-controlled trial. Semin Arthritis Rheum 2011;41:194–202.

62. Harrison MJ, Morris KA, Horton R, Toglia J, Barsky J, Chait S, et al. Results of intervention for lupus patients with self-perceived cognitive difficulties. Neurology 2005;65:1325–7.

63. Kozora E, Zell J, Swigris J, Strand M, Duggan EC, Burleson A, et al. Cardiopulmonary correlates of cognition in systemic lupus erythematosus. Lupus 2015;24:164–73.

64. Wagshul ME, Fleysher R, Stock A, Branch CA, Putterman C. Dynamic contrast enhancement in a mouse model of neuropsychiatric systemic lupus erythematosus. Proc Intl Soc Magn Reson Med 2013;21:2861.

65. Neuwelt A, Sidhu N, Hu CA, Mlady G, Eberhardt SC, Sillerud LO. Iron-based superparamagnetic nanoparticle contrast agents for MRI of infection and inflammation. AJR Am J Roentgenol 2015;204:W302–13.

66. Hammoud DA. Molecular imaging of inflammation: current status. J Nucl Med 2016;57:1161–5.

67. American Association for Cancer Research. Abstract: evaluating immunotherapy effects using preclinical molecular imaging tools for quantitative immune cell tracking. 2017. URL: http://cancerres.aacr-journals.org/content/77/13_Supplement/873.

68. Stam CJ. Use of magnetoencephalography (MEG) to study functional brain networks in neurodegenerative disorders. J Neurol Sci 2010;289:128–34.

69. Brookes MJ, Woolrich M, Luckhoo H, Price D, Hale JR, Stephenson MC, et al. Investigating the electrophysiological basis of resting state networks using magnetoencephalography. Proc Natl Acad Sci U S A 2011;108:16783–8.

70. Avolio C, Filippi M, Tortorella C, Rocca MA, Ruggieri M, Agosta F, et al. Serum MMP-9/TIMP-1 and MMP-2/TIMP-2 ratios in multiple sclerosis: relationships with different magnetic resonance imaging measures of disease activity during IFN-β-1a treatment. Mult Scler 2005;11:441–6.

71. Traenka C, Disanto G, Seiffge DJ, Gensicke H, Hert L, Grond-Ginsbach C, et al. Serum neurofilament light chain levels are associated with clinical characteristics and outcome in patients with cervical artery dissection. Cerebrovasc Dis 2015;40:222–7.

72. Rojas JC, Karydas A, Bang J, Tsai RM, Blennow K, Liman V, et al. Plasma neurofilament light chain predicts progression in progressive supranuclear palsy. Ann Clin Transl Neurol 2016;3:216–25.

73. Piehl F, Kockum I, Khademi M, Blennow K, Lycke J, Zetterberg H, et al. Plasma neurofilament light chain levels in patients with MS switching from injectable therapies to fingolimod. Mult Scler 2018;24:1046–54.

74. Wang S, Summers RM. Machine learning and radiology. Med Image Anal 2012;16:933–51.

75. Trysberg E, Blennow K, Zachrisson O, Tarkowski A. Intrathecal levels of matrix metalloproteinases in systemic lupus erythematosus with central nervous system engagement. Arthritis Res Ther 2004;6:R551–6.

76. Chehaibi K, le Maire L, Bradoni S, Escola JC, Blanco-Vaca F, Slimane MN. Effect of PPAR-β/δ agonist GW0742 treatment in the acute phase response and blood-brain barrier permeability following brain injury. Transl Res 2017;182:27–48.

77. Niego B, Lee N, Larsson P, De Silva TM, Au AE, McCutcheon F, et al. Selective inhibition of brain endothelial Rho-kinase-2 provides optimal protection of an in vitro blood-brain barrier from tissue-type plasminogen activator and plasmin. PLoS One 2017;12:e0177332.

78. Vazana U, Veksler R, Pell GS, Prager O, Fassler M, Chassidim Y, et al. Glutamate-mediated blood-brain barrier opening: implications for neuroprotection and drug delivery. J Neurosci 2016;36:7727–39.

79. Fukuyama T, Tschernig T, Qi Y, Volmer DA, Baumer W. Aggression behaviour induced by oral administration of the Janus-kinase inhibitor tofacitinib, but not oclacitinib, under stressful conditions. Eur J Pharmacol 2015;764:278–82.

80. Van der Meulen PM, Barendregt AM, Cuadrado E, Magro-Checa C, Steup-Beekman GM, Schonenberg-Meinema D, et al. Protein array autoantibody profiles to determine diagnostic markers for neuropsychiatric systemic lupus erythematosus. Rheumatology (Oxford) 2017;56:1407–16.

AMERICAN COLLEGE
OF RHEUMATOLOGY
EDUCATION · TREATMENT · RESEARCH

BRIEF REPORT

Influence of Disease Activity in Rheumatoid Arthritis on Radiographic Progression of Concomitant Interphalangeal Joint Osteoarthritis

Christian A. Lechtenboehmer,[1] (iD) Veronika K. Jaeger,[1] Diego Kyburz,[1] (iD) Ulrich A. Walker,[1] and Thomas Hügle[2]

Objective. Distal interphalangeal (DIP) joints are commonly considered to be unaffected by rheumatoid arthritis (RA). Despite synovitis and bone marrow edema being associated with radiographic progression in hand osteoarthritis (OA) and hand RA, radiographic courses differ substantially. This study was undertaken to analyze incidence and progression of radiographically evident DIP joint OA in RA patients, in relation to RA activity and patient characteristics.

Methods. In sequential radiographs of 1,988 RA patients in the Swiss Clinical Quality Management in Rheumatic Diseases registry, we evaluated and scored 15,904 DIP joints. Scoring was based on the presence of central erosions and subchondral sclerosis and on the severity of osteophytes and joint space narrowing, according to the modified Kellgren/Lawrence (K/L) grade. The presence of DIP joint OA was defined as ≥1 joint with a K/L grade of ≥2, and progression was defined as an increase in a summed K/L grade. Adjusted odds ratios (ORs) and 95% confidence intervals (95% CIs) were calculated.

Results. The median follow-up time was 4.5 years (interquartile range 3.1–7.0), and the mean ± SD age was 56.1 ± 11.1 years. DIP joint OA was present in 60% of patients at baseline. Higher mean age (OR 1.09 [95% CI 1.08–1.10]), female sex (OR 1.37 [95% CI 1.08–1.74]), and higher mean body mass index (OR 1.03 [95% CI 1.00–1.06]) were associated with the presence of DIP joint OA, but neither the presence of anti–citrullinated protein antibodies (ACPAs) (OR 0.72 [95% CI 0.50–1.03]) nor the presence of rheumatoid factor (OR 1.01 [95% CI 0.74–1.38]) were associated with it. Disease Activity Score using the erythrocyte sedimentation rate and metacarpophalangeal (MCP) joint erosions were not associated with DIP joint OA progression. RA disease duration had no relevant effect size associated with DIP joint OA progression (OR 0.97 [95% CI 0.96–0.99]).

Conclusion. Known risk factors for DIP joint OA were replicated in patients with RA. The observation that RA activity, the presence of ACPA, and MCP joint erosions were not associated with the prevalence or progression of DIP joint OA indicates that there are distinct roles of inflammation in the pathogenesis of RA and DIP joint OA.

INTRODUCTION

Distal interphalangeal (DIP) joint osteoarthritis (OA) is one of the most common articular diseases in elderly populations (1). DIP joints can be affected by psoriatic arthritis but are considered to be unaffected by rheumatoid arthritis (RA). The radiographic course differs between joints affected by DIP joint OA and those affected by RA, as there are fewer erosions in DIP joint OA and, unlike in RA, it is characteristically associated with new bone formation (2). Furthermore, joints affected by RA typically exhibit progressive erosive destruction, whereas erosive episodes of OA of the hand are followed by phases of bone remodeling (3). Similar to findings in RA, bone marrow edema and synovitis are also associated with the radiographic progression

of hand OA (4), indicating that inflammation may participate in its pathogenesis. However, antiinflammatory biologics such as tumor necrosis factor inhibitors or interleukin-1 inhibitors have demonstrated only minimal effectiveness in treating DIP joint OA (5,6). Thus, the role of inflammation on osseous changes in OA of the hand remains unclear. The influence of an active underlying inflammatory disorder, such as RA, on DIP joint OA has not been systematically studied. The present study was conducted to cross-sectionally characterize the prevalence of DIP joint OA in patients with concomitant RA and to assess the influence of RA's inflammatory activity on the radiographic incidence and progression of DIP joint OA.

PATIENTS AND METHODS

Ethics approval. Ethics approval was obtained from all of the respective local ethics committees. All study patients provided informed written consent.

Study population. We analyzed patients who were clinically diagnosed as having RA by their rheumatologist and who were monitored via the Swiss Clinical Quality Management in Rheumatic Diseases (SCQM) registry. The SCQM is a national, multicenter registry collecting patient information and clinical data longitudinally; it acquires radiographic images from enrolled patients at regular intervals (7). Patients were included in our study if they had 8 radiographically scorable joints (DIP joints 2–5 bilaterally) and ≥2 subsequent hand radiographs obtained in an interval of ≥2 years apart. Radiographs were obtained between November 1983 and October 2014.

Radiographic assessment. A trained radiology resident (CAL), blinded with regard to patient data, assessed conventional posteroanterior hand radiographs from each patient, with known time order. Before scoring patient images, the resident analyzed 100 radiographs as a training set. The Osteoarthritis Research Society International (OARSI) atlas (8) was used as the standard for interpreting DIP joint OA. DIP joints were scored for the severity of osteophytes (range 0–3), joint space narrowing (range 0–3), the presence of subchondral sclerosis, and central erosions, to assign the modified Kellgren/Lawrence (K/L) grade (grades 0–4) (9).

Following an initial assessment of 7,499 hand radiographs from 2,870 RA patients, the radiographs were rescored in the same order, in groups of 200 images and with an average of 60 patients, until the prespecified intrarater reliability of Cohen's kappa coefficient (defined as κ ≥0.70) was reached, taking into account repeated measures at the patient level. This cutoff was exceeded after 800 radiographs, and the reevaluated scores were used for the final analysis. In the final 200 rescored radiographs, kappa values were recorded as follows: K/L grade 0.90, osteophyte severity 0.77, joint space narrowing 0.83,

subchondral sclerosis 0.91, and central erosions 0.92. The percentage of erosive joint surface destruction (in 10% increments) of bilateral metacarpophalangeal (MCP) joints 2–5 (with an unknown chronology) was assessed by the SCQM Foundation using a similar scoring method to that described by Rau et al (10). For this analysis, percentages of erosive joint surface destruction in all 8 MCP joints were summed (range 0–800%) and categorized. The intraclass correlation coefficient was 0.98.

The presence of DIP joint OA was defined as ≥1 joint with a K/L grade of ≥2; K/L grade 1 was not rated as OA for further analyses. In patients without DIP joint OA at baseline, incident OA was defined as the development of a K/L grade of ≥2 in ≥1 DIP joint during follow-up. In patients with DIP joint OA at baseline, progression was defined as an increase in the summed K/L grade of all 8 DIP joints by ≥1 point, between baseline and the latest follow-up radiograph. The smallest detectable change recorded was a K/L grade of 0.13, and the kappa value of the reliability of change was 0.84.

Statistical analysis. Frequencies and percentages were calculated for categorical variables, and means/SDs or medians/interquartile ranges (IQRs) were calculated for continuous variables. Between-group comparisons were carried out using chi-square tests, Student's t-tests, or Wilcoxon-Mann-Whitney tests. Multiple logistic regression analyses were applied, including potentially confounding variables defined a priori, such as age, sex, body mass index (BMI), anti–citrullinated protein antibodies (ACPAs), rheumatoid factor (RF), erythrocyte sedimentation rate (ESR), tender joints, swollen joints, patient assessments of their general health, RA duration, and MCP erosions. Follow-up time and the severity of DIP joint OA at baseline were included in the DIP joint OA progression analysis. Additionally, instead of analyzing RA activity in terms of the individual components within the Disease Activity Score in 28 joints using ESR (DAS28-ESR) (11), we included DAS28-ESR scores in the multiple logistic regression models (see Supplementary Tables 1–3, available on the *Arthritis & Rheumatology* web site at http://onlinelibrary.wiley.com/doi/10.1002/art.40684/abstract). Missing baseline values were imputed using multiple imputation with chained equations ($m = 50$) under a missing-at-random assumption. All multiple regression analyses were based on the imputed data. All analyses were performed using Stata/IC 13.1 software.

RESULTS

Patient characteristics. The mean age of the study population was 56.1 ± 11.1 years, 76% of patients were female, and the median duration of RA was 6.1 years (IQR 2.2–13.1). The 2010 American College of Rheumatology and European League Against Rheumatism (ACR/EULAR) classification criteria for RA

Table 1. Baseline characteristics of and multivariable logistic regression analysis for RA patients without DIP joint OA versus RA patients with DIP joint OA*

	No DIP joint OA (n = 789)	DIP joint OA (n = 1,199)	P	Adjusted OR (95% CI)	Adjusted P
Clinical and demographic characteristics					
Fulfill 2010 ACR/EULAR criteria for RA, % of patients	80	81	–	–	–
Age, mean ± SD years	50.4 ± 10.0	59.9 ± 10.1	<0.001	1.09 (1.08–1.10)	<0.001
Female, % of patients	75	77	0.20	1.37 (1.08–1.74)	0.010
BMI, mean ± SD kg/m²	24.8 ± 4.6	25.7 ± 4.7	<0.001	1.03 (1.00–1.06)	0.025
Laboratory parameters					
ACPA+, % of patients	73	65	0.010	0.72 (0.50–1.03)	0.070
RF+, % of patients	79	77	0.21	1.01 (0.74–1.38)	0.96
ESR, median (IQR) mm/hour	16 (8–30)	18 (10–32)	0.006	1.00 (1.00–1.01)	0.45
RA characteristics					
Duration since first symptoms, median (IQR) years	5.5 (2.0–11.5)	6.4 (2.4–13.7)	0.001	1.00 (0.99–1.02)	0.55
Tender joints (range 0–28), median (IQR) no.	4 (1–10)	3 (1–9)	0.067	1.00 (0.98–1.02)	0.98
Swollen joints (range 0–28), median (IQR) no.	5 (2–9)	4.5 (1–9)	0.20	0.98 (0.96–1.01)	0.18
Patient-assessed general health (0–10 VAS), mean ± SD	4.3 ± 2.8	4.1 ± 2.7	0.059	0.99 (0.95–1.03)	0.61
Summed % erosive joint surface destruction in 8 MCP joints (maximum 100% per joint), % of patients			<0.001		
0	37	28		Referent	–
10–20	38	36		0.99 (0.77–1.28)	0.96
30–70	14	19		1.26 (0.89–1.76)	0.19
80–800	11	17		1.32 (0.88–1.97)	0.18

* Univariable analyses were based on complete cases, whereas multivariable analysis was based on the multiple imputed data. The logistic regression model included all of the characteristics listed in the table. Distal interphalangeal (DIP) joint osteoarthritis (OA) at baseline was defined as having a Kellgren/Lawrence grade of ≥2 in ≥1 of 8 DIP joints. RA = rheumatoid arthritis; OR = odds ratio; 95% CI = 95% confidence interval; ACR = American College of Rheumatology; EULAR = European League Against Rheumatism; BMI = body mass index; ACPA = anti–citrullinated protein antibody; RF = rheumatoid factor; ESR = erythrocyte sedimentation rate; IQR = interquartile range; VAS = visual analog scale; MCP = metacarpophalangeal.

(12) were met by 81% of patients. Ninety-five percent of patients of the study population were treated with a conventional, synthetic, or biologic disease-modifying antirheumatic drug (DMARD) at least once during the study period, and 71% were receiving such treatment at baseline. Glucocorticoid use was reported in 60% of patients during the radiographic follow-up period.

Prevalence of DIP joint OA. In the baseline radiographic images, 21% of the 15,904 DIP joints of 1,988 RA patients showed osteophytes. Joint space narrowing was observed in 13% of joints, subchondral sclerosis in 9%, and central erosions in 1%. Of all the joints examined, 13% had a K/L grade of 1, 22% had a K/L grade of 2, 4% had a K/L grade of 3, and 1% had a K/L grade of 4. At the patient level, 1,199 (60%) of the 1,988 RA patients had ≥1 DIP joint with OA (i.e., K/L grade ≥2);

the median summed K/L grade (sum for all DIP joints examined) among patients with ≥1 OA-affected joint was 6 (IQR 4–12) at baseline. The median number of affected joints per patient was 1 (IQR 0–4). Patients with DIP joint OA were on average 9.5 years older than patients without, and they had a significantly higher mean BMI (Table 1). Longer duration of RA was associated with DIP joint OA; at baseline, patients with DIP joint OA had a higher mean RA duration than patients without DIP joint OA (6.4 years [IQR 2.4–13.7] versus 5.5 years [IQR 2.0–11.5]; P = 0.001).

In univariable analysis, ACPA positivity was more frequent among RA patients with DIP joint OA than among those without DIP joint OA (65% versus 73%; P = 0.010). The presence of RF was not associated with DIP joint OA (P = 0.21) (Table 1). In multivariable analysis, RA duration and lack of ACPA were not significantly associated with DIP joint OA (OR 1.00 [95% CI 0.99–
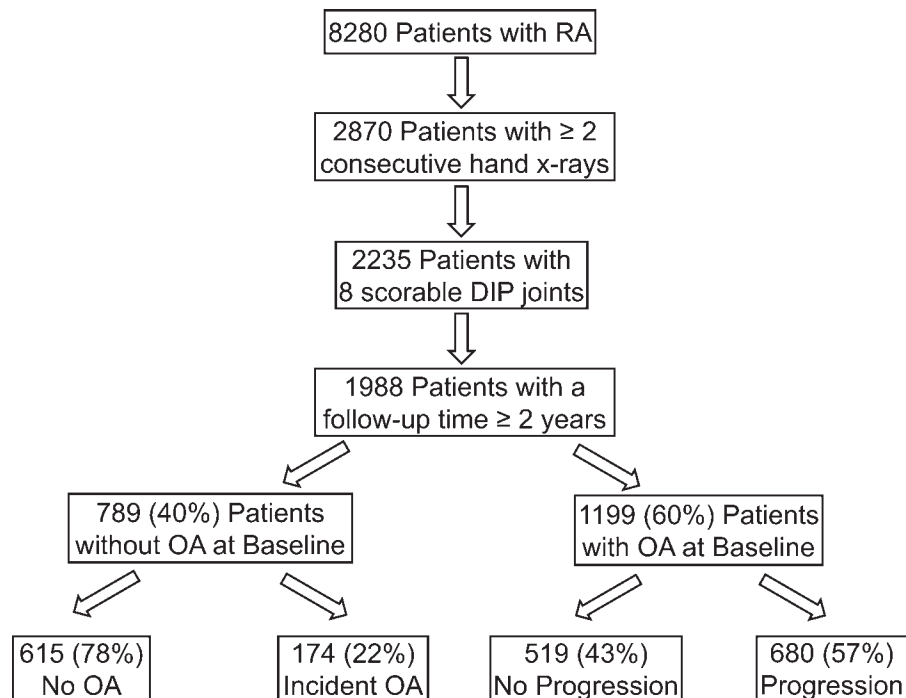
Figure 1. Patient selection process and distal interphalangeal (DIP) joint osteoarthritis (OA) development and progression rates. RA = rheumatoid arthritis.

1.02] and OR 0.72 [95% CI 0.50–1.03], respectively). RA activity, in terms of the DAS28-ESR score (OR 0.95 [95% CI 0.88–1.02]) and ESR alone (OR 1.00 [95% CI 1.00–1.01], was not associated with the presence of DIP joint OA (Table 1 and Supplementary Table 1, http://onlinelibrary.wiley.com/doi/10.1002/art.40684/abstract). However, age, sex, and BMI remained associated with the presence of DIP joint OA seen on baseline radiographs (OR 1.09 [95% CI 1.08–1.10], OR 1.37 [95% CI 1.08–1.74], and OR 1.03 [95% CI 1.00–1.06], respectively) (Table 1).

Development and progression of radiographic DIP joint OA. During follow-up (median 4.5 years [IQR 3.1–7.0]), 174 of 789 patients (22%) without DIP joint OA at baseline developed OA (K/L grade ≥2) in ≥1 DIP joint (Figure 1). In contrast, among the 1,199 patients who did have DIP joint OA at baseline, 680 (57%) experience worsening of the summed K/L grade over the follow-up period.

Patients who developed DIP joint OA during the observation period (i.e., incident OA) had a longer duration of RA than patients without incident DIP joint OA (7.8 years [IQR 2.5–11.7] versus 4.9 years [IQR 1.9–11.4]; P = 0.034) (see Supplementary Table 4, http://onlinelibrary.wiley.com/doi/10.1002/art.40684/abstract). However, in multivariable analysis, a longer duration of RA was not associated with the risk of incident OA (OR 1.02 [95% CI 0.99–1.05]), nor was the presence of RF or ACPA (OR 1.06 [95% CI 0.63–1.80] and OR 1.13 [95% CI 0.63–2.03], respectively) (Supplementary Table 4). RA activity as measured by the DAS28-ESR (OR 0.85 [95% CI 0.75–0.96]) and by ESR alone

(OR 0.98 [95% CI 0.98–1.00]) were negatively associated with the development of DIP joint OA (Supplementary Tables 2 and 4). The multivariable analysis demonstrated no significant association between the number of tender or swollen joints and the risk of incident OA. Patient assessments of their general health at baseline, using a visual analog scale (0–10, with 0 for best and 10 for worst health status), were not associated with the development of OA (OR 1.04 [95% CI 0.96–1.12]). The multivariable analysis showed that higher age and female sex were associated with a risk of OA (OR 1.03 [95% CI 1.01–1.05] and OR 1.67 [95% CI 1.08–2.58], respectively) (Supplementary Table 4).

Patients with OA progression during the follow-up period had a shorter duration of RA than patients without OA progression (5.7 years [IQR 2.2–12.7] versus 7.5 years [IQR 2.9–15.5]; P = 0.001) (Table 2). A longer duration of RA was associated with a reduced risk of OA progression after adjustment, although the effect size was low (OR 0.97 [95% CI 0.96–0.99]). Neither DAS28-ESR scores (OR 1.02 [95% CI 0.94–1.11]) nor ESR alone (OR 1.00 [95% CI 1.00–1.01]) was significantly associated with the progression of DIP joint OA (see Supplementary Tables 1 and 3, http://onlinelibrary.wiley.com/doi/10.1002/art.40684/abstract). An increased number of tender joints was associated with a reduced risk of OA progression, whereas an increased number of swollen joints was associated with an increased risk (OR 0.97 [95% CI 0.94–1.00] and OR 1.05 [95% CI 1.01–1.08], respectively) (Table 2). Higher age was not associated with progression of OA in the multivariable analysis (OR 0.99 [95% CI 0.98–1.01]), nor was the presence of RF or ACPA

Table 2. Univariable and multivariable logistic regression analysis of RA patients without DIP joint OA progression versus RA patients with DIP joint OA progression*

	No OA progression (n = 519)	OA progression (n = 680)	P	Adjusted OR (95% CI)	Adjusted P
Clinical and demographic characteristics					
Summed K/L grade in 8 joints at baseline, % of patients			0.68		
2–4	40	39		Referent	–
5–10	30	31		1.45 (1.07–1.95)	0.015
11–24	30	30		1.32 (0.96–1.81)	0.091
Radiographic observation time, median (IQR) years	4.0 (2.8–5.7)	5.4 (3.5–7.9)	<0.001	1.22 (1.16–1.29)	<0.001
Age, mean ± SD years	60.5 ± 10.5	59.4 ± 9.8	0.050	0.99 (0.98–1.01)	0.28
Female, % of patients	75	79	0.10	1.34 (1.00–1.79)	0.050
BMI, mean ± SD kg/m²	25.4 ± 4.7	26.0 ± 4.7	0.094	1.03 (1.00–1.06)	0.037
Laboratory parameters					
ACPA+, % of patients	65	66	0.86	1.06 (0.72–1.55)	0.77
RF+, % of patients	77	76	0.57	0.79 (0.55–1.12)	0.19
ESR, median (IQR) mm/hour	18 (9–32)	18 (10–32)	0.49	1.00 (1.00–1.01)	0.30
RA disease characteristics					
Duration since first symptoms, median (IQR) years	7.5 (2.9–15.5)	5.7 (2.2–12.7)	0.001	0.97 (0.96–0.99)	0.001
Tender joints (range 0–28), median (IQR) no.	3 (1–9)	3 (1–9)	0.85	0.97 (0.94–1.00)	0.024
Swollen joints (range 0–28), median (IQR) no.	4 (1–8)	5 (1–9)	0.094	1.05 (1.01–1.08)	0.004
Patient-assessed general health (0–10 VAS), mean ± SD	4.1 ± 2.8	4.0 ± 2.7	0.62	0.99 (0.93–1.04)	0.65
Summed % erosive joint surface destruction in 8 MCP joints (maximum 100% per joint), % of patients			0.11		
0	25	31		Referent	–
10–20	38	35		0.82 (0.60–1.13)	0.23
30–70	19	19		0.86 (0.59–1.26)	0.45
80–800	18	15		0.84 (0.53–1.33)	0.45

* Univariable analyses were based on complete cases, whereas multivariable analysis was based on the multiple imputed data. Progression was defined as an increase in summed Kellgren/Lawrence (K/L) grade of ≥1 in patients with distal interphalangeal (DIP) joint osteoarthritis (OA) at baseline. The logistic regression model included all of the characteristics listed in the table. RA = rheumatoid arthritis; OR = odds ratio; 95% CI = 95% confidence interval; IQR = interquartile range; BMI = body mass index; ACPA = anti–citrullinated protein antibody; RF = rheumatoid factor; ESR = erythrocyte sedimentation rate; VAS = visual analog scale; MCP = metacarpophalangeal.

(OR 0.79 [95% CI 0.55–1.12] and OR 1.06 [95% CI 0.72–1.55], respectively) (Table 2). Higher BMI was associated with DIP joint OA progression (OR 1.03 [95% CI 1.00–1.06]). Patients with a summed baseline K/L grade of 5–10 had significantly higher odds of progression (OR 1.45 [95% CI 1.07–1.95]) than patients with a summed score of 2–4.

DISCUSSION

In this study, we systematically investigated the radiographic progression of DIP joint OA in patients with concomitant RA.

We found that neither RA activity nor seropositivity was associated with progression of DIP joint OA, which is consistent with the notion of a distinct pathogenesis of the respective cartilage and bone loss in the 2 disorders. In fact, the multivariable analysis revealed an association of a longer duration of RA with lower risk of progression in DIP joint OA, and higher RA activity with lower incidence of DIP joint OA. At first glance, these results are surprising, as systemic low-grade inflammation is believed to foster OA and the inflammatory cytokines present in RA. For instance, tumor necrosis factor, among other cytokines, has been implicated in both OA and RA (13). Furthermore, in an earlier,

smaller study that enrolled patients with recent-onset RA and likely greater disease activity, a high ESR and progressive erosive damage were revealed as risk factors for incident erosions and osteophytes in DIP joints (14).

Despite these data, and although synovitis and bone marrow edema have been documented in DIP joint OA and RA (4), our results do not support the argument that systemic inflammation has a general pathogenic role in OA. This conclusion is supported by a previous study (15) that included patients with early RA, and in which underlying OA of the hand (as assessed using a composite score including proximal interphalangeal joints and the first carpometacarpal joints) was not associated with RA activity, and by another study (16) that showed no association between C-reactive protein levels at baseline and progression of erosive hand OA.

In our established RA cohort, central DIP joint erosions were observed in 5% of patients, which is similar to the proportion of DIP joint erosions in OA patients without RA (1,9). At this point, however, we cannot exclude the potential antierosive effects of methotrexate or other DMARDs in DIP joint OA. Furthermore, radiographic progression of preexisting DIP joint OA in our RA cohort reached 57%, which is lower than the rate of DIP joint OA progression among individuals without RA (9). Aside from the longer observation time in the Framingham Osteoarthritis Study (9) (8.7 years, versus 4.5 years in our study), one reason for the lower proportion of radiographic progression of DIP joint OA among RA patients could be the use of disease-modifying treatments. We also cannot rule out the idea that RA patients limit their manual activity and therefore diminish the mechanical stress on their osteoarthritic joints. The present study results favor the still-uncertain notion that obesity could be a risk factor for hand OA (17) by showing that patients with a higher BMI had a significantly higher risk of development and progression of DIP joint OA.

There are several potential limitations to our investigation. Not all patients fulfilled the 2010 ACR/EULAR classification criteria for RA due to some of its components not being assessed. However, when limiting our analysis to those patients who did fulfill the criteria, the results remained unchanged. Furthermore, possible associations in the incident OA analysis could have been missed due to the limited sample size. We were, however, able to identify highly significant associations of incident hand OA with the known risk factors of higher age and female sex. Sensitive techniques such as magnetic resonance imaging and ultrasound to detect signs of local inflammation in DIP joints (4) were not used in this cohort. We had no reliable data on metabolic factors such as the lipid profile, which might act as a potential modifier of radiographic progression. The effects of DMARDs on the course of hand OA warrant further studies. Interrater reliability was not assessed due to good intrarater reliability, but also due to a lack of resources.

Despite these limitations, the comprehensive radiographic assessment of DIP joints in this large RA cohort contributes to the understanding of DIP joint OA. The results demonstrate that RA activity and autoantibody levels are not involved in the radiographic course of OA in the DIP joints.

ACKNOWLEDGMENTS

AUTHOR CONTRIBUTIONS

All authors were involved in drafting the article or revising it critically for important intellectual content, and all authors approved the final version to be published. Mr. Lechtenboehmer had full access to all of the data in the study and takes responsibility for the integrity of the data and the accuracy of the data analysis.
Study conception and design. Lechtenboehmer, Jaeger, Kyburz, Walker, Hügle.
Acquisition of data. Lechtenboehmer.
Analysis and interpretation of data. Lechtenboehmer, Jaeger, Kyburz, Walker, Hügle.

REFERENCES

1. Kwok WY, Kloppenburg M, Rosendaal FR, van Meurs JB, Hofman A, Bierma-Zeinstra SM. Erosive hand osteoarthritis: its prevalence and clinical impact in the general population and symptomatic hand osteoarthritis. Ann Rheum Dis 2011;70:1238–42.

2. Figueiredo CP, Simon D, Englbrecht M, Haschka J, Kleyer A, Bayat S, et al. Quantification and impact of secondary osteoarthritis in patients with anti–citrullinated protein antibody-positive rheumatoid arthritis. Arthritis Rheumatol 2016;68:2114–21.

3. Verbruggen G, Veys EM. Erosive and non-erosive hand osteoarthritis: use and limitations of two scoring systems. Osteoarthritis Cartilage 2000;8 Suppl A:S45–54.

4. Damman W, Liu R, Bloem JL, Rosendaal FR, Reijnierse M, Kloppenburg M. Bone marrow lesions and synovitis on MRI associate with radiographic progression after 2 years in hand osteoarthritis. Ann Rheum Dis 2017;76:214–7.

5. Chevalier X, Ravaud P, Maheu E, Baron G, Rialland A, Vergnaud P, et al. Adalimumab in patients with hand osteoarthritis refractory to analgesics and NSAIDs: a randomised, multicentre, double-blind, placebo-controlled trial. Ann Rheum Dis 2015;74:1697–705.

6. Kloppenburg M, Peterfy C, Haugen IK, Kroon FP, Chen S, Wang L, et al. A phase 2A, placebo-controlled, randomized study of ABT-981, an anti–interleukin-1α and -1β dual variable domain immunoglobulin, to treat erosive hand osteoarthritis [abstract]. Arthritis Rheumatol 2017; 69 Suppl 10. URL: https://acrabstracts.org/abstract/a-phase-2a-placebo-controlled-randomized-study-of-abt-981-an-anti-interleukin-1alpha-and-1beta-dual-variable-domain-immunoglobulin-to-treat-erosive-hand-osteoarthritis/.

7. Uitz E, Fransen J, Langenegger T, Stucki G. Clinical quality management in rheumatoid arthritis: putting theory into practice. Swiss clinical quality management in rheumatoid arthritis. Rheumatology (Oxford) 2000;39:542–9.

8. Altman RD, Gold GE. Atlas of individual radiographic features in osteoarthritis, revised. Osteoarthritis Cartilage 2007;15 Suppl A:A1–56.

9. Haugen IK, Englund M, Aliabadi P, Niu J, Clancy M, Kvien TK, et al. Prevalence, incidence and progression of hand osteoarthritis in the general population: the Framingham Osteoarthritis Study. Ann Rheum Dis 2011;70:1581–6.

10. Rau R, Wassenberg S, Herborn G, Stucki G, Gebler A. A new method of scoring radiographic change in rheumatoid arthritis. J Rheumatol 1998;25:2094–107.

11. Prevoo ML, van 't Hof MA, Kuper HH, van Leeuwen MA, van de Putte LB, van Riel PL. Modified disease activity scores that include twenty-eight–joint counts: development and validation in a prospective longitudinal study of patients with rheumatoid arthritis. Arthritis Rheum 1995;38:44–8.

12. Aletaha D, Neogi T, Silman AJ, Funovits J, Felson DT, Bingham CO III, et al. 2010 rheumatoid arthritis classification criteria: an American College of Rheumatology/European League Against Rheumatism collaborative initiative. Arthritis Rheum 2010;62:2569–81.

13. Charlier E, Relic B, Deroyer C, Malaise O, Neuville S, Collée J, et al. Insights on molecular mechanisms of chondrocytes death in osteoarthritis. Int J Mol Sci 2016;17:E2146.

14. Güler-Yüksel M, Allaart CF, Watt I, Goekoop-Ruiterman YP, de Vries-Bouwstra JK, van Schaardenburg D, et al. Treatment with TNF-α inhibitor infliximab might reduce hand osteoarthritis in patients with rheumatoid arthritis. Osteoarthritis Cartilage 2010;18:1256–62.

15. McWilliams DF, Marshall M, Jayakumar K, Doherty S, Doherty M, Zhang W, et al. Erosive and osteoarthritic structural progression in early rheumatoid arthritis. Rheumatology (Oxford) 2016;55: 1477–88.

16. Bijsterbosch J, van Bemmel JM, Watt I, Meulenbelt I, Rosendaal FR, Huizinga TW, et al. Systemic and local factors are involved in the evolution of erosions in hand osteoarthritis. Ann Rheum Dis 2011;70:326–31.

17. Frey N, Hügle T, Jick SS, Meier CR, Spoendlin J. Hyperlipidemia and incident osteoarthritis of the hand: a population-based case-control study. Osteoarthritis Cartilage 2017;25:1040–5.

Therapeutic Effects of a TANK-Binding Kinase 1 Inhibitor in Germinal Center–Driven Collagen-Induced Arthritis

Cynthia Louis,[1] Devi Ngo,[1] Damian B. D'Silva,[1] Jacinta Hansen,[1] Louisa Phillipson,[1] Helene Jousset,[1] Patrizia Novello,[1] David Segal,[1] Kate E. Lawlor,[1] Christopher J. Burns,[2] and Ian P. Wicks[3]

Objective. The production of class-switched high-affinity autoantibodies derived from organized germinal centers (GCs) is a hallmark of many autoimmune inflammatory diseases, including rheumatoid arthritis (RA). TANK-binding kinase 1 (TBK-1) is a serine/threonine kinase involved in the maturation of GC follicular helper T (Tfh) cells downstream of inducible costimulator signaling. We undertook this study to assess the therapeutic potential of TBK-1 inhibition using the small-molecule inhibitor WEHI-112 in antibody-dependent models of inflammatory arthritis.

Methods. Using the models of collagen-induced arthritis (CIA), antigen-induced arthritis (AIA), and K/BxN serum-transfer–induced arthritis (STIA), we determined the effectiveness of WEHI-112 at inhibiting clinical and histologic features of arthritis in C57BL/6 and DBA/1 mice. We used immunohistochemistry to characterize GC populations during CIA development, and we used enzyme-linked immunosorbent assays to determine levels of Ig autoantibodies in WEHI-112–treated mice compared to vehicle-treated mice.

Results. WEHI-112, a tool compound that is semiselective for TBK-1 but that also has activity against IKKε and JAK2, abolished TBK-1–dependent activation of interferon (IFN) regulatory factor 3 and inhibited type I IFN responses in vitro. In vivo, treatment with WEHI-112 selectively abrogated clinical and histologic features of established, antibody-dependent CIA, but had minimal effects on an antibody-independent model of AIA or on K/BxN STIA. In keeping with these findings, WEHI-112 reduced arthritogenic type II collagen–specific IgG1 and IgG2b antibody production. Furthermore, WEHI-112 altered the GC Tfh cell phenotype and GC B cell function in CIA.

Conclusion. We report that TBK-1 inhibition using WEHI-112 abrogated antibody-dependent CIA. As WEHI-112 failed to inhibit non–antibody-driven joint inflammation, we conclude that the major effect of this compound was most likely the targeting of TBK-1–mediated mechanisms in the GC reaction. This approach may have therapeutic potential in RA and in other GC-associated autoantibody-driven inflammatory diseases.

INTRODUCTION

The presence of high-affinity autoantibodies, such as anti–citrullinated protein antibodies (ACPAs) in rheumatoid arthritis (RA) (1) and antinuclear antibodies in systemic lupus erythematosus (SLE) (2), is a common feature of humorally mediated autoimmune diseases and has been linked to the induction of autoimmune inflammation (3,4). The pathogenicity of high-affinity autoantibodies is exemplified in the K/BxN serum–transfer model of RA (5). Transfer of serum or purified autoantibodies generated

from autoimmune K/BxN-transgenic arthritic mice alone is sufficient to induce arthritis in naive recipients (5). Key cytokines, such as tumor necrosis factor (TNF) and interleukin-1β (IL-1β), are downstream amplifiers of joint inflammation in this model (6).

Germinal center (GC) formation in secondary lymphoid tissues plays a major role in humoral autoimmunity (7). In the inductive phase of an antibody response, GC follicular helper T (Tfh) cells and GC B cells cooperate to mediate Ig class-switching, affinity selection, and the generation of GC-derived memory B cells and antibody-secreting plasma cells. GC reactions,

including production of cytokines by Th17 cells within GCs, also induce posttranslational modification of antibodies produced by recently generated, GC-derived plasma cells and thereby influence the pathogenicity of arthritogenic autoantibodies in the autoimmune collagen-induced arthritis (CIA) model (8).

Biologic therapies to deplete B cells and antagonize key inflammatory cytokines such as TNF have been used clinically with success in treating RA. Small-molecule kinase inhibitors targeting JAKs have also been approved for RA (9). Nevertheless, important challenges remain in the treatment of RA. Responsiveness to these therapies varies in different patients, reflecting the heterogeneity of underlying pathogenic mechanisms and stage of disease. Additionally, TNF antagonism and JAK inhibitors exert effects on the immune response that increase the risk of infection. Thus, therapies aimed at curbing humoral autoimmunity while balancing immune competence are required. We propose that targeting key pathways involved in autoantibody development may be one such approach.

High-affinity autoantibodies arise from GC reactions occurring in B cell follicles, following iterative rounds of somatic hypermutation of GC B cells and selection/maturation facilitated by Tfh cells (7). GC B cells with high affinity for antigen eventually form antibody-producing plasma cells (10). Accordingly, we reasoned that by targeting regulators of the GC reaction, the production of pathogenic autoantibodies could be limited, thereby inhibiting inflammation. Three target pathways are of relevance in this context. First, elevated type I interferon (IFN) activity (the so-called type I IFN signature) is a remarkable feature of SLE that can also be observed in some patients with RA and Sjögren's syndrome, and it is associated with high-affinity autoantibodies, disease progression, and poor prognosis (11,12). Type I IFN signaling through the common receptor IFN-α/β/ω receptor 1 can prime dendritic cells (DCs) to produce IL-6 in secondary lymphoid tissues. Second, IL-6 supports the development of Tfh cells and Th17 cells in secondary lymphoid tissues as well as the maintenance of terminally differentiated antibody-secreting plasma cells (13). Third, the inducible costimulator (ICOS) is required for the differentiation and maintenance of GC Tfh cells, which mediate GC interactions and facilitate antibody responses (14–16). Loss or inhibition of these pathways has been shown to abrogate disease in humorally mediated autoimmune disease models (17–20).

TANK-binding kinase 1 (TBK-1) is an IKK-related serine/threonine kinase that is critical for the induction of IFN regulatory factor 3 (IRF-3)–driven type I IFN responses in nucleic acid sensing pathways, such as the Toll-like receptor 3 (TLR-3)/TLR-4/TRIF, retinoic acid–inducible gene 1/melanoma differentiation–associated protein 5/mitochondrial antiviral signaling protein, and cyclic GMP-AMP synthase (cGAS)/stimulator of IFN genes (STING) pathways (21). TBK-1 also regulates IL-6 expression in response to TLR-3 ligands (22) and in response to cytosolic DNA downstream of STING, but not to TLR-9 ligands (23). Because TBK-1$^{-/-}$ mice have the phenotype of embryonic lethality, by using viable TBK-1$^{-/-}$TNF$^{-/-}$ mice (24) and STING$^{-/-}$ mice (23), TBK-1–dependent induction of type I IFNs and IL-6, respectively, has been shown to be required for humoral responses in vivo. TBK-1 was also recently identified as a critical kinase for ICOS signaling in Tfh cells (25).

Given the involvement of TBK-1 in regulating the production of type I IFNs and IL-6, as well as ICOS signaling, we hypothesized that TBK-1 inhibition might provide an alternative approach to treatment of antibody-mediated inflammatory diseases. To explore this hypothesis, we generated WEHI-112 (a relatively selective small-molecule inhibitor of TBK-1) as a tool compound. TBK-1 inhibition by WEHI-112 was confirmed by effective suppression of TRIF/TBK-1–dependent IRF-3 activation and IRF-3–associated mediators in macrophage cell culture. In vivo, TBK-1 inhibition alleviated the progression of established autoantibody-mediated CIA, but not antibody-independent, antigen-induced arthritis (AIA) and not K/BxN serum-transfer–induced arthritis (STIA). TBK-1 inhibition reduced cytokine signaling and arthritogenic GC-driven humoral responses in CIA in conjunction with lowered serum type II collagen (CII)–specific IgG1 levels. TBK-1 inhibition may therefore provide an alternative therapeutic approach in RA and other autoantibody-mediated inflammatory diseases.

MATERIALS AND METHODS

Mice. C57BL/6 and DBA/1 mice ages 8–10 weeks were obtained from Walter and Eliza Hall Institute of Medical Research (WEHI) Animal Supplies. Mice were housed under standard conditions in the WEHI Animal Facility. All procedures were approved by the WEHI Animal Ethics Committee.

Chemical compounds. MRT67307 (26) was purchased from Sigma. Baricitinib (a JAK2 inhibitor) was purchased from SelleckChem. WEHI-112 was synthesized at WEHI. All compounds were dissolved in DMSO and diluted in 20% Captisol saline carrier solution.

Induction of arthritis and inhibitor treatment. For CIA, DBA/1 mice were immunized intradermally with chicken CII (2 mg/ml; Sigma-Aldrich) emulsified in an equal volume of Freund's complete adjuvant (CFA) containing 5 mg/ml heat-killed *Mycobacterium tuberculosis* H37RA (Difco) on day 0 and day 21. Intraperitoneal (IP) injection of vehicle or WEHI-112 (30 mg/kg) was initiated upon disease onset, and mice were randomly enrolled into treatment and control groups.

For AIA, C57BL/6 mice were immunized intradermally with methylated bovine serum albumin (mBSA) (2 mg/ml; Sigma-Aldrich) emulsified in an equal volume of CFA on day 0. Arthritis was induced on day 7 by an intraarticular (IA) injection of 200 μg mBSA in 10 μl of 0.9% weight/volume saline into the left knee. IP injection of vehicle or WEHI-112 (30 mg/kg) was initiated immediately after IA injection, and mice were randomly enrolled into treatment and control groups.

For K/BxN STIA, C57BL/6 mice were injected with 100 μl serum from K/BxN mice on day 0. IP injection of vehicle or WEHI-112 (30 mg/kg) was initiated on day 1 and continued daily for 8 consecutive days.

Antigen-specific antibody enzyme-linked immuno sorbent assay. Serial dilutions of sera were added to 96-well PolySorb microtiter plates (Nunc) coated with 5 μg/ml CII (Sigma-Aldrich) and incubated at room temperature for 2 hours, followed by incubation with horseradish peroxidase–conjugated secondary antibodies against mouse IgG1 (1144-05), IgG2a (1155-05), IgG2b (1186-05), and IgM (1140-05) (SouthernBiotech). The plates were developed with tetramethylbenzidine substrate solution (BD Biosciences), and optical densities were read at 450 nm. A mixture of sera from hyperimmunized DBA/1 mice with CIA was used to establish standard curves, and antibody levels are shown as relative titers.

Immunofluorescence. Lymph nodes (LNs) were fixed in 4% paraformaldehyde overnight, immersed in 20% sucrose for 1 hour, and embedded in TissueTek OCT compound, and 8-μm cryostat sections were prepared. After blocking of nonspecific binding sites with Avidin, Biotin, and Protein Block solutions (Dako) supplemented with 2.4G2 (100 μg/ml), sections were stained with Alexa Fluor 488–coupled anti–GL-7 (GL-7) and Alexa Fluor 647–coupled anti-B220 (RA3-6B2) (both from BioLegend). Nuclei were stained with DAPI. Images of whole LN sections were captured using an LSM780 confocal microscope system with ZEN2010 imaging software using the tile-scan function (Carl Zeiss).

T cell restimulation assay. Primary CD4+ T cell populations were isolated from pooled LNs of DBA/1 mice with CIA. CD4+ T cells were pregated as CD3+CD4+CD25– cells and sorted into CD44high and CD44intermediate populations. T cells were cultured in RPMI 1640 medium supplemented with 10% fetal bovine serum, L-glutamine (4 mM), HEPES (10 mM), sodium pyruvate (1 mM), β-mercaptoethanol (50 μM), penicillin (100 units/ml), and streptomycin (100 units/ml). Cells were left unstimulated or preconditioned with vehicle or WEHI-112 for 30 minutes. Vehicle- or WEHI-112–treated cells were stimulated with combinations of purified endotoxin-low and azide-free anti-CD3 (3 μg/ml, 2C11; BioLegend) and anti-ICOS (3 μg/ml, C398.4A; BioLegend). The antibodies were crosslinked at 37°C by goat antibody to hamster IgG (20 μg/ml, 127-005-099; Jackson ImmunoResearch). For immunoblotting, cells were lysed in radioimmunoprecipitation assay buffer after in vitro stimulation for 10 minutes, and cell lysates were probed for phospho-FoxO1 or β-actin. For ImageStream analysis, sorted CD44high cells were collected after stimulation for 30 minutes, stained for total FoxO1 (C29H4; Cell Signaling Technology), counterstained with DAPI, acquired using an ImageStream[x]

Mark II instrument (Amnis), and analyzed using IDEAS software (Merck).

Quantitative reverse transcriptase–polymerase chain reaction (RT-PCR). Total RNA was extracted from cells using an ISOLATE II RNA Mini Kit (Bioline), digested with RNase-free DNase I (Bioline), and reverse transcribed into complementary DNA using SuperScript III reverse transcriptase (Invitrogen) and oligo(dT) primers (Promega). Quantitative RT-PCR was performed using Fast SYBR Green Master Mix (ThermoFisher Scientific) on a ViiA 7 PCR System (ThermoFisher Scientific). Primers for the genes assessed are shown in Supplementary Table 1, available on the *Arthritis & Rheumatology* web site at http://onlinelibrary.wiley.com/doi/10.1002/art.40670/abstract. Gene expression levels were normalized to cellular GAPDH messenger RNA (mRNA) levels.

Statistical analysis. Data are expressed as the mean ± SEM. Statistical differences were assessed by Student's unpaired *t*-test or Student's paired *t*-test, as indicated, using GraphPad Prism 6.0 software. *P* values less than or equal to 0.05 were considered significant.

Additional information is available in Supplementary Methods, http://onlinelibrary.wiley.com/doi/10.1002/art.40670/abstract.

RESULTS

In vitro assessment of WEHI-112 as a TBK-1 inhibitor. Current pharmacologic TBK-1 inhibitors display off-target inhibition on other major kinases and some are poorly stable for in vivo use (26,27). We identified WEHI-112 as a tool compound inhibitor of TBK-1 with improved selectivity and bioactivity. WEHI-112 potently inhibited TBK-1 and its homolog IKKε (see Supplementary Table 2, http://onlinelibrary.wiley.com/doi/10.1002/art.40670/abstract), owing to a high degree of sequence homology. Cell-free biochemical assays revealed that WEHI-112 and the literature standard TBK-1 inhibitor MRT67307 (26) blocked TBK-1 activity with a 50% inhibition concentration (IC$_{50}$) of ~0.01 μM and ~0.05 μM, respectively (Figure 1A). WEHI-112 and MRT67307 also inhibited IKKε activity at an IC$_{50}$ of 0.003 μM and 0.03 μM, respectively, and JAK2 activity at an IC$_{50}$ of 0.01 μM and 0.08 μM, respectively (Figure 1A). WEHI-112 and MRT67307 inhibited lipopolysaccharide (LPS)–induced IRF-3 phosphorylation of the TRIF/TBK-1/IRF-3 pathway (21) in RAW 264.7 macrophages (Figure 1B). Consistent with other TBK-1 inhibitors, both WEHI-112 and MRT67307 paradoxically enhanced the phosphorylation of TBK-1 and IKKε (Figure 1B), despite efficient inhibition of TBK-1 activity (28). The induction of LPS-induced, TRIF/TBK-1/IRF-3–dependent genes (*Ifnb*, *Cxcl10*, and *Ccl5*) was reduced in macrophages in the presence of either WEHI-112 or MRT67307 (Figure 1C). WEHI-112 and MRT67307 did not affect the induction of LPS-induced *Tnf* or *Il1b*, but suppressed *Il6* transcription in RAW 264.7 mac-
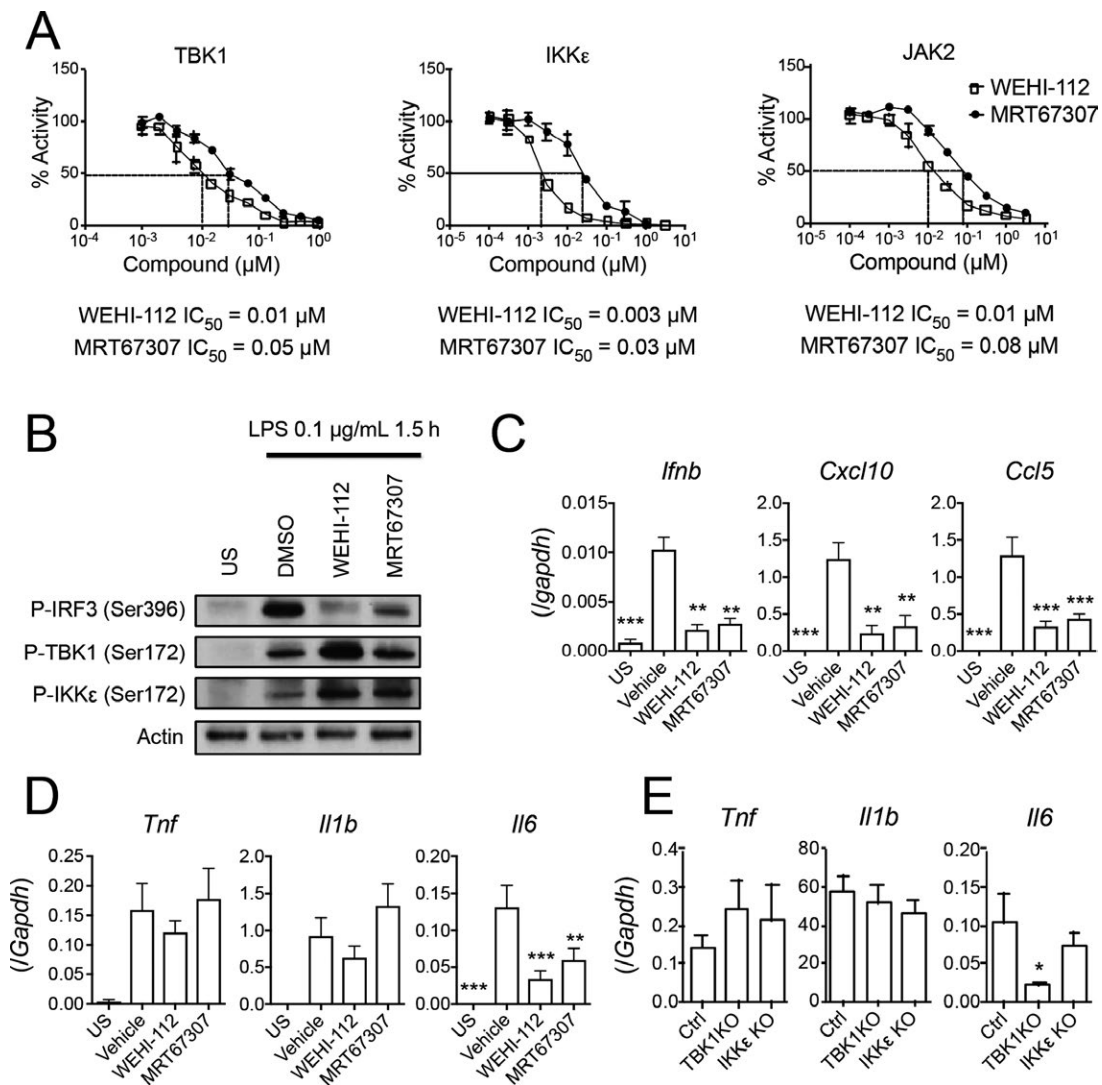
Figure 1. WEHI-112 is a potent inhibitor of TANK-binding kinase 1 (TBK-1). **A,** Dose-response curves showing inhibition of TBK-1, IKKε, and JAK2 activity in the presence of WEHI-112 or MRT67307. Percentage activity was calculated using the no-inhibitor control as 100% activity. Data are representative of 2 independent experiments. Broken lines indicate 50% inhibition concentration (IC_{50}) of each compound. **B,** Immunoblot analysis of phosphorylated interferon regulatory factor 3 (IRF-3), TBK-1, and IKKε in whole-cell lysates of RAW 264.7 macrophages that were unstimulated (US) or preconditioned with vehicle (DMSO), 0.25 μ*M* WEHI-112, or 0.25 μ*M* MRT67307 for 1 hour prior to stimulation with lipopolysaccharide (LPS). Data show results of 1 experiment representative of 2 independent experiments. **C** and **D,** Reverse transcriptase–polymerase chain reaction (RT-PCR) analysis of *Ifnb*, *Cxcl10*, and *Ccl5* (**C**) and of *Tnf*, *Il1b*, and *Il6* (**D**) in RAW 264.7 macrophages left unstimulated or preconditioned with vehicle or 0.25 μ*M* inhibitor (WEHI-112 or MRT67307) for 1 hour followed by stimulation for 4 hours with 0.1 μg/ml LPS. Data are pooled from 5 independent experiments. ∗∗ = $P \leq 0.01$; ∗∗∗ = $P \leq 0.005$ versus vehicle, by Student's paired *t*-test. **E,** RT-PCR analysis of *Tnf*, *Il1b*, and *Il6* in THP-1 human monocyte–derived macrophages stimulated for 4 hours with 0.1 μg/ml LPS following clustered regularly interspaced short palindromic repeat (CRISPR)/CRISPR-associated protein 9–mediated knockout (KO) of endogenous TBK-1 or IKKε. Data are pooled from 5 independent experiments. ∗ = $P \leq 0.05$ versus control, by Student's paired *t*-test. Values in **A** and **C–E** are the mean ± SEM.

rophages (Figure 1D). Additionally, TBK-1, rather than IKKε, was required for optimal *Il6* induction in response to LPS (Figure 1E). In summary, WEHI-112 is a potent and relatively selective inhibitor of TBK-1.

WEHI-112 ameliorates T cell– and B cell–dependent CIA but has minimal effect on B cell–independent AIA or T cell– and B cell–independent STIA. To test the therapeutic potential of TBK-1 inhibition using WEHI-112, we used the autoimmune

CIA model of inflammatory arthritis. The CIA model is dependent on both cellular and humoral responses to CII (29,30). Vehicle or WEHI-112 was administered immediately upon clinically evident signs of arthritis in immunized DBA/1 mice. Vehicle-treated mice developed progressive arthritis, but this was markedly inhibited in WEHI-112–treated mice (Figure 2A). A myeloperoxidase-based Lumina In Vivo Imaging System imaging spectrum showed markedly attenuated inflammation in the limbs of mice treated with WEHI-112 (Figure 2B). Histologic
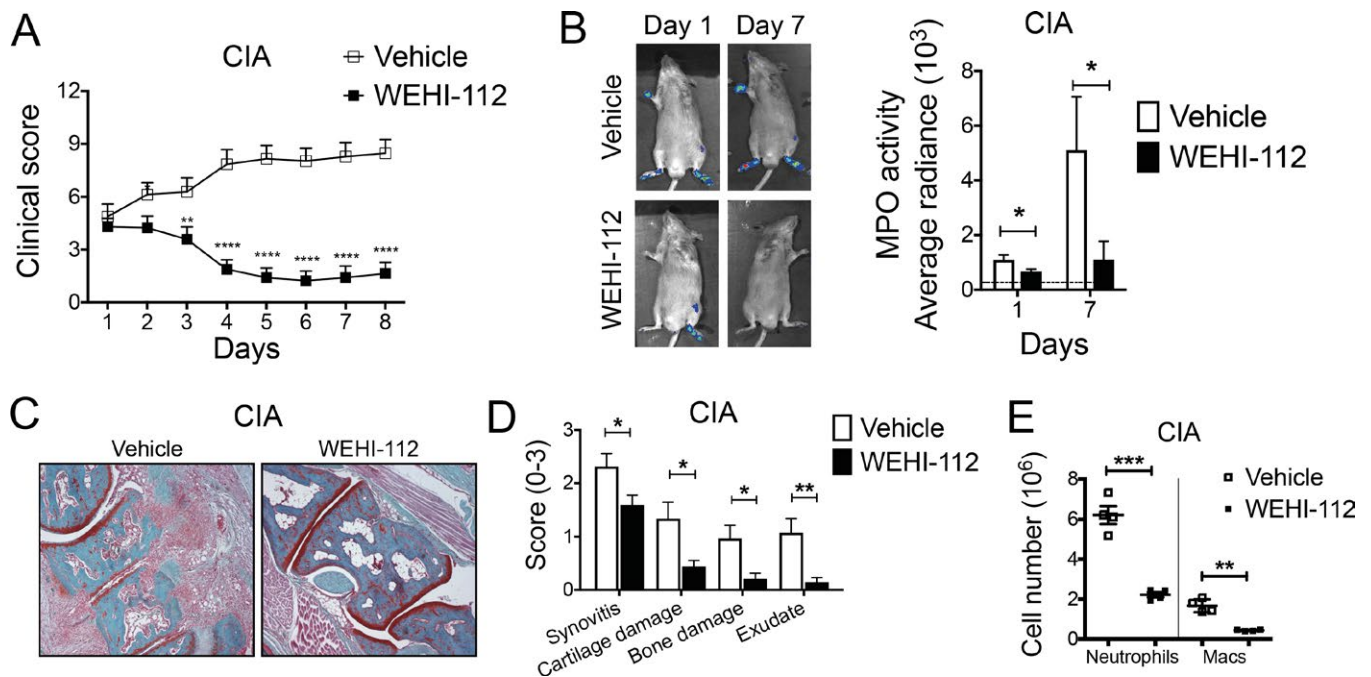
Figure 2. WEHI-112 markedly inhibits the progression of established collagen-induced arthritis (CIA) but has minimal effects on antigen-induced arthritis (AIA) or K/BxN serum-transfer–induced arthritis (STIA). **A**–**E** and **J**–**L,** DBA/1 mice with CIA were randomly enrolled into treatment or control groups at arthritis onset (day 1) to receive WEHI-112 (30 mg/kg) or vehicle intraperitoneally (IP) daily for 7 days. **A,** Clinical features in mice with CIA, evaluated daily. Data are pooled from 4 independent experiments with 4–5 mice per group per experiment. ∗∗ = $P \leq 0.01$; ∗∗∗∗ = $P \leq 0.0001$ versus vehicle, by Student's unpaired t-test. **B,** Representative bioluminescent images and quantification of myeloperoxidase (MPO) activity in arthritic DBA/1 mice (described in **A**) at the indicated times. ∗ = $P \leq 0.05$ by Student's unpaired t-test. **C,** Representative Safranin O staining of histologic joint sections from mice with CIA treated with vehicle or WEHI-112. Original magnification × 10. **D,** Histologic evaluation of total arthritis clinical scores (0 = normal; 1 = mild; 2 = moderate; 3 = severe). ∗ = $P \leq 0.05$; ∗∗ = $P \leq 0.01$ by Student's unpaired t-test. **E,** Quantification of joint-infiltrating neutrophils and macrophages (Macs) in ankle joints of DBA/1 mice with CIA. ∗∗ = $P \leq 0.01$; ∗∗∗ = $P \leq 0.005$ by Student's unpaired t-test. **F**–**H,** C57BL/6 mice were immunized with the antigen methylated bovine serum albumin (mBSA) in Freund's complete adjuvant on day 0. Arthritis was induced by intraarticular injection of mBSA into the knee on day 7. Vehicle or WEHI-112 was given daily IP from day 7 to day 13, and knee joints were collected for analysis on day 14. **F,** Representative Safranin O staining of histologic joint sections from mice with AIA treated with vehicle or WEHI-112. Original magnification × 5. **G,** Macroscopic scores of histologic changes in affected knee joints of mice with AIA (0 = normal; 1 = mild; 2 = moderate; 3 = severe). Data are pooled from 2 independent experiments with 4–5 mice per group per experiment. **H,** Quantification of joint-infiltrating neutrophils and macrophages in knee joints of C57BL/6 mice with AIA. Data are pooled from 2 independent experiments with 4–5 mice per group per experiment. **I,** Clinical arthritis severity in C57BL/6 mice receiving K/BxN serum on day 0, followed by WEHI-112 or vehicle IP daily for the next 8 days. Data are pooled from 2 independent experiments with 4–5 mice per group per experiment. **J,** Ig isotypes specific for type II collagen (CII) in serum from mice with CIA collected at study end point, determined by enzyme-linked immunosorbent assay. Data are pooled from 3 independent experiments. ∗ = $P \leq 0.05$; ∗∗∗ = $P \leq 0.005$ by Student's unpaired t-test. **K** and **L,** *Ifnb*, *Cxcl10*, and *Ccl5* (**K**) and *Tnf*, *Il1b*, and *Il6* (**L**) in total lymph node cells derived from mice with CIA, determined by reverse transcriptase–polymerase chain reaction analysis. Data are representative of 2 independent experiments. ∗ = $P \leq 0.05$; ∗∗ = $P \leq 0.01$ by Student's unpaired t-test. In **A**, **B**, **D**, **G**, and **I**–**L**, values are the mean ± SEM. In **E** and **H**, symbols represent individual mice; bars show the mean ± SEM.

evaluation of the inflammatory cell influx, cartilage damage, and bone degradation supported these observations (Figures 2C and D). There were significant reductions in tissue-infiltrating neutrophils (CD45+Ly-6G+CD88+CD64−CD11b+) and macrophages (CD45+Ly-6G−CD88+CD64+CD11b+) (see Supplementary Figure 1, http://onlinelibrary.wiley.com/doi/10.1002/art.40670/abstract) in mice with CIA treated with WEHI-112 relative to those treated with vehicle (Figure 2E).

WEHI-112 was next evaluated in the AIA model. AIA is T cell dependent but independent of B cells and antibody production (31). Vehicle or WEHI-112 was given immediately after

IA antigen challenge to induce AIA. WEHI-112 failed to inhibit inflammatory arthritis in the AIA model, as demonstrated by histology (Figures 2F and G) and fluorescence-activated cell sorting analysis of the inflamed joint (Figure 2H). Additionally, WEHI-112 did not prevent the evolution of inflammatory arthritis in the K/BxN STIA model (which develops independently of adaptive immune mechanisms) (5), but may have had a modest effect on the severity of disease at later time points (Figure 2I). Collectively, these well-described arthritis models show that WEHI-112 targets specific arthritogenic event(s) in CIA, to a much greater extent than in AIA or STIA.
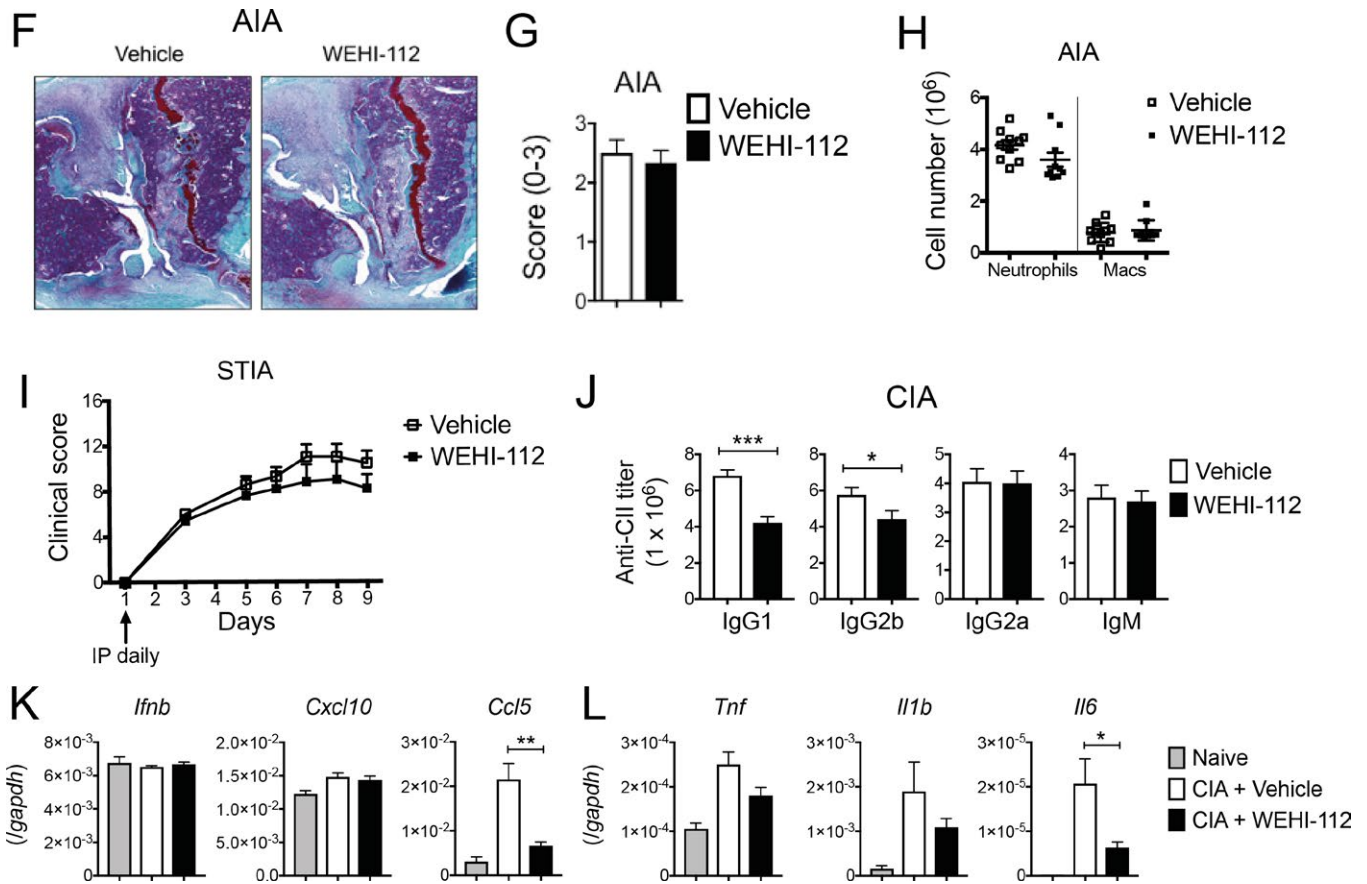
Figure 2. (*Cont'd*)

CIA development relies on efficient priming of humoral responses for the generation of arthritogenic CII-specific IgG1 autoantibodies, and to a lesser extent, IgG2b autoantibodies (5). Consistent with reduced arthritis, there was a significant reduction in pathogenic IgG1 anticollagen antibodies and a modest reduction in IgG2b isotypes in WEHI-112–treated mice compared to vehicle-treated mice. IgG2a and IgM anti-CII isotypes were not affected (Figure 2J).

Relative to naive LNs, there was no alteration in *Ifnb* or *Cxcl10* in LNs of mice with CIA (Figure 2K). In contrast, *Ccl5* was increased in LNs of mice with CIA relative to naive LNs, but this was reduced upon treatment with WEHI-112 (Figure 2K). *Tnf*, *Il1b*, and *Il6* were all elevated in LNs of mice with CIA compared to naive LNs, but only *Il6* was reduced upon treatment with WEHI-112 (Figure 2L), consistent with reduced IL-6 induction in vitro with WEHI-112 or deletion of TBK-1 (Figures 1D and E). Thus, the alleviation of CIA following TBK-1 inhibition with WEHI-112 could be due to reduced levels of particular cytokines and chemokines in secondary lymphoid tissues.

Characterization of GC populations during development of CIA. Given the effect of WEHI-112 in reducing CII-specific IgG1 titers in CIA (Figure 2J), the importance of GCs for development of CIA (32), and the requirement for TBK-1 in

mediating ICOS signaling during Tfh cell maturation (25), we examined the GC response following WEHI-112 treatment in the CIA model. Immunohistochemistry revealed an overall reduction in GC size as determined by GC area relative to total LN size (Figures 3A and B), although GC numbers were not affected by WEHI-112 (Figure 3C).

We defined mature GC Tfh cells as CD3+CD4+GL-7+ cells, and we defined activated ICOS+CD4+ T cells as CD3+CD4+GL-7–ICOS+ cells (33). Compared to LNs of naive mice, LNs of mice with CIA had expanded numbers of ICOS+CD4+ T cells and GC Tfh cells (see Supplementary Figure 2A, http://onlinelibrary.wiley.com/doi/10.1002/art.40670/abstract). Up-regulation of ICOS and GL-7 expression in the draining LNs of mice with active CIA was restricted to CD4+ T cells (Supplementary Figure 2A). GL-7+CD4+ GC Tfh cells had the highest expression of *Bcl6* (regulates Tfh cell differentiation and GC reactions), followed by GL-7–ICOS+CD4+ T cells and GL-7–ICOS–CD4+ T cells (Supplementary Figure 2B). Markers of Tfh cells (*Cxcr5* and *Tnfsf5* [encodes CD40L]) were also higher both in GC Tfh cells and in GL-7–ICOS+CD4+ T cells (Supplementary Figure 2B), which suggests that the GL-7–ICOS+CD4+ T cells likely contain pre–Tfh cells that have acquired CXCR5. *Il4* (for IgG1 class-switching) was exclusively enriched in the GC Tfh cell population (Supplementary Figure 2C), consistent with a

Figure 3. WEHI-112 treatment contracts the established germinal center (GC) response. DBA/1 mice with collagen-induced arthritis (CIA) were randomly enrolled into treatment or control groups at arthritis onset. WEHI-112 (30 mg/kg) was given daily for the next 4 days. GCs were analyzed by immunofluorescence analysis of draining lymph nodes (LNs) on day 34. **A,** Representative images of whole LN sections from mice with CIA treated with vehicle or WEHI-112. B cells (B220+) are shown in red, GC cells (GL-7+) are shown in green, and nuclear DAPI staining is shown in blue. Original magnification × 20. **B** and **C,** Quantification of GC size (GC area relative to total LN area) (**B**) and numbers of GCs per LN (**C**). Data are representative of 2 experiments with 4–5 mice per group per experiment. Symbols represent individual mice; bars show the mean ± SEM. ∗∗ = $P \leq 0.01$ by Student's unpaired t-test.

previous report (34). There was no difference in the expression level of $Il21$ (for GC B cell proliferation) (35). $Ifng$ (for IgG2a class-switching) was enriched both in GC Tfh cells and in ICOS+CD4+ T cells, but there was no clear demarcation between the 2 subsets (Supplementary Figure 2C). $Csf2$ (encodes granulocyte–macrophage colony-stimulating factor [GM-CSF]) and $Il17a$ (encodes IL-17) transcripts were less restricted to the GC Tfh cell population, compared to $Il4$ (Supplementary Figure 2C).

Thus, GL-7 expression defines a population of IL-4–producing GC Tfh cells that might drive IL-4–dependent IgG1 responses in LNs of mice with CIA. Indeed, ICOS-dependent GC Tfh cells have been shown to be indispensable for optimal maturation and selection of high-affinity IgG1 antibodies via the secretion of IL-4 (34). Complementary to the expanded GC Tfh cell population (Supplementary Figure 2A), LNs of mice with established CIA had an expanded CD19+GL-7high GC B cell population (Supplementary Figure 2D). A large proportion of GC B cells from LNs of mice with CIA had undergone IgG1 class-switching, as these cells expressed membrane-bound IgG1 (IgG1+) and were actively cycling, as shown by bromodeoxyuridine uptake (35)

(Supplementary Figure 2E). These GC B cells also exclusively expressed $Bcl6$ (a master regulator of GC B cells) and $Aicda$ (encoding activation-induced cytidine deaminase for class-switch recombination and somatic hypermutation) (36) (Supplementary Figure 2F).

WEHI-112 disrupts the established GC response in CIA. TBK-1–dependent ICOS signaling is required for GC Tfh cell differentiation from the pre–Tfh cell stage (25). In turn, GC Tfh cells support affinity maturation and selection of GC B cells for optimal production of high-affinity antibody (7,37). We examined whether WEHI-112 impaired the differentiation of CD4+ T cell populations in reactive LNs of mice with CIA. WEHI-112 did not affect the frequency of GC Tfh cells or the frequency of ICOS+CD4+ T cells during CIA (Figure 4A and B). Nevertheless, the absolute numbers of GC Tfh cells and ICOS+CD4+ T cells were reduced (Figure 4B). WEHI-112 did not alter the expression levels of $Il4$, $Il21$, or $Tnfsf5$ relative to Tfh cells taken from vehicle-treated mice (Figure 4C). However, $Ccr7$ and $Sell$ (encoding CD62L) were increased in Tfh cells from WEHI-112–treated mice (Figure 4D), which suggests relocation of GC Tfh cells away from the B cell follicle and presumably toward the T cell zone (37,38). $Klf2$ (a zinc-finger transcription factor, the down-regulation of which is associated with the ICOS-dependent Tfh cell phenotype) and $Tbx21$ (encoding the Th1 inducer T-bet transcription factor) were also increased in GC Tfh cells from WEHI-112–treated mice compared to control mice (Figure 4D), which indicates phenotypic reversion to a pre–Tfh cell stage (15,37,38). This pre–Tfh cell reversion has been noted with ICOSL blockade (15).

There was no obvious difference in $Bcl6$, $Cxcr4$, $S1P1R$, or $Cxcr5$ expression in the sorted GC Tfh cells (Figure 4E), which is consistent with CXCR5 induction being independent of ICOS (39). $Bcl6$ mRNA levels can be a poor indicator of Bcl-6 expression (40). We assessed changes in Bcl-6 protein expression by flow cytometry, comparing WEHI-112 with baricitinib (a JAK2/JAK1 inhibitor that has negligible inhibitory activity toward TBK-1) (41), to separate TBK-1– and JAK2-mediated events seen with WEHI-112. WEHI-112 or baricitinib was given for a short duration (4 days) to examine direct effects on GC responses. Consistent with gene expression profiling (see Supplementary Figure 2B, http://onlinelibrary.wiley.com/doi/10.1002/art.40670/abstract), GC Tfh cells (GL-7+ICOS+CD4+) had the highest level of Bcl-6 protein, followed by GL-7−ICOS+CD4+ and GL-7−ICOS−CD4+ T cell subsets (Figure 4F). WEHI-112, but not baricitinib, reduced Bcl-6 expression significantly both in GC Tfh cells and in GL-7−ICOS+CD4+ T cells (Figure 4F). The suppression of Bcl-6 by WEHI-112 most likely occurs through the inhibition of TBK-1 downstream of ICOS signaling, consistent with Bcl-6 induction being dependent on ICOS signaling (16). The reduction of Bcl-6 protein expression upon treatment with WEHI-112 is also consistent with increased expression of mediators of T cell migration ($Ccr7$ and $Sell$), as well as with increased expression of $Klf2$ and
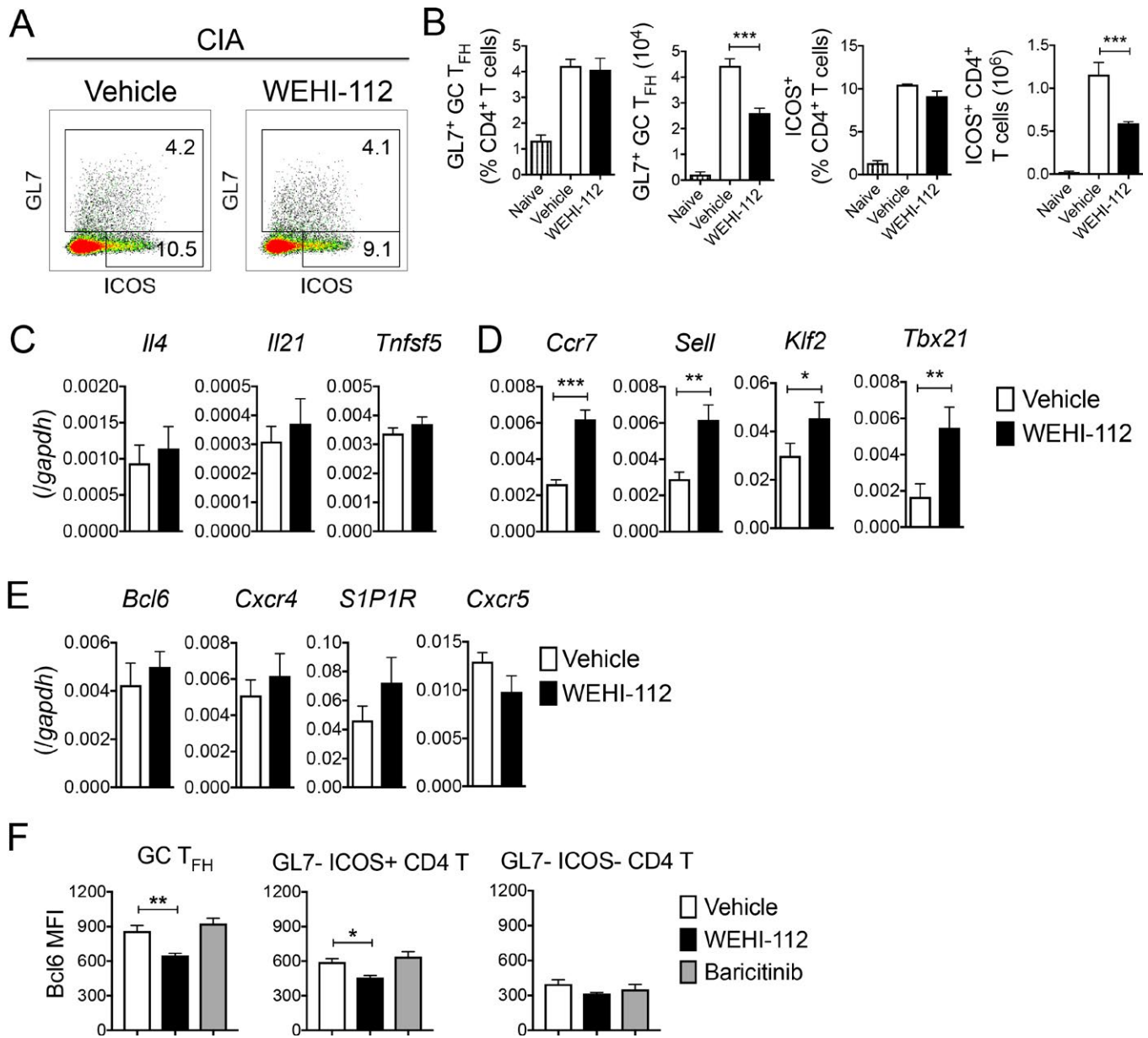
Figure 4. Reversal of the germinal center (GC) follicular helper T (Tfh) cell phenotype with WEHI-112. DBA/1 mice with collagen-induced arthritis (CIA) were randomly enrolled into treatment or control groups at arthritis onset. **A–E,** Vehicle or WEHI-112 (30 mg/kg) was given daily for the next 4 days. GC Tfh cells and inducible costimulator–positive (ICOS+) CD4+ T cells in the draining lymph nodes (LNs) were analyzed by flow cytometry. **A,** Representative flow cytometry plots indicating the frequency of GL-7+ GC Tfh cells and ICOS+ populations among CD4+ T cells. **B,** Shown are frequency and numbers of GL-7+ GC Tfh cells (left) and ICOS+CD4+ T cells (right). **C–E,** Shown is reverse transcriptase–polymerase chain reaction analysis of Tfh cell–associated genes in sorted GL-7+ GC Tfh cells isolated from vehicle- or WEHI-112–treated LNs. Data are from 2 experiments with 3–4 mice per group per experiment. **F,** Vehicle, WEHI-112, or baricitinib (30 mg/kg) was given daily for the next 4 days. Shown is the mean fluorescence intensity (MFI) of Bcl-6 on gated CD4+ T cell populations from LNs of mice treated with vehicle, WEHI-112, or baricitinib. Data are from 2 experiments with 3–4 mice per group per experiment. Values are the mean ± SEM. ∗ = $P \leq 0.05$; ∗∗ = $P \leq 0.01$; ∗∗∗ = $P \leq 0.005$ by Student's unpaired t-test. Color figure can be viewed in the online issue, which is available at http://onlinelibrary.wiley.com/doi/10.1002/art.40670/abstract.

Tbx21. This profile is suggestive of phenotypic reversion, as Bcl-6 is known to repress programming of these alternative effector T cells (42).

Of note, both WEHI-112 and baricitinib were able to suppress expression of osteoclast-associated genes, most notably *Mmp9* (see Supplementary Figure 3, http://onlinelibrary.wiley.com/doi/10.1002/art.40670/abstract). Taken together, these results also suggest that TBK-1 inhibition with WEHI-112 suppressed the GC components, while JAK inhibition alone may not be sufficient to exert such an effect in the short period of time observed.

Sustained ICOS signaling is required for maintenance of the GC Tfh cell phenotype through the inactivation of FoxO1, as
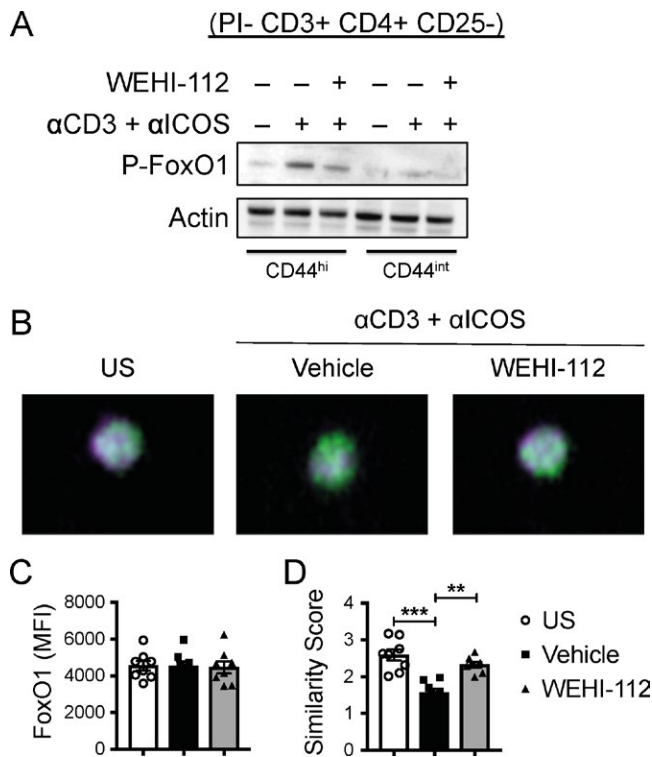
Figure 5. WEHI-112 inhibits inducible costimulator (ICOS)–mediated FoxO1 phosphorylation and inactivation. **A,** Immunoblot analysis of lysates of CD4+ T cell populations (CD44^high or CD44^intermediate) sorted as CD3+CD4+CD25– from lymph nodes (LNs) of DBA/1 mice with collagen-induced arthritis (CIA). Sorted cells were cultured and left unstimulated (US) or pretreated with vehicle or WEHI-112 for 30 minutes and stimulated with anti-CD3 (3 μg/ml) and anti-ICOS (3 μg/ml) for 10 minutes. Lysates were probed for phospho-FoxO1 or actin. Data are representative of 2 independent experiments. PI = propidium iodide. **B,** ImageStream analysis of CD4+CD44^high T cells sorted as CD3+CD4+CD25– from LNs of DBA/1 mice with CIA. Sorted cells were cultured and conditioned as described in **A**, then restimulated with anti-CD3 and anti-ICOS for 30 minutes. Total FoxO1 (in green) in unstimulated CD44^highCD4+ T cells was mainly intranuclear (nuclear stain in purple). Original magnification × 40. **C** and **D,** Mean fluorescence intensity (MFI) of green fluorescent protein (GFP)–FoxO1 (**C**) and score of similarity between DAPI and GFP–FoxO1 (**D**). In **B**–**D**, results are representative of 2 independent experiments, each of which was performed in quadruplicate. Symbols represent individual mice; bars show the mean ± SEM. ∗∗ = $P ≤ 0.01$; ∗∗∗ = $P ≤ 0.005$ by Student's paired t-test.

FoxO1 inhibits Tfh cell differentiation (14). Inactivation of FoxO1 occurs through its phosphorylation, which induces cytosolic localization and thereby relieves the negative regulation of Bcl-6 imposed by nuclear FoxO1 (14,15). We sorted CD3+CD4+CD25– T cells from LNs of mice with CIA into CD44^high and CD44^intermediate populations. Consistent with published findings (43), engagement of ICOS enhanced phosphorylation of FoxO1 in CD44^highCD4+ T cells, but not in CD44^intermediateCD4+ T cells (Figure 5A). Pretreatment with WEHI-112 reduced ICOS-driven FoxO1 phosphorylation in CD44^highCD4+ T cells (Figure 5A), consistent

with maintenance of nonphosphorylated FoxO1 in the nucleus and negative regulation of Bcl-6. This was also confirmed using ImageStream analysis. Total FoxO1 in unstimulated CD44^high-CD4+ T cells was mainly intranuclear. Agonistic anti-CD3 and anti-ICOS monoclonal antibodies induced FoxO1 cytoplasmic translocation, but nuclear egress was prevented in the presence of WEHI-112 (Figures 5B and D), without affecting overall FoxO1 expression (Figure 5C).

Proportion and absolute number of established secondary GC B cells were reduced with WEHI-112 treatment in LNs of mice with CIA (Figure 6A). However, proliferative activity of the secondary GC B cells was not altered (Figure 6B). Further supporting the possibility of phenotypic reversion of GC Tfh cells, sorted GC B cells from WEHI-112–treated mice with CIA expressed lower mRNA levels of GC function regulators, *Aicda* and *Bcl6*, but not *Cxcr5*, relative to cells isolated from vehicle-treated mice (Figure 6C). Bcl-6 protein in GC B cells was also reduced with WEHI-112 treatment, but not with baricitinib treatment (Figure 6D). These observations in the CIA model (Figures 4 and 5) are similar to the alterations of Tfh cell and GC B cell phenotypes following ICOSL blockade (15), as TBK-1 inhibition with WEHI-112 resulted in the induction of chemokine receptor genes associated with alternative effector T cell fate. Consistent with GC size being directly linked with the magnitude and quality of humoral responses (44), inhibition of the GC reaction in CIA with WEHI-112 correlated with reduced arthritogenic antibody levels and a marked therapeutic effect on inflammatory arthritis.

DISCUSSION

Although the pathogenic sequence of events leading to breaches of immunologic tolerance is likely to vary between RA patients, most patients have circulating, class-switched autoantibodies (e.g., ACPAs), and this is a well-documented risk factor for greater disease severity (45). Therapeutic B cell depletion using anti-CD20 antibody (rituximab) underscores the importance of B cells in maintaining disease activity in RA. However, rituximab mainly targets short-lived antibody-secreting CD20+ plasma cells, leaving long-lived plasma cells intact (46). GC-mediated somatic mutations and clonal selection are responsible for the generation of affinity-matured, autoantibody-producing long-lived plasma cells (7,47,48). Thus, inhibition of ongoing GCs that contribute to autoreactive plasma cell development offers therapeutic potential (3).

Optimal GC development and maintenance is positively regulated by type I IFNs, IL-6, and ICOS signaling (13–16,49,50). Because TBK-1 is a common denominator of these pathways (24,25), TBK-1 inhibition might be therapeutically effective, even in established autoimmune diseases. To this end, we assessed the therapeutic use of a semiselective tool compound inhibitor—WEHI-112. We confirmed WEHI-112 as a TBK-1 inhibitor in vitro, as it suppressed the induction of *Ifnb*
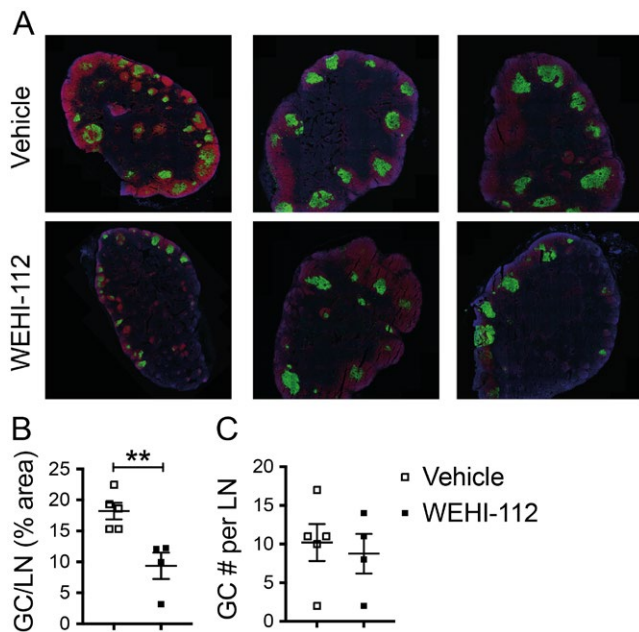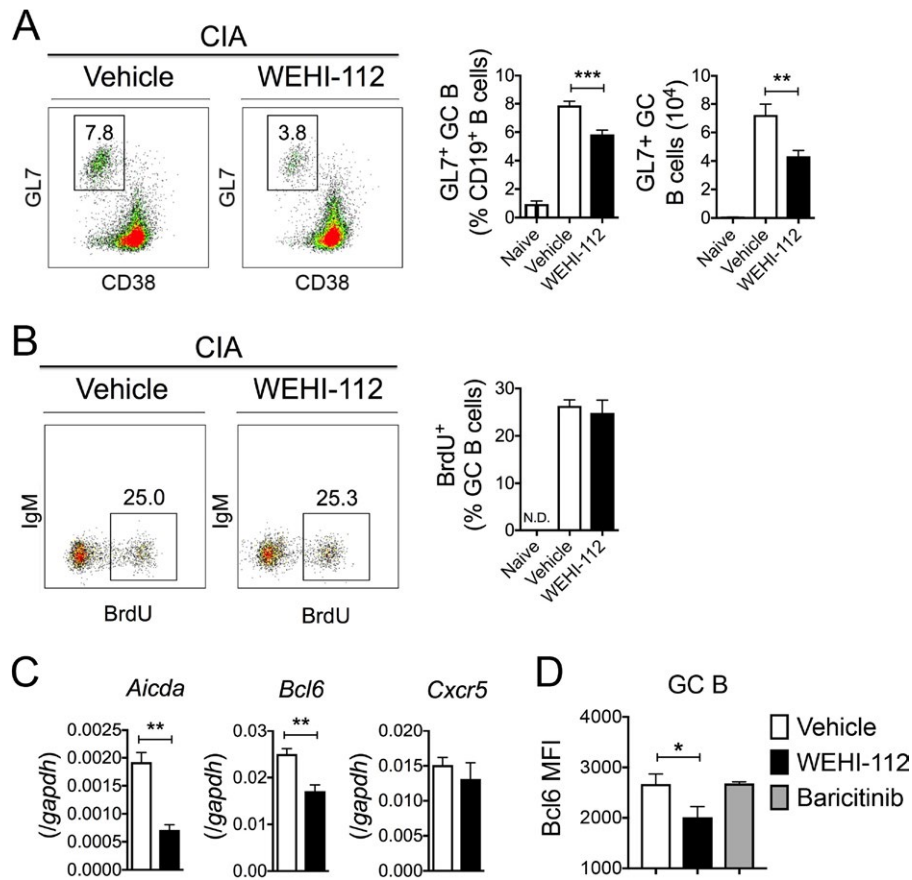
Figure 6. WEHI-112 disrupts the established germinal center (GC) B cell response. DBA/1 mice with collagen-induced arthritis (CIA) were randomly enrolled at arthritis onset into treatment or control groups. Vehicle or WEHI-112 (30 mg/kg) was given daily for the next 4 days. GC B cells in the lymph nodes (LNs) were analyzed by flow cytometry. **A,** Representative flow cytometry plots and bar graph indicating the frequency of GL-7+ GC B cells among CD19+ B cells and numbers of GL-7+ GC B cells. **B,** Representative flow cytometry plots and bar graph indicating the frequency of bromodeoxyuridine-positive (BrdU+) cells among GC B cells. ND = not detectable. **C,** Reverse transcriptase–polymerase chain reaction analysis of GC-associated genes in sorted GL-7+ GC B cells isolated from LNs of mice treated with vehicle or WEHI-112. **D,** Mean fluorescence intensity (MFI) of Bcl-6 on gated GC B cells from LNs of mice treated with vehicle, WEHI-112, or baricitinib. Data are from 2 experiments with 3–4 mice per group per experiment. Values are the mean ± SEM. $* = P \leq 0.05$; $** = P \leq 0.01$; $*** = P \leq 0.005$ by Student's unpaired t-test. Color figure can be viewed in the online issue, which is available at http://onlinelibrary.wiley.com/doi/10.1002/art.40670/abstract.

and *Il6*. In vivo, WEHI-112 suppressed arthritis in autoantibody-dependent CIA, but had much less effect in T cell–mediated AIA or in the T cell– and B cell–independent K/BxN STIA model. The varied effects seen in these arthritis models indicate that discrete immune mechanisms are differentially impacted by WEHI-112 treatment. CIA is a T cell– and B cell–dependent, GC-driven, autoantibody-mediated arthritis model, while the AIA model is entirely independent of the B cell compartment and antibody responses (29–31), and the STIA model is entirely independent of adaptive immune mechanisms (5).

Abrogated CIA was accompanied by reduced levels of arthritogenic, collagen-specific IgG1 and IgG2b isotypes, *Il6* and *Ccl5* expression, and GC size in reactive LNs. While IL-6 is well known for its importance in humoral responses and inflammation (13), CCL5 (RANTES) has not been extensively described in the context of humoral autoimmunity. Nevertheless, CCL5 blockade has been shown to reduce antigen-specific antibody respons-

es through unknown mechanisms (51). Although we could not detect type I IFN induction at the time point examined in LNs of mice with CIA, TBK-1 inhibition has been shown to reduce the type I IFN signature and alleviate disease in the three-prime repair exonuclease 1–knockout murine model of SLE, through inhibition of the cGAS/STING pathway (52). Other studies demonstrate synergies between IL-6 and type I IFN by driving optimal Tfh cell polarization (50) and type I IFN–dependent IL-6 induction in DCs that supports GC-driven affinity maturation of antibodies (49). Taken together, we propose that TBK-1 inhibition reduces production of cytokines associated with humoral immunity, particularly IL-6, but likely type I IFNs as well.

The magnitude and quality of humoral responses is directly linked with GC size (44). Consistent with this notion, inhibition of the GC reaction with WEHI-112 corresponded to reduced arthritogenic antibody levels and disease severity in CIA. Productive GC maintenance requires cooperative signals of GC Tfh cells

and GC B cells through cytokines and costimulatory molecules (7,48). While the differentiation of naive CD4+ T cells into Bcl-6+ nascent Tfh cells requires ICOS/phosphatidylinositol 3-kinase signaling, mature Bcl-6^{high} GC Tfh cell differentiation and maintenance require ICOS/ICOSL signaling through TBK-1 (15,25).

Bcl-6 maintains Tfh cell commitment by repressing effector T cell programs (42). We showed that GC Tfh cells from WEHI-112–treated mice with CIA displayed phenotypic reversion toward an effector, Th1-like population, as indicated by the up-regulation of *Tbx21*, *Ccr7*, and *Sell* (which are normally repressed in Tfh cells) and by accompanying reduction of Bcl-6 protein expression. These findings are consistent with the reacquisition of an effector T cell phenotype in the absence of ICOS/ICOSL signaling (15) and with reduced Bcl-6–mediated repression of effector T cell genes (42). This effect of WEHI-112 on the GC response is most likely mediated through TBK-1 inhibition, because in our study the JAK2 inhibitor baricitinib did not alter Bcl-6 expression in Tfh cells or GC B cells, although it did inhibit expression of matrix metalloproteinase 9 to a similar degree in an osteoclastogenesis assay. Of note, conditional TBK-1 deletion in CD4+ T cells has been shown to augment effector Th1 responses, and it renders these effector T helper cells incapable of exiting the secondary lymphoid tissue in experimental autoimmune encephalomyelitis (a model of multiple sclerosis), due to the greatly enhanced expression of CCR7 and CD62L (53).

Tfh cell differentiation also requires FoxO1 inactivation downstream of ICOS (14). WEHI-112 blocked ICOS-mediated phosphorylation and subsequent nuclear egress (inactivation) of FoxO1, consistent with TBK-1 being downstream of ICOS signaling (25). Enforced nuclear retention of FoxO1 inhibits Tfh cell development through negative regulation of Bcl-6 (14), and WEHI-112 recapitulated this phenotype. Complementing the changes in GC Tfh cells with WEHI-112, GC B cell responses were also abrogated in the CIA model. The effect of WEHI-112 in the CIA model resembles ICOSL blockade or deficiency, with reversion of the Tfh cell phenotype, dissolution of GCs, and abrogation of downstream GC-dependent IgG antibody responses to T cell–dependent antigens (15). It has been shown that even late-stage blockade of the ICOSL/ICOS pathway ameliorates autoantibody-driven disease models, including CIA, spontaneous K/BxN arthritis, proteoglycan-induced arthritis, (NZB × NZW)F1 lupus mice, and spontaneous lupus in sanroque mice (17–19). Thus, TBK-1 inhibition with WEHI-112 may recapitulate similar therapeutic effects of ICOSL blockade in humoral autoimmunity driven by GCs.

Although the effects of WEHI-112 observed in this study appear to be relatively selective to TBK-1 inhibition and downstream cytokine and GC responses, it is important to note that WEHI-112 is not completely TBK-1 selective, as it also targets IKKε and JAK2. The JAK2 inhibitor baricitinib did not abrogate Bcl-6 expression in GC Tfh cells and GC B cells, which suggests that JAK2 inhibition is unlikely to explain the efficacy of WE-

HI-112 in the GC reaction of CIA. The observed effects on Tfh cell phenotype may also be mediated through the IKKε pathway. However, we could not separate TBK-1– and/or IKKε-mediated effects of WEHI-112 on the Tfh cell phenotype as there are no IKKε-specific inhibitors. Comparative studies using targeted deletion of TBK-1 or IKKε in CD4+ T cells would be of interest. Although these inhibitory effects on IKKε and JAK2 seem unlikely to explain the therapeutic effect of WEHI-112, some inhibition of IKKε and JAK2 may actually provide synergistic therapeutic benefit. For example, IKKε appears to be involved in optimal Th17 function in response to IL-1β (54), and JAK2 is known to be downstream of several key inflammatory cytokines, such as IL-6, IL-12/23, GM-CSF, and IFNγ (55,56). Th17 cells in the early GC have been shown to modulate sialylation and thus the arthritogenicity of GC-derived autoantibodies (8). In summary, we propose that TBK-1 inhibition in RA, and potentially in other GC-associated humoral autoimmune diseases, may exert beneficial effects by reducing the pool of GC-derived, autoreactive long-lived plasma cell and memory B cell populations, as well as by inhibiting inflammatory cytokine signaling.

AUTHOR CONTRIBUTIONS

All authors were involved in drafting the article or revising it critically for important intellectual content, and all authors approved the final version to be published. Dr. Wicks had full access to all of the data in the study and takes responsibility for the integrity of the data and the accuracy of the data analysis.
Study conception and design. Louis.
Acquisition of data. Louis, Ngo, D'Silva, Hansen, Phillipson, Jousset, Novello.
Analysis and interpretation of data. Louis, Ngo, D'Silva, Hansen, Phillipson, Jousset, Novello, Segal, Lawlor, Burns, Wicks.

REFERENCES

1. Smolen JS, Aletaha D, McInnes IB. Rheumatoid arthritis. Lancet 2016;388:2023–38.

2. Arbuckle MR, McClain MT, Rubertone MV, Scofield RH, Dennis GJ, James JA, et al. Development of autoantibodies before the clinical onset of systemic lupus erythematosus. N Engl J Med 2003;349:1526–33.

3. Suurmond J, Diamond B. Autoantibodies in systemic autoimmune diseases: specificity and pathogenicity. J Clin Invest 2015;125:2194–202.

4. Rutgers A, Meyers KE, Canziani G, Kalluri R, Lin J, Madaio MP. High affinity of anti-GBM antibodies from Goodpasture and transplanted Alport patients to α3(IV)NC1 collagen. Kidney Int 2000;58:115–22.

5. Maccioni M, Zeder-Lutz G, Huang H, Ebel C, Gerber P, Hergueux J, et al. Arthritogenic monoclonal antibodies from K/BxN mice. J Exp Med 2002;195:1071–7.

6. Ji H, Pettit A, Ohmura K, Ortiz-Lopez A, Duchatelle V, Degott C, et al. Critical roles for interleukin 1 and tumor necrosis factor α in antibody-induced arthritis. J Exp Med 2002;196:77–85.

7. Ueno H, Banchereau J, Vinuesa CG. Pathophysiology of T follicular helper cells in humans and mice. Nat Immunol 2015;16:142–52.

8. Pfeifle R, Rothe T, Ipseiz N, Scherer HU, Culemann S, Harre U, et al. Regulation of autoantibody activity by the IL-23-TH17 axis determines the onset of autoimmune disease. Nat Immunol 2017;18:104–13.

9. Semerano L, Minichiello E, Bessis N, Boissier MC. Novel immunotherapeutic avenues for rheumatoid arthritis. Trends Mol Med 2016;22:214–29.

10. Phan TG, Paus D, Chan TD, Turner ML, Nutt SL, Basten A, et al. High affinity germinal center B cells are actively selected into the plasma cell compartment. J Exp Med 2006;203:2419–24.

11. Rönnblom L, Alm GV, Eloranta ML. Type I interferon and lupus. Curr Opin Rheumatol 2009;21:471–7.

12. Nordmark G, Eloranta ML, Ronnblom L. Primary Sjogren's syndrome and the type I interferon system. Curr Pharm Biotechnol 2012;13:2054–62.

13. Hunter CA, Jones SA. IL-6 as a keystone cytokine in health and disease. Nat Immunol 2015;16:448–57.

14. Stone EL, Pepper M, Katayama CD, Kerdiles YM, Lai CY, Emslie E, et al. ICOS coreceptor signaling inactivates the transcription factor FOXO1 to promote Tfh cell differentiation. Immunity 2015;42:239–51.

15. Weber JP, Fuhrmann F, Feist RK, Lahmann A, Al Baz MS, Gentz LJ, et al. ICOS maintains the T follicular helper cell phenotype by downregulating Kruppel-like factor 2. J Exp Med 2015;212:217–33.

16. Choi YS, Kageyama R, Eto D, Escobar TC, Johnston RJ, Monticelli L, et al. ICOS receptor instructs T follicular helper cell versus effector cell differentiation via induction of the transcriptional repressor Bcl6. Immunity 2011;34:932–46.

17. Hamel KM, Cao Y, Olalekan SA, Finnegan A. B cell-specific expression of inducible costimulator ligand is necessary for the induction of arthritis in mice. Arthritis Rheumatol 2014;66:60–7.

18. Hu YL, Metz DP, Chung J, Siu G, Zhang M. B7RP-1 blockade ameliorates autoimmunity through regulation of follicular helper T cells. J Immunol 2009;182:1421–8.

19. Iwai H, Kozono Y, Hirose S, Akiba H, Yagita H, Okumura K, et al. Amelioration of collagen-induced arthritis by blockade of inducible costimulator-B7 homologous protein costimulation. J Immunol 2002;169:4332–9.

20. Wong SC, Oh E, Ng CH, Lam KP. Impaired germinal center formation and recall T-cell-dependent immune responses in mice lacking the costimulatory ligand B7-H2. Blood 2003;102:1381–8.

21. Liu S, Cai X, Wu J, Cong Q, Chen X, Li T, et al. Phosphorylation of innate immune adaptor proteins MAVS, STING, and TRIF induces IRF3 activation. Science 2015;347:aaa2630.

22. Herman M, Ciancanelli M, Ou YH, Lorenzo L, Klaudel-Dreszler M, Pauwels E, et al. Heterozygous TBK1 mutations impair TLR3 immunity and underlie herpes simplex encephalitis of childhood. J Exp Med 2012;209:1567–82.

23. Ishikawa H, Ma Z, Barber GN. STING regulates intracellular DNA-mediated, type I interferon-dependent innate immunity. Nature 2009;461:788–92.

24. Ishii KJ, Kawagoe T, Koyama S, Matsui K, Kumar H, Kawai T, et al. TANK-binding kinase-1 delineates innate and adaptive immune responses to DNA vaccines. Nature 2008;451:725–9.

25. Pedros C, Zhang Y, Hu JK, Choi YS, Canonigo-Balancio AJ, Yates JR III, et al. A TRAF-like motif of the inducible costimulator ICOS controls development of germinal center TFH cells via the kinase TBK1. Nat Immunol 2016;17:825–33.

26. Clark K, Peggie M, Plater L, Sorcek RJ, Young ER, Madwed JB, et al. Novel cross-talk within the IKK family controls innate immunity. Biochem J 2011;434:93–104.

27. Reilly SM, Chiang SH, Decker SJ, Chang L, Uhm M, Larsen MJ, et al. An inhibitor of the protein kinases TBK1 and IKK-varepsilon improves obesity-related metabolic dysfunctions in mice. Nat Med 2013;19:313–21.

28. Clark K, Plater L, Peggie M, Cohen P. Use of the pharmacological inhibitor BX795 to study the regulation and physiological roles of TBK1 and IκB kinase epsilon: a distinct upstream kinase mediates Ser-172 phosphorylation and activation. J Biol Chem 2009;284:14136–46.

29. Svensson L, Jirholt J, Holmdahl R, Jansson L. B cell-deficient mice do not develop type II collagen-induced arthritis (CIA). Clin Exp Immunol 1998;111:521–6.

30. Corthay A, Johansson A, Vestberg M, Holmdahl R. Collagen-induced arthritis development requires α β T cells but not γ δ T cells: studies with T cell-deficient (TCR mutant) mice. Int Immunol 1999;11:1065–73.

31. Wong PK, Quinn JM, Sims NA, van Nieuwenhuijze A, Campbell IK, Wicks IP. Interleukin-6 modulates production of T lymphocyte-derived cytokines in antigen-induced arthritis and drives inflammation-induced osteoclastogenesis. Arthritis Rheum 2006;54:158–68.

32. Dahdah A, Habir K, Nandakumar KS, Saxena A, Xu B, Holmdahl R, et al. Germinal center B cells are essential for collagen-induced arthritis. Arthritis Rheumatol 2018;70:193–203.

33. Kerfoot SM, Yaari G, Patel JR, Johnson KL, Gonzalez DG, Kleinstein SH, et al. Germinal center B cell and T follicular helper cell development initiates in the interfollicular zone. Immunity 2011;34:947–60.

34. Reinhardt RL, Liang HE, Locksley RM. Cytokine-secreting follicular T cells shape the antibody repertoire. Nat Immunol 2009;10:385–93.

35. Zotos D, Coquet JM, Zhang Y, Light A, D'Costa K, Kallies A, et al. IL-21 regulates germinal center B cell differentiation and proliferation through a B cell-intrinsic mechanism. J Exp Med 2010;207:365–78.

36. Basso K, Schneider C, Shen Q, Holmes AB, Setty M, Leslie C, et al. BCL6 positively regulates AID and germinal center gene expression via repression of miR-155. J Exp Med 2012;209:2455–65.

37. Hardtke S, Ohl L, Förster R. Balanced expression of CXCR5 and CCR7 on follicular T helper cells determines their transient positioning to lymph node follicles and is essential for efficient B-cell help. Blood 2005;106:1924–31.

38. Haynes NM, Allen CD, Lesley R, Ansel KM, Killeen N, Cyster JG. Role of CXCR5 and CCR7 in follicular Th cell positioning and appearance of a programmed cell death gene-1high germinal center-associated subpopulation. J Immunol 2007;179:5099–108.

39. Odegard JM, Marks BR, DiPlacido LD, Poholek AC, Kono DH, Dong C, et al. ICOS-dependent extrafollicular helper T cells elicit IgG production via IL-21 in systemic autoimmunity. J Exp Med 2008;205:2873–86.

40. Kitano M, Moriyama S, Ando Y, Hikida M, Mori Y, Kurosaki T, et al. Bcl6 protein expression shapes pre-germinal center B cell dynamics and follicular helper T cell heterogeneity. Immunity 2011;34:961–72.

41. Klaeger S, Heinzlmeir S, Wilhelm M, Polzer H, Vick B, Koenig PA, et al. The target landscape of clinical kinase drugs. Science 2017;358:eaan4368.

42. Hatzi K, Nance JP, Kroenke MA, Bothwell M, Haddad EK, Melnick A, et al. BCL6 orchestrates Tfh cell differentiation via multiple distinct mechanisms. J Exp Med 2015;212:539–53.

43. Xiao N, Eto D, Elly C, Peng G, Crotty S, Liu YC, et al. The E3 ubiquitin ligase Itch is required for the differentiation of follicular helper T cells. Nat Immunol 2014;15:657–66.

44. Baumjohann D, Preite S, Reboldi A, Ronchi F, Ansel KM, Lanzavecchia A, et al. Persistent antigen and germinal center B cells sustain T follicular helper cell responses and phenotype. Immunity 2013;38:596–605.

45. Willemze A, Trouw LA, Toes RE, Huizinga TW. The influence of ACPA status and characteristics on the course of RA. Nat Rev Rheumatol 2012;8:144–52.

46. Huang H, Benoist C, Mathis D. Rituximab specifically depletes short-lived autoreactive plasma cells in a mouse model of inflammatory arthritis. Proc Natl Acad Sci U S A 2010;107:4658–63.

47. Hiepe F, Dörner T, Hauser AE, Hoyer BF, Mei H, Radbruch A. Long-lived autoreactive plasma cells drive persistent autoimmune inflammation. Nat Rev Rheumatol 2011;7:170–8.

48. Victora GD, Nussenzweig MC. Germinal centers. Annu Rev Immunol 2012;30:429–57.

49. Cucak H, Yrlid U, Reizis B, Kalinke U, Johansson-Lindbom B. Type I interferon signaling in dendritic cells stimulates the development of lymph-node-resident T follicular helper cells. Immunity 2009;31:491–501.

50. Riteau N, Radtke AJ, Shenderov K, Mittereder L, Oland SD, Hieny S, et al. Water-in-oil-only adjuvants selectively promote T follicular helper cell polarization through a type I IFN and IL-6-dependent pathway. J Immunol 2016;197:3884–93.

51. Palaniappan R, Singh S, Singh UP, Singh R, Ades EW, Briles DE, et al. CCL5 modulates pneumococcal immunity and carriage. J Immunol 2006;176:2346–56.

52. Hasan M, Dobbs N, Khan S, White MA, Wakeland EK, Li QZ, et al. Cutting edge: inhibiting TBK1 by compound II ameliorates autoimmune disease in mice. J Immunol 2015;195:4573–7.

53. Yu J, Zhou X, Chang M, Nakaya M, Chang JH, Xiao Y, et al. Regulation of T-cell activation and migration by the kinase TBK1 during neuroinflammation. Nat Commun 2015;6:6074.

54. Gulen MF, Bulek K, Xiao H, Yu M, Gao J, Sun L, et al. Inactivation of the enzyme GSK3α by the kinase IKKi promotes AKT-mTOR signaling pathway that mediates interleukin-1-induced Th17 cell maintenance. Immunity 2012;37:800–12.

55. O'Shea JJ, Kontzias A, Yamaoka K, Tanaka Y, Laurence A. Janus kinase inhibitors in autoimmune diseases. Ann Rheum Dis 2013;72 Suppl 2:ii111–5.

56. Schwartz DM, Bonelli M, Gadina M, O'Shea JJ. Type I/II cytokines, JAKs, and new strategies for treating autoimmune diseases. Nat Rev Rheumatol 2016;12:25–36.

AMERICAN COLLEGE
OF RHEUMATOLOGY
EDUCATION · TREATMENT · RESEARCH

ADAM15 in Apoptosis Resistance of Synovial Fibroblasts: Converting Fas/CD95 Death Signals Into the Activation of Prosurvival Pathways by Calmodulin Recruitment

Tomasz Janczi,[1] Beate B. Böhm,[1] Yuliya Fehrl,[1] Pangrazio DeGiacomo,[1] Raimund W. Kinne,[2] and Harald Burkhardt[3]

Objective. To investigate mechanisms underlying the capability of ADAM15 to transform FasL-mediated death-inducing signals into prosurvival activation of Src and focal adhesion kinase (FAK) in rheumatoid arthritis synovial fibroblasts (RASFs).

Methods. Caspase 3/7 activity and apoptosis rate were determined in RASFs and ADAM15-transfected T/C28a4 cells upon Fas/CD95 triggering using enzyme assays and annexin V staining. Phosphorylated Src and FAK were analyzed by immunoblotting. Interactions of ADAM15 and CD95 with calmodulin (CaM), Src, or FAK were analyzed by pull-downs using CaM–Sepharose and coimmunoprecipitations with specific antibodies. Protein binding assays were performed using recombinant CaM and ADAM15. Immunofluorescence was performed to investigate subcellular colocalization of ADAM15, Fas/CD95, and CaM.

Results. The antiapoptotic effect of ADAM15 in FasL-stimulated cells was demonstrated either by increased apoptosis of cells transfected with an ADAM15 construct lacking the cytoplasmic domain compared to cells transfected with full-length ADAM15 or by reduced apoptosis resistance of RASFs upon RNA interference silencing of ADAM15. Fas ligation triggered a Ca^{2+} release-activated Ca^{2+}/calcium release-activated calcium channel protein 1 (CRAC/Orai1) channel–dependent CaM recruitment to Fas/CD95 and ADAM15 in the cell membrane. Simultaneously, Src associated with CaM was shown to become engaged in the ADAM15 complex also containing cytoplasmic-bound FAK. Accordingly, Fas ligation in RASFs led to ADAM15-dependent phosphorylation of Src and FAK, which was associated with increased survival. Pharmacologic interference with either the CaM inhibitor trifluoperazine or the CRAC/Orai inhibitor BTP-2 simultaneously applied with FasL synergistically enhanced Fas-mediated apoptosis in RASFs.

Conclusion. ADAM15 provides a scaffold for formation of CaM-dependent prosurvival signaling complexes upon CRAC/Orai coactivation by FasL-induced death signals and a potential therapeutic target to break apoptosis resistance in RASFs.

INTRODUCTION

ADAM15 is a transmembrane-anchored multidomain protein belonging to the family of disintegrin metalloproteinases (1). Its extracellular part is composed of several domains, mainly a metalloproteinase domain that is kept inactive by a prodomain, a disintegrin domain, and a cytosolic tail. Its expression is up-regulated not only in several solid tumors, where it is tightly associated with the progression of aggressive forms of cancer (2,3), but also in inflamed synovial membranes of rheuma-

toid arthritis (RA), with high levels in the hyperplastic lining (4). ADAM15 has been shown to contribute significantly to apoptosis resistance of RA synovial fibroblasts (RASFs) by inducing prosurvival Src and focal adhesion kinase (FAK) signaling (5). Down-regulation of ADAM15 and/or inhibition of Src/FAK by tyrosine kinase inhibitors (e.g., dasatinib) markedly sensitized RASFs to apoptotic cell death. Moreover, ADAM15 is capable of up-regulating X-linked inhibitor of apoptosis protein (XIAP), a potent inhibitor of activated caspase 3, under conditions of genotoxic stress (6).

Address correspondence to Harald Burkhardt, MD, Goethe University Frankfurt, Department of Internal Medicine II, Division of Rheumatology, Theodor-Stern-Kai 7, 60590 Frankfurt am Main, Germany. E-mail: harald.burkhardt@kgu.de.

RA is a systemic immune-mediated disease predominantly manifesting in diarthrodial joints as a chronic inflammatory process inevitably leading to destruction of cartilage and bone if left improperly treated. Synovial inflammation is fueled by infiltrating cells of innate and adaptive immunity in concert with activated resident RASFs that display an aggressive/transformed phenotype (7). These RASFs critically contribute to tissue destruction in RA pathogenesis by producing proinflammatory cytokines as well as extracellular matrix–degrading proteinases (8). Their inherent capability to resist a repellent synovial environment enriched with oxygen radicals and other toxic metabolites at low oxygen tension resembles cellular phenotypes in malignancies. Despite the fact that RASFs do not fulfill cytologic criteria of malignancy, they share with tumor cells the property of increased resistance to apoptosis that contributes to hyperplasia and invasive growth of the inflamed synovial tissue into the adjacent cartilage and bone (9). Currently available disease-modifying drugs do not directly target the dysregulated RASF phenotype and leave a therapeutic gap as a challenge for the development of new treatment approaches.

Potential new pharmacologic strategies need to address the phenotypic characteristic of RASFs to resist apoptosis induction via the membrane-anchored tumor necrosis factor receptor (TNFR) superfamily member Fas/CD95 (10,11). Interaction with its trimeric ligand FasL initiates homotrimerization of the inactive monomeric Fas/CD95 and subsequent trimer clustering in a polarized plasma membrane structure known as the CD95-Cap (12). Further recruitment of FADD and formation of a death-inducing signaling complex (DISC) is triggered to activate a caspase cascade (12). However, Fas/CD95 ligation also triggers Ca^{2+} influx through specialized plasma membrane Ca^{2+} release-activated Ca^{2+} (CRAC) channels formed by subunits of calcium release-activated calcium channel protein 1 (Orai1), thus allowing Ca^{2+} to selectively enter the cell (13). This Fas-mediated Ca^{2+} influx delays the first steps in apoptosis execution by preventing the recruitment of FADD into the DISC and subsequent transmission of the apoptotic signal (14).

Calmodulin (CaM), a ubiquitious, highly conserved protein, is a crucial calcium sensor that plays a major role in the transmission of calcium signals and regulation of diverse target proteins in eukaryotes (15,16). CaM exists in 2 different conformations, both of which can be involved in protein interactions—a Ca^{2+}-free apo-CaM with an overall more compact, closed structure, and a Ca^{2+}-bound form, as the most frequently characterized in CaM–protein interactions (17).

Previously, we demonstrated that Fas stimulation by FasL led to enhanced phosphorylation of Src and FAK in RASFs that disappeared upon RNA interference (RNAi) silencing of ADAM15, and that ADAM15-mediated Src/FAK activation was associated with significantly reduced rates of apoptosis (5). The purpose of the current study was to elucidate how ADAM15 can transform FasL-induced death signals into prosurvival triggering of Src/FAK phosphorylation. Our results reveal that the cytoplasmic domain of ADAM15 provides a scaffold for FAK and Src

binding complemented by the engagement of CaM following its coactivation in the context of the apoptotic signal. Thus, Fas ligation triggers a CRAC/Orai-dependent CaM recruitment to Fas/CD95 and ADAM15 in the cell membrane. Simultaneously, Src associated with CaM was shown to become engaged in the ADAM15 complex that also contains cytoplasmic-bound FAK. This ADAM15-dependent formation of a prosurvival signaling complex in the CD95-Cap was associated with increased survival. The pathway, however, was shown to be sensitive to pharmacologic inhibition by either the CaM inhibitor trifluoperazine (TFP) or the CRAC/Orai channel inhibitor BTP-2 that synergistically enhanced Fas-mediated apoptosis in RASFs upon simultaneous application with the death-inducing FasL.

MATERIALS AND METHODS

Materials. Mouse and goat anti-ADAM15 antibodies were from R&D Systems. Rabbit anti–p-Y416 Src, rabbit anti-Src, and rabbit anti–p-ERK1/2 were from Cell Signaling Technology. Anti–p-Y397 FAK was from BD Biosciences. Anti–p-Y576/577 FAK, anti–p-Y861 FAK, and rabbit antitubulin were from Abcam. Rabbit anti-CD95 (C-20) and mouse anti-CD95 (B-10) were from Santa Cruz Biotechnology. Activating anti-Fas/CD95 (CH-11) and mouse anti-FAK (4.47) were from Merck Millipore, and mouse anti-CaM (2D1) was from Invitrogen. TFP and BTP-2 were from Santa Cruz Biotechnology. FasL and recombinant CaM were from Enzo Life Sciences.

Cell culture. The ADAM15-transfected chondrocyte cell line T/C28a4 (18) and the synovial fibroblast cell line K4IM (5) were grown in Dulbecco's modified Eagle's medium (DMEM) supplemented with 10% heat-inactivated fetal calf serum (FCS) to a density of ~4×10^6 cells/75 cm^2 tissue culture flask. All tissue culture reagents were from Invitrogen.

RA synovial cell culture. Synovial tissue was obtained during joint replacement/arthroscopic synovectomy at the Clinic of Orthopedics, University Hospital Jena. All patients met the American College of Rheumatology 1987 criteria for RA (19) and had established RA of >3 years' duration with an erosive disease course. Seventy percent of patients were positive for rheumatoid factor and/or anti–cyclic citrullinated peptide. Eighty percent of patients were treated with conventional disease-modifying antirheumatic drugs (DMARDs) (methotrexate [MTX] or leflunomide); 1 patient received combined treatment with both DMARDs, and 1 patient received etanercept plus MTX. DMARD therapy was tapered prior to joint surgery according to the recommendations of the German Society for Orthopedic Rheumatology. Thus, none of the patients were receiving any antirheumatic treatment besides nonsteroidal antiinflammatory drugs and/or prednisolone at a dosage of ≤10 mg/day at the time point when synovial tissue specimens were obtained. RASFs were isolated and grown

in DMEM containing 10% FCS, as previously described (5), and cells at passages 3–6 were used for all experiments.

Determination of caspase 3/7 activity. ADAM15-transfected T/C28a4 cells (1×10^4) and RASFs (2.5×10^3) were seeded into wells of half area 96-well plates and grown in DMEM containing 10% FCS for 24 hours. After removal of the medium, cells were treated with FasL (100 ng/ml) for various time intervals at 37°C. Caspase 3/7 activity was measured with a CaspaseGlo 3/7 Assay from Promega using a Mithras LB940 plate reader (Berthold).

Preparation of cell lysates and Western blotting. Cell lysates were prepared and immunoblotted as described previously (5). Signals were obtained with chemiluminescence reader Fusion FX (Vilber Lourmat), and signal densities were evaluated using ImageJ software (National Institutes of Health). Results of the densitometric analysis were used to calculate changes in protein levels.

CaM–Sepharose pull-down. Cells were lysed in lysis buffer (25 mM HEPES, pH 7.2, 150 mM NaCl, 1% Triton X-100, and proteinase inhibitor cocktail; Sigma-Aldrich) and incubated with Calmodulin Sepharose 4B (GE Healthcare) or with control Sepharose CL-4B (GE Healthcare) for 2 hours at 4°C, and either 1 mM CaCl$_2$ or 1 mM EDTA was added. The beads were washed 5 times with lysis buffer and analyzed by immunoblotting.

Immunoprecipitation. Cell lysates (500 μg) were incubated with anti-CD95 (CH-11), goat anti-ADAM15, anti-Src, and anti-CaM antibodies (1 μg/ml each) overnight at 4°C and precipitated using IgM–sepharose (Sigma) for CH-11 and protein G–agarose for all other antibodies, washed 3 times in lysis buffer, and analyzed by immunoblotting. For analysis of Fas-triggered protein complexes, cells were trypsinized, and suspended cells (2×10^6) were stimulated with anti-CD95 (CH-11; 1 μg/ml) for various time intervals at 37°C and lysed in lysis buffer for 1 hour on ice. In control cells, CH-11 was added to lysates at a final concentration of 1 μg/ml to immunoprecipitate unstimulated Fas receptors. After centrifugation at 15,000g for 10 minutes, supernatants were precipitated with 20 μl goat anti-mouse IgM–Sepharose overnight at 4°C.

Determination of total apoptosis. Apoptosis was analyzed using an annexin V–fluorescein isothiocyanate (FITC) assay kit according to the supplier's instructions (Cayman Chemical). RASFs (1×10^4) were grown in chamber slides (Sarstedt) for 24 hours and stimulated with FasL (100 ng/ml) at the indicated time points. Apoptotic cells were stained using FITC-conjugated annexin V. At least 200 cells were counted, and the percentage of cells staining positive for annexin V was determined.

RNAi silencing of ADAM15 in RASFs. ADAM15 was silenced in RASFs using Silencer Select predesigned and validated small interfering RNAs (siRNAs) for ADAM15 (Ambion/Applied Biosystems) as described previously (5). Nonsilencing siRNA Control #1 from Ambion was used as the negative control.
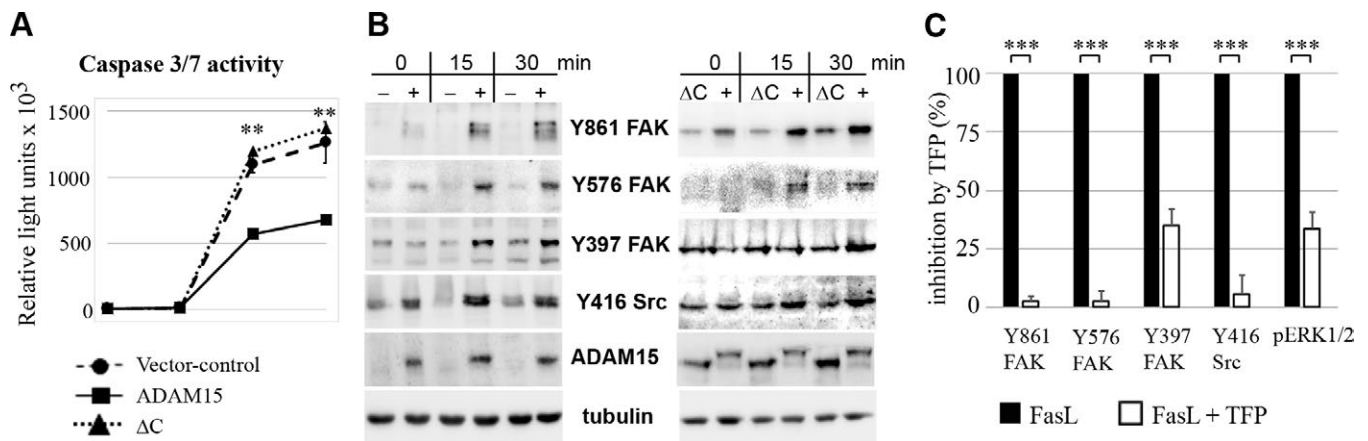
Figure 1. ADAM15-mediated reduced FasL-induced caspase 3/7 activity and increased phosphorylation of focal adhesion kinase (FAK) and Src inhibited by the calmodulin antagonist trifluoperazine (TFP). **A,** Caspase 3/7 activity (triplicates from 3 independent experiments) in T/C28a4 cells transfected with full-length ADAM15 (+), with a deletion mutant that lacks the cytoplasmic tail (ΔC), or with vector control (−) is shown. Cells were stimulated with FasL for 12–30 hours. Caspase activity was significantly increased in mutant- and vector control–transfected cells. **B,** Cells transfected with full-length ADAM15, with the cytoplasmic tail deletion mutant, or with vector control were stimulated with FasL for 15–30 minutes and analyzed by immunoblotting using anti–phospho-FAK and anti–phospho-Src antibodies. Fas-mediated increase of FAK and Src phosphorylation was found exclusively in cells transfected with full-length ADAM15. **C,** Densitometric evaluation of immunoblots of cell lysates from rheumatoid arthritis synovial fibroblasts (n = 3 donors) stimulated with FasL and FasL/TFP (25 μM) for 0 and 60 minutes shows significant inhibition of phosphorylation of FAK, Src, and ERK1/2 by TFP. The evaluated immunoblots are shown in Supplementary Figure 1, available on the *Arthritis & Rheumatology* web site at http://onlinelibrary.wiley.com/doi/10.1002/art.40667/abstract. Values in **A** and **C** are the mean ± SD. ∗∗ = $P < 0.002$ for vector control–transfected cells versus cells transfected with full-length ADAM15, by Student's t-test; ∗∗∗ = $P < 0.0002$ by Student's t-test.

Immunofluorescence. RASFs were grown in chamber slides for 3 hours and stimulated with CH-11 (2 μg/ml) for 15 minutes. After fixation in 4% paraformaldehyde and blocking in phosphate buffered saline containing 1% bovine serum albumin and 0.1% Triton X-100, cells were double-stained with rabbit anti-CD95 (1:100) and mouse anti-CaM (1:50) or goat anti-ADAM15 (1:50) overnight at 4°C and immunodetected by appropriate Alexa Fluor 488– and Alexa Fluor 594–conjugated secondary antibodies (Invitrogen). Cells were mounted in Pro-Long Gold Antifade Reagent with DAPI and analyzed using a Leica SP8 confocal laser scanning microscope. Images were processed using ImageJ Fiji software.

Statistical analysis. Data are presented as the mean ± SD of triplicates of at least 3 independently performed assays. Statistical significance was determined using Student's t-test or the Wilcoxon signed rank test.

RESULTS

Influence of ADAM15 on caspase 3/7 activity upon FasL-induced apoptosis. To complement our earlier results showing increased Fas-mediated apoptosis of RASFs after down-regulation of ADAM15 (5), we analyzed the effect of FasL stimulation on the induction of caspase activity for up to 30 hours in a cell line (T/C28a4) transfected with full-length ADAM15, a mutant lacking the cytoplasmic tail (Δcyto), or an empty vector as control. Transfected cells had been controlled for expression by immunoblotting and fluorescence-activated cell sorting analysis as described previously (20). Significantly reduced caspase 3/7 activity was determined in cells transfected with full-length ADAM15 compared to those expressing the cytoplasmic tail deletion mutant (Figure 1A). The latter displayed caspase activities comparable to those in vector control–transfected cells, underlining the functional importance of the cytoplasmic domain in ADAM15-mediated apoptosis resistance.

Moreover, a marked increase of phosphorylation of Src at Y416 and of FAK at Y576, Y861, and Y397 was detected in cells transfected with full-length ADAM15 by immunoblotting upon stimulation with FasL for 15 and 30 minutes. This demonstrates a crucial role of ADAM15 in Fas-triggered activation of FAK and Src not detectable in vector-transfected cells (Figure 1B). A direct comparison of Fas-stimulated ADAM15- and Δcyto-transfected cells revealed that in Δcyto-transfected cells, levels of phosphorylation of Src at Y416 and of FAK at all 3 tyrosines did not increase above baseline in the unstimulated state (Figure 1B). Taken together, these results provide evidence for a mechanism of ADAM15-mediated apoptosis resistance accom-
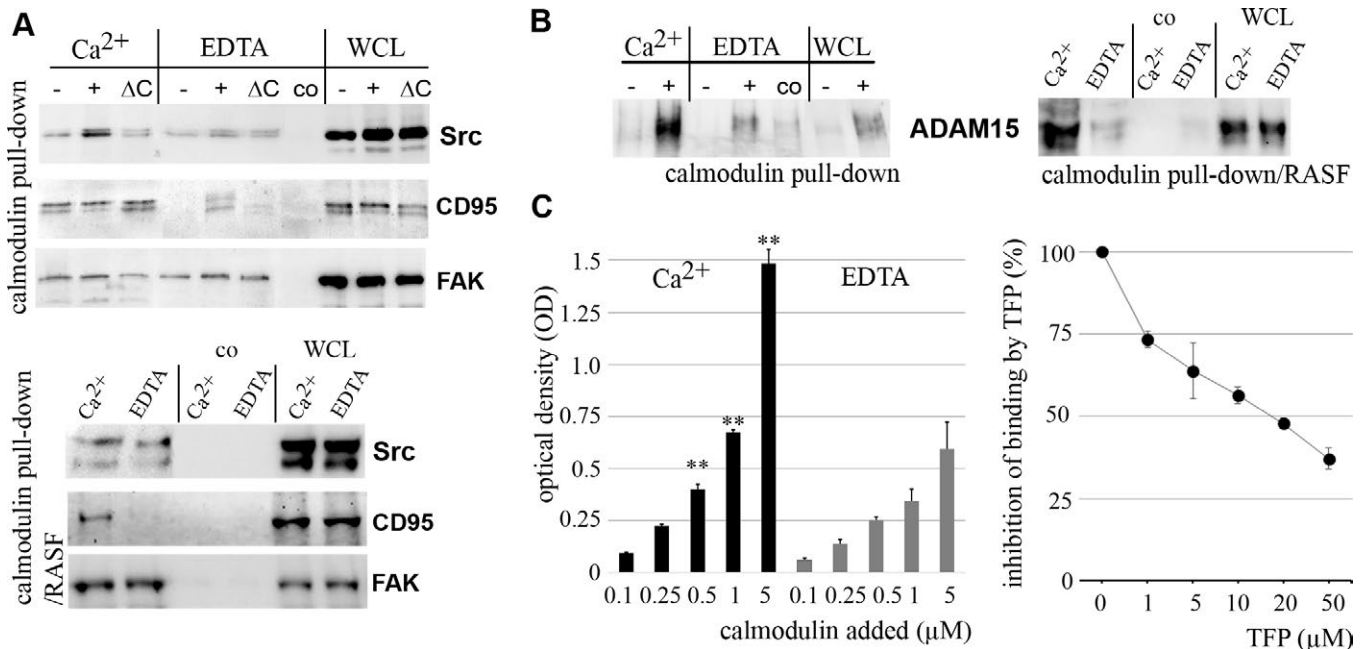
Figure 2. Interaction of Src, Fas/CD95, focal adhesion kinase (FAK), and ADAM15 with calmodulin (CaM). **A,** CaM pull-downs using CaM–Sepharose and subsequent immunodetection of Src, CD95, and FAK in chondrocytes transfected with ADAM15 (+), with a deletion mutant that lacks the cytoplasmic tail (ΔC), or with vector control (–) (top) and in primary rheumatoid arthritis synovial fibroblasts (RASFs) (bottom) in the presence of either Ca²⁺ ions or EDTA. WCL = whole cell lysate. Pull-downs on Sepharose CL-4B served as a control (co). **B,** ADAM15 binding to CaM–Sepharose in ADAM15- and vector control–transfected cells (left) and in RASFs (right), showing significant binding in the presence of Ca²⁺. **C,** Binding of increasing concentrations of recombinant CaM to the recombinant cytoplasmic domain of ADAM15 (cytoADAM) immobilized to a 96-well plate in triplicates in the presence of Ca²⁺ or EDTA (left). **C,** Binding of CaM (5 μ*M*) to immobilized cytoADAM, with increasing amounts of trifluoperazine (TFP) added during binding (right). Values are the mean ± SD. ** = $P < 0.002$ versus the respective CaM concentration in the presence of EDTA, by Student's t-test. All experiments were performed at least 3 times.

panied by Src/FAK signaling that is critically dependent on the cytoplasmic domain of ADAM15.

Inhibition of Src and FAK phosphorylation by a CaM antagonist. Since Fas ligation leads to Ca^{2+} influx bound by CaM (13), we analyzed whether CaM inhibition might impact Src/FAK signaling. ADAM15-transfected cells, the synovial cell line, and RASFs were stimulated with FasL for 0–60 minutes following preincubation with TFP. Immunoblot analysis revealed that TFP at a concentration of 25 μM efficiently reduced the phosphorylation of FAK at Y576 and Y861 and of Src at Y416 by >90% in both cell lines as well as in RASFs (Figure 1C; also see Supplementary Figure 1, available on the *Arthritis & Rheumatology* web site at http://onlinelibrary.wiley.com/doi/10.1002/art.40667/abstract). The phosphorylation of FAK at Y397 was inhibited ~60%, as was the phosphorylation of ERK1/2, both of which are downstream signaling effector kinases of the FAK/Src pathway.

Interaction of CaM with CD95, Src, and FAK. To analyze the Ca^{2+} dependency of CaM interactions, we performed pull-downs with CaM–Sepharose in ADAM15-, Δcyto-, and vector-transfected cells as well as in RASFs in the presence of either Ca^{2+} or EDTA, followed by immunoblotting using anti-Src, anti-FAK, and anti-CD95 antibodies. All cell types revealed binding of CaM to Src in the presence of Ca^{2+} that was slightly weaker in

the presence of EDTA, which suggests that apo-CaM as well as the Ca^{2+}-bound conformation of CaM binds to Src (Figure 2A). Moreover, in all independently performed CaM pull-down experiments (n = 5 donors), the strongest signals of precipitated Src became detectable in T/C28a4 cells transfected with full-length ADAM15, and signals remained considerably weaker in vector control– or Δcyto-transfected cells, strongly indicating the impact of ADAM15 on Src–CaM binding. A Ca^{2+}-independent interaction with CaM was also found for FAK in all transfected cells and RASFs. However, the pull-downs revealed that the interaction of CaM with CD95 was Ca^{2+} dependent, since it was nearly exclusively detectable in the presence of Ca^{2+} in the cell lines and RASFs.

Binding of ADAM15 to Ca^{2+}–CaM. The demonstrated influence of ADAM15 on promoting Src–CaM interaction led us to analyze whether ADAM15 itself binds to CaM. CaM pull-downs revealed a strong interaction of ADAM15 with CaM in the presence of Ca^{2+} but only minimal binding upon Ca^{2+} depletion with EDTA both in ADAM15-transfected cells and in RASFs (Figure 2B). For further characterization, protein binding assays were performed using recombinant proteins. The cytoplasmic tail of ADAM15 (cytoADAM), expressed as glutathione S-transferase–tagged fusion protein, was purified upon proteolytic tag removal as described previously (20) and immobilized to a 96-well plate for subsequent incubation with increasing concentrations of recombinant CaM.
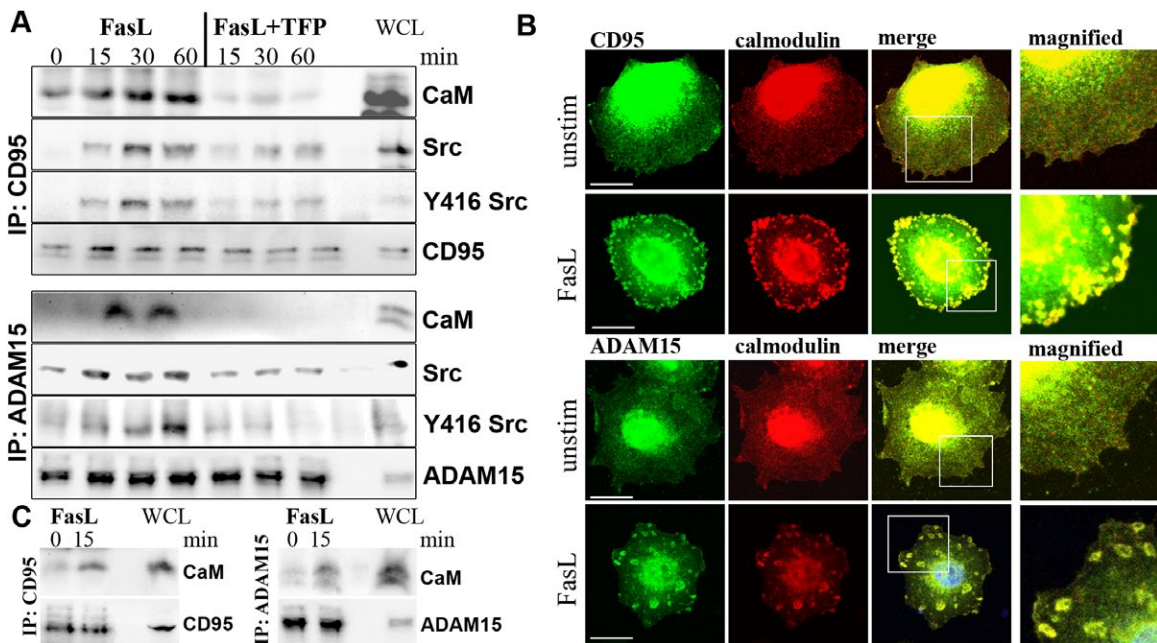
Figure 3. Recruitment of Src and calmodulin (CaM) to Fas/CD95 and ADAM15 upon Fas ligation is inhibited by the CaM inhibitor trifluoperazine (TFP). **A,** Immunoprecipitation (IP) of ADAM15-transfected T/C28a4 cells (from 3 independent experiments) using either anti-Fas/CD95 or anti-ADAM15 antibodies. Shown is the increased interaction of CaM, Src, and phospho-Src upon Fas stimulation. Parallel coincubation with TFP inhibits these interactions. WCL = whole cell lysate. **B,** Confocal microscopy of double immunofluorescence staining of rheumatoid arthritis synovial fibroblasts (RASFs) either unstimulated or stimulated with Fas-activating CH-11 antibody for 10 minutes, using specific antibodies to either ADAM15 and CaM or CD95 and CaM. Shown is the association of CaM with both ADAM15 and CD95 upon Fas ligation. Bars = 20 μm. Boxed areas in merged images are shown at higher magnification at right. **C,** Immunoprecipitation of cell lysates of RASFs (n = 2 donors) stimulated with FasL, using either anti-CD95 or anti-ADAM15 antibodies. Shown is the interaction of CaM with either molecule upon Fas ligation.

A concentration-dependent binding of CaM to cytoADAM at a low micromolar range could be detected in the presence of Ca^{2+}, which was significantly reduced by EDTA (Figure 2C). Also, the addition of TFP to the CaM–cytoADAM ligand pair inhibited their interaction in a concentration-dependent manner, with a half-maximal inhibitory concentration of ~20 μM (Figure 2C). Collectively, the results demonstrate a pharmacologically modifiable binding of ADAM15 to the Ca^{2+} conformation of CaM.

Recruitment of CaM and Src to both Fas/CD95 and ADAM15 upon Fas ligation. To analyze whether Fas ligation induced by anti-CD95 IgM (CH-11) in ADAM15-transfected T/C28a4 and K4IM cells leads to redistribution of CaM and Src to ADAM15 and Fas, coimmunoprecipitations were performed. Immunoblots of complexes precipitated with either anti-Fas/CD95 or anti-ADAM15 antibodies revealed increasing signal intensities for CaM during Fas stimulation for 15–60 minutes (Figure 3A). These Fas-triggered interactions were efficiently inhibited by TFP, suggesting that Ca^{2+} influxes elicited by Fas ligation promote conformational changes in CaM for subsequent recruitment to Fas as well as ADAM15. Concomitantly, the detectable signal intensities for Src and its phosphorylation at Y416 in Fas- and ADAM15-containing immunoprecipitates were markedly induced upon Fas ligation above the unstimulated baseline level and were proved to be sensitive to pretreatment with TFP. TFP efficiently reduced the amount of total as well as phosphorylated Src coprecipitated with ADAM15 and Fas (Figure 3A), which suggests that Ca^{2+}–CaM and its interaction with ADAM15 and/or Fas is critical for recruitment and efficient activation of Src.

Next, we investigated whether Fas ligation also induces CaM recruitment to Fas and ADAM15 in RASFs. Following Fas stimulation for 10 minutes, RASFs were analyzed by double immunofluorescence staining using specific antibodies to either ADAM15 and CaM or CD95 and CaM. Fas stimulation led to a staining pattern of colocalized CaM and ADAM15 in patches at the cell surface which was not detectable in unstimulated RASFs (Figure 3B). Correspondingly, an induced colocalization of CaM with Fas/CD95 in cell surface foci was observed to depend on preceding Fas stimulation as it was not detectable in unstimulated cells (Figure 3B). To confirm the Fas-induced interaction of CaM with CD95 and/or ADAM15, cell lysates of RASFs stimulated for 0 and 15 minutes with FasL were immunoprecipitated using anti-CD95 and anti-ADAM15 antibodies. Immunoblot analysis revealed coprecipitated CaM with CD95 and ADAM15 upon Fas ligation only (Figure 3C).

Enhanced interaction of Src and CaM upon Fas stimulation. Based on the detected interaction of Src with CaM (Figure 2A), we further investigated its modulation by Fas ligation and pharmacologic interference with the CaM inhibitor TFP. Following stimulation with anti-Fas antibody in the presence or absence of TFP for 0–60 minutes, ADAM15-transfected cells and K4IM cells (results not shown) were lysed, immunoprecipitated
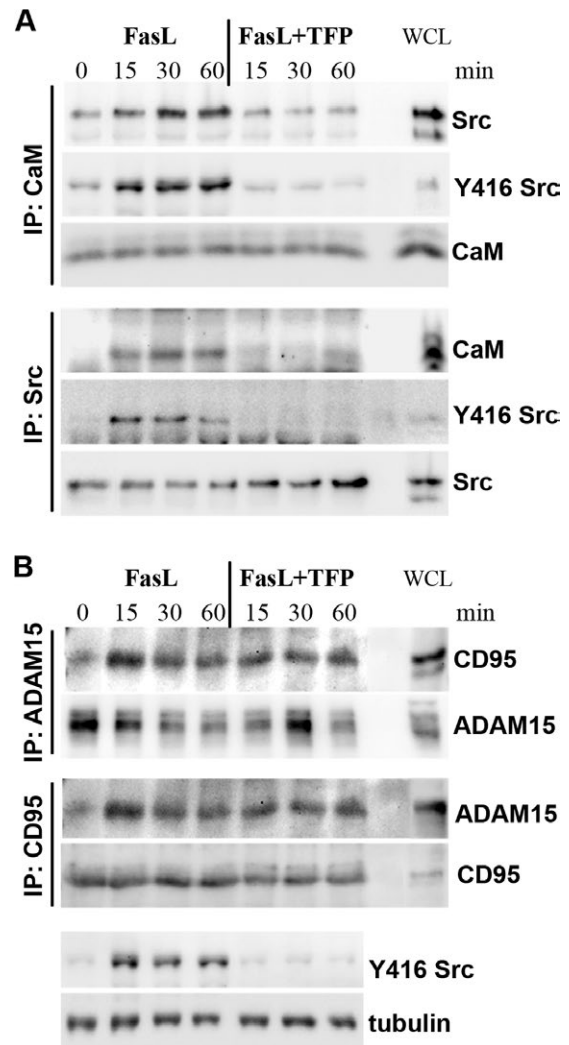
Figure 4. Enhanced interaction of calmodulin (CaM) and Src and an induced association of ADAM15 and Fas/CD95 upon Fas ligation. ADAM15-transfected T/C28a4 cells were stimulated with FasL and FasL/trifluoperazine (TFP) and either immunoprecipitated (IP) using anti-CaM antibodies and immunodetection of Src and phospho-Src, and vice versa using anti-Src IgG and detection of CaM by immunoblotting (**A**), or immunoprecipitated using anti-ADAM15 antibodies and detection of Fas/CD95, and vice versa (**B**). Bottom, As a control for functionality of TFP, whole cell lysates (WCL) were stimulated with FasL, which yielded phosphorylation of Src at Y416 and its inhibition by TFP. Tubulin served as a loading control. Experiments were performed 3 times.

using Src- or CaM-specific antibodies, and analyzed by immunoblotting. A marked increase of coprecipitated total and phosphorylated Src was observed in the CaM immunoprecipitates after 30 and 60 minutes (Figure 4A), demonstrating an increased interaction of Src and CaM by Fas ligation that was efficiently inhibited by TFP in accordance with a strict dependence on the Ca^{2+}-activated conformation of CaM (Figure 4A). The vice versa immunoprecipitation using antibodies to Src and subsequent detection of CaM confirmed the Fas-triggered interaction of Src with CaM and its inhibition by TFP (Figure 4A).

Redistribution of ADAM15 into CD95-Cap. In addition, we investigated whether Fas stimulation might also promote clustering of ADAM15 and Fas/CD95. In immunoprecipitations parallel to those described above, Fas-stimulated lysates of T/C28a4 and K4IM cells were coprecipitated using anti-ADAM15 or anti-CD95 antibodies, and the respective binding of CD95 or ADAM15 was visualized by immunoblotting. An association of ADAM15 with Fas/CD95 was detectable during Fas stimulation for 15–60 minutes in both immunoprecipitates, but not in unstimulated cells (Figure 4B). Moreover, TFP did not exert any inhibitory effect on Fas-triggered ADAM15–Fas interaction (Figure 4B), showing that their clustering is independent of Ca^{2+}-dependent conformational changes of CaM upon Fas ligation. Since all immunoprecipitations performed yielded identical results, representative data obtained in T/C28a4 cells are shown.

Apoptosis induction by CRAC/Orai channel and CaM inhibition upon Fas ligation in RASFs. Next, we analyzed whether inhibition of CRAC/Orai channels might influence Fas-mediated Src and FAK phosphorylation as well as apoptosis induction. RASFs were stimulated with FasL or FasL plus the CRAC inhibitor BTP-2 (25 and 50 μM), and lysates were analyzed by immunoblotting using specific anti–phospho-Src and anti–phospho-FAK antibodies. All FasL-stimulated phosphoryla-

tion of Src at Y416 and of FAK at Y576 and Y861 that was detectable after 30 minutes was efficiently inhibited >90% by BTP-2 at 25 μM and completely blocked by BTP-2 at 50 μM, while phosphorylation of FAK at Y397 was inhibited ~70% (Figure 5A).

Next, we analyzed whether CaM as well as Ca^{2+} influx inhibition could reduce the resistance of RASFs to Fas-mediated apoptosis. RASFs from 10 different donors were treated with TFP, BTP-2, FasL, or FasL in combinations with each inhibitor for 18 hours. Caspase 3/7 measurements are depicted in a dot plot (Figure 5B) with each dot representing the calculated mean of triplicate measurements for 1 donor. RASFs from 8 of 10 donors responded to FasL stimulation with an increase of their caspase activity, while RASFs from 2 donors remained rather unresponsive (Figure 5B). RASFs from all donors did not show any induction of caspase activity upon incubation with either TFP (25 μM) or BTP-2 (25 and 50 μM) compared to DMEM control. However, coincubation of TFP or BTP-2 with FasL led to statistically significant increases in caspase activity above the level induced by FasL alone (Figure 5B), indicating their synergistic death-inducing potential in combination with Fas ligation.

Accordingly, total apoptosis rates were determined by annexin V stainings of RASFs (n = 4 donors) incubated with TFP or BTP-2 or treated with either FasL or FasL/inhibitor cocktails for 18 hours. We determined the percentage of annexin V–positive
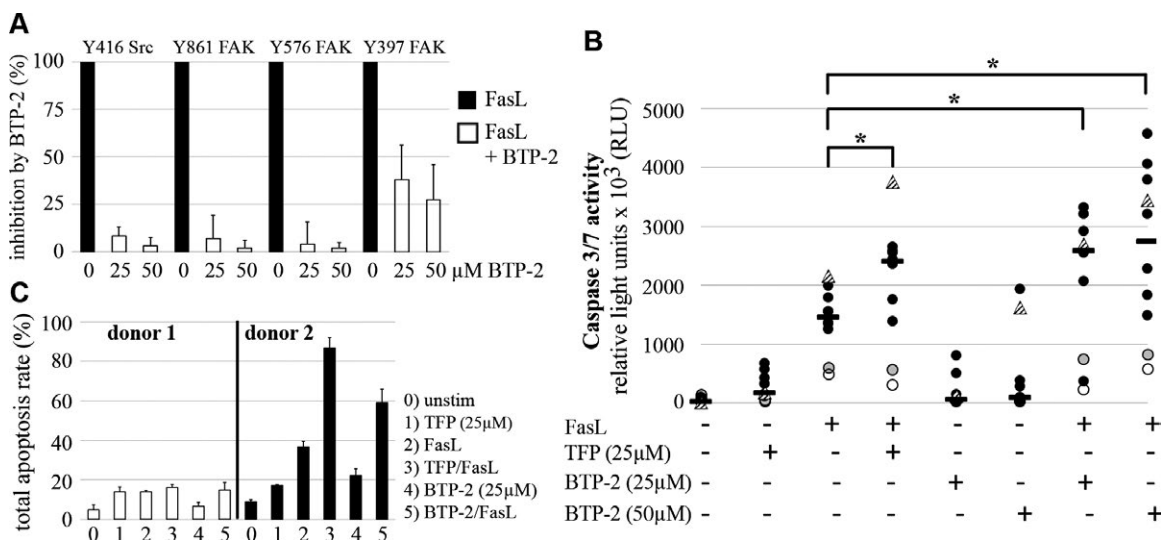
Figure 5. Increased apoptosis rate upon inhibition of FasL-induced phosphorylation of focal adhesion kinase (FAK) and Src by the calmodulin (CaM) inhibitor trifluoperazine (TFP) and by the Ca^{2+} release-activated Ca^{2+}/calcium release-activated calcium channel protein 1 channel inhibitor BTP-2 (commonly known as CRAC/Orai channel inhibitor BTP-2) in rheumatoid arthritis synovial fibroblasts (RASFs). **A,** Densitometric evaluation of immunoblots probed with anti–phospho-Src and anti–phospho-FAK antibodies in RASF lysates (n = 3 donors) stimulated with FasL for 30 minutes and coincubated with BTP-2 is shown. **B,** FasL-induced apoptosis in RASFs results in significantly and synergistically enhanced caspase 3/7 activity (measured in triplicates) in RASFs upon coincubation with TFP or BTP-2 for 18 hours. **Open circles** represent donors whose RASFs did not respond well to any agent. **Solid circles** represent donors whose RASFs yielded high caspase activities. Each symbol represents the calculated mean of triplicate measurements for 1 donor; horizontal lines indicate the median for 10 different donors. ∗ = $P < 0.05$ by Wilcoxon signed rank test. **C,** RASFs with low caspase activity from donor 1 (**open circle without shading** in **B**) and RASFs with high caspase activity from donor 2 (**triangle** in **B**) were untreated, incubated with TFP or BTP-2, or treated with either FasL or FasL/inhibitor cocktails for 18 hours, and total apoptosis rate was determined by correlating cells that stained positive for annexin V to the whole cell population. Results from 3 independent experiments are shown. Values in **A** and **C** are the mean ± SD.
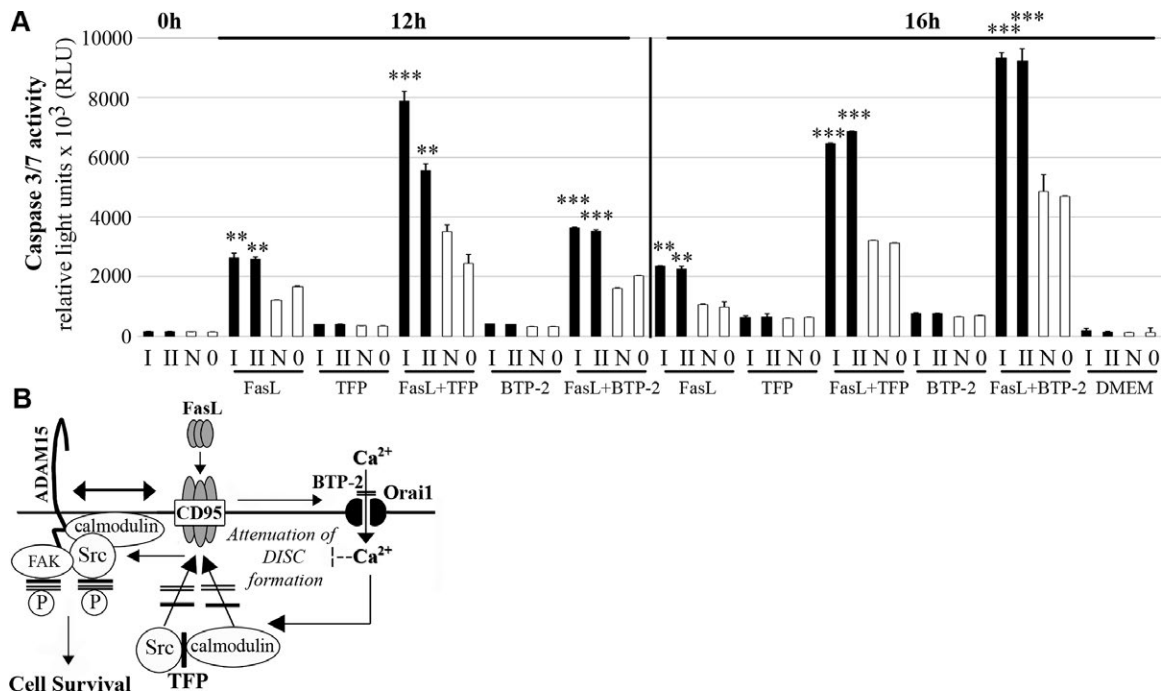
Figure 6. Higher caspase 3 activity upon apoptosis induction with FasL and calmodulin (CaM) and calcium-channel inhibitors following ADAM15 silencing in rheumatoid arthritis synovial fibroblasts (RASFs). **A,** After ADAM15 was silenced for 40 hours in triplicates with specific small interfering RNA I (siRNA I) and siRNA II, RASFs were incubated for 12 and 16 hours with FasL (100 ng/ml), trifluoperazine (TFP) (25 μ*M*), BTP-2 (25 μ*M*), and combinations of FasL with either inhibitor. Apoptosis induction by either FasL/TFP or FasL/BTP-2 resulted in significantly increased caspase 3 activity in ADAM15-silenced RASFs as compared to treatment with a nonsilencing siRNA control (N) or transfection agent alone (0). Dulbecco's modified Eagle's medium (DMEM) served as an incubation control. Results are from RASFs from a representative donor (of 5 donors tested). Values are the mean ± SD. ** = $P < 0.002$; *** = $P < 0.0002$ versus nonsilencing controls at the same time point, by Student's *t*-test. **B,** Schematic diagram shows ADAM15-mediated survival signaling upon FasL stimulation and inhibitory effects on Src and focal adhesion kinase (FAK) phosphorylation as well as the recruitment of CaM to CD95 by the CaM inhibitor TFP (single black line) and the Ca^{2+} release-activated Ca^{2+} channel inhibitor BTP-2 (double black line). P = tyrosine phosphorylation; DISC = death-inducing signaling complex; Orai1 = calcium release-activated calcium channel protein 1.

cells from the 2 donors that did not respond well to any agent and from 2 donors whose cells yielded high caspase activities, and representative results from 1 donor in each group are shown (Figure 5C). RASFs from donor 2 displayed a total apoptosis rate of ~90% when incubated with FasL and 25 μ*M* TFP, and they displayed a total apoptosis rate of ~60% with FasL and 25 μ*M* BTP-2, while they displayed an ~40% apoptosis rate when stimulated with FasL alone (Figure 5C). However, low responding RASFs from donor 1 only displayed apoptosis rates well below 20% independent of the compound applied (Figure 5C). Collectively, pharmacologic antagonism of either CRAC/Orai or CaM can synergistically enhance FasL-induced apoptosis induction in RASFs.

Protective effect of ADAM15 against synergistic caspase induction by FasL and CaM or CRAC inhibitors in RASFs. We performed additional studies to elucidate the impact of ADAM15 on apoptosis induction by FasL with concomitant CRAC/Orai channel or CaM inhibition. ADAM15 expression was silenced by specific ADAM15 siRNAs I and II using a nonsilencing RNA and

a transfection reagent as controls. Transfection efficiency was ~80%, as shown previously (5). After silencing, RASFs were stimulated with FasL (100 ng/ml), TFP (25 μ*M*), FasL/TFP, BTP-2 (25 μ*M*), and FasL/BTP-2 for 18 hours and subsequently analyzed for caspase 3/7 activity. Neither TFP alone nor BTP-2 alone elicited any caspase activity in RASFs, nor did DMEM, which served as an incubation control (Figure 6A). However, RASFs silenced with ADAM15 siRNAs I and II displayed significantly higher caspase activity upon FasL stimulation in comparison to the nonsilencing RNA and the transfection reagent. Moreover, apoptosis induction with FasL cocktails containing either inhibitor resulted in significantly and synergistically increased caspase activity in ADAM15–down-regulated RASFs compared to nonsilenced cells. Thus, ADAM15 is crucially involved in Ca^{2+}-triggered survival signaling elicited by Fas stimulation.

DISCUSSION

In the present study we identified CaM as a "cross-talk" protein linking death-inducing Fas/CD95 ligation to ADAM15-

dependent activation of survival pathways. Previously, we had reported that Fas stimulation induced Src/FAK-mediated survival signaling in RASFs that was virtually deleted upon down-regulation of ADAM15. Using T/C28a4 cells transfected with full-length ADAM15 or a mutant lacking the cytoplasmic tail, we could provide unequivocal evidence that Src/FAK activation elicited by Fas ligation is critically dependent on the cytoplasmic domain of ADAM15.

Our data show for the first time Ca^{2+}-dependent binding of ADAM15 to CaM. Thus, in vitro binding of the recombinant cytoplasmic domain of ADAM15 to CaM was efficiently blocked by EDTA and by the CaM inhibitor TFP in a concentration-dependent manner. TFP, a highly specific CaM antagonist binding to the Ca^{2+}-activated CaM conformation in 2 hydrophobic pockets adjacent to the Ca^{2+}-coordinating residues, efficiently inhibits protein interactions at these sites (21,22). Moreover, our investigations also provide clear evidence for interaction of CaM with ADAM15 in the living cell; however, this requires a preceding Fas ligation for triggering recruitment of Ca^{2+}–CaM to ADAM15. The implication of Ca^{2+}-induced CaM activation in this process is supported by an efficient inhibitory effect of TFP.

However, how can interaction of Ca^{2+}–CaM with ADAM15 contribute to the transformation of FasL-induced death signals into prosurvival triggering of Src/FAK phosphorylation? Previously, the direct binding of ADAM15 to the C-terminus of FAK has been shown to enhance phosphorylation of FAK/Src in response to apoptosis-inducing genotoxic stress, thereby reinforcing counter-regulatory survival pathways (20). Thus, the cytoplasmic domain of ADAM15 provides a scaffold for FAK and Src binding complemented by the engagement of CaM following its coactivation in the context of the apoptotic signal. Our data clearly show association of ADAM15 with Fas/CD95 upon Fas stimulation, providing unequivocal evidence for recruitment of ADAM15 into the CD95-Cap at the cell membrane. Concomitantly, cytosolic CaM is recruited to both membrane proteins upon Fas triggering. Thus, binding of CaM to the cytoplasmic death domain of Fas has been reported previously to occur at a 2:1 ratio in a Ca^{2+}-dependent manner sensitive to TFP inhibition (23) and was hypothesized to antagonize apoptosis execution (24) by blocking FADD binding to Fas in DISC formation (25,26). This mechanism initiated by CRAC/Orai1-dependent Ca^{2+} fluxes elicited by Fas ligation (13) might delay the immediate cell death execution to allow for simultaneous recruitment of CaM-associated Src to the ADAM15 scaffold containing already engaged cytoplasmic FAK. Accordingly, this instantaneous formation of an ADAM15-dependent prosurvival signaling complex in the CD95-Cap enables rapid activation of a variety of antiapoptotic pathways (e.g., up-regulation of the caspase inhibitor XIAP [6]), thereby increasing the likelihood of surviving Fas-transmitted death-inducing signals.

To allow for the rapid temporospatial formation of this ADAM15-dependent prosurvival signaling complex, a physical interaction of CaM with all of its components is required, and indeed our investigations demonstrate not only binding of CaM to Src and cytoplasmic ADAM15 but also to FAK in transfected T/C28a4 cells. Contrary to the strict Ca^{2+} dependency of CaM binding to CD95 and ADAM15, our investigations also reveal Ca^{2+}-independent interaction with both kinases, consistent with already published studies of Src in pancreatic and breast cancer cells (27,28).

Thus, our results can be summarized as follows describing a potential scenario for Fas-elicited ADAM15 survival signaling (Figure 6B). Upon binding of FasL (or agonistic antibodies), Fas receptors undergo homotrimerization and/or subsequent trimer clustering accompanied by localized Ca^{2+} fluxes into the cell via CRAC/Orai1 channels that lead to attenuation of DISC formation (14). Upon Fas ligation, ADAM15 is redistributed into the CD95-Cap. CaM and Src are recruited to the plasma membrane, where they bind (dependent on the Ca^{2+}-activated CaM conformation) to ADAM15 and the Fas receptor. Subsequently, FAK associated with cytoplasmic ADAM15 (20) and capable of interacting with CaM gets phosphorylated at its tyrosine residues Y576 and Y861 by activated Src. This Fas-triggered formation of ADAM15-dependent prosurvival signaling complexes in the CD95-Cap can be blocked efficiently by an antagonism of either the Ca^{2+} influx by BTP-2 or the Ca^{2+}-sensing CaM by TFP, leading to an abrogation of Src and FAK phosphorylation.

To date, a variety of antiapoptotic molecules have already been implicated as constituents of the apoptosis-resistant phenotype of RASFs, like FLIP, an important component of the DISC (29); POSH, an SH3 domain–containing protein involved in JNK activation (30); sentrin, a Fas- and TNFR type I–interacting protein (31); or small ubiquitin-like modifier 1 (32). As ADAM15 has been demonstrated to be highly up-regulated in RASFs (4), the above-described newly identified mechanism is likely to add an interesting facet to the spectrum of already-described pathways of apoptosis resistance since it opens potential new avenues for pharmacologic interference.

Previously, we had shown that FAK/Src signal transduction inhibitors, FAK inhibitor 14 and dasatinib, sensitize RASFs to apoptosis induction. In the present study, we demonstrate for the first time that simultaneous application of either the CaM inhibitor TFP or the CRAC/Orai inhibitor BTP-2 with death-inducing FasL synergistically enhances Fas-mediated apoptosis in RASFs. The death-promoting effect of both compounds is critically dependent on synergistic Fas ligation, which is provided under patho-physiologic conditions in RA by high FasL concentrations in the synovial fluid of inflamed joints (33). While TFP, applied in our study for its CaM-blocking effects, is a Food and Drug Administration–approved antipsychotic drug with preferred therapeutic use for schizophrenia, CRAC antagonists have recently already been tested for their antiarthritis potential in murine collagen-induced arthritis resulting in ameliorated disease development, relief from pain, and a 50% reduction of structural joint damage (34,35). In this context, the newly discovered role of CaM and

CRAC/Orai channels as pharmacologic targets to break Fas-mediated apoptosis resistance in RASFs might encourage further studies aiming at new treatment options in RA.

AUTHOR CONTRIBUTIONS

All authors were involved in drafting the article or revising it critically for important intellectual content, and all authors approved the final version to be published. Dr. Burkhardt had full access to all of the data in the study and takes responsibility for the integrity of the data and the accuracy of the data analysis.

Study conception and design. Böhm, Kinne, Burkhardt.
Acquisition of data. Janczi, Fehrl, DeGiacomo, Kinne.
Analysis and interpretation of data. Janczi, Böhm, Burkhardt.

REFERENCES

1. Edwards DR, Handsley MM, Pennington CJ. The ADAM metalloproteinases. Mol Aspects Med 2008;29:258–89.

2. Lucas N, Day ML. The role of the disintegrin metalloproteinase ADAM15 in prostate cancer progression. J Cell Biochem 2009;106:967–74.

3. Duffy MJ, McKiernan E, O'Donovan N, McGowan PM. Role of ADAMs in cancer formation and progression. Clin Cancer Res 2009;15:1140–4.

4. Böhm BB, Aigner T, Blobel CP, Kalden JR, Burkhardt H. The expression of the disintegrin-metalloproteinase MDC15 (metargidin) is highly enhanced in rheumatoid synovial tissue. Arthritis Rheum 2001;44:2046–54.

5. Böhm BB, Freund I, Krause K, Kinne RW, Burkhardt H. ADAM15 adds to apoptosis resistance of synovial fibroblasts by modulating focal adhesion kinase signaling. Arthritis Rheum 2013;65:2826–34.

6. Böhm B, Hess S, Krause K, Schirner A, Ewald W, Aigner T, et al. ADAM15 exerts an antiapoptotic effect on osteoarthritic chondrocytes via up-regulation of the X-linked inhibitor of apoptosis. Arthritis Rheum 2010;62:1372–82.

7. Müller-Ladner U, Pap T, Gay RE, Neidhart M, Gay S. Mechanisms of disease: the molecular and cellular basis of joint destruction in rheumatoid arthritis. Nat Clin Pract Rheumatol 2005;1:102–10.

8. Malemud CJ. Apoptosis resistance in rheumatoid arthritis synovial tissue. J Clin Cell Immunol 2011;S3:006.

9. Müller-Ladner U, Ospelt C, Gay S, Distler O, Pap T. Cells of the synovium in rheumatoid arthritis: synovial fibroblasts. Arthritis Res Ther 2007;9:223–32.

10. Liu H, Pope RM. Apoptosis in rheumatoid arthritis: friend or foe. Rheum Dis Clin North Am 2004;30:603–25.

11. Peng SL. Fas (CD95)-related apoptosis and rheumatoid arthritis. Rheumatology (Oxford) 2006;45:26–30.

12. Peter ME, Krammer PH. The CD95(APO-1/Fas) DISC and beyond. Cell Death Differ 2003;10:26–35.

13. Cahalan MD. STIMulating store-operated Ca(2+) entry. Nat Cell Biol 2009;11:669–77.

14. Khadra N, Bresson-Bepoldin L, Penna A, Chaigne-Delalande B, Ségui B, Levade T, et al. CD95 triggers Orai1-mediated localized Ca2+ entry, regulates recruitment of protein kinase C (PKC) β2, and prevents death-inducing signaling complex formation. Proc Natl Acad Sci U S A 2011;108:19072–7.

15. Berridge MJ, Bootman MD, Roderick HL. Calcium signaling: dynamics, homeostasis and remodeling. Nat Rev Mol Cell Biol 2003;4:517–29.

16. Kursula P. The many structural faces of calmodulin: a multitasking molecular jackknife. Amino Acids 2014;46:2295–304.

17. Tidow H, Nissen P. Structural diversity of calmodulin binding to its target sites. FEBS J 2013;280:5551–65.

18. Goldring MB, Birkhead JR, Suen LF, Yamin R, Mizuno S, Glowacki J, et al. Interleukin-1-β-modulated gene expression in immortalized human chondrocytes. J Clin Invest 1994;94:2307–16.

19. Arnett FC, Edworthy SM, Bloch DA, McShane DJ, Fries JF, Cooper NS, et al. The American Rheumatism Association 1987 revised criteria for the classification of rheumatoid arthritis. Arthritis Rheum 1988;31:315–24.

20. Fried D, Böhm BB, Krause K, Burkhardt H. ADAM15 protein amplifies focal adhesion kinase phosphorylation under genotoxic stress conditions. J Biol Chem 2012;287:21214–23.

21. Vandonselaar M, Hickie RA, Quail W, Delbaere LT. Trifluoperazine-induced conformational change in Ca^{2+}-calmodulin. Nat Struct Biol 1994;1:795–801.

22. Halling DB, Liebeskind BJ, Hall AW, Aldrich RW. Conserved properties of individual Ca2+-binding sites in calmodulin. Proc Natl Acad Sci U S A 2016;113:E1216–25.

23. Fernandez TF, Samal AB, Bedwell GJ, Chen Y, Saad JS. Structural and biophysical characterization of the interactions between the death domain of Fas receptor and calmodulin. J Biol Chem 2013;288:21898–908.

24. Wu X, Ahn EY, McKenna MA, Yeo H, McDonald JM. Fas binding to calmodulin regulates apoptosis in osteoclasts. J Biol Chem 2005;280:29964–70.

25. Chen Y, Pawar P, Pan G, Ma L, Liu H, McDonald JM. Calmodulin binding to the Fas-mediated death-inducing signaling complex in cholangiocarcinoma cells. J Cell Biochem 2008;103:788–99.

26. Pawar PS, Micoli KJ, Ding H, Cook WJ, Kappes JC, Chen Y, et al. Calmodulin binding to cellular FLICE-like inhibitory protein modulates Fas-induced signaling. Biochem J 2008;412:459–68.

27. Yuan K, Jing G, Chen J, Liu H, Zhang K, Li Y, et al. Calmodulin mediates Fas-induced FADD-independent survival signaling in pancreatic cancer cells via activation of Src-extracellular signal-regulated kinase (ERK). J Biol Chem 2011;286:24776–84.

28. Stateva SR, Salas V, Anguita E, Benaim G, Villalobo A. Ca^{2+}/calmodulin and apo-calmodulin both bind to and enhance the tyrosine kinase activity of c-Src. PLoS One 2015;10:e0128783.

29. Palao G, Santiago B, Galindo M, Payá M, Ramirez JC, Pablos JL. Down-regulation of FLIP sensitizes rheumatoid synovial fibroblasts to Fas-mediated apoptosis. Arthritis Rheum 2004;50:2803–10.

30. Tsuda M, Kawaida R, Kobayashi K, Shinagawa A, Sawada T, Yamada R, et al. POSH promotes cell survival in Drosophila and in human RASF cells. FEBS Lett 2010;584:4689–94.

31. Franz JK, Pap T, Hummel KM, Nawrath M, Aicher WK, Shigeyama Y, et al. Expression of sentrin, a novel antiapoptotic molecule, at sites of synovial invasion in rheumatoid arthritis. Arthritis Rheum 2000;43:599–607.

32. Meinecke I, Cinski A, Baier A, Peters MA, Dankbar B, Wille A, et al. Modification of nuclear PML protein by SUMO-1 regulates Fas-induced apoptosis in rheumatoid arthritis synovial fibroblasts. Proc Natl Acad Sci U S A 2007;104:5073–8.

33. Hashimoto H, Tanaka M, Suda T, Tomita T, Hayashida K, Takeuchi E, et al. Soluble Fas ligand in the joints of patients with rheumatoid arthritis and osteoarthritis. Arthritis Rheum 1998;41:657–62.

34. Blair HC, Soboloff J, Robinson LJ, Tourkova IL, Larrouture QC, Witt MR, et al. Suppression of arthritis-induced bone erosion by a CRAC channel antagonist. RMD Open 2016;2:e000093.

35. Gao XH, Gao R, Tian YZ, McGonigle P, Barrett JE, Dai Y, et al. A store-operated calcium channel inhibitor attenuates collagen-induced arthritis. Br J Pharmacol 2015;172:2991–3002.

AMERICAN COLLEGE
OF RHEUMATOLOGY
EDUCATION · TREATMENT · RESEARCH

Association of Changes in Effusion-Synovitis With Progression of Cartilage Damage Over Eighteen Months in Patients With Osteoarthritis and Meniscal Tear

Lindsey A. MacFarlane,[1] Heidi Yang,[2] Jamie E. Collins,[1] Mohamed Jarraya,[3] Ali Guermazi,[3] Lisa A. Mandl,[4] Scott D. Martin,[5] John Wright,[6] Elena Losina,[1] Jeffrey N. Katz,[1] and the MeTeOR Investigator Group

Objective. Synovitis is a feature of knee osteoarthritis (OA) and meniscal tear and has been associated with articular cartilage damage. This study was undertaken to examine the associations of baseline effusion-synovitis and changes in effusion-synovitis with changes in cartilage damage in a cohort with OA and meniscal tear.

Methods. We analyzed data from the Meniscal Tear in Osteoarthritis Research (MeTeOR) trial of surgery versus physical therapy for treatment of meniscal tear. We performed semiquantitative grading of effusion-synovitis and cartilage damage on magnetic resonance imaging, and dichotomized effusion-synovitis as none/small (minimal) and medium/large (extensive). We assessed the association of baseline effusion-synovitis and changes in effusion-synovitis with changes in cartilage damage size and depth over 18 months, using Poisson regression models. Analyses were adjusted for patient demographic characteristics, treatment, and baseline cartilage damage.

Results. We analyzed 221 participants. Over 18 months, effusion-synovitis was persistently minimal in 45.3% and persistently extensive in 21.3% of the patients. The remaining 33.5% of the patients had minimal synovitis on one occasion and extensive synovitis on the other. In adjusted analyses, patients with extensive effusion-synovitis at baseline had a relative risk (RR) of progression of cartilage damage depth of 1.7 (95% confidence interval [95% CI] 1.0–2.7). Compared to those with persistently minimal effusion-synovitis, those with persistently extensive effusion-synovitis had a significantly increased risk of progression of cartilage damage depth (RR 2.0 [95% CI 1.1–3.4]).

Conclusion. Our findings indicate that the presence of extensive effusion-synovitis is associated with subsequent progression of cartilage damage over 18 months. The persistence of extensive effusion-synovitis over time is associated with the greatest risk of concurrent cartilage damage progression.

INTRODUCTION

Osteoarthritis (OA) of the knee is a prevalent and disabling disorder traditionally ascribed to degeneration of articular cartilage. OA is increasingly recognized as a disorder of the entire joint, in which inflammation plays a prominent role, manifesting as synovitis. The presence of synovitis has been associated with pain, incidence and progression of OA, and meniscal tears (1–8).

An estimated 91% of patients with symptomatic knee OA will have meniscal tear on magnetic resonance imaging (MRI) (9). Since synovitis is a prominent feature of both OA and meniscal tear, the role of synovitis in patients with concurrent OA and meniscal tear warrants investigation.

Synovitis is posited to stem from intraarticular damage, including debris from cartilage destruction or meniscal tear (5,6). Even in patients without evidence of articular cartilage damage

on MRI, the presence of meniscal tear confers twice the odds of joint effusion compared to patients without meniscal tear (5). Synovitis further contributes to a catabolic intraarticular milieu and the presence of inflammatory cytokines, leading to cartilage damage (3,10,11). Thus, intraarticular damage appears to provoke synovitis, which in turn can incite further damage. Previous research has demonstrated an association between synovitis and cartilage damage; however, those studies included both patients with and those without OA and did not examine the effect of longitudinal changes (including persistence or intermittence) of synovitis on cartilage damage (3,12,13). Further research is needed to determine whether persistent versus intermittent synovitis over time is associated with the progression of cartilage destruction, since this relationship may offer insights for treating patients with synovitis, meniscal tear, and OA.

MRI provides a noninvasive method to longitudinally investigate intraarticular structures of the knee, including synovitis. In large studies, non–contrast-enhanced MRI is often used in lieu of contrast-enhanced imaging to reduce cost and avoid adverse reactions; however, non–contrast-enhanced MRI cannot distinguish effusion from synovitis (14). Thus, effusion-synovitis, hyperintense fluid-equivalent signal in the joint cavity comprising effusion and synovial thickening, has been used in non–contrast-enhanced studies as a proxy for synovitis (14).

The aim of this study was to examine the association between changes in effusion-synovitis and cartilage damage over time in a population with both OA and meniscal tear. We hypothesized that the persistence of extensive effusion-synovitis over time would be associated with greater progression of cartilage damage.

PATIENTS AND METHODS

Study sample. We used data from participants enrolled in the Meniscal Tear in Osteoarthritis Research (MeTeOR) trial, a randomized clinical trial of arthroscopic partial meniscectomy (APM) versus physical therapy (PT) for the treatment of symptomatic meniscal tear in patients with knee OA (15). See Appendix A for members of the MeTeOR Investigator Group. Details of the trial design have been published previously (16). Three hundred and fifty-one participants were recruited from 7 academic referral centers between June 2008 and August 2011. Men and women ≥45 years old with evidence of meniscal tear extending to the meniscal surface on knee MRI were enrolled. To be eligible, subjects had to have OA changes on imaging studies, including the presence of an osteophyte or joint space narrowing on plain radiograph, or of full-thickness cartilage defect on at least one tibial or femoral surface on MRI. We used the MRI OA Knee Score (MOAKS) criteria to assess cartilage damage on MRI, using water-sensitive sequences (such as intermediate-weighted sequences with and without fat suppression), which

are known to be more sensitive than gradient-echo sequences for cartilage focal defects (14,17).

All participants had ongoing knee symptoms at study enrollment that had been present for at least 4 weeks, including pain and at least one of the following symptoms: clicking, catching, popping, giving way, pain with pivot or torque, pain that was episodic, and pain that was acute and localized to one joint line. Exclusion criteria included a chronically locked knee, inflammatory arthritis (i.e., rheumatoid arthritis, acute crystal-induced arthritis, or spondyloarthritis), or prior surgery on the index knee. Patients with clinically symptomatic chondrocalcinosis were excluded, since this could be an alternative source of pain and swelling. Those with radiographic Kellgren/Lawrence (K/L) grade 4 OA (>50% loss of tibiofemoral joint space) were excluded; those with K/L grade 0–3 disease were eligible. Patients with bilateral symptomatic meniscal tears were excluded; therefore, the participants each contributed 1 index knee to the study based on reported symptoms. Participants were randomized to receive APM with PT or PT alone. Two-hundred and twenty-seven participants had paired MRIs at both baseline and 18-month follow-up available for central reading. Six participants lacked MRI scoring for effusion-synovitis or cartilage damage and were excluded; thus, our cohort consisted of 221 participants (Figure 1).

Our study was approved by the Partners HealthCare Human Research Committee. The MeTeOR clinical trial is registered at ClinicalTrials.gov (identifier: NCT00597012).
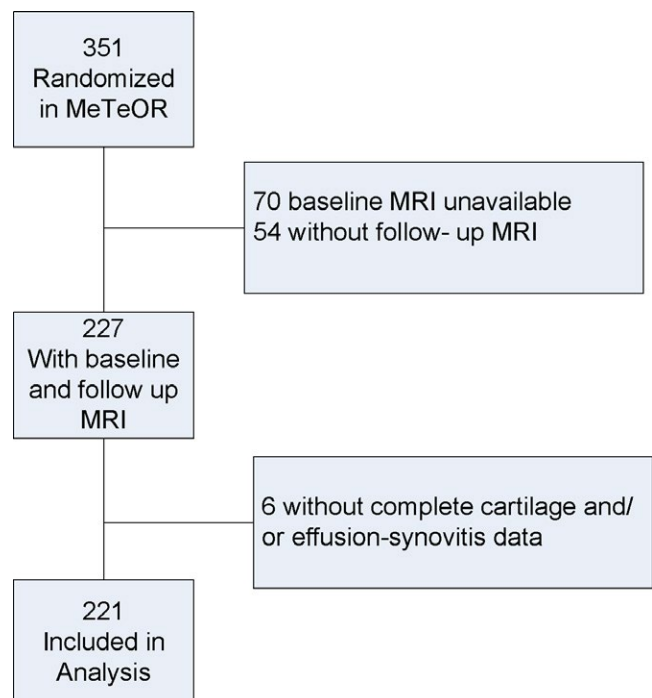
Figure 1. Flow diagram illustrating the selection of subjects for the analysis of associations of baseline effusion-synovitis and changes in effusion-synovitis with changes in cartilage damage in patients with osteoarthritis and meniscal tear. MeTeOR = Meniscal Tear in Osteoarthritis Research; MRI = magnetic resonance imaging.
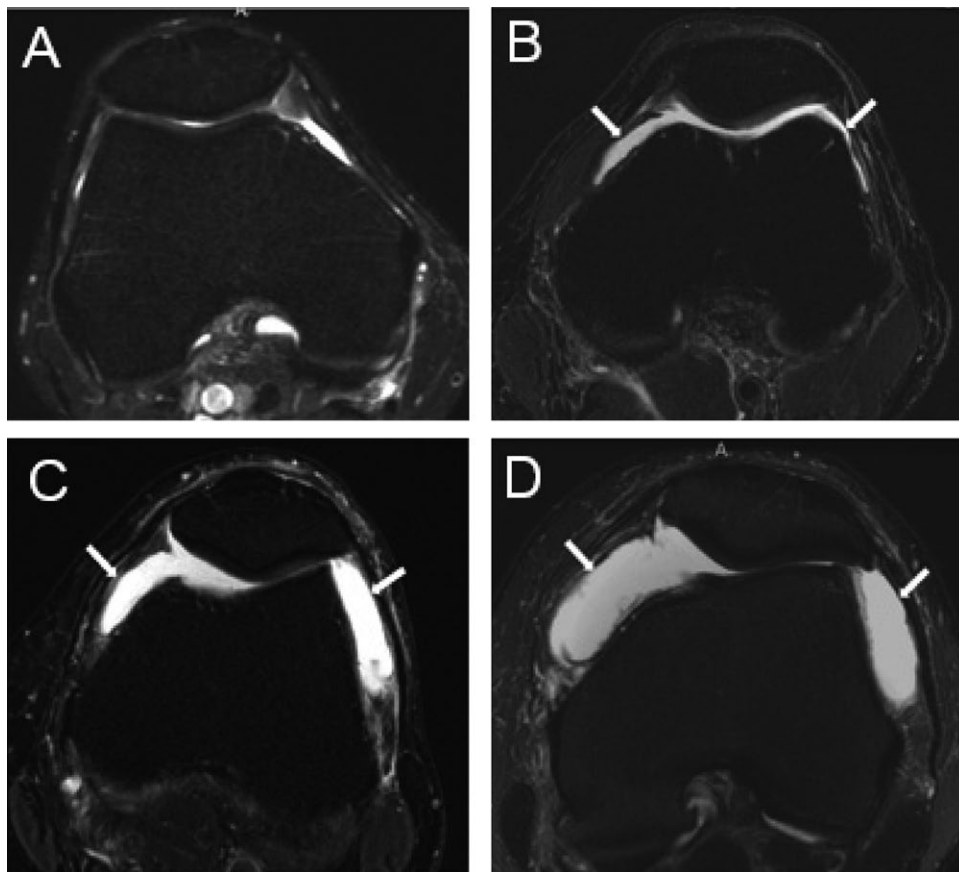
Figure 2. Axial fat-suppressed proton density–weighted magnetic resonance images of the suprapatellar pouch in patients with osteoarthritis and meniscal tear, showing different grades of effusion-synovitis. **A,** Grade 0, with no joint effusion-synovitis. **B,** Grade 1 effusion-synovitis with mild distension of the joint cavity indicated by fluid-equivalent signal within the suprapatellar pouch (**arrows**). **C,** Grade 2 effusion-synovitis with moderate distension of the joint cavity (**arrows**). **D,** Grade 3 effusion-synovitis with marked capsular distension (**arrows**).

Patient data. Data on age, sex, and body mass index (BMI; kg/m^2) were collected at baseline. The Knee Injury and Osteoarthritis Outcome Score (KOOS) Pain and Function scales were determined at baseline and 18 months to assess overall patient-reported knee pain in the past week. KOOS Pain and Function scores were transformed to a 0–100 scale, where 0 represents the least amount of pain/best function and 100 represents the greatest amount of pain/worst function (18). The K/L radiographic grade was used as an indication of baseline OA severity, where 0 = normal, 1 = questionable osteophyte, 2 = definite osteophyte, and 3 = definite narrowing of joint space not exhibiting a bone-on-bone appearance with or without osteophyte (19).

Imaging features. *Effusion-synovitis.* Both baseline and 18-month follow-up MRIs were reread by a single experienced musculoskeletal radiologist and scored according to the MOAKS criteria (14). In a reliability study of 10 subjects read by another highly experienced reader (AG), the interrater reliability intraclass correlation coefficient was 0.98 for the MOAKS total OA score.

Effusion-synovitis was detected by hyperintensity in the joint cavity on fat-suppressed T2-weighted or fat-suppressed proton density–weighted MRI (14). We chose to use effusion-synovitis as our measure of synovitis rather than Hoffa-synovitis (hyperintensity in Hoffa's fat pad), since effusion-synovitis may be more sensitive than Hoffa-synovitis for evaluating synovial thickness on non-contrast MRI (20). The interreader weighted kappa for MOAKS-based effusion-synovitis is 0.72 (14). At both baseline and 18 months, effusion-synovitis was graded on a scale of 0–3, where 0 = none (physiologic amount), 1 = small (fluid continuous in the retropatellar space), 2 = medium (slight convexity of the suprapatellar space), and 3 = large (evidence of capsular distension) (Figure 2). For all analyses, we dichotomized effusion-synovitis as none to small effusion-synovitis (termed "minimal") or medium to large effusion-synovitis (termed "extensive"). Change in effusion-synovitis from baseline to 18-month follow-up was categorized as persistently minimal (graded as none to small at both baseline and at 18 months), intermittent (graded as none to small at one time point and as medium to large at the other), or persistently
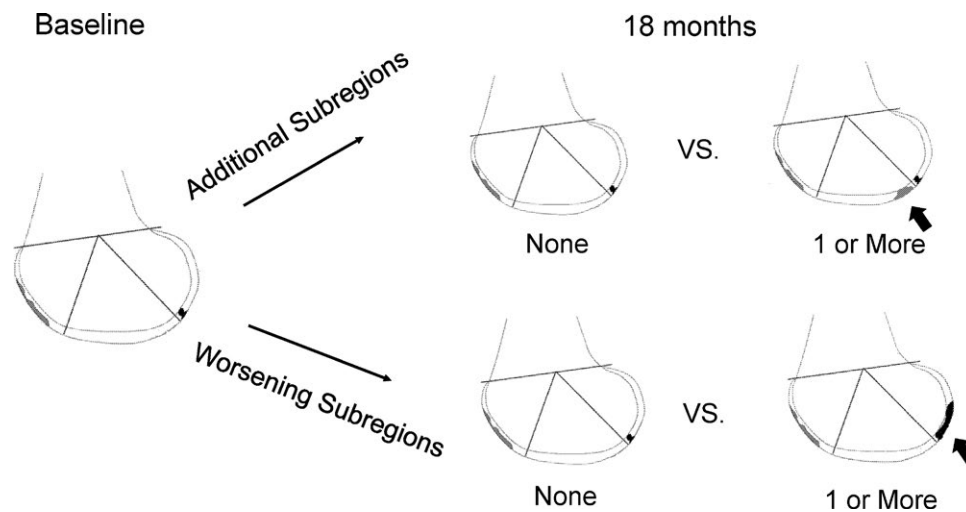
Figure 3. Diagram of outcomes in changes in cartilage damage over time in patients with osteoarthritis and meniscal tear. The number of additional subregions affected was classified as no additional subregions affected versus 1 or more additional subregions affected (**thick arrow**) at 18 months. The number of subregions with worsening damage was classified as no subregions with worsening versus 1 or more subregions with worsening (**thick arrow**) at 18 months. Adapted, with permission, from ref. 14.

extensive (graded as medium to large both at baseline and at 18 months).

Cartilage damage. We used MOAKS to assess articular cartilage damage (size and depth). MOAKS divides the articular region of the knee into 14 subregions to grade cartilage. Cartilage damage was quantified as size of any cartilage loss (percent of surface area in a subregion) and depth of cartilage damage (percent of loss that is full thickness in a subregion). For each subregion, both cartilage damage size and cartilage damage depth were categorized as 0 = none, 1 = <10%, 2 = 10–75%, and 3 = >75%. At baseline we used the maximum cartilage damage size and depth across the 14 regions for analysis. Due to small numbers in some categories and based on the baseline distributions of these variables, the MOAKS baseline cartilage damage size was dichotomized to ≤75% and >75%, while baseline cartilage damage depth was dichotomized to <10% and ≥10%.

The outcome of interest, progression of cartilage damage, was analyzed in two ways. First, we assessed the number of additional subregions affected, defined as the number of subregions with MOAKS grade 0 damage at baseline and grade ≥1 at 18-month follow-up. Second, we analyzed the number of subregions with worsening, defined as the number of subregions with an increase of ≥1 MOAKS grade at 18-month follow-up. Both cartilage damage size and depth were evaluated in this manner, as has been described previously (4,21). The number of additional subregions affected and the number of subregions with worsening damage were dichotomized as those with no additional subregion affected versus any additional subregions affected and those with no subregions with worsening versus those with any subregion with worsening (Figure 3).

Statistical analysis. Baseline characteristics were analyzed using means and percentages. We used a modified Poisson regression with robust error variance to estimate the relative risk (RR) of baseline effusion-synovitis and binary change in cartilage damage and the relationship of change in effusion-synovitis and binary change in cartilage damage over 18 months (22). We chose this approach given the high prevalence of the outcome; when the rare event rate assumption is violated, odds ratios generated from logistic regression generally overestimate risk ratios. Because binomial regression may lead to problems with convergence, Poisson regression with modification to ensure accurate variance estimations has been used to calculate RR from binary data (22,23). All analyses were adjusted for age, sex, BMI, and baseline cartilage damage (depth or size). Given that the outcome, worsening cartilage damage, occurred frequently in this sample, we present our results as RRs instead of odds ratios. APM has been associated with increased cartilage damage in this cohort; thus, all analyses were also adjusted for treatment received (APM versus no APM) (24). Over the 18-month follow-up period, 5 patients assigned to APM did not have surgery and were classified as "no APM". A total of 44 patients crossed over from the PT to the APM arm. Forty-three crossed over between baseline and 14 months and were classified as "APM" in this analysis. One patient crossed over from PT to APM at 30 months and was thus classified as "no APM" in this analysis.

In a sensitivity analysis, we reexamined the association between both baseline and change in effusion-synovitis and change in cartilage damage over 18 months after stratifying by 3 treatment groups: those randomized to APM and receiving APM, those randomized to PT and receiving PT, those who crossed over (randomized to PT and received APM or randomized to APM and not receiving APM).

In a second sensitivity analysis, we dichotomized effusion-synovitis as none versus any (small, medium, or large). Change in effusion-synovitis over 18 months was defined as never developed (graded as none at baseline and at 18 months), intermittent (none at one time point and any at the other time point), or persistent (any both at baseline and at 18 months). We then reexamined the association between both baseline and change in effusion-synovitis and change in cartilage damage over 18 months after adjusting for age, sex, BMI, and baseline cartilage damage (depth or size).

In a third sensitivity analysis, we redefined our change in effusion-synovitis categories, since participants with "resolution" of effusion-synovitis over 18 months may differ from those who have persistent effusion-synovitis or develop effusion-synovitis over 18 months. For this analysis, change in effusion-synovitis was defined as persistently minimal (none to small at both time points), resolving (medium to large at baseline and none to small at 18 months), or extensive at 18 months (medium to large at baseline and at 18 months or none to small at baseline and medium to large at 18 months). We then reexamined the association between change in effusion-synovitis and change in cartilage damage over 18 months after adjusting for age, sex, BMI, and baseline cartilage damage (depth or size).

RESULTS

Baseline effusion-synovitis and change in cartilage damage. The sample consisted of 221 participants. The mean age was 59 years, 58% were female, and the mean BMI was 30. Compared to men, women had a similar age and BMI, but a higher mean baseline KOOS Pain score (50 points compared to 40 points for men). At baseline, 48% of the patients had extensive effusion-synovitis and 52% had minimal effusion-synovitis. Thirty-nine percent of the participants had cartilage damage size >75%, and 40% had cartilage damage depth ≥10% (Table 1). There were no statistically significant associations between baseline effusion-synovitis and cartilage damage size. In the adjusted model, extensive effusion-synovitis was associated with a 1.4-fold increased risk of having additional subregions with damage (95% confidence interval [95% CI] 1.0–2.0) and a 1.2-fold increased risk of cartilage worsening (95% CI 0.8–1.6) compared to minimal effusion-synovitis. There was a significant association between baseline effusion-synovitis and cartilage damage depth. Those with extensive effusion-synovitis had a 1.7 times increased risk of additional subregions with damage (95% CI 1.1–2.6) and a 1.5 times increased risk of subregions with worsening damage (95% CI 1.0–2.2) compared to those with minimal effusion-synovitis (Table 2).

Table 1. Baseline characteristics of the cohort with osteoarthritis and meniscal tear*

		Change in effusion-synovitis over 18 months		
	All patients (n = 221)	Persistently minimal (n = 100)	Intermittent (n = 74)	Persistently extensive (n = 47)
Age, years	59 ± 7	59 ± 7	58 ± 8	58 ± 8
Sex, no. (%) female	129 (58)	59 (59)	33 (45)	37 (79)
BMI, kg/m²	30 ± 6	28 ± 5	30 ± 6	31 ± 7
KOOS Pain score	46 ± 16	44 ± 16	44 ± 15	54 ± 15
KOOS Function score	37 ± 18	34 ±17	35 ± 17	45 ± 20
Received APM, no. (%)	143 (65)	64 (64)	46 (62)	33 (70)
K/L grade, no. (%)				
0	50 (23)	26 (26)	17 (23)	7 (15)
1	51 (23)	24 (24)	23 (31)	4 (9)
2	58 (26)	27 (27)	14 (19)	17 (36)
3	62 (28)	23 (23)	20 (27)	19 (40)
Cartilage damage size, no. (%)				
≤75	135 (61)	65 (65)	46 (62)	24 (51)
>75%	86 (39)	35 (35)	28 (38)	23 (49)
Cartilage damage depth, no. (%)				
<10%	132 (60)	73 (73)	39 (53)	20 (43)
≥10%	89 (40)	27 (27)	35 (47)	27 (57)

* Except where indicated otherwise, values are the mean ± SD. BMI = body mass index; KOOS = Knee Injury and Osteoarthritis Outcome Score; APM = arthroscopic partial meniscectomy; K/L = Kellgren/Lawrence.

Table 2. Relative risk of cartilage damage according to baseline effusion-synovitis or change in effusion-synovitis*

	Cartilage damage size		Cartilage damage depth	
	Additional subregions affected	Subregions with worsening	Additional subregions affected	Subregions with worsening
Baseline effusion-synovitis				
Minimal	Reference	Reference	Reference	Reference
Extensive	1.4 (1.0–2.0)	1.2 (0.8–1.6)	1.7 (1.1–2.6)†	1.5 (1.0–2.2)†
Change in effusion-synovitis				
Persistently minimal	Reference	Reference	Reference	Reference
Intermittent	1.6 (1.0–2.4)†	1.3 (0.9–1.8)	1.6 (0.9–2.6)	1.5 (1.0–2.3)
Persistently extensive	1.6 (1.0–2.6)	1.2 (0.8–1.9)	2.0 (1.1–3.4)†	1.7 (1.0–2.7)†

* Values are the relative risk (95% confidence interval).
† $P < 0.05$.

Change in effusion-synovitis and change in cartilage damage. Over 18 months, effusion-synovitis was persistently minimal (none to small at baseline and 18 months) in 45% of the participants, intermittent (none to small at one time point and medium to large at the other) in 33% of the participants, and persistently extensive (medium to large at baseline and 18 months) in 21% of the participants. Of the participants with intermittent effusion-synovitis, 78% had effusion-synovitis at baseline only. The group with persistently minimal effusion-synovitis was 59% female and had a mean BMI of 28. Those with intermittent effusion-synovitis were 45% female and had a mean BMI of 30. Participants with persistently extensive effusion-synovitis were 79% female and had a mean BMI of 31. The percent of participants in the effusion-synovitis categories who received APM ranged from 62% to 70%, but these differences were not statistically significant (Table 1).

The reduction in reported pain scores from baseline to 18 months was similar across the effusion-synovitis categories, with those with persistently minimal effusion-synovitis sustaining a reduction in KOOS Pain score of 24 points, compared to 26 points in those with intermittent effusion-synovitis and 27 points in those with persistently extensive effusion-synovitis. The KOOS Function score improved by 21 points in patients with persistently minimal effusion-synovitis, 23 points in patients with intermittent effusion-synovitis, and 25 points in those with persistent effusion-synovitis.

Over 18 months, 74% of the patients had worsening cartilage damage size, and 53% had additional subregions affected by cartilage damage size. Fifty-seven percent had worsening cartilage damage depth, and 46% had additional subregions affected by cartilage damage depth. In participants with K/L grade 0–1 at baseline, 73% had worsening cartilage damage size, and 51% had additional regions affected by cartilage damage size, compared to 75% and 55%, respectively, in those with K/L grades 2–3. Of those with K/L grades 0–1, 50% had worsening cartilage damage depth, and 42% had additional regions affect-

ed by cartilage damage depth, compared to 64% and 49%, respectively, in those with K/L grades 2–3 at baseline.

In adjusted models, intermittent and persistent effusion-synovitis over 18 months were associated with concurrent increases in cartilage damage for both size and depth (Table 2 and Figure 4). Those with intermittent effusion-synovitis (RR 1.6 [95% CI 1.0–2.4]) and those with persistently extensive effusion-synovitis (RR 1.6 [95% CI 1.0–2.6]) had an increased risk of having additional subregions affected by cartilage damage size compared to patients with persistently minimal effusion-synovitis, but there were no significant associations between either synovitis category and the number of subregions with worsening damage size. Those with intermittent effusion-synovitis (RR 1.6 [95% CI 0.9–2.6]) and those with persistently extensive effusion-synovitis (RR 2.0 [95% CI 1.1–3.4]) had an increased risk of having additional subregions affected by cartilage damage depth. Finally, intermittent synovitis was associated with a 1.5 times increased risk of having subregions with worsening in cartilage damage depth (95% CI 1.0–2.3), and persistently extensive synovitis was associated with a 1.7 times increased risk of having subregions with worsening in cartilage damage depth (95% CI 1.0–2.7), compared with persistently minimal effusion-synovitis.

In the sensitivity analysis adjusted for the 3 treatment groups, the associations of baseline effusion-synovitis and change in effusion-synovitis with change in cartilage damage were similar to those observed in the main analysis in each treatment stratum (Supplementary Table 1, available on the *Arthritis & Rheumatology* web site at http://onlinelibrary.wiley.com/doi/10.1002/art.40660/abstract).

In the second sensitivity analysis, in which effusion-synovitis was dichotomized as any versus none, 20% of the participants had no effusion-synovitis and 80% had any effusion-synovitis at baseline. Over 18 months, 11% never developed effusion-synovitis, 19% had intermittent effusion-synovitis, and 71% had persistent effusion-synovitis (Supplementary Table 2, http://onlinelibrary.wiley.com/doi/10.1002/art.40660/abstract).
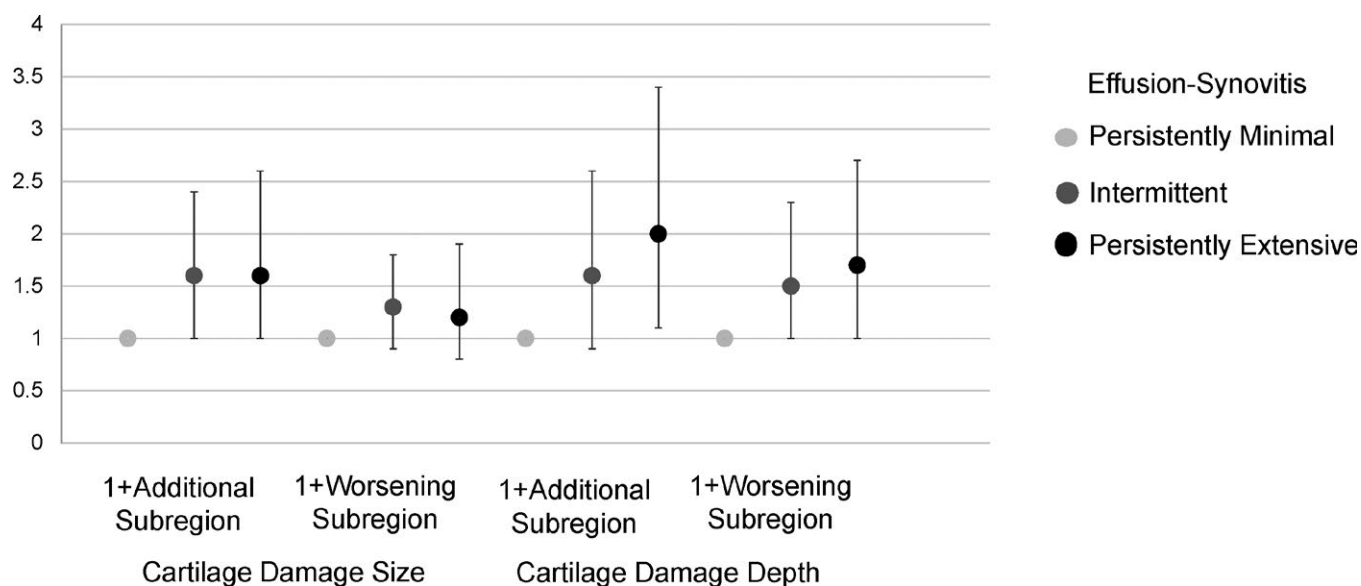
Figure 4. Relative risk of cartilage damage according to change in effusion-synovitis over 18 months in patients with osteoarthritis and meniscal tear. Effusion-synovitis was classified as persistently minimal (graded as none or small at both baseline and 18 months), intermittent (graded as none or small at one time point and medium or large at the other), or persistently extensive (graded as medium or large at both baseline and 18 months). The analysis was adjusted for age, sex, body mass index, and baseline cartilage damage and treatment. Circles represent relative risk; vertical lines indicate the 95% confidence interval.

In the third sensitivity analysis, assessing resolution of effusion-synovitis over 18 months, effusion-synovitis was persistently minimal in 45% of the patients, resolved in 26% of the patients, and was extensive at 18 months in 29% of the patients (Supplementary Table 3, http://onlinelibrary.wiley.com/doi/10.1002/art.40660/abstract). In the second and third sensitivity analyses, the associations of baseline effusion-synovitis and change in effusion-synovitis with change in cartilage damage were similar to those found in the main analysis.

DISCUSSION

Our study demonstrates a positive association between the presence and persistence of extensive effusion-synovitis and progression of cartilage damage depth over 18 months. Extensive effusion-synovitis at baseline conferred an ~50–70% increased risk of worsening cartilage damage depth. Over 18 months, intermittent and persistently extensive effusion-synovitis were associated with greater cartilage damage in analyses that adjusted for baseline cartilage damage. Participants with persistently extensive effusion-synovitis demonstrated the greatest risk of subsequent cartilage damage, with a 70–100% increased risk of progression of cartilage damage depth.

In our analyses, effusion-synovitis was associated with a non–statistically significant 20–30% increased risk of worsening cartilage damage size. The notable effect of effusion-synovitis on worsening cartilage damage depth but not on worsening cartilage damage size may be due to a threshold effect, since many participants had subregions with extensive cartilage damage size at baseline.

Several prior studies of patients both with and without OA have investigated the relationship between synovitis and cartilage damage (3,12,13,25). A study using the Multicenter Osteoarthritis Study (MOST) cohort of patients with or at risk of OA documented that baseline MRI-defined effusion or synovitis was associated with a 3-fold increased odds of more rapid cartilage loss (3). A subsequent study using the MOST cohort and contrast-enhanced MRI demonstrated that patients with synovitis had twice the odds of cartilage damage in a cross-sectional analysis (25).

Wang et al used MRI to assess the association of synovitis grade and cartilage damage both cross-sectionally and longitudinally in a cohort of older adults (12). In those longitudinal analyses over 2.7 years, baseline effusion-synovitis was associated with a small risk of worsening cartilage defects (RR 1.1) after adjustment for baseline bone marrow lesions and cartilage defects (12). The results of those analyses are consistent with the findings of our study. Furthermore, the majority of participants that we characterized as having intermittent effusion-synovitis had effusion-synovitis at baseline only (78%). Thus, it appears that "resolving" effusion-synovitis still confers a greater risk of future cartilage damage than no synovitis at all. Wang et al also evaluated a quantitative measure of cartilage volume on MRI and demonstrated a significant negative association between baseline effusion-synovitis and cartilage volume longitudinally (12). Interestingly, no significant association was documented between baseline effusion-synovitis and change in measured cartilage volume after adjustment for baseline bone marrow lesions and cartilage volume (12).

In the study by Wang et al described above, ~60% of the study population had any cartilage defect on MRI. In contrast, our cohort represents an important and prevalent subset of patients with greater intraarticular pathology, since all had imaging evidence of cartilage damage and concurrent meniscal tear. We contribute to the prior knowledge base by demonstrating that the presence of effusion-synovitis over time (persistent or intermittent) appears to be associated with worsening cartilage damage.

A second study, also by Wang et al, used a quantitative measure of MRI-defined effusion-synovitis in the same cohort in which ~60% had cartilage defects on MRI. Change in effusion-synovitis over 2.7 years was calculated, with 29% increasing in size, 50% remaining stable, and 22% decreasing in size. Over 2.7 years, baseline effusion-synovitis area was associated with increased cartilage defects and decreasing cartilage volume (13). The effect of change in effusion-synovitis on change in cartilage parameters was not assessed. It is of interest that in our study only 7% of the participants developed extensive effusion-synovitis over the 18-month period, while 26% had a decrease in grade from extensive to minimal. We cannot rule out the possibility that treatment (APM or PT) affected the presence of effusion-synovitis over time.

Our study has several limitations. We used semiquantitative grades for effusion-synovitis and cartilage, which have less granularity than a strictly quantitative score. However, our semiquantitative results appear to be consistent with those of prior studies using quantitative measures (13). We also recategorized the baseline effusion-synovitis into none versus any and observed similar findings. MOAKS was developed to score knee OA on MRI; thus, the clinical relevance or correlation of progressive cartilage damage on MRI is unknown. Since our cohort had baseline OA and meniscal tear, we were unable to ascertain whether intraarticular damage (cartilage and meniscal damage) incited synovitis, though we demonstrated that these pathologies are highly associated. We demonstrated that changes in effusion-synovitis potentially contribute to cartilage damage over time.

In summary, our study demonstrates that, in patients with OA and meniscal tear, changes in synovitis, whether persistently extensive or intermittent, are associated with cartilage damage over time. Since synovitis is a potentially modifiable intraarticular feature, further research is warranted to assess whether treatment of synovitis mitigates cartilage degradation.

AUTHOR CONTRIBUTIONS

All authors were involved in drafting the article or revising it critically for important intellectual content, and all authors approved the final version to be published. Dr. MacFarlane had full access to all of the data in the study and takes responsibility for the integrity of the data and the accuracy of the data analysis.

Study conception and design. MacFarlane, Yang, Collins, Guermazi, Losina, Katz.

Acquisition of data. Yang, Collins, Jarraya, Guermazi, Losina, Katz.

Analysis and interpretation of data. MacFarlane, Yang, Collins, Jarraya, Guermazi, Mandl, Martin, Wright, Losina, Katz.

ADDITIONAL DISCLOSURES

Author Wright is an employee of Johnson & Johnson.

REFERENCES

1. Neogi T, Guermazi A, Roemer F, Nevitt MC, Scholz J, Arendt-Nielsen L, et al. Association of joint inflammation with pain sensitization in knee osteoarthritis: the Multicenter Osteoarthritis Study. Arthritis Rheumatol 2016;68:654–61.

2. Felson DT, Niu J, Neogi T, Goggins J, Nevitt MC, Roemer F, et al. Synovitis and the risk of knee osteoarthritis: the MOST Study. Osteoarthritis Cartilage 2016;24:458–64.

3. Roemer FW, Zhang Y, Niu J, Lynch JA, Crema MD, Marra MD, et al. Tibiofemoral joint osteoarthritis: risk factors for MR-depicted fast cartilage loss over a 30-month period in the multicenter osteoarthritis study. Radiology 2009;252:772–80.

4. Collins JE, Losina E, Nevitt MC, Roemer FW, Guermazi A, Lynch JA, et al. Semiquantitative imaging biomarkers of knee osteoarthritis progression: data from the Foundation for the National Institutes of Health Osteoarthritis Biomarkers Consortium. Arthritis Rheumatol 2016;68:2422–31.

5. Roemer FW, Guermazi A, Hunter DJ, Niu J, Zhang Y, Englund M, et al. The association of meniscal damage with joint effusion in persons without radiographic osteoarthritis: the Framingham and MOST osteoarthritis studies. Osteoarthritis Cartilage 2009;17:748–53.

6. Roemer FW, Felson DT, Yang T, Niu J, Crema MD, Englund M, et al. The association between meniscal damage of the posterior horns and localized posterior synovitis detected on T1-weighted contrast-enhanced MRI—the MOST study. Semin Arthritis Rheum 2013;42:573–81.

7. Scanzello CR, McKeon B, Swaim BH, DiCarlo E, Asomugha EU, Kanda V, et al. Synovial inflammation in patients undergoing arthroscopic meniscectomy: molecular characterization and relationship to symptoms. Arthritis Rheum 2011;63:391–400.

8. Wallace G, Cro S, Dore C, King L, Kluzek S, Price A, et al. Associations between clinical evidence of inflammation and synovitis in symptomatic knee osteoarthritis: a cross-sectional substudy. Arthritis Care Res (Hoboken) 2017;69:1340–8.

9. Bhattacharyya T, Gale D, Dewire P, Totterman S, Gale ME, McLaughlin S, et al. The clinical importance of meniscal tears demonstrated by magnetic resonance imaging in osteoarthritis of the knee. J Bone Joint Surg Am 2003;85-A:4–9.

10. Sellam J, Berenbaum F. The role of synovitis in pathophysiology and clinical symptoms of osteoarthritis. Nature Rev Rheumatol 2010;6:625–35.

11. Sokolove J, Lepus CM. Role of inflammation in the pathogenesis of osteoarthritis: latest findings and interpretations. Ther Adv Musculoskelet Dis 2013;5:77–94.

12. Wang X, Blizzard L, Halliday A, Han W, Jin X, Cicuttini F, et al. Association between MRI-detected knee joint regional effusion-synovitis and structural changes in older adults: a cohort study. Ann Rheum Dis 2016;75:519–25.

13. Wang X, Blizzard L, Jin X, Chen Z, Zhu Z, Han W, et al. Quantitative assessment of knee effusion-synovitis in older adults: association with knee structural abnormalities. Arthritis Rheumatol 2016;68:837–44.

14. Hunter DJ, Guermazi A, Lo GH, Grainger AJ, Conaghan PG, Boudreau RM, et al. Evolution of semi-quantitative whole joint as-

sessment of knee OA: MOAKS (MRI Osteoarthritis Knee Score). Osteoarthritis Cartilage 2011;19:990–1002.

15. Katz JN, Brophy RH, Chaisson CE, de Chaves L, Cole BJ, Dahm DL, et al. Surgery versus physical therapy for a meniscal tear and osteoarthritis. N Engl J Med 2013;368:1675–84.

16. Katz JN, Chaisson CE, Cole B, Guermazi A, Hunter DJ, Jones M, et al. The MeTeOR trial (Meniscal Tear in Osteoarthritis Research): rationale and design features. Contemp Clin Trials 2012;33:1189–96.

17. Roemer FW, Kwoh CK, Hannon MJ, Crema MD, Moore CE, Jakicic JM, et al. Semiquantitative assessment of focal cartilage damage at 3T MRI: a comparative study of dual echo at steady state (DESS) and intermediate-weighted (IW) fat suppressed fast spin echo sequences. Eur J Radiol 2011;80:15.

18. Roos EM, Roos HP, Lohmander LS, Ekdahl C, Beynnon BD. Knee Injury and Osteoarthritis Outcome Score (KOOS)–development of a self-administered outcome measure. J Orthop Sports Phys Ther 1998;28:88–96.

19. Kellgren JH, editor. Atlas of standard radiographs of arthritis. Vol. II. Oxford: Blackwell Scientific; 1963.

20. Crema MD, Roemer FW, Li L, Alexander RC, Chessell IP, Dudley AD, et al. Comparison between semiquantitative and quantitative methods for the assessment of knee synovitis in osteoarthritis using non-enhanced and gadolinium-enhanced MRI. Osteoarthritis Cartilage 2017;25:267–71.

21. Roemer FW, Guermazi A, Collins JE, Losina E, Nevitt MC, Lynch JA, et al. Semi-quantitative MRI biomarkers of knee osteoarthritis progression in the FNIH biomarkers consortium cohort: methodo-logic aspects and definition of change. BMC Musculoskeletal Disord 2016;17:466.

22. Zou G. A modified poisson regression approach to prospective studies with binary data. Am J Epidemiol 2004;159:702–6.

23. McNutt LA, Wu C, Xue X, Hafner JP. Estimating the relative risk in cohort studies and clinical trials of common outcomes. Am J Epidemiol 2003;157:940–3.

24. Collins JE, Losina E, Guermazi A, Katz JN. The risk of osteoarthritis progression after arthroscopic partial meniscectomy (APM): data from an rct of APM vs. physical therapy. Osteoarthritis Cartilage 2017;25 Suppl 1:S59.

25. Guermazi A, Hayashi D, Roemer FW, Zhu Y, Niu J, Crema MD, et al. Synovitis in knee osteoarthritis assessed by contrast-enhanced magnetic resonance imaging (MRI) is associated with radiographic tibiofemoral osteoarthritis and MRI-detected widespread cartilage damage: the MOST study. J Rheumatol 2014;41:501–8.

APPENDIX A: THE MeTeOR INVESTIGATOR GROUP

Members of the MeTeOR Investigator Group are as follows: Robert H. Brophy, MD, Bruce A. Levy, MD, Robert G. Marx, MD, Mathew Matava, MD, Clare Safran-Norton, PT, PhD, Kurt P. Spindler, MD, Michael Stuart, MD, Diane L. Dahm, MD, and Rick Wright, MD.

Impact of Tumor Necrosis Factor Inhibitor Versus Nonsteroidal Antiinflammatory Drug Treatment on Radiographic Progression in Early Ankylosing Spondylitis: Its Relationship to Inflammation Control During Treatment

Jun Won Park,[1] ![iD] Min Jung Kim,[1] Jeong Seok Lee,[1] ![iD] You-Jung Ha,[2] Jin Kyun Park,[1] Eun Ha Kang,[2] Yun Jong Lee,[2] Yeong Wook Song,[1] and Eun Young Lee[1] ![iD]

Objective. To investigate the impact of tumor necrosis factor inhibitor (TNFi) treatment and inflammation control on radiographic progression in early ankylosing spondylitis (AS) over 4 years.

Methods. We included a total of 215 patients with early AS (symptom duration <10 years) treated with TNFi (the TNFi group; n = 135) or with nonsteroidal antiinflammatory drugs (NSAIDs) (the control group; n = 80). Two blinded readers assessed radiographic progression using the modified Stoke Ankylosing Spondylitis Spine Score (mSASSS). Inflammation control was inferred from C-reactive protein (CRP) levels time-averaged between 2 radiologic assessments. Linear mixed modeling was used to estimate mSASSS changes over radiographic intervals as well as the impact of clinical factors on outcomes.

Results. The TNFi group had longer disease duration, a higher baseline CRP level, and a higher Bath Ankylosing Spondylitis Disease Activity Index than did controls. The time-averaged CRP level over radiographic intervals was lower with TNFi treatment than with NSAID treatment (mean ± SD 0.27 ± 0.30 mg/dl versus 0.61 ± 0.68 mg/dl; $P <$ 0.001). Overall, mean ± SD mSASSS change over the 2-year interval was 1.30 ± 2.97 units. In the multivariable model adjusted for age, smoking status, baseline CRP level, and the presence of syndesmophytes at baseline, the TNFi group showed less mSASSS change over the 2-year interval (β = −0.90 [95% confidence interval {95% CI} −1.51, −0.29]). However, when a time-averaged CRP level was additionally included, it significantly influenced the mSASSS change (β = 1.02 [95% CI 0.32, 1.71]), decreasing the estimated group difference (β = −0.52 [95% CI −1.17, 0.14]). NSAID indices of both groups were not associated with either time-averaged CRP levels or mSASSS changes.

Conclusion. Effective suppression of inflammation by TNFi treatment decreases radiographic progression in early AS.

INTRODUCTION

It remains uncertain whether tumor necrosis factor inhibitors (TNFi) delay radiographic progression of ankylosing spondylitis (AS). Although TNFi effectively decrease spinal inflammation, previous studies from randomized controlled trials did not show any difference in radiographic progression between patients receiving TNFi and those using only nonsteroidal antiinflammatory drugs (NSAIDs) (1–4). However, recent cohort studies suggest-

ed that early or long-term TNFi treatment could slow down the process (5–7).

Some studies have supported the notion of a link between inflammation and pathologic new bone formation, especially during the early phase of the disease. Maksymowych et al showed that advanced inflammatory vertebral corner lesions on magnetic resonance imaging (MRI) are more likely to progress to syndesmophytes through a process of fat metaplasia in spite of TNFi treatment, while early lesions could be resolved without pro-

University College of Medicine, Department of Internal Medicine, Division of Rheumatology, 101 Daehak-ro, Jongno-gu, Seoul 03080, Republic of Korea. E-mail: elee@snu.ac.kr.

gression (8). In the Infliximab As First Line Therapy in Patients with Early Active Axial Spondyloarthritis Trial, which enrolled patients with axial spondyloarthritis of <3 years duration, ~70% of resolved vertebral inflammatory lesions did not progress to new fatty lesions (9). These results indicate that early, effective anti-inflammatory treatment may reduce radiographic progression in AS. However, since these studies had relatively short observation periods, it was still uncertain whether TNFi treatment in the early phase of disease can lead to decreased syndesmophyte formation, the final end point of radiographic progression, compared with conventional NSAID treatment.

In the present study, we compared radiographic progression over 4 years of observation between TNFi and conventional NSAID treatment in patients with early AS. In addition, to disentangle the relationships among inflammation, treatment strategy, and radiographic progression, we also investigated the extent to which inflammation control contributes to the suppression of radiographic progression by TNFi versus NSAIDs.

PATIENTS AND METHODS

Patients. Patients' clinical and radiographic data were extracted from 2 independent observational cohorts. AS patients receiving TNFi treatment (the TNFi group) were from a consecutive, single-center cohort in Seoul National University Hospital, and patients receiving conventional NSAID treatment (the control group) were from another single-center cohort in Seoul National University Bundang Hospital. All patients fulfilled the modified New York criteria for AS (10) at diagnosis. To precisely investigate radiographic progression in early AS, we included patients with initial onset of inflammatory back pain <10 years from the starting date of specific TNFi treatment (the TNFi group) or NSAID treatment (the control group) and with available sets of spine radiographs at baseline (defined as a starting date of group-specific treatment) and after 2 and/or 4 years of their respective treatments (11).

The study was approved by the Institutional Review Boards (IRBs) of Seoul National University Hospital (approval no. 1611-119-810) and Seoul National University Bundang Hospital (approval no. B-1604-343-112) and was conducted in accordance with the principles of the Declaration of Helsinki and Good Clinical Practice guidelines. The requirement for patient consent was waived by the IRBs due to the retrospective character of the study.

Clinical assessment during observation. All demographic and clinical data were extracted from the electronic medical database of each institution using common case report forms. Patients' demographic factors, body mass index (BMI), smoking status, Bath Ankylosing Spondylitis Disease Activity Index (BASDAI) (12), and serum C-reactive protein (CRP) level were assessed at baseline. Disease activity was regularly monitored every

3 or 6 months in accordance with the preference of the treating physician. In the TNFi group, the BASDAI was regularly checked, and continuation of treatment was mainly determined based on whether a patient fulfilled the BASDAI criteria for 50% improvement (BASDAI 50) (13). In contrast, the BASDAI was not routinely scored in the NSAID group. Physicians in both hospitals routinely checked the name and dose of the prescribed NSAIDs as well as the average number of days per week that the NSAIDs were taken. Quantification of NSAID intake during the 2-year interval was calculated as proposed in the Assessment of SpondyloArthritis international Society recommendations (14). Longitudinal control of inflammation during the 2-year interval was estimated using time-averaged CRP values, that is, the mean value of CRP levels determined every 6 months. The observation period in this study was 4 years from the baseline visit. However, for the precise estimation of treatment effect on radiographic progression and inflammation, observation was terminated if a patient stopped the TNFi, switched to another TNFi (the TNFi group), or started a new TNFi (the control group). Spine radiographs obtained during the observation period for each patient were used for analysis.

Measurement of serum CRP level. Serum high-sensitivity CRP (hsCRP) level in patients in both centers was measured using a chemistry autoanalyzer latex-enhanced turbidimetric immunoassay with CRP-Latex reagent (Denkaseiken). This assay permitted the measurement of hsCRP levels as low as 0.01 mg/dl in both centers. Four times each year, both centers also perform external quality control for hsCRP for the College of American Pathologists.

Assessment of radiographic progression. Spine radiographs obtained in the 2 hospitals were given a unique code after all clinical information (including name of patient and hospital and date of examination) was deleted. After this processing, all radiographs were collected and delivered to each assessor in the form of a Digital Imaging and Communication in Medicine file. Radiographic progression was assessed using the modified Stoke Ankylosing Spondylitis Spine Score (mSASSS) (15). Two trained assessors (JWP and MK) scored radiographs independently. If a radiograph had ≤3 missing vertebral corners, missing scores were replaced by the mean score of the corresponding corners of the visible segments. Radiographs with >3 missing vertebral corners were excluded from the scoring. The mean mSASSS of both readers was used for analysis. If a difference between scores measured by the 2 readers was >5 units (defined as a major disagreement), the same assessors rescored those radiographs. In case of persistent major disagreement after rescoring, an independent adjudicator (EYL) assigned a final score.

Statistical analysis. Interobserver reliability of the mSASSS was assessed using an intraclass correlation coefficient (ICC). The smallest detectable change (SDC) between the 2 readers

was calculated to estimate reliably detectable radiographic progression given measurement error (16).

Progression of the mSASSS over time and impact of clinical factors on outcome were estimated using a linear mixed model. A "compound symmetry" correlation structure was selected based on Pearson correlation coefficients of the mSASSS at different time points. To estimate the impact of longitudinal inflammation control on radiographic progression, we constructed 2 different models. First, mSASSS changes over radiographic intervals were correlated with the baseline features of age, sex, BMI, smoking status (never versus ever), symptom duration, CRP level (mg/dl), BASDAI, HLA–B27 status, concomitant NSAID treatment, and the presence of syndesmophytes on baseline radiographs. Any clinical factors that showed relevant influence ($P < 0.1$) on the outcome were included in the multivariable model (model 1). Next, time-averaged CRP level was added to this model, and changes in the effects of other covariates were analyzed (model 2). A Sobel test was also performed to estimate the indirect effect of TNFi on the outcome (17). Fitness of the model was estimated using Akaike's information criterion. To consider the bias due to measurement error between the assessors, mSASSS progression ≥2 units in 2 years (defined as definite radiographic progression) was also used as a dichotomous outcome and was modeled using a generalized linear mixed model.

Table 1. Baseline characteristics of the patients*

	TNFi group (n = 135)	Control group (n = 80)	P
Age, years	32.8 ± 11.5	34.4 ± 11.9	0.335
Male sex, no. (%)	110 (81.5)	61 (76.2)	0.358
Body mass index	23.3 ± 3.3	23.3 ± 3.5	0.980
Symptom duration, years†	4.3 ± 2.7	4.1 ± 2.9	0.679
Disease duration, years	2.7 ± 2.6	0.7 ± 1.8	<0.001
Ever smoker, no. (%)	53 (39.3)	32 (40.0)	0.914
HLA–B27 positive, no. (%)	119 (88.1)	71 (88.8)	0.894
BASDAI, 0–10	6.7 ± 1.6	3.2 ± 1.6	<0.001
Serum CRP level, mg/dl	2.2 ± 2.7	1.1 ± 1.3	<0.001
Presence of syndesmophytes, no. (%)	37 (27.4)	19 (23.8)	0.555
Number of syndesmophytes	1.6 ± 3.4	1.4 ± 3.1	0.591
mSASSS, 0–72	6.2 ± 9.9	7.3 ± 10.8	0.445

* Except where indicated otherwise, values are the mean ± SD. TNFi = tumor necrosis factor inhibitor; BASDAI = Bath Ankylosing Spondylitis Disease Activity Index; CRP = C-reactive protein; mSASSS = modified Stoke Ankylosing Spondylitis Spine Score.
† Time interval between initial onset of inflammatory back pain and baseline visit.

Table 2. Impact of time-averaged CRP level on difference of mSASSS progression between TNFi treatment and NSAID treatment during 2-year radiographic interval*

	β (95% CI)†	P
Model 1‡		
Age, years	0.02 (−0.004, 0.05)	0.092
Ever smoking (vs. never)	0.30 (−0.30, 0.89)	0.326
Baseline CRP level, mg/dl	0.16 (0.03, 0.29)	0.019
Presence of syndesmophytes at baseline (vs. absence)	2.09 (1.32, 2.86)	<0.001
TNFi group (vs. control group)	−0.90 (−1.51, −0.29)	0.004
Model 2‡		
Age, years	0.03 (−0.002, 0.05)	0.066
Ever smoking (vs. never)	0.28 (−0.31, 0.86)	0.356
Baseline CRP level, mg/dl	0.12 (−0.01, 0.25)	0.079
Presence of syndesmophytes at baseline (vs. absence)	1.86 (1.09, 2.63)	<0.001
TNFi group (vs. control group)	−0.52 (−1.17, 0.14)	0.123
Time-averaged CRP level in 2-year interval, mg/dl	1.02 (0.32, 1.71)	0.004

* TNFi = tumor necrosis factor inhibitor; NSAID = nonsteroidal antiinflammatory drug; 95% CI = 95% confidence interval.
† Indicates difference in modified Stoke Ankylosing Spondylitis Spine Score (mSASSS) change in 2-year radiographic interval between the 2 groups (dichotomous variable) or when a covariate increases by 1 unit (continuous variable).
‡ Any clinical factors that showed significant association ($P < 0.1$) in the univariable analysis were included in the multivariable model (model 1). Time-averaged C-reactive protein (CRP) level was then added to this model, and changes in the effects of other covariates were analyzed (model 2). Akaike's information criterion, an estimate of model fitness, was 1,473.740 for model 1 and 1,457.817 for model 2.

Since patients mostly started TNFi treatment after the failure of first-line NSAID treatment, it was expected that baseline features between the 2 groups were different. To minimize this confounding by indication, we performed 1:1 propensity score matching. This was carried out using age, disease duration, baseline CRP level, smoking status, and baseline mSASSS as predictors for choosing treatment, with a caliper of 0.2. Baseline BASDAI could not be included because its discrepancy between the 2 groups was so marked that propensity score matching including it as a covariate discarded most of the study population. Instead, the multivariable model performed after the matching was adjusted for the baseline BASDAI. After matching, 62 patients in each group were selected as the postmatched populations. In addition, the same analysis was performed in the sub-

group of 88 patients (58 in the TNFi group and 30 in the NSAID group) who had a complete set of radiographs at all follow-up time points during the observation period.

All statistical analyses were performed using IBM SPSS Statistics 20. *P* values less than 0.05 were considered significant.

RESULTS

Patient characteristics. A total of 215 patients were included (135 in the TNFi group and 80 controls). The number of evaluated sets of radiographs was 328 in the TNFi group and 190 in the control group. The mean ± SD symptom duration was 4.2 ± 2.8 years. One hundred seventy-one patients were male (79.5%), and 190 patients (88.4%) were HLA–B27 positive.

Clinical and radiographic features of included patients are presented in Table 1. Briefly, patients in the TNFi group had significantly longer disease duration (mean ± SD 2.7 ± 2.6 years versus 0.7 ± 1.8 years) and higher CRP levels (mean ± SD 2.2 ± 2.7 mg/dl versus 1.1 ± 1.3 mg/dl). However, other clinical factors such as age, sex, BMI, smoking status, and HLA–B27 positivity were comparable between the 2 groups. The mean ± SD baseline mSASSS was 6.2 ± 9.9 in the TNFi group and 7.3 ± 10.8 in the control group, which was not significantly different. In the postmatched population, baseline CRP level and disease duration were well balanced between the 2 groups, but imbalances

in the BASDAI persisted (see Supplementary Table 1, available on the *Arthritis & Rheumatology* web site at http://onlinelibrary. wiley.com/doi/10.1002/art.40661/abstract).

Radiographic progression over time. Among a total of 518 evaluations of sets of radiographs, mSASSS scores in 66 sets yielded major disagreement, and subsequently 12 of them were ultimately scored by the adjudicator. Interobserver ICCs for individual mSASSS scores, and for mSASSS change over time intervals, were 0.95 (95% confidence interval [95% CI] 0.92, 0.97) and 0.90 (95% CI 0.88, 0.92), respectively. The SDC for all mSASSS changes was 1.86. A Bland-Altman plot is shown in Supplementary Figure 1, http://onlinelibrary.wiley.com/doi/10.1002/art.40661/abstract.

The mean ± SD mSASSS change over 2 years in the whole population was 1.30 ± 2.97 units. Estimated rates of progression in the univariable mixed model during the 0–2-year interval and 2–4-year interval were comparable (1.36 [95% CI 0.82, 1.89] and 1.25 [95% CI 0.82, 1.68], respectively; *P* = 0.757). Among a total of 321 radiographic intervals, definite radiographic progression occurred in 81 (25.2%). The proportion of intervals showing definite radiographic progression was higher in the TNFi group (37 of 119 [31.1%] versus 44 of 202 [21.8%]; *P* = 0.064).

In the univariable analysis, age (β = 0.07 [95% CI 0.04, 0.10]), baseline CRP level (β = 0.15 [95% CI 0.01, 0.29]), ever
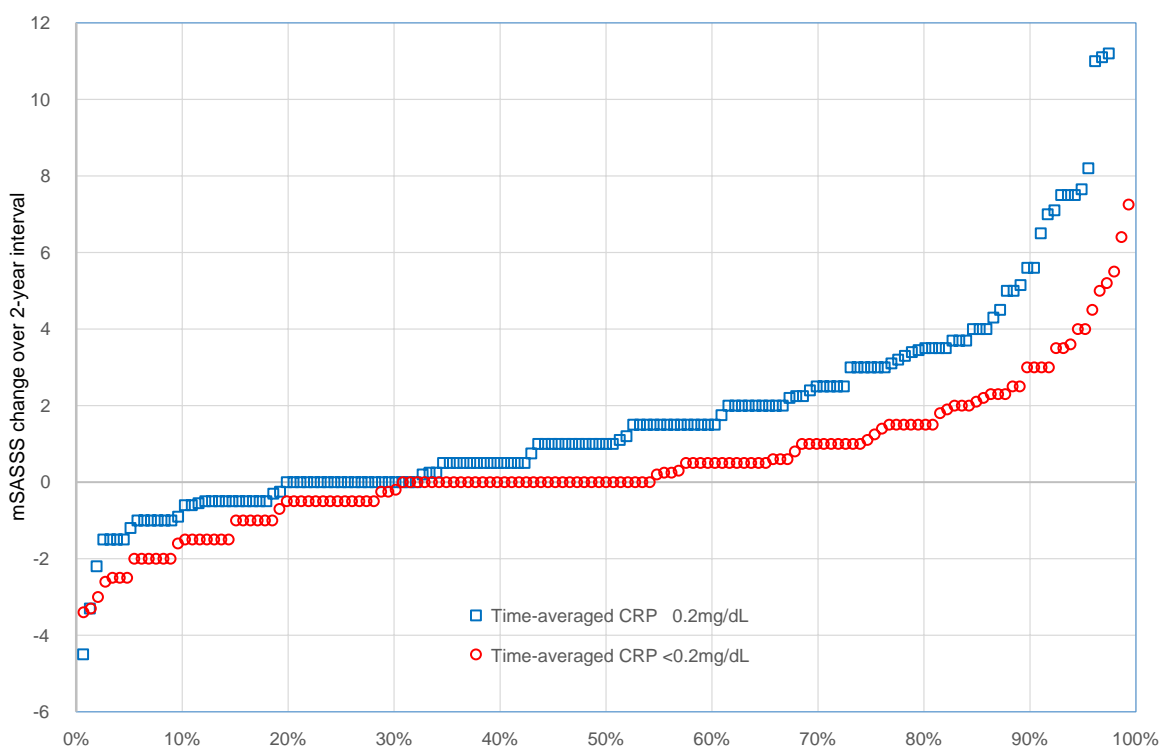
Figure 1. Cumulative probability plot showing radiographic progression during 2-year time intervals according to time-averaged C-reactive protein (CRP) levels (<0.2 mg/dl versus ≥0.2 mg/dl) over individual intervals. mSASSS = modified Stoke Ankylosing Spondylitis Spine Score.

smoking (β = 0.81 [95% CI 0.15, 1.47]), and the presence of syndesmophytes at baseline (β = 2.49 [95% CI 1.83, 3.16]) were significantly associated with rapid radiographic progression. Patients' sex, BMI, HLA–B27 positivity, and baseline BASDAI did not show any relevant effect (see Supplementary Table 2, http://onlinelibrary.wiley.com/doi/10.1002/art.40661/abstract). The TNFi group showed numerically less mSASSS change over radiographic intervals than did the control group (β = −0.68 [95% CI −1.36, 0.002]). In model 1, which included age, baseline CRP level, smoking status, and the presence of syndesmophytes at baseline, the TNFi group showed significantly slower radiographic progression over 2-year intervals than did the control group (β = −0.90 [95% CI −1.51, −0.29]) (Table 2).

Influence of time-averaged CRP level on radiographic progression. The time-averaged CRP level over radiographic intervals was lower with TNFi treatment than with NSAID treatment (mean ± SD 0.27 ± 0.30 mg/dl versus 0.61 ± 0.68 mg/dl; $P < 0.001$). And also, it was significantly lower in the TNFi group in both the 0–2-year interval and 2–4-year interval (mean ± SD 0.24 ± 0.27 mg/dl versus 0.62 ± 0.61 mg/dl and 0.31 ± 0.36 mg/dl versus 0.59 ± 0.78 mg/dl, respectively). The proportion of radiographic intervals with time-averaged CRP level <0.2 mg/dl was also significantly higher in the TNFi group (57.3% versus 27.5%; $P < 0.001$).

The time-averaged CRP level was significantly associated with rapid radiographic progression over relevant radiographic intervals (β = 1.68 [95% CI 1.00, 2.36]). When all intervals were stratified by time-averaged CRP level status, the mean ± SD mSASSS change in intervals with time-averaged CRP level <0.2 mg/dl was 0.58 ± 2.42 units, while it was 1.98 ± 3.28 units in the remaining intervals (Figure 1). Furthermore, definite radiographic progression also occurred significantly less frequently in the intervals with lower time-averaged CRP level (15.7% versus 33.7%; $P < 0.001$).

Interestingly, when mSASSS progression was analyzed after stratification by the presence of syndesmophytes at baseline and time-averaged CRP level (based on 0.2 mg/dl), each subgroup showed a significantly different course of radiographic progression (Figure 2). In patients without syndesmophytes at baseline, the estimated mSASSS change in radiographic intervals with time-averaged CRP level <0.2 mg/dl was 0.23 units (95% CI −0.22, 0.69) per 2-year interval, and definite radiographic progression occurred in only 10% of patients. However, this progression rate was significantly increased in those with a higher time-averaged CRP level (1.12 units [95% CI 0.61, 1.62]). The effect of time-averaged CRP level in patients with syndesmophytes at baseline was also consistent.

In multivariable model 2, an increase of 1 mg/dl in time-averaged CRP level resulted in an increase of 1.02 mSASSS
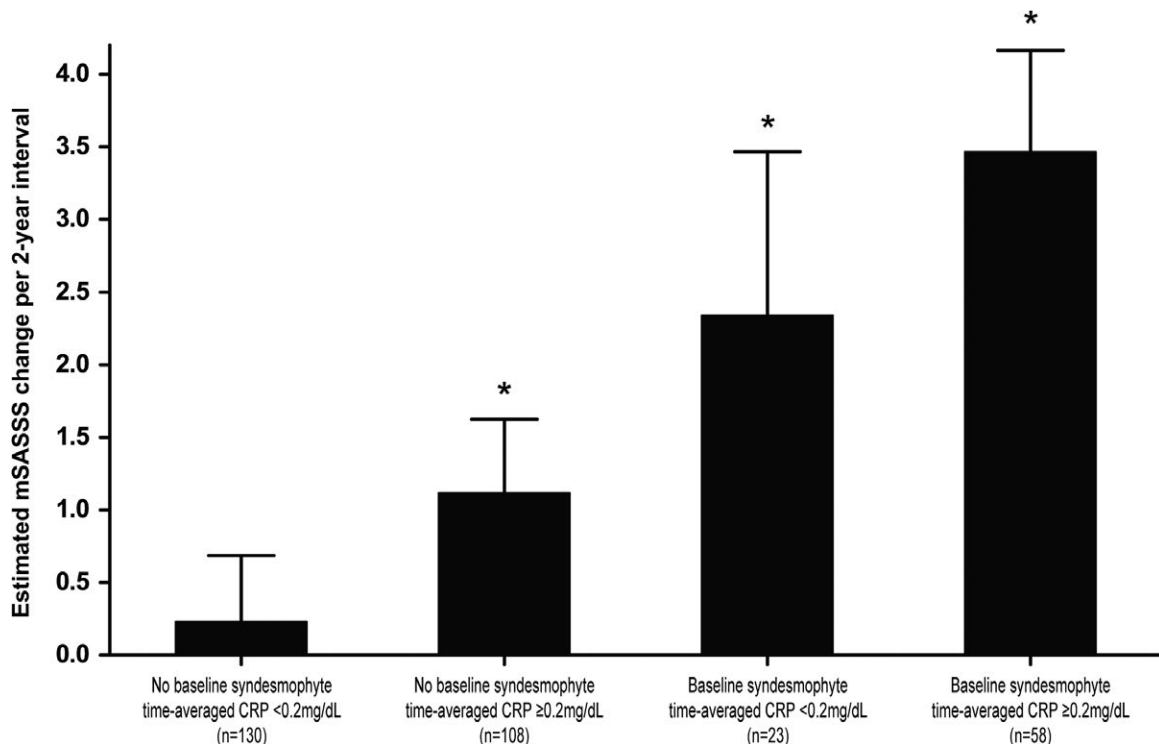
Figure 2. Different radiographic progression in 2-year intervals according to the presence or absence of syndesmophytes at baseline and time-averaged C-reactive protein (CRP) level (<0.2 mg/dl or ≥0.2 mg/dl). Values are the mean and upper margin of the 95% confidence interval. * = $P < 0.05$ versus patients without syndesmophytes at baseline and with lower time-averaged CRP levels. mSASSS = modified Stoke Ankylosing Spondylitis Spine Score.
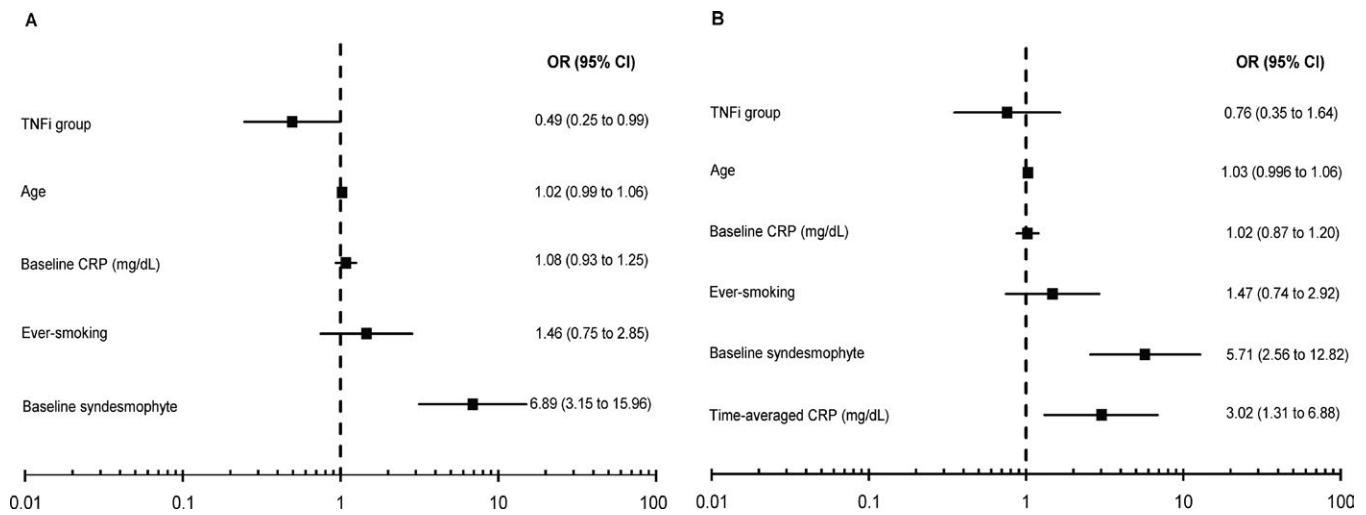
Figure 3. Forest plots indicating effect of clinical factors in 2 different multivariable models on odds of the occurrence of definite radiographic progression (defined as change of ≥2 units in modified Stoke Ankylosing Spondylitis Spine Score over 2 years). **A,** In model 1 including relevant baseline factors, treatment with tumor necrosis factor inhibitors (TNFi) was associated with significantly reduced odds of radiographic progression. **B,** This effect was decreased when the factor of time-averaged C-reactive protein (CRP) level was added (model 2). OR = odds ratio; 95% CI = 95% confidence interval.

units (95% CI 0.32, 1.72) per 2-year interval. In contrast, the impact of TNFi treatment (versus NSAID treatment) was decreased and lost its statistical significance (β = −0.52 [95% CI −1.17, 0.14]) (Table 2). Mediation analysis also showed that TNFi treatment significantly reduced radiographic progression through an indirect effect mediated by time-averaged CRP level (Z score for indirect effect = −2.08, P = 0.037). The effect of the interaction between treatment group and time-averaged CRP level on mSASSS progression was not significant (P = 0.309), which suggests that the effect of time-averaged CRP level did not differ by treatment regimen.

The impact of time-averaged CRP level was consistent in the generalized linear mixed model, in which definite radiographic progression was used as the outcome variable. The presence of syndesmophytes at baseline and time-averaged CRP level were associated with increased odds of progression (odds ratios [ORs] of 5.71 and 3.02, respectively). In contrast, TNFi treatment did not significantly reduce the probability of definite radiographic progression (OR 0.76 [95% CI 0.35, 1.64]) (Figure 3).

Impact of NSAID index on radiographic progression. The mean ± SD NSAID index for the control group during 0–2-year and 2–4-year intervals was 46.3 ± 23.3 and 42.0 ± 24.2, respectively (difference not significant). The proportion of users of high amounts of NSAIDs (NSAID index ≥50) was lower in the 2–4-year interval than in the 0–2-year interval (31.5% versus 46.6%). In the control group, the NSAID index for radiographic intervals was not associated with mSASSS change irrespective of the time effect (β = −0.006 [95% CI −0.03, 0.02]) (see Supplementary Table 2, http://onlinelibrary.wiley.com/doi/10.1002/art.40661/abstract).

Among the 268 2-year intervals in the TNFi group, concomitant NSAID therapy was administered in 190 (70.9%). The NSAID index (mean ± SD) of these 190 intervals was 23.3 ± 23.6, without any difference between 0–2-year and 2–4-year intervals. As in the control group, both concomitant NSAID use and NSAID index were not associated with mSASSS progression during radiographic intervals in the TNFi group (unadjusted β = −0.11 [95% CI −0.97, 0.74] and −0.007 [95% CI −0.03, 0.01], respectively) (see Supplementary Table 2, http://onlinelibrary.wiley.com/doi/10.1002/art.40661/abstract).

Interestingly, in the linear mixed model to investigate clinical factors affecting time-averaged CRP level, the presence of syndesmophytes at baseline (adjusted β = 0.20 [95% CI 0.07, 0.33]), higher baseline CRP level (adjusted β = 0.05 [95% CI 0.03, 0.08]), and the control group (adjusted β = 0.36 [95% CI 0.16, 0.56]) were associated with increased time-averaged CRP level. However, the NSAID index, irrespective of the group, did not significantly influence the outcome (adjusted β = 0.15 [95% CI −0.18, 0.49]).

Sensitivity analysis. In the postmatched population, the TNFi group showed numerically less radiographic progression than did the control group in model 1 (β = −0.64 [95% CI −1.84, 0.56]). The effect of TNFi treatment on the outcome was significantly decreased after adjustment for time-averaged CRP level (β = −0.02 [95% CI −1.28, 1.24]). In contrast, the significant effect of time-averaged CRP level on mSASSS progression was not changed (β = 1.15 [95% CI 0.27, 2.03]) (see Supplementary Table 3, http://onlinelibrary.wiley.com/doi/10.1002/art.40661/abstract). Other sensitivity analyses performed in the subgroup of 88 patients with complete sets of radiographs also showed consistent results (see Supplementary Table 4, http://onlinelibrary.wiley.com/doi/10.1002/art.40661/abstract).

Since the correlation between baseline and time-averaged CRP level could influence the result of multivariable model 2, we further analyzed their relationship and its significance. The correlation between baseline and time-averaged CRP level was significant, but the strength of correlation was very weak ($r = 0.18$, $P = 0.001$). In addition, when interaction between baseline and time-averaged CRP level was added to multivariable model 2 as a covariate, it was not statistically significant ($\beta = -0.01$ [95% CI -0.29, 0.27]), and the effect of time-averaged CRP level showed little change ($\beta = 1.04$ [95% CI 0.05, 2.04]). Correlations between age and symptom duration and between age and disease duration were also not significant ($r = 0.11$, $P = 0.106$ and $r = 0.03$, $P = 0.717$, respectively), and neither of these interactions influenced radiographic progression (data not shown).

DISCUSSION

Finding the answer to the question of whether radiographic progression can be prevented through effective treatment of AS is a task still remaining for rheumatologists (18). To the best of our knowledge, this is the first study that analyzes the relative contributions to radiographic progression, in early AS, of time-averaged CRP levels and direct TNFi treatment effects. Patients in the TNFi group showed less radiographic progression than those receiving conventional NSAID treatment. This was mainly linked to the differences in time-averaged CRP levels between the 2 groups.

Overall, an increase of 1 mg/dl time-averaged CRP level led to an increase of 1.02 mSASSS units per 2-year interval. In contrast, a previous study that investigated a longitudinal relationship between disease activity and mSASSS progression in the Outcome in AS International Study (OASIS) cohort showed that an increase of 1 mg/dl time-averaged CRP level led to additional mSASSS progression of 0.2 units over the same interval (19). Considering that patients in the OASIS cohort had significantly longer symptom durations (~20 years), it is probable that tight control of inflammation during the early phase of the disease is key to minimizing radiographic progression, supporting the notion of a "window of opportunity" (8). In fact, patients with low time-averaged CRP levels between radiologic assessments and with no syndesmophytes at baseline showed a minimal mSASSS change over time, and definite radiographic progression occurred in only 10% of them.

In the present study, the control group showed significantly higher time-averaged CRP levels than the TNFi group, which mediated rapid radiographic progression. However, the NSAID index was not significantly associated with time-averaged CRP level or mSASSS change, irrespective of the treatment group. It would be premature to conclude that NSAIDs alone cannot reduce the time-averaged CRP level based on this result, because this study did not compare the effect of NSAIDs with that of no treatment on time-averaged CRP level. However, this result is consistent with that of a recent randomized clinical trial that compared radiographic progression in patients receiving continuous NSAID treatment with that in patients receiving NSAID treatment on demand (20). The proportion of patients with a high NSAID index was only 39% over all radiographic intervals in the control group, so inadequate dosages of NSAIDs could have led to less-than-optimal therapeutic effects. However, maintaining a high NSAID index is not well tolerated in daily clinical practice (21). Furthermore, a recent study showed that full-dose NSAID treatment did not achieve a favorable response or a relevant decrease in sacroiliitis on MRI (22). Therefore, if a patient showed elevated CRP levels despite conventional NSAID treatment, timely switching to or adding TNFi treatment could be a proper strategy for inflammation control and inhibition of radiographic progression in early AS.

Some previous studies suggested that the Ankylosing Spondylitis Disease Activity Score (ASDAS) (23), which includes patient-reported outcome and CRP level, could be better than CRP level alone for predicting radiographic progression (24,25). Although a statistical model using the ASDAS showed a slightly better fit than one using CRP level in those studies, it would be premature to generalize from this result because patient-reported outcome could be influenced by clinical factors unrelated to disease activity such as concomitant fibromyalgia (26). In contrast, a previous study by Machado et al showed that spinal inflammation detected by MRI correlated better with CRP level than with other measures of disease activity (27). Therefore, we think that time-averaged CRP level could optimally represent the degree of inflammation during treatment and could help us to estimate the precise contribution of inflammation in radiographic progression. Unfortunately, the ASDAS was not routinely measured in our study, so we could not compare the power of the 2 markers to predict radiographic progression.

It is also interesting that only 57.3% of total radiographic intervals in the TNFi group had time-averaged CRP values <0.2 mg/dl. This result suggests that significant numbers of patients receiving TNFi treatment did not achieve an optimal antiinflammatory effect in the real world. In contrast, all patients in the TNFi group fulfilled the BASDAI 50 response criteria over the entire observation period. This discrepancy could explain why patient-reported outcomes could not precisely predict radiographic progression (19). Therefore, to minimize radiographic progression in AS, switching to other TNFi or interleukin-17–blocking agents should be considered based on the objective degree of anti-inflammatory effectiveness rather than on subjective outcome. This is consistent with the recently updated "treat-to-target" strategy, which consists of measuring disease activity, optimally using the ASDAS, and adjusting therapy accordingly (24,28).

Our study has some limitations. First, the baseline features between the 2 groups were significantly different, and this could lead to confounding by indication. This was a major, but not unexpected, drawback of the study, because starting TNFi treat-

ment in patients with AS is indicated after encountering intolerance or inadequate response to NSAID treatment in daily clinical practice. Although we performed propensity score matching to minimize this bias, the BASDAI could not be used in the matching process because there was little overlap in the ranges of these factors between the 2 groups. A randomized, head-to-head comparison of TNFi treatment with conventional NSAID treatment as initial treatment in patients with early AS would be optimal to demonstrate the different effect of time-averaged CRP level on radiographic progression in the 2 groups. However, such a study is less than feasible under real-world conditions. Second, since this was not a randomized study, radiographic progression could be influenced by a number of unmeasured confounders such as patient compliance with treatment and physician preferences. For example, patients in the control group did not regularly complete the BASDAI during treatment, so it is possible that patient-reported outcomes could differ between the 2 groups. However, in daily clinical practice, a physician would consider TNFi treatment if a patient does not fulfill the BASDAI 50 response criteria under NSAID treatment, so this imbalance should not be significant. In addition, it is possible that the NSAID index might have been underestimated because of use of over-the-counter NSAIDs. However, all AS patients in the Republic of Korea are covered by a national medical insurance system, and the patient pays only 10% of the price of all prescribed medication for the treatment of AS. Because of easy access to low-cost medical care in the Republic of Korea, we think that underestimation of the NSAID index due to use of over-the-counter medicine is less likely (29). Finally, because the present study included a relatively small number of patients in the control group, the effect of NSAID treatment could be insignificant due to Type II error. Although the 95% CI of the beta value regarding the effect of the NSAID index on the time-averaged CRP level was relatively far from the criterion for statistical significance, this result should be confirmed in future studies with a larger sample size.

In conclusion, we show that TNFi treatment in early AS can reduce radiographic progression, mainly by effective inflammation control. Although these results should be replicated in future (preferably randomized) studies, they may support the notion that early effective suppression of inflammation using TNFi could inhibit pathologic new bone formation in AS.

AUTHOR CONTRIBUTIONS

All authors were involved in drafting the article or revising it critically for important intellectual content, and all authors approved the final version to be published. Dr. E. Y. Lee had full access to all of the data in the study and takes responsibility for the integrity of the data and the accuracy of the data analysis.

Study conception and design. J. W. Park, E. Y. Lee.

Acquisition of data. J. W. Park, Kim, Ha, J. K. Park, Kang, Y. J. Lee, Song, E. Y. Lee.

Analysis and interpretation of data. J. W. Park, Kim, J. S. Lee, Y. J. Lee, E. Y. Lee.

REFERENCES

1. Braun J, Landewe R, Hermann KG, Han J, Yan S, Williamson P, et al. Major reduction in spinal inflammation in patients with ankylosing spondylitis after treatment with infliximab: results of a multicenter, randomized, double-blind, placebo-controlled magnetic resonance imaging study. Arthritis Rheum 2006;54:1646–52.

2. Van der Heijde D, Landewe R, Baraliakos X, Houben H, van Tubergen A, Williamson P, et al. Radiographic findings following two years of infliximab therapy in patients with ankylosing spondylitis. Arthritis Rheum 2008;58:3063–70.

3. Van der Heijde D, Landewe R, Einstein S, Ory P, Vosse D, Ni L, et al. Radiographic progression of ankylosing spondylitis after up to two years of treatment with etanercept. Arthritis Rheum 2008;58:1324–31.

4. Van der Heijde D, Salonen D, Weissman BN, Landewé R, Maksymowych WP, Kupper H, et al. Assessment of radiographic progression in the spines of patients with ankylosing spondylitis treated with adalimumab for up to 2 years. Arthritis Res Ther 2009;11:R127.

5. Haroon N, Inman RD, Learch TJ, Weisman MH, Lee M, Rahbar MH, et al. The impact of tumor necrosis factor α inhibitors on radiographic progression in ankylosing spondylitis. Arthritis Rheum 2013;65:2645–54.

6. Baraliakos X, Haibel H, Listing J, Sieper J, Braun J. Continuous long-term anti-TNF therapy does not lead to an increase in the rate of new bone formation over 8 years in patients with ankylosing spondylitis. Ann Rheum Dis 2014;73:710–5.

7. Maas F, Arends S, Brouwer E, Essers I, van der Veer E, Efde M, et al. Reduction in spinal radiographic progression in ankylosing spondylitis patients receiving prolonged treatment with tumor necrosis factor inhibitors. Arthritis Care Res (Hoboken) 2017;69:1011–9.

8. Maksymowych WP, Morency N, Conner-Spady B, Lambert RG. Suppression of inflammation and effects on new bone formation in ankylosing spondylitis: evidence for a window of opportunity in disease modification. Ann Rheum Dis 2013;72:23–8.

9. Poddubnyy D, Listing J, Sieper J. Brief report: course of active inflammatory and fatty lesions in patients with early axial spondyloarthritis treated with infliximab plus naproxen as compared to naproxen alone: results from the infliximab as first line therapy in patients with early active axial spondyloarthritis trial. Arthritis Rheumatol 2016;68:1899–903.

10. Van der Linden S, Valkenburg HA, Cats A. Evaluation of diagnostic criteria for ankylosing spondylitis: a proposal for modification of the New York criteria. Arthritis Rheum 1984;27:361–8.

11. Rudwaleit M, Haibel H, Baraliakos X, Listing J, Märker-Hermann E, Zeidler H, et al. The early disease stage in axial spondylarthritis: results from the German Spondyloarthritis Inception Cohort. Arthritis Rheum 2009;60:717–27.

12. Garrett S, Jenkinson T, Kennedy LG, Whitelock H, Gaisford P, Calin A. A new approach to defining disease status in ankylosing spondylitis: the Bath Ankylosing Spondylitis Disease Activity Index. J Rheumatol 1994;21:2286–91.

13. Braun J, Davis J, Dougados M, Sieper J, van der Linden S, van der Heijde D. First update of the international ASAS consensus statement for the use of anti-TNF agents in patients with ankylosing spondylitis. Ann Rheum Dis 2006;65:316–20.

14. Dougados M, Simon P, Braun J, Burgos-Vargas R, Maksymowych WP, Sieper J, et al. ASAS recommendations for collecting, analysing and reporting NSAID intake in clinical trials/epidemiological studies in axial spondyloarthritis. Ann Rheum Dis 2011;70:249–51.

15. Creemers MC, Franssen MJ, van't Hof MA, Gribnau FW, van de Putte LB, van Riel PL. Assessment of outcome in ankylosing spondylitis: an extended radiographic scoring system. Ann Rheum Dis 2005;64:127–9.

16. Bruynesteyn K, Boers M, Kostense P, van der Linden S, van der Heijde D. Deciding on progression of joint damage in paired films of individual patients: smallest detectable difference or change. Ann Rheum Dis 2005;64:179–82.

17. Mackinnon DP, Warsi G, Dwyer JH. A simulation study of mediated effect measures. Multivariate Behav Res 1995;30:41.

18. Machado P. Anti–tumor necrosis factor and new bone formation in ankylosing spondylitis: the controversy continues. Arthritis Rheum 2013;65:2537–40.

19. Ramiro S, van der Heijde D, van Tubergen A, Stolwijk C, Dougados M, van den Bosch F, et al. Higher disease activity leads to more structural damage in the spine in ankylosing spondylitis: 12-year longitudinal data from the OASIS cohort. Ann Rheum Dis 2014;73:1455–61.

20. Sieper J, Listing J, Poddubnyy D, Song IH, Hermann KG, Callhoff J, et al. Effect of continuous versus on-demand treatment of ankylosing spondylitis with diclofenac over 2 years on radiographic progression of the spine: results from a randomised multicentre trial (ENRADAS). Ann Rheum Dis 2016;75:1438–43.

21. Molto A, Granger B, Wendling D, Dougados M, Gossec L. Use of nonsteroidal anti-inflammatory drugs in early axial spondyloarthritis in daily practice: data from the DESIR cohort. Joint Bone Spine 2017;84:79–82.

22. Varkas G, Jans L, Cypers H, Van Praet L, Carron P, Elewaut D, et al. Six-week treatment of axial spondyloarthritis patients with an optimal dose of nonsteroidal antiinflammatory drugs: early response to treatment in signal intensity on magnetic resonance imaging of the sacroiliac joints. Arthritis Rheumatol 2016;68:672–8.

23. Lukas C, Landewé R, Sieper J, Dougados M, Davis J, Braun J, et al, for the Assessment of SpondyloArthritis international Society. Development of an ASAS-endorsed disease activity score (ASDAS) in patients with ankylosing spondylitis. Ann Rheum Dis 2009;68:18–24.

24. Molnar C, Scherer A, Baraliakos X, de Hooge M, Micheroli R, Exer P, et al. TNF blockers inhibit spinal radiographic progression in ankylosing spondylitis by reducing disease activity: results from the Swiss Clinical Quality Management cohort. Ann Rheum Dis 2018;77:63–9.

25. Poddubnyy D, Protopopov M, Haibel H, Braun J, Rudwaleit M, Sieper J. High disease activity according to the Ankylosing Spondylitis Disease Activity Score is associated with accelerated radiographic spinal progression in patients with early axial spondyloarthritis: results from the GErman SPondyloarthritis Inception Cohort. Ann Rheum Dis 2016;75:2114–8.

26. Molto A, Etcheto A, Gossec L, Boudersa N, Claudepierre P, Roux N, et al. Evaluation of the impact of concomitant fibromyalgia on TNF α blockers' effectiveness in axial spondyloarthritis: results of a prospective, multicentre study. Ann Rheum Dis 2018;77:533–40.

27. Machado P, Landewe RB, Braun J, Baraliakos X, Hermann KG, Hsu B, et al. MRI inflammation and its relation with measures of clinical disease activity and different treatment responses in patients with ankylosing spondylitis treated with a tumour necrosis factor inhibitor. Ann Rheum Dis 2012;71:2002–5.

28. Smolen JS, Schols M, Braun J, Dougados M, FitzGerald O, Gladman DD, et al. Treating axial spondyloarthritis and peripheral spondyloarthritis, especially psoriatic arthritis, to target: 2017 update of recommendations by an international task force. Ann Rheum Dis 2018;77:3–17.

29. Park K, Park J, Kwon YD, Kang Y, Noh JW. Public satisfaction with the healthcare system performance in South Korea: universal healthcare system. Health Policy 2016;120:621–9.

AMERICAN COLLEGE OF RHEUMATOLOGY
EDUCATION · TREATMENT · RESEARCH

BRIEF REPORT

How Do Patients With Newly Diagnosed Systemic Lupus Erythematosus Present? A Multicenter Cohort of Early Systemic Lupus Erythematosus to Inform the Development of New Classification Criteria

Marta Mosca,[1] Karen H. Costenbader,[2] Sindhu R. Johnson,[3] Valentina Lorenzoni,[4] Gian Domenico Sebastiani,[5] [ID]
Bimba F. Hoyer,[6] Sandra Navarra,[7] Eloisa Bonfa,[8] [ID] Rosalind Ramsey-Goldman,[9] Jorge Medina-Rosas,[3]
Matteo Piga,[10] Chiara Tani,[1] Sara K. Tedeschi,[2] Thomas Dörner,[11] Martin Aringer,[12] and Zahi Touma[3]

Objective. Systemic lupus erythematosus (SLE) presents with nonspecific signs and symptoms that are also found in other conditions. This study aimed to evaluate manifestations at disease onset and to compare early SLE manifestations to those of diseases mimicking SLE.

Methods. Academic lupus centers in Asia, Europe, North America, and South America collected baseline data on patients who were referred to them during the previous 3 years for possible SLE and who had a symptom duration of <1 year. Clinical and serologic manifestations were compared between patients diagnosed as having SLE and those diagnosed as having SLE-mimicking conditions. Diagnostic performance of the 1997 American College of Rheumatology (ACR) SLE classification criteria and the 2012 Systemic Lupus International Collaborating Clinics (SLICC) SLE classification criteria was tested.

Results. Data were collected on 389 patients with early SLE and 227 patients with SLE-mimicking conditions. Unexplained fever was more common in early SLE than in SLE-mimicking conditions (34.5% versus 13.7%, respectively; $P < 0.001$). Features less common in early SLE included Raynaud's phenomenon (22.1% versus 48.5%; $P < 0.001$), sicca symptoms (4.4% versus 34.4%; $P < 0.001$), dysphagia (0.3% versus 6.2%; $P < 0.001$), and fatigue (28.3% versus 37.0%; $P = 0.024$). Anti–double-stranded DNA, anti–β_2-glycoprotein I antibodies, positive Coombs' test results, autoimmune hemolytic anemia, hypocomplementemia, and leukopenia were more common in early SLE than in SLE-mimicking conditions. Symptoms detailed in the ACR and SLICC classification criteria were significantly more frequent among those with early SLE. Fewer patients with early SLE were not identified as having early SLE with use of the SLICC criteria compared to the ACR criteria (16.5% versus 33.9%), but the ACR criteria demonstrated higher specificity than the SLICC criteria (91.6% versus 82.4%).

Conclusion. In this multicenter cohort, clinical manifestations that could help to distinguish early SLE from SLE-mimicking conditions were identified. These findings may aid in earlier SLE diagnosis and provide information for ongoing initiatives to revise SLE classification criteria.

INTRODUCTION

Systemic lupus erythematosus (SLE) is a multifaceted and complex condition with variable phenotypes and clinical manifestations and a relapsing–remitting course. It is acknowledged that early recognition of SLE can be beneficial for long-term outcomes, allowing early intervention and reducing damage accrual (1). New therapies for SLE offer the opportunity to prevent serious sequelae, and limiting inclusion to only those with longstanding disease may underestimate the effectiveness of a new treatment, as late-stage disease may be more difficult to treat and/or irreversible (2). Because accurate classification is a prerequisite for including SLE patients in clinical trials, the difficulty in classifying patients with early SLE may limit the conduct of clinical and translational studies on early disease.

Because SLE onset is often insidious, with clinically evident disease developing over years, the classification and diagnosis of SLE may be delayed (3). Both the American College of Rheumatology (ACR) SLE classification criteria (4,5) and the Systemic Lupus International Collaborating Clinics (SLICC) SLE classification criteria (6) demonstrate lower sensitivity in identifying early disease, compared to established disease (7). Ines et al reported a higher sensitivity of the 2012 SLICC criteria (94%) compared to the 1997 ACR criteria (86%). Importantly, while the gap between the sensitivity of the SLICC and ACR criteria was maximal for patients with SLE duration of ≤5 years (89% versus 76%, respectively) and decreased with longer duration from the time of diagnosis, both sets of criteria performed suboptimally in the initial years after diagnosis. In addition, SLE diagnosis is often challenging due to a variety of conditions that may mimic SLE, including early phases of connective tissue diseases, infectious diseases, and hematologic diseases. Therefore, the identification of clinical and serologic manifestations at disease onset that could lead the physician to a potential SLE diagnosis and an early referral is important in clinical practice.

Despite differences in the aims and means of classification and diagnosis, classification criteria enhance physicians' ability to accurately identify and recognize SLE (8). The goals of the current multicenter study were to 1) evaluate the characteristics of patients with early SLE compared to non-SLE patients, 2) identify manifestations at disease onset that may support the early diagnosis of SLE, and 3) inform the development of new classification criteria, which could potentially and accurately identify more patients in the early stages of SLE. The performance of conventional classification criteria in early SLE against the diagnosis made by rheumatologists was also evaluated.

PATIENTS AND METHODS

Patients. Seven academic centers in Asia (Manila), Europe (Berlin and Pisa), North America (Boston, Chicago, and Toronto), and South America (São Paulo) with experience in the diagnosis and management of SLE took part in the study. Patients from a multicenter cohort collected by the Study Group on Early SLE of the Italian Society of Rheumatology (ISR) were also included. Personnel at the participating centers were asked to collect data on clinical and serologic manifestations in patients with early SLE and patients with conditions mimicking SLE, at disease onset.

Patients included in the present study had been referred to these centers for evaluation of possible SLE within the previous 3 years. Early SLE was diagnosed by experienced rheumatologists, based on clinical experience and judgment, and patients did not necessarily fulfill existing classification criteria. Non-SLE patients were those who were referred during the same period of time due to suspected SLE, but who ultimately did not receive a diagnosis of SLE by the center's experienced rheumatologists. Non-SLE conditions detected included infections, hematologic diseases (e.g., lymphoma), other defined connective tissue diseases (e.g., Sjögren's syndrome, primary antiphospholipid [aPL] syndrome, mixed connective tissue disease, systemic sclerosis), other rheumatic diseases (e.g., early rheumatoid arthritis), other autoimmune diseases (e.g., antinuclear antibody [ANA]–positive thyroiditis, autoimmune hepatitis, interstitial lung disease), and fibromyalgia. Patients with undifferentiated connective tissue disease (UCTD) who had a follow-up visit after ≥3 years were also included in the non-SLE group. This time requirement was applied due to the potential for UCTD to evolve into SLE, which occurs in the majority of cases within the first 3 years of disease (9).

Data collection. A standardized data extraction form to be used with the 1997 ACR criteria, the 2012 SLICC criteria, and an additional list of 30 items including clinical and serologic manifestations attributable to systemic autoimmune diseases was developed. Patient medical records were reviewed and investigators were asked to add to the list any other presenting manifestation that they considered relevant to the diagnosis. Standardized definitions of the clinical symptoms (e.g., pleuritis, alopecia, etc.) were not provided, since this study aimed to collect real-life data. If clinically feasible, physicians were asked to report only manifestations that were attributable to possible SLE, after excluding other explanations (e.g., fever in the presence of infection). Further analysis was carried out by attributing fever to SLE only in the setting of a normal C-reactive protein (CRP) level. Similarly, no specific requirements were made for autoantibody testing assays; negative results reported in clinical charts were also recorded.

Operating characteristics of conventional criteria in early disease. Performance characteristics of the 1997 ACR criteria and the 2012 SLICC criteria were evaluated compared to the gold standard of the diagnoses made by the lupus center rheumatologists in terms of accuracy, sensitivity, specificity,

Table 1. Demographic characteristics of the enrolled patients*

Characteristic	SLE (n = 389)	Non-SLE mimicking conditions (n = 227)	Total (n = 616)	P
Female	345 (88.9)	220 (96.9)	565 (91.9)	<0.001
Age at first symptom, mean ± SD years	31.4 ± 12.3	33.9 ± 13.5	32.3 ± 12.7	0.011
Ethnicity				<0.001
Caucasian	212 (54.5)	203 (89.4)	415 (67.7)	
Asian	113 (29.0)	14 (6.2)	127 (20.7)	
African descent	30 (7.7)	6 (2.6)	36 (5.9)	
American Indian	1 (0.3)	0	1 (0.2)	
Other	7 (1.8)	0	7 (1.1)	
Unknown	26 (6.7)	4 (1.8)	27 (4.4)	

* Except where indicated otherwise, values are the number (%) of patients. Non–systemic lupus erythematosus (non-SLE) mimicking conditions include undifferentiated connective tissue disease, Sjögren's syndrome, systemic sclerosis, primary Raynaud's phenomenon, fibromyalgia, antinuclear antibody–positive thyroiditis, rheumatoid arthritis, mixed connective tissue disease, hematologic diseases, infections, autoimmune hepatitis, psoriatic arthritis, miscellaneous diagnoses including rosacea, osteoarthritis, and erythema nodosum.

positive predictive value (PPV) and negative predictive value (NPV), and their 95% confidence intervals (95% CIs).

Statistical analysis. Demographic and clinical characteristics of SLE cases and non-SLE cases were tabulated. The proportion of patients with each clinical and laboratory manifestation were calculated. The distribution of variables in patients with early SLE was compared to the distribution of variables in non-SLE patients, using chi-square or Fisher's exact test. To assess the potential to improve performance of conventional criteria in correctly identifying SLE patients at early onset, 2 different multivariable logistic regression models (which added variables to the dummy variables used to indicate that ACR or SLICC criteria have been met) were developed. Covariate selection in multivariable analysis was done using clinical and statistical criteria; specifically, all variables with a P value of <0.10 in univariable analysis were considered for multivariable models. Backward and forward stepwise selections were used to assess model stability using P values less than 0.10 as a threshold to include or exclude a variable. The variance inflation factor was used to assess collinearity. The discrimination ability of the different models was assessed by calculating the area under the receiver operating characteristic curve and asymptotic 95% CI, and the C statistic was used to make comparisons. All analyses were performed using Stata 12 (StataCorp) and R version 3.2; in descriptive statistics, P values less than 0.05 were considered significant.

RESULTS

A total of 616 patients were evaluated (Manila: 80 patients, Berlin: 30 patients, Pisa and ISR group: 294 patients, Boston: 32 patients, Chicago: 6 patients, Toronto: 124 patients, São Paulo: 50 patients), 389 with early SLE and 227 with SLE-mimicking conditions. The SLE-mimicking conditions were identified as

UCTD (n = 136 [59.9% of non-SLE patients]), Sjögren's syndrome (n = 21 [9.3%]), systemic sclerosis (n = 11 [4.8%]), primary Raynaud's phenomenon (RP) (n = 10 [4.4%]), fibromyalgia (n = 8 [3.5%]), ANA-positive thyroiditis (n = 7 [3.1%]), rheumatoid arthritis (n = 6 [2.6%]), mixed connective tissue disease (n = 4 [1.8%]), hematologic diseases (n = 2 [0.9%]), infections (n = 2 [0.9%]), autoimmune hepatitis (n = 1 [0.4%]), psoriatic arthritis (n = 1 [0.4%]), and 18 miscellaneous diagnoses including rosacea, osteoarthritis, and erythema nodosum. Demographic data on the patients are shown in Table 1. The female:male ratio was higher among patients with mimicking conditions ($P < 0.001$), while age at first diagnosis was significantly lower among subjects with early SLE ($P = 0.011$) (Table 1).

Manifestations of early SLE. ACR and SLICC criteria items were detected significantly more frequently in early SLE than in mimicking conditions (Table 2). Seizures were uncommon at disease onset, reported in 11 SLE patients (2.8%) and in 0 non-SLE patients ($P = 0.009$). No patients with early SLE presented with peripheral neuropathy. Stroke and myocardial infarction occurred in SLE patients only, but were uncommon (n = 4 [1.0%] and n = 3 [0.8%], respectively). Unexplained fever was significantly more common in SLE patients than in patients with mimicking conditions (34.5% versus 13.7%, respectively; $P < 0.001$); significance was maintained when fever in association with a normal CRP level was considered (27.5% versus 7.9%; $P < 0.001$). Additional differentiating variables between SLE patients and patients with mimicking conditions were alopecia (30.6% versus 11.9%, respectively; $P < 0.001$), weight loss (13.1% versus 4.4%; $P < 0.001$), and ascites (3.1% versus 0%; $P = 0.005$).

Some symptoms that differed significantly between the 2 groups were detected more frequently in patients with mimicking conditions than in patients with SLE. Among these symptoms

Table 2. Clinical manifestations at disease onset in patients with early SLE and patients with SLE-mimicking conditions*

Manifestation	SLE (n = 389)	SLE-mimicking conditions (n = 227)	P
Fever	134 (34.5)	31 (13.7)	<0.001
Fatigue	110 (28.3)	84 (37.0)	0.02
Weight Loss	51 (13.1)	10 (4.4)	<0.001
Malar rash	193 (49.6)	14 (6.2)	<0.001
Subacute cutaneous lupus	9 (2.3)	8 (3.5)	0.37
Discoid lesions	36 (9.3)	11 (4.9)	0.04
Other rash	23 (5.9)	27 (11.9)	0.009
Photosensitivity	123 (31.6)	42 (18.5)	<0.001
Oral ulcers	84 (21.6)	12 (5.3)	<0.001
Alopecia	119 (30.6)	27 (11.9)	<0.001
Skin ulcers	8 (2.1)	3 (1.3)	0.75
Telangiectasias	4 (1.0)	5 (2.2)	0.30
Inflammatory arthritis	224 (57.6)	60 (26.4)	<0.001
Arthralgias	79 (20.3)	97 (42.7)	0.001
Pleuritis	87 (22.4)	6 (2.6)	<0.001
Pericarditis	73 (18.8)	7 (3.1)	<0.001
Ascites	12 (3.1)	0	0.005
Kidney involvement†	51 (13.1)	0	<0.001
Dry eyes	15 (3.9)	63 (27.8)	<0.001
Dry mouth	14 (3.6)	67 (29.5)	<0.001
Dysphagia	1 (0.3)	14 (6.2)	<0.001
Pneumonia	6 (1.5)	0	0.09
Alveolar hemorrhage	2 (0.5)	0	0.53
Pulmonary fibrosis	2 (0.5)	3 (1.3)	0.36
Pulmonary hypertension	5 (1.3)	5 (2.2)	0.51
Valvular disease	1 (0.3)	0	1.00
Myocardial infarction	3 (0.8)	0	0.30
Thrombosis	14 (3.6)	2 (0.9)	0.06
Swollen fingers	14 (3.6)	11 (4.9)	0.52
Raynaud's phenomenon	86 (22.1)	110 (48.5)	<0.001
Livedo reticularis	12 (3.1)	11 (4.9)	0.27
Stroke	4 (1.0)	0	0.30
Transitory ischemic attack	1 (0.3)	1 (0.4)	1.00
Cognitive impairment	6 (1.5)	1 (0.4)	0.43
Seizures	11 (2.8)	0	0.009
Psychosis	4 (1.0)	2 (0.9)	1.00
Migraine	10 (2.6)	5 (2.2)	1.00
Intestinal vasculitis	3 (0.8)	0	0.30

* Values are the number (%) of patients. SLE = systemic lupus erythematosus.
† Includes proteinuria, hematuria, pyuria, and casts.

were RP (22.1% in SLE patients versus 48.5% in non-SLE patients; $P < 0.001$), sicca symptoms (4.4% versus 34.4%, respectively; $P < 0.001$), dysphagia (0.3% versus 6.2%; $P < 0.001$), and fatigue (28.3% versus 37.0%; $P = 0.024$). Rashes outside the typical SLE symptom spectrum, such as skin vasculitis, were also slightly more frequent among patients with mimicking con-

ditions than among those with SLE (11.9% in non-SLE patients versus 5.9% in SLE patients; $P = 0.009$).

Serologic findings. Serologic results at disease onset are reported in Table 3. Only 2 patients with early SLE (0.5%) were ANA-negative at disease onset. One patient had a completely

Table 3. Serologic abnormalities and autoantibodies detected*

	SLE (n = 389)	SLE-mimicking conditions (n = 227)	P
ANA	387 (99.5)	216 (95.1)	<0.001
Anti-dsDNA	251 (71.7)	14 (6.9)	<0.001
Anti-Sm	90 (30.2)	5 (2.6)	<0.001
Anti-Ro	98 (33.2)	53 (25.6)	0.06
Anti-La	41 (15.1)	20 (9.9)	0.09
Anti-RNP	85 (28.5)	12 (5.9)	<0.001
IgG aCL	50 (18.1)	24 (12.1)	0.07
IgM aCL	36 (13.2)	4 (2.0)	<0.001
LAC	31 (12.7)	27 (17.6)	0.17
Anti-β_2GPI	30 (17.0)	5 (4.4)	0.001
Coombs' test positive	48 (12.3)	13 (5.7)	0.008
Low complement	243 (73.4)	104 (48.4)	<0.001
Thrombocytopenia	23 (6.6)	10 (4.8)	0.37
Leukopenia	61 (16.2)	21 (9.8)	0.02
Hemolytic anemia	18 (4.6)	1 (0.4)	0.003

* Values are the number (%) of patients. SLE = systemic lupus erythematosus; ANA = antinuclear antibody; anti-dsDNA = anti–double-stranded DNA; aCL = anticardiolipin; LAC = lupus anticoagulant; anti-β_2GPI = anti–β_2-glycoprotein.

negative autoantibody panel, and the second tested positive for anti-Sm and anti–double-stranded DNA (anti-dsDNA) antibodies, with negative ANA test results. Although positivity for ANA was the most common reason for referral of patients with mimicking conditions, 11 of the non-SLE patients (4.9%) tested negative for ANA at a cutoff titer of 1:80. Compared to patients with mimicking conditions, patients with early SLE were much more likely to have antibodies to dsDNA (71.7% of SLE patients versus 6.9% of non-SLE patients) and to Sm (30.2% versus 2.6%, respectively). Anticardiolipin IgM and anti–β_2-glycoprotein I antibodies were also more frequent in early SLE, as were positive Coombs' test results, autoimmune hemolytic anemia, hypocomplementemia, and leukopenia (Table 3). Antibodies to Ro/SSA and La/SSB did not differentiate between early SLE (33.2% anti-Ro–positive and 15.1% anti-La–positive) and mimicking conditions (25.6% and 9.9%, respectively). Thrombocytopenia was present in only 6.6% of SLE patients and 4.8% of those with mimicking conditions.

Performance characteristics of conventional criteria. Sensitivity and specificity of the 1997 ACR criteria and the 2012 SLICC criteria for early diagnosis were calculated with the physician diagnosis as the gold standard. At diagnosis, sensitivity of the ACR criteria was calculated as 66.1%, compared to 83.5% for the SLICC criteria. Of the 132 patients with early SLE who did not meet classification by ACR criteria (33.9%), 89 fulfilled 3 components of the ACR criteria, and 37 fulfilled 2 components of the ACR criteria. Six patients met only 1 ACR criteria component. Of the 64 patients with early SLE who did not meet classification by SLICC criteria (16.5%), 39 patients

fulfilled 3 components of the SLICC criteria, and 19 patients fulfilled 2 components of the SLICC criteria. The 1997 ACR criteria showed a specificity of 91.6%, while the specificity of the 2012 SLICC criteria was 82.4%. Accordingly, the accuracy was 75.5% for the ACR criteria and 83.1% for the SLICC criteria. The PPV and NPV for the ACR criteria were 93.1% and 61.2%, respectively, and 89.0% and 74.5%, respectively, for the SLICC criteria.

Improvement of the 1997 ACR criteria and the 2012 SLICC criteria diagnostic performance. Based on univariable analysis (Table 4), multivariable models were used to assess improvement of current criteria with the addition of other variables. When alopecia, fever, hypocomplementemia, and anti-RNP were added to the 1997 ACR criteria, accuracy in classification of patients improved significantly ($P < 0.001$), with the area under the curve (AUC) being 0.862 (95% CI 0.830–0.895). In the multivariable logistic models, the inclusion of anti-RNP, arthralgia, dry mouth, other rash, and weight loss in the 2012 SLICC criteria resulted in an AUC of 0.899 (95% CI 0.871–0.927), with a significant improvement of the discrimination ability, compared to the SLICC criteria alone ($P < 0.001$).

DISCUSSION

In the present study, we investigated clinical symptoms and serologic findings (at disease onset) from a large multicenter, multiethnic cohort of 389 SLE patients who received initial diagnoses at lupus referral centers and compared them to the findings in 227 patients referred for possible SLE, who were ulti-

Table 4. Univariable logistic regression models for the association with SLE*

	OR	95% CI	P
Clinical manifestation			
Malar rash	14.981	8.42–26.65	<0.001
Discoid rash	2.003	1–4.02	0.051
Photosensitivity	2.037	1.37–3.03	<0.001
Oral ulcer	4.934	2.63–9.26	<0.001
Inflammatory arthritis	3.779	2.64–5.4	<0.001
Kidney involvement†	16.975	4.09–70.43	<0.001
Pericarditis	7.260	3.28–16.07	<0.001
Peripheral edema	30.309	4.15–221.34	0.001
Alopecia	3.265	2.07–5.15	<0.001
Fever	3.322	2.16–5.12	<0.001
Fatigue	0.671	0.47–0.95	0.025
Weight loss	3.274	1.63–6.59	0.001
Other rash	0.465	0.26–0.83	0.010
Dry eyes	0.104	0.06–0.19	<0.001
Dry mouth	0.089	0.05–0.16	<0.001
Arthralgia	0.613	0.44–0.86	0.005
Dysphagia	0.039	0.01–0.3	0.002
Hypertension	15.522	2.09–115.34	0.007
Raynaud's phenomenon	0.302	0.21–0.43	<0.001
Neurologic involvement‡	4.512	1.02–19.91	0.047
CNS symptom (≥1)	2.721	1.18–6.29	0.019
Serositis	6.624	3.55–12.35	<0.001
Serologic manifestation			
ANA	9.854	2.16–44.87	0.003
Anti-dsDNA	34.046	18.86–61.46	<0.001
Anti-Sm	16.269	6.47–40.9	<0.001
IgG aCL	1.597	0.94–2.7	0.081
IgM aCL	7.329	2.56–20.95	<0.001
LAC	0.679	0.39–1.19	0.177
Anti-β_2GPI	4.438	1.67–11.81	0.003
Anti-Ro	1.445	0.97–2.15	0.068
Anti-La	1.624	0.92–2.87	0.095
Anti-RNP	6.352	3.37–11.99	<0.001
Leukopenia	1.789	1.06–3.03	0.031
Piastrinopenia	1.411	0.66–3.03	0.376
Coombs' test	2.317	1.23–4.38	0.010
Hypocomplementemia	3.016	2.15–4.23	<0.001

* OR = odds ratio; 95% CI = 95% confidence interval; CNS = central nervous system; ANA = antinuclear antibody; anti-dsDNA = anti–double-stranded DNA; aCL = anticardiolipin; LAC = lupus anticoagulant; anti-β_2GPI = anti–β_2-glycoprotein.
† Includes proteinuria, hematuria, pyuria, and casts.
‡ As defined in the American College of Rheumatology systemic lupus erythematosus (SLE) classification criteria.

mately given another diagnosis after clinical and serologic evaluation at the same centers. We identified parameters that could help in identifying patients with early SLE and could guide the physician in a differential diagnosis with mimicking conditions. In addition, we identified items relevant for the development of new classification criteria for SLE, with specific interest in improving sensitivity and specificity for the classification of early disease.

Descriptive statistical analyses revealed that some symptoms were more prevalent in SLE than in SLE-mimicking conditions. As expected, among clinical manifestations, standard items in existing classification criteria were more prevalent in SLE than in SLE-mimicking conditions; some signs and symptoms that are not part of current classification criteria were also associated with early SLE, including fever and weight loss. Noninfectious fever was more prevalent in early SLE than in SLE-mimicking conditions (34.5% versus 13.7%). Of the serologic variables, ANAs, anti-dsDNA antibodies, anti-RNP antibodies, and aPL antibodies were also more prevalent in the SLE subgroups, in addition to a positive Coombs' test result and hemolytic anemia. However, no differences between the groups were observed with respect to leukopenia, thrombocytopenia, or anti-Ro/La antibodies.

In our cohort of 616 patients, the 1997 ACR criteria demonstrated a sensitivity of 66.1% and a specificity of 91.6%, and the 2012 SLICC criteria demonstrated a sensitivity of 83.5% and a specificity of 82.4% for early diagnosis (8,10,11). As a result, 132 patients with a clinical diagnosis of SLE (33.9%) were not classified as having SLE according to the ACR criteria, and 64 with a clinical diagnosis of SLE (16.5%) did not fulfill the SLICC classification criteria. These patients were more likely to present milder cases, which included conditions such as arthritis, hematologic manifestations, malar rash, lymphadenopathy, noninfectious fever, alopecia, ANA-positive thyroiditis, and the presence of anti-dsDNA or aPL antibodies. In contrast, some patients were inaccurately classified as having SLE by the ACR criteria (n = 19) and SLICC criteria (n =40). The accuracy of the 1997 ACR criteria and the 2012 SLICC criteria was 75.5% and 83.1%, respectively.

SLE is a disease characterized by a large variety of autoantibodies, and their production has been shown to increase shortly before disease onset (10). A fundamental decision made in the development of the SLICC criteria was that patients were required to have serologic evidence of antibodies or immune complex deposition (6). Within the current SLE classification criteria approach, a meta-analysis of published data showed that ANA positivity by HEp-2 testing, at a titer of ≥1:80, was 98% sensitive for SLE (11). Our cohort results support the idea that ANA positivity might be an important discriminant variable in the assessment of patients in whom SLE is clinically suspected. In fact, at disease onset, only 2 patients diagnosed as having SLE were recorded to be ANA-negative, and in 1 of the 2 this was apparently a false-negative result.

In addition to negativity for ANA, manifestations such as fatigue, dysphagia, RP, and some skin lesions (i.e., purpura and skin vasculitis), especially in serologically negative patients, are either not useful to distinguish from SLE-mimicking conditions or may steer toward alternative diagnoses. These data also emphasize that the differential diagnosis process for SLE is long and requires comprehensive experience with other autoimmune and related diseases. In recent years, several studies have characterized SLE patients in the early phases of the disease, highlighting the importance of non–classification criteria symptoms (12–16).

Recently, Rees et al examined the clinical manifestations in SLE patients at onset, in order to develop a risk prediction model for SLE that can be used at the time of referral to a general practitioner, rather than at a later referral to a rheumatologist or lupus expert (12). This study showed that SLE patients consult their physicians frequently in the 5 years preceding their diagnosis, for manifestations such as arthralgias, rash, and alopecia. While the median time from clinical presentation of SLE to SLE diagnosis was >1 year, manifestations like thrombocytopenia and nephrotic syndrome were more likely to be associated with acute care management (i.e., hospital admission or urgent referral) and an earlier diagnosis of SLE. Since 1990, different studies have examined clinical manifestations and serologic features at SLE onset; among non-criteria symptoms, arthralgias, fever, alopecia, RP, non-hemolytic anemia, and lymphadenopathy were the most frequently reported (13–16).

There are some inconsistencies between the results of these studies and ours; presumably, differences in inclusion criteria and disease duration limit the comparability of the results. We enrolled patients independent of whether they fulfilled ACR classification criteria or SLICC classification criteria. In contrast to other cohort studies that enrolled patients upon fulfillment of classification criteria (mainly the 1997 ACR criteria), our study design allowed for the inclusion of patients at very early disease onset, even before the accrual of standard classification criteria. This methodology was crucial for identifying variables that could distinguish patients with very early SLE, particularly in the absence of disease-specific markers such as lupus nephritis, disease-specific skin manifestations, or autoantibodies that might develop later in the course of disease.

Some limitations of our study need to be acknowledged. Due to its observational nature, some of the variables included in the analysis were collected in different ways among the diverse centers, according to local clinical practice. For instance, the SLE group and the SLE-mimicking condition group were compared in order to explore factors that may help identify SLE patients, and no sample size calculation was performed a priori, because patients in the 2 groups were selected on the basis of availability. Thus, group sample sizes were different (i.e., the non-SLE group was smaller than the SLE group), which can potentially affect the results and power of the analysis. Other methodologic limitations to be acknowledged when interpreting results include the limited sample size for some manifestations and the bivariate nature of almost all of the analyses, such that instead of taking into account the overall spectrum of variables, they are limited to pairwise comparisons.

Additionally, the fact that patients were enrolled after visiting expert rheumatologic centers might constitute a bias, as patients may present differently to different specialists. However, since the disease diagnosis was considered the gold standard in this study, we also believe this selection has the advantage of additional information (e.g., patient sex, race, and age at onset) being integrated into the diagnostic decision. Relying on expert diagnosis also has the advantage of a clear-cut, binary response, which allows for analysis of every submitted case, instead of an adjudication process that would have led to the exclusion of certain patients. A final limitation of the study might be the relatively small number of patients identified as Hispanic or of African descent; these patients might have a different disease expression or severity, and our results need further confirmation in these ethnic groups.

In conclusion, the present study has identified clinical and serologic characteristics of patients with early SLE that may help physicians differentiate between SLE and SLE-mimicking conditions. Additionally, we identified features at symptom onset that may help in the identification of early SLE. Limitations of the 1997 ACR criteria and the 2012 SLICC criteria in the accurate classification of early SLE were also identified in this cohort. This study is an element in the item-generation phase of an ongoing international effort to devise new SLE classification criteria with a focus on early disease, consecutively informing both the nominal group technique exercise for item reduction and the multivariable decision analysis for item weighting.

ACKNOWLEDGMENT

AUTHOR CONTRIBUTIONS

All authors were involved in drafting the article or revising it critically for important intellectual content, and all authors approved the final version to be published. Dr. Mosca had full access to all of the data in the study and takes responsibility for the integrity of the data and the accuracy of the data analysis.

Study conception and design. Mosca, Costenbader, Johnson, Lorenzoni, Hoyer, Ramsey-Goldman, Tani, Tedeschi, Dörner, Aringer, Touma.

Acquisition of data. Mosca, Costenbader, Johnson, Sebastiani, Hoyer, Navarra, Bonfa, Ramsey-Goldman, Medina-Rosas, Piga, Tani, Tedeschi, Dörner, Touma.

Analysis and interpretation of data. Mosca, Costenbader, Johnson, Lorenzoni, Sebastiani, Hoyer, Navarra, Bonfa, Ramsey-Goldman, Medina-Rosas, Piga, Tani, Tedeschi, Dörner, Aringer, Touma.

REFERENCES

1. Oglesby A, Korves C, Laliberte F, Dennis G, Rao S, Suthoff ED, et al. Impact of early versus late systemic lupus erythematosus diagnosis on clinical and economic outcomes. Appl Health Econ Health Policy 2014;12:179–90.

2. Touma Z, Gladman DD. Current and future therapies for systemic lupus erythematosus: obstacles and recommendations for the development of novel treatments. Lupus Sci Med 2017;4: e000239.

3. Urowitz MB, Gladman DD, Ibanez D, Sanchez-Guerrero J, Romero-Diaz J, Gordon C, et al. American College of Rheumatology criteria at inception, and accrual over 5 years in the SLICC inception cohort. J Rheumatol 2014;41:875–80.

4. Tan EM, Cohen AS, Fries JF, Masi AT, McShane DJ, Rothfield NF, et al. The 1982 revised criteria for the classification of systemic lupus erythematosus. Arthritis Rheum 1982;25:1271–7.

5. Hochberg MC. Updating the American College of Rheumatology revised criteria for the classification of systemic lupus erythematosus [letter]. Arthritis Rheum 1997;40:1725.

6. Petri M, Orbai AM, Alarcon GS, Gordon C, Merrill JT, Fortin PR, et al. Derivation and validation of the Systemic Lupus International Collaborating Clinics classification criteria for systemic lupus erythematosus. Arthritis Rheum 2012;64:2677–86.

7. Ines L, Silva C, Galindo M, Lopez-Longo FJ, Terroso G, Romao VC, et al. Classification of systemic lupus erythematosus: Systemic Lupus International Collaborating Clinics versus American College of Rheumatology Criteria. A comparative study of 2,055 patients from a real-life, international systemic lupus erythematosus cohort. Arthritis Care Res (Hoboken) 2015;67:1180–5.

8. Aringer M, Dorner T, Leuchten N, Johnson SR. Toward new criteria for systemic lupus erythematosus—a standpoint. Lupus 2016;25:805–11.

9. Mosca M, Tani C, Bombardieri S. Undifferentiated connective tissue diseases (UCTD): a new frontier for rheumatology. Best Pract Res Clin Rheumatol 2007;21:1011–23.

10. Arbuckle MR, McClain MT, Rubertone MV, Scofield RH, Dennis GJ, James JA, et al. Development of autoantibodies before the clinical onset of systemic lupus erythematosus. N Engl J Med 2003;349:1526–33.

11. Leuchten N, Hoyer A, Brinks R, Schoels M, Schneider M, Smolen J, et al. Performance of antinuclear antibodies for classifying systemic lupus erythematosus: a systematic literature review and meta-regression of diagnostic data. Arthritis Care Res (Hoboken) 2018;70:428–38.

12. Rees F, Doherty M, Lanyon P, Davenport G, Riley RD, Zhang W, et al. Early clinical features in systemic lupus erythematosus: can they be used to achieve earlier diagnosis? A risk prediction model. Arthritis Care Res (Hoboken) 2017;69:833–41.

13. Cervera R, Khamashta MA, Font J, Sebastiani GD, Gil A, Lavilla P, et al, and the European Working Party on Systemic Lupus Erythematosus. Systemic lupus erythematosus: clinical and immunologic patterns of disease expression in a cohort of 1,000 patients. Medicine (Baltimore) 1993;72:113–24.

14. Pons-Estel BA, Catoggio LJ, Cardiel MH, Soriano ER, Gentiletti S, Villa AR, et al. The GLADEL multinational Latin American prospective inception cohort of 1,214 patients with systemic lupus erythematosus: ethnic and disease heterogeneity among "Hispanics". Medicine (Baltimore) 2004;83:1–17.

15. Sebastiani GD, Prevete I, Piga M, Iuliano A, Bettio S, Bortoluzzi A, et al. Early Lupus Project—a multicentre Italian study on systemic lupus erythematosus of recent onset. Lupus 2015;24:1276–82.

16. Canora J, García M, Mitjavila F, Espinosa G, Suárez S, González-León R, et al. Clinical characteristics during diagnosis of a prospective cohort of patients with systemic lupus erythematosus treated in Spanish departments of internal medicine: the RELES study. Rev Clin Esp 2017;217:7–14.

Signaling Lymphocytic Activation Molecule Family Member 1 Engagement Inhibits T Cell–B Cell Interaction and Diminishes Interleukin-6 Production and Plasmablast Differentiation in Systemic Lupus Erythematosus

Maria P. Karampetsou,[1] Denis Comte,[2] Abel Suárez-Fueyo,[1] Eri Katsuyama,[1] Nobuya Yoshida,[1] Michihito Kono,[1] Vasileios C. Kyttaris,[1] and George C. Tsokos[1]

Objective. Signaling lymphocytic activation molecule family member 1 (SLAMF1) homophilic interactions promote immunoglobulin production and T cell–B cell cross-talk. SLAMF1 is overexpressed on T and B cells in patients with systemic lupus erythematosus (SLE). This study was undertaken to determine the role of SLAMF1 monoclonal antibody (mAb) in modulating T cell–B cell interaction and B cell activation.

Methods. Anti-IgM–prestimulated naive or total B cells from either healthy donors or patients with SLE were cocultured with autologous T cells under CD3/CD28 stimulation, in the presence or absence of the SLAMF1 mAb. Naive B cells were stimulated with anti-IgM and CD40L in the presence of the SLAMF1 antibody. Cytokine production by CD4+ T cells and B cells was examined by flow cytometry and/or quantitative polymerase chain reaction. Plasmablast formation and T cell and B cell conjugates were assessed by flow cytometry. IgG and antinuclear antibody production was determined by enzyme-linked immunosorbent assay.

Results. SLAMF1 ligation in a human peripheral blood T cell–B cell culture system reduced the following in both healthy controls and patients with SLE: conjugate formation, interleukin-6 (IL-6) production by B cells, IL-21 and IL-17A production by T cells, and Ig and autoantibody production. Whereas the SLAMF1 mAb directly affected the function of isolated peripheral B cells by decreasing IL-6 and Ig production in vitro, it did not affect cytokine production by isolated T cells stimulated in vitro.

Conclusion. The SLAMF1 antibody inhibits T cell–B cell interaction and suppresses B cell cytokine production and differentiation, thereby acting as a potential therapeutic tool in the treatment of patients with SLE.

INTRODUCTION

Systemic lupus erythematosus (SLE) is characterized by alterations in B cell subset distribution in the peripheral blood (1), defects in early B cell receptor (BCR)–initiated signaling events (2), and spontaneous autoantibody and interleukin-6 (IL-6) production (3,4). The pathophysiologic significance of B cells in SLE is underscored by the beneficial clinical outcomes of treatment with belimumab, an antibody that inhibits B cell–stimulating cytokines known to affect the survival of B cells and plasma cells (5).

Signaling lymphocytic activation molecule family members 1–9 (SLAMF1–9) are type I transmembrane glycoprotein cell surface receptors that deliver downstream signals upon their engagement and modulate the magnitude of the immune response. The SLAMF-encoding genes are located on chromosome 1 within q23, a region known to be associated with increased susceptibility to SLE development (6,7).

SLAMF1 is expressed on T cells, B cells, and dendritic cells, but not on monocytes or natural killer cells (8,9). Under physiologic conditions, SLAMF1 acts as a self ligand. The −262 A/G and −188 A/G polymorphisms in the promoter region of SLAMF1 are linked to an increase in SLAMF1 messenger RNA (mRNA) expression following stimulation of SLE peripheral blood mononuclear cells with

phytohemagglutinin, and may contribute to increased SLE susceptibility (10). Moreover, SLAMF1 is up-regulated on the cell surface of both T cells and B cells in the peripheral blood of patients with SLE, suggesting its potential role in SLE immunopathogenesis (11,12).

In B cells, SLAMF1 is up-regulated following activation, and it has been shown that coengagement with membrane forms or soluble forms of recombinant SLAMF1 may promote B cell proliferation and differentiation into immunoglobulin-secreting cells (ISCs) (13). Interestingly, it has been shown that the SLAMF1 monoclonal antibody (mAb) A12 and its F(ab')$_2$ fragment slightly diminished B cell proliferation induced by *Staphylococcus aureus* Cowan 1 (SAC) or anti-CD40, suggesting that SLAMF1 mAb may have an inhibitory effect on B cell activation (13).

We found that the presence of SLAMF1 mAb in human peripheral blood T cell and B cell cultures reduces both T cell–B cell interaction and IL-6 production by B cells. As a result, IL-21 and IL-17A production by T cells and Ig and autoantibody production by B cells are diminished in both healthy subjects and patients with SLE.

While the SLAMF1 mAb directly affects the function of isolated peripheral B cells by decreasing IL-6 and Ig production in vitro, it does not affect cytokine production by isolated T cells stimulated in vitro. These data suggest that SLAMF1 engagement may have an unrecognized beneficial effect in conditions where T cell–B cell interaction is crucial in disease pathogenesis.

PATIENTS AND METHODS

SLE patients and healthy controls. Patients (n = 26) who fulfilled the American College of Rheumatology criteria for SLE (14) were recruited from the Rheumatology Department at Beth Israel Deaconess Medical Center. Disease activity scores were measured using the SLE Disease Activity Index (SLEDAI) scoring system (15) (see Supplementary Table 1, on the *Arthritis & Rheumatology* web site at http://onlinelibrary.wiley.com/doi/10.1002/art.40682/abstract). Age-, sex-, and ethnicity-matched healthy individuals were evaluated as controls. Informed consent was obtained from all participants in accordance with the Declaration of Helsinki.

Cell isolation. Peripheral blood mononuclear cells were isolated by density-gradient centrifugation using Lymphocyte Separation Medium (Corning Life Sciences). Total T cells and B cells were isolated by negative selection using RosetteSep (Stem Cell Technologies). Naive B cells were negatively selected from total B cells using a Human Naive B Cell Isolation Kit II (Miltenyi Biotec). The positive fractions representing memory B cells were also collected. Naive CD4+ T cell purification was performed with a Human Naive CD4+ T Cell Isolation Kit II (Miltenyi Biotec).

T cell stimulation. Reagents used for T cell and B cell in vitro stimulation are listed in Supplementary Table 2 (http://onlinelibrary.wiley.com/doi/10.1002/art.40682/abstract). Total or naive CD4+ T cells were stimulated in complete RPMI medium (supplemented with 10% fetal bovine serum, 100 μg/ml streptomycin, and 100 units/ml penicillin), with precoated antibodies (1 μg/ml anti-CD3, 1 μg/ml anti-CD28, 5 μg/ml anti-SLAMF1, or 5 μg/ml isotype control). Where indicated, cells were restimulated for 6 hours with 25 ng/ml phorbol 12-myristate 13-acetate (PMA) and 0.5 μg/ml ionomycin in the presence of Brefeldin A (1 μg/ml GolgiPlug; BD Biosciences).

B cell stimulation. Total, naive, or memory peripheral blood B cells were stimulated with the F(ab')$_2$ fragment of an affinity-purified mouse anti-human heavy chain μ antibody (1 μg/ml), followed by stimulation with soluble CD40L (2 μg/ml), in the presence of either mouse anti-human SLAMF1 mAb (5 μg/ml) or mouse IgG1κ isotype control mAb (5 μg/ml), for the indicated amount of time. In some experiments, cells were cultured in the presence of a pharmacologic inhibitor against SHP-2 (SHP099; Cayman Chemical).

For cytokine detection, cells were restimulated with PMA (25 ng/ml) and ionomycin (0.5 μg/ml) in the presence of Brefeldin A (1 μg/ml) for the final 6 hours of culture. For B cell differentiation, naive B cells were stimulated as described above in the presence of 10 ng/ml IL-4 (PeproTech) for 7 days, with IL-4 replenished every 3 days. For immunoglobulin production, naive B cells (50 × 10^3/200 μl in complete medium in 96-well U-bottomed plates) were stimulated for 12 days with F(ab')$_2$ anti-IgM (1 μg/ml), CD40L (2 μg/ml), and IL-4 (10 ng/ml), in the presence of SLAMF1 mAb (5 μg/ml) or isotype control.

T cell–B cell coculture. Total or naive B cells were prestimulated for 48 hours with F(ab')$_2$ anti-IgM (1 μg/ml). Following this, cells were cocultured with autologous total T cells or naive CD4+ T cells, as indicated, in complete medium in 48-well plates (precoated with 1 μg/ml anti-CD3 and 1 μg/ml anti-CD28) for 5 days at 37°C with 5% CO$_2$. Soluble SLAMF1 mAb (5 μg/ml) or isotype control was added to the culture. Where indicated, we used a F(ab')$_2$ fragment generated from either SLAMF1 mAb (5 μg/ml) or normal isotype control (5 μg/ml), using a F(ab')$_2$ Fragmentation Kit according to the instructions of the manufacturer (G-Biosciences).

On day 5, cells were restimulated with PMA (25 ng/ml) and ionomycin (0.5 μg/ml) in the presence of Brefeldin A (1 μg/ml) for 6 hours. Cytokine production was examined by flow cytometry. Alternatively, cocultures were maintained for 12 hours and then examined for conjugate formation, or they were maintained for 7 days to examine follicular helper T (Tfh) cell–like formation and plasmablast differentiation.

Th17 cell differentiation. Freshly isolated naive CD4+ T cells were cultured in complete medium with precoated anti-CD3 mAb (1 μg/ml) and anti-CD28 mAb (1 μg/ml) in the presence of either soluble SLAMF1 mAb (5 μg/ml) or isotype control

(5 μg/ml), under the previously described Th17-polarizing conditions (16). On day 5, cells were restimulated for 6 hours with PMA (25 ng/ml) and ionomycin (0.5 μg/ml) in the presence of Brefeldin A (1 μg/ml). Cytokine production was examined by flow cytometry. All cytokines were purchased from PeproTech.

Flow cytometry and proliferation experiments. Cells were stained to detect dead cells (Zombie Aqua/UV/NIR Fixable Viability Kit; BioLegend) and then labeled for surface antibodies (see Supplementary Table 2, on the *Arthritis & Rheumatology* web site at http://onlinelibrary.wiley.com/doi/10.1002/art.40682/abstract). For cytokine detection, cells were permeabilized (Cytofix/Cytoperm; BD Biosciences) and stained with the indicated antibodies (Supplementary Table 2). Data were acquired with an LSR II SORP (BD Biosciences) and analyzed using FlowJo. Cells were labeled with 1 μ*M* carboxyfluorescein succinimidyl ester (CFSE) for 5 minutes at 37°C, and were then activated with appropriate stimuli. The CFSE dilution was examined by flow cytometry.

Enzyme-linked immunosorbent assay (ELISA), real-time quantitative reverse transcriptase–polymerase chain reaction (qRT-PCR), and Western immunoblotting. ELISA was used to determine secretion of IgG (eBioscience) and antinuclear antibody (ANA; NeoScientific) in culture supernatants, according to the manufacturers' instructions. Real-time qRT-PCR was performed as previously described (17). Primer sequences are shown in Supplementary Table 3 (http://onlinelibrary.wiley.com/doi/10.1002/art.40682/abstract). Western immunoblotting was performed as previously described (18).

Statistical analysis. Data are presented as the mean ± SEM. Statistical significance was determined by Wilcoxon matched pairs signed rank test, or for multiple comparisons, by one-way analysis of variance followed by post hoc analysis with Tukey's test. Analyses were performed using GraphPad Prism version 7. *P* values less than or equal to 0.05 were considered significant.

RESULTS

SLAMF1 ligation reduces IL-21 and IL-17A production by healthy and SLE CD4+ T cells in a T cell–B cell coculture system. B cells are potent antigen-presenting cells that are able to initiate and maintain T cell responses, through both cell–cell contact and cytokine release. SLAMF1 is up-regulated on both T cells and B cells in patients with SLE (12). We examined the effect of SLAMF1 ligation using a specific anti-human SLAMF1 mAb in the context of T cell–B cell interactions in vitro. Total B cells were isolated from the peripheral blood of healthy donors and patients with SLE, and stimulated

with F(ab')$_2$ anti-IgM for 48 hours to mimic the initial capture of antigen by the B cells. Stimulated B cells were then cocultured for 5 days with autologous T cells, in the presence or absence of soluble SLAMF1 mAb.

We examined the production of IL-21, IL-17A, interferon-γ (IFNγ), tumor necrosis factor (TNF), IL-4, IL-10, and IL-2 by CD4+ T cells on day 5, following restimulation with PMA and ionomycin for the final 6 hours of the culture. In cultures in which SLAMF1 mAb was added, we observed a significant decrease in the percentage of IL-21– and IL-17A–producing CD4+ T cells in both SLE patients and healthy subjects, compared to cultures treated with isotype control mAb (Figures 1A–C). Production of IFNγ, TNF, IL-4, IL-10, and IL-2 remained unaffected by SLAMF1 mAb (Supplementary Figures 1 and 2, http://onlinelibrary.wiley.com/doi/10.1002/art.40682/abstract). For certain coculture experiments, a F(ab')$_2$ fragment of either anti-SLAMF1 or isotype control was used, yielding results similar to those observed with regard to IL-21 and IL-17 production (Supplementary Figure 3).

When T cells were cultured in the absence of autologous B cells, we failed to detect differences in the percentage of IL-21+ CD4+ T cells following SLAMF1 coengagement, and IL-17A production under non–Th17 polarization conditions was minimal (Supplementary Figures 4A and B, http://onlinelibrary.wiley.com/doi/10.1002/art.40682/abstract). To further assess the potential effect of SLAMF1 coengagement on IL-17A production and Th17 differentiation, naive CD4+ T cells from healthy controls were incubated with SLAMF1 mAb under Th17-polarizing conditions. We did not observe any differences in the percentages of IL-17A–producing cells following Th17 differentiation in the presence of anti-SLAMF1 mAb compared to isotype control mAb (Supplementary Figures 4C and D).

Finally, we assessed the effects of SLAMF1 mAb on CD4+ T cell activation and proliferation. No differences were observed in the degree of up-regulation of CD69 and CD25 on the surface of CD4+ T cells following 48 hours of stimulation or in percentages of proliferating CFSE^{low} cells following 6 days of culture, between cells treated with anti-SLAMF1 and those treated with isotype control mAb (Supplementary Figure 5, http://onlinelibrary.wiley.com/doi/10.1002/art.40682/abstract).

The above data suggest that the decrease in the percentage of IL-17A– and IL-21–producing CD4+ T cells in the coculture system does not represent a direct effect of SLAMF1 mAb on T cells. Rather, the SLAMF1 mAb exerts its effect on T cell–B cell interaction.

SLAMF1 ligation inhibits plasmablast differentiation in a T cell–B cell coculture system in vitro. Production of IL-21 is instrumental in driving differentiation of B cells into ISCs (19,20). Because SLAMF1 ligation resulted in reduced IL-21 production from CD4+ T cells in our T cell–B cell coculture system, we assessed the effect of SLAMF1 mAb on the progres-
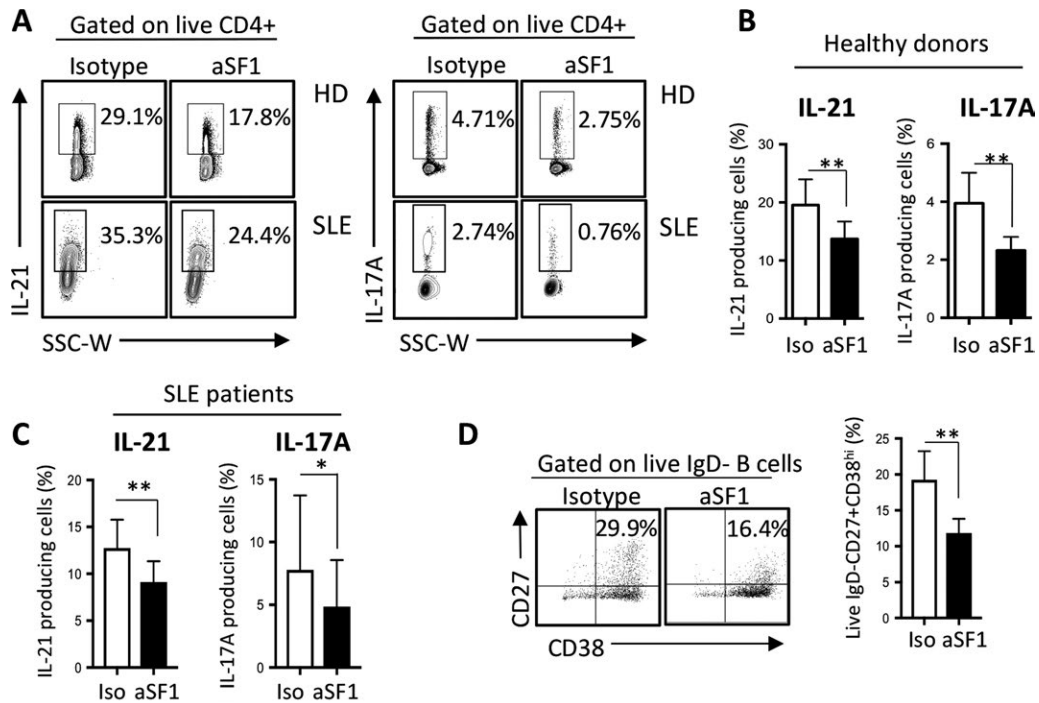
Figure 1. Reduction of interleukin-21 (IL-21) and IL-17A cytokine production from healthy and systemic lupus erythematosus (SLE) CD4+ T cells and inhibition of plasmablast formation in a T cell–B cell coculture system. **A–C,** Peripheral blood B cells from healthy donors (HDs; n = 8–10) or SLE patients (n = 9) were prestimulated with a F(ab′)$_2$ anti-IgM for 48 hours, and were plated with autologous total T cells at a 1:1 ratio under anti-CD3/CD28 stimulation for 5 days, in the presence of soluble signaling lymphocytic activation molecule family member 1 monoclonal antibodies (aSF1) or isotype control. On day 5, cells were restimulated with phorbol myristate acetate and ionomycin for 6 hours. Cytokine production by CD4+ T cells was evaluated by intracellular flow cytometry. Results of a representative experiment for IL-21 and IL-17A production in healthy individuals and SLE patients (**A**), as well as cumulative results for healthy donors (**B**) and SLE patients (**C**), are shown. **D,** Prestimulated naive B cells (n = 12) were cocultured with total T cells under anti-CD3/CD28 stimulation for 7 days. Representative flow plot (left) and cumulative results (right) of the frequency of plasmablasts (defined as IgD–CD27+CD38^{high}) are shown. Values are the mean ± SEM. * = P < 0.05; ** = P < 0.01. Iso = isotype control.

sion of naive B cells into plasmablasts. We isolated and prestimulated (for 48 hours) healthy naive peripheral blood B cells and then cocultured them with autologous total T cells for 7 days. Formation of plasmablasts (defined as IgD–CD27+CD38^{high}) was assessed by flow cytometry. In the presence of SLAMF1 mAb, the frequency of plasmablasts was significantly reduced, compared to that observed with isotype control mAb, after 7 days of culture (Figure 1D).

Because IL-21 production mainly characterizes CD4+ Tfh cells, a distinct subset of CD4+ helper T cells that drives antigen-specific humoral immune responses within germinal centers, we examined the effect of anti-SLAMF1 ligation on CD4+T cell differentiation toward Tfh-like cells. F(ab′)$_2$ anti-IgM–prestimulated B cells were cocultured for 7 days with naive CD4+ T cells in the presence or absence of SLAMF1 mAb. The frequency of naive CD4+ T cells that acquired a Tfh-like phenotype (defined by high expression of inducible costimulator [ICOS], programmed cell death 1 [PD-1], and chemokine receptor 5 [CXCR5]) remained unaltered (21,22).

SLAMF1 ligation with SLAMF1 mAb diminishes IL-6 cytokine production by B cells. It has been reported that

SLAMF1 coengagement inhibits the production of proinflammatory cytokines, such as TNF and IL-6, by CD40L-activated human dendritic cells (23). Moreover, production of IL-17A and IL-21 by CD4+ T cells depends on IL-6 (24). We sought to examine whether SLAMF1 coengagement exerts a similar effect on cytokine production in human B cells. As SLAMF1 is expressed at higher levels on naive B cells compared to memory B cells (8), we assessed cytokine expression following F(ab′)$_2$ anti-IgM– and/or CD40-mediated stimulation in sorted naive and memory peripheral blood B cells, in the presence of SLAMF1 mAb or isotype control. It has been reported that a sequential activation of B cells through the BCR followed by CD40 engagement leads to increased IL-6 and TNF production (25). We found that, in the presence of soluble SLAMF1 mAb, naive B cells that were submitted to dual stimulation exhibited significantly decreased IL-6 production, whereas the frequency of memory IL-6–producing B cells remained unaffected (Figures 2A and B).

On the other hand, the percentage of TNF-producing naive and memory B cells was not significantly affected by SLAMF1 coengagement (Supplementary Figures 6A and B, http://onlinelibrary.wiley.com/doi/10.1002/art.40682/abstract). Reduced IL-6
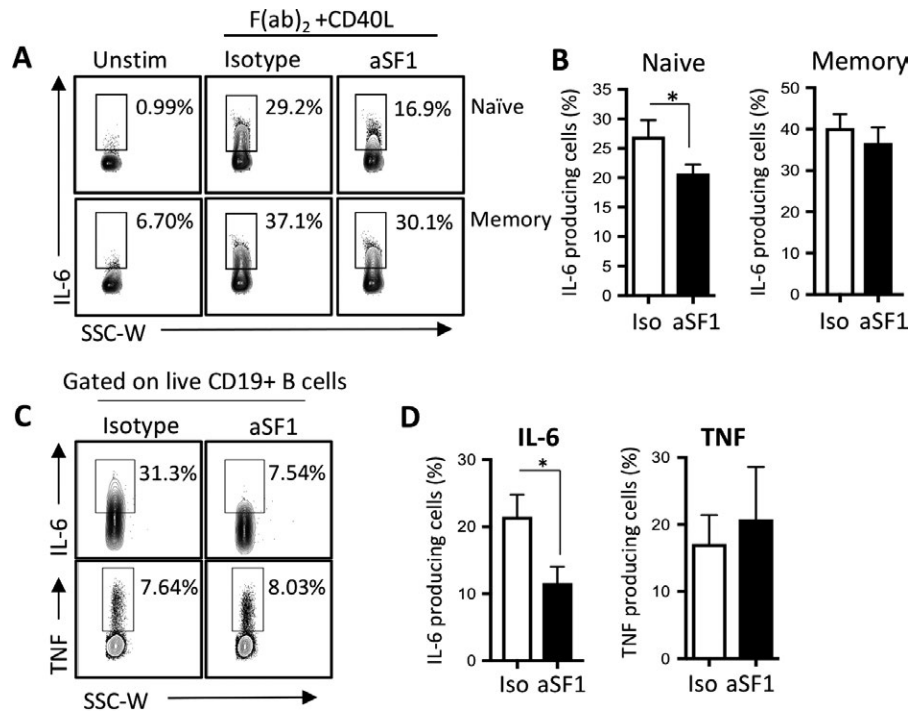
Figure 2. Reduction of IL-6 production by healthy naive B cells. **A** and **B,** Naive and memory B cells were isolated from the peripheral blood of healthy donors (n = 7) and were left unstimulated (Unstim) or were stimulated with F(ab')$_2$ anti-IgM and CD40L for 72 hours in the presence of signaling lymphocytic activation molecule family member 1 (SLAMF1) monoclonal antibodies. Cells were then restimulated with phorbol myristate acetate (PMA) and ionomycin for 6 hours. Results of a representative experiment (**A**) and cumulative results (**B**) for IL-6 production are shown. **C** and **D,** Total B cells were prestimulated with F(ab')$_2$ anti-IgM for 48 hours and were plated with autologous total T cells at a 1:1 ratio under anti-CD3/CD28 stimulation for 5 days, in the presence of soluble SLAMF1 monoclonal antibodies or isotype control. On day 5, cells were restimulated with PMA and ionomycin for 6 hours. Results of a representative experiment (**C**) and cumulative results (**D**) for IL-6 and tumor necrosis factor (TNF) expression are shown. Values are the mean ± SEM. * = $P < 0.05$. See Figure 1 for other definitions.

production was validated by qRT-PCR (Supplementary Figure 6C). We did not record any differences in TNF mRNA levels (Supplementary Figure 6D). IL-6 production and TNF production by B cells were also examined in the T cell–B cell coculture system. As expected, we observed a significant reduction in the frequency of IL-6–producing B cells, whereas TNF production remained unchanged following SLAMF1 ligation (Figures 2C and D). Based on the above data, in addition to inhibiting T cell–B cell interaction, SLAMF1 ligation may have a direct effect on B cells.

SLAMF1 coengagement inhibits B cell differentiation toward plasmablasts and ISCs. It is well established that IL-6 promotes B cell growth and terminal differentiation to Ig-producing cells both directly and indirectly (3,24). Because SLAMF1 coengagement results in reduced IL-6 production by naive B cells, we hypothesized that treatment with SLAMF1 mAb would negatively affect B cell differentiation. We differentiated naive B cells from the peripheral blood of healthy donors toward plasmablasts, with consecutive dual BCR- and CD40-mediated stimulation in the presence or absence of SLAMF1 mAb. Plasmablast formation was evaluated on day 7 as the percentage of IgD−CD27+CD38high cells. We found that in the presence of SLAMF1 mAb, the percentage of IgD−CD27+

CD38high plasmablasts was significantly diminished compared to that observed with isotype control (Figures 3A and B). Moreover, IgG production was reduced when B cells were differentiated toward plasmablasts in the presence of anti-SLAMF1 (versus in the presence of isotype control mAb) (Figure 3C), which can be explained, in part, by reduced IL-6 production by B cells.

A reduction in the percentage of plasmablast-like cells and diminished IgG production following SLAMF1 coengagement in vitro was not the result of increased cell death, because the percentage of live cells (defined as Aqua− cells) at the end of culture was similar among anti-SLAMF1–treated cells and isotype control–treated cells (Figure 3D). In addition, the inhibitory effect of SLAMF1 mAb on plasmablast differentiation and Ig secretion was not due to a generalized B cell unresponsiveness. B cells up-regulated CD69 and CD86 at 12 hours and 72 hours of stimulation, respectively, in the presence of SLAMF1 mAb as effectively as in the presence of isotype control (Supplementary Figures 7A and B, http://onlinelibrary.wiley.com/doi/10.1002/art.40682/abstract). Moreover, B cells proliferated normally in the presence of SLAMF1 mAb (Supplementary Figures 7C and D).

To better assess the effect of SLAMF1 mAb on B cells, we incubated healthy B cells with F(ab')$_2$ anti-IgM in the presence of either anti-SLAMF1 or isotype control for 5 minutes,
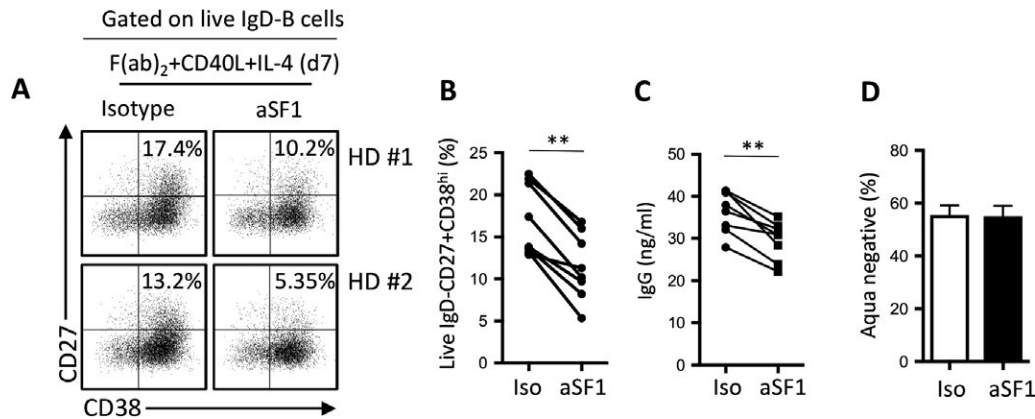
Figure 3. Inhibition of B cell differentiation toward plasmablasts and prevention of IgG secretion in healthy controls. **A** and **B,** Naive B cells were isolated from the peripheral blood of healthy donors (n = 8). Cells were stimulated with F(ab′)$_2$ anti-IgM and CD40L, in the presence of signaling lymphocytic activation molecule family member 1 monoclonal antibodies or isotype control. IL-4 (10 ng/ml) was added on day 1 and replenished every 3 days. Formation of plasmablasts (defined as IgD–CD27+CD38^{high}) was assessed by flow cytometry on day 7. Results of a representative experiment (**A**) and individual results in each subject (**B**) are shown. **C,** IgG production in culture supernatants was assessed by enzyme-linked immunosorbent assay on day 12. **D,** B cell survival in culture was evaluated on day 7. Values are the mean ± SEM. ** = *P* < 0.01. See Figure 1 for other definitions.

10 minutes, or 30 minutes, and we examined protein tyrosine phosphorylation by Western immunoblotting. In the presence of anti-SLAMF1, pTyr levels were decreased, suggesting a possible inhibitory effect of SLAMF1 mAb on B cells via BCR-mediated signaling regulation (Supplementary Figure 8).

It has been reported that SLAMF1 mediates signaling via SH2 domain–containing phosphatase 2 (SHP-2) (26). To further address the mechanism by which anti-SLAMF1 affects BCR-initiated signaling, we cultured healthy B cells with F(ab′)$_2$ anti-IgM in the presence of SLAMF1 mAb and an SHP-2 inhibitor (SHP099) and assessed pTyr levels by Western immunoblotting. Indeed, in the presence of SHP099, pTyr levels were restored following SLAMF1 coengagement. This indicates that BCR-mediated signaling can be directly modulated in the presence
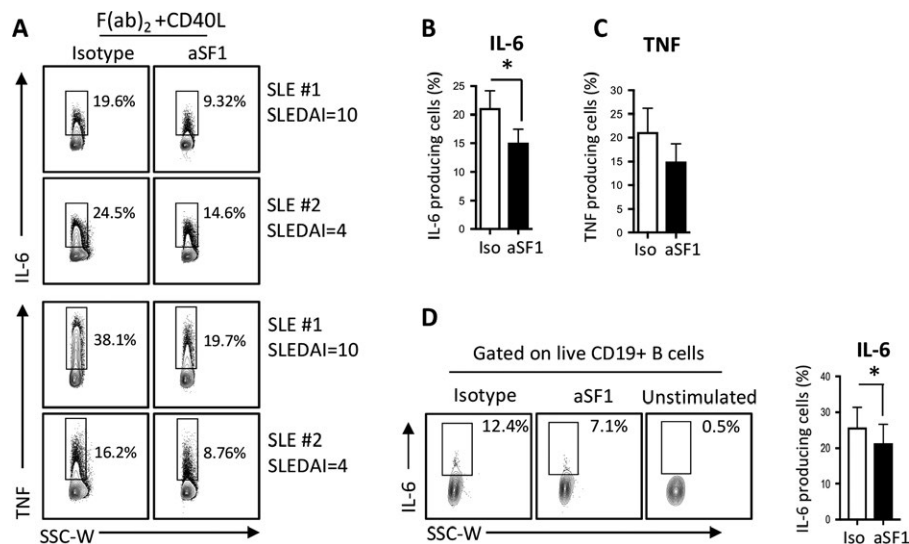
Figure 4. Decreased IL-6 production in SLE B cells. **A–C,** B cells were isolated from the peripheral blood of SLE patients (n = 6) and were stimulated with F(ab′)$_2$ anti-IgM and CD40L for 72 hours, in the presence of signaling lymphocytic activation molecule family member 1 (SLAMF1) monoclonal antibodies (mAb) or isotype control. Cells were then restimulated with phorbol myristate acetate (PMA) and ionomycin for 6 hours. IL-6 and tumor necrosis factor (TNF) production was evaluated by intracellular flow cytometry. Representative flow plots from 2 SLE patients (**A**) and cumulative results (**B** and **C**) are shown. **D,** Peripheral blood B cells from SLE patients (n = 6) were prestimulated with F(ab′)$_2$ anti-IgM for 48 hours and were plated with autologous total T cells at a 1:1 ratio under anti-CD3/CD28 stimulation for 5 days, in the presence of soluble SLAMF1 mAb or isotype control. On day 5, cells were restimulated with PMA and ionomycin for 6 hours. IL-6 production by B cells was evaluated by intracellular flow cytometry. A representative flow cytometry panel (left) and cumulative results (right) are shown. Values are the mean ± SEM. * = *P* < 0.05. SLEDAI = SLE Disease Activity Index (see Figure 1 for other definitions).
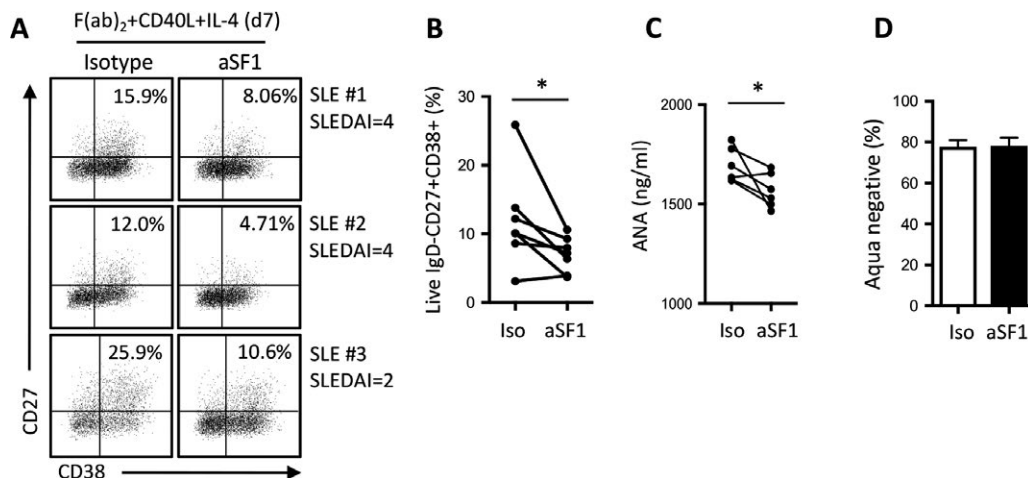
Figure 5. Reduction in B cell differentiation toward plasmablasts and reduced antinuclear antibody (ANA) production in SLE patients. Naive B cells were isolated from the peripheral blood of patients with SLE (n = 6). Cells were stimulated with F(ab′)$_2$ anti-IgM and CD40L in the presence of signaling lymphocytic activation molecule family member 1 monoclonal antibodies or isotype control. IL-4 (10 ng/ml) was added on day 1 and replenished every 3 days. **A,** Representative flow cytometry plots of formation of plasmablasts (IgD–CD27+CD38^{high}) from the naive B cells from 3 SLE patients are shown. **B,** Individual results from each patient are also shown. **C,** Naive SLE B cells were maintained in culture for 12 days, and ANA production in culture supernatants was evaluated by enzyme-linked immunosorbent assay. **D,** B cell survival in culture was evaluated on day 7 by examining the percentage of Aqua– cells. Values are the mean ± SEM. * = $P < 0.05$. SLEDAI = SLE Disease Activity Index (see Figure 1 for other definitions).

of SLAMF1 mAb in an SHP-2–dependent manner in single cell population cultures (Supplementary Figure 9, http://onlinelibrary.wiley.com/doi/10.1002/art.40682/abstract).

SLAMF1 ligation regulates IL-6 production and plasmablast differentiation of SLE B cells. SLE B cells spontaneously produce IL-6 in vitro, which drives B cell differentiation and autoantibody production (3). We examined whether treatment of peripheral blood SLE B cells with anti-SLAMF1 regulated IL-6 production and differentiation of naive SLE B cells. Naive B cells from SLE patients were stimulated for 72 hours with F(ab′)$_2$ anti-IgM followed by CD40L in the presence of either SLAMF1 mAb or isotype control. We observed that the frequency of IL-6–producing B cells was significantly decreased when cells were coengaged with anti-SLAMF1 versus isotype control mAb, whereas no significant differences in TNF production were detected (Figures 4A–C). IL-6 production by SLE B cells was also examined in the T cell–B cell coculture system. We observed a statistically significant reduction in the percentage of IL-6–producing SLE B cells in the presence of anti-SLAMF1 (Figure 4D). Finally, when we differentiated naive SLE B cells toward ISCs, both the percentage of IgD–CD27+CD38^{high} plasmablasts and the production of ANA were significantly reduced in the presence of anti-SLAMF1, compared to cells treated with isotype control (Figure 5).

SLAMF1 mAb prevents T cell–B cell conjugate formation in vitro. Considering that the presence of SLAMF molecules is important for cell–cell interactions, we hypothesized that SLAMF1 mAb could inhibit the formation of T cell–B

cell conjugates (27). B cells isolated from the peripheral blood of healthy subjects or SLE patients were cocultured with autologous total T cells for 12 hours in the presence or absence of soluble SLAMF1 mAb. Conjugate frequencies were measured by flow cytometry. In the presence of SLAMF1 mAb, the formation of CD4+CD19+ T cell–B cell conjugates was decreased in both healthy individuals and patients with SLE (Figure 6).

DISCUSSION

B cells in SLE are able to stimulate T cells via up-regulation of costimulatory molecules, and reciprocally activated T cells provide substantial help to autoreactive B cells, thus driving autoantibody production (28). Relying on inhibition of T cell–B cell interaction and costimulation to constrain activation of adaptive immunity is an appealing therapeutic approach for patients with SLE and/or other autoimmune diseases. Treatment with mAb directed against costimulatory molecules such as CD28, ICOS, and CD40L has been attempted in patients with SLE with variable results in efficacy and safety (5), or is currently under evaluation.

In this study, we showed that in the context of an in vitro T cell–B cell coculture system, SLAMF1 ligation with a SLAMF1 mAb limits the frequency of IL-21– and IL-17A–producing CD4+ T cells in healthy controls and, more importantly, in patients with SLE. Our data suggest that this inhibition occurs in two ways: 1) through inhibition of direct interaction between T cells and B cells, and 2) through modulation of B cell activation and BCR signaling, which affects the production of IL-6 by B cells.

Because SLAMF1 acts through homophilic interaction, ligation of SLAMF1 with a specific monoclonal antibody or its
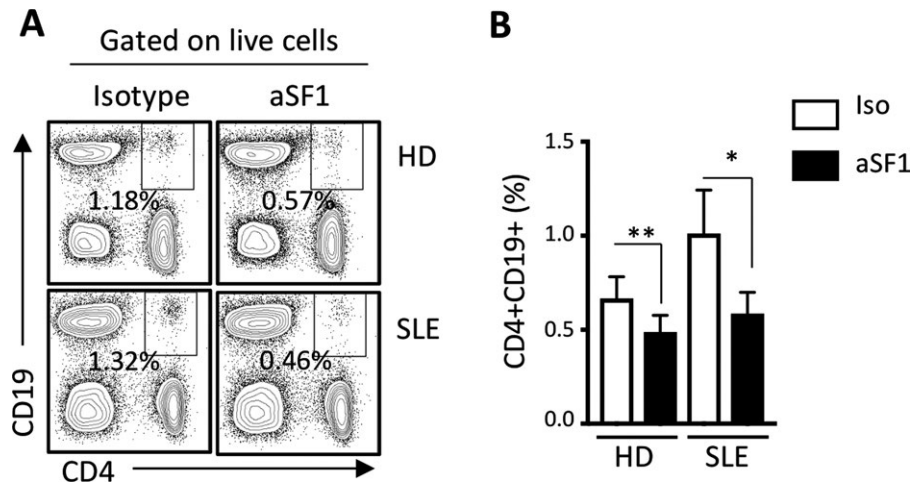
Figure 6. Inhibition of T cell–B cell conjugate formation in vitro. Total B cells isolated from the peripheral blood of healthy individuals (n = 8) and SLE patients (n = 5) were prestimulated with F(ab′)$_2$ anti-IgM for 48 hours and then cocultured for 12 hours with autologous total T cells in 96-well U-bottomed plates (precoated with anti-CD3/CD28), in the presence of signaling lymphocytic activation molecule family member 1 monoclonal antibodies or isotype control. Cells were stained with anti-CD4 and anti-CD19, and conjugate formation (CD4+CD19+) was assessed by flow cytometry. Results of representative experiments with cells from a healthy donor (top) and an SLE patient (bottom) (**A**) and cumulative results (**B**) are shown. Values are the mean ± SEM. * = $P < 0.05$; ** = $P < 0.01$. See Figure 1 for other definitions.

F(ab′)$_2$ fragment could affect cell–cell interaction and interfere with T cell activation, proliferation, and differentiation. Several observations in the literature indicate that anti–SLAMF1-specific antibodies may interfere with SLAMF1 homotypic interactions. Initial in vitro studies conducted in human preactivated Th0, Th1, and Th2 clones suggested that SLAMF1 ligation (with the use of SLAMF1 mAb or its F[ab′]$_2$ fragment) strongly up-regulated IFNγ production and was even found to redirect Th2 clones to acquire a Th1-like phenotype (29,30). On the contrary, antigen receptor–dependent production of IFNγ, following anti-CD3 activation, was inhibited on T cell clone BI-141, expressing a constitutively activated SLAMF1–SLAM-associated protein pathway (31). Because SLAMF1 mAb clone A12 recognizes the external V1 domain of SLAMF1, it likely disrupts SLAMF1–SLAMF1 homotypic interactions.

In support of the above, we observed that in the presence of SLAMF1 mAb, the formation of T cell–B cell conjugates was significantly reduced in healthy individuals, and more importantly, in patients with SLE. We further characterized the effect of SLAMF1 ligation on direct B cell activation and BCR signaling. In our coculture system (and single cell assays), we noted a significant decrease in IL-6, but not in TNF, production by B cells in healthy controls and SLE patients, when cells were incubated with SLAMF1 mAb.

Indeed, upon stimulation, B cells are known to become a rich of source of cytokines that contribute to the outcome of the immune response. B cells may promote or inhibit T cell immune responses and differentiation via cytokine production (32). B cells from patients with SLE can produce significant amounts of IL-6, even in the absence of stimulation (33). A fundamental function of IL-6 is to promote B cell maturation into Ig-secreting cells in an autocrine/paracrine manner (3). However, IL-6 also indirectly

affects B cell progression to antibody-producing cells as it drives CD4+ T cells to secrete IL-21, a cytokine that plays a major role in differentiation, Ig secretion, and the B cell antibody class switch process (19,34). Data from studies in murine lupus and in humans with SLE have shown that IL-6 plays an important role in sustaining B cell overactivity and autoantibody production, and in mediating tissue damage (24,35). When we differentiated naive B cells from healthy donors and patients with SLE, either alone or with autologous T cells, plasmablast formation and IgG and ANA production were reduced in the presence of anti-SLAMF1.

The failure of B cells to differentiate into ISCs was not due to a general unresponsiveness following treatment with SLAMF1 mAb. B cell proliferation, as well as up-regulation of activation markers, was not affected by SLAMF1 mAb. This is consistent with previously published data demonstrating that B cell stimulation with SLAMF1 mAb, or its F(ab′)$_2$ fragment, had no effect on proliferation and activation, whereas soluble and membrane forms of SLAMF1 protein promoted human B cell proliferation and Ig synthesis (13). Our data also indicate that SLAMF1 ligation with mAb may have a direct effect on BCR-mediated signaling, as it diminished overall pTyr levels following BCR stimulation via SHP-2 (13,31).

IL-6 is known to drive Th17 differentiation (36) and promote IL-21 production by activated CD4+ T cells (37,38). SLE is characterized by increased serum IL-21 and IL-17 levels that correlate with disease activity (39–41). Moreover, IL-17–producing T cells are expanded in the periphery in SLE patients and detected in the kidneys of lupus nephritis patients, indicating a link between IL-17 production and lupus immunopathogenesis (39). When we cultured human naive CD4+ T cells under Th17-polarizing conditions, the presence of SLAMF1 mAb did not affect IL-17 production. In contrast, we observed a reduction in

IL-17A production by CD4+ T cells upon SLAMF1 ligation, detected only when T cells were cocultured with autologous B cells. This indicates a regulatory effect of SLAMF1 mAb on IL-17A production, either by directly inhibiting T cell–B cell interaction and/or by suppressing IL-6 production by B cells.

Production of IL-21 mainly characterizes CD4+ Tfh cells, a subset of CD4+ helper T cells that drives antigen-specific humoral immune responses within germinal centers (21,22). IL-21–producing CD4+ T cells and CXCR5+ICOS+PD-1+ Tfh-like cells are expanded in the peripheral blood of SLE patients and are found in kidney sections from lupus nephritis patients (42–45). In our study, SLAMF1 ligation did not interfere with the generation of Tfh-like CD4+ T cells in vitro. This is consistent with previously published data using SLAM$^{-/-}$ mice, which demonstrated that even though Tfh differentiation in germinal centers remained intact, cytokine production by Tfh was nevertheless affected (46).

Although total B cell depletion therapies failed to deliver the expected results in the treatment of patients with SLE in controlled clinical trials (5), the role of B cells in the immunopathogenesis of lupus should not be overlooked, and more targeted treatments need to be explored. The efficacy of tocilizumab, a human monoclonal antibody directed against the IL-6 receptor α-chain, has already been assessed in an open-label phase I dose-escalation study in patients with moderately active SLE (47). Treatment with tocilizumab resulted in an improvement of Safety of Estrogens in Lupus Erythematosus National Assessment–SLEDAI scores (48) and a reduction of double-stranded DNA antibody titers. However, the concurrent development of neutropenia and severe infections posed a significant limiting factor to continuation of treatment. Therefore, newer and safer treatments targeting the IL-6 pathway should be explored. Moreover, SLAMF1 mAb inhibits T cell–B cell interaction, which may have a beneficial effect in the context of autoimmunity.

In summary, we have shown that SLAMF1 coengagement in vitro regulates IL-6 cytokine production and inhibits differentiation of naive B cells toward ISCs in both healthy individuals and patients with SLE. More notably, we have demonstrated that in a T cell–B cell coculture system, the presence of SLAMF1 mAb reduces T cell–B cell interaction, thus interfering with IL-21 and IL-17A production by T cells.

AUTHOR CONTRIBUTIONS

All authors were involved in drafting the article or revising it critically for important intellectual content, and all authors approved the final version to be published. Dr. Tsokos had full access to all of the data in the study and takes responsibility for the integrity of the data and the accuracy of the data analysis.
Study conception and design. Karampetsou, Comte, Tsokos.
Acquisition of data. Karampetsou, Comte, Suárez-Fueyo, Katsuyama, Yoshida, Kono, Kyttaris, Tsokos.

Analysis and interpretation of data. Karampetsou, Comte, Suárez-Fueyo, Katsuyama, Yoshida, Kono, Tsokos.

REFERENCES

1. Dorner T, Jacobi AM, Lee J, Lipsky PE. Abnormalities of B cell subsets in patients with systemic lupus erythematosus. J Immunol Methods 2011;363:187–97.

2. Liossis SN, Kovacs B, Dennis G, Kammer GM, Tsokos GC. B cells from patients with systemic lupus erythematosus display abnormal antigen receptor-mediated early signal transduction events. J Clin Invest 1996;98:2549–57.

3. Kitani A, Hara M, Hirose T, Harigai M, Suzuki K, Kawakami M, et al. Autostimulatory effects of IL-6 on excessive B cell differentiation in patients with systemic lupus erythematosus: analysis of IL-6 production and IL-6R expression. Clin Exp Immunol 1992;88:75–83.

4. Nagafuchi H, Suzuki N, Mizushima Y, Sakane T. Constitutive expression of IL-6 receptors and their role in the excessive B cell function in patients with systemic lupus erythematosus. J Immunol 1993;151:6525–34.

5. Kyttaris VC. Novel treatments in lupus. Curr Rheumatol Rep 2017;19:10.

6. Wakeland EK, Liu K, Graham RR, Behrens TW. Delineating the genetic basis of systemic lupus erythematosus. Immunity 2001;15:397–408.

7. Tsao BP. The genetics of human systemic lupus erythematosus. Trends Immunol 2003;24:595–602.

8. Romero X, Benitez D, March S, Vilella R, Miralpeix M, Engel P. Differential expression of SAP and EAT-2-binding leukocyte cell-surface molecules CD84, CD150 (SLAM), CD229 (Ly9) and CD244 (2B4). Tissue Antigens 2004;64:132–44.

9. Castro AG, Hauser TM, Cocks BG, Abrams J, Zurawski S, Churakova T, et al. Molecular and functional characterization of mouse signaling lymphocytic activation molecule (SLAM): differential expression and responsiveness in Th1 and Th2 cells. J Immunol 1999;163:5860–70.

10. You Y, Wang Z, Deng GH, Liu Y, Hao F. Detection and functional evaluation of -262A/T and -188A/G polymorphisms of SLAM gene in patients with systemic lupus erythematosus. J Rheumatol 2010;37:2268–72.

11. Linan-Rico L, Hernandez-Castro B, Doniz-Padilla L, Portillo-Salazar H, Baranda L, Cruz-Munoz ME, et al. Analysis of expression and function of the co-stimulatory receptor SLAMF1 in immune cells from patients with systemic lupus erythematosus (SLE). Lupus 2015;24:1184–90.

12. Karampetsou MP, Comte D, Kis-Toth K, Kyttaris VC, Tsokos GC. Expression patterns of signaling lymphocytic activation molecule family members in peripheral blood mononuclear cell subsets in patients with systemic lupus erythematosus. PLoS One 2017;12:e0186073.

13. Punnonen J, Cocks BG, Carballido JM, Bennett B, Peterson D, Aversa G, et al. Soluble and membrane-bound forms of signaling lymphocytic activation molecule (SLAM) induce proliferation and Ig synthesis by activated human B lymphocytes. J Exp Med 1997;185:993–1004.

14. Tan EM, Cohen AS, Fries JF, Masi AT, McShane DJ, Rothfield NF, et al. The 1982 revised criteria for the classification of systemic lupus erythematosus. Arthritis Rheum 1982;25:1271–7.

15. Bombardier C, Gladman DD, Urowitz MB, Caron D, Chang CH, and the Committee on Prognosis Studies in SLE. Derivation of the SLEDAI: a disease activity index for lupus patients. Arthritis Rheum 1992;35:630–40.

16. Comte D, Karampetsou MP, Kis-Toth K, Yoshida N, Bradley SJ, Mizui M, et al. Engagement of SLAMF3 enhances CD4+ T-cell sensi-

tivity to IL-2 and favors regulatory T-cell polarization in systemic lupus erythematosus. Proc Natl Acad Sci U S A 2016;113:9321–6.

17. Comte D, Karampetsou MP, Yoshida N, Kis-Toth K, Kyttaris VC, Tsokos GC. SLAMF7 engagement restores defective effector CD8+ T cells activity in response to foreign antigens in systemic lupus erythematosus. Arthritis Rheumatol 2017;69:1035–44.

18. Karampetsou MP, Comte D, Kis-Toth K, Terhorst C, Kyttaris VC, Tsokos GC. Decreased SAP expression in T cells from patients with systemic lupus erythematosus contributes to early signaling abnormalities and reduced IL-2 production. J Immunol 2016;196:4915–24.

19. Ettinger R, Sims GP, Fairhurst AM, Robbins R, da Silva YS, Spolski R, et al. IL-21 induces differentiation of human naive and memory B cells into antibody-secreting plasma cells. J Immunol 2005;175:7867–79.

20. Ding BB, Bi E, Chen H, Yu JJ, Ye BH. IL-21 and CD40L synergistically promote plasma cell differentiation through upregulation of Blimp-1 in human B cells. J Immunol 2013;190:1827–36.

21. Gensous N, Schmitt N, Richez C, Ueno H, Blanco P. T follicular helper cells, interleukin-21 and systemic lupus erythematosus. Rheumatology (Oxford) 2017;56:516–23.

22. Blanco P, Ueno H, Schmitt N. T follicular helper (Tfh) cells in lupus: activation and involvement in SLE pathogenesis. Eur J Immunol 2016;46:281–90.

23. Rethi B, Gogolak P, Szatmari I, Veres A, Erdos E, Nagy L, et al. SLAM/SLAM interactions inhibit CD40-induced production of inflammatory cytokines in monocyte-derived dendritic cells. Blood 2006;107:2821–9.

24. Hunter CA, Jones SA. IL-6 as a keystone cytokine in health and disease. Nat Immunol 2015;16:448–57.

25. Duddy ME, Alter A, Bar-Or A. Distinct profiles of human B cell effector cytokines: a role in immune regulation? J Immunol 2004;172:3422–7.

26. Wang N, Halibozek PJ, Yigit B, Zhao H, O'Keeffe MS, Sage P, et al. Negative regulation of humoral immunity due to interplay between the SLAMF1, SLAMF5, and SLAMF6 receptors. Front Immunol 2015;6:158.

27. Cannons JL, Tangye SG, Schwartzberg PL. SLAM family receptors and SAP adaptors in immunity. Annu Rev Immunol 2011;29:665–705.

28. Moulton VR, Tsokos GC. T cell signaling abnormalities contribute to aberrant immune cell function and autoimmunity. J Clin Invest 2015;125:2220–7.

29. Cocks BG, Chang CC, Carballido JM, Yssel H, de Vries JE, Aversa G. A novel receptor involved in T-cell activation. Nature 1995;376:260–3.

30. Aversa G, Chang CC, Carballido JM, Cocks BG, de Vries JE. Engagement of the signaling lymphocytic activation molecule (SLAM) on activated T cells results in IL-2-independent, cyclosporin A-sensitive T cell proliferation and IFN-γ production. J Immunol 1997;158:4036–44.

31. Latour S, Gish G, Helgason CD, Humphries RK, Pawson T, Veillette A. Regulation of SLAM-mediated signal transduction by SAP, the X-linked lymphoproliferative gene product. Nat Immunol 2001;2:681–90.

32. Bao Y, Cao X. The immune potential and immunopathology of cytokine-producing B cell subsets: a comprehensive review. J Autoimmun 2014;55:10–23.

33. Kitani A, Hara M, Hirose T, Norioka K, Harigai M, Hirose W, et al. Heterogeneity of B cell responsiveness to interleukin 4, interleukin 6 and low molecular weight B cell growth factor in discrete stages of

34. Ozaki K, Spolski R, Ettinger R, Kim HP, Wang G, Qi CF, et al. Regulation of B cell differentiation and plasma cell generation by IL-21, a novel inducer of Blimp-1 and Bcl-6. J Immunol 2004;173:5361–71.

35. Tackey E, Lipsky PE, Illei GG. Rationale for interleukin-6 blockade in systemic lupus erythematosus. Lupus 2004;13:339–43.

36. Acosta-Rodriguez EV, Napolitani G, Lanzavecchia A, Sallusto F. Interleukins 1β and 6 but not transforming growth factor-β are essential for the differentiation of interleukin 17-producing human T helper cells. Nat Immunol 2007;8:942–9.

37. Dienz O, Eaton SM, Bond JP, Neveu W, Moquin D, Noubade R, et al. The induction of antibody production by IL-6 is indirectly mediated by IL-21 produced by CD4+ T cells. J Exp Med 2009;206:69–78.

38. Diehl SA, Schmidlin H, Nagasawa M, Blom B, Spits H. IL-6 triggers IL-21 production by human CD4+ T cells to drive STAT3-dependent plasma cell differentiation in B cells. Immunol Cell Biol 2012;90:802–11.

39. Crispin JC, Tsokos GC. IL-17 in systemic lupus erythematosus. J Biomed Biotechnol 2010;2010:943254.

40. Wang L, Zhao P, Ma L, Shan Y, Jiang Z, Wang J, et al. Increased interleukin 21 and follicular helper T-like cells and reduced interleukin 10+ B cells in patients with new-onset systemic lupus erythematosus. J Rheumatol 2014;41:1781–92.

41. Lan Y, Luo B, Wang JL, Jiang YW, Wei YS. The association of interleukin-21 polymorphisms with interleukin-21 serum levels and risk of systemic lupus erythematosus. Gene 2014;538:94–8.

42. Chang A, Henderson SG, Brandt D, Liu N, Guttikonda R, Hsieh C, et al. In situ B cell-mediated immune responses and tubulointerstitial inflammation in human lupus nephritis. J Immunol 2011;186:1849–60.

43. Zhang X, Lindwall E, Gauthier C, Lyman J, Spencer N, Alarakhia A, et al. Circulating CXCR5+CD4+helper T cells in systemic lupus erythematosus patients share phenotypic properties with germinal center follicular helper T cells and promote antibody production. Lupus 2015;24:909–17.

44. Terrier B, Costedoat-Chalumeau N, Garrido M, Geri G, Rosenzwajg M, Musset L, et al. Interleukin 21 correlates with T cell and B cell subset alterations in systemic lupus erythematosus. J Rheumatol 2012;39:1819–28.

45. Choi JY, Ho JH, Pasoto SG, Bunin V, Kim ST, Carrasco S, et al. Circulating follicular helper–like T cells in systemic lupus erythematosus: association with disease activity. Arthritis Rheumatol 2015;67:988–99.

46. Yusuf I, Kageyama R, Monticelli L, Johnston RJ, Ditoro D, Hansen K, et al. Germinal center T follicular helper cell IL-4 production is dependent on signaling lymphocytic activation molecule receptor (CD150). J Immunol 2010;185:190–202.

47. Illei GG, Shirota Y, Yarboro CH, Daruwalla J, Tackey E, Takada K, et al. Tocilizumab in systemic lupus erythematosus: data on safety, preliminary efficacy, and impact on circulating plasma cells from an open-label phase I dosage-escalation study. Arthritis Rheum 2010;62:542–52.

48. Petri M, Kim MY, Kalunian KC, Grossman J, Hahn BH, Sammaritano LR, et al. Combined oral contraceptives in women with systemic lupus erythematosus. N Engl J Med 2005;353:2550–8.

B cell activation in patients with systemic lupus erythematosus. Clin Exp Immunol 1989;77:31–6.

AMERICAN COLLEGE
OF RHEUMATOLOGY
EDUCATION · TREATMENT · RESEARCH

Macrophage Migration Inhibitory Factor Regulates U1 Small Nuclear RNP Immune Complex–Mediated Activation of the NLRP3 Inflammasome

Min Sun Shin,[1] Youna Kang,[1] Elizabeth R. Wahl,[2] Hong-Jai Park,[1] Rossitza Lazova,[3] Lin Leng,[1] Mark Mamula,[1] Smita Krishnaswamy,[1] Richard Bucala,[1] and Insoo Kang[1]

Objective. High-expression alleles of macrophage migration inhibitory factor (MIF) are linked genetically to the severity of systemic lupus erythematosus (SLE). The U1 small nuclear RNP (snRNP) immune complex containing U1 snRNP and anti–U1 snRNP antibodies, which are found in patients with SLE, activates the NLRP3 inflammasome, comprising NLRP3, ASC, and procaspase 1, in human monocytes, leading to the production of interleukin-1β (IL-1β). This study was undertaken to investigate the role of the snRNP immune complex in up-regulating the expression of MIF and its interface with the NLRP3 inflammasome.

Methods. MIF, IL-1β, NLRP3, caspase 1, ASC, and MIF receptors were analyzed by enzyme-linked immunosorbent assay, Western blotting, quantitative polymerase chain reaction, and cytometry by time-of-flight mass spectrometry (CytoF) in human monocytes incubated with or without the snRNP immune complex. MIF pathway responses were probed with the novel small molecule antagonist MIF098.

Results. The snRNP immune complex induced the production of MIF and IL-1β from human monocytes. High-dimensional, single-cell CytoF analysis established that MIF regulates activation of the NLRP3 inflammasome, including findings of a quantitative relationship between MIF and its receptors and IL-1β levels in the monocytes. MIF098, which blocks MIF binding to its cognate receptor, suppressed the production of IL-1β, the up-regulation of NLRP3, which is a rate-limiting step in NLRP3 inflammasome activation, and the activation of caspase 1 in snRNP immune complex–stimulated human monocytes.

Conclusion. The U1 snRNP immune complex is a specific stimulus of MIF production in human monocytes, with MIF having an upstream role in defining the inflammatory characteristics of activated monocytes by regulating NLRP3 inflammasome activation and downstream IL-1β production. These findings provide mechanistic insight and a therapeutic rationale for targeting MIF in subgroups of lupus patients, such as those classified as high genotypic *MIF* expressers or those with anti-snRNP antibodies.

INTRODUCTION

Macrophage migration inhibitory factor (MIF), produced primarily from activated monocytes and macrophages, is an upstream activator of innate immune responses (1–3). In addition to its inhibition of monocyte migration and macrophage mobility, MIF promotes inflammatory responses by counter-regulating the inhibitory effect of glucocorticoids on the production of inflammatory cytokines from macrophages, and by suppressing p53-dependent cell death (4,5). The MIF receptor complex is composed of the transmembrane ligand-binding component CD74 and the CD44 signaling component (6,7). MIF also competes with cognate ligands for CXCR4 and CXCR2, and directly binds to CXCR2 in a macromolecular receptor complex with CD74 (8).

Findings from human and animal studies have supported a role of MIF in the pathogenesis of infectious and inflammatory conditions, including septic shock, malaria, rheumatoid arthritis, and systemic lupus erythematosus (SLE; lupus) (9–13). MIF is overexpressed in lupus-prone mice, and MIF-deficient lupus-prone MRL/*lpr* mice are protected from glomerular injury (14). In addition, the therapeutic efficacy of blocking MIF in lupus-prone mice has previously been demonstrated (11). An association between high-expression *MIF* alleles and susceptibility to lupus and deep organ involvement has been reported (12,15). In patients with lupus, circulatory MIF levels are increased (15) and these augmented levels are correlated with disease damage, as has been observed both cross-sectionally and longitudinally (16,17). These findings support the pathogenic role of MIF and the therapeutic value of targeting MIF-dependent pathways in lupus, which is currently under study with the clinical testing of anti-CD74 (18).

The pathologic hallmarks of SLE are altered immune responses to nuclear autoantigens, manifested as production of autoantibodies and subsequent tissue injury (19,20). Experimental studies support the critical role of innate immunity, in addition to that of adaptive immunity, in the development of lupus and in the pathologic progression of disease. Plasmacytoid dendritic cells recognize lupus self antigens via Toll-like receptors (TLRs), leading to the production of interferon-α (IFNα), which is linked to the pathogenesis of lupus and its clinical manifestations (21–23). For instance, TLRs 7 and 8 recognize the single-stranded RNA of the self antigen U1 small nuclear RNP (snRNP), which is targeted by anti–U1 snRNP antibodies in lupus (21). In support of a role of this pathway, studies in experimental models have demonstrated ameliorated disease in TLR-7–deficient lupus-prone mice (24). Moreover, we recently showed that interleukin-1β (IL-1β) is produced by human monocytes in response to serum containing a combination of U1 snRNP and anti–U1 snRNP antibodies (referred to as the snRNP immune complex). This process was attributed to activation of the NLRP3 inflammasome, comprising NLRP3, the adaptor protein ASC (apoptosis-associated speck-like protein containing a caspase recruitment domain), and pro-caspase 1 (25).

NLRP3 recruits ASC and procaspase 1, leading to assembly of the NLRP3 inflammasome, which cleaves pro–IL-1β to mature IL-1β (26). NLRP3 appears to act as a rate-limiting molecule in the process of inflammasome activation, because the protein level of NLRP3 is relatively low in resting macrophages, a phenomenon that has been observed in murine and immortalized human macrophages (27,28). Of note, patients with SLE have increased activation of the NLRP3 inflammasome in monocytes, which may be related to exposure to IFNα (29). Lupus-prone mice treated with an NLRP3 inflammasome inhibitor or those deficient in caspase 1 also show reduced disease severity (30,31), further supporting the pathogenic role of innate immunity and the NLRP3 inflammasome pathway in lupus.

Although genetic, clinical, and mouse modeling data implicate MIF and the NLRP3 inflammasome in the pathogenesis and clinical progression of lupus, little is known about the possible interface between the 2 pathways at the molecular level. In the present study, we demonstrate that the lupus snRNP immune complex is a specific stimulus of human MIF production, and our findings support the upstream regulatory role of MIF in activating the NLRP3 inflammasome and subsequent production of IL-1β. In addition, we define the molecular characteristics of these activated monocyte populations.

MATERIALS AND METHODS

Human monocytes and sera. Human peripheral blood was obtained from healthy adult donors after informed consent had been provided. Fresh monocytes were purified from the blood using a negative cell purification kit (Stem Cell Technologies). Anti–U1 snRNP antibody–positive sera were obtained from the L2 Diagnostic Laboratory. Anti–U1 snRNP antibodies were measured in the serum by enzyme-linked immunosorbent assay (ELISA) (DiaSorin). Healthy control serum samples were obtained from the peripheral blood of healthy donors. This work was approved by the institutional review committee of Yale University.

Stimulation of monocytes. Purified monocytes (1×10^5) were resuspended in 200 μl of RPMI 1640 medium supplemented with 10% fetal calf serum, penicillin, and streptomycin. Monocytes were treated for 30 minutes with the MIF antagonist 3-(3-hydroxybenzyl)-5-methylbenzooxazol-2-one, designated MIF098 (at a dose of 20 μ*M*, as determined on the basis of a previous dose kinetics study [32]), followed by stimulation for 3, 7, or 18 hours with or without U1 snRNP (5 μg/ml; AroTec Diagnostics Limited) in the presence or absence of anti–U1 snRNP antibody–positive serum or healthy control serum (final concentration of 5%) (25). Some cells were treated for 18 hours with U1 snRNP and anti–U1 snRNP antibody–positive serum in the presence or absence of recombinant human MIF (40 μg/ml; R&D Systems).

ELISA, quantitative polymerase chain reaction (qPCR), flow cytometry, and lactate dehydrogenase (LDH)–based cytotoxicity assay. Levels of IL-1β and MIF in culture supernatants were measured by sandwich ELISA with the use of a commercially available IL-1β kit (eBioscience) and specific antibodies for MIF (33), respectively. *IL1B*, *NLRP3*, *MIF*, *MARCH7*, and *TRIM31* genes were determined by qPCR. Primer sequences for the qPCR analyses are shown in Supplementary Table 1 (available on the *Arthritis & Rheumatology* web site at http://onlinelibrary.wiley.com/doi/10.1002/art.40672/abstract). Total RNA was extracted from cells using an RNeasy Plus Midi kit (Qiagen), and complementary DNA (cDNA) was synthesized. Each real-time PCR reaction was performed on a 10-μl reaction

mixture containing cDNA, 2× Brilliant SYBR Green Master Mix (Stratagene), and 3 μM of each primer. The reaction mixture was denatured for 10 minutes at 94°C and incubated for 40 cycles (denaturing for 15 seconds at 95°C, and annealing and extending for 1 minute at 60°C) using an Mx3005P QPCR system (Stratagene). *GAPDH* was amplified as an internal control. The relative messenger RNA levels for each gene were calculated using the 2$^{-\Delta\Delta Ct}$ algorithm.

Freshly isolated monocytes were stained with antibodies to fluorescein isothiocyanate (FITC)–conjugated CD44, phyoerythrin (PE)–conjugated CD74, FITC-conjugated CXCR2, or PE-conjugated CXCR4 (all from BioLegend). Following staining, the cells were analyzed using an LSRII flow cytometer (BD Biosciences), with results analyzed using FlowJo software. An LDH-based cytotoxicity assay (Promega) was performed on the culture supernatants of monocytes incubated for 18 hours with U1 snRNP (5 μg/ml) and anti–U1 snRNP antibody–positive serum (5% final concentration) in the presence or absence of the MIF antagonist MIF098 (20 μM), in accordance with the manufacturer's instructions (34).

Western blotting. Protein extracts that were separated by sodium dodecyl sulfate–polyacrylamide gel electrophoresis and transferred onto PVDF membranes were probed with antibodies against total NF-κB p65, phospho–NF-κB p65, caspase 1 p20, ASC (all from Cell Signaling Technology), NLRP3 (Enzo Life Sciences), IL-1β, and GAPDH (both from Santa Cruz Biotechnology). The probed membranes were washed and incubated with horseradish peroxidase–labeled secondary antibodies (Santa Cruz Biotechnology). The bands were visualized with a Pierce ECL Western blotting substrate (Thermo Scientific).

Immunofluorescence staining. Formalin-fixed paraffin-embedded sections of skin tissue from patients with acute cutaneous lupus and healthy donors were obtained from the Department of Pathology at Yale Medical School. The skin sections were dewaxed and rehydrated with serial ethanol treatments, and then heat-induced antigen retrieval was performed. After blocking, skin tissue specimens on slides were serially incubated overnight at 4°C with rabbit anti-CD14 (Invitrogen), mouse anti-CD74 (R&D Systems), and goat anti-NLRP3 antibodies (R&D Systems), followed by staining with secondary antibodies (Alexa 594–conjugated donkey anti-rabbit, Alexa 488–conjugated goat anti-mouse, and Alexa 647–conjugated rabbit anti-goat antibodies; Molecular Probes) and with Hoechst 33342 dye (Immuno-Chemistry Technologies). Some sections were incubated with mouse anti-MIF antibodies (R&D Systems) and subsequently stained with secondary antibodies (Alexa 488–conjugated goat anti-mouse). Cells staining positive in response to the antibodies were detected with a Leica DM6000 FS fluorescence microscope, with results analyzed using Leica Microsystems software (version 5.0).

Cytometry by time-of-flight mass spectrometry (CytoF) analysis. All mass cytometry reagents were purchased from Fluidigm, unless otherwise noted. Monocytes (5 × 10^5) were treated for 30 minutes with or without MIF098, followed by 5 hours of incubation with U1 snRNP (5 μg/ml) in the presence of anti–U1 snRNP antibody–positive serum (5% final concentration). Incubated cells were stained with a panel of metal-tagged antibodies (as listed in Supplementary Table 2, available on the *Arthritis & Rheumatology* web site at http://onlinelibrary.wiley.com/doi/10.1002/art.40672/abstract) and Cisplatin. For intracellular staining, cells were fixed and permeabilized with Maxpar Fix 1 buffer and Maxpar Perm-S buffer, respectively. Stained cells were washed and kept overnight in the MaxPar Fix & Perm Buffer containing intercalator-Ir. Cells were resuspended with MaxPar Water containing EQ Four Element Calibration Beads, and acquired on a Helios CytoF system (Fluidigm). All flow cytometry standard files were normalized and analyzed using the CYT, an open source analytic tool for CytoF data, and FlowJo software. PhenoGraph, *t*-distributed stochastic neighbor embedding (*t*-SNE), and the computational algorithms conditional-density resampled estimate of mutual information (DREMI) and conditional-density rescaled visualization (DREVI) were performed on gated cells (35,36).

Statistical analysis. Data were statistically compared using a paired *t*-test and two-way analysis of variance, as appropriate, using Microsoft Excel and GraphPad Prism version 7.0 software, respectively. *P* values less than 0.05 were considered significant.

RESULTS

Induction of MIF from human monocytes by the lupus snRNP immune complex, leading to promotion of IL-1β production. We explored whether MIF could be released from human monocytes in response to the snRNP immune complex, and whether this could modulate the production of IL-1β. High levels of MIF were detected in the culture supernatants of monocytes incubated with the snRNP immune complex (Figure 1A). In contrast, incubations with U1 snRNP alone, anti–U1 snRNP antibody–positive serum, or a combination of U1 snRNP and serum from healthy donors induced relatively low levels of MIF.

Given the evident coexpression of the MIF binding and signaling receptors CD74 and CD44 in human monocytes (Figure 1B), we next determined whether the released MIF, acting in an autocrine and/or paracrine manner, could affect the production of IL-1β. MIF098 is a potent and orally bioavailable small molecule that blocks MIF binding to the extracellular domain of CD74 (32,37). Monocytes activated with the snRNP immune complex in the presence of MIF098 showed decreased production of IL-1β (Figure 1C). The addition of recombinant human MIF to the snRNP immune complex resulted in a trend toward increased production of IL-1β by monocytes, although
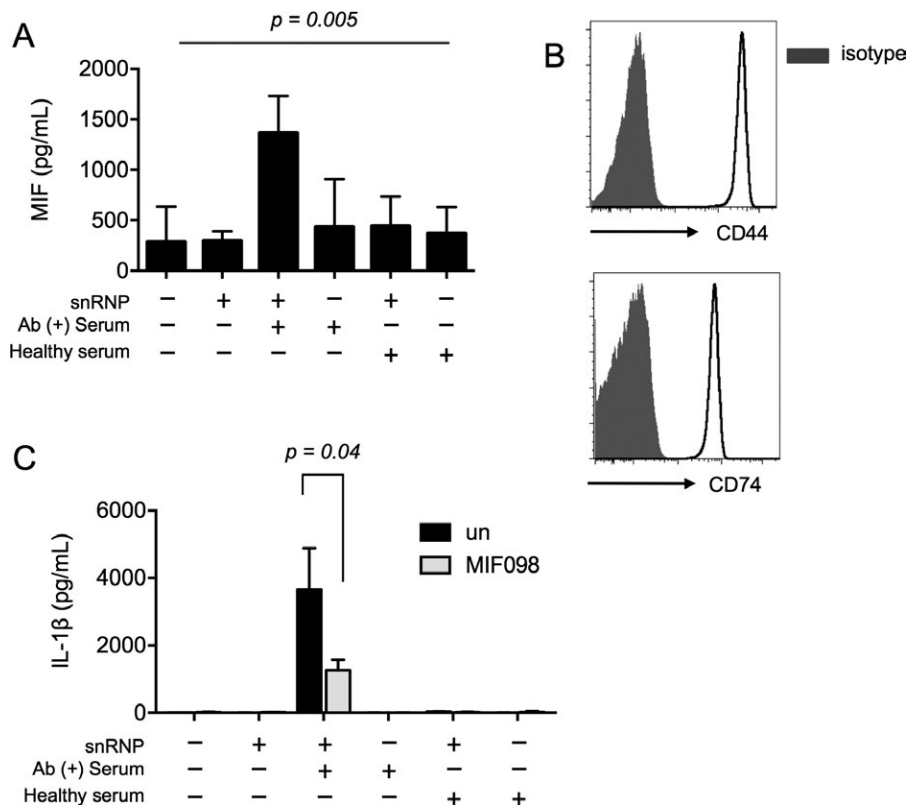
Figure 1. The lupus small nuclear RNP (snRNP) immune complex induces macrophage migration inhibitory factor (MIF) release from human monocytes, leading to the promotion of interleukin-1β (IL-1β) production. **A,** MIF levels in culture supernatants of monocytes incubated with or without U1 snRNP (5 µg/ml) in the presence or absence of healthy serum or anti–U1 snRNP antibody–positive (Ab⁺) serum (5% final concentration) were determined by enzyme-linked immunosorbent assay (ELISA) after 18 hours of culture. Results are the mean ± SEM (n = 15 donors). *P* values were obtained by analysis of variance. **B,** Expression of CD44 and CD74 was determined by flow cytometry on monocytes freshly isolated from the peripheral blood of a healthy donor. Results are representative of 2 donors. **C,** IL-1β levels were determined by ELISA at 18 hours in culture supernatants of human monocytes incubated with or without U1 snRNP (5 µg/ml) and/or healthy serum or anti–U1 snRNP antibody–positive serum (5% final concentration) in the presence or absence (untreated [un]) of the MIF antagonist MIF098 (20 µ*M*). Results are the mean ± SEM (n = 6 donors). *P* values were obtained by paired *t*-test.

the difference was not statistically significant (see Supplementary Figure 1, available on the *Arthritis & Rheumatology* web site at http://onlinelibrary.wiley.com/doi/10.1002/art.40672/abstract). Monocytes treated with recombinant human MIF alone had no production of IL-1β (data not shown). Taken together, these findings support an upstream regulatory role of autocrine/paracrine MIF release, in that it enabled high levels of IL-1β production from human monocytes stimulated with the snRNP immune complex.

MIF-dependent NLRP3 up-regulation in human monocytes in response to the snRNP immune complex. Because NLRP3 acts as a rate-limiting molecule in inflammasome activation (since studies have demonstrated low NLRP3 protein levels in resting murine and immortalized human macrophages [27,28]), we explored whether the decreased production of IL-1β from snRNP immune complex–activated monocytes in culture supernatants with the MIF antagonist MIF098 was related to altered NLRP3 expression. Although unstimulated human monocytes had barely detect-

able levels of NLRP3 protein, the snRNP immune complex induced high levels of NLRP3 protein expression, as measured by Western blotting (Figure 2A). The expression of NLRP3 protein in these cells was substantially suppressed by MIF098 (Figures 2A and B). Furthermore, expression levels of the *NLRP3* gene, which were up-regulated by the snRNP immune complex, also were decreased in the same cells by MIF098 (Figure 2C).

It is known that MIF may contribute to the activation of NF-κB, which also up-regulates NLRP3 (28). The snRNP immune complex activated NF-κB in monocytes (Figure 2D), as has been reported previously (25), and MIF098 moderately reduced the activation of NF-κB in snRNP immune complex–stimulated monocytes (Figures 2D and E).

We also determined the levels of the E3 ubiquitin ligase genes *MARCH7* (for membrane-associated RING-CH-type finger 7) and *TRIM31* (for tripartite motif–containing 31) in the same cells, since these molecules were reported to participate in the degradation of NLRP3 via ubiquitination (38,39). We could not detect *TRIM31* (data not shown), but did note a
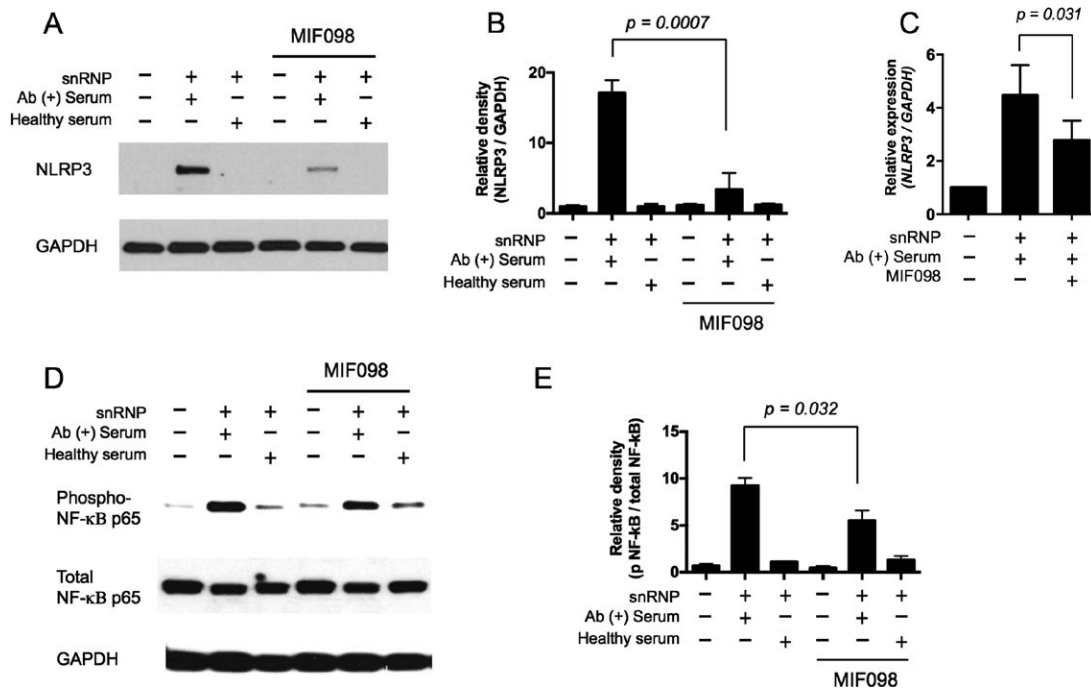
Figure 2. The lupus snRNP immune complex induces NLRP3 expression and NF-κB activation in human monocytes, while blockade of MIF suppresses these effects. **A** and **B,** Western blotting was used to determine NLRP3 expression in human monocytes incubated for 7 hours with or without U1 snRNP (5 μg/ml) and/or healthy serum or anti–U1 snRNP antibody–positive serum (5% final concentration) in the presence or absence of the MIF antagonist MIF098 (20 μ*M*). **A,** Representative data from 4 independent experiments with 4 donors are shown. **B,** Relative density of phospho-NLRP3 in cells from 4 donors is shown. **C,** Quantitative polymerase chain reaction was used to assess *NLRP3* gene expression in monocytes treated in the same manner as in **A** and **B** (n = 4 donors). **D** and **E,** Expression of phospho–NF-κB p65 and total NF-κB p65 was assessed by Western blotting in human monocytes incubated for 1 hour with or without U1 snRNP (5 μg/ml) and/or healthy serum or anti–U1 snRNP antibody–positive serum (5% final concentration) in the presence or absence of the MIF antagonist MIF098 (20 μ*M*). **D,** Representative data from 4 independent experiments with 4 donors are shown. **E,** Relative density of phospho–NF-κB p65/total NF-κB p65 in cells from 4 donors is shown. Results are the mean ± SEM. *P* values were obtained by paired *t*-test. See Figure 1 for definitions.

trend toward increased levels of *MARCH7* in monocytes stimulated with the snRNP immune complex which was not affected by the addition of MIF098 to the culture supernatants (see Supplementary Figure 2, available on the *Arthritis & Rheumatology* web site at http://onlinelibrary.wiley.com/doi/10.1002/art.40672/abstract). Overall, these findings indicate that MIF has an up-stream regulatory role in controlling the expression of NLRP3 in human monocytes in response to the snRNP immune complex.

Decrease in snRNP immune complex–mediated caspase 1 activation in human monocytes by MIF antagonism. We next determined whether antagonizing MIF suppresses the activation of the NLRP3 inflammasome component caspase 1 by reducing NLRP3 expression. In monocytes incubated with the snRNP immune complex, generation of the caspase 1 p20 subunit, an indicator of the activation of caspase 1, was decreased by MIF098 (Figures 3A and B). Moreover, the mature form of IL-1β, which is processed from the immature form, pro–IL-1β, by activated caspase 1, was decreased in monocytes incubated in the same conditions, which included incubation with the snRNP immune complex and MIF098 (results

in Supplementary Figure 3, available on the *Arthritis & Rheumatology* web site at http://onlinelibrary.wiley.com/doi/10.1002/art.40672/abstract).

We explored whether activation of caspase 1 in monocytes by the snRNP immune complex induced pyropotosis. which is a form of cell death mediated by the activation of caspase 1 (40). We noticed modest levels of cell death (~20%) in monocytes incubated with the snRNP immune complex, which was not affected by antagonizing MIF (results in Supplementary Figure 4, available on the *Arthritis & Rheumatology* web site at http://onlinelibrary.wiley.com/doi/10.1002/art.40672/abstract).

We also analyzed the adaptor molecule ASC, which is a component of the NLRP3 inflammasome, in human monocytes stimulated with or without the snRNP immune complex in the presence or absence of MIF098. Unstimulated human monocytes showed substantial expression of ASC, which was not affected by stimulation with the snRNP immune complex and/or incubation with MIF098 (Figures 3C and D). These findings suggest that MIF-mediated up-regulation of the rate-limiting molecule NLRP3 is essential for activation of the NLRP3 inflammasome in monocytes upon snRNP immune complex stimulation (as depicted in Figure 3E).
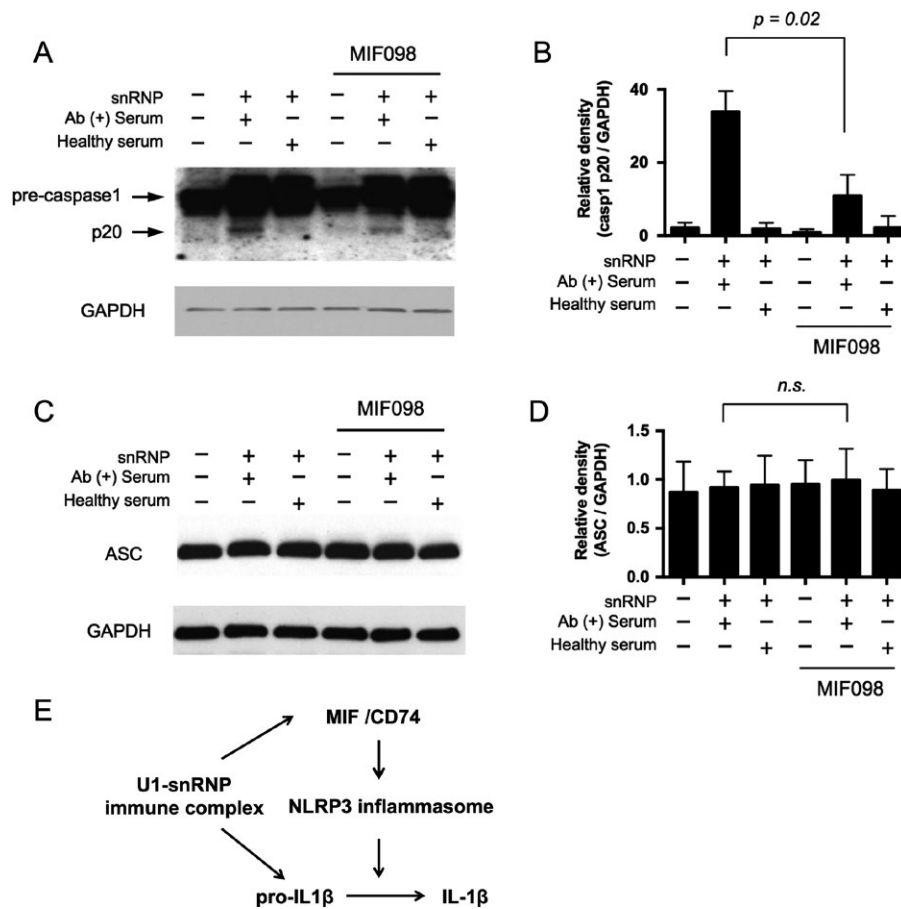
Figure 3. Activation of caspase 1 in human monocytes in response to the lupus snRNP immune complex is decreased by blocking MIF. **A** and **C,** Expression of pro–caspase 1 and caspase 1 p20 (**A**) and ASC (**C**) was assessed by Western blotting in human monocytes incubated for 18 hours with or without U1 snRNP (5 μg/ml) and/or healthy serum or anti–U1 snRNP antibody–positive serum (5% final concentration) in the presence or absence of the MIF antagonist MIF098 (20 μM). Representative data from 4 independent experiments with 4 donors are shown. **B** and **D,** Relative density of caspase 1 p20 (**B**) and ASC (**D**) was determined by Western blotting (each n = 4). Results are the mean ± SEM. P values were obtained by paired t-test. **E,** The model shows the possible role of MIF in the production of IL-1β from human monocytes upon stimulation with U1 snRNP immune complex. The U1 snRNP immune complex induces the secretion of MIF. The secreted MIF binds MIF receptor CD74 on monocytes, leading to the activation of the NLRP3 inflammasome by promoting NLRP3 gene and protein expression. The activated NLRP3 inflammasome cleaves pro–IL-1β into bioactive IL-1β. NS = not significant (see Figure 1 for other definitions).

Expression of NLRP3 and CD74 by CD14+ cells in skin lesions from patients with acute cutaneous lupus. Increased levels of MIF are detected in the kidney tissue of patients with lupus proliferative glomerulonephritis, as well as in both skin and kidney lesions from lupus-prone MRL/*lpr* mice (14,41). However, the relationship between the MIF receptor CD74 and NLRP3 expression in lupus skin lesions has not been explored. Thus, using immunofluorescence staining, we measured the expression of CD74 and NLRP3 by CD14+ cells, as well as the expression of MIF, in skin lesions from patients with acute cutaneous lupus. Our findings revealed the presence of CD14+ cells, including monocytes, that expressed CD74 and NLRP3, as well as MIF, in the lupus skin lesions (Figures 4A and B, and Supplementary Figure 5 [available on the *Arthritis & Rheumatology* web site at http://onlinelibrary.wiley.com/doi/10.1002/art.40672/abstract]).

Characterization of the unique cellular traits of snRNP immune complex–stimulated monocytes altered by antagonizing MIF, using high-dimensional, single-cell analyses. We explored whether monocytes stimulated with the snRNP immune complex develop unique cellular traits, as determined by CytoF analysis together with high-dimensional computational analysis at the single-cell level. CytoF utilizes heavy metal ions and mass spectrometry as labels and a readout, respectively, which allows the measurement of multiple molecules in a single analysis (42). High-dimensional CytoF data can be analyzed to demonstrate the multidimensional relationships of molecules expressed by single cells, using computational methods such as the nonlinear dimensionality-reduction tool t-SNE. This tool can be utilized in combination with PhenoGraph clustering analysis to robustly identify distinct cellular subsets (35,43).
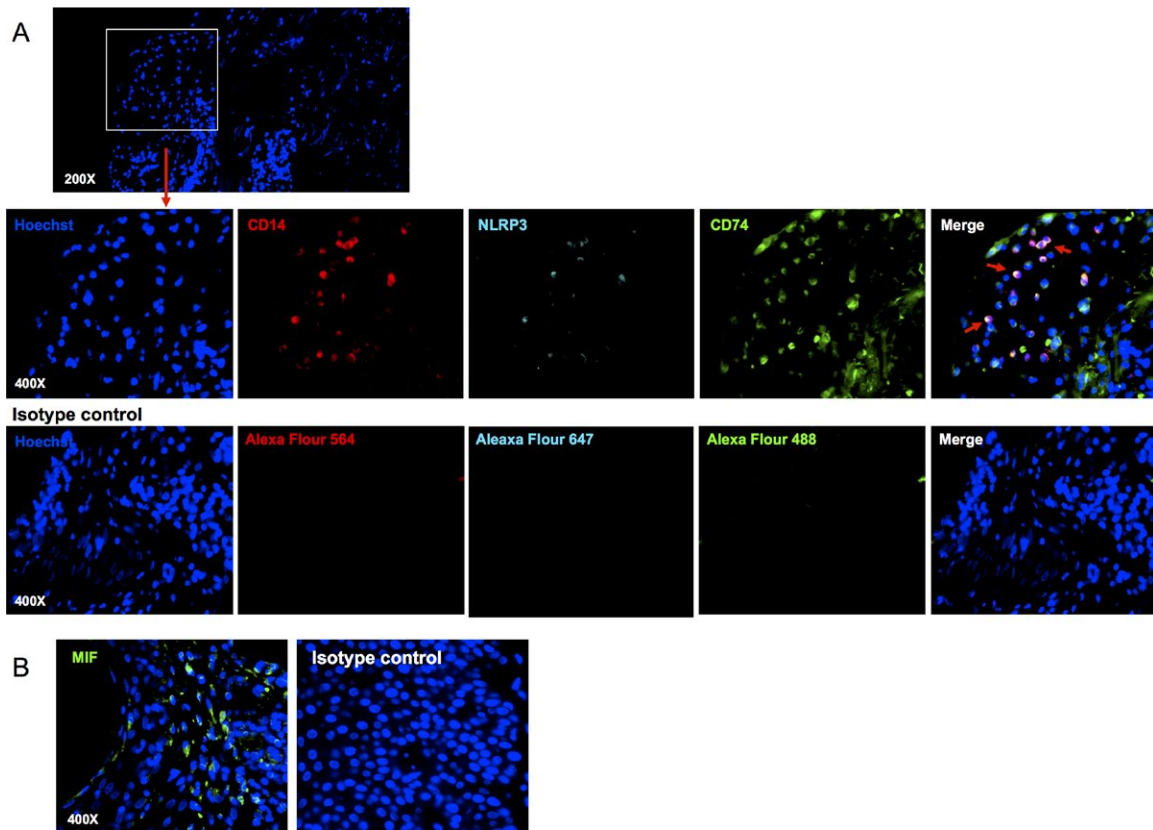
Figure 4. NLRP3 and CD74 are expressed by CD14+ cells in skin lesions from patients with acute cutaneous lupus. **A,** Immunofluorescence staining with antibodies to CD14 (red), NLRP3 (cyan), and CD74 (green) was used to assess human acute cutaneous lupus lesions. All nuclei were counterstained with Hoechst 33342. IgG was used as an isotype control. The upper panel shows nucleus staining (original magnification × 200), while lower panels are higher-magnification images (original magnification × 400) of the area denoted in the upper panel. **Arrows** indicate triple-stained cells. **B,** Human acute cutaneous lupus lesions were assessed for MIF expression by immunofluorescence staining with antibodies to MIF (green) or control IgG. All nuclei were counterstained with Hoechst 33342. Representative data from 2 independent experiments are shown. See Figure 1 for definitions.

Analyses using the *t*-SNE dimensionality-reduction tool showed a segregation of snRNP immune complex–stimulated monocytes from unstimulated monocytes, based on the expression of 17 molecules, including MIF, CD74, CD44, CXCR4, CXCR2, and IL-1β (Figures 5A and F). PhenoGraph clustering revealed subsets of cells within the monocytes that were incubated with or without snRNP immune complex and in the presence or absence of MIF098 (Figures 5B–D and G–I). Of note, compared to stimulated cells, unstimulated cells expressed high levels of CXCR2, CD32, CXCR4, and CD62L (Figures 5D and E and 5I and J), whereas stimulated cells had higher levels of intracellular cytokines, including IL-1β and the activation marker CD80.

A group of monocytes stimulated with the snRNP immune complex in the presence of MIF098 were segregated from the same stimulated cells in the absence of MIF098. Such cell clusters had decreased expression levels of IL-23, CD80, and p53 (Figures 5D and E and 5I and J). Some unstimulated monocytes expressed MIF, indicating that MIF was constitutively expressed, as has been reported previously (44). IL-1β was not detected

in unstimulated monocytes, and the expression levels of intracellular IL-1β, including both the pro and active forms of IL-1β, appeared largely similar in monocytes activated with the snRNP immune complex in the presence or absence of MIF098 (Figures 5D and E and 5I and J). This finding, which is consistent with the results of *IL1B* gene expression analysis in the same cells (see Supplementary Figure 2 [http://onlinelibrary.wiley.com/doi/10.1002/art.40672/abstract]), supports the conclusion that the suppressive effect of MIF098 on the production of IL-1β is mediated primarily by the decrease in activation of the NLRP3 inflammasome and the subsequent generation of the active form of IL-1β.

We determined how the expression levels of MIF and MIF receptors changed at the single-cell level, using the computational algorithms DREMI and DREVI (36). DREMI computes mutual information that describes how the state of "Y" alters with different states of "X" (36), while DREVI visualizes the function underlying such interactions (36). DREMI scores show the strength of the statistical dependency between 2 molecules. CD74 and CD44 increased as the expression levels of MIF
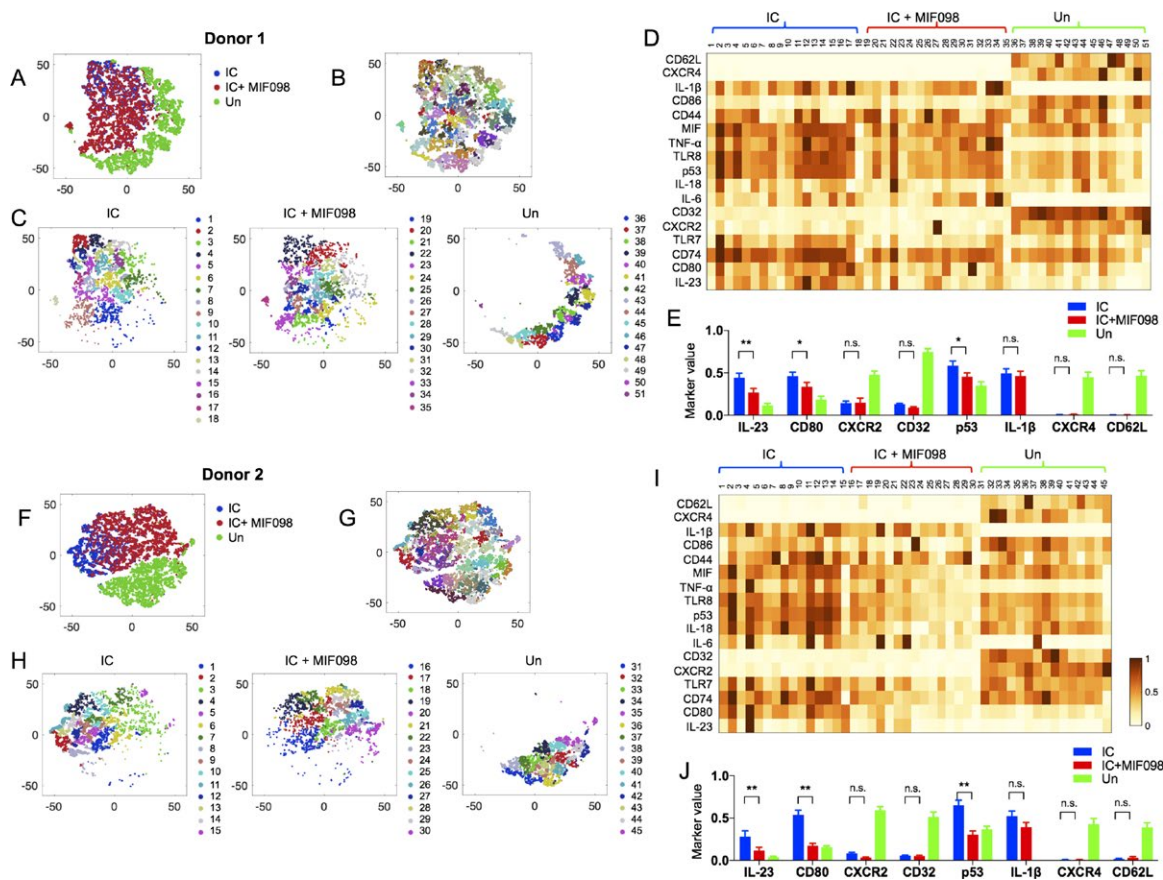
Figure 5. High-dimensional, single-cell analysis shows the unique cellular traits of monocytes stimulated with the snRNP immune complex (IC) that were altered by antagonizing MIF. Monocytes were incubated for 5 hours without IC (unstimulated [Un]) or with IC (U1 snRNP at 5 µg/ml/anti–U1 snRNP antibody–positive serum [5% final concentration]) alone or with MIF098 (20 µM), followed by cytometry by time-of-flight mass spectrometry analysis. PhenoGraph clustering was performed on monocytes based on the expression of 17 molecules (as listed in **D** and **I**). The *t*-distributed stochastic neighbor embedding plots in **A–C** (donor 1) and **F–H** (donor 2) show a landscape of cell subsets and their relationships in the incubated monocytes. **C** and **H** show subsets identified by PhenoGraph clustering on monocytes incubated in the indicated conditions. Numbers and matched color dots represent individual cell subsets. **D** and **I,** The mean levels of 17 molecules expressed by the individual cell subsets identified in **C** and **H** are shown for donor 1 (**D**) and donor 2 (**I**), respectively. Values are scaled between 0 and 1 for each molecule. **E** and **J,** Bar graphs show the intensity of each molecule expressed by individual subsets of the incubated monocytes identified in **C** and **H**, respectively. Results are the mean ± SEM. * = $P < 0.05$; ** = $P < 0.005$, by two-way analysis of variance (controlled for multiple comparisons by the Benjamin, Krieger, and Yekutieli method, false discovery rate 0.05). NS = not significant (see Figure 1 for other definitions).

increased in monocytes stimulated with or without the snRNP immune complex (Figures 6A and B), thus supporting the notion that MIF has both autocrine and paracrine effects on monocyte activation. A similar relationship with MIF expression was noted with regard to the expression levels of CXCR4, but not CXCR2 (Figures 6C and D).

DISCUSSION

The present study identifies the snRNP immune complex as an up-regulator of MIF production in human monocytes that is relevant to innate immune activation in lupus, and provides the first evidence to support the notion of an upstream role of MIF in promoting NLRP3 expression, which represents a rate-limiting step in the formation of the NLRP3 inflammasome.

Previous studies indicated that MIF-deficient mice express decreased levels of IL-1β (45), thereby supporting the upstream regulatory role of MIF in inducing this cytokine. In accordance with this finding, we noted a decrease in the production of IL-1β from snRNP immune complex–stimulated human monocytes in the presence of the MIF antagonist MIF098. Our findings of decreased NLRP3 expression and NLRP3 inflammasome activation in the same cells indicate that MIF likely functions upstream by enabling NLRP3 expression and subsequent formation of the NLRP3 inflammasome, which cleaves pro–IL-1β into bioactive IL-1β. Of interest, the expression levels of ASC, which was highly expressed at the basal level, were not different between monocytes stimulated with the snRNP immune complex and those left unstimulated. MIF antagonism did not alter the expression of ASC, further supporting the role of MIF in regulating the NLRP3
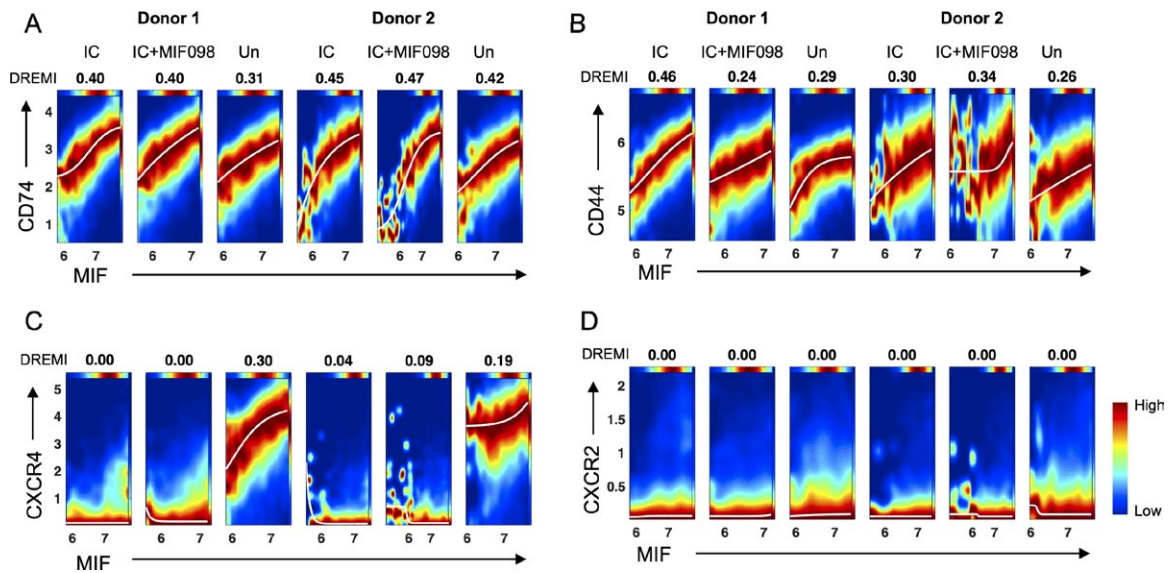
Figure 6. MIF has a robust quantitative relationship with the expression of CD74 and CD44 at the single-cell level in monocytes stimulated with the lupus snRNP immune complex. Monocytes purified from healthy donors were incubated for 5 hours with U1 snRNP (5 µg/ml) and anti–U1 snRNP antibody–positive serum (5% final concentration) (referred to as the immune complex [IC]) or incubated without IC (untreated [Un]) in the presence or absence of the MIF antagonist MIF098 (20 µ*M*). The cells were then stained with a set of antibodies, and run on a Helios cytometry by time-of-flight mass spectrometer. The computational algorithms conditional-density resampled estimate of mutual information (DREMI) and conditional-density rescaled visualization (DREVI) were performed on the incubated monocytes. DREVI plots show the quantitative relationship of MIF with CD74 (**A**), CD44 (**B**), CXCR4 (**C**), and CXCR2 (**D**). DREMI scores indicating the strength of the statistical dependency between 2 molecules are shown above the DREVI plots. Representative data from 4 independent experiments with 4 donors are shown. See Figure 1 for other definitions.

inflammasome through its specific control of the expression of NRLP3, a rate-limiting molecule in forming the NLRP3 inflammasome in monocytes.

NF-κB is known to promote the expression of the *NLRP3* gene (28). Our results demonstrated that NF-κB activation and *NLRP3* gene expression was suppressed in snRNP immune complex–stimulated monocytes when MIF expression was antagonized with MIF098. Previous studies have shown that NF-κB is activated by MIF in murine B cells in a CD74/CD44-dependent manner (46), as well as in HEK 293 cells transfected with human CD74 (47). The latter findings support the autocrine and paracrine activation effects of MIF on the up-regulation of NLRP3 in snRNP immune complex–stimulated monocytes through the CD74/CD44 receptor complex and subsequent NF-κB activation. *IL1B* gene expression was also modestly decreased in monocytes activated with the snRNP immune complex in the presence of MIF098, although such a decrease was not statistically significant. It is possible that MIF regulates NLRP3 expression through mechanisms that are redundant to those modulating NF-κB activation. We noted that there were no changes in the expression of *MARCH7* and *TRIM31*, both of which are reported to be involved in degrading NLRP3 in snRNP immune complex–stimulated monocytes (38,39). Our findings imply that the effect of MIF on IL-1β production takes place, in part, through NF-κB–mediated regulation of the *NLRP3* gene and subsequent expression of the NLRP3 protein.

We explored how the cellular phenotype of monocytes, especially those molecules related to MIF, changed upon stimulation with the snRNP immune complex at the single-cell level, using high-dimensional CytoF analysis. The dimensional reduction analysis using *t*-SNE showed a segregation of unstimulated monocytes from stimulated monocytes based on the expression levels of 17 cytokines, chemokine receptors, and activation markers. Monocytes stimulated with the snRNP immune complex in the presence of the MIF antagonist MIF098 were segregated from both stimulated monocytes and unstimulated monocytes without MIF antagonism. These findings support the interpretation that the actions of MIF on monocytes upon stimulation with the snRNP immune complex are more extensive than simple regulation of the NLRP3 pathway and IL-1β production. Furthermore, the effect of MIF on individual monocytes and molecules is not uniform, as distinct subsets of unstimulated and stimulated monocytes with diverse characteristics can be identified, including expression of the MIF cognate receptors (CD74/CD44) and noncognate receptors (CXCR2/CXCR4). Analysis using the DREMI and DREVI algorithms further supported the autocrine and paracrine activation effects of MIF through the CD74/CD44 receptor complex in stimulated and resting monocytes at the single-cell level.

The results of this study identify the snRNP immune complex as a specific trigger of MIF production and NLRP3 inflammasome activation in human monocytes, which has downstream biologic significance as indicated by our evidence of a decrease in the ac-

tivation of caspase 1 and IL-1β production following MIF receptor blockade. Genetic deficiency or pharmacologic MIF antagonism has previously been shown to reduce functional and histologic indices of disease severity in glomerulonephritis, and inflammatory cytokine and chemokine expression in lupus-prone MRL/*lpr* mice or (NZB × NZW)F1 mice (11,14). In pristane-induced murine lupus, genetic caspase 1 deficiency also reduces the severity of disease (48), while hyperactivation of the NLRP3 inflammasome produces more severe renal disease and increased mortality (49). Inhibitiion of the NLRP3/ASC/caspase 1 pathway also suppressed nephritis in MRL/*lpr* mice with lupus (30), although, paradoxically, genetic lack of NLRP3 or ASC appeared to trigger lupus-like disease in C57BL/6-*lpr/lpr* mice (50).

Of note, MIF was 1 of the 77 molecules with decreased levels in ultraviolet B–irradiated keratinocytes in the presence of the caspase 1 inhibitor YVAD, as measured by a mass spectrometry–based method (51). However, this phenomenon is likely attributable to an indirect mechanism, since MIF secretion is not required, nor is it necessary for MIF to have a caspase cleavage site for secretion, unlike IL-1β. A possible molecular link between the snRNP immune complex and MIF production could exist in the TLR-7 pathway, in that snRNP can activate this pathway (52). Previous studies in vitro have demonstrated a posttranslational modification of N-terminal proline in MIF, which is targeted by MIF098, that can be linked to dietary isothiocyanates or myeloperoxidase-derived oxidants of neutrophils (for review, see ref. 53). This modification impaired the tautomerase activity, but not immunomodulatory activity, of MIF (54). However, in the present study, we assessed only monocytes, without adding these molecules. MIF098 targets the region encompassing the N-terminal proline in MIF, which mediates its tautomerase activity and also participates in binding to the MIF receptor CD74 (32,37). Our data suggest that MIF098 primarily blocks extracellular MIF, since MIF098 does not inhibit MIF tautomerase activity intracellularly, in contrast to the previously described MIF inhibitor 4-IPP (55) (Bucala R, et al: unpublished observations).

Given the longstanding observations that anti-snRNP autoantibody responses are associated with distinct inflammatory sequelae (e.g., a mixed connective tissue disease phenotype), our findings suggest a rationale for specific targeting of the NLRP3 inflammasome or MIF signaling, potentially focusing on SLE patients classified as high genotypic *MIF* expressers. In addition, high-dimensional CytoF analysis could be applied to identify patient subsets with relevant monocyte populations (e.g., high MIF or MIF receptor expression) in whom responsiveness to MIF- or inflammasome-directed therapies may be warranted.

ACKNOWLEDGMENTS

REFERENCES

1. Lang T, Foote A, Lee JP, Morand EF, Harris J. MIF: implications in the pathoetiology of systemic lupus erythematosus. Front Immunol 2015;6:577.

2. Bucala R. MIF, MIF alleles, and prospects for therapeutic intervention in autoimmunity. J Clin Immunol 2013;33 Suppl 1:S72–8.

3. Calandra T, Roger T. Macrophage migration inhibitory factor: a regulator of innate immunity. Nat Rev Immunol 2003;3:791–800.

4. Calandra T, Bernhagen J, Metz CN, Spiegel LA, Bacher M, Donnelly T, et al. MIF as a glucocorticoid-induced modulator of cytokine production. Nature 1995;377:68–71.

5. Fingerle-Rowson G, Petrenko O, Metz CN, Forsthuber TG, Mitchell R, Huss R, et al. The p53-dependent effects of macrophage migration inhibitory factor revealed by gene targeting. Proc Natl Acad Sci U S A 2003;100:9354–9.

6. Leng L, Metz CN, Fang Y, Xu J, Donnelly S, Baugh J, et al. MIF signal transduction initiated by binding to CD74. J Exp Med 2003;197:1467–76.

7. Shi X, Leng L, Wang T, Wang W, Du X, Li J, et al. CD44 is the signaling component of the macrophage migration inhibitory factor-CD74 receptor complex. Immunity 2006;25:595–606.

8. Bernhagen J, Krohn R, Lue H, Gregory JL, Zernecke A, Koenen RR, et al. MIF is a noncognate ligand of CXC chemokine receptors in inflammatory and atherogenic cell recruitment. Nat Med 2007;13:587–96.

9. Ayoub S, Hickey MJ, Morand EF. Mechanisms of disease: macrophage migration inhibitory factor in SLE, RA and atherosclerosis. Nat Clin Pract Rheumatol 2008;4:98–105.

10. McDevitt MA, Xie J, Ganapathy-Kanniappan S, Griffith J, Liu A, McDonald C, et al. A critical role for the host mediator macrophage migration inhibitory factor in the pathogenesis of malarial anemia. J Exp Med 2006;203:1185–96.

11. Leng L, Chen L, Fan J, Greven D, Arjona A, Du X, et al. A small-molecule macrophage migration inhibitory factor antagonist protects against glomerulonephritis in lupus-prone NZB/NZW F1 and MRL/lpr mice. J Immunol 2010;186:527–38.

12. Sreih A, Ezzeddine R, Leng L, LaChance A, Yu G, Mizue Y, et al. Dual effect of the macrophage migration inhibitory factor gene on the development and severity of human systemic lupus erythematosus. Arthritis Rheum 2011;63:3942–51.

13. Calandra T, Echtenacher B, Roy DL, Pugin J, Metz CN, Hultner L, et al. Protection from septic shock by neutralization of macrophage migration inhibitory factor. Nat Med 2000;6:164–70.

14. Hoi AY, Hickey MJ, Hall P, Yamana J, O'Sullivan KM, Santos LL, et al. Macrophage migration inhibitory factor deficiency attenuates macrophage recruitment, glomerulonephritis, and lethality in MRL/lpr mice. J Immunol 2006;177:5687–96.

15. De la Cruz-Mosso U, Bucala R, Palafox-Sanchez CA, Parra-Rojas I, Padilla-Gutierrez JR, Pereira-Suarez AL, et al. Macrophage migration inhibitory factor: association of –794 CATT5–8 and –173 G>C polymorphisms with TNF-α in systemic lupus erythematosus. Hum Immunol 2014;75:433–9.

16. Foote A, Briganti EM, Kipen Y, Santos L, Leech M, Morand EF. Macrophage migration inhibitory factor in systemic lupus erythematosus. J Rheumatol 2004;31:268–73.

17. Connelly KL, Kandane-Rathnayake R, Hoi A, Nikpour M, Morand EF. Association of MIF, but not type I interferon-induced chemokines, with increased disease activity in Asian patients with systemic lupus erythematosus. Sci Rep 2016;6:29909.

18. Wallace DJ, Weisman MH, Wegener WA, Horne H, Goldenberg DM. THU0288 IMMU-115 (humanized anti-CD74 antibody) for subcutaneous (SC) administration: a phase Ib study in patients with systemic lupus erythematosus (SLE). Ann Rheum Dis 2016;75 Suppl 2:291.

19. Shin MS, Lee N, Kang I. Effector T-cell subsets in systemic lupus erythematosus: update focusing on Th17 cells. Curr Opin Rheumatol 2011;23:444–8.

20. Tsokos GC. Systemic lupus erythematosus. N Engl J Med 2011; 365:2110–21.

21. Marshak-Rothstein A. Toll-like receptors in systemic autoimmune disease. Nat Rev Immunol 2006;6:823–35.

22. Theofilopoulos AN, Baccala R, Beutler B, Kono DH. Type I interferons (α/β) in immunity and autoimmunity. Annu Rev Immunol 2005;23:307–36.

23. Guiducci C, Gong M, Xu Z, Gill M, Chaussabel D, Meeker T, et al. TLR recognition of self nucleic acids hampers glucocorticoid activity in lupus. Nature 2010;465:937–41.

24. Christensen SR, Shupe J, Nickerson K, Kashgarian M, Flavell RA, Shlomchik MJ. Toll-like receptor 7 and TLR9 dictate autoantibody specificity and have opposing inflammatory and regulatory roles in a murine model of lupus. Immunity 2006;25:417–28.

25. Shin MS, Kang Y, Lee N, Kim SH, Kang KS, Lazova R, et al. U1-small nuclear ribonucleoprotein activates the NLRP3 inflammasome in human monocytes. J Immunol 2012;188:4769–75.

26. Tschopp J, Schroder K. NLRP3 inflammasome activation: the convergence of multiple signalling pathways on ROS production? Nat Rev Immunol 2010;10:210–5.

27. Haneklaus M, O'Neill LA, Coll RC. Modulatory mechanisms controlling the NLRP3 inflammasome in inflammation: recent developments. Curr Opin Immunol 2013;25:40–5.

28. Bauernfeind FG, Horvath G, Stutz A, Alnemri ES, MacDonald K, Speert D, et al. Cutting edge: NF-κB activating pattern recognition and cytokine receptors license NLRP3 inflammasome activation by regulating NLRP3 expression. J Immunol 2009;183: 787–91.

29. Liu J, Berthier CC, Kahlenberg JM. Enhanced inflammasome activity in systemic lupus erythematosus is mediated via type I interferon-induced up-regulation of interferon regulatory factor 1. Arthritis Rheumatol 2017;69:1840–9.

30. Zhao J, Wang H, Dai C, Wang H, Zhang H, Huang Y, et al. P2X7 blockade attenuates murine lupus nephritis by inhibiting activation of the NLRP3/ASC/caspase 1 pathway. Arthritis Rheum 2013;65:3176–85.

31. Kahlenberg JM, Carmona-Rivera C, Smith CK, Kaplan MJ. Neutrophil extracellular trap-associated protein activation of the NLRP3 inflammasome is enhanced in lupus macrophages. J Immunol 2013;190:1217–26.

32. Yoo SA, Leng L, Kim BJ, Du X, Tilstam PV, Kim KH, et al. MIF allele-dependent regulation of the MIF coreceptor CD44 and role in rheumatoid arthritis. Proc Natl Acad Sci U S A 2016;113:E7917–E26.

33. Grigorenko EL, Han SS, Yrigollen CM, Leng L, Mizue Y, Anderson GM, et al. Macrophage migration inhibitory factor and autism spectrum disorders. Pediatrics 2008;122:e438–45.

34. Park E, Na HS, Song YR, Shin SY, Kim YM, Chung J. Activation of NLRP3 and AIM2 inflammasomes by Porphyromonas gingivalis infection. Infect Immun 2014;82:112–23.

35. Levine JH, Simonds EF, Bendall SC, Davis KL, Amir ED, Tadmor MD, et al. Data-driven phenotypic dissection of aml reveals progenitor-like cells that correlate with prognosis. Cell 2015;162:184–97.

36. Krishnaswamy S, Spitzer MH, Mingueneau M, Bendall SC, Litvin O, Stone E, et al. Systems biology: conditional density-based analysis of T cell signaling in single-cell data. Science 2014;346:1250689.

37. Sauler M, Zhang Y, Min JN, Leng L, Shan P, Roberts S, et al. Endothelial CD74 mediates macrophage migration inhibitory factor protection in hyperoxic lung injury. FASEB J 2015;29:1940–9.

38. Yan Y, Jiang W, Liu L, Wang X, Ding C, Tian Z, et al. Dopamine controls systemic inflammation through inhibition of NLRP3 inflammasome. Cell 2015;160:62–73.

39. Song H, Liu B, Huai W, Yu Z, Wang W, Zhao J, et al. The E3 ubiquitin ligase TRIM31 attenuates NLRP3 inflammasome activation by promoting proteasomal degradation of NLRP3. Nat Commun 2016;7:13727.

40. Fink SL, Cookson BT. Apoptosis, pyroptosis, and necrosis: mechanistic description of dead and dying eukaryotic cells. Infect Immun 2005;73:1907–16.

41. Lan HY, Yang N, Nikolic-Paterson DJ, Yu XQ, Mu W, Isbel NM, et al. Expression of macrophage migration inhibitory factor in human glomerulonephritis. Kidney Int 2000;57:499–509.

42. Bendall SC, Simonds EF, Qiu P, Amir ED, Krutzik PO, Finck R, et al. Single-cell mass cytometry of differential immune and drug responses across a human hematopoietic continuum. Science 2011;332:687–96.

43. Amir ED, Davis KL, Tadmor MD, Simonds EF, Levine JH, Bendall SC, et al. ViSNE enables visualization of high dimensional single-cell data and reveals phenotypic heterogeneity of leukemia. Nat Biotechnol 2013;31:545–52.

44. Lu Y, Xue Q, Eisele MR, Sulistijo ES, Brower K, Han L, et al. Highly multiplexed profiling of single-cell effector functions reveals deep functional heterogeneity in response to pathogenic ligands. Proc Natl Acad Sci U S A 2015;112:E607–15.

45. Stosic-Grujicic S, Stojanovic I, Maksimovic-Ivanic D, Momcilovic M, Popadic D, Harhaji L, et al. Macrophage migration inhibitory factor (MIF) is necessary for progression of autoimmune diabetes mellitus. J Cell Physiol 2008;215:665–75.

46. Gore Y, Starlets D, Maharshak N, Becker-Herman S, Kaneyuki U, Leng L, et al. Macrophage migration inhibitory factor induces B cell survival by activation of a CD74-CD44 receptor complex. J Biol Chem 2008;283:2784–92.

47. Binsky I, Haran M, Starlets D, Gore Y, Lantner F, Harpaz N, et al. IL-8 secreted in a macrophage migration-inhibitory factor- and CD74-dependent manner regulates B cell chronic lymphocytic leukemia survival. Proc Natl Acad Sci U S A 2007;104:13408–13.

48. Kahlenberg JM, Yalavarthi S, Zhao W, Hodgin JB, Reed TJ, Tsuji NM, et al. An essential role of caspase 1 in the induction of murine lupus and its associated vascular damage. Arthritis Rheumatol 2014;66:152–62.

49. Lu A, Li H, Niu J, Wu S, Xue G, Yao X, et al. Hyperactivation of the NLRP3 inflammasome in myeloid cells leads to severe organ damage in experimental lupus. J Immunol 2017;198:1119–29.

50. Lech M, Lorenz G, Kulkarni OP, Grosser MO, Stigrot N, Darisipudi MN, et al. NLRP3 and ASC suppress lupus-like autoimmunity by driving the immunosuppressive effects of TGF-β receptor signalling. Ann Rheum Dis 2014;74:2224–35.

51. Keller M, Ruegg A, Werner S, Beer HD. Active caspase-1 is a regulator of unconventional protein secretion. Cell 2008;132: 818–31.

52. Savarese E, Chae OW, Trowitzsch S, Weber G, Kastner B, Akira S, et al. U1 small nuclear ribonucleoprotein immune complexes induce type I interferon in plasmacytoid dendritic cells through TLR7. Blood 2006;107:3229–34.

53. Schindler L, Dickerhof N, Hampton MB, Bernhagen J. Post-translational regulation of macrophage migration inhibitory factor: basis for functional fine-tuning. Redox Biol 2018;15:135–42.

54. Dickerhof N, Schindler L, Bernhagen J, Kettle AJ, Hampton MB. Macrophage migration inhibitory factor (MIF) is rendered enzymatically inactive by myeloperoxidase-derived oxidants but retains its immunomodulatory function. Free Radic Biol Med 2015;89:498–511.

55. Winner M, Meier J, Zierow S, Rendon BE, Crichlow GV, Riggs R, et al. A novel, macrophage migration inhibitory factor suicide substrate inhibits motility and growth of lung cancer cells. Cancer Res 2008;68:7253–7.

Clinical Images: Arthritis mutilans in systemic sclerosis
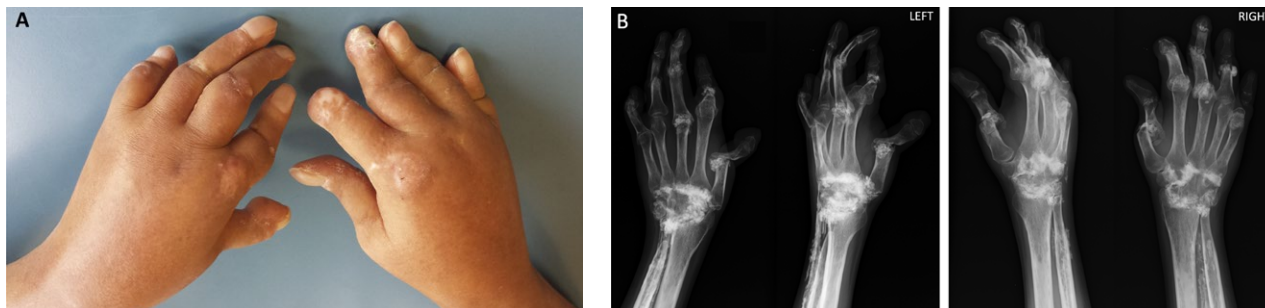
The patient, a 40-year-old man, was diagnosed as having diffuse cutaneous systemic sclerosis (SSc) with anti–topoisomerase I antibody. Raynaud's phenomenon, diffuse skin sclerosis, and severe interstitial lung disease (ILD) were present at onset. He subsequently developed inflammatory polyarthritis of the hands and wrists. His brother had psoriasis. Physical examination showed pitting scars of the fingertips, subcutaneous calcinosis, skin sclerosis with hyper- and hypopigmentation, flexion and extension contractures, and shortened fingers (**A**). Radiography of the hands and wrists revealed bilateral destructive arthropathy, acro-osteolysis, and calcified deposits consistent with joint and skin calcinosis (**B**). Joint destruction, most typical of psoriatic arthritis (PsA) mutilans (1,2), was evident, with diffuse bone loss of the left second and fifth and right fifth proximal interphalangeal (PIP) joints, multiple subluxations of the left first and second and right first through third metacarpophalangeal (MCP) joints, whittling of the left first MCP joint, and pencil-in-cup–like deformity of the left second PIP joint and left fifth MCP joint (**B**). A previous EUSTAR cross-sectional analysis revealed frequent articular involvement in SSc (3). However, finger shortening caused by destructive inflammatory polyarthritis is not common and should be distinguished from acro-osteolysis secondary to ischemia in order to guide treatment. Since SSc diagnosis, our patient has received nifedipine, intravenous prostanoids, and bosentan to treat digital ischemia and prevent ulceration, and several immunosuppressive agents (low-dose glucocorticoids, cyclophosphamide, azathioprine, and mycophenolate mofetil) to target both skin involvement and ILD. Methotrexate failed to control rapidly progressive articular damage. The patient is currently undergoing rituximab therapy to target SSc-related skin involvement and severe ILD and to control joint symptoms. An earlier diagnosis of PsA mutilans may have changed treatment escalation in favor of cytokine inhibition. However, since therapies that reliably target both SSc and PsA are not currently available, treatment choice should be driven by the severity and presence of life-threatening manifestations.

1. McGonagle D, Conaghan PG, Emery P. Psoriatic arthritis: a unified concept twenty years on. Arthritis Rheum 1999;42:1080–6.
2. Haddad A, Johnson SR, Somaily M, Fazelzad R, Kron AT, Chau C, et al. Psoriatic arthritis mutilans: clinical and radiographic criteria—a systematic review. J Rheumatol 2015;42:1432–8.
3. Avouac J, Walker U, Tyndall A, Kahan A, Matucci-Cerinic M, Allanore Y, et al. Characteristics of joint involvement and relationships with systemic inflammation in systemic sclerosis: results from the EULAR Scleroderma Trial and Research Group (EUSTAR) database. J Rheumatol 2010;37:1488–501.

Giuseppina Abignano, MD, PhD
Rheumatology Institute of Lucania (IReL), San Carlo Hospital
Potenza, Italy
LIRMM, University of Leeds
Leeds, UK
Gianna A. Mennillo, MD
IReL, San Carlo Hospital
Giovanni Lettieri, MD
Radiology Department
San Giovanni di Dio e Ruggi d'Aragona University Hospital
Salerno, Italy
Angela Padula, MD
IReL, San Carlo Hospital
Dennis McGonagle, FRCPI, PhD
LIRMM, University of Leeds and NIHR LBRC
Leeds Teaching Hospitals NHS Trust
Salvatore D'Angelo, MD, PhD
IReL, San Carlo Hospital

AMERICAN COLLEGE
OF RHEUMATOLOGY
EDUCATION · TREATMENT · RESEARCH

Tissue-Resident Memory CD8+ T Cells Acting as Mediators of Salivary Gland Damage in a Murine Model of Sjögren's Syndrome

Cai-Yue Gao,[1] Yuan Yao,[1] Liang Li,[1] Shu-Han Yang,[1] Hui Chu,[2] Koichi Tsuneyama,[3] Xiao-Mei Li,[2] M. Eric Gershwin,[4] and Zhe-Xiong Lian[1]

Objective. Although a role for CD4+ T cells in the pathogenesis of Sjögren's syndrome (SS) has been documented, the pathogenic significance of CD8+ T cells is unclear. The aim of this study was to investigate the role of CD8+ T cells in the development of SS.

Methods. Flow cytometry and immunofluorescence analyses were utilized to detect T cell infiltration within the labial salivary glands of patients with primary SS. In parallel, p40$^{-/-}$CD25$^{-/-}$ mice were used as a murine model of SS. In addition, mice with genetic knockout of CD4, CD8a, or interferon-γ (IFNγ) were crossed with p40$^{-/-}$CD25$^{-/-}$ mice to study the pathogenic significance of specific lineage subpopulations, including functional salivary gland tests as well as histopathologic and serologic data. A CD8+ T cell–specific depletion antibody was used in this murine SS model to evaluate its potential as a therapeutic strategy.

Results. CD8+ T cells with a tissue-resident memory phenotype outnumbered CD4+ T cells in the labial salivary glands of patients with SS, and were primarily colocalized with salivary duct epithelial cells and acinar cells. Furthermore, infiltrating CD8+ T cells with a CD69+CD103+/− tissue-resident phenotype and with a significant elevation of IFNγ production were dominant in the submandibular glands of mice in this murine SS model. CD8a knockout abrogated the development of SS in these mice. Knockout of IFNγ decreased CD8+ T cell infiltration and gland destruction. More importantly, depletion of CD8+ T cells fully protected mice against the pathologic manifestations of SS, even after the onset of disease.

Conclusion. These data reveal the pathogenic significance of CD8+ T cells in the development and progression of SS in the salivary glands. Treatment directed against CD8+ T cells may be a rational therapy for the management of SS in human subjects.

INTRODUCTION

Sjögren's syndrome (SS) is a chronic systemic autoimmune disease that is characterized by mononuclear cell infiltration in the exocrine glands. Clinically, SS manifests as sicca symptoms on mucosal surfaces, including oral and ocular dryness due to the destruction of secretory glands by lymphocytic foci with T cells and B cells (1–3). Serologically, the most notable autoantibodies are those recognizing antinuclear antigens (ANAs), RNP complexes (Ro/SSA and La/SSB), and type 3 muscarinic acetylcholine receptors (M3Rs) (4–7).

Genome-wide association scans and meta-analyses of SS have revealed a strong association of the disease with several HLA molecules (8,9), implicating T cells as a major driver of SS. Although previous studies have found that CD4+ T cells constitute the majority of infiltrating cells, recent findings have suggested that CD8+ T cells are just as abundant as CD4+ T cells and may play an equally critical role in SS (10–12). However, the

CD8+ T cell subpopulations implicated in the pathologic development and progression of SS have not yet been identified.

One of the subpopulations that may play an important role in chronic autoimmune diseases are memory T cells, which coordinate a specific, timely, and highly effective immune response against reencountered pathogens. An important subset of memory T cells was recently discovered, referred to as tissue-resident memory T (Trm) cells. Trm cells are phenotypically defined as CD69+CD103+/– T cells and mainly reside in epithelial barrier tissues, such as the respiratory tract (13), gastrointestinal tract (14), reproductive tract (15), skin (16), and secretory glands (17). Salivary glands can function as a depot for CD8+ Trm cells and protect against viral infections through degranulation and production of interferon-γ (IFNγ) (17). CD103 expressed on the surface of CD8+ Trm cells also acts as a molecular tether that attaches to E-cadherin–expressing epithelial cells in murine salivary glands (18–20). It is thus logical that Trm cells may be involved in the pathologic processes of SS.

SS is similar to primary biliary cholangitis in that activated infiltrating T cells can cause severe damage in epithelial structures; therefore, both diseases are considered to be an autoimmune epithelitis with overlapping features (21,22). In the present study, we observed that p40$^{-/-}$CD25$^{-/-}$ mice exhibiting severe autoimmune cholangitis, including hepatic fibrosis (23), also recapitulated key features of human SS. A striking discovery was that CD8+ T cells constituted the majority of infiltrating T cells in the salivary glands both from p40$^{-/-}$CD25$^{-/-}$ mice and from human patients with SS. Furthermore, these CD8+ T cells exhibited a Trm phenotype with high capacity for IFNγ production. Knockout of CD8a by crossing p40$^{-/-}$CD25$^{-/-}$ mice with CD8a$^{-/-}$ mice or by targeted antibody depletion of CD8+ T cells in vivo alleviated disease manifestations in the salivary glands and restored saliva secretion in this murine model of SS. Our data thus demonstrate that infiltrating CD8+ Trm cells in the salivary glands play a dominant role in the pathogenesis of SS and suggest a novel therapeutic strategy for the management of SS in human subjects.

MATERIALS AND METHODS

Mice. CD25$^{-/-}$ (B6.129S4-*Il2ra*^{tm1Dw}/J), p40$^{-/-}$ (B6.129S1-*Il12b*^{tm1Jm}/J), CD4$^{-/-}$ (B6.129S2-*Cd4*^{tm1Mak}/J), CD8a$^{-/-}$ (B6.129S2-*Cd8a*^{tm1Mak}/J), and IFNγ$^{-/-}$ (B6.129S7-*Ifng*^{tm1Ts}/J) mice on a C57BL/6J background were purchased from The Jackson Laboratory. The mice were maintained under specific pathogen–free conditions in individually ventilated cages at the Laboratory Animal Center in the School of Life Sciences at the University of Science and Technology of China (USTC). Polymerase chain reaction (PCR) was used to identify the interleukin-12p40 (IL-12p40) wild-type gene in mice, and flow cytometry was used to identify the surface markers CD25, CD4, and CD8a. Mice of both sexes and at different serial ages were used; there were no between-sex differences, unless noted otherwise. All animal experiments were performed in conformity with the requirements of the USTC guidelines for Care and Use of Laboratory Animals.

Patients. Labial salivary gland and peripheral blood samples from patients with SS were obtained from Anhui Provincial Hospital (Hefei, China). Our cohort included 8 patients (7 female and 1 male) who were diagnosed as having primary SS. All patients were naive to treatment, and none of the patients had features of another connective tissue disease. The study was approved by the ethics committee of Anhui Medical University (approval no. 20131172), and informed consent was obtained from all patients.

Histologic and immunofluorescence analyses. Mouse submandibular glands were fixed in 4% paraformaldehyde and embedded in paraffin. Tissues were then cut into 4-μm slices, deparaffinized, and stained with hematoxylin and eosin for microscopic examination. Lymphocytic foci, defined as areas of the submandibular gland tissue containing more than 50 lymphocytes per 4 mm^2, were identified. Scores for the presence of acinar atrophy and fibrosis were classified as 0 or 1, with a score of 0 indicating no acinar atrophy or fibrosis, and a score of 1 indicating mild acinar atrophy or fibrosis. Scores for salivary duct and vascular damage were also assessed, classified as follows: 0 = no salivary duct or vascular damage, 0.5 = presence of only salivary duct damage, and 1 = presence of both salivary duct damage and vascular damage. For analysis of the effects of antibody treatment, the treated samples were assessed for the presence of damage or fibrosis with scores of 0–4, representing no damage or fibrosis (score 0) to minimal, mild, moderate, or severe damage or fibrosis (scores of 1, 2, 3, or 4, respectively). All samples were scored by a single pathologist (KT) in a blinded manner.

For immunofluorescence analysis, mouse submandibular glands or human labial salivary glands were fixed with 4% paraformaldehyde for 4 hours and then dehydrated in 30% sucrose solution overnight. Dehydrated tissue samples were embedded in Tissue-Tek OCT compound, frozen in liquid nitrogen, and cut into 6-μm slices. After blocking with 10% goat serum for 2 hours at room temperature, the slices were incubated with a fluorescent antibody overnight under humidified conditions at 4°C. DAPI was used to stain the nucleus. Sections were visualized using an LSM 710 confocal microscope (Carl Zeiss). Staining of the mouse submandibular glands was performed using phycoerythrin (PE)–conjugated B220 (RA3-6B2; BioLegend), allophycocyanin (APC)–conjugated CD3 (17A2; BioLegend), and BV421-conjugated CD4 (RM4-5; BioLegend), and human labial salivary glands were stained with Alexa Fluor 594–conjugated CD8a antibodies (C8/144B; BioLegend), Alexa Fluor 647–conjugated CD3 antibodies (UCHT1; BioLegend), and DAPI (Boster).

Indirect immunofluorescence analysis. An IgG ANA kit (IIFT; Hautmont) was purchased to detect ANAs in the serum

of mice. Briefly, sera from p40$^{-/-}$CD25$^{+/-}$ and p40$^{-/-}$CD25$^{-/-}$ mice were diluted in a 1:100 ratio, added onto slides coated with HEp-2 cells, and then incubated for 30 minutes at room temperature. After washing with 1× phosphate buffered saline (PBS)–Tween (containing 0.05% Tris buffered saline), Alexa Fluor 647–conjugated goat anti-mouse IgG (1:500; BioLegend) was added and incubated for 30 minutes at room temperature. Slides were washed and visualized using an LSM 710 confocal microscope.

Cell isolation. In mouse submandibular glands, draining lymph nodes were dissociated and homogenized with PBS containing 0.2% bovine serum albumin. Cell suspensions were then passed through a 74-μm nylon mesh. After removal of the lymph nodes, the submandibular glands were harvested, cut into small pieces, and digested using type II collagenase (1 mg/ml). Human labial salivary glands were prepared and digested in the same manner and under the same conditions. Cell suspensions were passed through a nylon mesh and isolated by centrifugation with 40% Percoll. In addition, peripheral blood samples were obtained from patients with SS and homogenized with an equal volume of 1× PBS. Peripheral blood mononuclear cells (PBMCs) were isolated by centrifugation with Ficoll.

The number of leukocytes in the mouse submandibular glands was calculated by flow cytometry. For assessment of cell viability, mouse draining lymph node cells and human PBMCs were stained with trypan blue.

Flow cytometry. Cell suspensions were incubated with purified anti-CD16/32 antibody (BioLegend) for 15 minutes at 4°C, and then stained for 20 minutes at 4°C with a cocktail of fluorochrome-conjugated antibodies against cell surface markers. The procedure for measurement of intracellular cytokines was performed as previously described (23), using the following monoclonal antibodies (mAb) (all from BioLegend): for mouse cells, Pacific Blue (PB)–conjugated CD3 (17A2), APC-conjugated NK1.1 (PK136), fluorescein isothiocyanate (FITC)–conjugated CD19 (6D5), PE–Cy7–conjugated CD138 (281-2), FITC-conjugated Fas (15A7), PerCP–Cy5.5–conjugated GL7 (GL7), PerCP–Cy5.5–conjugated CD4 (GK1.5), APC–Cy7–conjugated CD8a (53-6.7), PerCP–Cy5.5–conjugated CD8b (YTS156.7.7), PE–Cy7–conjugated CD11b (M1/70), PE-conjugated F4/80 (BM8), anti-CD16/32 (93), FITC-conjugated CD69 (H1.2F3), PE–Cy7–conjugated CD103 (2E7), PE-conjugated CXCR3 (CXCR3-173), PE-conjugated CXCR6 (SA051D1), APC-conjugated CD49a (HMa1), and PE-conjugated IFNγ (XMG1.2); for human cells, APC–Cy7–conjugated CD45 (HI30), PE-conjugated CD56 (5.1H11), PB-conjugated CD3 (SK7), PerCP–Cy5.5–conjugated CD8 (HIT8α), FITC-conjugated CD69 (FN50),
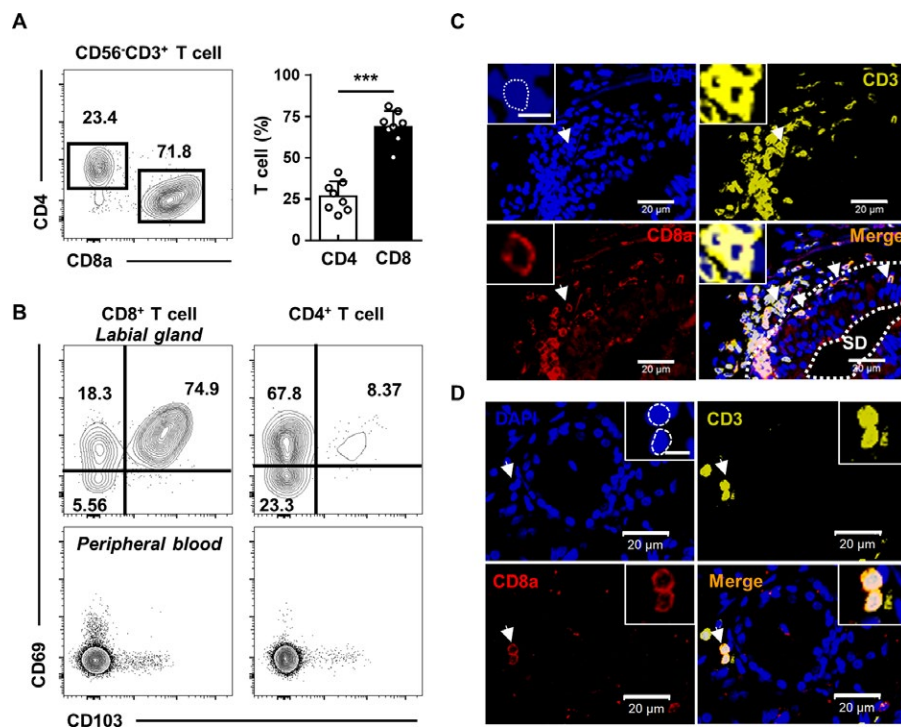
Figure 1. CD8+ T cells are the dominant infiltrating T cells in the labial salivary glands of patients with Sjögren's syndrome (SS). **A,** Percentages of CD4+ and CD8+ T cells in labial salivary glands of patients with SS (n = 8). Symbols represent individual patients; bars show the mean ± SD. **B,** Expression of CD69 and CD103 on CD4+ and CD8+ T cells in labial salivary glands and peripheral blood of patients with SS. **C** and **D,** Results of immunofluorescence microscopy demonstrating the presence of CD8+ T cells (**arrows**) near the duct (**C**) and acinar cells (**D**) in labial salivary glands from a representative patient with SS. DAPI was used to stain the nuclei. Bars = 20 μm; bars in **insets** = 2 μm. In **A** and **C**, the experiment was performed 3 times. SD = salivary duct. *** = P < 0.001.

and APC-conjugated CD103 (Ber-ACT8). In addition, mAb against mouse V500-conjugated CD45.2 (104), mouse V500-conjugated B220 (RA3-6B2), and human V500-conjugated CD4 (RPA-T4) were purchased from BD Biosciences.

Saliva collection. Mice were anesthetized with pentobarbital sodium, and then injected intraperitoneally with pilocarpine (Sigma-Aldrich) at 5 mg/kg body weight to induce saliva secretion. Saliva was collected from the oral cavity for 15 minutes at room temperature into a 20-μl pipette tip, and the volume of saliva in the tip was calculated.

Quantitative real-time PCR. Total RNA was extracted from the mouse submandibular glands using TRIzol reagent (Invitrogen). A PrimeScript reverse transcription reagent kit with gDNA Eraser (Takara) was used for reverse transcription.

SYBR Premix Ex Taq II (Takara) was used to perform quantitative real-time PCR. Gene expression values were normalized to the values for a control gene encoding GAPDH, with results calculated using the $2^{-\Delta\Delta Ct}$ method. The following oligonucleotides were used: for *cxcl9*, 5′-AATGCACGATGCTCCTGCA-3′ (sense) and 5′-AGGTCTTTGAGGGATTTGTAGTGG-3′ (antisense); for *cxcl10*, 5′-GCCGTCATTTTCTGCCTCA-3′ (sense) and 5′-CG TCCTTGCGAGAGGGATC-3′ (antisense); for *Ifng*, 5′-TAGCCA AGACTGTGATTGCGG-3′ (sense) and 5′-AGACATCTCCTCC CATCAGCAG-3′ (antisense); for *gapdh*, 5′-AAATGGTGAAGGTC GGTGTGAAC-3′ (sense) and 5′-CAACAATCTCCACTTTGCCAC TG-3′ (antisense).

Enzyme-linked immunosorbent assay (ELISA). Ready-Set-Go! ELISA kits (eBioscience) were used to detect the serum concentrations of IgG1, IgG2a, IgG2b, IgG3, and IgM. Se-
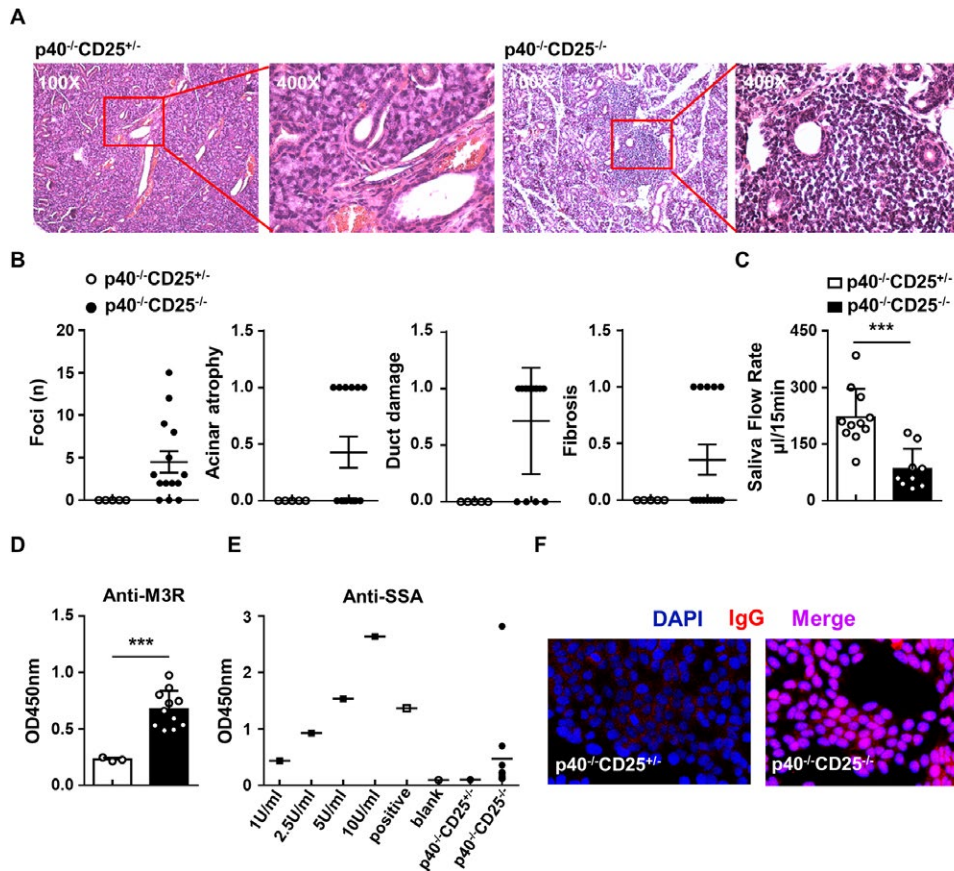
Figure 2. Characteristics of p40$^{-/-}$CD25$^{-/-}$ mice as a model of Sjögren's syndrome. **A,** Hematoxylin and eosin staining of the submandibular glands from a representative p40$^{-/-}$CD25$^{+/-}$ and p40$^{-/-}$CD25$^{-/-}$ mouse. **B,** Numbers of infiltrating lymphocytic foci and histopathologic scores for acinar atrophy, duct damage, and fibrosis in the submandibular glands from p40$^{-/-}$CD25$^{+/-}$ (n = 5) and p40$^{-/-}$CD25$^{-/-}$ mice (n = 13). Symbols represent individual mice; horizontal lines with bars show the mean ± SEM. **C,** Saliva flow rate in p40$^{-/-}$CD25$^{+/-}$ (n = 11) and p40$^{-/-}$CD25$^{-/-}$ mice (n = 9). **D** and **E,** Serum levels of anti–type 3 muscarinic acetylcholine receptor (anti-M3R) (**D**) and anti-SSA antibodies (**E**) as measured by enzyme-linked immunosorbent assay in p40$^{-/-}$CD25$^{+/-}$ (n = 3) and p40$^{-/-}$CD25$^{-/-}$ mice (n = 11). In **C** and **D**, symbols represent individual mice; bars show the mean ± SD. In **E**, horizontal lines show the mean. **F,** Serum from p40$^{-/-}$CD25$^{+/-}$ and p40$^{-/-}$CD25$^{-/-}$ mice (n = at least 5 mice per group) was incubated with HEp-2 cells, followed by incubation with Alexa Fluor 647–conjugated goat anti-mouse IgG (red) and DAPI (blue). Examples of negative and speckled staining patterns are demonstrated. Findings were derived from at least 3 separate experiments. Original magnification × 200. *** = $P < 0.001$. Color figure can be viewed in the online issue, which is available at http://onlinelibrary.wiley.com/doi/10.1002/art.40676/abstract.

rum samples were analyzed for autoantibodies against the salivary gland protein M3R. Peptides encoding murine M3R extracellular domains (VLVNTFCDSCIPKTYWNLGY) were synthesized chemically and purified (Sangon Biotech). Serum antibodies were measured using a standard ELISA (24). Serum levels of SSA and SSB were assayed using commercially available ELISA kits (Alpha Diagnostic) according to the manufacturer's instructions.

Depletion of CD8+ T cells in vivo. To deplete CD8+ T cells, 200 μg of *InVivoMAb* anti-mouse CD8α antibody (clone 2.43; BioXCell) was injected intraperitoneally 3 times per week into p40$^{-/-}$CD25$^{-/-}$ mice starting at age 8 weeks to age 12 weeks. As a control, an *InVivoMAb* rat IgG2b isotype control (clone LTF-2; BioXCell) was used.

Statistical analysis. Statistical analyses were performed using Student's 2-tailed unpaired *t*-tests in GraphPad Prism version 5. Results are expressed as the mean ± SD or mean ± SEM.

RESULTS

Dominance of infiltrating CD8+ Trm cells in the labial salivary glands of patients with SS. Flow cytometry analysis of the labial salivary glands from patients with primary SS indicated that the percentage of CD8+ T cells was significantly higher than that of CD4+ T cells (Figure 1A and Supplementary Figure 1, available on the *Arthritis & Rheumatology* web site at http://onlinelibrary.wiley.com/doi/10.1002/art.40676/abstract). Interestingly, compared to peripheral blood T cells, the majority of infiltrating T cells in the labial salivary glands of patients with SS were Trm cells, expressing CD69 and CD103. This pattern was especially evident in CD8+ T cells (Figure 1B), which were in close proximity to salivary duct epithelial cells and acinar cells (Figures 1C and D). These results suggest that CD8+ T cells, rather than CD4+ T cells, are the dominant infiltrating lymphocytes in the labial salivary glands of patients with SS and may play an important role in the destruction of the salivary duct and acinus.

Murine model of SS using p40$^{-/-}$CD25$^{-/-}$ mice. Given that SS can coexist in patients with primary biliary cholangitis, we investigated whether p40$^{-/-}$CD25$^{-/-}$ mice with primary biliary cholangitis (23) could also develop symptoms of SS. Distinct lymphocytic foci were found around the salivary ducts of p40$^{-/-}$CD25$^{-/-}$ mice (Figures 2A and B), and the scores of acinar atrophy, duct damage, and even fibrosis were notably higher in the submandibular glands of p40$^{-/-}$CD25$^{-/-}$ mice compared to p40$^{-/-}$CD25$^{+/-}$ control mice (Figure 2B). In addition, the saliva flow rate was significantly decreased in p40$^{-/-}$CD25$^{-/-}$ mice compared to control mice (Figure 2C).

We also noted significantly higher serologic levels of anti-M3R antibody in p40$^{-/-}$CD25$^{-/-}$ mice compared to control mice (Figure 2D). Anti-SSA antibodies were detectable in the serum from

2 of 11 p40$^{-/-}$CD25$^{-/-}$ mice, but not in the serum from control mice (Figure 2E), while anti-SSB antibodies were undetectable (data not shown). ANAs were also detectable in the serum of p40$^{-/-}$CD25$^{-/-}$ mice (Figure 2F). Taken together, these data demonstrate that p40$^{-/-}$CD25$^{-/-}$ mice exhibit characteristics of SS.

Accumulation of CD8+ Trm cells in the submandibular glands of p40$^{-/-}$CD25$^{-/-}$ mice. Consistent with the results of histopathology, the number of leukocytes in the submandibular glands was significantly higher in p40$^{-/-}$CD25$^{-/-}$ mice compared to control mice (Figure 3A). Analysis of the leukocyte subpopulations in the submandibular glands of p40$^{-/-}$CD25$^{-/-}$ mice and control mice demonstrated that T cells and B cells were the major infiltrating immune cells in p40$^{-/-}$CD25$^{-/-}$ mice (Figures 3B–D and Supplementary Figure 2A, available on the *Arthritis & Rheumatology* web site at http://onlinelibrary.wiley.com/doi/10.1002/art.40676/abstract), just as in patients with SS (25).

These data were also confirmed by immunofluorescence microscopy of submandibular gland tissue sections (results in Supplementary Figure 2C [http://onlinelibrary.wiley.com/doi/10.1002/art.40676/abstract]). Among leukocytes, the percentages of macrophages and natural killer (NK) cells were significantly lower in p40$^{-/-}$CD25$^{-/-}$ mice compared to control mice (Figure 3B). The macrophage numbers in the submandibular glands of p40$^{-/-}$CD25$^{-/-}$ mice were decreased, but NK cell numbers did not change (Figure 3C). Among T cell subsets, the numbers of CD4+ T cells and CD8+ T cells were higher in p40$^{-/-}$CD25$^{-/-}$ mice compared to control mice (Figure 3D). Similar to that in patients with SS, there was a much higher CD8:CD4 T cell ratio in p40$^{-/-}$CD25$^{-/-}$ mice (Figure 3E).

Likewise, in the draining lymph nodes of p40$^{-/-}$CD25$^{-/-}$ mice, the numbers of leukocytes, including T cells, were significantly increased compared to those in control mice (Figures 3F and G). The CD8:CD4 T cell ratio in the draining lymph nodes was also higher in p40$^{-/-}$CD25$^{-/-}$ mice compared to control mice (Figure 3H). Although there was no significant difference in the number of B cells, the germinal center response in the draining lymph nodes was increased considerably in p40$^{-/-}$CD25$^{-/-}$ mice compared to control mice (results in Supplementary Figures 2D–F [http://onlinelibrary.wiley.com/doi/10.1002/art.40676/abstract]).

Interestingly, the majority of the infiltrating T lymphocytes in the submandibular glands of p40$^{-/-}$CD25$^{-/-}$ mice, as well as control mice, expressed CD69 and CXCR6, with a proportion of CD8+ T cells coexpressing CD103 and CD49a (Figure 3I and Supplementary Figure 2B [http://onlinelibrary.wiley.com/doi/10.1002/art.40676/abstract] or data not shown). While a comparably large amount of infiltrating CD4+ T cells were CD69+, very few were CD69+CD103+ (Figure 3I). Our results thus demonstrate that CD8+ T cells, rather than CD4+ T cells, are the main infiltrating cells in the submandibular glands of these mice and exhibit a Trm phenotype.
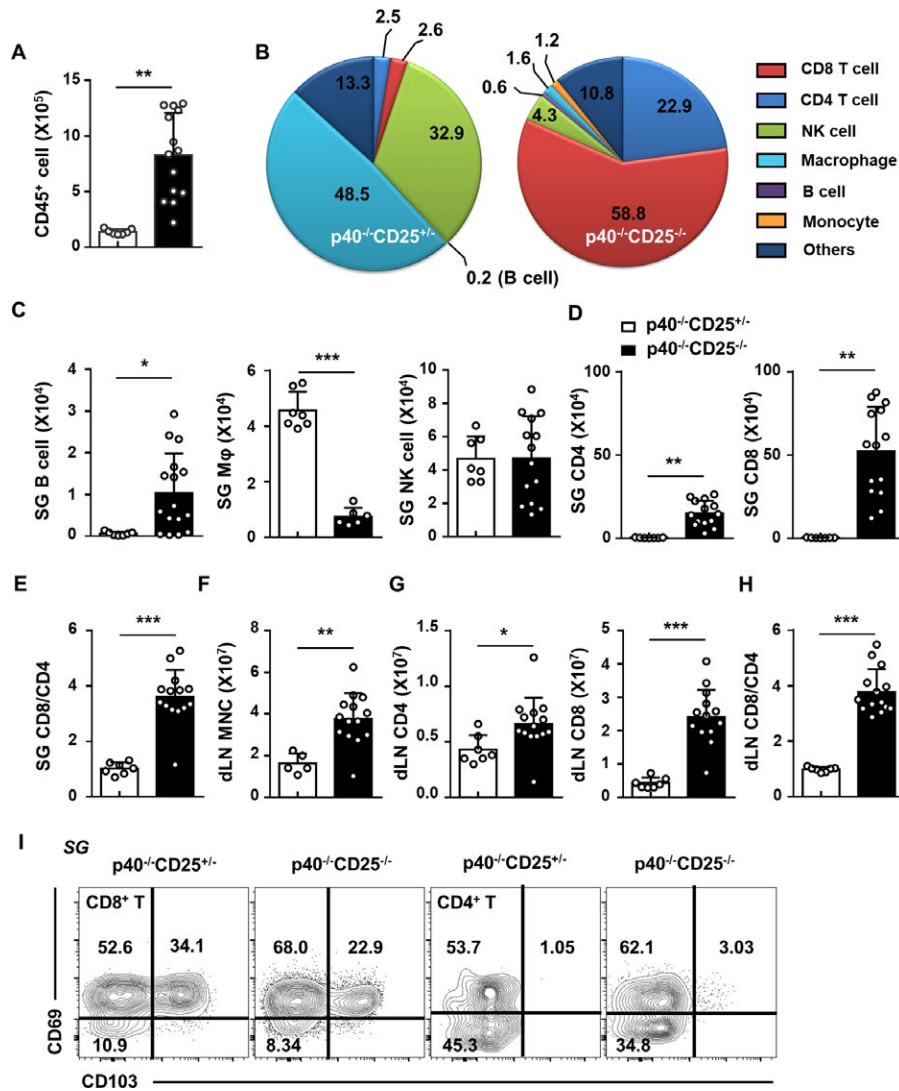
Figure 3. CD8+ tissue-resident memory T cells accumulate in the submandibular glands of p40$^{-/-}$CD25$^{-/-}$ mice. **A, C,** and **F,** Numbers of total mononuclear cells (MNCs) (**A**) and B cells, macrophages (Mφ), and natural killer (NK) cells (**C**) in the submandibular glands (SGs) and numbers of draining lymph node (dLN) MNCs (**F**) from p40$^{-/-}$CD25$^{+/-}$ mice (n = 7) and p40$^{-/-}$CD25$^{-/-}$ mice (n = 14, or n = 6 for macrophages). **B,** Percentages of each cell subset in the submandibular glands from p40$^{-/-}$CD25$^{+/-}$ mice (n = 5) and p40$^{-/-}$CD25$^{-/-}$ mice (n = 6). Values in the individual slices indicate the percentage of each subset among leukocytes. **D** and **G,** Numbers of CD4+ T cells and CD8+ T cells in the SGs (**D**) and dLNs (**G**) from p40$^{-/-}$CD25$^{+/-}$ mice (n = 7) and p40$^{-/-}$CD25$^{-/-}$ mice (n = 14). **E** and **H,** Ratio of CD8+ T cells to CD4+ T cells in the SGs (**E**) and dLNs (**H**) from p40$^{-/-}$CD25$^{+/-}$ mice (n = 7) and p40$^{-/-}$CD25$^{-/-}$ mice (n = 14). In **A** and **C–H,** symbols represent individual mice; bars show the mean ± SD. **I,** Expression of CD69 and CD103 on CD4+ and CD8+ T cells in the SGs of p40$^{-/-}$CD25$^{+/-}$ and p40$^{-/-}$CD25$^{-/-}$ mice. Values were derived from at least 3 separate experiments. * = $P < 0.05$; ** = $P < 0.01$; *** = $P < 0.001$. Color figure can be viewed in the online issue, which is available at http://onlinelibrary.wiley.com/doi/10.1002/art.40676/abstract.

Tissue damage mediated primarily by CD8+ Trm cells in murine SS. Knowing that T cells constituted the majority of the infiltrating foci in the salivary glands of human patients with SS and in our murine model of SS, we crossed p40$^{-/-}$CD25$^{-/-}$ mice with CD4$^{-/-}$ and CD8a$^{-/-}$ mice to examine the role of CD4+ and CD8+ T cells in the development of SS. The number of infiltrating foci was decreased when either CD4 or CD8a was knocked out (Figure 4B). There was a diffuse infiltration, rather than the classic focal infiltration, in the submandibular glands of p40$^{-/-}$CD25$^{-/-}$CD4$^{-/-}$ mice (Figures 4A and B). In contrast, when CD8a was knocked out, it completely abrogated the development of acinar atrophy, duct damage, and fibrosis, whereas knocking out CD4 only mildly alleviated symptoms (Figure 4B). More importantly, knockout of CD8a, but not of CD4, in p40$^{-/-}$CD25$^{-/-}$ mice restored the secretory function of the salivary glands (Figure 4C).

The number of leukocytes was significantly decreased in both p40$^{-/-}$CD25$^{-/-}$CD8a$^{-/-}$ and p40$^{-/-}$CD25$^{-/-}$CD4$^{-/-}$ mice compared to p40$^{-/-}$CD25$^{-/-}$ mice, but this decrease was greater in mice with knockout of CD8a (Figure 4D). Similarly, the
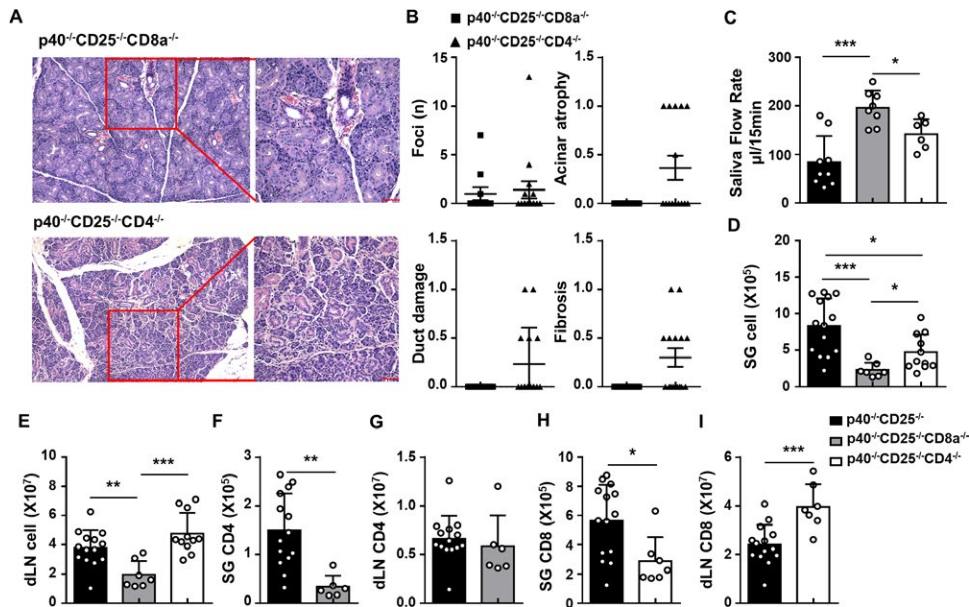
Figure 4. Tissue damage is mediated primarily by CD8+ tissue-resident memory T cells in murine Sjögren's syndrome. **A,** Hematoxylin and eosin staining of the submandibular glands (SGs) from a representative $p40^{-/-}CD25^{-/-}CD8a^{-/-}$ and $p40^{-/-}CD25^{-/-}CD4^{-/-}$ mouse. Bars = 50 μm. **B,** Numbers of infiltrating lymphocytic foci and histopathologic scores for acinar atrophy, duct damage, and fibrosis in the SGs from $p40^{-/-}CD25^{-/-}CD8a^{-/-}$ (n = 11) and $p40^{-/-}CD25^{-/-}CD4^{-/-}$ mice (n = 15). **C,** Saliva flow rate in $p40^{-/-}CD25^{-/-}$ (n = 9), $p40^{-/-}CD25^{-/-}CD8a^{-/-}$ (n = 8), and $p40^{-/-}CD25^{-/-}CD4^{-/-}$ mice (n = 6). **D** and **E,** Numbers of total mononuclear cells in the SGs (**D**) and draining lymph nodes (dLNs) (**E**) from $p40^{-/-}CD25^{-/-}$ (n = 14), $p40^{-/-}CD25^{-/-}CD8a^{-/-}$ (n = 7), and $p40^{-/-}CD25^{-/-}CD4^{-/-}$ mice (n = 11). **F** and **G,** Numbers of CD4+ T cells in the SGs (**F**) and dLNs (**G**) from $p40^{-/-}CD25^{-/-}$ (n = 14) and $p40^{-/-}CD25^{-/-}CD8a^{-/-}$ mice (n = 6). **H** and **I,** Numbers of CD8+ T cells in the SGs (**H**) and dLNs (**I**) from $p40^{-/-}CD25^{-/-}$ (n = 14) and $p40^{-/-}CD25^{-/-}CD4^{-/-}$ mice (n = 7). Symbols represent individual mice; horizontal lines with bars show the mean ± SEM in **B** or bars show the mean ± SD in **C–I**. Values were derived from at least 3 separate experiments. * = $P < 0.05$; ** = $P < 0.01$; *** = $P < 0.001$. Color figure can be viewed in the online issue, which is available at http://onlinelibrary.wiley.com/doi/10.1002/art.40676/abstract.

numbers of total draining lymph node mononuclear cells were significantly decreased in $p40^{-/-}CD25^{-/-}CD8a^{-/-}$ mice, but not in $p40^{-/-}CD25^{-/-}CD4^{-/-}$ mice, compared to $p40^{-/-}CD25^{-/-}$ mice (Figure 4E). There were fewer CD4+ T cells in the submandibular glands of $p40^{-/-}CD25^{-/-}CD8a^{-/-}$ mice compared to $p40^{-/-}CD25^{-/-}$ mice (Figures 4F and G). The number of CD8+ T cells was also significantly decreased in the submandibular glands, but increased in the draining lymph nodes, of $p40^{-/-}CD25^{-/-}CD4^{-/-}$ mice (Figures 4H and I).

Although tissue damage was significantly alleviated in the absence of CD8+ T cells, a high germinal center response was still noted (results in Supplementary Figures 3A and B, available on the *Arthritis & Rheumatology* web site at http://onlinelibrary.wiley.com/doi/10.1002/art.40676/abstract). In mice with CD8a deficiency, serum levels of IgM, IgG1, and IgG3 were all increased in comparison to $p40^{-/-}CD25^{-/-}$ mice (results in Supplementary Figure 3C [http://onlinelibrary.wiley.com/doi/10.1002/art.40676/abstract]). In contrast, knockout of CD4 impaired the germinal center response and antibody production in $p40^{-/-}CD25^{-/-}$ mice (results in Supplementary Figures 3A and C). Taken together, these findings suggest that tissue damage is primarily mediated by CD8+ T cells, and that CD4+ T cells may be important for CD8+ T cell infiltration for specific destruction of the salivary duct.

Required presence of IFNγ for CD8+ T cell infiltration in the submandibular glands. T cells infiltrating the submandibular glands and draining lymph nodes of $p40^{-/-}CD25^{-/-}$ mice had high IFNγ production (Figures 5A and B). Levels of IFNγ messenger RNA (mRNA) were also up-regulated in the submandibular gland tissue of these mice (Figure 5C). We therefore generated $p40^{-/-}CD25^{-/-}IFNγ^{-/-}$ mice to investigate the role of IFNγ in SS. Significantly fewer leukocytes were found in the submandibular glands of $p40^{-/-}CD25^{-/-}IFNγ^{-/-}$ mice compared to $p40^{-/-}CD25^{-/-}$ mice (Figure 5D). Whereas knockout of IFNγ in $p40^{-/-}CD25^{-/-}$ mice resulted in only a slightly decreased number of infiltrated foci and slightly lower scores for duct damage and fibrosis, the absence of IFNγ in these mice alleviated the severity of acinar atrophy and restored the secretory function of the salivary glands (Figures 5E and F). These data demonstrate the pathogenic role of IFNγ in $p40^{-/-}CD25^{-/-}$ mice.

Notably, $p40^{-/-}CD25^{-/-}$ mice with IFNγ knockout had dramatically enlarged draining lymph nodes (Figure 5G), which was attributable to increased numbers of CD8+ and CD4+ T cells (Figure 5H). However, in the submandibular glands of $p40^{-/-}CD25^{-/-}IFNγ^{-/-}$ mice, the number of CD8+ T cells was decreased (Figure 5I), suggesting that IFNγ may promote CD8+ T cell migration from the draining lymph nodes to the submandibular glands.
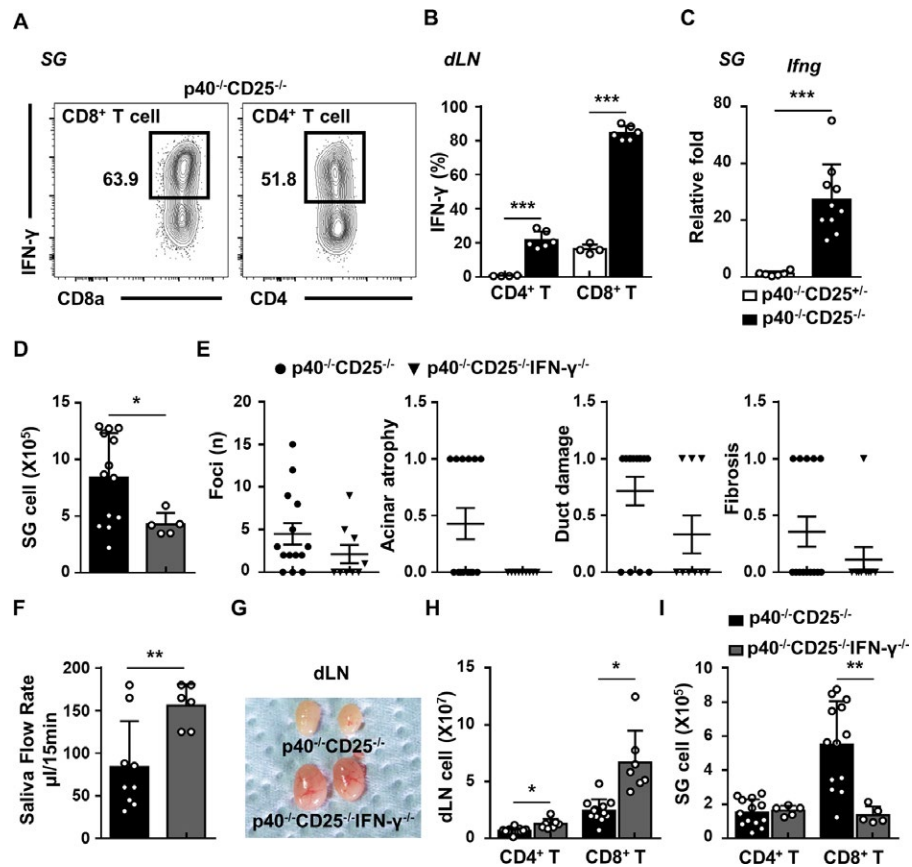
Figure 5. CD8+ T cell infiltration in the salivary glands requires the presence of interferon-γ (IFNγ). **A** and **B,** IFNγ+ T cells in the submandibular glands (SGs) (**A**) and draining lymph nodes (dLNs) (**B**) from p40$^{-/-}$CD25$^{+/-}$ mice (n = 4) and p40$^{-/-}$CD25$^{-/-}$ mice (n = 6). **C,** Results of quantititative polymerase chain reaction showing *Ifng* gene expression in the SGs from p40$^{-/-}$CD25$^{+/-}$ mice (n = 6) and p40$^{-/-}$CD25$^{-/-}$ mice (n = 10). **D,** Numbers of total mononuclear cells in the SGs from p40$^{-/-}$CD25$^{-/-}$ mice (n = 13) and p40$^{-/-}$CD25$^{-/-}$IFNγ$^{-/-}$ mice (n = 5). **E,** Numbers of infiltrating lymphocytic foci and histopathologic scores for acinar atrophy, duct damage, and fibrosis in the SGs from p40$^{-/-}$CD25$^{-/-}$ mice (n = 14) and p40$^{-/-}$CD25$^{-/-}$IFNγ$^{-/-}$ mice (n = 9). **F,** Saliva flow rate in p40$^{-/-}$CD25$^{-/-}$ mice (n = 9) and p40$^{-/-}$CD25$^{-/-}$IFNγ$^{-/-}$ mice (n = 6). **G,** Microscopic images of the dLNs from a representative p40$^{-/-}$CD25$^{-/-}$ mouse and p40$^{-/-}$CD25$^{-/-}$IFNγ$^{-/-}$ mouse. **H** and **I,** Numbers of CD4+ and CD8+ T cells in the dLNs (**H**) and SGs (**I**) from p40$^{-/-}$CD25$^{-/-}$ mice (n = 13) and p40$^{-/-}$CD25$^{-/-}$IFNγ$^{-/-}$ mice (n = 5). Symbols represent individual mice; bars show the mean ± SD in **B–D**, **F**, **H**, and **I** or horizontal lines with bars show the mean ± SEM in **E**. Values were derived from at least 3 separate experiments. * = $P < 0.05$; ** = $P < 0.01$; *** = $P < 0.001$. Color figure can be viewed in the online issue, which is available at http://onlinelibrary.wiley.com/doi/10.1002/art.40676/abstract.

We also observed that the germinal center response in the draining lymph nodes was completely abolished after knockout of IFNγ in p40$^{-/-}$CD25$^{-/-}$ mice (results in Supplementary Figure 3D [http://onlinelibrary.wiley.com/doi/10.1002/art.40676/abstract]), indicating that the absence or presence of IFNγ determined the germinal center response.

Considering that previous studies have demonstrated an effect of IFNγ on the CXCR3–CXCL9/10 axis (26), we next measured the expression of CXCR3 on T lymphocytes in the draining lymph nodes of mice, and the expression of CXCL9/CXCL10 in the mouse submandibular glands. A significantly higher frequency of CXCR3+ T lymphocytes, especially among CD8+ T cells, was observed in the draining lymph nodes of p40$^{-/-}$CD25$^{-/-}$ mice compared to control mice (results in Supplementary Figure 4A, available on the *Arthri-*

tis & Rheumatology web site at http://onlinelibrary.wiley.com/doi/10.1002/art.40676/abstract). However, knockout of IFNγ in p40$^{-/-}$CD25$^{-/-}$ mice did not decrease the percentage of CXCR3+ T lymphocytes in the draining lymph nodes (Supplementary Figure 4A).

Furthermore, the levels of mRNA for *Cxcl9* and *Cxcl10* were each significantly increased in the submandibular glands of both p40$^{-/-}$CD25$^{-/-}$ and p40$^{-/-}$CD25$^{-/-}$CD4$^{-/-}$ mice compared to control mice (results in Supplementary Figure 4B [http://onlinelibrary.wiley.com/doi/10.1002/art.40676/abstract]). In contrast, mRNA expression of these chemokines was significantly decreased in p40$^{-/-}$CD25$^{-/-}$CD8a$^{-/-}$ and p40$^{-/-}$CD25$^{-/-}$IFNγ$^{-/-}$ mice compared to p40$^{-/-}$CD25$^{-/-}$ mice (Supplementary Figure 4B). Our findings thus suggest that IFNγ contributes to CD8+ T cell infiltration in the submandibular glands through a CXCR3-dependent mechanism.
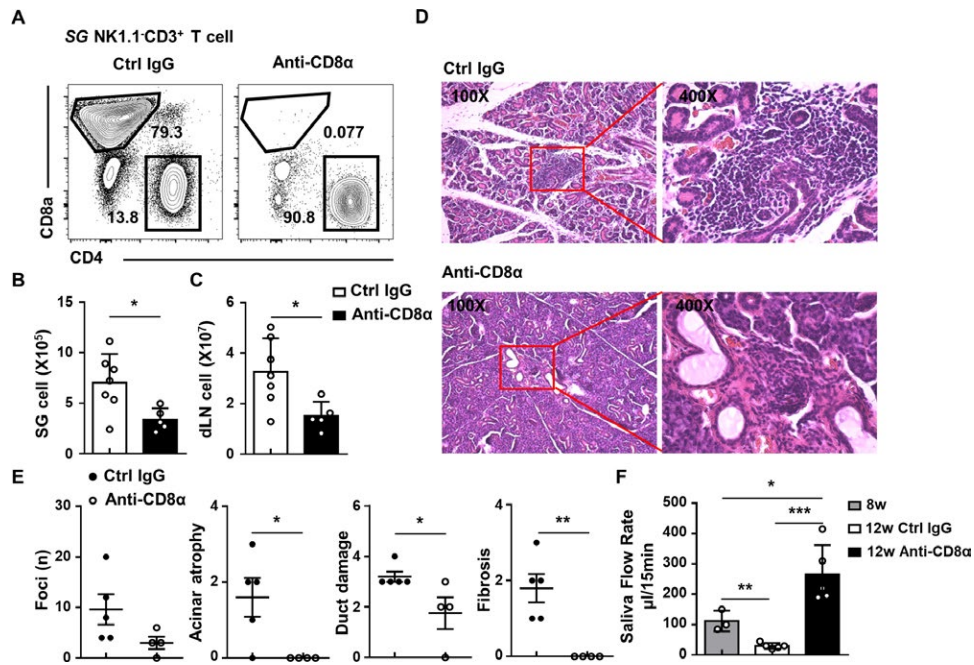
Figure 6. CD8+ T cell depletion therapy alleviates tissue damage in a murine model of Sjögren's syndrome. **A,** Expression of T cell subsets in the submandibular glands (SGs) from p40$^{-/-}$CD25$^{-/-}$ mice treated with the CD8+ T cell depletion antibody or control IgG. **B** and **C,** Numbers of total mononuclear cells in the SGs (**B**) or draining lymph nodes (dLNs) (**C**) from p40$^{-/-}$CD25$^{-/-}$ mice treated with CD8+ T cell depletion antibody (n = 5) or control IgG (n = 7). **D,** Hematoxylin and eosin staining of the SGs from a representative p40$^{-/-}$CD25$^{-/-}$ mouse treated with CD8+ T cell depletion antibody or control IgG. **E,** Numbers of infiltrating lymphocytic foci and histopathologic scores for acinar atrophy, duct damage, and fibrosis in the SGs from p40$^{-/-}$CD25$^{-/-}$ mice treated with CD8+ T cell depletion antibody (n = 4) or control IgG (n = 5). **F,** Saliva flow rate in untreated 8-week-old p40$^{-/-}$CD25$^{-/-}$ mice (n = 3), 12-week-old p40$^{-/-}$CD25$^{-/-}$ mice treated with CD8+ T cell depletion antibody (n = 5), or 12-week-old p40$^{-/-}$CD25$^{-/-}$ mice treated with control IgG (n = 5). Symbols represent individual mice; bars show the mean ± SD in **B**, **C**, and **F** or horizontal lines with bars show the mean ± SEM in **E**. Values were derived from at least 3 separate experiments. * = $P < 0.05$; ** = $P < 0.01$; *** = $P < 0.001$. Color figure can be viewed in the online issue, which is available at http://onlinelibrary.wiley.com/doi/10.1002/art.40676/abstract.

Alleviation of tissue damage by CD8+ T cell depletion therapy in murine SS. Given that CD8+ T cells contribute to the pathogenesis of SS, we depleted CD8+ T cells after disease onset as a therapeutic strategy. We began CD8+ T cell–specific antibody treatment in p40$^{-/-}$CD25$^{-/-}$ mice at age 8 weeks, when severe lymphocyte infiltration and tissue damage had already appeared in the submandibular glands (see Supplementary Figures 5A and B, available on the *Arthritis & Rheumatology* web site at http://onlinelibrary.wiley.com/doi/10.1002/art.40676/abstract). The depletion antibody effectively eliminated CD8+ T cells in the submandibular glands of mice and in the peripheral blood of patients with SS (Figure 6A and Supplementary Figure 5C [http://onlinelibrary.wiley.com/doi/10.1002/art.40676/abstract]). Furthermore, the number of total mononuclear cells in the mouse submandibular glands was significantly reduced by the depletion antibody treatment (Figure 6B). The number of infiltrated foci as well as the scores for acinar atrophy, duct damage, and fibrosis were all decreased after treatment with the CD8+ T cell depletion antibody (Figures 6D and E).

More importantly, the secretory function of the mouse salivary glands was restored after antibody therapy (Figure 6F). For example, untreated 8-week-old mice secreted more saliva than

did 12-week-old mice treated with control IgG, but did not show as much saliva secretion as mice treated with the anti-CD8a antibody for 4 weeks (Figure 6F). The number of total mononuclear cells in the draining lymph nodes was significantly decreased in the treated mice but not in the control mice (Figure 6C), but the number of B cells and the germinal center response in the draining lymph nodes were not affected by the antibody treatment (results in Supplementary Figures 5D–F [http://onlinelibrary.wiley.com/doi/10.1002/art.40676/abstract]). There was no difference in the serum levels of either anti-M3R antibodies or ANAs between anti-CD8a depletion antibody–treated mice and control mice (results in Supplementary Figures 5G and H [http://onlinelibrary.wiley.com/doi/10.1002/art.40676/abstract]). Taken together, our results demonstrate that an antibody treatment aimed at depleting CD8+ T cells can effectively improve the disease manifestations of SS, even in animals with established disease.

DISCUSSION

The results of this study show that CD8+ T cells constitute the majority of T cells infiltrating the labial salivary glands of pa-

tients with primary SS. Using a mouse model that recapitulates many of the features of human SS, we documented a critical role of CD8+ T cells in the development of SS. Most importantly, targeted depletion of CD8+ T cells appears to significantly reduce tissue damage and restore salivary gland functions even in mice with established disease, providing a new therapeutic strategy for human SS.

SS is characterized by extensive lymphocytic infiltration in the exocrine glands or other epithelial elements, most prominently in the salivary glands, by CD4+ and CD8+ T cells (10). However, the role of CD8+ T cells has not been well studied. A recent study using mass flow cytometry demonstrated the presence of a large number of activated CD8+ T cells in the labial salivary glands of patients with SS (10). A multiomics study with blood and tissue samples from patients with SS indicated that cytotoxic CD8+ T cells are associated with SS gene signatures (12).

Cytotoxic CD8+ T cells can induce apoptosis and lysis of target cells through the Fas/FasL pathway or can induce degranulation and IFNγ production (27). Patients with SS have high expression levels of Fas and FasL in acinar and ductal epithelial cells and infiltrating cells in their salivary glands (28). CD8+ T cells localize around the apoptotic acinar epithelial cells in patients with SS (29). Another recent study found that CD8+ T cells can promote dacryoadenitis and mediate epithelial cell damage in NOD mice (11). In this study, we found that CD8+ T cells were dominant both in the labial salivary glands of patients with SS and in the salivary glands of p40$^{-/-}$CD25$^{-/-}$ mice. However, CD8+ T cell infiltration in the submandibular glands became more diffuse in CD4-knockout mice with SS-like disease, suggesting that CD4+ T cells were involved in cell clustering and in the formation of infiltrating foci during the pathogenesis of SS.

Trm cells manifest up-regulated expression of CD69, which antagonizes the sphingosine 1-phosphate receptor 1 (a receptor for S1P) to maintain tissue-resident features (30–32). CD103, also coined αEβ7, is associated with the Trm phenotype and can bind to E-cadherin (14,33,34). CD103 expression on Trm cell precursors depends on transforming growth factor β (TGFβ) (14,33,35,36). Transcripts of *Tgfb1–3* are highly expressed in the salivary glands, allowing CD8+ T cells infiltrating the salivary glands to be activated by TGFβ signaling and express CD103, thus becoming CD103+CD8+ Trm cells (37). Indeed, we observed that a large proportion of CD8+ T cells in the labial salivary glands of patients with SS or in the murine model of SS were CD103+CD8+ Trm cells. Acinar cells and salivary duct epithelial cells both have high E-cadherin expression (38). CD8+ T cells can therefore colocalize with acinar cells and salivary duct epithelial cells via the interaction between CD103 on CD8+ Trm cells and E-cadherin on epithelial cells.

Compared to subjects without SS, the salivary glands and saliva from patients with SS exhibit elevated levels of IFNγ (39,40). The labial salivary glands from patients with SS exhibit a high gene expression of *cxcl9* and *cxcl10*, which are induced by IFNγ and encode the ligands of CXCR3 (41). As noted above, IFNγ production by infiltrating mononuclear cells was increased in the submandibular glands of mice in our murine model of SS. Although the presence of IL-12p40 is critical for IFNγ production, the production of IFNγ in CD25$^{-/-}$ mice may occur independent of IL-12 and may be limited by the presence of IL-23, which prevents Th1 responses or inhibits Th1 development (21). Our results suggest that increased expression of *cxcl9* and *cxcl10* may enable IFNγ to promote CD8+ T cells, displaying a high expression of CXCR3 in draining lymph nodes and subsequent infiltration into the submandibular glands. Nevertheless, we noticed that infiltrating CD8+ T cells were significantly decreased in the submandibular glands of p40$^{-/-}$CD25$^{-/-}$CD4$^{-/-}$ mice despite their high expression of *cxcl9* and *cxcl10*, which suggests that CD4+ T cells recruit CD8+ T cells via a different mechanism during SS development.

In addition, increased production of IFNγ can induce the expression of apoptosis-related molecules, such as Fas, on ductal epithelial cells in the salivary glands of patients with SS (42). IFNγ can also induce immunoproteasomes and promote the presentation of class I major histocompatibility complex–associated peptides on human salivary gland cells (43), enhancing CD8+ T cell–mediated immune responses.

In addition to T cells, activated B cells also infiltrate the salivary glands of patients with SS (23). Autoantibody production can begin at a very early stage, well before the onset of clinical manifestations (44). However, autoantibodies do not appear to play a direct role in the pathogenesis of SS (45). Rituximab, an anti–B cell therapy, was not clinically effective in patients with SS (46). IFNγ has been reported to promote autoimmune germinal centers via interaction with the B cell IFNγ receptor (47,48). However, knockout of CD8a or deletion of CD8+ T cells did not suppress germinal center responses and antibody secretion, suggesting that IFNγ derived from other cells is sufficient to maintain the autoimmune germinal center response.

In this study, we found that although the germinal center response and antibody production were suppressed in CD4-knockout or IFNγ-knockout p40$^{-/-}$CD25$^{-/-}$ mice, tissue damage still occurred. Furthermore, CD8+ T cell deficiency did not decrease antibody production, despite our observation that it improved the structure and physiologic function of the target tissue.

In conclusion, CD8+ T cells appear to play a significant role in the immunopathology of SS both in this murine model and in humans. This study also demonstrates that the majority of infiltrating CD8+ T cells are Trm cells (as depicted in Supplementary Figure 6, available on the *Arthritis & Rheumatology* web site at http://onlinelibrary.wiley.com/doi/10.1002/art.40676/abstract). Furthermore, depletion of CD8+ T cells even after the onset of disease improves the pathologic manifestations of SS. These data collectively enhance our understanding of the pathogenesis of SS and suggest a new therapeutic strategy for the management of SS in human subjects.

AUTHOR CONTRIBUTIONS

REFERENCES

1. Peri Y, Agmon-Levin N, Theodor E, Shoenfeld Y. Sjögren's syndrome, the old and the new. Best Pract Res Clin Rheumatol 2012;26:105–17.

2. Fisher BA, Brown RM, Bowman SJ, Barone F. A review of salivary gland histopathology in primary Sjögren's syndrome with a focus on its potential as a clinical trials biomarker. Ann Rheum Dis 2015;74:1645–50.

3. Rusakiewicz S, Nocturne G, Lazure T, Semeraro M, Flament C, Caillat-Zucman S, et al. NCR3/NKp30 contributes to pathogenesis in primary Sjögren's syndrome. Sci Transl Med 2013;5:195ra96.

4. Naito Y, Matsumoto I, Wakamatsu E, Goto D, Sugiyama T, Matsumura R, et al. Muscarinic acetylcholine receptor autoantibodies in patients with Sjögren's syndrome. Ann Rheum Dis 2005;64:510–1.

5. Iizuka M, Wakamatsu E, Tsuboi H, Nakamura Y, Hayashi T, Matsui M, et al. Pathogenic role of immune response to M3 muscarinic acetylcholine receptor in Sjögren's syndrome-like sialoadenitis. J Autoimmun 2010;35:383–9.

6. Moutsopoulos HM, Zerva LV. Anti-Ro (SSA)/La (SSB) antibodies and Sjögren's syndrome. Clin Rheumatol 1990;9 Suppl 1:123–30.

7. Ma WT, Chang C, Gershwin ME, Lian ZX. Development of autoantibodies precedes clinical manifestations of autoimmune diseases: a comprehensive review. J Autoimmun 2017;83:95–112.

8. Lessard CJ, Li H, Adrianto I, Ice JA, Rasmussen A, Grundahl KM, et al. Variants at multiple loci implicated in both innate and adaptive immune responses are associated with Sjögren's syndrome. Nat Genet 2013;45:1284–92.

9. Cruz-Tapias P, Rojas-Villarraga A, Maier-Moore S, Anaya JM. HLA and Sjögren's syndrome susceptibility: a meta-analysis of worldwide studies. Autoimmun Rev 2012;11:281–7.

10. Mingueneau M, Boudaoud S, Haskett S, Reynolds TL, Nocturne G, Norton E, et al. Cytometry by time-of-flight immunophenotyping identifies a blood Sjögren's signature correlating with disease activity and glandular inflammation. J Allergy Clin Immunol 2016;137:1809–21.

11. Barr JY, Wang X, Meyerholz DK, Lieberman SM. CD8 T cells contribute to lacrimal gland pathology in the nonobese diabetic mouse model of Sjögren syndrome. Immunol Cell Biol 2017;95:684–94.

12. Tasaki S, Suzuki K, Nishikawa A, Kassai Y, Takiguchi M, Kurisu R, et al. Multiomic disease signatures converge to cytotoxic CD8 T cells in primary Sjögren's syndrome. Ann Rheum Dis 2017;76:1458–66.

13. Hogan RJ, Zhong W, Usherwood EJ, Cookenham T, Roberts AD, Woodland DL. Protection from respiratory virus infections can be mediated by antigen-specific CD4(+) T cells that persist in the lungs. J Exp Med 2001;193:981–6.

14. Casey KA, Fraser KA, Schenkel JM, Moran A, Abt MC, Beura LK, et al. Antigen-independent differentiation and maintenance of effector-like resident memory T cells in tissues. J Immunol 2012;188:4866–75.

15. Steinert EM, Schenkel JM, Fraser KA, Beura LK, Manlove LS, Igyarto BZ, et al. Quantifying memory CD8 T cells reveals regionalization of immunosurveillance. Cell 2015;161:737–49.

16. Gebhardt T, Wakim LM, Eidsmo L, Reading PC, Heath WR, Carbone FR. Memory T cells in nonlymphoid tissue that provide enhanced local immunity during infection with herpes simplex virus. Nat Immunol 2009;10:524–30.

17. Thom JT, Weber TC, Walton SM, Torti N, Oxenius A. The salivary gland acts as a sink for tissue-resident memory CD8(+) T cells, facilitating protection from local cytomegalovirus infection. Cell Rep 2015;13:1125–36.

18. Smith CJ, Caldeira-Dantas S, Turula H, Snyder CM. Murine CMV infection induces the continuous production of mucosal resident T cells. Cell Rep 2015;13:1137–48.

19. Woyciechowski S, Hofmann M, Pircher H. alpha4 beta1 integrin promotes accumulation of tissue-resident memory CD8(+) T cells in salivary glands. Eur J Immunol 2017;47:244–50.

20. Hofmann M, Pircher H. E-cadherin promotes accumulation of a unique memory CD8 T-cell population in murine salivary glands. Proc Natl Acad Sci U S A 2011;108:16741–6.

21. Selmi C, Meroni PL, Gershwin ME. Primary biliary cirrhosis and Sjögren's syndrome: autoimmune epithelitis. J Autoimmun 2012;39:34–42.

22. Sun Y, Zhang W, Li B, Zou Z, Selmi C, Gershwin ME. The coexistence of Sjögren's syndrome and primary biliary cirrhosis: a comprehensive review. Clin Rev Allergy Immunol 2015;48:301–15.

23. Yao Y, Yang W, Yang YQ, Ma HD, Lu FT, Li L, et al. Distinct from its canonical effects, deletion of IL-12p40 induces cholangitis and fibrosis in interleukin-2Rα(−/−) mice. J Autoimmun 2014;51:99–108.

24. Chen Y, Zheng J, Huang Q, Deng F, Huang R, Zhao W, et al. Autoantibodies against the second extracellular loop of M3R do neither induce nor indicate primary Sjögren's syndrome. PLoS One 2016;11:e0149485.

25. Jonsson R, Gordon TP, Konttinen YT. Recent advances in understanding molecular mechanisms in the pathogenesis and antibody profile of Sjögren's syndrome. Curr Rheumatol Rep 2003;5:311–6.

26. Carter SL, Muller M, Manders PM, Campbell IL. Induction of the genes for Cxcl9 and Cxcl10 is dependent on IFN-γ but shows differential cellular expression in experimental autoimmune encephalomyelitis and by astrocytes and microglia in vitro. Glia 2007;55:1728–39.

27. Russell JH, Ley TJ. Lymphocyte-mediated cytotoxicity. Annu Rev Immunol 2002;20:323–70.

28. Polihronis M, Tapinos NI, Theocharis SE, Economou A, Kittas C, Moutsopoulos HM. Modes of epithelial cell death and repair in Sjögren's syndrome (SS). Clin Exp Immunol 1998;114:485–90.

29. Fujihara T, Fujita H, Tsubota K, Saito K, Tsuzaka K, Abe T, et al. Preferential localization of CD8+ αE β7+ T cells around acinar epithelial cells with apoptosis in patients with Sjögren's syndrome. J Immunol 1999;163:2226–35.

30. Cyster JG, Schwab SR. Sphingosine-1-phosphate and lymphocyte egress from lymphoid organs. Annu Rev Immunol 2012;30:69–94.

31. Matloubian M, Lo CG, Cinamon G, Lesneski MJ, Xu Y, Brinkmann V, et al. Lymphocyte egress from thymus and peripheral lymphoid organs is dependent on S1P receptor 1. Nature 2004;427:355–60.

32. Skon CN, Lee JY, Anderson KG, Masopust D, Hogquist KA, Jameson SC. Transcriptional downregulation of S1pr1 is required for the establishment of resident memory CD8+ T cells. Nat Immunol 2013;14:1285–93.

33. Mackay LK, Rahimpour A, Ma JZ, Collins N, Stock AT, Hafon ML, et al. The developmental pathway for CD103(+)CD8+ tissue-resident memory T cells of skin. Nat Immunol 2013;14:1294–301.

34. Cepek KL, Shaw SK, Parker CM, Russell GJ, Morrow JS, Rimm DL, et al. Adhesion between epithelial cells and T lymphocytes mediated by E-cadherin and the αEβ7 integrin. Nature 1994;372:190–3.

35. Sheridan BS, Pham QM, Lee YT, Cauley LS, Puddington L, Lefrancois L. Oral infection drives a distinct population of intestinal resident memory CD8(+) T cells with enhanced protective function. Immunity 2014;40:747–57.

36. Zhang N, Bevan MJ. Transforming growth factor-β signaling controls the formation and maintenance of gut-resident memory T cells by regulating migration and retention. Immunity 2013;39:687–96.

37. Cortez VS, Cervantes-Barragan L, Robinette ML, Bando JK, Wang Y, Geiger TL, et al. Transforming growth factor-β signaling guides the differentiation of innate lymphoid cells in salivary glands. Immunity 2016;44:1127–39.

38. Walker JL, Menko AS, Khalil S, Rebustini I, Hoffman MP, Kreidberg JA, et al. Diverse roles of E-cadherin in the morphogenesis of the submandibular gland: insights into the formation of acinar and ductal structures. Dev Dyn 2008;237:3128–41.

39. Jin JO, Yu Q. T cell-associated cytokines in the pathogenesis of Sjögren's syndrome. J Clin Cell Immunol 2013;S!:11742.

40. Hall JC, Casciola-Rosen L, Berger AE, Kapsogeorgou EK, Cheadle C, Tzioufas AG, et al. Precise probes of type II interferon activity define the origin of interferon signatures in target tissues in rheumatic diseases. Proc Natl Acad Sci U S A 2012;109:17609–14.

41. Ogawa N, Ping L, Zhenjun L, Takada Y, Sugai S. Involvement of the interferon-γ-induced T cell-attracting chemokines, interferon-γ-inducible 10-kd protein (CXCL10) and monokine induced by interferon-γ (CXCL9), in the salivary gland lesions of patients with Sjögren's syndrome. Arthritis Rheum 2002;46:2730–41.

42. Matsumura R, Umemiya K, Goto T, Nakazawa T, Ochiai K, Kagami M, et al. Interferon γ and tumor necrosis factor α induce Fas expression and anti-Fas mediated apoptosis in a salivary ductal cell line. Clin Exp Rheumatol 2000;18:311–8.

43. Arellano-Garcia ME, Misuno K, Tran SD, Hu S. Interferon-γ induces immunoproteasomes and the presentation of MHC I-associated peptides on human salivary gland cells. PLoS One 2014;9:e102878.

44. Theander E, Vasaitis L, Baecklund E, Nordmark G, Warfvinge G, Liedholm R, et al. Lymphoid organisation in labial salivary gland biopsies is a possible predictor for the development of malignant lymphoma in primary Sjögren's syndrome. Ann Rheum Dis 2011;70: 1363–8.

45. Nocturne G, Mariette X. Advances in understanding the pathogenesis of primary Sjögren's syndrome. Nat Rev Rheumatol 2013;9: 544–56.

46. Bowman SJ, Everett CC, O'Dwyer JL, Emery P, Pitzalis C, Ng WF, et al. Randomized controlled trial of rituximab and cost-effectiveness analysis in treating fatigue and oral dryness in primary Sjögren's syndrome. Arthritis Rheumatol 2017;69:1440–50.

47. Jackson SW, Jacobs HM, Arkatkar T, Dam EM, Scharping NE, Kolhatkar NS, et al. B cell IFN-γ receptor signaling promotes autoimmune germinal centers via cell-intrinsic induction of BCL-6. J Exp Med 2016;213:733–50.

48. Domeier PP, Chodisetti SB, Soni C, Schell SL, Elias MJ, Wong EB, et al. IFN-γ receptor and STAT1 signaling in B cells are central to spontaneous germinal center formation and autoimmunity. J Exp Med 2016;213:715–32.

AMERICAN COLLEGE
OF RHEUMATOLOGY
EDUCATION · TREATMENT · RESEARCH

Salivary Gland Stem Cells Age Prematurely in Primary Sjögren's Syndrome

Sarah Pringle,[1] Xiaoyan Wang,[1] Gwenny M. P. J. Verstappen,[1] Janneke H. Terpstra,[1] Clarence K. Zhang,[2] Aiqing He,[3] Vishal Patel,[3] Rhiannon E. Jones,[4] Duncan M. Baird,[4] Fred K. L. Spijkervet,[1] Arjan Vissink,[1] Hendrika Bootsma,[1] Robert P. Coppes,[1] and Frans G. M. Kroese[1]

Objective. A major characteristic of the autoimmune disease primary Sjögren's syndrome (SS) is salivary gland (SG) hypofunction. The inability of resident SG stem cells (SGSCs) to maintain homeostasis and saliva production has never been explained and limits our comprehension of mechanisms underlying primary SS. The present study was undertaken to investigate the role of salivary gland stem cells in hyposalivation in primary SS.

Methods. SGSCs were isolated from parotid biopsy samples from controls and patients classified as having primary SS or incomplete primary SS, according to the American College of Rheumatology/European League Against Rheumatism criteria. Self-renewal and differentiation assays were used to determine SGSC regenerative potential, RNA was extracted for sequencing analysis, single telomere length analysis was conducted to determine telomere length, and frozen tissue samples were used for immunohistochemical analysis.

Results. SGSCs isolated from primary SS parotid gland biopsy samples were regeneratively inferior to healthy control specimens. We demonstrated that SGSCs from samples from patients with primary SS are not only lower in number and less able to differentiate, but are likely to be senescent, as revealed by telomere length analysis, RNA sequencing, and immunostaining. We further found that SGSCs exposed to primary SS–associated proinflammatory cytokines we induced to proliferate, express senescence-associated genes, and subsequently differentiate into intercalated duct cells. We also localized p16+ senescent cells to the intercalated ducts in primary SS SG tissue, suggesting a block in SGSC differentiation into acinar cells.

Conclusion. This study represents the first characterization of SGSCs in primary SS, and also the first demonstration of a linkage between an autoimmune disease and a parenchymal premature-aging phenotype. The knowledge garnered in this study indicates that disease-modifying antirheumatic drugs used to treat primary SS are not likely to restore saliva production, and should be supplemented with fresh SGSCs to recover saliva production.

INTRODUCTION

Between 0.4 and 3.1 million people in the US have been diagnosed as having the autoimmune disease primary Sjögren's syndrome (SS) (1). Presenting clinically predominantly in women (9:1 ratio), primary SS is a multifaceted syndrome most often associated with production of autoantibodies (SSA/Ro and SSB/La), infiltration of the salivary glands (SGs) with lymphocytes, and hyposalivation (reduced secretory function of the SGs). Other symptoms may include neurologic involvement, lung symptoms,

and chronic fatigue. Lymphocytic infiltration of SGs is characterized and measured clinically by the presence of immune foci, defined as a gathering of >50 lymphocytes in the SGs, associated with the striated ducts. The periductal infiltrates may evolve into ectopic lymphoid tissue harboring germinal centers (sites of memory B cell formation). In addition, the relative number of IgA plasma cells decreases, in parallel with glandular dominance of IgG-producing plasma cells. Mucosa-associated lymphoid tissue lymphomas are also frequently observed in the SG tissue of patients with primary SS. These features of salivary gland infiltration

reflect the B cell–dominated phenotype of primary SS (2). Given these characteristic lymphocytic infiltrates, the logical conclusion is that lymphocytic infiltration of SGs is the causative factor underlying hyposalivation. However, recent detailed research has clearly demonstrated that the correlation between salivary flow and degree of inflammation is weak (3–11).

In healthy SGs, homeostasis is maintained by proliferation and differentiation of tissue-resident SGSCs. According to one of the prevailing views in the field, these cells reside in striated ducts, from where they differentiate first toward intercalated ducts and subsequently to acinar cells (12–16). Other studies have identified progenitor cell populations within the acinar cell subset, and, alternatively, have suggested that acinar cells themselves are capable of maintaining SG homeostasis through self-replication (17,18). Regardless of the predominant viewpoints, the apparent lack of ability of SGSCs to maintain SG homeostasis in primary SS has never been explained, and likely contributes to hyposalivation development in primary SS. In this study, we used protocols for SGSC isolation recently developed by us and others (12–14,16,19) to probe the involvement of SGSCs in primary SS. We demonstrate that SGSCs in primary SS are likely to be senescent, a phenotype that may be induced by exposure to primary SS–associated proinflammatory cytokines.

PATIENTS AND METHODS

Source of SG tissue. For healthy control specimens, biopsy samples of parotid SG tissue were obtained from donors (after informed consent and institutional review board [IRB] approval) who were treated for a squamous cell carcinoma of the oral cavity. In these patients, an elective head and neck dissection procedure was performed. During this procedure, a parotid SG is exposed and removed. This tissue does not contain malignant cells, as oral squamous cell carcinoma does not disseminate to the parotid SG. To obtain study samples from patients with primary and incomplete primary SS, specimens were obtained during the routine diagnostic evaluation for primary SS. Patients were classified as having primary SS if they fulfilled the 2016 American College of Rheumatology (ACR)/European League Against Rheumatism (EULAR) criteria (20). Patients classified as having incomplete primary SS did not fulfill these criteria and were not taking hyposalivation-inducing medication, but they did demonstrate either objective symptoms of dry mouth or SSA autoantibody presence. IRB approval was obtained, and all patients with primary SS and incomplete primary SS provided informed consent (METc 2016/010).

Stem cell isolation. Parotid SG biopsy samples harvested from oral squamous cell cancer patients with healthy parotid gland tissue and samples obtained from patients with primary SS and incomplete primary SS after surgery were processed in Hanks' balanced salt solution (HBSS) containing 1% bovine serum albumin (BSA; Invitrogen). Biopsy samples were digest-

ed mechanically using a gentleMACS dissociator (Miltenyi Biotec) or manually with scissors and simultaneously digested in HBSS/1% BSA buffer containing 0.63 mg/ml type II collagenase (Invitrogen) and 0.5 mg/ml hyaluronidase (Sigma-Aldrich), as well as calcium chloride at a final concentration of 6.25 mM, for 30 minutes at 37°C. Forty milligrams of tissue was processed per 1 ml buffer volume; total volume was adjusted according to biopsy sample weight. Digested cells were collected by centrifugation, washed twice in HBSS/1% BSA solution, and passed through 100-μm cell strainers (BD Biosciences).

The resultant cell suspensions were collected again by centrifugation and resuspended in SGSC medium consisting of 40% Dulbecco's modified Eagle's medium/F-12 medium, penicillin/streptomycin antibiotics (Invitrogen), Glutamax (Invitrogen), 50% Wnt-3a–conditioned medium, 10% R-spondin–conditioned medium (derived from the RSPO1 cell line; AMSBIO), 20 ng/ml epidermal growth factor (Sigma-Aldrich), 20 ng/ml fibroblast growth factor 2 (Sigma-Aldrich), N2 (Invitrogen), 10 mg/ml insulin (Sigma-Aldrich), 1 mM dexamethasone (Sigma-Aldrich), 10 μM Rho kinase inhibitor (Abcam), 5 μM transforming growth factor β inhibitor (catalog no. A8301; ToCris Bioscience), and 12.5 ng/ml Noggin (PeproTech). A total of 800,000 primary isolate cells were resuspended in 25 μl of SGSC medium combined with 50 μl of basement membrane Matrigel (BD Biosciences) and deposited in the center of 12-well tissue culture plates. After the gels were allowed to solidify (20 minutes at 37°C), 1 ml of stem cell medium was added per well. After 3–5 days of culture, the formed primary spheres were released from Matrigel by incubation in 1 mg/ml Dispase (Sigma) (1 hour at 37°C). Primary spheres of a minimum size of 50 μM were counted and used to establish primary sphere yield per milligram of biopsy material. To correct primary sphere yield for the site of biopsy, the primary sphere yields for healthy control samples and primary SS samples were multiplied by factors of 4.1 and 11.95, respectively. Multiplication factors were derived from the yield of primary spheres isolated from the SGSC-rich area, as described by van Luijk et al (21).

Cytospot preparation and quantification. A total of 100 μl of cell suspension obtained after SGSC isolation was added into a cytospin funnel, after prewetting of coated microscope slides with 1% BSA/phosphate buffered saline (PBS) solution. After centrifugation at 300 revolutions per minute for 2 minutes, slides were air dried and fixed with 4% paraformaldehyde (PFA) at room temperature for 20 minutes. Hematoxylin and eosin staining was then performed according to standard protocols. The number of acinar and ductal cells was determined by capturing images of 3 areas of the cytospot per sample. The total cell number in each area was determined by counting hematoxylin-stained nuclei. Acinar cells were identified by characteristic triangular morphology and predominant hematoxylin staining. Ductal cells were identified by heavily eosin-stained cytoplasm. The proportion of each cell type was expressed as

the percentage of total cells. For CD45+ cell quantification, cytospots were fixed as described above, then permeabilized in 100% ethanol (20 minutes at –20°C), washed in PBS, and then incubated in mouse anti-CD45 antibody (Dako) (1 hour at room temperature), diluted 1:100 in 1% BSA containing 0.05% Tween. Following PBS washing, Alexa Fluor 488–conjugated goat anti-mouse secondary antibody was added onto cytospots at 1:300 dilution in 1% BSA/0.05 PBS containing Tween and incubated at room temperature for 1 hour. Following final PBS washes, nuclei were counterstained with DAPI, and cytospots were visualized using a Leica 6000 Series microscope.

Flow cytometry and fluorescence-activated cell sorting (FACS) of SG isolate. After isolation, cell suspensions were dispersed to single cells. Cells were immunolabeled with antibodies against the following human proteins, conjugated to fluorophores as indicated: eFluor 660–conjugated epithelial cell adhesion molecule (EpCAM) (1:20; eBioscience), phycoerythrin (PE)–Cy5–conjugated CD45 (1:50; BioLegend), BUV737-conjugated CD19 (1:50; eBioscience), allophycocyanin (APC)–eF700–conjugated CD3 (1:50; eBioscience), PE-Cy7–conjugated CD56 (1:50; BioLegend), APC-eF780–conjugated CD4 (1:50; eBioscience), PE-Cy7–CD24 (1:20; BioLegend), and fluorescein isothiocyanate –conjugated Ki-67 (1:200; ThermoFisher Scientific). For intranuclear staining for Ki-67, a Foxp3 Transcription Factor Buffer Set was used, according to the instructions of the manufacturer (eBioscience). Staining for K14 and smooth muscle actin (SMA) was performed in 2 steps using rabbit anti-human K14 (1:100; Abcam) and mouse anti-human SMA (1:100; Dako) and Alexa Fluor 647–conjugated secondary antibody (1:300). Antibodies were added in a total volume of 100 µl 0.5% BSA/PBS with 2 mM EDTA (staining buffer), containing a maximum of 1 million cells. Staining was performed for 20 minutes on ice. Cells were collected by centrifugation and resuspended in staining buffer for analysis with an LSRII flow cytometer (BD Bioscience).

Living–dead discrimination was performed using 80 ng/ml propidium iodide (ThermoFisher). For FACS sorting of EpCAM+ cells from SG isolate, staining was performed as described above, with the addition of 0.1M magnesium sulfate and 50 µg/ml DNase (both from Sigma) into cell suspension to prevent cell clumping. Collected CD45+ cells were harvested into stem cell medium collected by centrifugation and plated into Matrigel as described above. The gating strategy for flow cytometric analysis and FACS is shown in Supplementary Figure 1, available on the Arthritis & Rheumatology web site at http://onlinelibrary.wiley.com/doi/10.1002/art.40659/abstract.

Self-renewal. Following the release of primary spheres from Matrigel as described above, cells were dispersed to form single-cell suspensions using 0.05% trypsin–EDTA (Invitrogen), enumerated, and concentrations adjusted to 0.4×10^6 cells per ml in SGSC medium. Twenty-five microliters of this cell solu-

tion was combined with 50-µl volumes of basement membrane Matrigel and deposited in the center of 12-well tissue culture plates. After the Matrigel was solidified for 20 minutes at 37°C, gels were covered in stem cell medium as described above. Organoids appeared 2–3 days after seeding of single cells in Matrigel. Ten days after seeding, Matrigel was dissolved by incubation with Dispase enzyme as described above. Organoids >50 µM in diameter were enumerated, cells were processed to a single-cell suspension using 0.05% trypsin–EDTA, and cell numbers were determined. These data were used to generate the organoid formation efficiency and population doublings. Population doublings (pds) were calculated according to the following formula:

$$pds = \frac{\ln 2 \ (\text{harvested cells/seeded cells})}{\ln 2}$$

Encapsulation in Matrigel was repeated to generate the next passage. This cycle was repeated 4 times (4 passages). At the end of each passage, an image of the cells was captured using an Olympus CKX53 microscope and DP2-SAL software.

Mature organoid formation assay. For mature organoid formation assays, organoid cultures were supplemented with 1 µM isoproterenol. Mature organoid formation was monitored over a 2-week period.

RNA sequencing. Total RNA was extracted from stem cells using an Absolutely RNA Miniprep Kit (catalog no. 400800), according to the instructions of the manufacturer (Agilent). The integrity of RNA was examined with an Agilent 2100 Bioanalyzer. Subsequent sequencing was performed using a SMART-Seq v4 Ultra Low Input RNA Kit (catalog no. 634890; Clontech) and a Nextera XT DNA Library Prep Kit (catalog no. FC-131-1096; Illumina) according to the instructions of the manufacturers, and prepared DNA libraries were sequenced on a HiSeq 2500 system. Data quality assessment was performed to understand the main source of variability, and differential expression analysis and visualization were performed in R (packages PVCA, EdgeR, and PHeatmap). The MetaCore pathway database was used for pathway enrichment analysis; data can be accessed via the NCBI Sequence Reads Archive (accession no. PRJNA506620).

Cytokine incubations with SGSCs. Cytokines were purchased as follows: human interleukin-6 (IL-6) (catalog no. 200-06A; PeproTech), human interferon-α (IFNα) (catalog no. 11100-1; R&D Systems), and human tumor necrosis factor (TNF) (catalog no. 300-01A; PeproTech) and reconstituted according to the instructions of the manufacturers. Dilutions for coculture with cytokines were performed in such a manner that the volume of cytokine added to the medium was always

1% of the total medium volume. The medium was refreshed 2 times within the passage (days 3 and 6), in parallel with control cultures.

Whole-mount and tissue immunocytochemistry. Mature organoids were released from Matrigel using Dispase, collected in round-bottomed 96-well plates, and fixed in 2% PFA for 10 minutes. Frozen tissue sections were cut at a thickness of 8 μ*M* and fixed in 2% PFA for 5 minutes. Staining for all samples was performed from this point, using a Tyramide Signal Amplification Kit according to the instructions of the manufacturer (ThermoFisher). After hydrogen peroxide blocking and general blocking, primary antibodies were incubated with organoids, mature organoids, or tissue sections overnight in PBS at 4°C. Dilutions of primary antibodies used for immunostaining were as follows: rabbit anti-human amylase (1:100) (catalog no. A2863; Sigma), rabbit anti-human aquaporin 5, rabbit anti-human EpCAM, mouse anti-human IL-6 receptor (1:100) (clone B-R6; ThermoFisher), mouse anti-human TNF receptor type I (clone H398;ThermoFisher), rabbit anti-human IFNα receptor (1:100) (catalog no. 62693; Abcam), mouse anti-human p16 (1:100) (catalog no. 54210; Abcam), and mouse anti-human SMA (1:100) (catalog no. M0851; Dako). Nuclear counterstaining was performed with Hoechst 33342, at a 1:300 dilution from 10 mg/ml stock solution, for 10 minutes at room temperature. Immunostainings were visualized using a Leica TCS SP8 confocal laser scanning microscope and Leica Application Suite software.

Telomere analysis. DNA was extracted from human SGSCs using a QIAamp DNA Micro Kit (Qiagen). Single telomere length analysis (STELA) was carried out at the XpYp telomere as described previously by Capper et al (22). Briefly, 1 μ*M* Telorette 2 linker was added to 10 ng of purified genomic DNA in a final volume of 40 μl per sample. Multiple polymerase chain reactions (PCRs) were performed for each test DNA in 10-μl volumes, incorporating 250 pg of DNA, 0.5 μ*M* telomere-adjacent and Tel-tail primers, 75 m*M* Tris HCl (pH 8.8), 20 m*M* (NH$_4$)$_2$SO$_4$, 0.01% Tween 20, 1.5 m*M* MgCl$_2$, and 0.5 units of a 10:1 mixture of Taq (ABgene) and Pwo polymerase (Roche Molecular Biochemicals). The reactions were processed in a Tetrad2 Thermal Cycler (Bio-Rad). DNA fragments were resolved by 0.5% Tris–acetate–EDTA agarose gel electrophoresis and identified by Southern hybridization with a random-primed a-^{33}P-labeled (PerkinElmer) TTAGGG repeat probe, together with probes specific for the 1 kb (Stratagene) and 2.5 kb (Bio-Rad) molecular weight markers. Hybridized fragments were detected using a Typhoon FLA 9500 Phosphorimager (GE Healthcare). The molecular weights of the DNA fragments were calculated using a Phoretix 1D Quantifier (Nonlinear Dynamics).

Quantitative PCR (qPCR). Total RNA was extracted from cultured cells using an RNeasy Microkit, including DNase incubation, according to the instructions of the manufacturer

(Qiagen). One microgram of total RNA was reverse transcribed to complementary DNA (cDNA) using 0.5 μg of oligo(dT)$_{15-18}$ primers, 1.0 m*M* dNTPs, 1× Reaction Buffer, 20 units of RiboLock, and 200 units of RevertAid reverse transcriptase (all from ThermoFisher Scientific) in a total volume of 20 μl per reaction. The cDNA product was diluted 10-fold in water and used at this concentration for qPCR. Qualitative PCR was performed using SsoAdvanced Universal SYBR Green qPCR Master Mix (Bio-Rad), with primers at a final concentration of 500 n*M* from a 10 μ*M* stock. Diluted cDNA (2.5 μl) was used per reaction, and all reactions were performed in triplicate in a total volume of 10 μl. Primer sequences are shown in Supplementary Table 1, available on the *Arthritis & Rheumatology* web site at http://onlinelibrary.wiley.com/doi/10.1002/art.40659/abstract. A 2-step qPCR cycle with a Bio-Rad iCycler qPCR machine was used for target amplification, according to the instructions of the manufacturer for SSoAdvanced Universal SYBR Green Master Mix, and CFX Manager was used for analysis.

RESULTS

Reduced regenerative potential shown by SGSCs from patients with primary SS. We began by isolating SGSCs from parotid SG biopsy samples from control patients with healthy SGs and patients with primary SS fulfilling the ACR/EULAR classification criteria (20). SGSCs were initially cultured from processed biopsy samples as primary spheres in Wnt-containing medium. Three to 5 days later, spheres were dispersed to single SGSCs and expanded in a "self-renewal assay." The cell suspension generated by the isolation process from primary SS biopsy samples contained significantly fewer epithelial cells than healthy control biopsy samples and significantly more CD45+ leukocytes, based on cell morphology and immunostaining on cytospots (Supplementary Figures 2 and 3A–C, available on the *Arthritis & Rheumatology* web site at http://onlinelibrary.wiley.com/doi/10.1002/art.40659/abstract). As previously reported for minor SGs (23), we detected a high proportion of B cells and a predominance of CD4+ T cells within the flow cytometry–defined CD45+ fraction of the biopsy isolate (Supplementary Figure 3D and E, available at http://onlinelibrary.wiley.com/doi/10.1002/art.40659/abstract). SGSCs are EpCAM[high] in nature. The number of both spheres generated per EpCAM[high] cell and yield of spheres per milligram of biopsy sample was significantly lower (a 10-fold difference) in samples from patients with primary SS compared to the healthy samples (Figures 1A and B, and Supplementary Figure 3F, available at http://onlinelibrary.wiley.com/doi/10.1002/art.40659/abstract).

(Data are presented as normalized to milligrams of tissue to take into account the larger size of the healthy SG biopsy samples obtained.) Primary sphere yield was not correlated with focus score (lymphocytic infiltration) (Supplementary Figure 3G, available at http://onlinelibrary.wiley.com/doi/10.1002/art.40659/
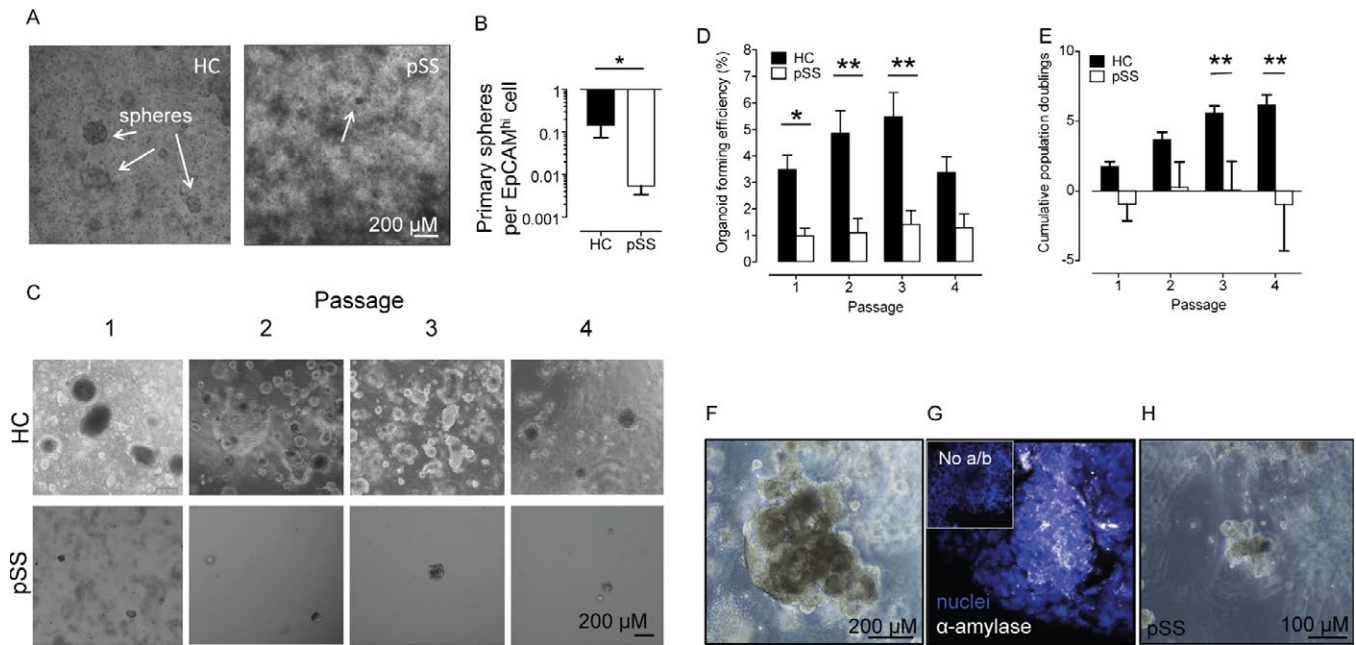
Figure 1. Salivary gland stem cells (SGSCs) from patients with primary Sjögren's syndrome (pSS) show reduced regenerative potential. **A**, Microscopy of primary spheres isolated from SGSCs from a healthy control (HC) (left) and a patient with primary SS (right). **Arrows** show organoids. **B**, Quantification of primary sphere yield per epithelial cell adhesion molecule (EpCAM^{high}) cell in SGSC isolates from biopsy samples from healthy controls (n = 6) and patients with primary SS (n = 9). * = $P < 0.05$ by Student's t-test. **C**, Microscopy of organoid cultures of SGSCs from a healthy control and a patient with primary SS. **D**, Organoid-forming efficiency of SGSCs in cultures of biopsy tissue from healthy controls (n = 27 at passages 1–4) and patients with primary SS (n = 12, 16, 9, and 6 at passages 1–4, respectively). * = $P < 0.05$; ** = $P < 0.01$ by two-way analysis of variance (ANOVA) with Bonferroni post hoc testing. **E**, Cumulative population doublings of SGSCs from healthy controls (n = 26 at passages 1–3; n = 24 at passage 4) and patients with primary SS (n = 10, 5, 4, and 2 at passages 1–4, respectively). ** = $P < 0.01$ by two-way ANOVA with Bonferroni post hoc testing. **F**, Phase-contrast microscopy of mature organoids formed from SGSCs from a healthy control. **G**, Immunocytochemical staining of acinar cell–associated amylase in a healthy control SG sample–derived mature organoid. **Inset** shows a healthy control SG sample without anti-amylase antibody (a/b) to demonstrate staining specificity. **H**, Diminished ability to form mature organoids from primary SS SGSCs. Values in **B**, **D**, and **E**, are the mean ± SEM.

abstract), supporting the notion that infiltration does not determine SG function. We have previously demonstrated that SGSC yield decreases with age and that more SGSCs are present closest to the facial nerve in the parotid gland (21,24). Neither donor age nor biopsy site was responsible for the decreased yield of SGSCs from primary SS biopsy samples (Supplementary Figures 3H and I, available at http://onlinelibrary.wiley.com/doi/10.1002/art.40659/abstract). Stem cells are classically defined by their ability to proliferate and differentiate. When SGSCs from primary SS biopsies were cultured as organoids to assess their proliferation capacity, we observed a significantly (up to 5 times) lower self-renewal capability compared to healthy samples (Figures 1C–E) Thus,. FACS selection of EpCAM^{high} cells from primary SS biopsies, after removal of infiltrating leukocytes, did not rescue the self-renewal potential of primary SS SGSCs (Supplementary Figure 3, http://onlinelibrary.wiley.com/doi/10.1002/art.40659/abstract), indicating that the sole presence of CD45+ cells in SGs of patients with primary SS is not responsible for the regenerative deficits observed.

Healthy SGSCs could be induced to proliferate and differentiate from organoids into α-amylase–expressing mature or-

ganoids (Figures 1F and G). The lack of proliferative capabilities of SGSCs from primary SS biopsies was reflected also in their greatly diminished ability to form mature organoids (Figure 1H). These data imply that the relatively few SGSCs present in primary SS SGs also harbor defects in differentiation ability.

Extensive replicative history of SGSCs in primary SS. In order to elucidate the early events in SG pathology development in primary SS that are not influenced by mass lymphocytic infiltration, we focused on patients classified as having incomplete primary SS. These patients have some hallmarks of primary SS (outlined in Supplementary Table 2, available on the *Arthritis & Rheumatology* web site at http://onlinelibrary.wiley.com/doi/10.1002/art.40659/abstract) but do not have a positive lymphocyte focus score. Also, the patients with incomplete primary SS were not taking medication known to cause dry mouth symptoms, they all had recorded symptoms of dry eyes and mouth associated with primary SS development, and they did not fulfill the ACR/EULAR criteria. We consider these features indicative of early SG pathology development in primary SS. When SGSCs were isolated from the patients with incomplete primary
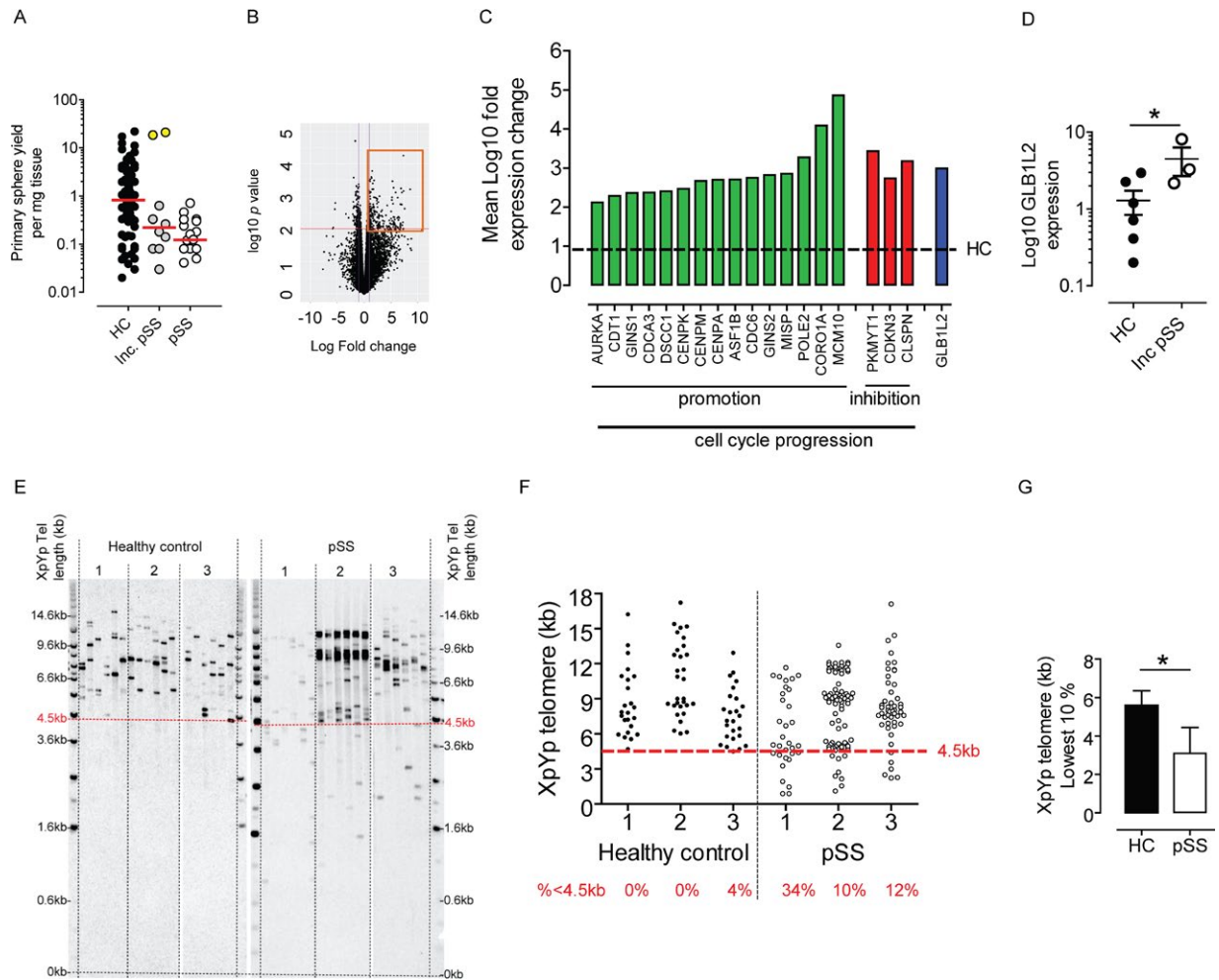
Figure 2. Salivary gland stem cells (SGSCs) from patients with primary Sjögren's syndrome (pSS) are more likely to be senescent. **A**, Primary sphere yield in SGSCs from healthy controls (HC) (n = 73), patients with incomplete (Inc.) primary SS (n = 10), and patients with primary SS (n = 18). Symbols represent individual spheres. Yellow circles show SGSCs with unusually high yield. Red lines show the median. The primary SS group from Figure 1B is used for comparison. **B**, Volcano plot resulting from RNA sequencing analysis comparing SGSC transcriptomes in biopsy samples from healthy controls and patients with incomplete primary SS. Boxed area denotes genes whose expression is $\geq \log_{10}$ 2-fold higher in primary SS SGSCs. Red line shows P value cutoff threshold ($P < 0.01$). **C**, Up-regulation of cell cycle progression promotion genes (green) and inhibition genes (red) identified from RNA sequencing, including the β-galactosidase–like gene (GLB1L2) (blue). Broken line represents the mean expression level in healthy controls (n = 6 individual samples from healthy controls; n = 3 samples from patients with primary SS). **D**, Raw expression values for GLB1L2. Symbols represent individual samples from healthy controls (n = 6) and patients with primary SS) (n = 3). Bars show the mean ± SEM. **E**, Single telomere length analysis of SGSC telomere lengths in biopsy samples from healthy controls and patients with biopsy-proven primary SS, showing outlying small (<4.5 kb) telomeres (red dotted line) in primary SS SGSCs. **F**, Quantification of telomere lengths in SGSCs from healthy controls and patients with primary SS. Red text denotes percentage of telomeres with length <4.5 kb (broken line). Symbols represent individual samples. **G**, Length analysis of lowest 10% of telomeres in SGSCs from healthy controls and patients with biopsy-proven primary SS (n = 3 per group). Values are the mean ± SEM. * = $P \leq 0.05$ by Student's t-test.

SS we observed that the primary sphere yield from a small proportion (2 of 10) of these biopsy samples was markedly greater than the median of the healthy control samples (Figure 2A). The yield of primary spheres from the remaining biopsy samples was comparable to the biopsy yield from the patients with primary SS. Reasoning that the 2 (of 10) patients with the high yield represent an earlier disease stage (25), we theorized that SGSCs receive mitotic stimuli early in primary SS. We performed RNA sequencing on organoids cultured from patients with incomplete primary SS to investigate early events in primary SS, and we observed

a cohort of 101 significantly up-regulated genes in SGSCs from biopsy-negative patients compared to healthy control samples ($P < 0.01$, $\log_{10}$-fold change ≥2) (Figure 2B).

On further examination, we found that 18 of these genes were involved in cell cycle progression (both its promotion and inhibition) and DNA replication (Figure 2C and Supplementary Figure 4, available on the *Arthritis & Rheumatology* web site at http://onlinelibrary.wiley.com/doi/10.1002/art.40659/abstract). As shown in Figures 2C and D, the β-galactosidase–like gene GLB1L2 was also significantly up-regulated. Beta galactosidase

expression is associated with cellular senescence and aging. Hypothesizing that SGSCs in primary SS disease progression become senescent, we examined the telomere lengths of organoids cultured from patients with primary SS with positive SG

biopsy evaluations (i.e., with lymphocytic infiltration), representing a later phase of primary SS in terms of SG pathology. STELA analysis of telomere length revealed short telomeres of <4.5 kb in length in SGSCs from biopsy-positive patients with primary SS
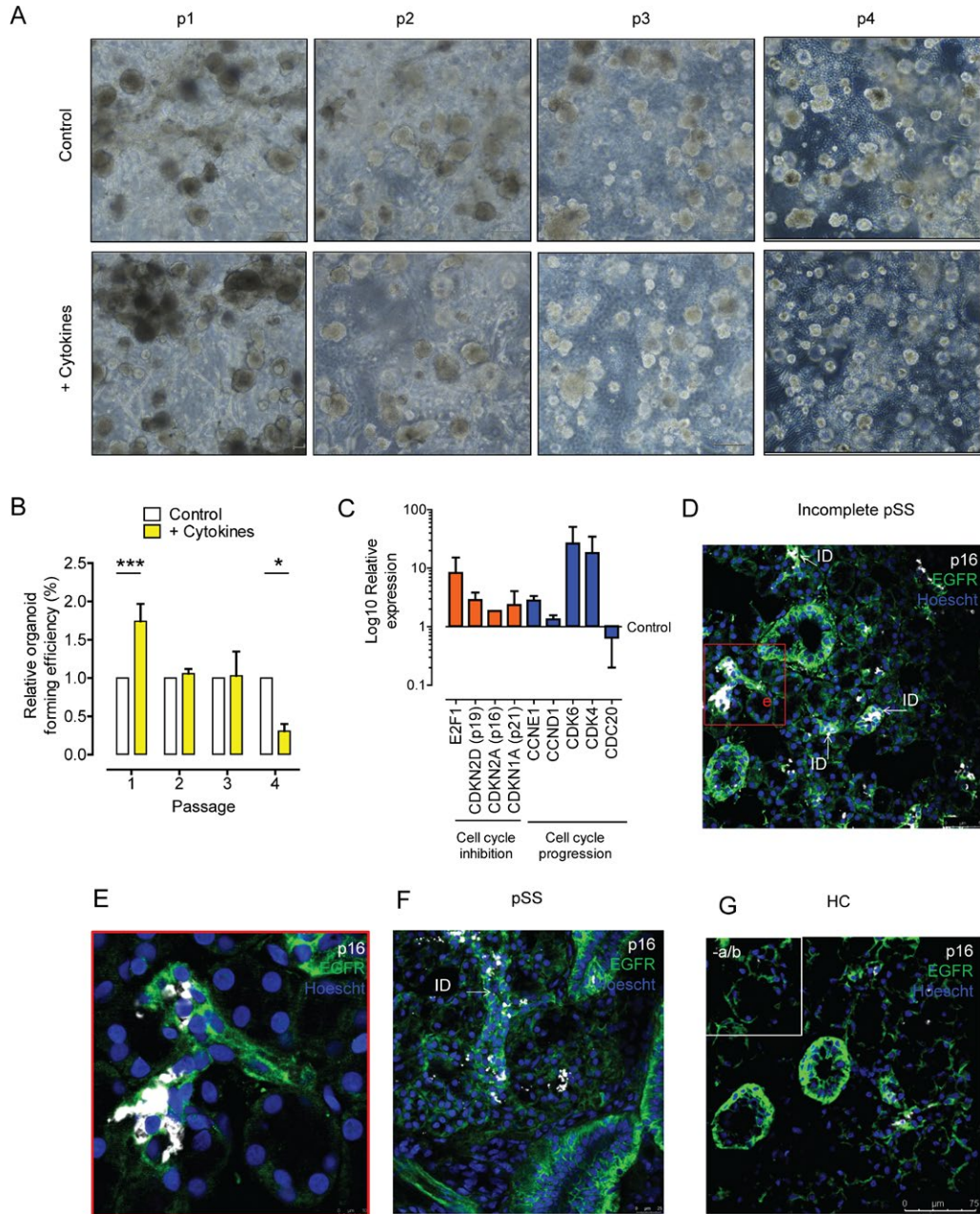
Figure 3. Parotid salivary gland stem cell (SGSC) organoid cultures proliferate upon exposure to a proinflammatory cytokine cocktail and express cell cycle and senescence genes. P16+ senescent cells localize to the intercalated ducts (IDs) in SG tissue from patients with incomplete primary Sjögren's syndrome (pSS) and patients with primary SS. **A**, Phase-contrast microscopy of SGSCs from a healthy control at passages 1–4, incubated with (+ Cytokines) and without (Control) the proinflammatory cytokine cocktail. **B**, Quantification of organoid formation efficiency of SGSCs exposed to proinflammatory cytokines compared to control cells; (n = ≥7 separate cell sample isolations at each passage). Bars show the mean ± SEM. * = $P < 0.05$; *** = $P < 0.001$ by two-way analysis of variance. **C**, Expression of cell cycle–associated genes in SGSCs exposed to proinflammatory cytokines. Cells were harvested at the end of passage 1 for quantitative polymerase chain reaction analysis. Bars show the mean ± SEM (n = 2 separate cell sample isolations). **D–G**, Immunohistochemical staining for p16 senescence marker in SG tissue from a patient with incomplete primary SS (**D**; **D inset** shown in **E**), a patient with primary SS (**F**), and a healthy control (HC) (**G**), counterstained with epithelial growth factor receptor (EGFR) to mark all ductal cells. **Inset** in **G** shows SG tissue from a healthy control without antibody (−a/b) staining, to demonstrate specificity. Ages of tissue donors were 50, 73, and 31 years for the healthy control, patient with incomplete primary SS, and patient with primary SS, respectively, indicating that the increase in p16+ ID cells could not be attributed to the advanced age of the donor.

(Figures 2E and F(and clinical characteristics shown in Supplementary Table 2, available on the *Arthritis & Rheumatology* web site at http://onlinelibrary.wiley.com/doi/10.1002/art.40659/abstract). The mean length of the lowest 10% of telomeres in the SGSCs of healthy control samples was significantly greater (5.58 kb) compared to primary SS SGSCs (3.10 kb) (Figure 2G), suggesting that primary SS SGSCs have a more extensive replicative history. The mean ages of healthy control sample donors and primary SS SGSC donors in whom telomere analysis was performed were 77.3 and 61.5 years, respectively, confirming that telomere difference was not due to the advanced age of SGSC donors with primary SS.

Proinflammatory cytokines include proliferation and differentiation of healthy SGSCs. Primary SS is an autoimmune disease associated with the glandular presence of classic proinflammatory cytokines, as exemplified by IFNα, TNF, and IL-6 (23). Proinflammatory cytokines within the glandular tissue could provide mitotic signals, driving SGSC exhaustion in primary SS and leading to a senescent, aging-like phenotype and ultimately hyposalivation. Considering the low yield of SGSCs from patients with primary SS, and in order to model the earliest phases of primary SS, we employed healthy control SGSC cultures to investigate this hypothesis. Quantitative PCR and immunostaining of healthy control SGSC organoids at passage 2 demonstrated that healthy control SGSCs express receptors for the proinflammatory cytokines IFNα, TNF, and IL-6 (see Supplementary Figure 5 and [for primers] Supplementary Table 1, available on the *Arthritis & Rheumatology* web site at http://onlinelibrary.wiley.com/doi/10.1002/art.40659/abstract). When healthy control SGSCs from passages 1–4 were incubated with a cocktail of proinflammatory cytokines at concentrations matching those found in the serum of patients with primary SS (IFNα 500 pg/ml, TNF 40 pg/ml, and IL-6 30 pg/ml) (26), we observed initially a significant increase in organoid formation efficiency, followed by a decrease to significantly below the levels in control cells (Figures 3A and B). Incubation with single cytokines did not induce significant proliferative effects, even at higher doses (see Supplementary Figure 6, available at http://onlinelibrary.wiley.com/doi/10.1002/art.40659/abstract).

At passage 1 following cytokine exposure, expression of genes promoting cell cycle progression (CDK4, CDK6, and CDC20), inhibiting cell cycle (E2F1 and CDKN2D), and promoting senescence (p16 and p21) was up-regulated (Figure 3C). Through definition of SGSC subsets using cell surface markers and costaining with the proliferation marker Ki-67 (see Supplementary Figures 7A and B, available at http://onlinelibrary.wiley.com/doi/10.1002/art.40659/abstract), we also showed that SGSCs resident in the basal layer of striated ducts (BSD cells) were responsible for the proliferation observed (Supplementary Figure 7C, available at http://onlinelibrary.wiley.com/doi/10.1002/art.40659/abstract). We also suggest that proin-

flammatory cytokines induce differentiation of BSD cells into intercalated ducts (ID cells) (Supplementary Figure s 7C and D. Finally, p16 immunostaining was performed on sections of SG tissue in order to determine where senescent cells were located in situ; p16+ cells were found mostly in intercalated ducts in incomplete and complete primary SS tissue. In contrast, p16+ cells in healthy SGs were found dispersed through the tissue (Figures 3D–G), illustrating their full differentiation potential.

DISCUSSION

The origins of hyposalivation development in primary SS have never been fully elucidated, although many studies have now firmly established that its development cannot be fully explained by the extent of lymphocytic infiltration (3–9). Using SGSCs as a tool to probe SG dysfunction in primary SS, we showed in the present study that parotid gland biopsy samples from patients with primary SS contain fewer SGSCs with reduced proliferation, differentiation potential, and shortened telomeres. Shortened telomeres imply that the SGSC pool has an extensive replicative history, the reason for which we propose is 2-fold.

First, the parenchymal epithelium, e.g., the non-stem ductal cells and saliva-producing acinar cells in primary SS, have been demonstrated to undergo enhanced levels of apoptosis, from sources intrinsic and extrinsic to the cells themselves. Extrinsically, the action of cytokines, cytotoxic T cells, and natural killer cells all promote apoptosis (27). Additionally, a disorganized extracellular matrix in primary SS SGs may account for acinar cell loss by anoikis (28). Epithelial cells have been shown to intrinsically express defective levels of the antiinflammatory mediator peroxisome proliferator–activated receptor γ, resulting in increased activity of the NF-κB and IL-6 pathways, but also rendering them more susceptible to cell death (29–34). Similarly, levels of the ubiquitin-editing protein A20, a negative regulator of NF-κB, were down-regulated in SG epithelial cells from patients with primary SS compared to healthy subjects (35). Therefore, depletion of the parenchymal cell pool via intrinsic and extrinsic mechanisms together likely stimulates SGSC proliferation and differentiation into acinar cells, in an attempt to maintain the saliva-producing capacity of the SGs.

Second, as we have demonstrated here, proinflammatory cytokines exert a direct effect on proliferation of SGSCs. In other model systems, and most extensively in the well-characterized intestinal stem cell niche, proinflammatory cytokines have also been shown to exert a proliferative effect, mediated by modulation of the stem cell–associated Wnt, Notch, and Yes-associated protein/transcriptional co-activator with PDZ-binding motif (YAP/TAZ) pathways, suggesting that cross-talk between stem cells and the elements of the immune system may underlie many disease manifestations (36–40). Cytokine production in the case of primary SS may be derived from neighboring epithelial cells signaling in

a paracrine manner. The production and secretion of proinflammatory cytokines by epithelial cells has been demonstrated in long-term epithelial culture systems and in situ (32,41–44). Following the release of damage- and pathogen-associated molecular patterns, e.g., molecules such as high mobility group box chromosomal protein 1 and viral antigens, pattern recognition receptors on epithelial cells may be activated, culminating in epithelial cell autonomous NF-κB pathway activity, cytokine production, and paracrine signaling to neighboring SGSCs (33,34). Indeed, the dysregulated NF-κB pathway seen in primary SS may account for the sustained proinflammatory cytokine production by glandular epithelial cells (33,35).

One prevailing theory regarding stem cells dictates that under healthy conditions, SGSCs reside in the striated ducts, proliferate and differentiate into intercalated ducts, and then finally into saliva-producing acinar cells. We have demonstrated the presence of senescent cells in intercalated ducts of primary SS SGs. This presence suggests a blockade in the ability of SGSCs to further differentiate into acinar cells, presumably due to having reached their regenerative limit, similar to the poor mature organoid differentiation potential we demonstrated in vitro. Clinically, our data suggest that screening patient SGs or saliva for senescence biomarker expression may indicate the extent of SGSC exhaustion. We further suggest that clinical interventions aimed at preventing hyposalivation development need to occur before the appearance of high levels of senescent markers in SGs or saliva. The present study findings also suggest, critically, that effective interventions to cure established hyposalivation by targeting the inflammatory process are not likely to involve only immune signal blockade, but rather the replenishment of SGSC stocks in conjunction with resolving the inflammation. Plausible strategies include the use of induced pluripotent stem cell technologies in the manufacture of SGSCs.

In conclusion, we have demonstrated for the first time an aging phenotype as a potential causative agent for the lack of SG repair in the autoimmune disease primary SS, and link this finding to possible future clinical strategies.

ACKNOWLEDGMENTS

AUTHOR CONTRIBUTIONS

All authors were involved in drafting the article or revising it critically for important intellectual content, and all authors approved the final version to be submitted for publication. Dr. Pringle had full access to all of the data in the study and takes responsibility for the integrity of the data and the accuracy of the data analysis.

Study conception and design. Pringle, Wang, Verstappen, Terpstra, Zhang, He, Patel, Jones, Baird, Spijkervet, Vissink, Bootsma, Coppes, Kroese.
Acquisition of data. Pringle, Wang, Verstappen, Terpstra, Zhang, He, Patel, Jones.
Analysis and interpretation of data. Pringle.

ROLE OF THE STUDY SPONSOR

REFERENCES

1. Helmick CG, Felson DT, Lawrence RC, Gabriel S, Hirsch R, Kwoh CK, et al. Estimates of the prevalence of arthritis and other rheumatic conditions in the United States: part I. Arthritis Rheum 2008;58: 15–25.

2. Kroese FG, Abdulahad WH, Haacke E, Bos NA, Vissink A, Bootsma H. B-cell hyperactivity in primary Sjögren's syndrome. Expert Rev Clin Immunol 2014;10:483–99.

3. Jonsson R, Kroneld U, Backman K, Magnusson M, Tarkowskit A. Progression of sialadenitis in Sjögren's sydrome. Br J Rheumatol 1993;32:578–81.

4. Dawson LJ, Fox PC, Smith PM. Sjögrens syndrome: the non-apoptotic model of glandular hypofunction. Rheumatology (Oxford) 2006;45:792–8.

5. Gannot G, Lancaster HE, Fox PC. Clinical course of primary Sjögren's syndrome: salivary, oral, and serologic aspects. J Rheumatol 2000;27: 1905–9.

6. Appel S, Le Hellard S, Bruland O, Brun JG, Omdal R, Kristjansdottir G, et al. Potential association of muscarinic receptor 3 gene variants with primary Sjögren's syndrome. Ann Rheum Dis 2011;70: 1327–9.

7. Theander E, Andersson SI, Manthorpe R, Jacobsson LT. Proposed core set of outcome measures in patients with primary Sjögren's syndrome: 5 year follow up. J Rheumatol 2005;32:1495–1502.

8. Haldorsen K, Moen K, Jacobsen H, Jonsson R, Brun JG. Exocrine function in primary Sjögren's syndrome: natural course and prognostic factors. Ann Rheum Dis 2008;67:949–54.

9. Pijpe J, Kalk WW, Bootsma H, Spijkervet FK, Kallenberg CG, Vissink A. Progression of salivary gland dysfunction in patients with Sjögren's syndrome. Ann Rheum Dis 2007;66:107–12.

10. Imrich R, Alevizos I, Bebris L, Goldstein DS, Holmes CS, Illei GG, et al. Predominant glandular cholinergic dysautonomia in patients with primary Sjögren's syndrome. Arthritis Rheumatol 2015;67:1345–52.

11. Nikolov NP, Illei GG. Pathogenesis of Sjögren's syndrome. Curr Opin Rheumatol 2009;21:465–70.

12. Lombaert IM, Brunsting JF, Wierenga PK, Faber H, Stokman MA, Kok T, et al. Rescue of salivary gland function after stem cell transplantation in irradiated glands. PLoS One 2008;3:e2063.

13. Pringle S, Maimets M, van der Zwaag M, Stokman MA, van Gosliga D, Zwart E, et al. Human salivary gland stem cells functionally restore radiation damaged salivary glands. Stem Cells 2016;34:640–52.

14. Pringle S, van Os R, Coppes RP. Adult salivary gland stem cells and a potential therapy for xerostomia. Stem Cells 2012;31:613–9.

15. Xiao N, Lin Y, Cao H, Sirjani D, Giaccia AJ, Koong AC, et al. Neurotrophic factor GDNF promotes survival of salivary stem cells. J Clin Invest 2014;124:3364–77.

16. Maimets M, Rocchi C, Bron R, Pringle S, Kuipers J, Giepmans BN, et al. Long-term in vitro expansion of salivary gland stem cells driven by Wnt signals. Stem Cell Reports 2016;6:150–62.

17. Emmerson E, May AJ, Berthoin L, Cruz-Pacheco N, Nathan S, Mattingly AJ, et al. Salivary glands regenerate after radiation injury through SOX2-mediated secretory cell replacement. EMBO Mol Med 2018;10:e8051.

18. Aure MH, Konieczny SF, Ovitt CE. Salivary gland homeostasis is maintained through acinar cell self-duplication. Dev Cell 2015;33:231–7.

19. Nanduri LS, Baanstra M, Faber H, Rocchi C, Zwart E, de Haan G, et al. Purification and ex vivo expansion of fully functional salivary gland stem cells. Cell Rep 2014;3:957–64.

20. Shiboski CH, Shiboski SC, Seror R, Criswell LA, Labetoulle M, Lietman TM, et al. 2016 American College of Rheumatology/European League Against Rheumatism classification criteria for primary Sjögren's syndrome: a consensus and data-driven methodology involving three international patient cohorts. Arthritis Rheumatol 2017;69:35–45.

21. Van Luijk P, Pringle S, Deasy JO, Moiseenko VV, Faber H, Hovan A, et al. Sparing the region of the salivary gland containing stem cells preserves saliva production after radiotherapy for head and neck cancer. Sci Transl Med 2015;7:305ra147.

22. Capper R, Britt-Compton B, Tankimanova M, Rowson J, Letsolo B, Man S, et al. The nature of telomere fusion and a definition of the critical telomere length in human cells. Genes Dev 2007;21:2495–508.

23. Mingueneau M, Boudaoud S, Haskett S, Reynolds TL, Nocturne G, Norton E, et al. Cytometry by time-of-flight immunophenotyping identifies a blood Sjögren's signature correlating with disease activity and glandular inflammation. J Allergy Clin Immunol 2016;137:1809–21.

24. Maimets M, Bron R, de Haan G, van Os R, Coppes RP. Similar ex vivo expansion and post-irradiation regenerative potential of juvenile and aged salivary gland stem cells. Radiother Oncol 2015;116:443–8.

25. Shiboski CH, Baer AN, Shiboski SC, Lam M, Challacombe S, Lanfranchi HE, et al. Natural history and predictors of progression to Sjögren's syndrome among participants of the SICCA registry. Arthritis Care Res (Hoboken) 2018;70:284–94.

26. Pollard RP, Abdulahad WH, Bootsma H, Meiners PM, Spijkervet FK, Huitema MG, et al. Predominantly proinflammatory cytokines decrease after B cell depletion therapy in patients with primary Sjögren's syndrome. Ann Rheum Dis 2013;72:2048–50.

27. Manganelli P, Fietta P. Apoptosis and Sjögren's syndrome. Semin Arthritis Rheum 2003;33:49–65.

28. Manoussakis MN, Spachidou MP, Maratheftis CI. Salivary epithelial cells from Sjogren's syndrome patients are highly sensitive to anoikis induced by TLR-3 ligation. J Autoimmun 2010;35:212–8.

29. Kyriakidis NC, Kapsogeorgou EK, Gourzi VC, Konsta OD, Baltatzis GE, Tzioufas AG. Toll-like receptor 3 stimulation promotes Ro52/TRIM21 synthesis and nuclear redistribution in salivary gland epithelial cells, partially via type I interferon pathway. Clin Exp Immunol 2014;178:548–60.

30. Manoussakis MN, Moutsopoulos HM. Sjögren's syndrome: autoimmune epithelitis. Baillieres Best Pract Res Clin Rheumatol 2000; 14:73–95.

31. Kapsogeorgou EK, Abu-Helu RF, Moutsopoulos HM, Manoussakis MN. Salivary gland epithelial cell exosomes: a source of autoantigenic ribonucleoproteins. Arthritis Rheum 2005;52:1517–21.

32. Spachidou MP, Bourazopoulou E, Maratheftis CI, Kapsogeorgou EK, Moutsopoulos HM, Tzioufas AG, et al. Expression of functional Toll-like receptors by salivary gland epithelial cells: increased mRNA expression in cells derived from patients with primary Sjögren's syndrome. Clin Exp Immunol 2007;147:497–503.

33. Vakrakou AG, Polyzos A, Kapsogeorgou EK, Thanos D, Manoussakis MN. Impaired anti-inflammatory activity of PPARγ in the salivary epithelia of Sjögren's syndrome patients imposed by intrinsic NF-κB activation. J Autoimmun 2018;86:62–74.

34. Goules AV, Kapsogeorgou EK, Tzioufas AG. Insight into pathogenesis of Sjögren's syndrome: dissection on autoimmune infiltrates and epithelial cells. Clin Immunol 2017;182:30–40.

35. Sisto M, Lisi S, Lofrumento DD, Ingravallo G, Maiorano E, D'Amore M. A failure of TNFAIP3 negative regulation maintains sustained NF-κB activation in Sjögren's syndrome. Histochem Cell Biol 2011;135: 615–25.

36. Nava P, Koch S, Laukoetter MG, Lee WY, Kolegraff K, Capaldo CT, et al. Interferon-γ regulates intestinal epithelial homeostasis through converging β-catenin signaling pathways. Immunity 2010;32:392–402.

37. Jeffery V, Goldson AJ, Dainty JR, Chieppa M, Sobolewski A. IL-6 signaling regulates small intestinal crypt homeostasis. J Immunol 2017;199:304–11.

38. Karin M, Clevers H. Reparative inflammation takes charge of tissue regeneration. Nature 2016;529:307–15.

39. Ando K, Kanazawa S, Tetsuka T, Ohta S, Jiang X, Tada T, et al. Induction of Notch signaling by tumor necrosis factor in rheumatoid synovial fibroblasts. Oncogene 2003;22:7796–803.

40. Cressman DE, Greenbaum LE, DeAngelis RA, Ciliberto G, Furth EE, Poli V, et al. Liver failure and defective hepatocyte regeneration in interleukin-6-deficient mice. Science 1996;274:1379–83.

41. Ittah M, Miceli-Richard C, Gottenberg JE, Lavie F, Lazure T, Ba N, et al. B cell-activating factor of the tumor necrosis factor family (BAFF) is expressed under stimulation by interferon in salivary gland epithelial cells in primary Sjögren's syndrome. Arthritis Res Ther 2006;8:R51.

42. Ittah M, Miceli-Richard C, Gottenberg JE, Sellam J, Eid P, Lebon P, et al. Viruses induce high expression of BAFF by salivary gland epithelial cells through TLR- and type-I IFN-dependent and -independent pathways. Eur J Immunol 2008;38:1058–64.

43. Ogawa N, Ping L, Zhenjun L, Takada Y, Sugai S. Involvement of the interferon-γ–induced T cell–attracting chemokines, interferon-γ–inducible 10-kd protein (CXCL10) and monokine induced by interferon-γ (CXCL9), in the salivary gland lesions of patients with Sjögren's syndrome. Arthritis Rheum 2002;46:2730–41.

44. Fox RI, Kang HI, Ando D, Abrams J, Pisa E. Cytokine mRNA expression in salivary gland biopsies of Sjögren's syndrome. J Immunol 1994;152:5532–9.

Efficacy and Safety of Febuxostat Extended and Immediate Release in Patients With Gout and Renal Impairment: A Phase III Placebo-Controlled Study

Kenneth G. Saag,[1] 🆔 Michael A. Becker,[2] Andrew Whelton,[3] Barbara Hunt,[4] Majin Castillo,[4] Krisztina Kisfalvi,[4] and Lhanoo Gunawardhana[4] 🆔

Objective. To assess the efficacy and safety of febuxostat extended release (XR) and immediate release (IR) in patients with gout and normal or impaired renal function.

Methods. This was a 3-month, phase III, multicenter, double-blind, placebo-controlled study. Patients (n = 1,790) with a history of gout and normal or impaired (mild-to-severe) renal function were randomized to receive placebo, febuxostat IR 40 or 80 mg, or febuxostat XR 40 or 80 mg once daily (1:1:1:1:1 ratio). End points included proportions of patients with a serum urate (UA) level of <5.0 mg/dl at month 3 (primary end point), a serum UA level of <6.0 mg/dl at month 3, and ≥1 gout flare requiring treatment over 3 months (secondary end points).

Results. Both febuxostat formulations led to significantly greater proportions of patients achieving a serum UA level of <5.0 mg/dl or <6.0 mg/dl at month 3 ($P < 0.001$ for all comparisons versus placebo). Equivalent doses of febuxostat XR and IR had similar treatment effects on serum UA level end points; however, a significantly greater proportion of patients achieved a serum UA level of <5.0 mg/dl with XR 40 mg versus IR 40 mg. Similar proportions of patients experienced ≥1 gout flare across treatment groups. Rates of treatment-emergent adverse events were low and evenly distributed between treatment arms. A preplanned subgroup analysis demonstrated that febuxostat formulations were well tolerated and generally effective on serum UA level end points (versus placebo) across all renal function subgroups.

Conclusion. Both formulations of febuxostat (XR and IR) were well tolerated and effective in patients with gout and normal or impaired renal function, including patients with severe renal impairment.

INTRODUCTION

Gout (urate crystal–induced arthritis) is a chronic disease associated with hyperuricemia, affecting approximately 8.3 million people in the US (1). Hyperuricemia is strongly linked to renal disease (2–7), and impaired renal function is an important risk factor for gout (8). It is estimated that approximately one-quarter of patients with gout have chronic stage ≥3 kidney disease (defined as an estimated glomerular filtration rate [eGFR] of <60 ml/minute/1.73 m²) (9). There is a clinical need for a well-tolerated

and effective treatment for hyperuricemia management in patients with gout and renal impairment.

Xanthine oxidase inhibitors, such as febuxostat immediate release (IR) and allopurinol, have been approved for the treatment of hyperuricemia (defined as serum urate [UA] levels above the limit of solubility [~6.8 mg/dl]) in patients with gout (10–13). Whereas febuxostat and allopurinol both lower urate levels by inhibiting xanthine oxidase, there are key differences in how they are metabolized and eliminated from the body in patients with renal impairment (10,13,14). Allopurinol and its principal active

metabolite (oxypurinol) are primarily removed through renal pathways, and concerns relating to high doses and increased risk of adverse events (AEs) have been reported (10,14,15).

However, a recent study evaluating allopurinol dose escalation using a treat-to-target approach demonstrated that higher doses of allopurinol significantly lowered serum UA levels and were well tolerated; dose escalation with allopurinol was not associated with any differences in renal function change compared with maintenance of allopurinol dose (16). Consequently, an initial dosage of <100 mg/day, followed by slow titration in line with renal function (to ≥300 mg/day), is suggested in patients with gout and moderate-to-severe kidney disease (11). Conversely, febuxostat is primarily eliminated via the liver through hepatobiliary conjugation, which is not affected by renal impairment (13,17).

The efficacy and tolerability of febuxostat IR 40 mg and 80 mg once daily are well established in patients with gout who have normal renal function or mild-to-moderate renal impairment (17–22). Additionally, results from a recent phase II study suggested that febuxostat IR (30 mg twice daily and 40/80 mg once daily [dosage based on serum UA level on study day 14: patients with serum UA <6.0 mg/dl continued on 40 mg once daily and those with serum UA ≥6.0 mg/dl received 80 mg once daily from month 1]) was well tolerated and associated with significant urate lowering, without any significant deterioration in renal function, versus placebo in patients with gout and moderate-to-severe renal impairment (12). However, further evidence of the efficacy and safety of febuxostat in patients with renal impairment is needed, especially for patients with severe renal impairment.

To reduce the potential risk of treatment-initiated gout flares caused by fluctuations in drug exposure levels with febuxostat IR, an extended release (XR) formulation of febuxostat was developed with the aim of providing comparable or greater urate lowering with more stable drug exposure. Results from a phase I trial demonstrated that the XR formulation was associated with reduced exposure to febuxostat compared with the IR formulation (23). It has been hypothesized that the more stable drug exposure and reduced variability in daily serum UA levels associated with febuxostat XR may reduce the incidence of urate crystal–mediated inflammation and development of gout flares. In a phase II trial, febuxostat IR 30 mg twice daily (used to mirror the effect of XR 80 mg once daily) was more effective at lowering serum UA compared with placebo in patients with moderate-to-severe renal impairment (12). A subsequent phase II proof-of-concept study demonstrated that both IR and XR formulations had comparable efficacy on serum UA levels; the only significant treatment difference was a greater proportion of patients achieving a serum UA level of <5.0 mg/dl with febuxostat XR 40 mg versus the IR 40 mg formulation (24).

In this study, we present results from a 3-month, phase III, placebo-controlled study to investigate the efficacy and safety of febuxostat IR and XR in patients with gout and normal or impaired renal function, including a preplanned subgroup analysis of treatment effects in patients stratified by baseline renal function (from normal to severely impaired).

PATIENTS AND METHODS

Patients. In this phase III study comparing the efficacy and safety of febuxostat IR and XR, methodologies overlapped considerably with the above- mentioned phase II study in patients with gout and moderate renal impairment (24). The key differences between the 2 studies were a larger number of patients and a much broader gout patient population in the current study, including patients with normal renal function or mild-to-severe renal impairment. Eligible patients were age ≥18 years, had a history or presence of gout (defined as fulfilling the American Rheumatism Association (now the American College of Rheumatology) gout classification criteria) (25), a serum UA level of ≥8.0 mg/dl on the day −4 screening visit, and ≥1 gout flare within 12 months prior to screening. Patients were required to have an eGFR of ≥15 ml/minute at screening, and the protocol specified that ≥30% of enrolled patients should have moderate-to-severe renal impairment (eGFR of ≥15–59 ml/minute), with ≥85 of these patients having severe renal impairment (eGFR ≥15–29 ml/minute). Exclusion criteria included secondary hyperuricemia, history of xanthuria, and known hypersensitivity to febuxostat (for more exclusion criteria details, see Supplementary Appendix A, available on the *Arthritis & Rheumatology* web site at http://onlinelibrary.wiley.com/doi/10.1002/art.40685/abstract).

Study design. This phase III, multicenter, randomized, double-blind, placebo-controlled study was conducted at 217 sites across the US from April 18, 2015 to November 18, 2016. The study was conducted in compliance with the principles of the Declaration of Helsinki and the International Conference on Harmonisation guidelines for Good Clinical Practice, along with all applicable local regulations. The study protocol and related documents received institutional review board or ethics committee approval. All participants provided written informed consent prior to entering the study. The study design was previously described in the report on the related phase II study (24); briefly, the study consisted of a 3-week screening/washout period, followed by a 3-month double-blind treatment period (Figure 1).

Eligible patients received placebo or febuxostat IR 40 mg, XR 40 mg, IR 80 mg, or XR 80 mg orally once daily (randomized in a 1:1:1:1:1 ratio) for 3 months. Patients were randomized within 2 population strata based on baseline renal function: patients with severe renal impairment (eGFR ≥15–29 ml/minute) and without severe renal impairment (eGFR ≥30 ml/minute). An interactive voice or web-response technology was used for randomization and assigning the study drug. The study drug was self-administered as previously described (24).

All patients systematically received gout flare prophylaxis for the duration of double-blind treatment from day 1 to the end of treatment; colchicine 0.6 mg was administered every other
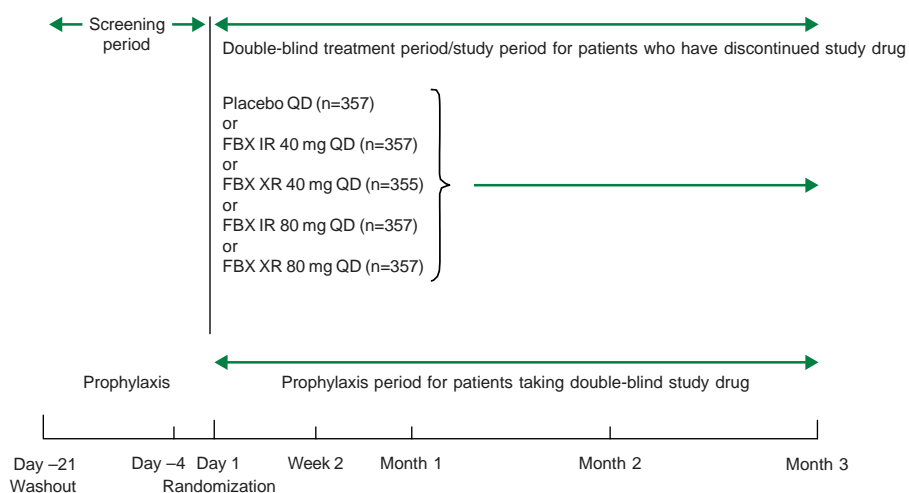
Figure 1. Study design. Subgroup numbers are from the full analysis set. In the safety analysis set, 1 patient was randomized to receive placebo but received febuxostat (FBX) immediate release (IR) 40 mg and so was included in the FBX IR 40 mg group. All patients received prophylaxis for gout flares over the 3-month double-blind treatment period. QD = once daily; XR = extended release.

day to patients with an eGFR of 15–59 ml/minute or once daily in patients with an eGFR of ≥60 ml/minute. However, if colchicine was not tolerated, naproxen 250 mg twice daily with lansoprazole 15 mg once daily was permitted in patients with an eGFR of ≥50 ml/minute; other nonsteroidal antiinflammatory drugs or prednisone were permitted at the discretion of the investigator. Beginning on the day –21 screening visit, patients discontinuing urate-lowering therapy received 0.6 mg colchicine every other day for gout flare prophylaxis until eGFR results were available.

Clinic visits occurred on days 1 and 14, and months 1 and 2; the final visit was on month 3 or with early termination. Clinical assessments (including vital signs, concomitant medication usage, and laboratory safety tests) were conducted during each of these visits, and samples were collected for clinical laboratory tests (including serum UA assessments) at all visits, except day 1.

Study end points. Primary and secondary end points were the same as those assessed in the related phase II study, i.e., the proportion of patients with a serum UA level of <5.0 mg/dl at month 3 was the primary end point, and the proportion of patients with a serum UA level of <6.0 mg/dl at month 3 and the proportion of patients with ≥1 gout flare requiring treatment during the 3-month treatment period were the secondary efficacy end points (24).

Based on the pharmacokinetic and pharmacodynamic characteristics of the XR formulation (23), greater serum UA level reductions were expected with febuxostat XR than with febuxostat IR; therefore, the more difficult-to-achieve target of a serum UA level of <5.0 mg/dl was selected for the primary end point to compare the efficacy of the XR and IR formulations. The recommended target level to ensure better disease control for patients receiving urate-lowering therapy with severe disease and high urate burden is a serum UA level of <5.0 mg/dl, and a serum

UA level of <6.0 mg/dl is the recommended target level for most patients with gout (11,26).

Safety and tolerability assessments included incidence of treatment-emergent AEs (TEAEs), findings from 12-lead electrocardiograms, clinical laboratory assessments, and vital signs. As in the related phase II study (24), a TEAE was defined as any AE, regardless of its relationship to the study drug, occurring from day 1 through 30 days after the last dose of the double-blind study drug. TEAEs were identified as reported by the investigators and summarized using the terminology of the Medical Dictionary for Regulatory Activities (version 18.0). AEs were summarized as any TEAE, treatment-related TEAEs, TEAEs leading to discontinuation of the study drug, serious TEAEs, and death.

Statistical analysis. Efficacy outcomes were assessed using the full analysis set, which included all patients who were randomized for treatment and received ≥1 dose of study drug. Notable changes to the original trial protocol are summarized in Supplementary Appendix B, available on the *Arthritis & Rheumatology* web site at http://onlinelibrary.wiley.com/doi/10.1002/art.40685/abstract. Efficacy outcomes were compared between treatment groups using the Cui, Hung, and Wang Z test statistic (see Supplementary Appendix C, available at http://onlinelibrary.wiley.com/doi/10.1002/art.40685/abstract). A closed testing strategy was prespecified for the primary and secondary end points to adjust for comparisons between the 2 doses (40 and 80 mg); only *P* values less than 0.025 were considered statistically significant. A gout flare was defined as previously described (24). Safety outcomes were evaluated using the safety analysis set (all patients who received ≥1 dose of study drug), and patients were analyzed according to the treatment they received.

A sample size of 1,750 patients (350 per treatment group) was targeted to provide ≥90% power to detect a 14% difference

between febuxostat XR and the corresponding febuxostat IR dose or placebo, using a 2-sided Fisher's exact test at a significance level of 2.5%.

For preplanned subgroup analysis, treatment effects on the proportion of patients achieving serum UA level targets and safety end points were also assessed in patient populations stratified by level of renal function at baseline. The classification of renal impairment was as follows: normal renal function, eGFR ≥90 ml/minute; mild renal impairment, eGFR ≥60–89 ml/minute; moderate renal impairment, eGFR ≥30–59 ml/minute; and severe renal impairment, eGFR ≥15–29 ml/minute.

RESULTS

Findings in the patient population. Of 3,654 patients screened, 1,097 (30.0%) and 767 (21.0%) were not enrolled due to screening failure and washout failure, respectively; the primary reason was failure to meet the entry criteria (870 of 1,097

patients [79.3%] and 487 of 767 patients [63.5%], respectively). Overall, 1,790 patients (49.0%) were enrolled and randomized to treatment (see Supplementary Figure 1, available on the *Arthritis & Rheumatology* web site at http://onlinelibrary.wiley.com/doi/10.1002/art.40685/abstract). A total of 1,783 randomized patients (99.6%) received ≥1 dose of study drug (full and safety analysis sets). The percentages of early discontinuations were similar across treatment groups (14.5–19.0%).

Patient characteristics at baseline were similar across treatment arms (Table 1). The patient cohort was predominantly male (88.4%) and white (64.3%), with a mean age of 55.1 years (range 24–94 years) and mean ± SD body mass index of 34.3 ± 7.8 kg/m^2. The overall mean ± SD serum UA level at baseline was 9.61 ± 1.27 mg/dl, and ~65.1% of patients had a baseline serum UA level of ≥9.0 mg/dl. Approximately 88% of patients had a gout flare within 6 months prior to study enrollment; the majority of patients (59.2%) had received prior treatment with urate-lowering therapy. The proportion of patients in each base-

Table 1. Demographic information and characteristics of the patients at baseline*

	Placebo (n = 357)	FBX IR 40 mg (n = 357)	FBX XR 40 mg (n = 355)	FBX IR 80 mg (n = 357)	FBX XR 80 mg (n = 357)
Age, mean ± SD years	54.4 ± 11.6	55.5 ± 11.1	55.1 ± 12.7	54.9 ± 11.3	55.4 ± 11.9
Sex, no. (%)					
Men	316 (88.5)	311 (87.1)	312 (87.9)	315 (88.2)	323 (90.5)
Women	41 (11.5)	46 (12.9)	43 (12.1)	42 (11.8)	34 (9.5)
Race, no. (%)†					
White	231 (64.7)	235 (65.8)	226 (63.7)	230 (64.4)	225 (63.0)
Black/African American	94 (26.3)	89 (24.9)	100 (28.2)	98 (27.5)	93 (26.1)
BMI, mean ± SD kg/m^2	34.9 ± 8.3‡	34.3 ± 8.0	34.3 ± 8.1	33.7 ± 7.5	34.1 ± 7.2
Baseline serum UA, mean ± SD mg/dl§	9.7 ± 1.4	9.6 ± 1.2	9.5 ± 1.2	9.6 ± 1.3	9.7 ± 1.3
Approximate gout flares during past year, no. (%)§					
1–3	196 (55.1)	200 (55.9)	213 (60.0)	203 (56.9)‡	214 (59.9)
4–6	102 (28.7)	97 (27.1)	92 (25.9)	93 (26.1)	85 (23.8)
>6	58 (16.3)	61 (17.0)	50 (14.1)	60 (16.8)	58 (16.2)
Renal function at baseline, no. (%)					
Severely impaired	18 (5.0)	23 (6.4)	21 (5.9)	20 (5.6)	18 (5.0)
Moderately impaired	93 (26.1)	91 (25.5)	93 (26.2)	106 (29.7)	100 (28.0)
Mildly impaired	194 (54.3)	192 (53.8)	196 (55.2)	185 (51.8)	198 (55.5)
Normal	52 (14.6)	51 (14.3)	45 (12.7)	46 (12.9)	41 (11.5)

* Except where indicated otherwise, data are from the full analysis set. BMI = body mass index; UA = urate.
† The total number (%) of patients classified as American Indian or Alaska Native, Asian, Native Hawaiian or Other Pacific Islander, and Other were 7 (0.4), 112 (6.3), 20 (1.1), and 23 (1.3), respectively.
‡ Data are missing for 1 patient for this variable in this treatment group.
§ Data are from the safety analysis set: placebo (n = 356), febuxostat (FBX) immediate release (IR) 40 mg (n = 358), FBX extended release (XR) 40 mg (n = 355), FBX IR 80 mg (n = 357), and FBX XR 80 mg (n = 357).
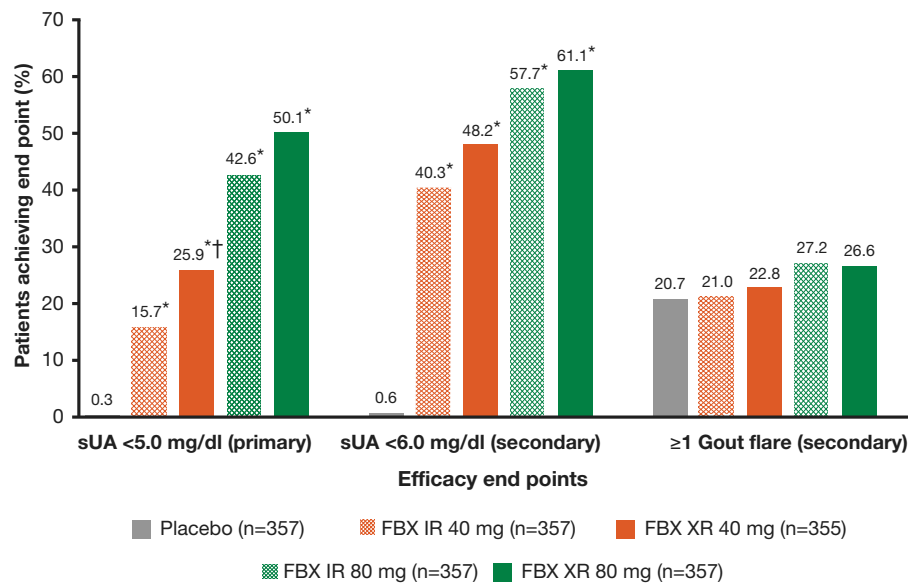
Figure 2. Percentage of patients (in full analysis set) who achieved primary and secondary outcomes. Based on multiplicity adjustment, the level of significance was set at $P < 0.025$ for primary comparisons. * = $P < 0.001$ versus placebo. † = $P = 0.001$ versus equivalent-dose immediate release (IR) formulation. FBX = febuxostat; XR = extended release.

line renal function subgroup category was comparable across treatment groups (Table 1).

Efficacy. *Primary efficacy end point*. Significantly greater proportions of patients treated with febuxostat (both formulations and doses) had achieved a serum UA level of <5.0 mg/dl at month 3 compared with patients who received placebo ($P < 0.001$ for all comparisons) (see Figure 2 and Supplementary Table 1, available on the *Arthritis & Rheumatology* web site at http://onlinelibrary.wiley.com/doi/10.1002/art.40685/abstract). Febuxostat XR 40 mg was associated with a significantly greater proportion of patients achieving a serum UA level of <5.0 mg/dl at month 3 versus IR 40 mg (25.9% versus 15.7%; $P = 0.001$). Although a numerically greater proportion of patients treated with febuxostat XR 80 mg achieved a serum UA level of <5.0 mg/dl at month 3 compared with patients treated with IR 80 mg, the difference was not statistically significant.

Secondary efficacy end points. Both formulations and doses of febuxostat treatment were associated with significantly greater proportions of patients achieving a serum UA level of <6.0 mg/dl at month 3 versus placebo ($P < 0.001$ versus placebo for all comparisons). However, there were no significant differences in the treatment effect of equivalent doses of XR and IR for this end point. The proportions of patients with ≥1 gout flare requiring treatment during the 3-month treatment period were similar across treatment groups (Figure 2 and Supplementary Table 1, available at http://onlinelibrary.wiley.com/doi/10.1002/art.40685/abstract).

Analysis of serum UA end points in renal function subgroups. Febuxostat IR and XR (both doses) were associated with significantly greater proportions of patients achieving the primary end point of a serum UA level of <5.0 mg/dl at month 3 versus placebo across all renal function subgroups with the exception of febuxostat XR 40 mg in patients with severe renal impairment ($P < 0.05$ for all other comparisons) (see Figure 3A and Supplementary Table 2, available at http://onlinelibrary.wiley.com/doi/10.1002/art.40685/abstract). Similarly, both formulations and doses of febuxostat were associated with consistent treatment benefits in the proportions of patients achieving a serum UA level of <6.0 mg/dl at month 3 across all renal function subgroups versus placebo ($P ≤ 0.001$ for all comparisons versus placebo) (see Figure 3B and Supplementary Table 2, available at http://onlinelibrary.wiley.com/doi/10.1002/art.40685/abstract).

Compared with febuxostat IR 40 mg, febuxostat XR 40 mg was associated with a significantly greater proportion of patients achieving a serum UA level of <5.0 mg/dl in patients with moderate renal impairment (26.9% versus 13.2%; $P = 0.02$) or mild renal impairment (29.1% versus 16.1%; $P = 0.001$), as well as with a greater proportion of patients achieving a serum UA level of <6.0 mg/dl in patients with mild renal impairment (49.5% versus 38.0%; $P = 0.016$) (see Figures 3A and B and Supplementary Table 2, available at http://onlinelibrary.wiley.com/doi/10.1002/art.40685/abstract). However, there were no other significant differences in the treatment effect of equivalent doses of XR and IR on these end points in any other renal function subgroups. The proportions of patients with ≥1 gout flare requiring treatment during the 3-month treatment period were generally comparable
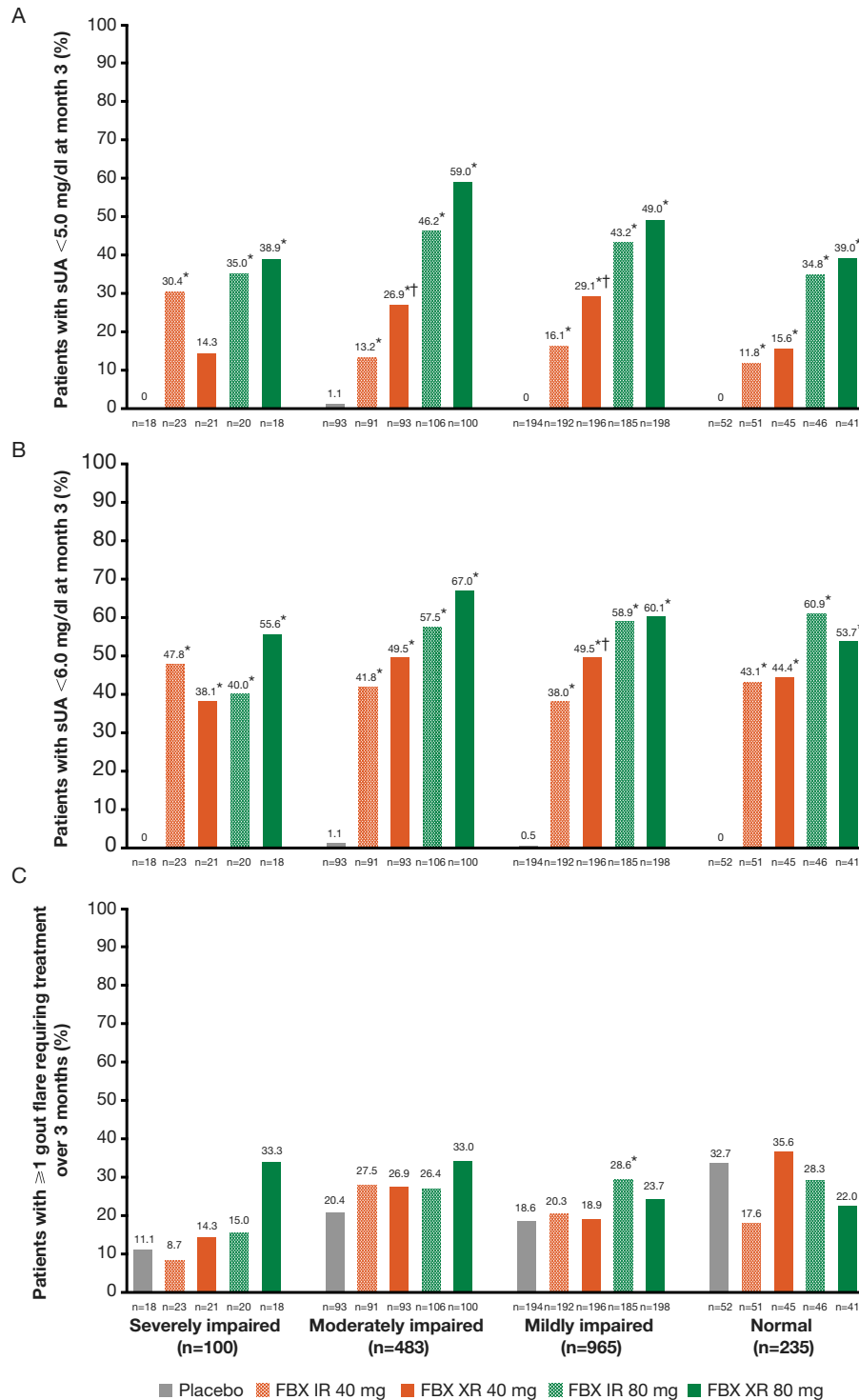
Figure 3. Renal subgroup analysis, with treatment group comparisons were based on the Cui, Hung, and Wang Z test statistic. **A,** Percentage of patients who achieved a serum urate (sUA) level of <5.0 mg/dl (primary end point) at month 3. * = $P < 0.05$ versus placebo; † = $P < 0.05$ versus equivalent-dose immediate release (IR) formulation. **B,** Percentage of patients who achieved a serum UA level of <6.0 mg/dl at month 3. * = $P \leq 0.001$ versus placebo; † = $P < 0.05$ versus equivalent-dose IR formulation. **C,** Percentage of patients who experienced ≥1 gout flare that required treatment over the 3-month study period. * = $P < 0.05$ versus placebo. Patients were stratified by baseline renal function; normal renal function was defined as an estimated glomerular filtration rate (eGFR) of ≥90 ml/minute, mild renal impairment as an eGFR of ≥60–89 ml/minute, moderate renal impairment as an eGFR of ≥30–59 ml/minute, and severe renal impairment as an eGFR of ≥15–29 ml/minute. FBX = febuxostat; XR = extended release.

Table 2. Overview of patients experiencing TEAEs, treatment-related TEAEs, and serious TEAEs*

	Placebo (n = 356)	FBX IR 40 mg (n = 358)	FBX XR 40 mg (n = 355)	FBX IR 80 mg (n = 357)	FBX XR 80 mg (n = 357)
Overall TEAEs	134 (37.6)	147 (41.1)	119 (33.5)	143 (40.1)	148 (41.5)
Related to treatment	25 (7.0)	29 (8.1)	21 (5.9)	22 (6.2)	32 (9.0)
Not related to treatment	109 (30.6)	118 (33.0)	98 (27.6)	121 (33.9)	116 (32.5)
TEAEs by severity					
Mild	59 (16.6)	70 (19.6)	53 (14.9)	69 (19.3)	84 (23.5)
Moderate	64 (18.0)	61 (17.0)	57 (16.1)	59 (16.5)	57 (16.0)
Severe	11 (3.1)	16 (4.5)	9 (2.5)	15 (4.2)	7 (2.0)
TEAEs leading to study drug discontinuation	9 (2.5)	9 (2.5)	10 (2.8)	13 (3.6)	6 (1.7)
Serious TEAEs	8 (2.2)	12 (3.4)	6 (1.7)	8 (2.2)	8 (2.2)
Related to treatment	0	1 (0.3)	1 (0.3)	1 (0.3)	1 (0.3)
Not related to treatment	8 (2.2)	11 (3.1)	5 (1.4)	7 (2.0)	7 (2.0)
Leading to study drug discontinuation	2 (0.6)	3 (0.8)	3 (0.8)	4 (1.1)	1 (0.3)
Deaths	1 (0.3)	0	1 (0.3)	1 (0.3)	0

* Values are the number (%) of patients in the safety analysis set experiencing any treatment-emergent adverse events (TEAEs). One patient was randomized to receive placebo but received febuxostat (FBX) immediate release (IR) 40 mg and so was included in the FBX IR 40 mg group. XR = extended release.

across treatment groups within each of the renal function subgroups (see Figure 3C and Supplementary Table 2, available at http://onlinelibrary.wiley.com/doi/10.1002/art.40685/abstract).

Safety and tolerability. TEAEs, treatment-related TEAEs, and serious TEAEs across treatment groups are summarized in Table 2. Overall, 38.8% of patients (691 of 1,783) experienced at least 1 TEAE. In most of these patients (633 of 691 [91.6%]), TEAEs were mild or moderate in intensity, and no apparent patterns were observed in relation to the dose level or formulation of febuxostat. The incidences of treatment-related TEAEs (129 of 1,783 [7.2%]) and serious TEAEs (42 of 1,783 [2.4%]) were low across all treatment groups.

The most common TEAEs (reported by ≥2% of patients in any treatment group) are described in Table 3, with diarrhea, nasopharyngitis, and hypertension most commonly experienced by patients. The overall incidence of treatment-related TEAEs was relatively low; among these, there were 2 cases of renal failure (reported as renal insufficiency or worsening renal insufficiency, with 1 patient each in the febuxostat XR 40 mg and IR 40 mg treatment groups), 1 case of acute kidney injury (reported as acute renal insufficiency [with febuxostat XR 40 mg]), and 1 case of renal impairment (reported as worsening kidney function [with febuxostat IR 40 mg]). The incidence of increased blood levels of creatinine appeared to be slightly higher with febuxostat IR 80 mg group (2%) compared with the other febuxostat treatment groups (0.8%).

The overall incidence of serious TEAEs was low and generally similar across treatment groups. Serious TEAEs included 3 fatal AEs, 2 of which were considered unrelated to the study drug (1 fatal cardiac arrest in a patient with severe renal impairment in the placebo group and 1 fatal worsening of hypertensive cardiovas-

cular disease in a patient with mild renal impairment in the febuxostat XR 40 mg group) and another that was considered to be related to the study drug (fatal cardiorespiratory arrest in a patient with severe renal impairment in the febuxostat IR 80 mg group). Three other patients had nonfatal serious TEAEs that were considered to be related to the study drug: with febuxostat IR 40 mg (severe renal impairment subgroup), 1 patient had serious TEAEs of renal impairment and abdominal pain: with febuxostat XR 40 mg (severe renal impairment subgroup), with 1 patient had acute respiratory failure and angioedema; and with febuxostat XR 80 mg (mild renal impairment subgroup), 1 patient had peripheral edema.

The medical histories of patients with fatal serious TEAEs and serious TEAEs related to treatment are summarized in Supplementary Table 3 (available on the *Arthritis & Rheumatology* web site at http://onlinelibrary.wiley.com/doi/10.1002/art.40685/abstract). The overall incidence of TEAEs leading to discontinuation of the study drug (47 of 1,783 [2.6%]) was low and similar across treatment groups (Table 2). The majority of TEAEs leading to discontinuation of the study drug were single occurrences and were generally distributed across treatment groups with no apparent trends.

Analysis of safety and tolerability in renal function subgroups. The overall incidence of TEAEs was similar across treatment groups within each of the renal function subgroups, as was the incidence of treatment-related TEAEs (see Supplementary Table 4, available at http://onlinelibrary.wiley.com/doi/10.1002/art.40685/abstract). There were no apparent trends observed between febuxostat dose or formulation and incidence of TEAEs. The incidences of the 5 most commonly reported TEAEs (diarrhea, hypertension, nasopharyngitis, arthralgia, and upper respiratory tract infection) were evenly distributed across the renal function sub-

Table 3. Most common TEAEs recorded in ≥2% of patients in any treatment group*

	Placebo (n = 356)	FBX IR 40 mg (n = 358)	FBX XR 40 mg (n = 355)	FBX IR 80 mg (n = 357)	FBX XR 80 mg (n = 357)
Gastrointestinal disorders					
Diarrhea	13 (3.7)	9 (2.5)	9 (2.5)	21 (5.9)	9 (2.5)
Infections and infestations					
Nasopharyngitis	11 (3.1)	7 (2.0)	7 (2.0)	9 (2.5)	4 (1.1)
Upper respiratory tract infection	4 (1.1)	6 (1.7)	6 (1.7)	5 (1.4)	8 (2.2)
Laboratory abnormalities					
Alanine aminotransferase increased	6 (1.7)	7 (2.0)	8 (2.3)	2 (0.6)	4 (1.1)
Aspartate aminotransferase increased	3 (0.8)	3 (0.8)	7 (2.0)	3 (0.8)	2 (0.6)
Blood creatinine increased	1 (0.3)	3 (0.8)	3 (0.8)	7 (2.0)	3 (0.8)
Gamma glutamyl transferase increased	3 (0.8)	6 (1.7)	6 (1.7)	7 (2.0)	5 (1.4)
Musculoskeletal and connective tissue disorders					
Arthralgia	7 (2.0)	8 (2.2)	5 (1.4)	6 (1.7)	4 (1.1)
Nervous system disorders					
Headache	6 (1.7)	6 (1.7)	8 (2.3)	4 (1.1)	4 (1.1)
Respiratory, thoracic, and mediastinal disorders					
Cough	5 (1.4)	9 (2.5)	2 (0.6)	3 (0.8)	1 (0.3)
Vascular disorders					
Hypertension	10 (2.8)	13 (3.6)	6 (1.7)	8 (2.2)	5 (1.4)

* Values are the number (%) of patients in the safety analysis set reporting any treatment-emergent adverse events (TEAEs; by system organ class/preferred term). One patient was randomized to receive placebo but received febuxostat (FBX) immediate release (IR) 40 mg and so was included in the FBX IR 40 mg group. XR = extended release.

groups (see Supplementary Table 5, available at http://onlinelibrary.wiley.com/doi/10.1002/art.40685/abstract). Not surprisingly, the overall incidence of TEAEs was higher in the severe renal impairment subgroup than in the other renal function subgroups.

DISCUSSION

The febuxostat XR formulations were developed with the aim of providing comparable or superior urate-lowering efficacy versus their febuxostat IR counterparts, with reductions in treatment-initiated flares due to a more stable drug exposure profile. The current phase III study assessed the tolerability and efficacy of febuxostat IR 40 and 80 mg once daily (currently approved dosages) compared with XR formulations at the same dosages. The inclusion of a placebo arm permitted comparisons of the safety and efficacy of all febuxostat treatment regimens versus placebo. In addition, preplanned subgroup analyses were conducted to evaluate treatment effects in patients stratified by baseline renal function.

Several key findings were demonstrated in this phase III study. First, both the XR and IR formulations of febuxostat were generally well tolerated and were associated with significant reductions in serum UA levels compared with placebo in patients with gout and normal or impaired renal function. The incidences of renal TEAEs were relatively low and evenly distributed across treatment groups, with 1 case of fatal cardiorespiratory arrest

in a patient with severe renal impairment (febuxostat IR 80 mg group) and 1 serious renal TEAE (a case of renal impairment in the febuxostat IR 40 mg group) considered to be related to febuxostat treatment. Second, the statistically significant treatment benefits in favor of febuxostat (versus placebo) were also generally seen across all renal function subgroups, including patients with severe renal impairment. Third, analysis of the safety data demonstrated that there were no large differences in TEAEs across treatment arms in patients with gout stratified by baseline renal function. These findings provide further evidence of the tolerability and efficacy of febuxostat in patients with gout and normal or impaired renal function, including patients with severe renal impairment.

The results of this study also indicated that equivalent doses of febuxostat XR and IR had similar treatment effects on serum UA levels; in the overall population, the only statistically significant treatment difference between formulations was the greater proportion of patients achieving a serum UA level of <5.0 mg/dl at month 3 seen with febuxostat XR 40 mg versus IR 40 mg. It is worth noting that febuxostat IR 80 mg was consistently more effective at controlling serum UA levels than febuxostat XR 40 mg, suggesting that dose titration from febuxostat IR 40 mg to febuxostat IR 80 mg would potentially represent a more effective treatment strategy than switching to febuxostat XR 40 mg. Febuxostat XR 80 mg was not associated with any statistically significant treatment benefits

on serum UA level <5.0 mg/dl or serum UA level <6.0 mg/dl treatment target end points compared with febuxostat IR 80 mg. In addition, the proportions of patients with ≥1 gout flare requiring treatment during the 3-month treatment period were similar across active treatment groups, suggesting that the XR formulation did not reduce the incidence of treatment-initiated gout flares compared with the IR formulation.

These results were similar to those from a 3-month phase II study in patients with moderate renal function, which demonstrated that treatment with febuxostat XR or IR led to significant urate lowering versus placebo, as well as indicated that equivalent doses of febuxostat XR and IR had similar treatment effects on serum UA levels (24). The only significant treatment difference between equivalent doses of febuxostat XR and IR was the greater proportion of patients achieving a serum UA level of <5.0 mg/dl at month 3 with febuxostat XR 40 mg versus IR 40 mg. Although febuxostat XR 40 mg was associated with a numerically lower proportion of patients with ≥1 gout flare requiring treatment compared with febuxostat IR 40 mg during the phase II study, the difference was not statistically significant. The absence of any significant treatment benefit in favor of febuxostat XR on the incidence of treatment-initiated gout flares is consistent with findings from the current phase III study.

The current results do, however, add to the growing evidence supporting the use of febuxostat in the management of hyperuricemia in patients with renal impairment. Data from clinical trials have demonstrated that febuxostat IR is effective and well tolerated in patients with mild-to-moderate renal impairment (19,20,27,28). Two long-term open-label studies demonstrated that febuxostat IR not only lowered serum UA levels, but was also associated with more stable and even improved renal function (27,28). In a 5-year open-label study, febuxostat (IR 40, 80, or 120 mg) was well tolerated and effective at reducing serum UA levels in patients with normal and impaired renal function (22). Subanalyses of data from a separate 4-year open-label trial demonstrated that febuxostat (IR 80 or 120 mg) consistently reduced serum UA levels from baseline by ~50% (28). In post hoc analyses of these long-term trials, it was estimated that each 1 mg/dl of sustained reduction of serum UA levels brought about by urate-lowering treatment could potentially lead to preservation of 1.0–1.15 ml/minute of eGFR (27,28).

While substantial evidence supports the efficacy and safety of febuxostat IR in patients with gout and normal or mildly impaired renal function, data regarding the effects of febuxostat IR treatment are less robust in patients with gout and moderate renal impairment, and are very limited in patients with severe renal impairment (12). Findings from a recent phase II study suggested that both febuxostat IR 30 mg twice daily and febuxostat IR 40 or 80 mg (depending on a serum UA level of <6.0 or ≥6.0 mg/dl on study day 14) once daily significantly

lowered serum UA levels compared with placebo in patients with gout and moderate-to-severe renal impairment (eGFR 15–50 ml/minute/1.73 m²). Critically, these treatment benefits were not associated with any significant deterioration in renal function (12). These findings are supported by those from the current renal subgroup analysis, which showed that, in general, all formulations and doses of febuxostat were effective and well tolerated across all renal function subgroups, including patients with severe renal impairment.

Treatment options for patients with gout and renal impairment are limited. Despite allopurinol being relatively well tolerated and effective at reducing serum UA in patients with gout (10), its elimination via the kidneys complicates its use in patients with impaired renal function. Previous publications have suggested that a dose reduction of allopurinol in patients with gout and renal impairment may limit its effectiveness on serum UA treatment targets (20,29,30) and potentially lead to suboptimal treatment in clinical practice (31). However, a recent study evaluating dose escalation with allopurinol suggested that higher doses were effective in lowering serum UA levels to treatment target in most people with gout and were well tolerated (16).

Febuxostat IR 80 mg or IR 120 mg has been shown to be more efficacious than allopurinol 300 mg (the most commonly used fixed daily dose) in lowering serum UA levels to <6.0 mg/dl and maintaining this level in patients with gout and mild to moderately impaired renal function (18).

The current phase III study has several benefits and limitations. This trial represents the largest investigation of febuxostat in patients with renal impairment, including severe renal impairment, and the stratification of randomization by renal function (severe or not severe) helped to maintain a balanced distribution of patients with various degrees of renal impairment across treatment groups at baseline. While the sample size was adequate to demonstrate the efficacy of both formulations of febuxostat in the overall patient population and across renal function subgroups, the small sample sizes seen in the renal function subgroups are associated with greater variability, and any significant differences, or lack thereof, should therefore be interpreted with caution. It is also important to note that the use of gout flare prophylaxis in this study is likely to have limited the possibility of detecting any benefits of the XR formulation over the IR formulation in reducing the incidence of treatment-initiated gout flares.

In conclusion, the results from this phase III study demonstrated that febuxostat IR and XR formulations were both well tolerated and effective in patients with gout and normal renal function or mild-to-severe renal impairment. However, the incidence of treatment-initiated gout flares was not reduced with the XR formulation compared with the IR formulation. The present findings, together with those from recent phase II trials in patients with gout and moderate or moderate-to-severe renal impairment (12,24), support the view that febuxostat IR has the

potential to help address the treatment of gout in patients with renal impairment.

REFERENCES

1. Zhu Y, Pandya BJ, Choi HK. Prevalence of gout and hyperuricemia in the US general population: the National Health and Nutrition Examination Survey 2007–2008. Arthritis Rheum 2011;63:3136–41.

2. Hsu CY, Iribarren C, McCulloch CE, Darbinian J, Go AS. Risk factors for end-stage renal disease: 25-year follow-up. Arch Intern Med 2009;169:342–50.

3. Iseki K, Oshiro S, Tozawa M, Iseki C, Ikemiya Y, Takishita S. Significance of hyperuricemia on the early detection of renal failure in a cohort of screened subjects. Hypertens Res 2001;24:691–7.

4. Kang DH, Nakagawa T. Uric acid and chronic renal disease: possible implication of hyperuricemia on progression of renal disease. Semin Nephrol 2005;25:43–9.

5. Obermayr RP, Temml C, Gutjahr G, Knechtelsdorfer M, Oberbauer R, Klauser-Braun R. Elevated uric acid increases the risk for kidney disease. J Am Soc Nephrol 2008;19:2407–13.

6. Sonoda H, Takase H, Dohi Y, Kimura G. Uric acid levels predict future development of chronic kidney disease. Am J Nephrol 2011;33: 352–7.

7. Zhu Y, Pandya BJ, Choi HK. Comorbidities of gout and hyperuricemia in the US general population: NHANES 2007-2008. Am J Med 2012;125:679–87.

8. Krishnan E. Reduced glomerular function and prevalence of gout: NHANES 2009-10. PLoS One 2012;7:e50046.

9. Roughley MJ, Belcher J, Mallen CD, Roddy E. Gout and risk of chronic kidney disease and nephrolithiasis: meta-analysis of observational studies. Arthritis Res Ther 2015;17:90.

10. Zyloprim (allopurinol) product monograph. Vaughan (ON): AA Pharma Inc.; 2010. URL: https://www.aapharma.ca/downloads/en/PIL/allopurinol_pm.pdf.

11. Khanna D, Fitzgerald JD, Khanna PP, Bae S, Singh MK, Neogi T, et al. 2012 American College of Rheumatology guidelines for management of gout. Part 1: systematic nonpharmacologic and pharmacologic therapeutic approaches to hyperuricemia. Arthritis Care Res (Hoboken) 2012;64:1431–46.

12. Saag KG, Whelton A, Becker MA, MacDonald P, Hunt B, Gunawardhana L. Impact of febuxostat on renal function in gout patients with moderate-to-severe renal impairment. Arthritis Rheumatol 2016;68:2035–43.

13. Uloric (febuxostat) prescribing information. Deerfield (IL): Takeda Pharmaceuticals America, Inc. 2013. URL: http://general.takedapharm.com/content/file.aspx?filetypecode=ULORICPI&cacheRandomizer=a9b8bc72-9cd9-42de-834a-d3d2ea6ef737.

14. Hande KR, Noone RM, Stone WJ. Severe allopurinol toxicity: description and guidelines for prevention in patients with renal insufficiency. Am J Med 1984;76:47–56.

15. Thurston MM, Phillips BB, Bourg CA. Safety and efficacy of allopurinol in chronic kidney disease. Ann Pharmacother 2013;47:1507–16.

16. Stamp LK, Chapman PT, Barclay ML, Horne A, Frampton C, Tan P, et al. A randomised controlled trial of the efficacy and safety of allopurinol dose escalation to achieve target serum urate in people with gout. Ann Rheum Dis 2017;76:1522–8.

17. Becker MA, Schumacher HR Jr, Wortmann RL, MacDonald PA, Palo WA, Eustace D, et al. Febuxostat, a novel nonpurine selective inhibitor of xanthine oxidase: a twenty-eight–day, multicenter, phase II, randomized, double-blind, placebo-controlled, dose-response clinical trial examining safety and efficacy in patients with gout. Arthritis Rheum 2005;52:916–23.

18. Becker MA, Schumacher HR Jr, Wortmann RL, MacDonald PA, Eustace D, Palo WA, et al. Febuxostat compared with allopurinol in patients with hyperuricemia and gout. N Engl J Med 2005;353:2450–61.

19. Becker MA, Schumacher HR, MacDonald PA, Lloyd E, Lademacher C. Clinical efficacy and safety of successful longterm urate lowering with febuxostat or allopurinol in subjects with gout. J Rheumatol 2009;36:1273–82.

20. Becker MA, Schumacher HR, Espinoza LR, Wells AF, MacDonald P, Lloyd E, et al. The urate-lowering efficacy and safety of febuxostat in the treatment of the hyperuricemia of gout: the CONFIRMS trial. Arthritis Res Ther 2010;12:R63.

21. Schumacher HR Jr, Becker MA, Wortmann RL, MacDonald PA, Hunt B, Streit J, et al. Effects of febuxostat versus allopurinol and placebo in reducing serum urate in subjects with hyperuricemia and gout: a 28-week, phase III, randomized, double-blind, parallel-group trial. Arthritis Rheum 2008;59:1540–8.

22. Schumacher HR Jr, Becker MA, Lloyd E, MacDonald PA, Lademacher C. Febuxostat in the treatment of gout: 5-yr findings of the FOCUS efficacy and safety study. Rheumatology (Oxford) 2009;48:188–94.

23. Febuxostat: study number. TMX-67_106. Clinical study report. Deerfield (IL): Takeda Pharmaceuticals America Inc.; 2012. URL: https://www.takedaclinicaltrials.com/files2/TMX-67-106-RDS-2014-10-26.pdf.

24. Gunawardhana L, Becker MA, Whelton A, Hunt B, Castillo M, Saag K. Efficacy and safety of febuxostat extended release and immediate release in patients with gout and moderate renal impairment: phase II placebo-controlled study. Arthritis Res Ther 2018;20:99.

25. Wallace SL, Robinson H, Masi AT, Decker JL, McCarty DJ, Yu TF. Preliminary criteria for the classification of the acute arthritis of primary gout. Arthritis Rheum 1977;20:895–900.

26. Richette P, Doherty M, Pascual E, Barskova V, Becce F, Castaneda-Sanabria J, et al. 2016 updated EULAR evidence-based recommendations for the management of gout. Ann Rheum Dis 2017;76:29–42.

27. Whelton A, MacDonald PA, Zhao L, Hunt B, Gunawardhana L. Renal function in gout: long-term treatment effects of febuxostat. J Clin Rheumatol 2011;17:7–13.

28. Whelton A, MacDonald PA, Chefo S, Gunawardhana L. Preservation of renal function during gout treatment with febuxostat: a quantitative study. Postgrad Med 2013;125:106–14.

29. Curiel RV, Guzman NJ. Challenges associated with the management of gouty arthritis in patients with chronic kidney disease: a systematic review. Semin Arthritis Rheum 2012;42:166–78.

30. Dalbeth N, Kumar S, Stamp L, Gow P. Dose adjustment of allopurinol according to creatinine clearance does not provide adequate control of hyperuricemia in patients with gout. J Rheumatol 2006;33:1646–50.

31. Sarawate CA, Brewer KK, Yang W, Patel PA, Schumacher HR, Saag KG, et al. Gout medication treatment patterns and adherence to standards of care from a managed care perspective. Mayo Clin Proc 2006;81:925–34.

The Risk of Gout Among Patients With Sleep Apnea: A Matched Cohort Study

Milica Blagojevic-Bucknall,[1] (iD) Christian Mallen,[1] (iD) Sara Muller,[1] (iD) Richard Hayward,[1] Sophie West,[2] Hyon Choi,[3] and Edward Roddy[1] (iD)

Objective. Obstructive sleep apnea (OSA) is associated with a range of serious comorbidities. This study was undertaken to investigate whether people with OSA are more likely to develop gout, in the short and long term, compared to those without OSA.

Methods. A matched retrospective cohort study was undertaken using the UK Clinical Practice Research Datalink. Individuals age ≥18 years who received a diagnosis of OSA between 1990 and 2010 were identified and matched on age, sex, and practice with up to 4 individuals without OSA; follow-up was until the end of 2015. Hazard ratios (HRs) were estimated using Cox regression adjusted for general health, lifestyle, and comorbidity characteristics. The risk of developing gout was assessed at different time points, and the body mass index (BMI) category–specific results were presented.

Results. The study sample included 15,879 patients with OSA and 63,296 without. The median follow-up was 5.8 years. We found that 4.9% of patients with OSA and 2.6% of patients without the disorder developed gout. The incidence rate per 1,000 person-years was 7.83 (95% confidence interval [95% CI] 7.29–8.40) and 4.03 (95% CI 3.84–4.23) among those with and without OSA, respectively. The adjusted HR was 1.42 (95% CI 1.29–1.56). The risk of developing gout among OSA patients compared to those without was highest 1–2 years after the index date (HR 1.64 [95% CI 1.30–2.06]). This finding persisted among those who were overweight and obese. For those with normal BMI, the highest significant HR (2.02 [95% CI 1.13–3.62]) was observed at 2–5 years after the index date.

Conclusion. In this study, patients with OSA continued to be at higher risk of developing gout beyond the first year following the diagnosis. Our results further indicate that peak incidences of gout vary according to BMI.

INTRODUCTION

Gout is the most prevalent inflammatory arthropathy, affecting 2.5% of adults in the UK in 2012 (1). In addition to being the most painful form of acute arthritis, it is associated with considerable comorbidity, including metabolic syndrome, hypertension, obesity, insulin resistance, and cardiovascular disease (2–4). Obstructive sleep apnea (OSA) is also a common problem in primary care settings, having a similar prevalence to gout (4–10%) (5), although there is evidence that it is underdiagnosed in this setting (6). As with gout, OSA is associated with a range of serious comorbidities (7–9).

Evidence suggests that elevated serum uric acid levels, the cause of gout, are also frequently identified in patients with OSA (10). However, despite prevalent hyperuricemia in patients with OSA, some shared risk factors with gout (obesity and alcohol consumption), and research identifying associations between gout and other comorbidities, few studies have addressed the possibility of an association between OSA and gout.

The intermittent hypoxia present in OSA enhances nucleotide turnover, generating purines which are metabolized to uric acid (11), providing a biologically plausible mechanism by which OSA predisposes patients to hyperuricemia and gout. In a small cross-sectional observational study undertaken in a lo-

Arthritis Research UK Primary Care Centre, Research Institute for Primary Care & Health Services, Newcastle-under-Lyme, UK; [2]Sophie West, PhD: Newcastle University, Freeman Hospital, Newcastle upon Tyne, UK; [3]Hyon Choi, MD, DrPH: Massachusetts General Hospital, Boston.

Address correspondence to Milica Blagojevic-Bucknall, PhD, Arthritis Research UK Primary Care Centre, Research Institute for Primary Care & Health Sciences, Keele University, Keele ST5 5BG, Staffordshire, UK. E-mail: m.bucknall@keele.ac.uk.

Submitted for publication October 26, 2017; accepted in revised form July 5, 2018.

cal primary care database, we found an association between gout and sleep disorders but the study had insufficient power to demonstrate an independent association between gout and OSA (12). A single-cohort study undertaken using a UK primary care database, The Health Improvement Network, showed that patients with OSA had a 50% higher risk of developing gout over a 1-year follow-up period than those without the disorder, regardless of sex or weight status (13). However, it is unclear whether such findings would persist beyond the relatively short follow-up period of 1 year, and whether the risk of gout is perhaps at its highest beyond the first year following the diagnosis of OSA. This study aimed to address these shortfalls of previous studies by reexamining the association between OSA and the subsequent development of gout over a longer follow-up period, assessing the risk at different time points after the diagnosis, and subgrouping according to body mass index (BMI), using a matched retrospective cohort study design in a sample from UK general practice.

PATIENTS AND METHODS

Clinical practice research datalink. Primary care is the most common first point of entry into the health system in the UK for those with a new symptom or illness, such as OSA or gout. Therefore, the Clinical Practice Research Datalink (CPRD; http://www.cprd.com) was chosen as the appropriate data source for this study. The CPRD is a large, validated, and extensively used ongoing UK database of routinely collected primary care information, such as consultations and prescriptions, on ~5.5 million registered patients (9% of the UK population) shown to be representative of the general UK population (14). General practitioners (GPs) enter the data using coding schemes, such as Read codes and British National Formulary codes, and practices that contribute data to the CPRD undergo regular cycles of training and audit. The data from a particular practice are only eligible for use once they have been deemed "up-to-standard." A systematic review of studies investigating the validation of diagnoses in the CPRD showed that a high proportion of cases were confirmed for >180 different diagnoses, with a median of 89% of Read code diagnoses confirmed via different validation methods (15).

OSA exposure. Exposed patients were those age ≤18 years with a first-ever diagnosis of OSA recorded between January 1, 1990 and December 31, 2010; the date of diagnosis was defined as the index date. The unexposed comparison group was drawn by matching each patient with OSA to up to 4 individuals without a diagnosis of OSA at any point (unexposed patients). In order to ensure that an adequate number of unexposed patients remained, 20 were initially assigned to each exposed patient. Unexposed patients were matched to exposed patients on the basis of general practice, sex, and year of birth

(within 3 years). The index date for unexposed patients was the date of OSA diagnosis of their matched OSA patient. Patients with a gout diagnosis or those prescribed allopurinol or colchicine in the period before the index date were removed from analysis. All patients were required to have 2 years of up-to-standard data prior to the index date.

Furthermore, unexposed patients were required to have consulted with the practice within a year of the index date. This ensured that those without OSA were active members of the practice and eliminated the possibility of artificially inflating any association between OSA and gout by comparing OSA patients to individuals who had not been seen at the practice in recent years.

Outcome measure. The outcome of interest was the time from the index date to the first diagnosis of gout, defined using relevant Read codes up to the end of March 2015. For those patients who had no record of gout, the end of study was defined as the earliest of the following: date of death, date of transfer from practice, date of last collection of records from the practice, or March 31, 2015.

Covariates. Covariates believed to potentially confound the relationship between OSA and gout were selected based on their previously established association with the incidence of gout and/or OSA (16–18). These included age and sex (largely accounted for through the matched study design), type 2 diabetes mellitus, ischemic heart disease, hypertension, hyperlipidemia, use of diuretic drugs, obesity, and alcohol consumption. Information on the presence of comorbidities, weight (used to calculate BMI), and alcohol consumption was identified in the period prior to the index date and denoted in terms of binary presence/absence indicators (assuming that no record implies absence of diagnosis) for comorbidities. Height measurements were considered valid regardless of the time point at which they were obtained. Alcohol consumption was categorized as never/ever, and BMI (kg/m^2) was categorized as normal (<25)/overweight (25–30)/obese (≥30). Weight entries of <30 kg or >250 kg and height entries of <1.2m or >2.2m were ignored in the calculation of BMI. Categories for missing data were defined for alcohol consumption and BMI in order to preserve sample size.

The lists of Read codes (used for identifying OSA, gout, diabetes, ischemic heart disease, hypertension, and hyperlipidemia) and product codes (used for identifying allopurinol, colchicine, and diuretic drugs) were compiled by a general practitioner (GP) (CM), a rheumatologist (ER), and, for OSA, a respiratory medicine consultant and another GP (SW and RH). Any disagreements were resolved by consensus. A list of all such codes used may be found in the morbidity section of the medical record data research repository at www.keele.ac.uk/mrr.

Statistical analysis. Characteristics of the subjects at the index date were summarized using descriptive statistics. Incidence rates of gout and corresponding 95% confidence intervals (95% CIs) were calculated per 1,000 person-years. Cox proportional hazards regression models were used to obtain associations between OSA status and time to diagnosis of gout in terms of hazard ratios (HRs). Corresponding 95% CIs were based on robust standard errors to account for any possible clustering due to matching. Initially crude HRs were obtained, followed by adjustments for age, sex, diabetes mellitus, ischemic heart disease, hypertension, hyperlipidemia, use of diuretic drugs, BMI, and alcohol consumption.

It has been previously shown that increased risk of gout due to OSA persists across obesity status (13). Therefore, models were refit with further adjustment for sleep apnea × BMI interaction and stratified effect sizes were obtained via the lincom command in Stata, which calculates appropriate linear combinations of coefficients and associated CIs. The association between OSA and gout was explored over the whole follow-up period, as well as 1, 2, 5, and 10 years post–index date, using the lincom command.

Assumption of proportionality of hazards was assessed using graphical methods and Schoenfeld residuals. If proportionality was not satisfied, interactions of corresponding covariates with appropriate functions of time were included in the model. Right censoring was assumed noninformative and was taken as the earliest date of death, date of transfer from practice, date of last collection of records from the practice, or March 31, 2015.

All analyses were performed using Stata software, version 13.1 (19). The study was approved by the CPRD Independent Scientific Advisory Committee (project 14-047).

Sensitivity analyses. The first sensitivity analysis assessed whether our main findings were influenced by the potential presence of unmeasured confounding, using a method proposed by Lin and colleagues (20). We assumed a binary unmeasured confounder with an associated HR of 2.5 among both exposed and unexposed patients (guided by the strongest association between the assessed covariates and gout, as observed in our data), and varied its prevalence among the exposed and unexposed patients. The second sensitivity analysis involved the assessment of results stemming from complete case analyses, with missing data ignored. Multiple imputations were not considered as it was suspected that missing data on BMI and alcohol consumption were not missing at random. Finally, we assessed whether our main findings were altered by the use of available alcohol and weight data recorded at any point rather than prior to the index date only. This is a common approach, though erroneous in studies of exposure effect, used in CPRD
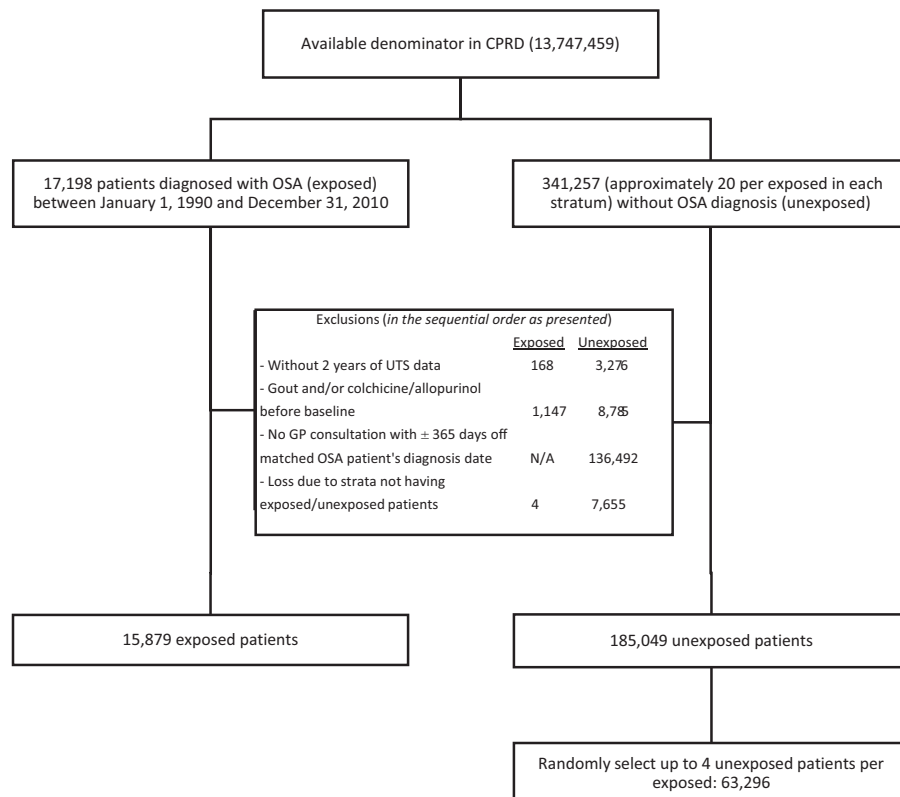

Figure 1. Selection of exposed and unexposed patients. CPRD = Clinical Practice Research Datalink; OSA = obstructive sleep apnea; UTS = up to standard date; GP = general practitioner; NA = not applicable.

analyses involving lifestyle characteristics to minimize the extent of missing data.

RESULTS

Analysis sample. We identified 17,198 patients with incident OSA between 1990 and 2010 who were matched at an ~1:20 ratio to 341,257 patients who had no record of OSA. Following the exclusion of those with an inadequate period of up-to-standard data, those prescribed allopurinol or colchicine prior to the index date, the unexposed patients who did not consult their practice within a year of their OSA patient's index date, and the patients who were left without a match following these exclusions, 15,879 OSA patients and 185,049 unexposed patients remained. Up to 4 available unexposed patients per OSA patient were then chosen at random, resulting in 63,296 unexposed patients (Figure 1).

The mean age and sex of the 2 exposure groups were the same (mean age 52.2 years and 76% male, in both) as expected due to the matched study design. Those with OSA had a higher prevalence of each comorbidity assessed, were more likely to have been prescribed diuretic medications, and were more likely to be obese and current alcohol drinkers. Furthermore, they

Table 1. Patient characteristics (covariates) at the index date*

Covariate	OSA (n = 15,879)	No OSA (n = 63,296)	P
Age, mean ± SD years	52.2 ±1.2	52.2 ±12.2	0.949
Male	12,108 (76)	48,260 (76)	0.986
BMI			<0.001
Normal	1,272 (8)	13,148 (21)	
Overweight	3,279 (21)	14,830 (23)	
Obese	8,059 (51)	8,857 (14)	
Data missing	3,269 (21)	26,461 (42)	
BMI, mean ± SD kg/m^2	34.0 ±8.1	27.4 ±5.1	
Alcohol			<0.001
No	1,748 (11)	4,968 (8)	
Ex-drinker	372 (2)	854 (1)	
Current drinker	9,841 (62)	31,823 (50)	
Data missing	3,918 (25)	25,651 (41)	
Diabetes	2,168 (14)	3,669 (6)	<0.001
Ischemic heart disease	741 (5)	1,691 (3)	<0.001
Hypertension	4,667 (29)	10,299 (16)	<0.001
Hyperlipidemia	2,288 (14)	4,942 (8)	<0.001
Diuretic use	4,499 (28)	7,587 (12)	<0.001

* Except where indicated otherwise, values are the number (%). OSA = obstructive sleep apnea.

were less likely to have missing information regarding BMI and alcohol use (Table 1).

Risk of gout. During follow-up, 782 OSA patients (4.9%) and 1,651 non-OSA patients (2.6%) developed gout, with a median time to gout diagnosis of 5.66 years (interquartile range [IQR] 3.58–8.28) and 5.83 years (IQR 3.93–8.55) in the 2 groups, respectively. The incidence rate per 1,000 person-years was 7.83 among those with OSA and 4.03 among those without OSA (unadjusted HR 1.94 [95% CI 1.78–2.12]). On adjustment for covariates considered in this study, the effect diminished but the statistically significant HR remained (1.42 [95% CI 1.29–1.56]) (Table 2).

The interaction between sleep apnea and BMI was statistically significant ($P < 0.001$); therefore, results are also presented by BMI group (Table 2). The increased risk of gout among patients with sleep apnea compared to those without sleep apnea was noted in all BMI categories, particularly in the normal BMI group (adjusted HR 1.76 [95% CI 1.22–2.53]). Corresponding HR estimates in the overweight and obese groups were 1.27 (95% CI 1.06–1.54) and 1.40 (95% CI 1.21–1.61), respectively.

There was also a significant connection between sleep apnea and time. The association between sleep apnea and development of gout was substantial across all time periods following the index date except for 0–1 years and >10 years post–index date, and was the strongest 1–2 years following the index date (adjusted HR 1.64 [95% CI 1.30–2.06]). Associations between sleep apnea and gout were similar across the 2–5-year and the 5–10-year period following the index date (Table 3).

In the normal BMI category, the risk of incident gout 2–5 years after the index date was more than twice as great among those with OSA than those without OSA (HR 2.02 [95% CI 1.13–3.62]); however, no significant differences were found for other time periods despite the HR being the highest 1–2 years post–index date (Table 3). For subjects who were overweight, the HR peaked to 1.73 in the period 1–2 years after the index date (95% CI 1.02–2.96), and for those who were obese, significant HRs were observed 1–2, 2–5, and 5–10 years post–index date, being the highest in the 1–2 year-time period (1.70 [95% CI 1.18–2.43]).

A sensitivity analysis to assess the effect of unmeasured confounding showed that adjustment for a confounder with a difference in prevalence of <20% (e.g., as seen in diabetes and hypertension) would result in a reduction in the bias of the estimated HR, but the significant association between OSA and gout would remain. The effect of restricting analyses to those with complete data on all covariates (i.e., complete case analysis) generally had minimal impact on our findings, as did using data on BMI and alcohol use recorded at any time point. Findings of all sensitivity analyses are presented in Supplementary Tables 1–3 (on the *Arthritis & Rheumatology* web site at

Table 2. Incidence rate and risk of gout by BMI category*

Sample (n)	No. of gout events	OSA	No OSA	Unadjusted HR (95% CI)	Adjusted HR (95% CI)
All (79,175)†	2,433	7.83 (7.29–8.39)	4.03 (3.84–4.23)	1.94 (1.78–2.12)‡	1.42 (1.29–1.56)‡
BMI§					
Normal (14,420)	222	4.16 (2.99–5.80)	2.24 (1.94–2.59)	1.84 (1.28–2.64)¶	1.76 (1.22–2.53)¶
Overweight (18,109)	608	6.76 (5.74–7.96)	5.00 (4.57–5.48)	1.34 (1.11–1.62)¶	1.27 (1.06–1.54)#
Obese (16,916)	808	9.77 (8.83–10.61)	6.70 (6.03–7.44)	1.44 (1.25–1.66)‡	1.40 (1.21–1.61)‡

* Values are the gout incidence rate per 1,000 person-years (95% confidence interval [95% CI]). OSA = obstructive sleep apnea.
† Hazard ratio (HR) was adjusted for age, sex, body mass index (BMI), alcohol, diabetes mellitus, ischemic heart disease, hypertension, hyperlipidemia, and use of diuretic drugs.
‡ $P < 0.0001$.
§ HR was adjusted for sleep apnea × BMI interaction (P for interaction < 0.001 by Wald's test) in addition to the factors for which the all-subjects HR was adjusted.
¶ $P < 0.005$.
# $P < 0.05$.

http://onlinelibrary.wiley.com/doi/10.1002/art.40662/abstract). The proportional hazards assumption was satisfied throughout.

DISCUSSION

The novelty of this study lies in its assessment of both the short- and long-term associations of OSA with incident gout in a large primary care–based population. It has previously been shown that people with OSA have a higher risk of developing gout in the first year following an OSA diagnosis (13). We showed that this increased risk persists beyond the first year after OSA diagnosis, with overall risk peaking 1–2 years after the index date. This statistically significant finding was seen in patients with normal BMI as well as in patients who were overweight or obese; however, the risk of incident gout in patients with OSA relative to those without OSA was greater in patients with normal BMI than in patients who were overweight or obese.

While there is potential for misclassification of OSA, this diagnosis is unlikely to be made solely in primary care and, as

such, will be entered into the patient's record only after a diagnosis has been made by a respiratory specialist in secondary care. Previous studies have shown that when a GP records a diagnosis of OSA, this diagnosis is usually correct (6,21,22). Therefore, it is likely that those identified as having OSA do indeed have the condition; however, OSA may be unrecognized in some patients (6,22,23), which could potentially bias our findings toward the null. Similarly, there is the possibility of the misclassification of gout if the GP diagnosis is not entirely accurate; however, previous studies have indicated that this is unlikely to occur frequently in the CPRD (24,25). Furthermore, a study by Meier and Jick showed the positive predictive value of a gout diagnosis in the CPRD to be 90% (26). Possible misclassification of confounding comorbidities may occur but is expected to occur at random, therefore not affecting our findings.

BMI may not be the best correlation with OSA. Neck and waist circumference may be better suited, as they take into account obesity distribution and are associated with visceral obesity, which is associated with the risk of OSA among other

Table 3. Adjusted risk of gout at different time points after the index date by BMI category*

Group	Years after index date				
	0–1	1–2	2–5	5–10	>10
All†	1.22 (0.97–1.53)	1.64 (1.30–2.06)‡	1.46 (1.25–1.70)‡	1.44 (1.22–1.70)‡	1.27 (0.95–1.70)
BMI§					
Normal	1.75 (0.67–4.54)	2.11 (0.71–6.26)	2.02 (1.13–3.62)¶	1.65 (0.82–3.32)	0.96 (0.29–3.22)
Overweight	1.22 (0.73–2.04)	1.73 (1.02–2.96)¶	1.05 (0.75–1.48)	1.38 (0.98–1.93)	1.31 (0.77–2.25)
Obese	1.24 (0.88–1.77)	1.70 (1.18–2.43)#	1.42 (1.12–1.79)#	1.41 (1.08–1.85)¶	0.82 (0.46–1.44)

* Reference category in each case is no obstructive sleep apnea. Values are the hazard ratio (HR) (95% confidence interval).
† HR was adjusted for sleep apnea × time interaction (P for interaction < 0.001 by Wald's test), age, sex, body mass index (BMI), alcohol, diabetes mellitus, ischemic heart disease, hypertension, hyperlipidemia, and use of diuretic drugs.
‡ $P < 0.0001$.
§ HR was adjusted for three-way sleep apnea × BMI × time interaction (P for interaction < 0.001 by Wald's test) in addition to the factors for which the all-subjects HR was adjusted.
¶ $P < 0.05$.
# $P < 0.005$.

subjects (27,28). However, these measures are not routinely collected in the CPRD.

It is important to know how reliable our estimates are. It is possible that the significant adjusted relationship between OSA and gout could be a result of residual confounding, due to possible exposure misclassification as explained above, and/or omission of important confounders such as genetic factors and dietary components that may be associated with both OSA and gout, but are unmeasurable or are not routinely recorded in primary care in the UK. We have tested the sensitivity of our overall estimated HR to the presence of some unobserved confounder (or a selection of confounders subsequently split into binary low/high risk) strongly associated with gout in both exposure groups, and found that it is robust provided that the absolute difference in the prevalence of such a confounder between exposed and unexposed subjects is approximately <20%. If, however, the prevalence among the exposed subjects is much higher, then it is possible that adjustment for such a confounder would have attenuated the observed association in this study. This should not take away from the importance of our findings, but rather be seen as a necessary component of any analysis using observational data, especially when medical record data are involved as they may be prone to incomplete and imprecise recording. A broad time frame was selected for identifying OSA, namely, from January 1, 1990 through December 31, 2010, in order to allow sufficient time to detect potential confounders prior to an OSA diagnosis and the development of gout after this index date.

Our study confirms the findings of earlier studies that people with OSA are at increased risk of incident gout. The most likely mechanism to explain this association is that, along with catecholamine surges and sustained hypertension (29), intermittent hypoxia increases nucleotide turnover, which enhances endogenous uric acid production (11). This raises the question as to whether the correction of hypoxia in OSA by treatment with continuous positive airways pressure (CPAP) lowers serum uric acid levels. Theoretically, this could reduce the risk of incident gout and treat existing gout. However, while observational studies have suggested that CPAP treatment leads to a reduction in serum uric acid levels (30), a secondary, although underpowered, analysis of data from a small randomized controlled trial of obese men with OSA and type 2 diabetes mellitus but not gout did not show any beneficial urate-lowering effect of CPAP compared to sham CPAP (31).

The risk of incident gout in patients with OSA persisted in all 3 BMI strata. However, the risk differed according to BMI, with those having normal BMI being at greater risk of developing gout than those who were overweight or obese. This suggests that the contribution of OSA to the risk of hyperuricemia and gout is independent of BMI, and clinicians should consider the possibility of gout in patients with sleep apnea regardless of obesity. The effect of CPAP in lowering urate and preventing or treating gout in patients with OSA remains unclear, and further adequately powered randomized controlled trials are required.

AUTHOR CONTRIBUTIONS

All authors were involved in drafting the article or revising it critically for important intellectual content, and all authors approved the final version to be published. Dr. Blagojevic-Bucknall had full access to all of the data in the study and takes responsibility for the integrity of the data and the accuracy of the data analysis.
Study conception and design. Blagojevic-Bucknall, Mallen, Muller, Hayward, West, Choi, Roddy.
Acquisition of data. Blagojevic-Bucknall.
Analysis and interpretation of data. Blagojevic-Bucknall, Mallen, Muller, Roddy.

REFERENCES

1. Kuo CF, Grainge MJ, Malled CD, Zhang W, Doherty M. Rising burden of gout in the UK but continuing suboptimal management: a nationwide population study. Ann Rheum Dis 2014;74:661–7.

2. Roddy E, Choi HK. Epidemiology of gout. Rheum Dis Clin North Am 2014;40:155–75.

3. McAdams-DeMarco MA, Maynard JW, Baer AN, Coresh J. Hypertension and the risk of incident gout in a population-based study: the Atherosclerosis Risk in Communities cohort. J Clin Hypertens (Greenwich) 2012;14:675–9.

4. Maynard JW, McAdams-DeMarco MA, Baer AN. Kottgen A, Folsom AR, Coresh J, et al. Incident gout in women and association with obesity in the Atherosclerosis Risk in Communities (ARIC) Study. Am J Med 2012;125:e9–717.

5. US Preventative Services Task Force, Bibbins-Domingo K, Grossman DC, Curry SJ, Davidson KW, Epling JW Jr, et al. Screening for obstructive sleep apnea in adults: US Preventive Services Task Force recommendation statement. JAMA 2017;317:407–14.

6. Ram S, Seirawan H, Kumar SK, Clark GT. Prevalence and impact of sleep disorders and sleep habits in the United States. Sleep Breath 2010;14:63–70.

7. Young T, Palta M, Dempsey J, Skatrud J, Weber S, Badr S. The occurrence of sleep-disordered breathing among middle-aged adults. N Engl J Med 1993;328:1230–5.

8. West SD, Nicikk DJ, Stradling JR. Prevalence of obstructive sleep apnea in men with type 2 diabetes. Thorax 2006;61:945–50.

9. Bazzano LA, Khan Z, Reynolds K, He J. Effect of nocturnal nasal continuous positive airway pressure on blood pressure in obstructive sleep apnea. Hypertension 2007;50:417–23.

10. Ruiz García A, Sánchez Armengol A, Luque Crespo E, Garcia Aguilar D, Romero Falcon A, Carmona Bernal C, et al. Blood uric acid levels in patients with sleep-disordered breathing. Arch Bronconeumol 2006;42:492–500.

11. Glantzounis GK, Tsimoyiannis EC, Kappas AM, Galaris DA. Uric acid and oxidative stress. Curr Pharm Des 2005;11:4145–51.

12. Roddy E, Muller S, Hayward R, Mallen C. The association of gout with sleep disorders: a cross-sectional study in primary care. BMC Musculoskelet Disord 2013;14:119.

13. Zhang Y, Peloquin CE, Dubreuil M, Roddy E, Lu N, Neogi T, et al. Sleep apnea and the risk of incident gout: a population-based, body mass index–matched cohort study. Arthritis Rheumatol 2015;67:3298–302.

14. Tate AR, Beloff N, Al-Radwan B, Wickson J, Puri S, Williams T, et al. Exploiting the potential of large databases of electronic health

records for research using rapid search algorithms and an intuitive query interface. J Am Med Inform Assoc 2014;21:292–8.

15. Herrett E, Thomas SL, Schoonen WM, Smeeth L, Hall AJ. Validation and validity diagnoses in the General Practice Research Databases: a systematic review. Br J Clin Pharmacol 2010;69:4–14.

16. Choi HK, Atkinson K, Karlson EW, Curhan G. Obesity, weight change, hypertension, diuretic use, and risk of gout in men: the health professionals follow-up study. Arch Intern Med 2005;165:742–8.

17. Zhu Y, Pandya BJ, Choi HK. Comorbidities of gout and hyperuricemia in the US general population: NHANES 2007-2008. Am J Med 2012;125:679–87.

18. Punjabi NM. The epidemiology of adult obstructive sleep apnea. Proc Am Thorac Soc 2008;15:136–43.

19. Stata statistical software: release 13. College Station (TX): StataCorp; 2013.

20. Lin DY, Psaty BM, Kronmal RA. Assessing the sensitivity of regression results to unmeasured confounding in observational studies. Biometrics 1998;54:948–63.

21. Kramer NR, Cook TE, Carlisle CC, Corwin RW, Millman RP. The role of the primary care physician in recognizing obstructive sleep apnea. Arch Intern Med 1999;159:965–8.

22. Mold JW, Quattlebaum C, Schinnerer E, Boeckman L, Orr W, Hollabaugh K. Identification of primary care clinicians of patients with obstructive sleep apnea: a practice-based research network (PBRN) study. J Am Board Fam Med 2011;24:138–145.

23. Roth T, Bogan RK, Culpepper L, Doghramji K, Doghramji P, Drake C, et al. Excessive sleepiness: under-recognized and essential marker for sleep/wake disorder management. Curr Med Res Opin 2010;26:S3–S24.

24. Roddy E, Zhang W, Doherty M. Concordance of the management of chronic gout in a UK primary-care population with the EULAR gout recommendation. Ann Rheum Dis 2007;66:1311–55.

25. Roddy E, Mallen CD, Hider SL, Jordan KP. Prescription and comorbidity screening following consultation for acute gout in primary care. Rheumatology (Oxford) 2010;49:105–11.

26. Meier CR, Jick H. Omeprazole, other antiulcer drugs and newly diagnosed gout. Br J Clin Pharmacol 1997;44:175–8.

27. Yusuf S, Hawken S, Ounpuu S, Bautista L, Franzosi MG, Commerford P, et al. Obesity and the risk of myocardial infarction in 27,000 participants from 52 countries: a case-control study. Lancet 2005;366:1640–9.

28. Romero-Corral A, Montori VM, Somers VK, Korinek J, Thomas RJ, Allison TG, et al. Association of bodyweight with total mortality and with cardiovascular events in coronary artery disease: a systematic review of cohort studies. Lancet 2006; 368:666–78.

29. Kohler M, Stradling JR. Mechanisms of vascular damage in obstructive sleep apnea. Nat Rev Cardiol 2010;7:677–85.

30. Seetho IW, Parker RJ, Craig S, Duffy N, Hardy KJ, Wilding JP, et al. Serum urate and obstructive sleep apnea in severe obesity. Chron Respir Dis 2015;12:238–46.

31. Prudon B, Roddy E, Stradling JR, West SD. Serum urate levels are unchanged with continuous positive airway pressure therapy for obstructive sleep apnea: a randomized controlled trial. Sleep Med 2013;14:1419–21.

AMERICAN COLLEGE
OF RHEUMATOLOGY
EDUCATION · TREATMENT · RESEARCH

BRIEF REPORT

Interferon-γ–Mediated Immunopathology Potentiated by Toll-Like Receptor 9 Activation in a Murine Model of Macrophage Activation Syndrome

Lehn K. Weaver, Niansheng Chu, and Edward M. Behrens

Objective. Macrophage activation syndrome (MAS) is a life-threatening cytokine storm syndrome that occurs in patients with underlying rheumatic diseases. Preclinical and clinical data suggest that interferon-γ (IFNγ) is pathogenic in MAS, but how IFNγ may be linked to disease pathogenesis remains unknown. This study was undertaken to determine whether IFNγ signals synergize with systemic innate immune responses to drive the cytokine storm in a murine model of MAS.

Methods. IFNγ-deficient mice were treated with 5 doses of the Toll-like receptor 9 (TLR-9) agonist CpG 1826, IFNγ, or a combination of the 2 stimuli over the course of 10 days. Immunopathologic features of MAS, including cytopenias, hepatitis, hepatosplenomegaly, and induction of inflammatory myelopoiesis, were assessed. Mixed bone marrow chimeras were created to determine whether TLR-9– and IFNγ receptor 1 (IFNγR1)–dependent signals induce enhanced myelopoiesis in a cell-intrinsic or cell-extrinsic manner.

Results. IFNγ-deficient mice did not develop features of MAS when treated with repeated doses of either the TLR-9 agonist or IFNγ alone. In contrast, IFNγ-deficient mice treated with both the TLR-9 agonist and IFNγ developed cytopenias, hepatitis, and hepatosplenomegaly, reproducing major clinical features of MAS. TLR-9– and IFNγR1-dependent signals synergized to enhance myeloid progenitor cell function and induce myelopoiesis in vivo, which occurred through cell-extrinsic mechanisms and correlated with the induction of disease.

Conclusion. These findings demonstrate that TLR-9–driven signals potentiate the effects of IFNγ to initiate murine MAS, and provide evidence that induction of inflammatory myelopoiesis is a common TLR-9– and IFNγ-dependent pathway that may contribute to the pathogenesis of MAS.

INTRODUCTION

Macrophage activation syndrome (MAS) is a life-threatening clinical syndrome resulting from immune dysregulation and uncontrolled inflammation in patients with rheumatic conditions (1). Morbidity and mortality from MAS remain high despite the advent of targeted immunosuppressive therapies and improvements in intensive care measures to support failing organs (1). The pathogenesis of this rare and devastating condition remains poorly defined, which impedes the development of rational and targeted therapies to treat patients with MAS.

Results of preclinical and translational studies have suggested that interferon-γ (IFNγ) is pathogenic in MAS (2–4), which prompted a clinical trial to study the safety and efficacy of IFNγ neutralization in patients with systemic juvenile idiopathic arthritis (JIA) who developed MAS (ClinicalTrials.gov identifier NCT03311854). Despite the growing interest in IFNγ as a therapeutic target, the mechanisms leading to IFNγ-mediated immunopathology in MAS remain unclear. Furthermore, high-dose IFNγ drives anemia and hemophagocytosis in mice, but is insufficient to recapitulate all of the manifestations of MAS by itself (5). These data suggest that additional inflammatory signals in

Address correspondence to Lehn K. Weaver, MD, PhD, The Children's Hospital of Philadelphia, 1107-C Abramson Research Center, 3615 Civic Center Boulevard, Philadelphia, PA 19104-4399. E-mail: weaverl1@email.chop.edu.

combination with IFNγ are required to induce MAS immunopathology.

Pattern-recognition receptors (PRRs) are expressed by innate immune cells and sense a diverse range of endogenous and exogenous danger signals. Toll-like receptors (TLRs) are the best-characterized PRRs and are implicated in the development of MAS. Preclinical models of disease suggest that chronic or exaggerated responses to systemic TLR activation lead to MAS in mice (2,6,7). Patients with systemic JIA, the rheumatic disease with the greatest predisposition to the development of MAS, have an interleukin-1 (IL-1) and TLR gene expression signature in their peripheral blood mononuclear cells (8). Furthermore, polymorphisms in IFN regulatory factor 5 (IRF-5), a signaling molecule downstream of TLR activation, results in higher IRF-5 gene expression and a 4-fold higher risk of MAS in patients with systemic JIA (9,10). These data suggest that TLRs and their downstream signaling pathways could contribute to the pathogenesis of MAS.

Previous investigations have established that repeated TLR-9 activation in wild-type mice induces clinical manifestations of MAS, including cytopenias, hepatosplenomegaly, hepatitis, and hypercytokinemia (2). This model is an IFNγ-dependent model of MAS, as neutralization of IFNγ abrogates disease and IFNγ$^{-/-}$ mice are protected from TLR-9–induced immunopathology (2). Inflammatory monocytes are the main producers of IL-12 and are key to disease pathogenesis in this model (11), since neutralization of IL-12 prevents TLR-9–induced production of IFNγ and ameliorates disease (12). Repeated doses of a TLR-9 agonist are required to induce disease, which leads to heightened systemic production of IL-12 after each dose of TLR-9 stimulus, and drives a feed-forward inflammatory response (11). This feed-forward inflammatory response correlates with the induction of inflammatory myelopoiesis, which skews the hematopoietic output of the host to accelerate the production of new inflammatory monocytes (11). Accumulation of TLR-9–responsive inflammatory monocytes correlates with heightened cytokine production following repeated activation of TLR-9 in vivo, a mechanism that is thought to drive disease (11).

It remains unclear whether repeated TLR-9 activation is required simply for the upstream, IL-12–mediated induction of high levels of pathogenic IFNγ or whether IFNγ-independent, TLR-9–dependent signals are additionally necessary for the induction of murine MAS. To differentiate between these possibilities, we stimulated IFNγ-deficient mice with repeated doses of the TLR-9 agonist CpG 1826 or IFNγ alone, or with a combination of the 2 stimuli. Consistent with our hypothesis, IFNγ-deficient mice develop MAS when treated with both the TLR-9 agonist and IFNγ, but not when treated with these inflammatory signals individually. We provide evidence that induction of inflammatory myelopoiesis requires both TLR-9– and IFNγ-dependent signals, which may contribute to disease by accelerating the production of new TLR-9–responsive monocytes. These findings add to our under-

standing of MAS pathogenesis, and reveal IFNγ-independent signals as potential therapeutic targets for the treatment of MAS.

MATERIALS AND METHODS

Vertebrate animals. Mice used in individual experiments were age- and sex-matched. Efforts were made to ensure equal use of male and female mice in all experiments. IFNγ-deficient, IFNγ receptor 1 (IFNγR1)–deficient, and congenically labeled Wild-type CD45.1 SJL C57BL/6 mice were purchased from The Jackson Laboratory. TLR-9–deficient mice were originally produced by Shizuo Akira (Osaka University). Mouse breeding, animal husbandry, and animal experiments occurred within the specific pathogen–free animal facilities at The Children's Hospital of Philadelphia. All animals were cared for according to each institution's animal facility guidelines, and procedures were performed after review and approval for all experiments had been obtained from each institution's ethics board.

Induction of murine MAS. The TLR-9 agonist and class B CpG oligonucleotide CpG 1826 (sequence TCCATG ACGTTCCTGACGTT) was synthesized with a phosphothioate backbone at Integrated DNA Technologies (Coralville, IA). Recombinant murine IFNγ was obtained from PeproTech. Eight-week-old IFNγ-deficient mice were treated with 5 intraperitoneal doses of vehicle (phosphate buffered saline [PBS]), 50 μg of the TLR-9 agonist CpG 1826, 10 μg of IFNγ, or a combination of CpG 1826 and IFNγ every other day over the course of 10 days. Mice were killed 24 hours after the last injection. The extent of splenomegaly and hepatomegaly was calculated by dividing the organ weight by the body weight of the mouse and multiplying by 100. Whole blood was obtained from the cheeks of mice for determination of complete blood cell counts on a Sysmex XT-2000iV Automated Hematology Analyzer. Whole livers from mice were fixed in 10% formaldehyde and embedded in paraffin, and individual slides containing hematoxylin and eosin–stained tissue were made at the Pathology Core at The Children's Hospital of Philadelphia. All histology images were obtained with the use of a Leica DM4000B microscope and SPOT Software version 5.1. Foci of >10 inflammatory cells per high-power field were counted using a 20× objective.

Processing of organs, whole blood, and serum. Bone marrow cells were flushed from the leg bones of mice using cold PBS, and single cell suspensions were generated by mechanical disruption through a 70-μm strainer. Whole spleens were digested with DNase I (Roche) and collagenase (Roche) at 37°C for 30 minutes prior to the generation of single cell suspensions of splenocytes, which was achieved by mechanical disruption of the spleen through a 70-μm strainer. Red blood cell lysis was performed on all harvested cells using ACK lysis buffer (Lonza).

Total cells per organ were counted on a Countess TM Automated Cell Counter (ThermoFisher Scientific).

Generation of mixed bone marrow chimeras. Wild-type CD45.1 SJL C57BL/6 mouse hosts were lethally irradiated with 950 rads (cGy) of x-ray irradiation, followed by rescue with injection of 2.5–5 × 10^6 mixed bone marrow cells using 90% wild-type cells (from CD45.1 mice) and 10% knockout cells (from TLR-9–deficient or IFNγR1-deficient mice). Mixed bone marrow–chimeric mice were allowed 4–5 weeks of bone marrow reconstitution prior to the induction of murine MAS.

Cellular immunophenotyping. Flow cytometry was performed on a Miltenyi MacsQuant, and cell sorting was performed using a BD FACSAria II. Data from fluoresence-activated cell sorting were analyzed using FlowJo software. Fluorescently labeled cells were gated on forward and side light-scatter patterns to limit the inclusion of dead cells, debris, and doublets. Live cells were identified by excluding cells staining positive for LIVE/DEAD Fixable Aqua Dead Cell Stain (ThermoFisher Scientific). Fc Block (anti-CD16/32, clone 2.4G2) was used prior to staining for all flow cytometry experiments, except for the myeloid progenitor panels, which included staining for the Fc receptor CD16/32. Inflammatory monocytes were identified as Ly-6G–Ly-6C^{high}CD115+ cells. Myeloid progenitors were identified as common myeloid progenitors (CMPs) (Lin–c-Kit+CD105– CD16/32^{intermediate}CD115–), granulocyte–monocyte progenitors (GMPs) (Lin–c-Kit+CD105–CD16/32^{high}CD115–), monocyte–dendritic cell progenitors (MDPs) (Lin–c-Kit+CD105–CD115+Ly-6C–), and committed monocyte progenitors (cMoPs) (Lin–c-Kit+CD105–CD115+Ly-6C+). The lineage panel included antibodies against B220, CD4, CD5, CD8a, CD11b, CD11c, CD90.2, CD49b, Ly-6G, NK1.1, and Ter119.

Myelopoiesis assays. Bone marrow myeloid progenitors were sorted from mice treated with 5 doses of PBS, CpG 1826, IFNγ, or a combination of both CpG 1826 and IFNγ, as described above. Myeloid progenitors (500–2,000 cells per well) were cultured in α-minimum essential medium (Gibco) supplemented with 20% heat-inactivated fetal bovine serum (Atlanta Biologicals) and penicillin–streptomycin–L-glutamine (Cellgro) at 37°C in 6% CO_2. Granulocyte–macrophage colony-stimulating factor (GM-CSF), M-CSF, IL-3, and stem cell factor were obtained from PeproTech and used to stimulate the division and differentiation of myeloid progenitor cells in liquid cultures. All cytokines were used at a concentration of 5 ng/ml, except GM-CSF, which was used at a concentration of 3.3 ng/ml. After 7 days in culture, myeloid progenitor cell progeny were harvested and stained for mature myeloid cell surface markers (Ly-6G, Ly-6C, and CD11b) using the cellular immunophenotyping protocol described above. Total myeloid cell counts were enumerated on

a Miltenyi MacsQuant flow cytometer and gated on individual cell populations in FlowJo.

Statistical analysis. The numbers of experimental replicates differed in each experiment. All statistical analyses were performed using Prism version 7.0a (GraphPad). The Mann-Whitney U test was used for all between-group comparisons. Two-way analysis of variance was used to analyze the interaction between 2 independent variables on a dependent variable. P values less than or equal to 0.05 were considered significant.

RESULTS

IFNγ-driven immunopathology potentiated by TLR-9–dependent signals in murine MAS. Studies in murine models have highlighted the role of TLR-driven chronic and exaggerated immune responses as potent inducers of murine MAS (2,6,7). In TLR-9–mediated MAS, high levels of IFNγ are stimulated downstream of systemic TLR activation, and induction of IFNγ is required to drive MAS immunopathology (2). It remains unclear whether TLR-9–driven signals are required solely for the induction of high levels of IFNγ or whether TLR-9–dependent signals must act in combination with high levels of IFNγ to induce murine MAS. To differentiate between these possibilities, IFNγ-deficient mice were treated with repeated doses of a TLR-9 agonist (CpG 1826) alone, IFNγ alone, or a combination of the 2 stimuli over the course of 10 days. The dose of IFNγ used in these experiments recapitulates the levels of serum IFNγ induced downstream of repeated TLR-9 activation in wild-type mice (mean ~10 ng/ml; Supplementary Figure 1B, available on the *Arthritis & Rheumatology* web site at http://onlinelibrary.wiley.com/doi/10.1002/art.40683/abstract) as indicated in a study by Behrens et al (2).

IFNγ-deficient mice stimulated with repeated doses of the TLR-9 agonist CpG 1826 or IFNγ alone did not develop clinical manifestations of MAS (Figures 1A–G). Importantly, the same dose of IFNγ that caused no disease manifestations in IFNγ-deficient mice became pathogenic when delivered in the context of repeated systemic activation of TLR-9, as evident in our experiments showing that IFNγ-deficient mice treated with repeated doses of both the TLR-9 agonist and IFNγ developed robust clinical manifestations of MAS, including cytopenias, hepatosplenomegaly, and hepatitis (Figures 1A–G). Increased production of ferritin was induced following repeated dosing with CpG 1826, and these levels were not further increased in the presence of both TLR-9– and IFNγ-dependent signals (Supplementary Figure 1A [http://onlinelibrary.wiley.com/doi/10.1002/art.40683/abstract]). These data demonstrate that TLR-9–dependent signals are required to potentiate IFNγ-dependent immunopathology in murine MAS.
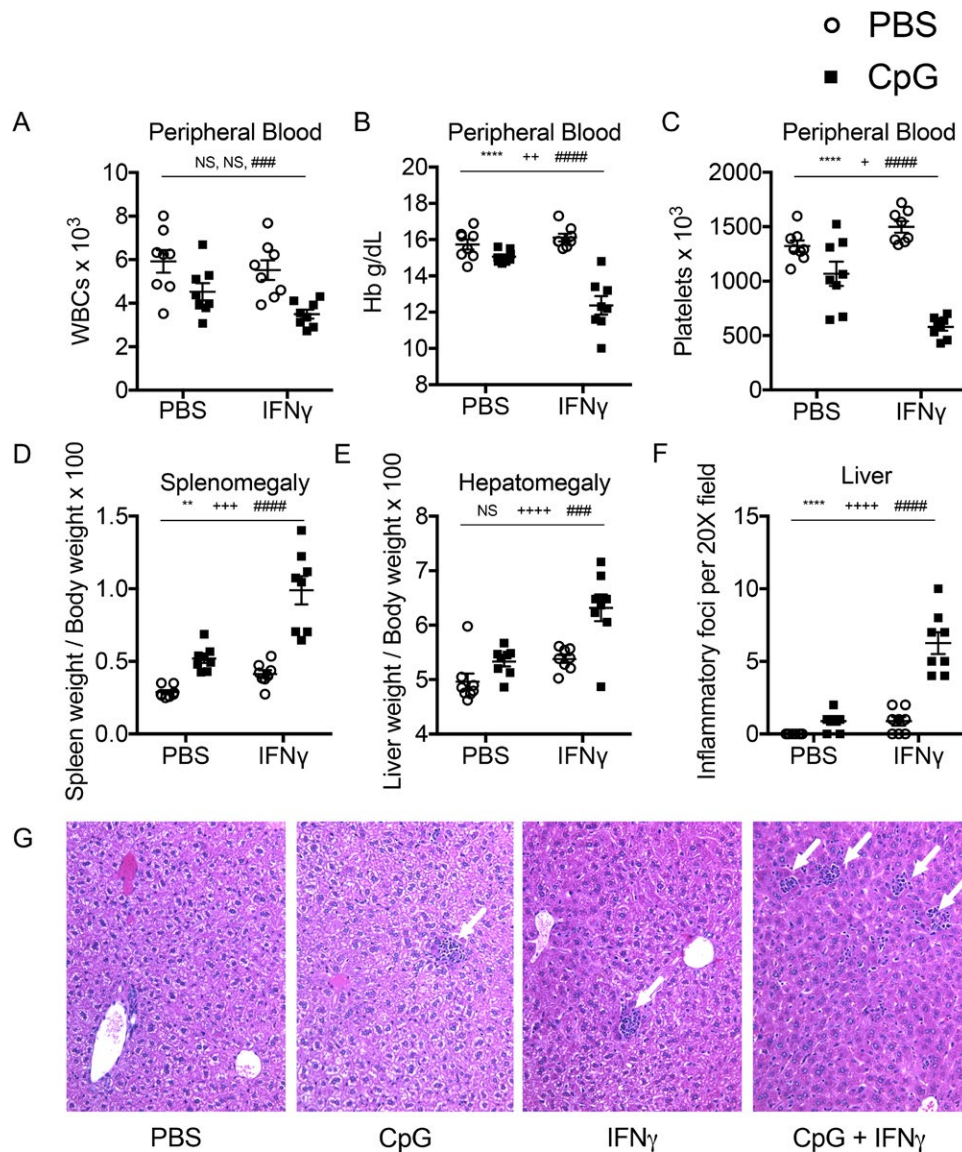
Figure 1. Toll-like receptor 9 (TLR-9)–dependent signals potentiate interferon-γ (IFNγ)–driven immunopathology in murine macrophage activation syndrome. IFNγ-deficient mice were treated with 5 doses of phosphate buffered saline (PBS), the TLR-9 agonist CpG 1826, IFNγ, or the combination of CpG 1826 and IFNγ every other day for 10 days. The mice were killed 24 hours after the fifth injection. **A–E,** Clinical manifestations of the cytokine storm were evaluated as peripheral white blood cell (WBC) counts (**A**), anemia (hemoglobin [Hb] levels) (**B**), thrombocytopenia (**C**), splenomegaly (**D**), and hepatomegaly (**E**). **F,** Livers from mice were sectioned and stained with hematoxylin and eosin, and the hepatic inflammatory foci per high-power field were enumerated. Original magnification × 20. **G,** Representative images from 1 mouse per treatment group show pathologic features of the liver. **Arrows** point to individual hepatic inflammatory foci. In **A–F,** symbols represent individual mice (n = 8 per group); horizontal lines with bars show the mean ± SD compiled from 3 independent experiments. All statistical comparisons were determined by two-way analysis of variance. For interaction within group, ** = $P < 0.01$ and **** = $P < 0.0001$. For IFNγ-treated mice versus mice not treated with IFNγ, + = $P < 0.05$; ++ = $P < 0.01$; +++ = $P < 0.001$; ++++ = $P < 0.0001$. For CpG-treated mice versus mice not treated with CpG, ### = $P < 0.001$; #### = $P < 0.0001$. NS = not significant.

Induction of inflammatory myelopoiesis by systemic TLR-9– and IFNγ-dependent signals, in a synergistic manner. Both TLR-9– and IFNγ-dependent signals have been implicated in the induction of myelopoiesis during systemic inflammatory responses (13,14). In TLR-9–mediated MAS, induction of enhanced myelopoiesis may be pathogenic, as myeloid progenitors (CMPs, GMPs, MDPs, and cMoPs) accumulate in the peripheral blood of TLR-9–activated mice, which correlates with the accumulation of TLR-9–responsive inflammatory monocytes (11). Accumulation of inflammatory monocytes leads to heightened cytokine production and MAS immunopathology, which occurs downstream of repeated TLR-9 activation in vivo (11). We therefore sought to determine whether TLR-9– and IFNγ-dependent signaling together may induce inflammatory
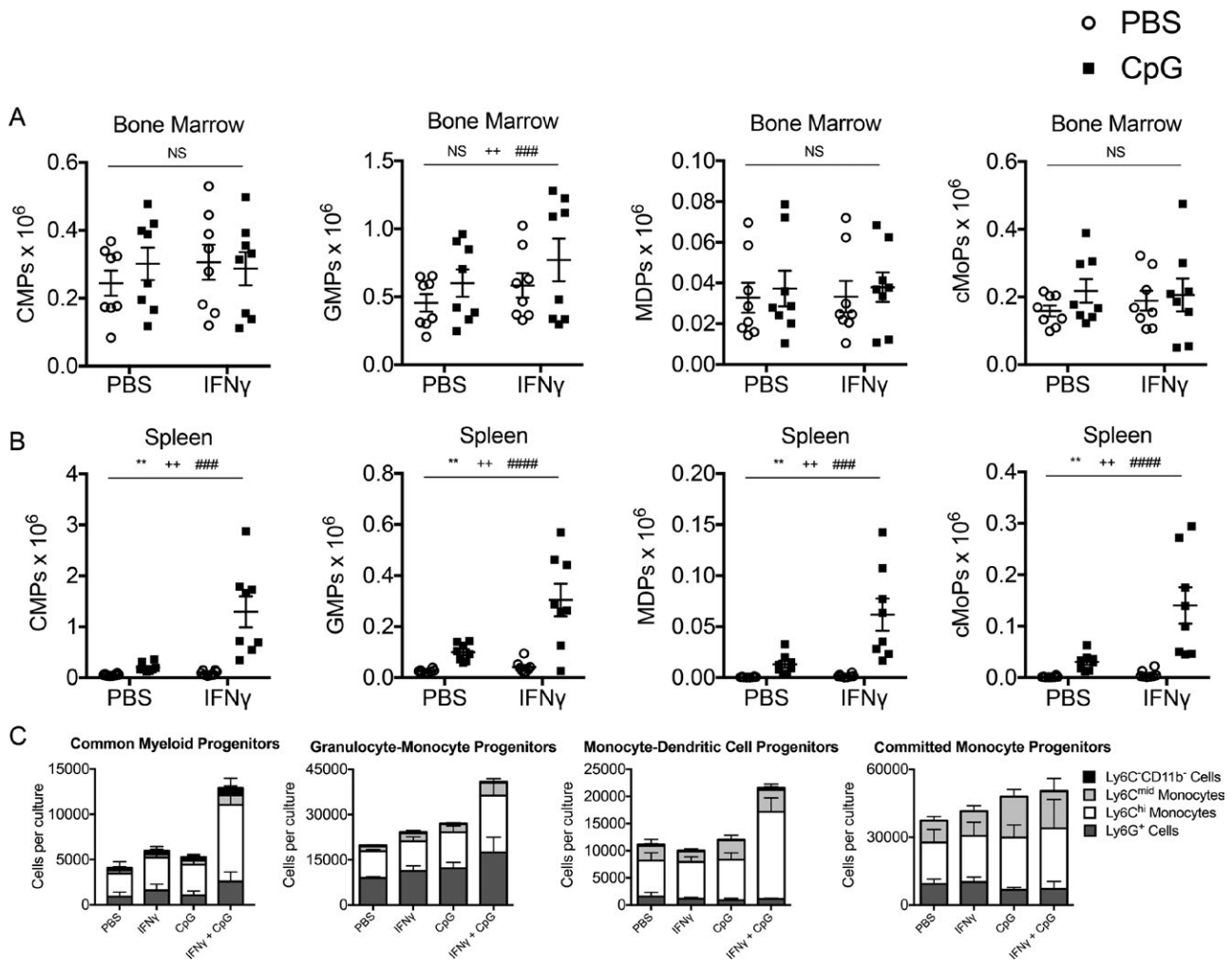
Figure 2. Systemic TLR-9– and IFNγ-dependent signals synergistically induce inflammatory myelopoiesis. IFNγ-deficient mice were treated with 5 doses of PBS, the TLR-9 agonist CpG 1826, IFNγ, or the combination of CpG 1826 and IFNγ every other day for 10 days. The mice were killed 24 hours after the fifth injection. **A** and **B,** The numbers of myeloid progenitors were determined in the bone marrow (**A**) and spleen (**B**) of mice in each treatment group. **C,** Individual populations of myeloid progenitors were sorted from the bone marrow of mice in each treatment group. Sorted myeloid progenitors were cultured in vitro for 7 days in medium containing macrophage colony-stimulating factor, granulocyte–macrophage colony-stimulating factor, interleukin-3, and stem cell factor. Mature myeloid cells were enumerated by flow cytometry. In **A** and **B**, compiled data from 3 independent experiments are shown. Symbols represent individual mice (n = 8 per group); horizontal lines with bars show the mean ± SD. In **C**, compiled data from 2 independent experiments are shown; bars show the mean and SD (n = 4 mice per group). All statistical comparisons were determined by two-way analysis of variance. For interaction within group, ** = $P < 0.01$. For IFNγ-treated mice versus mice not treated with IFNγ, ++ = $P < 0.01$. For CpG-treated mice versus mice not treated with CpG, ### = $P < 0.001$; #### = $P < 0.0001$. See Figure 1 for definitions.

myelopoiesis to promote immunopathology in murine MAS. Treatment with repeated doses of the TLR-9 agonist alone, IFNγ alone, or a combination of the TLR-9 agonist and IFNγ had minimal effects on the numbers of bone marrow myeloid progenitors (Figure 2A). In contrast, in the spleen, treatment of IFNγ-deficient mice with repeated doses of both the TLR-9 agonist and IFNγ synergistically induced the accumulation of extramedullary myeloid progenitors, whereas treatment with the TLR-9 agonist alone or IFNγ alone failed to have this effect in the spleen (Figure 2B).

Furthermore, individual populations of sorted myeloid progenitor cells (CMPs, GMPs, MDPs, or cMoPs) exhibited enhanced output of mature myeloid cells, as determined in ex vivo myelopoiesis assays, when the cells were isolated from IFNγ-deficient mice treated with both the TLR-9 agonist and IFNγ, but not when the cells were isolated from IFNγ-deficient mice treated with the TLR-9 agonist or IFNγ individually (Figure 2C). These data demonstrate that systemic TLR-9– and IFNγ-dependent signals lead to enhanced production of mature myeloid cells from myeloid progenitors in vitro, and this effect correlates with the accumulation of myeloid progenitors and MAS immunopathology in vivo. Our findings thus support a model that involves inflammatory myelopoiesis in the pathogenesis of MAS in which both TLR-9– and IFNγ-dependent signals work in conjunction to accelerate the production of new inflammatory monocytes that

accumulate in the periphery and heighten systemic immune responses to repeated TLR-9 activation in vivo.

Indirect, cell-extrinsic mechanisms for the induction of inflammatory myelopoiesis by TLR-9– and IFNγ-dependent signals in murine MAS. To determine whether TLR-9– and IFNγ-dependent signals either directly or indirectly induce inflammatory myelopoiesis, we generated 2 cohorts

of bone marrow–chimeric mice: 1 cohort injected with mixed wild-type:TLR-9–deficient mouse bone marrow, and 1 cohort injected with mixed wild-type:IFNγR1-deficient mouse bone marrow. We used a ratio of 90% wild-type and 10% knockout mouse bone marrow for the mixed bone marrow–chimeras to ensure that robust MAS immunopathology was generated in the chimeric mice (Supplementary Figures 2A and B, available on the *Arthritis & Rheumatology* web site at http://onlineli-
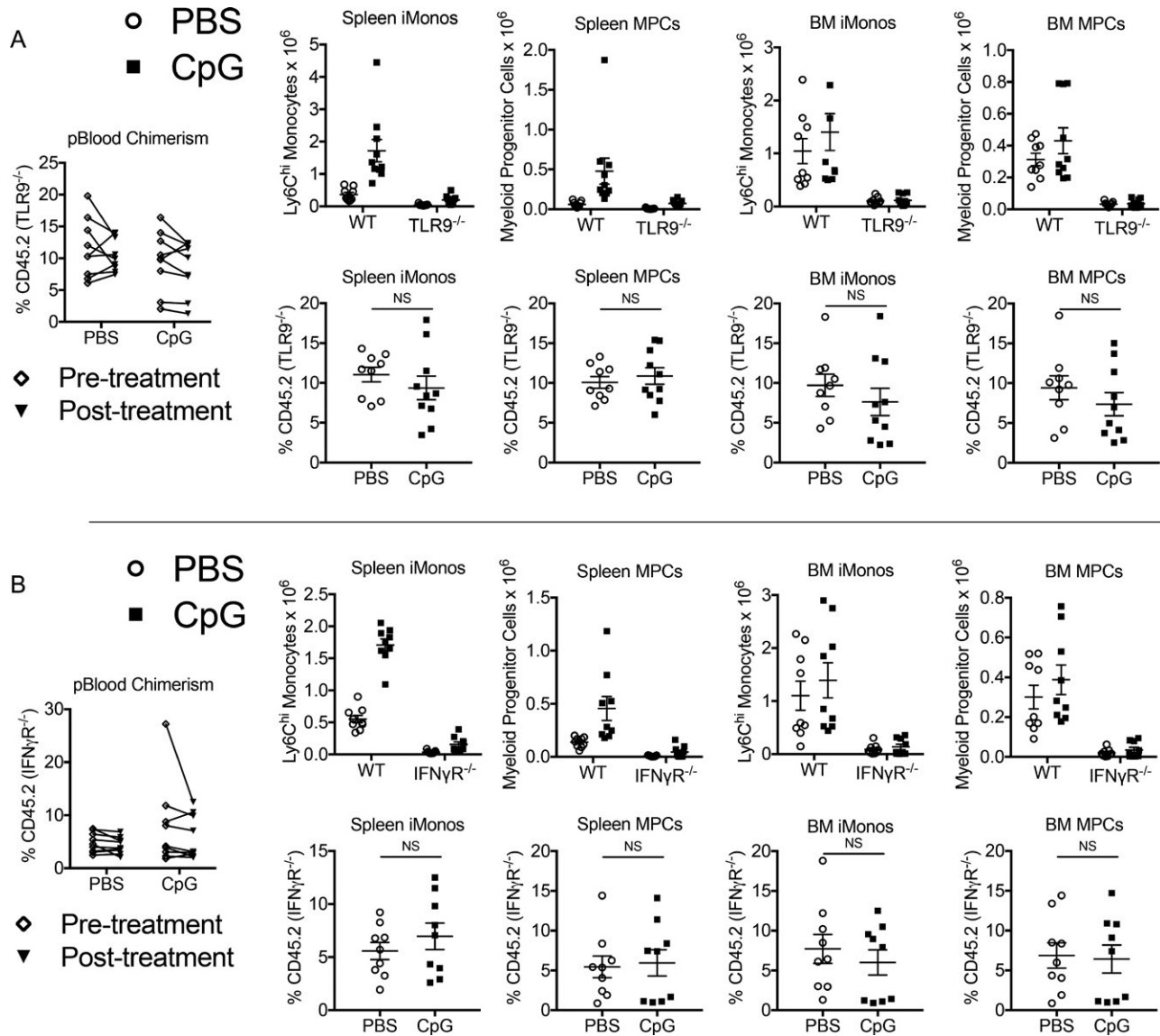
Figure 3. TLR-9– and IFNγ-dependent signals indirectly induce inflammatory myelopoiesis in murine macrophage activation syndrome. Congenically labeled CD45.1 wild-type (WT) SJL mouse hosts were lethally irradiated and reconstituted with mixed bone marrow (BM) from CD45.1 wild-type mice and CD45.2 TLR-9–deficient mice (**A**) or CD45.1 wild-type mice and CD45.2 IFNγR1-deficient mice (**B**) at a ratio of 9:1. After 4–5 weeks of bone marrow reconstitution, chimeric mice were treated with 5 doses of PBS or CpG 1826 over the course of 10 days. **A** and **B,** Left, Peripheral blood (pBlood) leukocyte chimerism was determined before and after treatment. **A** and **B,** Right, The numbers of wild-type (CD45.1) and TLR-9– or IFNγR1-deficient (CD45.2) spleen and bone marrow inflammatory monocytes (iMonos) and total myeloid progenitor cells (MPCs) were enumerated (top panels), and the percentages of wild-type (CD45.1) and TLR-9–or IFNγR1-deficient (CD45.2) spleen and bone marrow monocytes and total myeloid progenitors were determined (bottom panels). Symbols in right panels represent individual mice (n = 9–10 chimeric mice per group); horizontal lines with bars show the mean ± SD. Data were compiled from 2 independent experiments. Statistical analyses were performed using Mann-Whitney U test, comparing percentages of TLR-9–deficient cells (**A**) or IFNγR1-deficient cells (**B**) between chimeric mice treated with repeated doses of PBS and those treated with repeated doses of CpG. See Figure 1 for other definitions.

brary.wiley.com/doi/10.1002/art.40683/abstract). Injection of TLR-9–deficient cells contributed to the production of similar percentages of myeloid progenitors and inflammatory monocytes in the spleen and bone marrow of mixed bone marrow–chimeric mice, regardless of whether the mice were treated with repeated doses of the TLR-9 agonist or with the vehicle control (Figure 3A). Similar results were observed in wild-type: IFNγR1-deficient mixed bone marrow–chimeric mice (Figure 3B), suggesting that activation of both TLR-9 and IFNγR1 induces enhanced myelopoiesis through hematopoietic progenitor cell–extrinsic mechanisms. These data imply that both TLR-9– and IFNγ-dependent signals stimulate the production of additional inflammatory factors that act indirectly to induce inflammatory myelopoiesis during murine MAS.

DISCUSSION

A growing body of preclinical and translational studies implicates IFNγ as a central mediator of MAS pathogenesis in patients with systemic JIA (2–4). However, the mechanisms leading to IFNγ-mediated immunopathology remain unclear, and observations from animal models suggest that IFNγ alone is insufficient to induce all manifestations of MAS (5). In the present study, we have provided evidence that systemic TLR-9–driven signals potentiate IFNγ-mediated immunopathology in a murine model of MAS, as removal of either TLR-9– or IFNγ-dependent signals abrogated the manifestations of disease in IFNγ-deficient mice. This study adds to our understanding of MAS pathogenesis by delineating a role for both TLR- and IFNγ-dependent processes in the induction of disease, and suggests that these independent signals may contribute to disease pathogenesis by synergistically inducing inflammatory myelopoiesis.

IFNγ is known to potently synergize with TLR-dependent signals to induce cell-intrinsic proinflammatory macrophage functions (15). Induction of enhanced myelopoiesis may be a cell-extrinsic correlate that is synergistically induced downstream of IFNγ- and TLR-dependent signals in vivo to drive murine MAS. Intriguingly, increased numbers of extramedullary myeloid progenitors are correlated with the induction of disease in TLR-9–mediated murine MAS, which both require combined IFNγ- and TLR-dependent signals (11). TLR-9– and IFNγ-dependent signals contribute to the induction of inflammatory myelopoiesis through cell-extrinsic mechanisms. These data suggest that additional signals produced downstream of TLR-9 and IFNγR activation indirectly induce the accumulation of myeloid progenitors and potentiate their function in vivo. Future efforts directed at identifying the factors and signaling cascades involved in the induction of inflammatory myelopoiesis will be crucial to delineate whether targeting this pathway has therapeutic potential in MAS.

Thus, the results of this study support a role for both TLR- and IFNγ-dependent signals in the pathogenesis of murine MAS,

and highlight how the induction of inflammatory myelopoiesis may be a common pathogenic pathway synergistically induced downstream of these inflammatory signals. Future efforts will be required to determine the relevance of these findings to patients with MAS, and to define the cellular and molecular mechanisms that lead to the induction of inflammatory myelopoiesis. Such efforts may reveal novel therapeutic targets to ameliorate the overwhelming inflammatory cascade that leads to the clinical syndrome of MAS.

AUTHOR CONTRIBUTIONS

All authors were involved in drafting the article or revising it critically for important intellectual content, and all authors approved the final version to be published. Dr. Weaver had full access to all of the data in the study and takes responsibility for the integrity of the data and the accuracy of the data analysis.
Study conception and design. Weaver, Behrens.
Acquisition of data. Weaver, Chu.
Analysis and interpretation of data. Weaver, Behrens.

REFERENCES

1. Weaver LK, Behrens EM. Weathering the storm: improving therapeutic interventions for cytokine storm syndromes by targeting disease pathogenesis. Curr Treatm Opt Rheumatol 2017;3:33–48.

2. Behrens EM, Canna SW, Slade K, Rao S, Kreiger PA, Paessler M, et al. Repeated TLR9 stimulation results in macrophage activation syndrome-like disease in mice. J Clin Invest 2011;121:2264–77.

3. Bracaglia C, de Graaf K, Pires Marafon D, Guilhot F, Ferlin W, Prencipe G, et al. Elevated circulating levels of interferon-γ and interferon-γ-induced chemokines characterise patients with macrophage activation syndrome complicating systemic juvenile idiopathic arthritis. Ann Rheum Dis 2017;76:166–72.

4. Prencipe G, Caiello I, Pascarella A, Grom AA, Bracaglia C, Chatel L, et al. Neutralization of IFN-γ reverts clinical and laboratory features in a mouse model of macrophage activation syndrome. J Allergy Clin Immunol 2018;141:1439–49.

5. Zoller EE, Lykens JE, Terrell CE, Aliberti J, Filipovich AH, Henson PM, et al. Hemophagocytosis causes a consumptive anemia of inflammation. J Exp Med 2011;208:1203–14.

6. Strippoli R, Carvello F, Scianaro R, De Pasquale L, Vivarelli M, Petrini S, et al. Amplification of the response to Toll-like receptor ligands by prolonged exposure to interleukin-6 in mice: implication for the pathogenesis of macrophage activation syndrome. Arthritis Rheum 2012;64:1680–8.

7. Avau A, Mitera T, Put S, Put K, Brisse E, Filtjens J, et al. Systemic juvenile idiopathic arthritis–like syndrome in mice following stimulation of the immune system with Freund's complete adjuvant: regulation by interferon-γ. Arthritis Rheumatol 2014;66:1340–51.

8. Fall N, Barnes M, Thornton S, Luyrink L, Olson J, Ilowite NT, et al. Gene expression profiling of peripheral blood from patients with untreated new-onset systemic juvenile idiopathic arthritis reveals molecular heterogeneity that may predict macrophage activation syndrome. Arthritis Rheum 2007;56:3793–804.

9. Yanagimachi M, Naruto T, Miyamae T, Hara T, Kikuchi M, Hara R, et al. Association of IRF5 polymorphisms with susceptibility to macrophage activation syndrome in patients with juvenile idiopathic arthritis. J Rheumatol 2011;38:769–74.

10. Graham RR, Kozyrev SV, Baechler EC, Reddy MV, Plenge RM, Bauer JW, et al. A common haplotype of interferon regulatory factor 5 (IRF5) regulates splicing and expression and is associated with increased risk of systemic lupus erythematosus. Nat Genet 2006;38:550–5.

11. Weaver LK, Chu N, Behrens EM. TLR9-mediated inflammation drives a Ccr2-independent peripheral monocytosis through enhanced extramedullary monocytopoiesis. Proc Natl Acad Sci U S A 2016;113:10944–9.

12. Canna SW, Wrobel J, Chu N, Kreiger PA, Paessler M, Behrens EM. Interferon-γ mediates anemia but is dispensable for fulminant Toll-like receptor 9–induced macrophage activation syndrome and hemophagocytosis in mice. Arthritis Rheum 2013;65:1764–75.

13. Burberry A, Zeng MY, Ding L, Wicks I, Inohara N, Morrison SJ, et al. Infection mobilizes hematopoietic stem cells through cooperative NOD-like receptor and Toll-like receptor signaling. Cell Host Microbe 2014;15:779–91.

14. De Bruin AM, Libregts SF, Valkhof M, Boon L, Touw IP, Nolte MA. IFNγ induces monopoiesis and inhibits neutrophil development during inflammation. Blood 2012;119:1543–54.

15. Hu X, Chakravarty SD, Ivashkiv LB. Regulation of interferon and Toll-like receptor signaling during macrophage activation by opposing feedforward and feedback inhibition mechanisms. Immunol Rev 2008;226:41–56.

AMERICAN COLLEGE OF RHEUMATOLOGY
EDUCATION · TREATMENT · RESEARCH

LETTERS

Rheumatoid factor reactivity of expanded CD21−/low B cells in patients with Sjögren's syndrome: comment on the article by Glauzy et al

To the Editor:

Populations of CD21−/low-expressing memory B cells in peripheral blood have been described in conditions involving persistent immune activation, such as autoimmune diseases including Sjögren's syndrome (SS), and in chronic infections, such as HIV, malaria, tuberculosis, hepatitis C virus (HCV), and schistosomiasis (1,2). CD21−/low memory B cells have also been designated as atypical or tissue-type memory B cells and have been detected in low numbers in peripheral blood of healthy donors and in chronically inflamed tonsils (2). Tissue-type memory B cells are characterized by high expression of CD11c and inhibitory receptors such as CD22 and CD72, unique patterns of chemokine receptors, and low or absent expression of CD21 and CD27 (1,2).

In a study reported in *Arthritis & Rheumatology*, Glauzy et al (3) showed that the frequency of CD21−/low B cells was increased in the peripheral blood of 5 of 8 SS patients. In 3 of these patients (patients SS59, SS03, and SS204), this B cell subset harbored clonally expanded B cells, which exhibited somatic mutations in their immunoglobulin heavy and light chain variable genes. Recombinant IgG antibodies derived from these expanded B cell clones from 2 of the patients (patients SS59 and SS03) showed HEp-2 reactivity and polyreactivity, with strong reactivity exhibited in the antibody from patient SS59. This result is consistent with the authors' earlier finding that B cell receptors (BCRs) of polyclonal CD21−/low memory B cells of SS patients, obtained using a single B cell cloning approach, frequently displayed polyreactivity and self-reactivity (1). However, the IgG derived from the clonally expanded B cells of patient SS204 did not show any reactivity, including rheumatoid factor (RF) activity (3).

We have previously shown that at least 40% of SS-related mucosa-associated lymphoid tissue lymphomas express stereotypic RFs with high affinity for IgG (4). Stereotypic RFs are IgM antibodies encoded by combinations of canonical immunoglobulin heavy chain variable (*IGHV*) and immunoglobulin light chain variable (*IGLV*) genes with distinct V_H third complementarity-determining regions (V_H-CDR3), which is the region that contributes most to the antigenic specificity of an Ig.

In light of this association, we also studied expanded B cell clones from patients SS59, SS03, and SS204, examining their Ig configuration. Interestingly, the memory B cell clone from patient SS204 expressed the combination of an *IGHV1–69/IGHJ4* heavy chain rearrangement and an *IGKV3–20* κ light chain rearrangement, which is typical for stereotypic V1–69 RFs. Moreover, the SS204 V_H-CDR3 was highly homologous with those of various V1–69 RFs (Figure 1).

Previously, we identified 4 cases of HCV-associated lymphomas, which were originally described by Ng et al (5), that also expressed stereotypic RFs, i.e., V4–59 RFs and V4–59/J_H5 RFs (6). From these lymphomas Ng and colleagues produced recombinant IgG antibodies, in the same system as that used by Glauzy et al (3), which were reported to have no in vitro RF activity. We also produced these 4 HCV-associated lymphoma-derived antibodies recombinantly—but as IgM, instead of IgG, antibodies. These IgM antibodies were not polyreactive in vitro and displayed strong RF activity, with K_D values ranging between 3.9 and 22.5 n*M* (6). Moreover, Charles and colleagues (7) recombinantly produced both IgM and IgG of 3 stereotypic V1–69 RFs, which were isolated from single B cells of HCV-infected patients with mixed cryoglobulinemia. In that study it was also found that the 3 IgM V1–69 RFs strongly bound to immobilized IgG while the 3 recombinant IgG V1–69 RFs did not (7). The lack of in vitro RF activity of IgG-RFs is most likely explained by self-binding and formation of IgG complexes, thereby

	IGHV	IGHV-CDR3 region	Homology	Genbank
SS204	V1-69/JH4	C AREGYGD-GNRPFDY WGQG	86%	
KAS-RF		C AKEGYGDYG-RPFDF WGQG		1313976B
SS204	V1-69/JH4	C AREG-YGDG-NRPFDY WGQG	79%	
MR13-RF		C AREGKAGDYSN-PFDY WGQG		CAA84385

Figure 1. V_H–third complementarity-determining region (CDR3) amino acid sequence homology of the clonally expanded CD21−/low B cell clones from Sjögren's syndrome patient SS204 with stereotypic V1–69 rheumatoid factors (RFs). Identical amino acids are shown in red; homologous amino acids are shown in blue.

precluding binding to the coated polyclonal IgG in the enzyme-linked immunosorbent assay.

Based on these observations, we expect that the antibody from patient SS204, when expressed as IgM, will display in vitro RF activity. We and others have shown on several occasions that these stereotypic V1–69 RFs all exhibit RF activity when expressed as IgM antibodies (4,6–9). Thus, all clonally expanded CD21$^{-/low}$ B cells from the 3 SS patients exhibit poly- and/or autoreactivity. These poly/autoreactive CD21$^{-/low}$ B cells likely will undergo chronic BCR ligation. In addition to BCR engagement, CD21 can bind complement fragments C3d, C3dg, and iC3b that are covalently bound to antigen or immune complexes. As CD21 forms a complex with CD19, this costimulation may lead to enhanced BCR signaling (10). By lowering CD21 expression and inducing various inhibitory receptors such as CD22 and CD72, these CD21$^{-/low}$ B cells may counteract the chronic BCR stimulation and enter a state of hyporesponsiveness.

Richard J. Bende, PhD
Carel J. M. van Noesel, MD, PhD
Amsterdam UMC
University of Amsterdam
Amsterdam, The Netherlands

1. Saadoun D, Terrier B, Bannock J, Vazquez T, Massad C, Kang I, et al. Expansion of autoreactive unresponsive CD21$^{-/low}$ B cells in Sjögren's syndrome–associated lymphoproliferation. Arthritis Rheum 2013;65:1085–96.

2. Karnell JL, Kumar V, Wang J, Wang S, Voynova E, Ettinger R. Role of CD11c$^+$ T-bet$^+$ B cells in human health and disease. Cell Immunol 2017;321:40–5.

3. Glauzy S, Boccitto M, Bannock JM, Delmotte FR, Saadoun D, Cacoub P, et al. Accumulation of antigen-driven lymphoproliferations in complement receptor 2/CD21$^{-/low}$ B cells from patients with Sjögren's syndrome. Arthritis Rheumatol 2018;70:298–307.

4. Bende RJ, Aarts WM, de Jong D, Pals ST, van Noesel CJ. Among B-cell non-Hodgkin's lymphomas, MALT lymphomas express a unique antibody repertoire with frequent rheumatoid factor reactivity. J Exp Med 2005;201:1229–41.

5. Ng PP, Kuo CC, Wang S, Einav S, Arcaini L, Paulli M, et al. B-cell receptors expressed by lymphomas of hepatitis C virus (HCV)-infected patients rarely react with the viral proteins. Blood 2014;123:1512–5.

6. Bende RJ, Janssen J, Wormhoudt TA, Wagner K, Guikema JE, van Noesel CJ. Identification of a novel stereotypic IGHV4-59/IGHJ5-encoded B-cell receptor subset expressed by various B-cell lymphomas with high affinity rheumatoid factor activity. Haematologica 2016;101:e200–3.

7. Charles ED, Orloff MI, Nishiuchi E, Marukian S, Rice CM, Dustin LB. Somatic hypermutations confer rheumatoid factor activity in hepatitis C virus–associated mixed cryoglobulinemia. Arthritis Rheum 2013;65:2430–40.

8. Newkirk MM, Mageed RA, Jefferis R, Chen PP, Capra JD. Complete amino acid sequences of variable regions of two human IgM rheumatoid factors, BOR and KAS of the Wa idiotypic family, reveal restricted use of heavy and light chain variable and joining region gene segments. J Exp Med 1987;166:550–64.

9. Borretzen M, Randen I, Zdarsky E, Forre O, Natvig JB, Thompson KM. Control of autoantibody affinity by selection against amino acid replacements in the complementarity-determining regions. Proc Natl Acad Sci U S A 1994;91:12917–21.

10. Van Noesel CJ, Lankester AC, van Lier RA. Dual antigen recognition by B cells. Immunol Today 1993;14:8–11.

Germinal centers in diagnostic biopsies of patients with primary Sjögren's syndrome are not a risk factor for non-Hodgkin's lymphoma but a reflection of high disease activity: comment on the article by Sène et al

To the Editor:

We read with interest the article by Sène et al (1) in which ectopic germinal centers (GCs) in labial gland biopsy samples from patients with primary Sjögren's syndrome (SS) were found to be predictive for non-Hodgkin's lymphoma (NHL) development later in the disease. In the univariate analysis, the presence of GCs in these biopsy specimens was not significantly different between patients with primary SS who developed NHL and those who did not. However, multivariate analysis revealed that the presence of GCs in biopsy tissue was an independent predictor for NHL development (1). This study adds to the ongoing discussion on whether the presence of ectopic GCs in SS diagnostic salivary gland biopsy samples is a risk factor for subsequent NHL development. Theander et al (2) reported that GCs in diagnostic labial gland biopsy tissue were predictive for NHL development in patients with primary SS, whereas we (3) and others (4,5) did not detect such an association. As discussed extensively (3,6), a major reason for the apparent discrepancy in the different studies was the variation in NHL subtypes that were included.

Of note, half of the patients with primary SS in the study by Sène et al (1) were male, whereas in other studies that evaluated the presence of GCs as risk factors, the majority of patients (>81%) were female (2–5). Whether the predictive value of the presence of GCs in diagnostic biopsy specimens differs between male patients and female patients is unknown.

A very unusual observation in the study by Sène and colleagues was that all patients with primary SS who developed NHL had monoclonal gammopathy. In patients with primary SS, in general, the prevalence of monoclonal gammopathy is 4–22% (1,7,8). We observed monoclonal gammopathy at the time of lymphoma diagnosis in 4 of 8 patients (50%) with primary SS and parotid mucosa-associated lymphoid tissue (MALT) lymphoma (Haacke EA, et al: unpublished observations). In another recent study, only 3 of 7 patients (43%) with primary SS and pulmonary MALT lymphoma exhibited monoclonal gammopathy (9). The presence of monoclonal gammopathy is known as a risk factor for NHL development, but is also associated with higher disease activity (8,10). Therefore, the presence of monoclonal gammopathy in patients with primary SS prior to development of

lymphoma in the study by Sène et al (1) could also be a reflection of high disease activity as indicated by the European League Against Rheumatism Sjögren's Syndrome Disease Activity Index (ESSDAI) (11), an independent predictor for NHL development (12).

The presence of GCs in biopsy tissue is also associated with high disease activity (13). Since disease activity, as measured by the ESSDAI, can change over time (14), the time point when the diagnostic primary SS biopsy sample is obtained is of crucial importance. If a labial gland biopsy specimen is obtained during a period of relatively low disease activity, the likelihood of the presence of GCs may consequently be low. On the other hand, when a diagnostic salivary gland biopsy sample is obtained in a period of high SS disease activity, the chance of finding GCs is higher.

Thus, both GCs and monoclonal gammopathy are associated with higher disease status, but there is no clear indication that the presence of ectopic GCs is a prerequisite for MALT lymphoma development. There are many patients with primary SS and GCs present in their salivary gland biopsy tissue who do not develop NHL. Notably, the presence of GCs is usually assessed in labial salivary glands, which are not the sites where MALT lymphoma preferentially develops.

We conclude that in order to predict which patients with primary SS are at risk for NHL development, clinical and laboratory factors such as low C4, rheumatoid factor positivity, the presence of cryoglobulin, high disease activity, purpura, lymphadenopathy and, especially, persistent parotid enlargement (5,12,15), are more important than the presence of GCs in diagnostic salivary gland biopsy samples.

Erlin A. Haacke, MD
Bert van der Vegt, MD, PhD
Arjan Vissink, DMD, MD, PhD
Fred K. L. Spijkervet, DMD, PhD
Hendrika Bootsma, MD, PhD
Frans G. M. Kroese, PhD
University of Groningen
Groningen, The Netherlands

1. Sène D, Ismael S, Forien M, Charlotte F, Kaci R, Cacoub P, et al. Ectopic germinal center–like structures in minor salivary gland biopsy tissue predict lymphoma occurrence in patients with primary Sjögren's syndrome. Arthritis Rheumatol 2018;70:1481–8.

2. Theander E, Vasaitis L, Baecklund E, Nordmark G, Warfvinge G, Liedholm R, et al. Lymphoid organisation in labial salivary gland biopsies is a possible predictor for the development of malignant lymphoma in primary Sjögren's syndrome. Ann Rheum Dis 2011;161:1363–8.

3. Haacke EA, van der Vegt B, Vissink A, Spijkervet FK, Bootsma H, Kroese FG. Germinal centres in diagnostic labial gland biopsies of patients with primary Sjögren's syndrome are not predictive for parotid MALT lymphoma development. Ann Rheum Dis 2017;76:1781–4.

4. Johnsen SJ, Gudlaugsson E, Skaland I, Janssen E, Jonsson MV, Helgeland L, et al. Low protein A20 in minor salivary glands is as-

sociated with lymphoma in primary Sjögren's syndrome. Scand J Immunol 2016;83:181–7.

5. Fragkioudaki S, Mavragani CP, Moutsopoulos HM. Predicting the risk for lymphoma development in Sjögren syndrome: an easy tool for clinical use. Medicine (Baltimore) 2016;95:e3766.

6. Kroese FG, Haacke EA, Bombardieri M. The role of salivary gland histopathology in primary Sjögren's syndrome: promises and pitfalls. Clin Exp Rheumatol 2018;36 Suppl 112:222–33.

7. Baimpa E, Dahabreh IJ, Voulgarelis M, Moutsopoulos HM. Hematologic manifestations and predictors of lymphoma development in primary Sjögren syndrome: clinical and pathophysiologic aspects. Medicine (Baltimore) 2009;88:284–93.

8. Brito-Zerón P, Kostov B, Fraile G, Caravia-Durán D, Maure B, Rascón FJ, et al. Characterization and risk estimate of cancer in patients with primary Sjögren syndrome. J Hematol Oncol 2017;10:90.

9. Yachoui R, Leon C, Sitwala K, Kreidy M. Pulmonary MALT lymphoma in patients with Sjögren's syndrome. Clin Med Res 2017;15:6–12.

10. Yang Y, Chen L, Jia Y, Liu Y, Wen L, Liang Y, et al. Monoclonal gammopathy in rheumatic diseases. Clin Rheumatol 2018;37:1751–62.

11. Seror R, Ravaud P, Bowman SJ, Baron G, Tzioufas A, Theander E, et al, on behalf of the EULAR Sjögren's Task Force. EULAR Sjögren's Syndrome Disease Activity Index: development of a consensus systemic disease activity index for primary Sjögren's syndrome. Ann Rheum Dis 2010;69:1103–9

12. Nocturne G, Virone A, Ng WF, Le Guern V, Hachulla E, Cornec D, et al. Rheumatoid factor and disease activity are independent predictors of lymphoma in primary Sjögren's syndrome. Arthritis Rheumatol 2016;68:977–85.

13. Risselada AP, Looije MF, Kruize AA, Bijlsma JW, van Roon JA. The role of ectopic germinal centers in the immunopathology of primary Sjögren's syndrome: a systematic review. Semin Arthritis Rheum 2013;42:368–76.

14. Gottenberg JE, Seror R, Saraux A, Devauchelle V, Labous E, Dieudé P, et al. Evolution of disease activity over a 5-year period in the 395 patients with primary Sjögren's syndrome of the assess prospective cohort [abstract]. Arthritis Rheumatol 2016;68 Suppl 10. URL: https://acrabstracts.org/abstract/evolution-of-disease-activity-over-a-5-year-period-in-the-395-patients-with-primary-sjogrens-syndrome-of-the-assess-prospective-cohort/.

15. Nishishinya MB, Pereda CA, Muñoz-Fernández S, Pego-Reigosa JM, Rúa-Figueroa I, Andreu JL, et al. Identification of lymphoma predictors in patients with primary Sjögren's syndrome: a systematic literature review and meta-analysis. Rheumatol Int 2015;35:17–26.

Reply

To the Editor:

We thank Dr. Haacke and colleagues for their interest in our study in which we identified ectopic GC structures in labial minor salivary glands as significant predictors of NHL in patients with primary SS. As discussed in our article, we agree that this finding is not consensual, with contradictory reports, and we have analyzed the factors that may explain these discrepancies.

While confirming the already recognized risk factors, including cryoglobulin, splenomegaly, and sensorimotor neuropathy, we have, for the first time, identified male sex as being a risk factor for NHL in primary SS. Contrary to the comments made by Haacke et al, only 13% of patients with primary SS included in the study were male (consistent with previous studies), and not 50% as they reported. Half of the patients with NHL, however, were male. As discussed, we are unable to explain this high prevalence. However, we do believe that the association between male sex and NHL in primary SS is not coincidental or linked to recruitment or selection bias. As noted by Haacke and colleagues, the risk of lymphoma is associated with higher disease activity (1,2), consensually assessed by the ESSDAI score (2,3). We want to bring to their attention that recent analyses of the largest international primary SS cohort, which included 9,974 patients, showed that male patients with primary SS, compared to female patients, are characterized by higher disease activity at diagnosis. This includes a higher mean ESSDAI (8.0 versus 5.9; $P < 0.001$) and clinESSDAI (8.4 versus 6.1; $P < 0.001$), and clinically by a higher prevalence of lymphadenopathy ($P < 0.001$) and glandular involvement ($P < 0.001$) (4), both manifestations being recognized as predictors of NHL in primary SS.

Haacke et al also pointed out the high prevalence of monoclonal gammopathy in patients with NHL. The prevalence of monoclonal gammopathy in our cohort (13%) was comparable to those previously reported (4–22%) (5). However, all 8 patients with NHL had monoclonal gammopathy, in contrast to approximately half of the patients in other studies. This may be explained by the presence of type II mixed cryoglobulin, which is characterized by the association of both a monoclonal gamma globulin component and polyclonal immunoglobulins in all patients.

To conclude, we agree that the presence of ectopic GCs is associated with, and may reflect, more active disease (6). The time point when the biopsy is performed may be crucial for the detection and the significance of GCs in labial minor salivary glands. This is why we do not consider that the presence of GCs per se is only sufficient to determine all the risk for NHL in patients with primary SS.

As reported in Tables 2 and 3 of our article, the other consensual risk factors for NHL, such as serum cryoglobulin, splenomegaly, parotid gland enlargement, sensorimotor neuropathy, low C4, and leukopenia, yielded higher predictive power than GCs. We agree with Haacke et al that the assessment of the risk of NHL should take into account all recognized clinical and laboratory risk factors, especially those that might be easily and regularly quantifiable throughout the patient's follow-up. All of the following parameters weighed heavily in the ESSDAI score: leukopenia, low C4 and C3 levels, rheumatoid factor positivity, the presence of cryoglobulin, purpura, sensorimotor neuropathy, lymphadenopathy, splenomegaly, and parotid enlargement (2,3).

Damien Sène, MD, PhD
Sophie Ismael, MD
*Lariboisière Fernand Widal Hospital
  and Paris-Diderot University*
Marine Forien, MD
Philippe Dieudé, MD, PhD
*Bichat Hospital
  and Paris-Diderot University*
Frédéric Charlotte, MD, PhD
Patrice Cacoub, MD (iD)
*Pitié-Salpêtrière Hospital
  and Pierre & Marie Curie University*
Rachid Kaci, MD
Abdourahmane Diallo, PhD
Lariboisière Fernand Widal Hospital
Frédéric Lioté, MD, PhD
*Lariboisière Fernand Widal Hospital
  and Paris Diderot University*
Paris, France

1. Brito-Zerón P, Kostov B, Fraile G, Caravia-Durán D, Maure B, Rascón FJ, et al. Characterization and risk estimate of cancer in patients with primary Sjögren syndrome. J Hematol Oncol 2017;10:90.
2. Nocturne G, Virone A, Ng WF, Le Guern V, Hachulla E, Cornec D, et al. Rheumatoid factor and disease activity are independent predictors of lymphoma in primary Sjögren's syndrome. Arthritis Rheumatol 2016;68:977–85.
3. Seror R, Ravaud P, Bowman SJ, Baron G, Tzioufas A, Theander E, et al. EULAR Sjögren's syndrome disease activity index: development of a consensus systemic disease activity index for primary Sjögren's syndrome. Ann Rheum Dis 2010;69:1103–9.
4. Retamozo S, Acar-Denizli N, Fai Ng W, Zeher M, Rasmussen A, Seror R, et al. Influence of epidemiology and ethnicity on systemic expression of primary Sjögren's syndrome in 9,974 patients. Ann Rheum Dis 2018;77:110.
5. Yang Y, Chen L, Jia Y, Liu Y, Wen L, Liang Y, et al. Monoclonal gammopathy in rheumatic diseases. Clin Rheumatol 2018;37:1751–62.
6. Risselada AP, Looije MF, Kruize AA, Bijlsma JW, van Roon JA. The role of ectopic germinal centers in the immunopathology of primary Sjögren's syndrome: a systematic review. Semin Arthritis Rheum 2013;42:368–76.

Arthritis prevalence: which case definition should be used for surveillance? Comment on the article by Jafarzadeh and Felson

To the Editor:

We read with interest the article by Jafarzadeh and Felson in which they presented an alternative estimate of arthritis prevalence (1). Specifically, using a new case definition for arthritis and applying Bayesian methods to correct misclassification, Jafarzadeh and Felson analyzed National Health Interview Survey (NHIS) data and estimated that in 2015, 91.2 million US adults had arthritis. In contrast, the Centers for Disease Control and Prevention (CDC) had estimated from the 2013–2015 NHIS that 54.4 million US adults had doctor-diagnosed arthritis (2). In this letter, we make 2 observations about their methods

and discuss implications for the public health surveillance of arthritis.

We believe that the primary difference between the authors' and CDC's prevalence estimates is attributable to the use of different case definitions. Compared with use of different case definitions, the effects of "correcting" for misclassification are quite minor. The CDC reported estimates for doctor-diagnosed arthritis based on the NHIS question, "Have you ever been told by a doctor or other health professional that you have some form of arthritis, rheumatoid arthritis, gout, lupus, or fibromyalgia?" Jafarzadeh and Felson added 2 more elements to this case definition: recent joint symptoms (case finding question: "During the past 30 days, have you had any symptoms of pain, aching, or stiffness in or around a joint?") and/or joint symptoms lasting more than 30 days (case finding question: "Did your joint symptoms first begin more than 3 months ago?"). An affirmative response to any of these 3 questions qualifies as a countable case of arthritis, according to Jafarzadeh and Felson. Whereas previous studies on case definitions that include joint symptoms (3–5) defined chronic joint symptoms as a positive response to both of the joint symptom questions above, the case definition used by the authors allows the inclusion of individuals with acute joint symptoms only (e.g., as a result of an acute injury).

Interestingly, when we simply, without any corrections, recalculated arthritis prevalence for 2015 from the NHIS using doctor-diagnosed arthritis and/or chronic joint symptoms based on positive responses to both joint symptom questions, the prevalence was 88.6 million (95% confidence interval [95% CI] 85.9–91.3) (2). The difference between this and Jafarzadeh and Felson's estimate is just under 3% (2.6 million people).

The sensitivity and specificity estimates used to correct the NHIS estimates in the authors' Bayesian analysis were obtained from a single validation study conducted in 2003, comprising 389 individuals from Massachusetts age ≥45 years who were predominantly white (97–98%) (4). This study's ethnic and racial homogeneity does not reflect the diversity of the US population or those with arthritis (2). For example, a validation study of doctor-diagnosed arthritis and chronic joint symptoms by Bombard et al (5), in which 41% of the study population was black, showed racial differences in specificity: compared with white participants, the odds of a false-positive report of arthritis among black participants were 60% lower (odds ratio 0.4 [95% CI 0.2–0.9]). Thus, the correction factors used in Jafarzadeh and Felson's study may be inappropriate when applied to a diverse population like that of the entire US.

The overarching purpose of public health surveillance is to facilitate the prevention or control of a health-related problem (6). For arthritis, a surveillance system should indicate the number of individuals in need of strategies to control arthritis and reduce adverse effects, such as pain, functional limitations, and depression.

The CDC Arthritis Program included chronic joint symptoms in its case definition of arthritis during its early years of surveillance. For example, the CDC reported that 69.9 million US adults had doctor-diagnosed arthritis and/or chronic joint symptoms in 2001 (7).

However, the CDC eliminated chronic joint symptoms from prevalence estimates after a series of studies showed that those with reported chronic joint symptoms only (i.e., without doctor-diagnosed arthritis), were unlikely to have arthritis or be a fruitful target group for arthritis control efforts. A study of adults age ≥45 years with chronic joint symptoms only showed that many individuals did not report an arthritis diagnosis because they had not sought medical attention for symptoms that were mild and ignorable (Aeffect Inc.: personal communication). Another study indicated that individuals with arthritis took action (e.g., by seeking medical care and participating in interventions) only after arthritis symptoms began to affect their daily activities (8). While the validation study of a very homogeneous group by Sacks et al showed that 1 in 3 individuals age ≥45 years with chronic joint symptoms only have arthritis (4), a population-based study of adults age ≥18 years by the CDC showed something different (7). Among those who reported having seen their health care provider about their joint symptoms, only 6.3% of those with chronic joint symptoms only had been diagnosed by their health care provider as having arthritis (3).

These results, based on a larger, population-based, racially and ethnically diverse sample of adults of all ages, suggest that including those with chronic joint symptoms only in a surveillance case definition results in a dramatic overestimate of arthritis prevalence (many false-positives). Thus, the evidence that those with chronic joint symptoms only do not take action on their symptoms indicates that inclusion of this group in prevalence estimates, which in turn is used to inform arthritis control efforts, would undermine the ability of the surveillance system to enumerate those ready for control efforts and potentially misdirect efforts and resources.

As of 2019, neither of the national and state surveillance surveys recommended for generating arthritis prevalence estimates will include questions about joint symptoms: the NHIS is eliminating the 2 questions related to joint symptoms starting in 2019 (9), and these questions were dropped from the state-level Behavioral Risk Factor Surveillance Survey (BRFSS) in 2005. Thus, Jafarzadeh and Felson's approach will not be possible in analyses of future BRFSS and NHIS data.

Jafarzadeh and Felson recommended that their methods be used for other studies, and specifically mentioned studies examining the cost of arthritis. While they did not provide details on how to implement these methods, we question their suggestion. A recent study of national medical expenditures and earnings losses for 2013 used multi-stage regression models and an International Classification of Diseases, Ninth Revision, Clinical Modification (ICD-9-CM)–based arthritis definition, in which national estimates were the product of the number of individuals with arthritis and the average cost per person as ascertained from a single data source—the Medical Expenditure Panel Survey (MEPS) (10). Multiplying the average cost per person for

those with ICD-9-CM–based arthritis from the MEPS by a prevalence estimate, derived from a different case definition and NHIS data, is likely to introduce its own biases (11).

Jafarzadeh and Felson also recommended changes to the doctor-diagnosed arthritis case-finding question. Specifically, they suggested that osteoarthritis (OA) be added to, and fibromyalgia be removed from, the list of conditions mentioned in the question. Evidence from studies examining the accuracy of self-reported OA suggests that most people with OA simply report what they have as arthritis, or misreport it as rheumatoid arthritis or a nonspecific type of arthritis (12,13). In 1994, the National Arthritis Data Workgroup expert panel recommended that fibromyalgia be included in standard arthritis surveillance because it is commonly treated by rheumatologists and its symptoms resemble those of arthritis (14).

We agree with Jafarzadeh and Felson that the CDC's NHIS-based estimate of 54.4 million US adults with arthritis is likely conservative (2). Individuals may be more likely to recall their arthritis diagnosis with increasing inquiries and/or if they are symptomatic at the time of the survey (4,15). The annual prevalence of arthritis in the 2011–12 MEPS was 26.1% (99% CI 25.0–27.2), compared with 23.5% (99% CI 22.9–24.1) in the 2011–12 NHIS (15). One reason for this difference may be that MEPS respondents were asked whether they had been diagnosed as having arthritis multiple times over a year, compared with only once in NHIS.

In conclusion, the crux of the issue seems to be how we define a case of arthritis for surveillance (i.e., whether to include joint symptoms), and not correction for misclassification. For all the reasons described above, we believe that the case definition and approach used by Jafarzadeh and Felson are not appropriate for the public health surveillance of arthritis. The CDC estimate, based on a conservative yet credible case definition, is more defensible than a broader definition whose estimate captures an additional 36.8 million individuals about whom little is known, including whether they have arthritis. Nevertheless, we share the desire expressed by Jafarzadeh and Felson and by Katz, in an editorial accompanying their article (16), to increase awareness of the prevalence and impact of arthritis. Despite the different perspectives on how to conduct arthritis surveillance, we believe there is a consensus that there is a very large number of adults with arthritis in the US who require strategies to reduce its adverse effects and improve their quality of life in a meaningful way.

Louise B. Murphy, PhD iD
Centers for Disease Control and Prevention
Atlanta, GA
Jeffrey J. Sacks, MD, MPH
Sue Binder Consulting, Inc.
Decatur, GA
Charles G. Helmick, MD
Teresa J. Brady, PhD

Kamil E. Barbour, PhD
Jennifer M. Hootman, PhD
Centers for Disease Control and Prevention
Atlanta, GA
Michael A. Boring, MS
Cutting Edge Technologies and Solutions
Mesa, AZ
Susan Moss, MSPH
G2S Corporation
San Antonio, TX
Dana Guglielmo, MPH
Centers for Disease Control and Prevention
Atlanta, GA
    and Oak Ridge Institute for Science and
        Education
    Oak Ridge, TN
Kristina A. Theis, PhD
Centers for Disease Control and Prevention
Atlanta, GA

1. Jafarzadeh SR, Felson DT. Updated estimates suggest a much higher prevalence of arthritis in United States adults than previous ones. Arthritis Rheumatol 2018;70:185–92.

2. Barbour KE, Helmick CG, Boring M, Brady TJ. Vital signs: prevalence of doctor-diagnosed arthritis and arthritis-attributable activity limitation—United States, 2013-2015. MMWR Morb Mortal Wkly Rep 2017;66:246–53.

3. Bolen J, Helmick CG, Sacks JJ, Gizlice Z, Potter C. Should people who have joint symptoms, but no diagnosis of arthritis from a doctor, be included in surveillance efforts? Arthritis Care Res (Hoboken) 2011;63:150–4.

4. Sacks JJ, Harrold LR, Helmick CG, Gurwitz JH, Emani S, Yood RA. Validation of a surveillance case definition for arthritis. J Rheumatol 2005;32:340–7.

5. Bombard JM, Powell KE, Martin LM, Helmick CG, Wilson WH. Validity and reliability of self-reported arthritis: Georgia senior centers, 2000-2001. Am J Prev Med 2005;28:251–8.

6. Centers for Disease Control and Prevention. Lesson 5: public health surveillance: Section 7: evaluating and improving surveillance 2012. URL: https://www.cdc.gov/ophss/csels/dsepd/ss1978/lesson5/section7.html.

7. Centers for Disease Control and Prevention. Prevalence of self-reported arthritis or chronic joint symptoms among adults—United States, 2001. MMWR Morb Mortal Wkly Rep 2002;51:948–50.

8. Brady TJ. Moving from identifying to addressing health disparities: a public health perspective. Arthritis Rheum 2007;57:544–6.

9. Centers for Disease Control and Prevention. 2019 Questionnaire Redesign, 2017. URL: https://www.cdc.gov/nchs/nhis/2019_quest_redesign.htm.

10. Murphy LB, Cisternas MG, Pasta DJ, Helmick CG, Yelin EH. Medical expenditures and earnings losses among US adults with arthritis in 2013. Arthritis Care Res (Hoboken) 2018;70:869–76.

11. Honeycutt AA, Segel JE, Hoerger TJ, Finkelstein EA. Comparing cost-of-illness estimates from alternative approaches: an application to diabetes. Health Serv Res 2009;44:303–20.

12. Cisternas MG, Murphy L, Sacks JJ, Solomon DH, Pasta DJ, Helmick CG. Alternative methods for defining osteoarthritis and the impact on estimating prevalence in a US population-based survey. Arthritis Care Res (Hoboken) 2016;68:574–80.

13. Machlin S, Cohen J, Elixhauser A, Beauregard K, Steiner C. Sensitivity of household reported medical conditions in the medical expenditure panel survey. Med Care 2009;47:618–25.

14. Helmick CG, Lawrence RC, Pollard RA, Lloyd E, Heyse SP, for the National Arthritis Data Workgroup. Arthritis and other rheumatic conditions: who is affected now, who will be affected later? Arthritis Care Res 1995;8:203–11.

15. Murphy LB, Cisternas MG, Greenlund KJ, Giles W, Hannan C, Helmick CG. Defining arthritis for public health surveillance: methods and estimates in four US population health surveys. Arthritis Care Res (Hoboken) 2017;69:356–67.

16. Katz JN. Prevalence of arthritis revisited [editorial]. Arthritis Rheumatol 2018;70:153–4.

Reply

To the Editor:

We thank Dr. Murphy et al for their interest in our study on arthritis prevalence. Murphy and colleagues asserted that 1 survey question asking participants whether they recall an arthritis diagnosis by a health professional is sufficient to accurately characterize the prevalence of arthritis. However, we used 3 survey questions, i.e., their question and 2 questions on joint pain, to increase the accuracy of arthritis prevalence estimation. Murphy et al also asserted that in our study, a positive response to any of the 3 arthritis-related questions in the NHIS qualified as a case of arthritis, and this is incorrect.

Our approach begins with the assumption that, using a survey alone, it is not possible to accurately characterize a person's arthritis status. When the true disease status of individuals is unknown, latent class methods offer an unbiased estimation of prevalence in the population. The methods are based on calculating true- and false-positive fractions for each or a combination of survey responses. Given the imperfect sensitivity and specificity of the questions used to screen for arthritis, the CDC's approach, which assumes that those who report doctor-diagnosed arthritis have arthritis, is fundamentally flawed. In this situation, the only method to provide accurate prevalence estimates is one that adjusts for misclassification. We briefly described how prevalence can be calculated from an imperfect screening instrument (e.g., a test, survey question, etc.), followed by a note on using multiple survey questions simultaneously to estimate prevalence. We will note some fundamental flaws in arguments presented by Murphy et al, describe how our approach was misunderstood, and conclude with comments and suggestions.

When the sensitivity and specificity of an imperfect instrument such as a single question to estimate arthritis prevalence are known, an unbiased estimate for prevalence can be calculated from apparent prevalence (i.e., the proportion who tested positive) by summing true- and false-positive fractions, i.e., $\Pr(T+) = \text{Prev Se} + ([1 - \text{Prev}] \times [1 - \text{Sp}])$, where $\Pr(T+)$ = proportion tested positive, Prev = true prevalence, Se = sensitivity, and Sp = specificity (1). Besides sensitivity and specificity, the only extra input required for unbiased estimation of prevalence is the proportion who tested positive. Unless a perfect instrument with both 100% sensitivity and 100% specificity is used, the proportion who tested positive produces a biased estimate of true prevalence, and this bias can be substantial when sensitivity and/or specificity is poor. Unfortunately, the survey question (self-reported recall of doctor-diagnosed arthritis) used by the CDC to derive national estimates of arthritis prevalence has consistently been shown to have poor sensitivity (2,3). This is exemplified by the validation study by Sacks et al (4) in which these questions were administered to a mixed group of patients who were then examined by trained rheumatology nurses asked to identify patients with treatable arthritis. Furthermore, while that study showed that the sensitivity of the "doctor-diagnosed arthritis" question was only 53% for persons ages 45–64, our own estimates (Table 3 in our article) suggested a sensitivity of 22% and 34% in men and women, respectively, implying that using this single question for arthritis surveillance would miss nearly 65–80% of persons with arthritis in this age group.

An estimate of apparent prevalence based on the proportion who tested positive by any screening instrument or survey question, which is the CDC's approach, should not be taken as an unbiased estimate of prevalence (5). For future studies, we encourage the use of adjusted estimates by, for example, application of the Rogan and Gladen formula (6) that accommodates true- and false-positive fractions.

Murphy and colleagues criticized the generalizability of the sensitivity and specificity reported by Sacks et al (4) for survey questions used in the NHIS. We agree that more comprehensive validation studies of arthritis-related survey questions are needed to provide assurance of surveillance instrument validity. However, we used estimates of sensitivity and specificity from the study by Sacks and colleagues only as guidance to construct prior probabilities for accuracy parameters. This means that we used this validation study to define a "distribution" of probable values for sensitivity and specificity (7), rather than using the exact values provided in the report. This distinguishes our Bayesian approach from a frequentist method in estimating arthritis prevalence.

When 3 tests (e.g., survey questions) are available, true- and false-positive fractions for all realizations of outcomes can be calculated in the same manner as the 1-test scenario. For example, one realization of survey outcomes could be the proportion who responded positively to all 3 arthritis-related NHIS questions, i.e., $\Pr(T_1+, T_2+, T_3+$, where T_1+ is a positive response to the first survey question). Using corresponding sensitivity and specificity, an unbiased estimate of prevalence can be derived from true- and false-positive fractions through $\Pr(T_1+, T_2+, T_3+) = \text{Prev Se}_1\, \text{Se}_2\, \text{Se}_3 + ([1\text{-Prev}] \times [1\text{-Sp}_1] \times [1\text{-Sp}_2] \times [1\text{-Sp}_3])$. As mentioned in our article, the observed frequency of each possible realization is modeled as a multinomial sampling distribution without the need to know the true disease status of each participant (8). Both models (the one with 1 test and the other with 3 tests) target the same parameter (i.e., arthritis prevalence).

We referred to this multiple testing technique as an expanded "surveillance definition" in our article. While we cannot know the arthritis status of each individual from survey questions, it is possible to provide an unbiased estimate of prevalence in the population by using all realizations of responses to survey questions, along with their corresponding sensitivity and specificity.

Although arthritis prevalence can be accurately estimated using 1 question adjusted for misclassification, there are two reasons the use of 3 questions about arthritis and joint pain is preferable. First, the misclassification of arthritis cases is less likely when multiple, overlapping questions about arthritis and its symptoms are used so that adjusting for misclassification produces a more accurate assessment of arthritis prevalence. Second, we are concerned about another public health consequence of the CDC's approach that identifies arthritis only in people who recall having been seen by a health practitioner and given an arthritis diagnosis. At a time when many in our society remain outside the medical care system, this approach will make it impossible to know whether a substantial number of people are living with undiagnosed arthritis.

Last, Murphy et al opposed our suggestion to improve NHIS questions by including osteoarthritis, the most common form of arthritis, and excluding fibromyalgia from the doctor-diagnosed arthritis question. We maintain our belief that NHIS questions, which aim to estimate the burden of arthritis, should not include questions about non-arthritis conditions. Regardless, the impact of this shortcoming can be minimized if techniques to adjust for misclassification bias are implemented.

In conclusion, we believe that reporting the proportion who responded positively to 1 survey question on doctor-diagnosed arthritis does not produce accurate national estimates of arthritis prevalence, and the consequence has been to grossly underestimate its prevalence. Furthermore, regardless of how many and which survey instruments are used, providing estimates that are adjusted for misclassification bias is essential to produce credible estimates that could guide efficient planning at federal and local levels and could be used to measure the burden of arthritis.

S. Reza Jafarzadeh, DVM, MPVM, PhD [iD]
David T. Felson, MD, MPH [iD]
Boston University School of Medicine
Boston, MA

1. McV Messam LL, Branscum AJ, Collins MT, Gardner IA. Frequentist and Bayesian approaches to prevalence estimation using examples from Johne's disease. Anim Health Res Rev 2008;9:1–23.
2. Bombard JM, Powell KE, Martin LM, Helmick CG, Wilson WH. Validity and reliability of self-reported arthritis: Georgia senior centers, 2000–2001. Am J Prev Med 2005;28:251–8.
3. Lo T, Parkinson L, Cunich M, Byles J. Discordance between self-reported arthritis and musculoskeletal signs and symptoms in older women. BMC Musculoskelet Disord 2016;17:494.
4. Sacks JJ, Harrold LR, Helmick CG, Gurwitz JH, Emani S, Yood RA. Validation of a surveillance case definition for arthritis. J Rheumatol 2005;32:340–7.
5. Enøe C, Georgiadis MP, Johnson WO. Estimation of sensitivity and specificity of diagnostic tests and disease prevalence when the true disease state is unknown. Prev Vet Med 2000;45:61–81.
6. Rogan WJ, Gladen B. Estimating prevalence from the results of a screening test. Am J Epidemiol 1978;107:71–6.
7. Branscum AJ, Gardner IA, Johnson WO. Estimation of diagnostic-test sensitivity and specificity through Bayesian modeling. Prev Vet Med 2005;68:145–63.
8. Collins J, Huynh M. Estimation of diagnostic test accuracy without full verification: a review of latent class methods. Stat Med 2014;33: 4141–69.

ACR Announcements

ACR Meetings

Annual Meetings
  November 8–13, 2019, Atlanta

Winter Rheumatology Symposium
  January 26–February 1, 2019, Snowmass

State-of-the-Art Clinical Symposium
  April 5–7, 2019, Chicago

For additional information, contact the ACR office.

ACR Open Rheumatology Accepting Submissions and Publishing Soon

The American College of Rheumatology will be publishing the first issue of its third official journal, *ACR Open Rheumatology* (*ACROR*), in early 2019. Editors-in-Chief Drs. Patricia P. Katz and Edward H. Yelin, and Clinical and Basic Science Deputy Editors Drs. David I. Daikh and Bruce N. Cronstein, will be heading *ACROR*'s editorial team.

ACROR will publish manuscripts describing potentially important findings of rigorously conducted studies in all aspects of rheumatology. As an open access journal, immediate access to full content of *ACROR* will be available to all readers. The electronic-only format of the journal, as well as other aspects of the review and production processes, will allow for faster review and publication, and liberal sharing of articles. The projected article publication fee (APC) for *ACROR* will be $2,500 with a discounted rate of $2,000 for articles in which the first or corresponding author is an ACR/ARP member. In addition, there will be waivers of the APC for all articles submitted through March 31, 2019.

For additional information, visit www.acropenrheum.org.

New Division Name

Rheumatology is truly a people specialty: We often develop lifelong relationships with our patients as well as our colleagues. We increasingly recognize that providing the best rheumatologic care requires a team effort. The collegial nature of our specialty is reflected in the ACR's mission statement: To empower rheumatology professionals to excel in their specialty.

In keeping with this mission, we are pleased to announce that our health professionals' membership division is changing its name to Association of Rheumatology Professionals (ARP). This name change highlights the dedication of the ACR to serve the entire rheumatology community. It also reflects our broadened base of interprofessional members (administrators, advanced practice nurses, health educators, nurses, occupational therapists, pharmacists, physical therapists, physician assistants, research teams, and more).

The name is new, but our commitment and promise remain the same: We are here for you, so you can be there for your patients.

ACR State-of-the-Art Clinical Symposium

The 2019 State-of-the-Art Clinical Symposium (SOTA), to be held April 5–7 in Chicago, Illinois, offers high-impact rheumatology education over the course of a single weekend. The symposium will provide more than 10 hours of nonconcurrent sessions with an emphasis on clinical application to rheumatology practice. Attendees will hear key opinion leaders speak on a range of content in areas such as therapeutic developments, recent research findings, and scientific advances. The program will include breakfast and lunch roundtable discussions to allow for personal interactions with experts.

The Fellows-in-Training (FIT) Educational Session at SOTA will be offered as a presymposium session encouraging FITs to explore career opportunities and participate in hands-on workshops designed to further their understanding of essential rheumatologic areas. (FIT travel scholarship recipients are required to attend this session.)

In addition, the presymposium program Rheumatology Documentation and Coding will provide guidance from expert coders on the changes to the 2019 payment policies and insight into difficult E&M coding situations. Be sure to register by the early-bird deadline of February 6 and book your hotel room by March 15. For additional information and to register, visit www.rheumatology.org/Learning-Center/Educational-Activities.